RLC

GEOLOGICAL SURVEY OF CANADA
DEPARTMENT OF ENERGY, MINES AND RESOURCES, OTTAWA

PAPER 74-1 Part B

REPORT OF ACTIVITIES
Part B, November 1973 to March 1974

1974

Energy, Mines and Resources Canada
Énergie, Mines et Ressources Canada

GEOLOGICAL SURVEY
PAPER 74-1 Part B

REPORT OF ACTIVITIES
Part B, November 1973 to March 1974

1974

Available by mail from *Information Canada*, Ottawa

from the Geological Survey of Canada
601 Booth St., Ottawa

and

Information Canada bookshops in

HALIFAX — 1683 Barrington Street
MONTREAL — 640 St. Catherine Street W.
OTTAWA — 171 Slater Street
TORONTO — 221 Yonge Street
WINNIPEG — 393 Portage Avenue
VANCOUVER — 800 Granville Street

or through your bookseller

A deposit copy of this publication is also available
for reference in public libraries across Canada

Price: $5.00 Catalogue No. M44-74-1B

Price subject to change without notice

Information Canada
Ottawa
1974

CONTENTS

GEOPHYSICS

MARINE GEOSCIENCE

A. Environmental Marine Geology

B. Sedimentary Basins

C. Regional Reconnaissance

Page

STRATIGRAPHY AND STRUCTURAL GEOLOGY

INTRODUCTION

The Geological Survey, founded in 1842, functions under the responsibilities assigned to the Minister of Energy, Mines and Resources as defined in the Resources and Technical Surveys Act. The Geological Survey has responsibility for investigating the geology, resource geophysics, geochemistry, geomorphology and physical geography of the Canadian landmass including the continental shelves and adjacent ocean floors. In addition to systematic mapping (carried out and published at various scales and including an extensive program of aeromagnetic mapping) and comprehensive topical studies, much attention is given to development of nationally consistent standards in geological cartography, geological time scales and stratigraphic correlation and to essential, mission-oriented paleontological, petrological and mineralogical studies. In the fields of geophysics and geochemistry, methods and equipment designed for Canadian conditions are developed and/or tested. The Geological Survey outlines and evaluates regions of high mineral or fuel potential. It appraises the national endowment of mineral wealth and participates with other agencies of the department in assessing the technical and socio-economic feasibility of their development and the impact of such development on the Canadian landmass.

The 107 reports that make up this publication reflect the broad range of investigations carried out by officers of the Geological Survey to meet these responsibilities. They represent the results of some of the studies carried out between November 1, 1973 and March 31, 1974. The reports are arranged in broad scientific categories that correspond only roughly to the formal organization of the Survey into divisions and sections. The illustrations are reproduced without change from material submitted by the authors. Manuscripts were accepted for inclusion in this report until May 13, 1974.

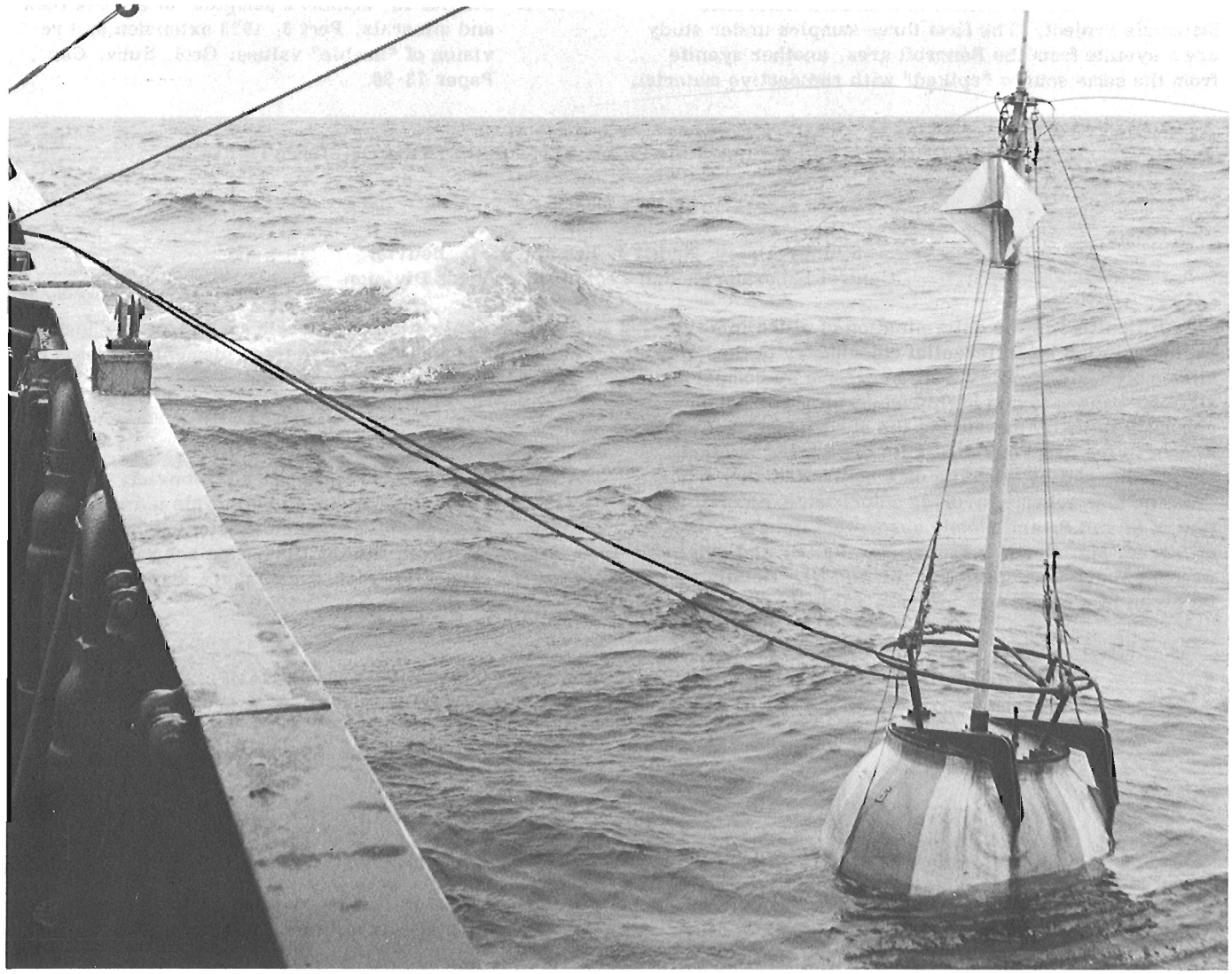

Sea Operations, Atlantic Geoscience Centre.
Lowering a telemetering refraction seismic buoy from CSS Dawson.

1. STUDIES IN "STANDARD SAMPLES" OF SILICATE ROCKS AND MINERALS

Project 690089

Sydney Abbey
Central Laboratories and Technical Services Division

Receipt of additional data from a variety of sources resulted in the publication of a revised and enlarged compilation of "usable" values. Since that publication appeared, data became available on some British samples, assigned values for two Japanese samples were re-calculated here, and some additional analytical work was done on proposed reference samples originating in Canada, France, the U.S.S.R. and South Africa. Additional proposed reference samples were received from Canada (see below), France and Czechoslovakia.

A "Task Force on Rock Samples" was launched in conjunction with the Canadian Standard Reference Materials Project. The first three samples under study are a syenite from the Bancroft area, another syenite from the same source "spiked" with radioactive material, and a gabbro from Mount Royal. Portions of all three samples have been distributed to over fifty laboratories in seventeen countries. The large number of collaborating laboratories was required in order to obtain at least some data on all elements of interest and as much data as possible for the delicate task of assigning reliable values for major components.

Reference

Abbey, Sydney
1973: Studies in "standard samples" of silicate rocks and minerals, Part 3, 1973 extension and revision of "usable" values; Geol. Surv. Can., Paper 73-36.

2. EXTENSION OF THE LITHIUM FLUOBORATE SYSTEM OF ANALYSIS OF SILICATE ROCKS

Project 690090

Sydney Abbey, Naomi J. Lee and J.-L. Bouvier
Central Laboratories and Technical Services Division

Difficulties in the determination of silica in a fluoborate solution by differential colorimetry of the beta-silicomolybdate complex were overcome by comparing all absorbances to one highly-absorbing potassium chromate null, by measuring the absorbance of the unknown in the same cuvette as its bracketing synthetic standards, and by working on a controlled-time basis.

The new scheme involves colorimetric determination of Si and P, and atomic absorption determination of Al, Fe, Mg, Ca, Na, K, Ti, Mn, Ba, Sr and where present above trace amounts, Cr and Ni. Details will be given in a paper now in press (Abbey, et al., 1974). Possible application of this scheme and/or the "neo-classical" system to certain trace elements remains to be investigated.

Reference

Abbey, Sydney, Lee, Naomi J. and Bouvier, J.-L.
1974: Analysis of rocks and minerals using an atomic absorption spectrophotometer. Part 5. An improved lithium fluoborate scheme for fourteen elements; Geol. Surv. Can., Paper 74-19, 26 p.

3. DETERMINATION OF LITHIUM, RUBIDIUM, CESIUM AND POTASSIUM IN SOLID SAMPLES BY ATOMIC ABSORPTION SPECTROMETRY

Project 690090

J.-L. Bouvier
Central Laboratories and Technical Services Division

The existing method for K, Li, Rb and Cs (Abbey, 1972) suffers from a number of shortcomings:

(a) the slow, tedious process of sample dissolution, dilution, aliquoting, etc;

(b) the need to run standard additions to overcome matrix effects on some samples;

(c) limited sensitivity for Cs, which frequently occurs at the 1 ppm level; and

(d) difficulty in treating resistant samples, such as tourmaline.

The "screw-rod" technique of Govindaraju et al. (1972, 1973) was, therefore, tried. It involves grinding and mixing the solid sample with twice its weight of sodium chloride (for L, Rb and K) or sodium carbonate (for Cs). The resulting powdered mixture is impregnated in the threads of the screw rod which is then inserted in the flame of the atomic absorption spectrometer. The resulting signal is recorded on a chart, and the area under the curve compared with similar signals obtained with reference samples subjected to the same treatment.

Although intended originally only for trace amounts of the rarer alkali metals, the method has been successfully applied to potassium determination by using a relatively insensitive spectrum line. According to Govindaraju, the technique should be applicable to such volatile trace elements as Cd, Zn and Pb. Determination of those elements will be attempted, as will also be that of strontium and possibly other elements.

References

Abbey, Sydney
1972: Analysis of rocks and minerals by atomic absorption and flame emission spectroscopy. Part 4. A composite scheme for the less common alkali and alkaline earth elements; Geol. Surv. Can., Paper 71-50.

Govindaraju, K., et al.
1972: Analyse directe sur poudre de roches et spectrométrie d'absorption atomique: Dosage du rubidium et du lithium; Bull. Soc. Fran. Céramique, v. 96, p. 47-52.

1973: Solid sampling flame atomic absorption determination of cesium in silicate rock samples; Atom. Absorpt. Newsletter, v. 12, p. 73-76.

4. IMPROVEMENTS IN SAMPLE PREPARATION TECHNIQUES FOR X-RAY FLUORESCENCE ANALYSIS OF ROCKS

Project 690090

J.-L. Bouvier
Central Laboratories and Technical Services Division

The resin-bonded sample disc, based on the work of Leake et al. (1969) has given satisfactory performance for over a year, providing more stability and freedom from boric acid "dusting" when compared to the method previously used. It was necessary, however, to perform the analysis by computer-controlled comparison with reference samples of similar composition in order to overcome inter-element effects. In using the new X-ray spectrometer (expected in the Spring of 1974), it will be possible to determine at least 12 elements instead of the present eight, and more computer storage would then be required if the same procedure were followed.

In an attempt at improving accuracy and simplifying calculation by eliminating both inter-element and particle-size effects (without introducing boric acid dusting), a fused glass disc method was examined (Harvey, et al., 1973). Samples were fused with lithium metaborate and an oxidant in gold-platinum crucibles and the melt poured into an aluminum ring lying on a titanium block on an electric hot plate. A titanium plunger was used to compress the disc, which was then annealed on the hot plate. The resulting disc appears reasonably stable and mechanically strong.

Work is continuing on studying the effect of overall sample composition, choice of oxidant, possible addition of an absorber, etc.

References

Harvey, P.K., et al.
1973: An accurate fusion method for the analysis of rocks and chemically related materials by X-ray fluorescence spectrometry; X-Ray Spectrometry, v. 2, p. 33-44.

Leake, B.E., et al.
1969: The chemical analysis of rock powders by X-ray fluorescence; Chem. Geol., v. 5, p. 7-86.

5. APPLICATION OF SPECTROCHEMICAL METHODS TO TRACE ELEMENT DETERMINATIONS IN GEOLOGICAL MATERIALS

Project 690090

W. H. Champ
Central Laboratories and Technical Services Division

A series of publications has been planned, which will describe in detail the optical emission spectrographic methods which have been developed in these laboratories for analysis of geological samples. The first of these, entitled "A Spectrochemical Analysis System using Controlled D.C. Arc for Quantitative Multi-element Trace Determinations in Rocks, Minerals and Ores" is nearing completion. It is expected to be available for distribution to interested persons later this year.

Detailed plans have been made for extending the optical capabilities of our direct-reading spectrometer from the current 22 element readout to 32 elements, and at the same time to discard the original electronic parts of the instrument and replace them with an improved solid state components package. The Datagen minicomputer and teletype system which presently controls the output will be re-programmed to incorporate the new elements, and we hope also to include various correction factors in this program which should bring about some increases in precision and accuracy to the analytical output.

In order to maintain and extend analytical working curves for some 40 elements determined by our various methods, both photographic and direct-reading, comprehensive series of synthetic standard samples have been planned and calculations made. These will be prepared by the laboratory staff on a continuing basis during the next year or more as required.

6. INVESTIGATION OF THE APPLICATION OF THE KARL FISCHER TITRATION METHOD FOR THE DETERMINATION OF TOTAL WATER IN ROCKS

Project 690090

Serge Courville
Central Laboratories and Technical Services Division

The K-F method would provide a direct determination of the water content of rocks. Experimental runs were made in order to investigate and establish the optimum operational parameters. Some areas of investigation were: methods of fusion, flux composition, flux to sample ratio, completeness of evolution and recovery, absorbing media, equipment modification, accuracy and precision.

Two methods are now proving suitable. "Method A" involves the fusion of a flux-sample mixture in an induction furnace, with a K-F titration of the absorbed water. In "method B", the condensed water from a Penfield determination is quantitatively transferred and titrated with the K-F reagent. Both methods give compatible results.

Work is continuing on modifications of Method A and in the accumulation of analytical data. A Geological Survey report is planned.

7. X-RAY DETERMINATION OF PYRRHOTITE COMPOSITIONS

Project 680023

G. J. Pringle
Central Laboratories and Technical Services Division

Procedures have been established in the X-ray laboratory for the routine determination of pyrrhotite compositions in either large or small samples. The technique is based on the curves for the spacing d(102) vs. composition of hexagonal pyrrhotite, as given in Arnold and Reichen (1962) and modified by Toulmin and Barton (1964). Spacings for samples large enough to prepare a smear mount are determined by diffractometer. Smaller samples are prepared as spindles and the spacings are determined using a large (114mm) powder camera. Optical densitometer measurements of the films using an Optronics Stripscan instrument give spacing values that compare favourably with the precision of the diffractometer method.

The smear mounts are prepared on a glass base using halite [d(220) = 1.994 ± .001 A] as an internal standard. One smear mount is prepared for each sample and the spacing d(102) for pyrrhotite is determined against halite (220) by taking the mode for six oscillations of the goniometer. Since the smallest chart division on the diffractometer is approximately equal to the variation between oscillations, the mode is a more convenient measure than the mean.

The powder mounts are prepared also using halite

Table 1

Pyrite d(220) in Å, determined by diffractometer. (CuK∝)

	Mount 1	Mount 2	Mount 3
	1.916	1.917	1.916
	1.917	1.916	1.916
	1.916	1.916	1.916
	1.916	1.916	1.916
	1.915	1.916	1.916
	1.916		1.917
Mode	1.916	1.916	1.916

Table 2

Pyrite d(220) in Å, determined on film. (FeK∝)

	Film 1	Film 2	Film 3
	1.9150	1.9154	1.9152
	1.9156	1.9156	1.9152
	1.9156	1.9156	1.9148
	1.9156	1.9156	1.9152
	1.9154	1.9154	1.9154
	1.9161	1.9152	1.9152
Mean	1.9156	1.9155	1.9152

Table 3

Pyrrhotite compositions

	Chart			Film		
Sample	d(102)* ±.001 Å	N ±.0025	Wt. % Fe** ±.1%	d(102)* ±.001 Å	N ±.0025	Wt. % Fe** ±.1%
1	2.065	.9450	60.9	2.065	.9450	60.9
2	2.068	.9500	61.2	2.067	.9475	61.1
3	2.072	.9575	61.5	2.071	.9550	61.4
4	2.075	.9625	61.8	2.073	.9600	61.7

*N = mol. fraction of FeS in the system FeS - S_2 from the curve in Toulmin and Barton (1964).

** Wt.% Fe = $\frac{(11169.4)\ (N)}{128.256 + (47.566)\ (N)}$

as an internal standard. One mount is prepared for each sample and the spacing d(102) for pyrrhotite is taken from the mean of six densitometer scans on the film.

Both the diffractometer and the film method were standardized against the (220) line of pyrite (d = 1.915 ± .001 A). Tables 1 and 2 list the result in each case for three mounts made from the same pyrite standard. The precision of both methods can be quoted as ± .001 A.

Table 3 lists measurements on four samples of synthetic hexagonal pyrrhotite that were supplied by K.L. Currie for use in comparing composition determinations by both techniques. The film method gives essentially the same results as the diffractometer and has the advantage that pyrrhotite compositions can be determined on single disseminated grains in a specimen without resorting to time consuming separation procedures.

References

Arnold, R.G., and Reichen, L.E.
1962: Measurement of the metal content of naturally occurring, metal-deficient hexagonal pyrrhotite by an X-ray spacing method; Amer. Mineral., v. 47, nos. 1 and 2, p. 105-111.

Toulmin, P. III, and Barton, P.B., Jr.
1964: A thermodynamic study of pyrite and pyrrhotite; Geochim. et Cosmochim. Acta, v. 28, no. 5, p. 641-671.

8. THE DETERMINATION OF RARE EARTHS, SCANDIUM, YTTRIUM AND LANTHANUM IN ROCKS AND MINERALS BY ATOMIC ABSORPTION AND FLAME EMISSION SPECTROSCOPY

Project 690090

J.G. Sen Gupta
Central Laboratories and Technical Services Division

A study with synthetic solutions of scandium, yttrium, lanthanum and rare earths indicates that it is possible to determine these elements except cerium, gadolinium, terbium and lutetium by a combination of atomic absorption and flame emission spectroscopy in a variety of geological materials. The sensitivity of determination of these elements is increased by aspirating a 100% ethanolic solution of the perchlorates in nitrous oxide-acetylene flame. Sodium (1000 ppm) or 1% lanthanum (when determination of this metal is not necessary) can be used as spectroscopic buffer to eliminate interferences.

From samples containing traces or low rare earths, it is necessary to preconcentrate the rare earths by oxalate precipitation with calcium as the carrier, followed by removal of calcium by hydroxide precipitation using mg amounts of iron or aluminum as carrier.

Geol. Surv. Can., Paper 74-1, Part B

9. CRUSTAL DELEVELLING IN NORTHERN NEWFOUNDLAND

Project 680130

L.M. Cumming[1] and D.R. Grant[2]

A raised beach observed at nearly 500 feet above sea level in the Hawke Bay area provides evidence of the minimum amount of crustal isostatic adjustment since the last glaciation (Figs. 1, 3 and 4). This feature is considerably higher in elevation than other evidence of postglacial marine overlap in western Newfoundland, ranges up to about 200 feet at Bonne Bay. Observations of raised marine features at comparable elevation farther north on the Northern Peninsula (Daly, 1921) could not be substantiated during recent surficial geological mapping (Grant, 1969a), although numerous trimlines on moraines between Bonne Bay and Hawke Bay generally increase in elevation (Grant, 1972).

The Hawke Bay feature is thus the highest and northernmost, precise evidence of postglacial marine overlap in Newfoundland. Its discovery, the first record of marine overlap in Newfoundland, is attributed to James Richardson who in 1860 wrote in part:

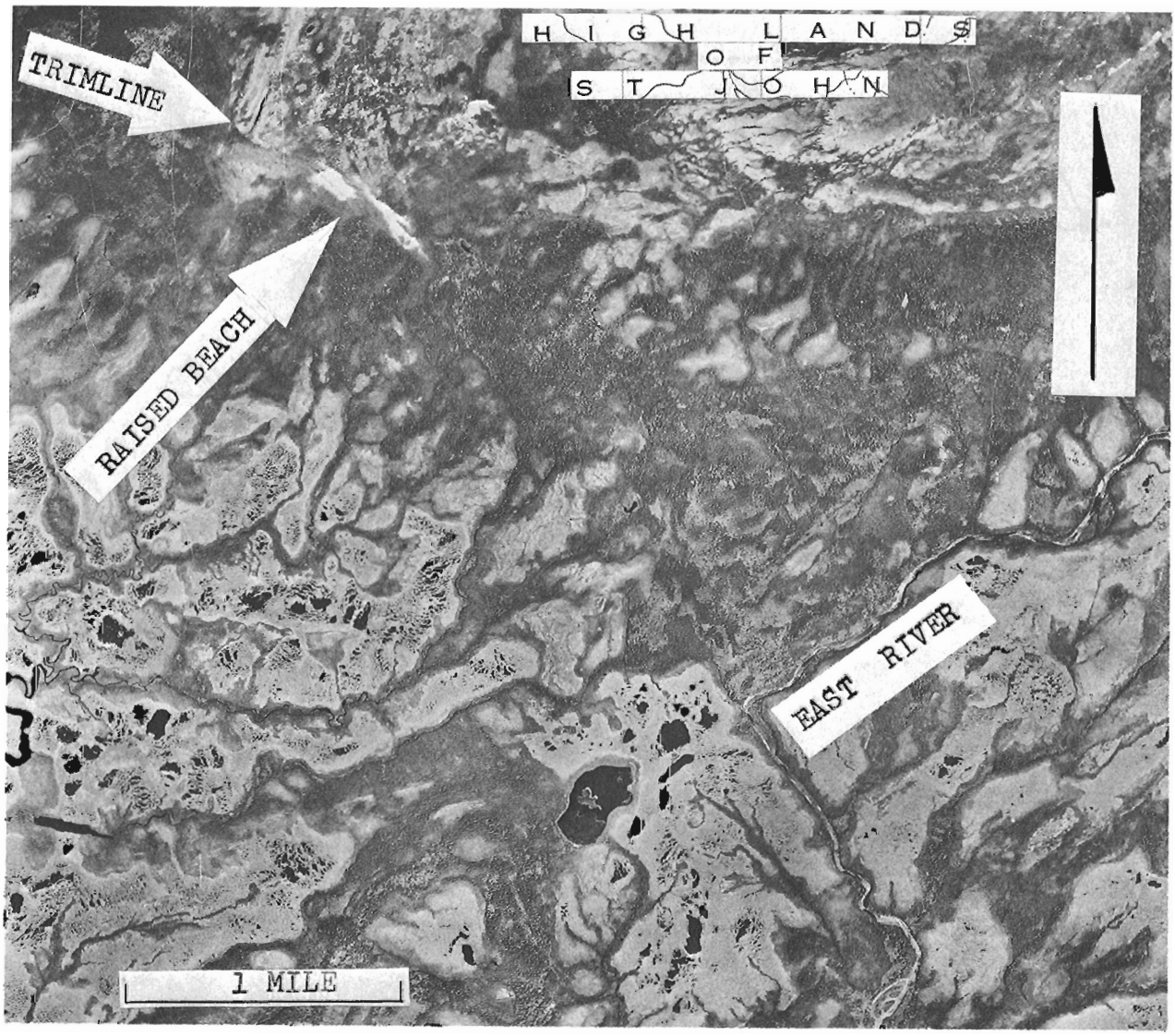

Figure 1. Location of raised beach in map-area 12I/11, at elevation 450 feet. The location is on the west flank of the Highlands of St. John and to the north of East River, which flows into Hawke Bay. EMR Photo NFL-5-185.

[1]Regional and Economic Geology Division, Ottawa.

[2]Terrain Sciences Division, Ottawa.

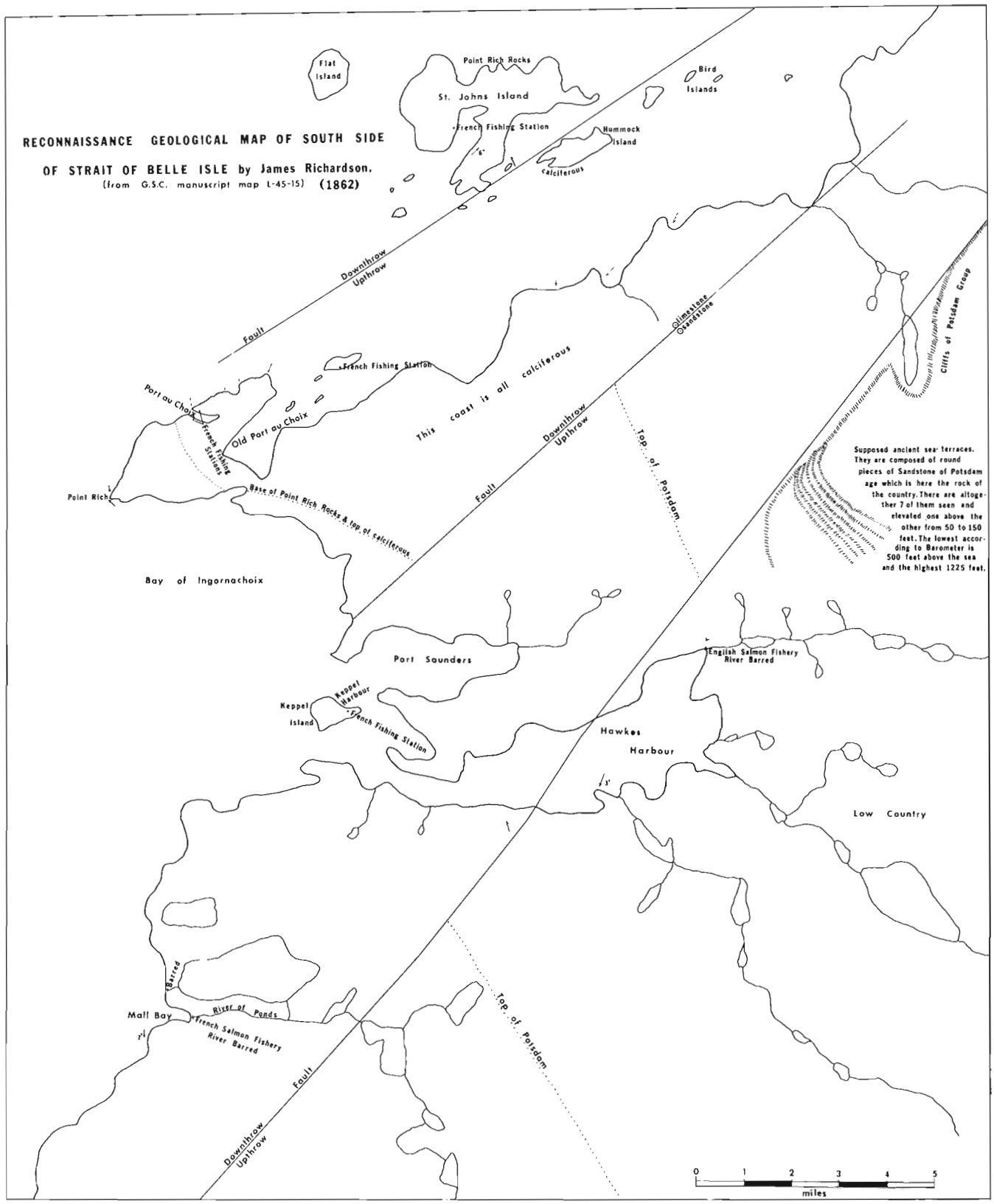

Figure 2. Geological sketch map of the Hawke Bay area by James Richardson, 1862, showing his notations concerning seven terraces. The arrows show the direction of the dip of the strata.

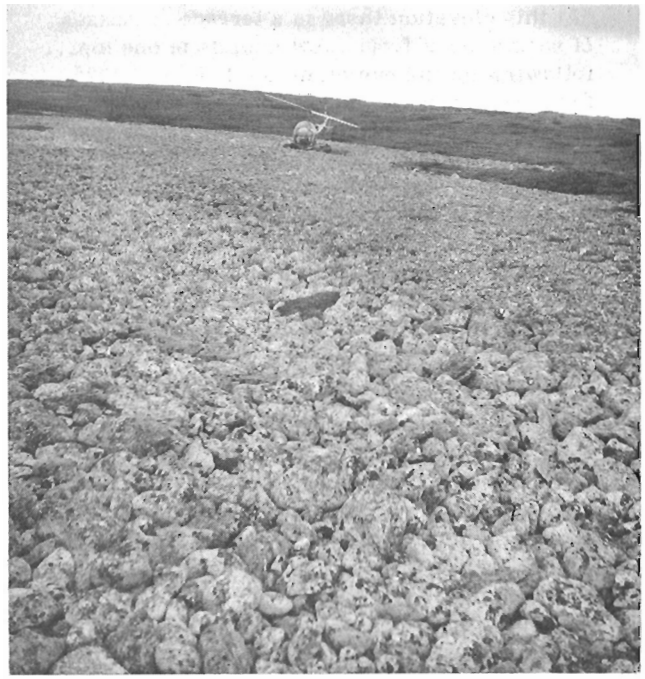

Figure 3.

Raised beach trending at 330 degrees at elevation Ca 450 feet above sea level at lat. 50°42'N., long. 57°08½'W. The water-worn cobbles are mainly white orthoquartzitic sandstone of the Hawke Bay Formation of Lower Cambrian age. GSC photo 161917.

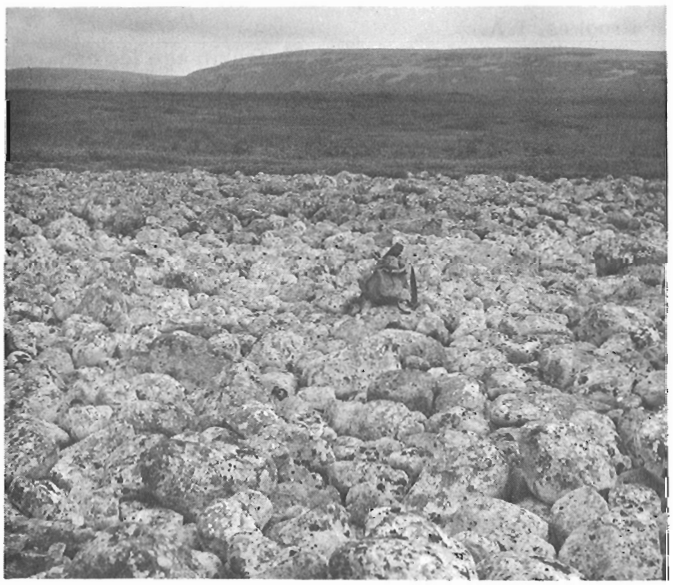

Figure 4.

Close-up view of cobbles on the raised beach at lat. 50°42'N., long. 57°08½'W. A packsack provides a scale. Occasional cobbles of Precambrian pink granite as well as Cambrian arkose of the Bradore Formation occur among the white sandstone cobbles. In the distance, with structural benches visible, are the Highlands of St. John capped by flat-lying sandstone of the Hawke Bay Formation. GSC photo 161918.

Figure 5.

Terrace composed of frost-heaved angular blocks of white sandstone of the Hawke Bay Formation. This terrace is near the summit of the Highlands of St. John and is formed along a bedding plane surface. GSC photo 161920.

"At this elevation there is a terrace of masses of sandstone of from a few pounds to one ton... following up the mountain to a height of 1225 feet, by barometer, seven of these terraces are passed at elevations of 50 to 150 feet apart – they are (made up of) bare pieces of sandstone of the above size and description, with now and then a Laurential boulder (which are) much more rounded. All these terraces show the pieces of sandstone lying on one another as if they had been beaten by the waves of the ocean, being overlain with one another (in a manner) that is peculiar to the action of waves or currents." (GSC notebook 1493, p. 88; see also Fig. 2.)

The cobble-strewn terraces above 500 feet, noted by Richardson, are clearly seen on airphotos to be very extensive, slightly subhorizontal and to follow the sedimentary stratification. They are now known to be bedrock structural benches with a veneer of frost-heaved debris also containing erratics, similar to that shown in Figure 5.

Richardson's intriguing description prompted a visit to the feature during bedrock studies of the Port Saunders area (12-I/11) in 1971. At the location of Figure 4, there are 8 distinct cobble beach berms, in a series of 21 that extend for one-half mile and cover 500 feet of slope (N.A.P.L. airphoto A20521-16; scale 1:18,000). They are developed on a salient of fractured Hawke Bay quartzite forming South Summit of the Highlands of St. John. The upper limit of the beach ridges is a conspicuous trimline cut across the steeply dipping sandstone ridges.

Three elevation determinations of the highest berm and the trimline by the stereotope photogrammetric method (by G. Mizerovsky, Terrain Sciences Division) yielded a figure for marine limit of 466 feet. The 450-foot contour on the topographic map is slightly lower. Though both determinations are subject to a nominal error of ± 25 feet, their comparability suggests the error is minimal. Marine limit here is therefore taken to be 460 feet.

This is the net amount by which the land has risen out of the sea by crystal rebound since deglaciation. To this may be added an approximately equal amount to include the isostatic rebound that occurred as the ice sheet was thinning and receding toward this site. Additionally world-wide sea level has risen about 450 feet (135 m) as glaciers melted. Thus the elevation of this raised beach marking the marine limit is only the latter third of the total 1,500 feet of deglacial crustal isostatic rebound.

This rebound in turn implies a former ice thickness of nearly a mile, and is indirect evidence that the extent of the Laurentide continental ice sheet extended at least far enough to affect the Hawke Bay area because 1) lower marine limits are known elsewhere in Newfoundland where only island ice cap activity is indicated (Brookes, 1970); 2) there are vague indications of comparably high marine overlap farther north of the Northern Peninsula where there is evidence of overriding by Laurentide ice (Grant, 1969b); and 3) marine limits to 500 feet are measured on the Quebec coast across the Strait of Belle Isle whence Laurentide ice apparently approached Newfoundland. In fact, striations trending southwestward along the coast are found on shoreline outcrops as far south as Port au Choix, presumably left by confluent Labrodorean and Newfoundland glaciers. Farther south, lower marine limits and only westward oriented striations imply thinner radially flowing island ice.

References

Brookes, I.A.
1970: New evidence for a Wisconsin age ice cap over Newfoundland; Can. J. Earth Sci., v. 7, no. 6, p. 1374-1382.

Daly, R.A.
1921: Postglacial warping of Newfoundland and Nova Scotia; Am. J. Sci., Ser. 5, v. 1, no. 5, p. 381-391.

Grant, D.R.
1969a: Late Pleistocene readvance of piedmont glaciers in western Newfoundland; Marit. Sediments, v. 5, no. 3, p. 126-128.

1969b: Surficial deposits, geomorphic features and late Quaternary history of the terminus of the Northern Peninsula of Newfoundland, and adjacent Quebec-Labrador; Marit. Sediments, v. 5, no. 3, p. 123-125.

1972: Postglacial emergence of northern Newfoundland; in Report of Activities, Part B, November, 1971 to March 1972; Geol. Surv. Can., Paper 72-1, pt. B, p. 100-102.

10. STRATIGRAPHIC FRAMEWORK OF VOLCANOGENIC MASSIVE SULPHIDE DEPOSITS, NORTHERN APPALACHIAN OROGEN[1]

W. H. Poole
Regional and Economic Geology Division

The northern Appalachian orogen is well endowed with volcanogenic massive sulphide deposits of copper, zinc and lead. The total size of bodies from significant mining camps, already mined, being mined and to be mined in the near future, exceeds 200 and perhaps 300 million tons. About three quarters of this is in the Bathurst camp of New Brunswick.

Throughout the northern Appalachians from the Hudson River to Notre Dame Bay are some 14 significant deposits and mining camps selected for purposes of this paper. Their host rocks range in age from Hadrynian to Devonian with the Ordovician the most favoured. The greatest number of deposits with largest tonnages are within mixed acid and basic volcanics ascribed to former volcanic island arc assemblages according to the plate tectonic model. These are generally polymetallic base metal sulphides in a pyrite and/or pyrrhotite matrix. Other deposits are smaller and are simple copper ores in a pyrite and/or pyrrhotite matrix; they occur within low-potash pillow basalt, generally in what we would call an ophiolite assemblage (basalts which pass downward through a sheeted dyke zone to gabbro and thence ultramafic rocks) and these rocks are believed to have formed at a mid-oceanic ridge or marginal basin.

In the first type, the host volcanics are presumed to have formed above a subduction zone of crustal consumption, and in the second, at a zone of crustal accretion or generation. If these hypotheses are correct, then both types of volcanogenic massive sulphides are genetically related to active margins of crustal blocks. However, some volcanic piles, judged to be related to subduction zones, have not as yet yielded massive sulphide deposits. To learn why one volcanic pile yields deposits is a challenge but to learn why another does not is a greater challenge.

Significant Volcanogenic Sulphide Deposits

Significant ophiolite-type deposits are found only along the northwest margin of the northern Appalachian belt (Fig. 1). In Newfoundland there is the Whalesback deposit and there are others in the district such as Tilt Cove, Betts Cove, Little Bay and Little Deer. The York Harbour deposit on the west coast occurs within an Ordovician allochthon. All but the Little Deer are now inactive. In Quebec there is the old Huntington mine. These deposits are found in basalts believed to be the upper part of the ophiolite suite.

Deposits of the calc-alkaline or island arc type are many and irregularly distributed when viewed over the entire northern Appalachians. In Newfoundland, the Rambler and Buchans mines are operating, the Gullbridge is closed, and the Point Leamington yet to be exploited. The Mindamar mine or Cape Breton Island is closed, and the Teahan mine in southern New Brunswick produced long ago. Northern New Brunswick has the queen of sulphide deposits in the northern Appalachian region: more than a dozen deposits totalling 130 million tons and probably much more. Four mines are operating: Brunswick No. 6 and No. 12, Heath Steele and Caribou. The Wedge is closed, and several await their time: Chester, Murray, Restigouche and others. The Bathurst camp is very large by Canadian standards, perhaps second only to the Kidd Creek mine near Timmins, Ontario. Many deposits in the Eastern Townships of Quebec have been mined since the 1860's, like those of the Notre Dame Bay district (Tilt Cove, Betts Cove, etc.) in Newfoundland. Among the Quebec deposits are the Eustis, Suffield, Weedon, Cupra-d'Estrie, and Solbec. To these must now be added the newly opened Clinton copper mine. The New England States, and areas about equivalent in size to New Brunswick and the Appalachian part of Quebec, has surprisingly few significant volcanogenic sulphide deposits. Two are shown on Figure 1, the Black Hawk and Elizabeth mine areas.

Thus over 200 million tons of major massive sulphide deposits have been found in the northern Appalachians. The value of metals produced approaches $150 million per year.

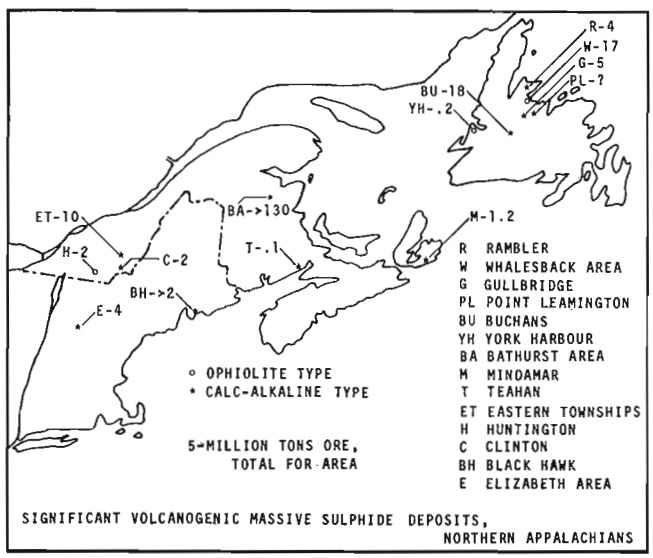

SIGNIFICANT VOLCANOGENIC MASSIVE SULPHIDE DEPOSITS, NORTHERN APPALACHIANS

[1]This paper is a shortened version of a talk given at McGill University on November 30, 1973 in a symposium on metavolcanic massive sulphide deposits of the northern Appalachians organized by the geology graduate students of the Adams Club. Tonnage and average grade figures of the mines and mining camps were provided by D. F. Sangster, Geological Survey of Canada, and are only approximate.

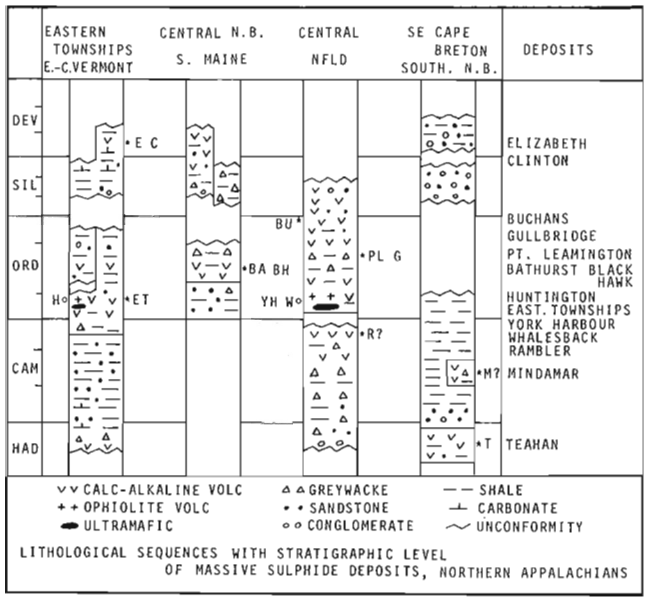

Stratigraphic Level of Deposits

A generalized chart of selected lithological sequences in the northern Appalachians is shown on Figure 2 with the 14 selected sulphide deposits. Most deposits occur within Ordovician rocks, which were formed during a time when crustal margins were most active. The ophiolite type is believed to be Early Ordovician in age. The largest deposits are of the volcanic island arc type and occur in Middle Ordovician and possibly Upper Ordovician rocks, deposits such as those at Bathurst, Gullbridge, Point Leamington, and possibly at Black Hawk. The Buchans mine host rocks are probably either Upper Ordovician or slightly younger, Lower Silurian. They could indeed be the same age as the Gullbridge and Point Leamington host rocks but of different environment, facies and tectonic setting. The age of the host rocks (Ascot and Weedon Groups) of the Eastern Townships polymetallic deposits is uncertain, probably either Late Cambrian or Early Ordovician

Five deposits on Figure 2 have host rocks not of Ordovician age. The Rambler host rocks are Hadrynian or Cambrian, although may be Early Ordovician. Middle Cambrian strata host the Mindamar mine and Hadrynian strata the Teahan. On the other hand, Lower Devonian host rocks contain the Elizabeth and Clinton mines.

Rocks younger than Early Devonian lack volcanogenic sulphide deposits apparently because their volcanics were not generated along oceanic ridges or in island arcs. Notable too is the lack of deposits in Silurian rocks (except possibly for Buchans).

In this paper the sulphide deposits or at least the protosulphide deposits are assumed to be the same age as the host rocks, i.e. they are essentially syngentic deposits regardless of later superposed processes (deformation and metamorphism, and resultant recrystallization, diffusion and/or flowage) which may have greatly changed the geometry, distribution of values etc. within the deposit.

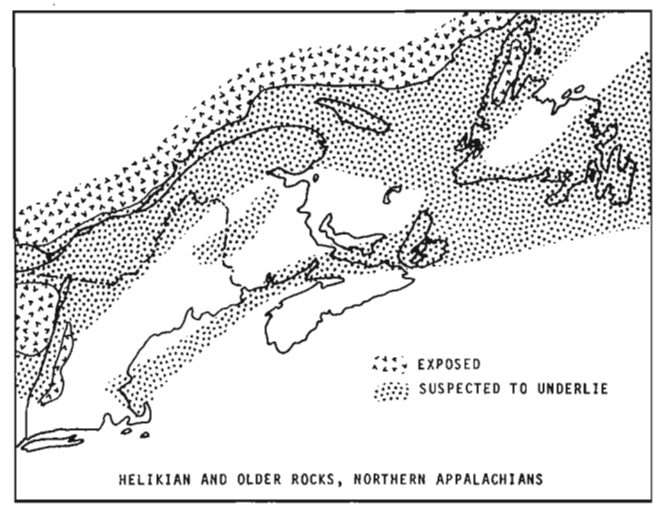

Geological Evolution and Sulphide Deposits

Helikian and Earlier

The distribution of exposed Grenfillian rocks and of those areas believed to be now underlain by Grenvillian rocks is depicted in Figure 3. To the northwest is the Canadian Shield, which forms inliers in western Newfoundland and the Green Mountains of Vermont, in large subject to part retrograde metamorphism during Paleozoic orogenies. Farther inside the Appalachian belt are two inliers in western Newfoundland, and possibly another in the Boundary Mountain anticlinorium in northwestern Maine. There, R.S. Naylor of M.I.T. obtained a discordant zircon age, in which the $^{207}Pb/^{206}Pb$ date is 1500 m.y. Thus I believe that the St. Lawrence Platform and most of the north west margin of the Appalachian belt is underlain by Grenville rocks. And, I also believe that the Avalon belt is underlain by a Grenville-type basement, nowhere now positively recognized in exposure. I further speculate that the Miramichi Anticlinorium in central New Brunswick is underlain by Grenville-type basement.

Hadrynian and Cambrian

The Helikian and older continent began to thin and pull apart during the Hadrynian along the site of two proto-Atlantic oceans, the one along the axial zone of the Appalachians between the Canadian Shield and the Avalon belt and the other between the Avalon belt and the African Shield. Along the northwestern flank of the Appalachian belt are mainly sediments derived from the Shield to the northwest (Fig. 4). Cambrian carbonate with a basal quartzite passed southeast (in a reconstructed model) through a bank-edge limestone breccia to "basinal" or continental slope greywacke, shale and minor volcanics which extend stratigraphically downward into the Hadrynian. The Cambrian strata are exposed in western Newfoundland and in New York State but are missing, and presumably covered by allochthonous geosynclinal rocks, along

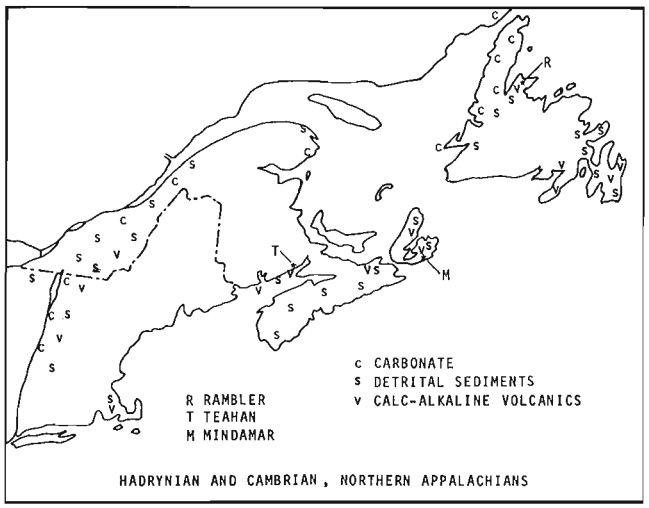

HADRYNIAN AND CAMBRIAN, NORTHERN APPALACHIANS

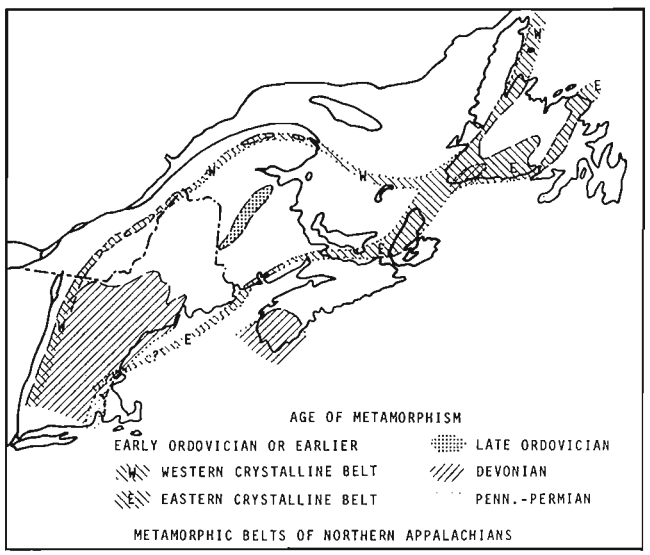

METAMORPHIC BELTS OF NORTHERN APPALACHIANS

the St. Lawrence River between these two areas. The "basinal" facies was polydeformed and metamorphosed in late Cambrian or early Ordovician and is now represented by the western (Fleur de Lys) crystalline belt. Much of this sub-belt was moved northwestward as allochthons during the Ordovician. Rather anomalously located are the unmetamorphosed platformal Cambrian siltstone and fossiliferous carbonate of the Corner-of-the-Beach and Murphy Creek strata in eastern Gaspé; these rocks probably represent the platform beneath the Quebec allochthon, either a window through the otherwise covered allochthon or a sample of the platform to the southeast of a Quebec klippe such as found east of the Humber Arm klippe near Corner Brook, Newfoundland.

In the Avalon belt of eastern Newfoundland, Cape Breton Island and southern New Brunswick, Hadrynian acid and basic volcanics of calc-alkaline to weakly alkaline affinity are interbedded with marine and non-marine terrigenous sediments, here and there intruded by granitic plutons presumably of subvolcanic origin. The stratified rocks pass upward into fluviatile red beds and conglomerates, and are capped by synclinal relics of orthoquartzite followed upward by Lower, Middle, and Upper Cambrian fossiliferous shales. Locally, the Cambrian rests unconformably upon Hadrynian rocks. The fossils here are of the Atlantic faunal realm, whereas those in correlative rocks in Quebec and western Newfoundland are of the Pacific faunal realm. The presence of this zone in eastern Massachusetts, albeit fragmentary, is indicated by fossiliferous Cambrian rocks in at least one locality resting upon granodiorite, presumably Hadrynian. Volcanic rocks appear locally in the Middle Cambrian part of the assemblage.

Small areas of older rocks — quartzite, slate and carbonate — appear in Cape Breton Island and southern New Brunswick as the George River and Green Head groups. Some of them are metamorphosed and everywhere they are in fault-contact with known Hadrynian volcanics. They could be Hadrynian or much older. If they are Hadrynian, they could represent cover strata upon a Grenville basement.

In the Meguma block, southeast of the Avalon belt and known only in Nova Scotia, there is a thick greywacke assemblage which was deposited during Cambrian from turbidity currents derived from the southeast in a source believed now to be the North African Shield.

The Hadrynian and Cambrian rocks lack volcanogenic massive sulphides except for two deposits which may be classed as volcanogenic. The Teahan deposit in southern New Brunswick consists of a thin, irregularly folded lens within chloritized Hadrynian andesitic and dacitic tuffs. Chalcopyrite, sphalerite, galena and minor tennantite replace and form veins in brecciated pyrite and quartz-carbonate-talc gangue. The host rocks are polydeformed and schistose. Over 100,000 tons of reserves run approximately 0.5% Cu, 1.5% Zn and nearly one ounce Ag per ton. The old Mindamar mine in southeast Cape Breton consisted of lenses in a "shear" zone marked by schistose rhyolite tuff and siltstone within an assemblage of rhyolite, rhyolite tuff and basic flows and dykes, all of Middle Cambrian age. The "shear" is nearly vertical and parallels bedding in the wall-rocks. The ore formed lenses of massive, fine-grained pyrite, sphalerite, galena, chalcopyrite and tennantite in a quartz-carbonate-talc gangue. About 1.2 million tons were mined, grading about 0.7% Cu, 1.3% Pb, 5.5% Zn, and 2 ounces of Ag per ton.

The Teahan and Mindamar deposits are similar in structural setting, mineralogy, and lithology of host rock, although different in age of host rock. R.D. Hutchinson who has studied the paleontology and stratigraphy of the Cape Breton Cambrian strata (see Geol. Surv. Can., Mem. 263) expressed doubt following the talk that the unfossiliferous host rocks of the Mindamar mine are indeed Cambrian as correlated lithologically by L.J. Weeks in Geological Survey Memoir 277. It is tempting to hypothesize that the Mindamar host rocks are Hadrynian like those of the Teahan, that the sulphides in both are of the volcanogenic type, and that the so-called "shearing", quartz-carbonate-talc gangue and paragenetic relations are the result of younger, superimposed tectonic, metamorphic and

hydrothermal processes. It also follows that the Hadrynian (and Cambrian?) volcanics of the Avalon belt ought not to be discarded as exploration target areas without careful consideration. The western margin of the Avalon belt in Newfoundland (Hermitage-Burin-Bonavista strip) may be worth prospecting.

The Rambler mine host-rocks, metamorphosed basic and minor acid volcanic rocks of the western crystalline zone, are of Hadrynian-Cambrian of Early Ordovician age. The deposits comprise about 3.7 million tons roughly averaging 2.2% Cu, 0.5% Zn, and significant values in silver and gold. The massive to disseminated form of the orebodies, and their association with acid volcanics and ferruginous chert suggest affinity with the calc-alkaline, island arc type. If the orebodies and host rocks are Hadrynian-Cambrian, they are unlike all other northern Appalachian deposits in that respect. Perhaps other Hadrynian-Cambrian volcanic assemblages in the belt deserve consideration as exploration targets.

Paleozoic Metamorphism

The age of metamorphism in some places particularly those of the middle and late Paleozoic age is reasonably well known. Examples are (Fig. 5) the Late in the Miramichi anticlinorium in New Brunswick; the Middle Devonian of the New England states, southern mainland Nova Scotia and southern Newfoundland; and the Pennsylvanian-Permian of Rhode Island in southern New England.

The main metamorphic belts, or crystalline belts, are long continuous belts which flank the core zone of the Appalachian belt. The western (Fleur de Lys) crystalline belt extends from Burlington Peninsula to southwest Newfoundland, thence it presumably passes beneath the Gulf of St. Lawrence and beneath Silurian and younger strata, to the Shickshocks and farther southwest passes beneath Siluro-Devonian cover rocks to re-appear as the Bennett Schist and Sutton Schist and thence southward along the Green Mounts. The belt contains inliers of "reworked" Grenvillian crystalline rocks. In southern New England, the belt loses definition through superposition of the Devonian metamorphic area. It is tempting to suppose that the metamorphism along this entire belt is the same age. It may just be, but stratigraphic and radiometric dating evidence is not totally convincing. Nevertheless in the Canadian part of the belt, the major metamorphism is certainly pre-Silurian, almost undoubtedly pre-Middle Ordovician, and possibly even within or just before the Early Ordovician.

The eastern (Gander) crystalline belt extends from the Wesleyville area in northeastern Newfoundland, southward to the coast and then arcs west to merge or to appear to merge with the western crystalline belt in southwest Newfoundland. It then passes under Cabot Strait to northwestern Cape Breton Island and southwestward beneath middle and upper Paleozoic strata to the Saint John area of southern New Brunswick. Southwest of Saint John the belt passes into the Gulf of Maine. It may cut through the Boston-Long Island area farther southwest. The age of this metamorphism is less well known. It would certainly be pre-Silurian, and probably pre-Middle Ordovician.

The western and eastern crystalline belts are very fundamental features. They are old and undoubtedly had a strong effect on evolution of the Appalachian belt. For this reason, these two belts will appear on subsequent figures depicting the various systems.

Ordovician

The Ordovician period was one of intense and complex tectonic activity, associated with movements of continental plates. It also marks the period during which most of the characteristic volcanogenic massive deposits were formed in the northern Appalachians.

In Early Ordovician time the pattern of deposition established during the Cambrian continued along the northwest margin of the Appalachians: carbonate on the platform, limestone breccia to the southeast at the bank-edge, and thick flysch derived from the Canadian Shield next to the southeast (Fig. 6). Still farther southeast was found the ophiolite sequences (Snooks Arm, Lushs Bight in part, Serpentine Belt of Quebec) presumably in oceanic crust within a newly opened marginal basin and/or open oceanic crust formed at a mid-ocean ridge. It seems too that island arc volcanism prevailed on the southeast side of the ophiolite belt; in Newfoundland these rocks are represented by the Catchers Pond assemblage and in Quebec perhaps by the Ascot-Weedon volcanic assemblage.

The ophiolitic rocks are host in Newfoundland to a multitude of generally small massive copper deposits in western Notre Dame Bay, the Whalesback, Tilt Cove, Betts Cove, Little Bay and Little Deer deposits. Some contain significant values in zinc. Six of these, before mining, had 17 million tons in total, averaging about 1.7% Cu. Within the crystalline belt is the similar Terra deposit in the Baie Verte ophiolite belt either originating in situ in a marginal basin, or downfaulted from a once-continuous overriding allochthonous ophiolite sheet above. Within the ophiolite slices in the Humber Arm klippe is the York Harbour deposit of one quarter million tons averaging 2% Cu and 5% Zn. Some of these ophiolite deposits, like that at York Harbour, are located within the basal part of the pillowed basalts at the top of the sheeted dyke zone. The old Huntington copper mine in the Eastern Townships probably of the ophiolite type, contained about 2 million tons of ore averaging 0.9% Cu.

Southeast of the ophiolite belt there was apparently an island arc which produced the acid and basic volcanics of the Ascot and Weedon Groups and, of course, the many massive sulphide deposits such as the Eustis, Suffield, Weedon, Cupra-d'Estrie and Solbec. The tonnage of these deposits before mining was 10 million tons, grading roughly 2% Cu, 0.3% Pb, and 3% Zn. The age of these unfossiliferous volcanic formations is unknown; they are certainly pre-Middle Ordovician and presumably latest Cambrian or like the Cathers Pond rocks, Early Ordovician. Similar island arc volcanic rocks, if present, would lie buried beneath Siluro-

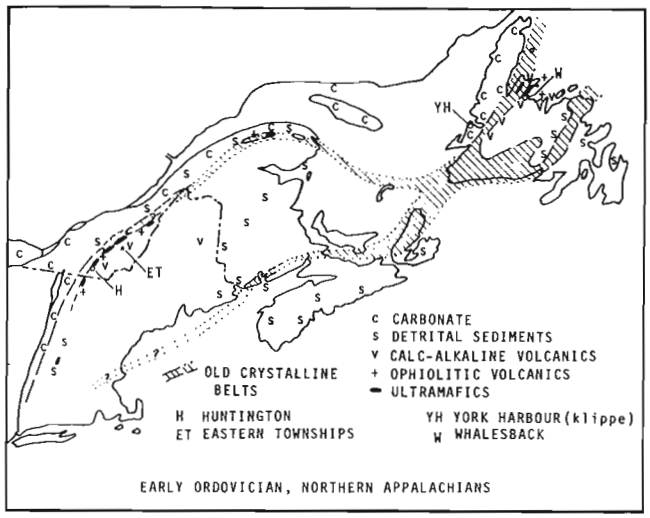

EARLY ORDOVICIAN, NORTHERN APPALACHIANS

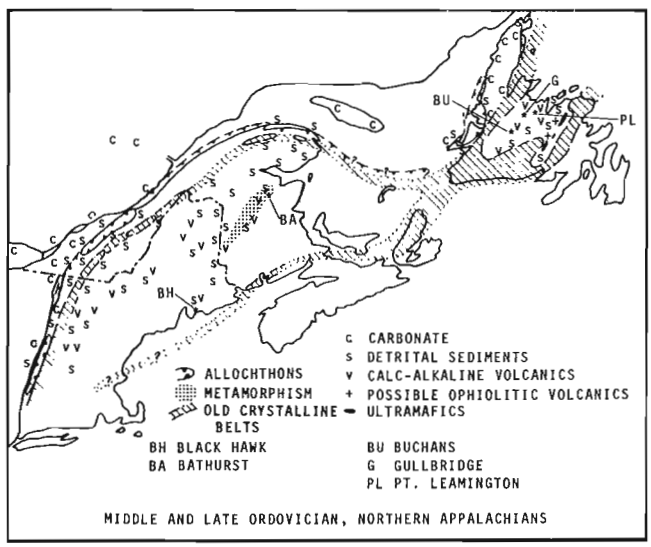

MIDDLE AND LATE ORDOVICIAN, NORTHERN APPALACHIANS

Devonian rocks northeast of the Ascot-Weedon rocks through Temiscouata region and axial Gaspé Peninsula. Lower Ordovician rocks occur elsewhere in the northern Appalachians, but none are known to be host to significant volcanogenic sulphide bodies to date. In central New Brunswick, the oldest rocks of the Miramichi anticlinorium are orthoquartzites, the maturity of which suggest a stable underlying unseen basement, possibly Grenville crust. Shale deposition continued in the Avalon belt conformably upon Cambrian shale, and in eastern Newfoundland, sandstone and iron-formation of the Wabana iron mine were deposited. Similar dark grey shale was also deposited in the Meguma belt.

Middle and Late Ordovician times were tectonically active. In Newfoundland and southern Quebec, the carbonate platform became depressed along the edge of the Appalachian zone, black shale and greywackes from the southeast were deposited in the trough or exogeosyncline, and allochthons of folded and partly metamorphosed rocks of Hadrynian to Early Ordovician age were driven westward out of the "geosyncline" onto the platform (Fig. 7). Ophiolite assemblages, bordering flysch deposits, metamorphic rocks of the western crystalline belt, and perhaps too the Ascot-Weedon volcanic rocks were moved northwestward as oceanic crust became subducted and/or obducted. The process took place during Early and early Middle Ordovician time in western Newfoundland, and during middle and late Middle Ordovician time in southern Quebec, where conditions were much more complex than those of Newfoundland and where the sequence is in in the process of being worked out. At present, I favour a model in which the entire pre-late Ordovician terrane in the Quebec Appalachians is allochthonous, and that the suture zone from which the allochthons were derived lies in a zone now almost entirely covered by younger rocks between the Boundary Mountains of northwestern Maine and Chaleur Bay (Maquereau Group).

Within the axial part of the Appalachian belt late Middle Ordovician calc-alkaline volcanism and sedimentation occurred. One such belt is the Ammonoosuc volcanics extending northeasterly into the northern Maine volcanic belt. In central New Brunswick these are the Tetagouche volcanics and associated sediments deposited gradationally upon the older orthoquartzites in en echelon relations with the northern Maine volcanic belt. Both belts were intruded in late Ordovician time by plutons of granodiorite and quartz monzonite. The New Brunswick rocks were deformed and regionally metamorphosed in later Ordovician time and uplifted to become the Miramichi Anticlinorium.

In central Newfoundland, calc-alkaline volcanism and sedimentation took place in the western part of the belt while dominantly shale was deposited in the eastern part. Along the eastern side of the shale belt are some volcanics and ultramafic rocks, whose age is thought to be Middle Ordovician.

Middle and Upper Ordovician rocks are lacking in the Avalon belt presumably reflecting a period of uplift. On the Meguma block, some volcanism and sedimentation may have occurred at this time.

Rocks of Middle and Late Ordovician age have produced the largest massive sulphide deposits. Most are in the Canadian sector of the belt. The largest assemblage of deposits is found in the Tetagouche rocks of

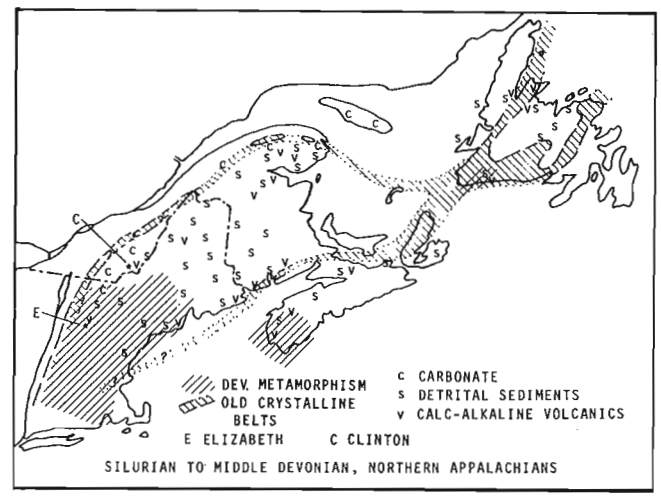

SILURIAN TO MIDDLE DEVONIAN, NORTHERN APPALACHIANS

the Bathurst Camp at the northern end of the Miramichi anticlinorium. The more than 130 million tons of sulphide deposits have grades of roughly 1% Cu, 5% Zn, and 3% Pb. Four are being mined presently — the Brunswick No. 6 and No. 12 deposits, and the Heath Steele and Caribou deposits. The rocks containing the smaller Black Hawk deposit in southeastern Maine may be Ordovician but its age is uncertain. The black quartzite, schist and metavolcanic host faintly resemble the Bathurst host rocks. The Black Hawk contains over 2 million tons of ore with values in Zn, Cu, Pb and Ag.

In Newfoundland there are at least three large deposits. The Gullbridge mine, now closed, contained 5 million tons of ore with 0.8% Cu. To the east is the newly found and yet to be mined Point Leamington deposit; tonnage and grade figures have not been published. Farther south is the rich Buchans mine. The host rock acid volcanics and minor sediments are of either Late Ordovician or Early Silurian age. More than a dozen individual orebodies in the camp totalled 18 million tons averaging about 1.8% Cu, 6% Zn, 1.3% Pb, 3.8 ounces of Ag per ton and some gold.

Silurian to Middle Devonian

Silurian to Middle Devonian was a time of basin-filling between and around the anticlinorial uplifts raised during the Ordovician. Sedimentation was widespread, generally of shallow-water aspect, and calc-alkaline volcanism localized (Fig. 8). In mid-Devonian, metamorphism was intense in the New England part of the belt, small, hot, gabbro-ultramafic bodies were intruded in a few localities in central Newfoundland, southern New Brunswick and southeastern Maine, and folding and granite intrusion widespread. This orogeny, the Acadian, changed the character of the belt profoundly.

Silurian carbonates were deposited upon the St. Lawrence Platform. Relics appear on Anticosti Island and in Ontario and eastern New York State. Lower and Middle Devonian sediments have been recovered from a Cretaceous diatreme near Montreal, evidence of widespread deposition on the platform. Red beds of latest Silurian age appear above the frontal edge of the Humber Arm klippe in western Newfoundland.

Silurian to Middle Devonian sediments in the Connecticut Valley — Gaspé Synclinorium in southern Quebec and northwestern New England are a very thick carbonate-terrigenous sequence, generally shallow-water, with calc-alkaline volcanics here and there. Carbonate is more common along the northwestern edge of the synclinorium. Near the top of this sequence, the Gaspé Sandstones of late Early Devonian and early Middle Devonian age were deposited in a marginal trough extending from Gaspé Peninsula to Eastern Townships. They became conglomeratic and partly nonmarine at the top. The trough formed in response to the beginnings of orogenic activity farther southeast. Volcanics and sediments extended southwesterly along the northwestern boundary of the Miramichi anticlinorium in northern and central New Brunswick. South of the anticlinorium is a non-volcanic deep-water Silurian greywacke assemblage which graded southeastward into a volcanic and sedimentary zone along the northern side of the old eastern crystalline belt. These central New Brunswick rocks extend southwesterly through Maine, south of the Ammonoosuc-northern Maine volcanic belt into the Merrimac Synclinorium.

Some sediments and acid and basic volcanics were deposited upon the Avalon belt in northern Nova Scotia and Cape Breton Island. In the Meguma block of mainland Nova Scotia were deposited a very thick assemblage of sediments and acid and basic volcanics of the White Rock Formation which became overlain by younger sediments.

The Siluro-Devonian development in Newfoundland was quite different from that of the mainland part of the northern Appalachians. The merging of the two crystalline belts in the Cabot Strait area may be an old feature, perhaps Ordovician, which served to separate two quite different terranes during the Siluro-Devonian. In east-central Newfoundland, in the Botwood belt, polymictic conglomerates overlain locally with some acid and basic volcanics pass upward into terrestrial shallow-water and fluviatile red and green sandstones. These rocks are dated by fossils and are Early and Middle Silurian in age. No younger Silurian or Devonian strata are known in this belt. To the west is the Springdale belt in which acid and some basic volcanics are grossly interbedded with red terrestrial polymictic conglomerates and sandstone. West again, on the western side of the western crystalline belt, are the fossiliferous lower and middle Silurian sediments and acid and basic volcanic rocks in western White Bay. In the southwest corner of Newfoundland, amongst the metamorphic rocks, are patches of acid volcanics thought to be Silurian, and shale, sandstone and polymictic conglomerate bearing Early to Middle Devonian plants suggestive of a Gaspé Sandstone equivalent.

These southwest Newfoundland rocks grade outward into metamorphic rocks, evidence there of Devonian regional metamorphism. The extent of this metamorphic overprint in Newfoundland is not known. The southern part of the northern Appalachians was also regionally metamorphosed in southwestern Nova Scotia and southern New England. It is tempting to link these two metamorphic areas across the Gulf of Maine.

Two possible volcanogenic massive sulphide deposits were formed during this period. One is the Elizabeth mine in east-central Vermont. Small bodies of massive and disseminated chalcopyrite and pyrrhotite lie concordantly within Lower Devonian amphibolite and schist. The grade of metamorphism is medium to high; kyanite and sillimanite occur locally. The other is the newly opened Clinton copper mine in the Eastern Townships; concordant pyrite-chalcopyrite zones lie within basic volcanics. Orebodies in the nearly 2 million tons grading 2% Cu and 1.5% Zn have been reported.

Conclusions

There are some interesting conclusions to be drawn from examination of the host rocks of the sulphide deposits.

1. There are two general types, the ophiolite type and the calc-alkaline type, and maybe some "intergradational" types yet to be properly defined.

2. The ophiolite type is mainly a simple copper ore. The bodies in the northern Appalachians are small in comparison to those of the calc-alkaline type.

3. The calc-alkaline type is mainly a polymetallic Cu, Zn and Pb assemblage, and the bodies range in size from small to very large. Those bodies with host rocks of higher proportion of acid volcanics contain higher proportions of Pb and Zn values.

4. Neither type can be identified on ore mineralogy along. The Gullbridge, for example, is of the calc-alkaline type, but is essentially a copper-only body. On the other hand, the York Harbour deposit is of the ophiolite type, but carries much more Zn than Cu.

5. Both types were formed during volcanism closely related to active crustal plate boundaries, the ophiolite type at an accretion boundary and the calc-alkaline type above a subduction boundary, according to the dictates of the plate tectonic model.

6. Most significant deposits are of Ordovician age.

7. Perhaps very significant are the occurrences in non-Ordovician host rocks — the Teahan in Hadrynian volcanics, the Mindamar in Cambrian (or Hadrynian?) volcanics, and the Elizabeth and Clinton in Devonian rocks. If these are indeed volcanogenic massive sulphide deposits, then large non-Ordovician terranes become possible host rocks of deposits, and ought not to be discarded from exploration programs without careful consideration. Hadrynian volcanics are plentiful in the Avalon belt of southern New Brunswick, Cape Breton and eastern Newfoundland. Silurian volcanics appear in all provinces and some states and appear to lack volcanogenic sulphide deposits for quite uncertain reasons.

11. RELATION OF PREDICTED TO EXPERIMENTALLY DETERMINED COKE STABILITIES FOR WESTERN CANADIAN COALS

Projects 610269, 680105

A.R. Cameron, P.R. Gunther, P.A. Hacquebard and T.F. Birmingham
Institute of Sedimentary and Petroleum Geology, Calgary

The regional petrological studies being carried out on coals of the Kootenay and Luscar Formations include attempts to evaluate the coking properties of these coals from their petrographic composition. The method used in this instance is that of Schapiro et al. (1961). Their procedure requires data on maceral content and reflectance, both determined microscopically. Reflectance is an index of coal rank. The macerals are grouped into reactives and inerts depending upon known or supposed behaviour in the coking process. Coals vary in terms of maceral content and rank and, provided oxidation has not been a significant factor, these variations contribute largely toward differences in coke properties including stability.

In the present report a comparison is made between predicted stabilities and stabilities actually determined on cokes. Maceral and reflectance data were obtained on 28 coals for which coking information was available. A summary of the maceral and reflectance data is given in Table I and the calculated stabilities are plotted against determined stabilities in Figure 1. The oblique line on this figure represents a position of perfect coincidence; that is, the calculated value coincides with the determined value. The greater the deviation from this line, the greater the difference between predicted and actual values. Figure 1 shows that three coals, represented by points 22, 23 and 28, fall far above the line. If these three samples are eliminated, the other 25 show differences which range from 0 to 14 in the comparison of predicted to actual values. Fifteen of these 25 samples differ by 5 or less from the actual values obtained. The three coals not from western Canada (samples 1, 2 and 5) gave a good comparison of predicted to determined stabilities. These three are Appalachian coals and it may be significant that the constants developed for use in the Schapiro and Gray procedure were largely based on experiments with Appalachian coals.

Samples 22, 23 and 28 are characterized by calculated stabilities which were far above those actually determined. The history of these samples is such that oxidation is suspected. Particles showing oxidation features were observed microscopically in these samples but were not evaluated quantitatively. Oxidation has a deleterious effect on coking properties and is difficult to evaluate microscopically, at least in its early stages. Also it should be noted that two of these samples (23 and 28) have high ash contents. The effect of ash on coke stability is difficult to predict. Schapiro and Gray based their formula and constants on an ash value of 12 per cent or less by weight (Schapiro and Gray, 1964). With the present suite of samples, those with ash contents of greater than 12 per cent show a mean difference of 14 in the calculated vs. the actual stabilities, while those with ash contents of 12 per cent or less show a mean difference of 6. An area for further research in connection with coke properties involves the influence of variations in ash content, distribution and quality.

In the Schapiro and Gray formula a group of macerals considered as semi-inerts are empirically assigned 1/3 to reactives and 2/3 to inerts. An attempt was made in the present study to bring the predicted values more into line with actual values by varying the proportions of semi-inert macerals (semi-fusinite, etc.) assigned to reactives and inerts. The first step in this attempt involved measuring the reflectance of the maceral semi-fusinite. The resulting data were used then in two ways. In the first approach, the actual reflectance values obtained were employed to divide the semi-inerts into "V" types after which coke calculations were made. In the second approach, the reflectance of the semi-fusinite was used to assign to reactives that proportion of the semi-inerts of which the reflectance values differed from the vitrinite in the coal by 0.20 or less. With both approaches, the differences between predicted and actual stabilities become smaller for some samples and

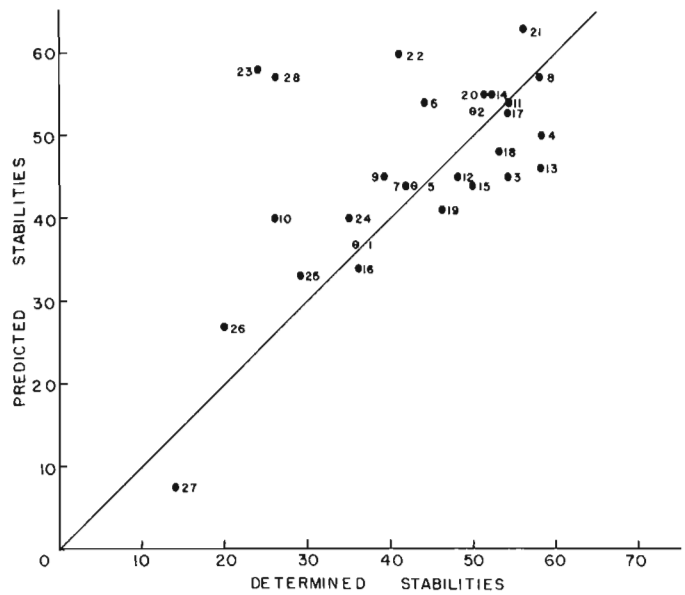

Figure 1. Relationship between predicted coke stabilities and actual stabilities determined on coke.

Table 1. Summary of Petrographic Data and Coke Stabilities.

Sample	Reactives[1] vol. pct.	Inerts[2] vol. pct.	Ash, dry wt. pct.	Mean Max R_o	Predicted Stabilities	Determined[3] Stabilities
1	63	37	4.6	0.98	37	36
2	69	31	6.6	1.59	53	50
3	63	37	5.8	1.58	45	54
4	63	37	6.5	1.53	50	58
5	82	18	6.4	1.00	44	43
6	54	46	8.3	1.35	54	44
7	72	28	9.6	0.92	44	43
8	71	29	9.0	1.09	57	58
9	62	38	12.5	1.57	45	39
10	54	46	11.1	1.59	40	26
11	75	25	10.6	1.06	54	54
12	80	20	7.5	1.00	45	48
13	58	42	10.4	1.48	46	58
14	66	34	8.2	1.50	55	52
15	56	44	8.5	1.48	44	50
16	50	50	9.0	1.46	34	36
17	62	38	8.5	1.50	53	54
18	56	44	6.8	1.43	48	53
19	52	48	7.2	1.41	41	46
20	64	36	6.3	1.34	55	52
21	81	19	9.0	1.27	63	56
22	72	28	12.0	1.15	60	41
23	69	31	18.1	1.17	58	24
24	53	47	10.3	1.46	40	35
25	50	50	10.9	1.48	33	29
26	47	53	15.8	1.46	27	20
27	40	60	15.4	1.46	8	14
28	67	33	14.4	1.47	57	26

[1] Reactives include vitrinite, exinite plus 1/3 semi-inert macerals.

[2] Inerts include inertinite, mineral matter plus 2/3 semi-inert macerals.

[3] Determined stabilities obtained from Metals Reduction and Energy Centre, Mines Branch, as results of tests in 500-lb. experimental oven.

larger for others. Thus, there was little or no overall improvement over the use of the conventional Schapiro and Gray procedure. However, it is felt that this is an area that should be explored further. It is reasonable to expect that the breakdown of the semi-inerts into 1/3 reactive and 2/3 inert does not hold invariably for every coal. For those coals with high contents of semi-inerts, and many of our western coals are in this category, a more precise measure of reactivity vs. inertness seems necessary.

In summary the results suggest that the Schapiro and Gray method can be used to give at least a semi-quantitative indication of strength properties of cokes produced from western Canadian coking coals. This assumes unoxidized coal and a relatively normal ash content.

References

Schapiro, N., Gray, R.J., and Eusner, G.R.
1961: Recent developments in coal petrography; Proc. Am. Inst. Mining Eng., v. 20, p. 89-112.

Schapiro, N., and Gray, R.J.
1964: The use of coal petrography in coke making; J. Inst. Fuel, v. 37, p. 234-242.

12. A COMPOSITE COALIFICATION CURVE OF THE MARITIME REGION AND ITS VALUE FOR PETROLEUM EXPLORATION

Project 680102

P. A. Hacquebard
Institute of Sedimentary and Petroleum Geology, Calgary

This composite coalification curve (Fig. 1) portrays the changes of coal rank with depth of a series of Mesozoic and Carboniferous coals. The rank data were obtained from vitrinite reflectance measurements, which are indicated on the abscissa at the top of Figure 1, while the corresponding contents of volatile matter and the A. S. T. M. rank classes are shown at the bottom.

The curve on the left (commencing near the top of the diagram) represents the rank changes of Mesozoic coals obtained on 29 samples from four offshore wells

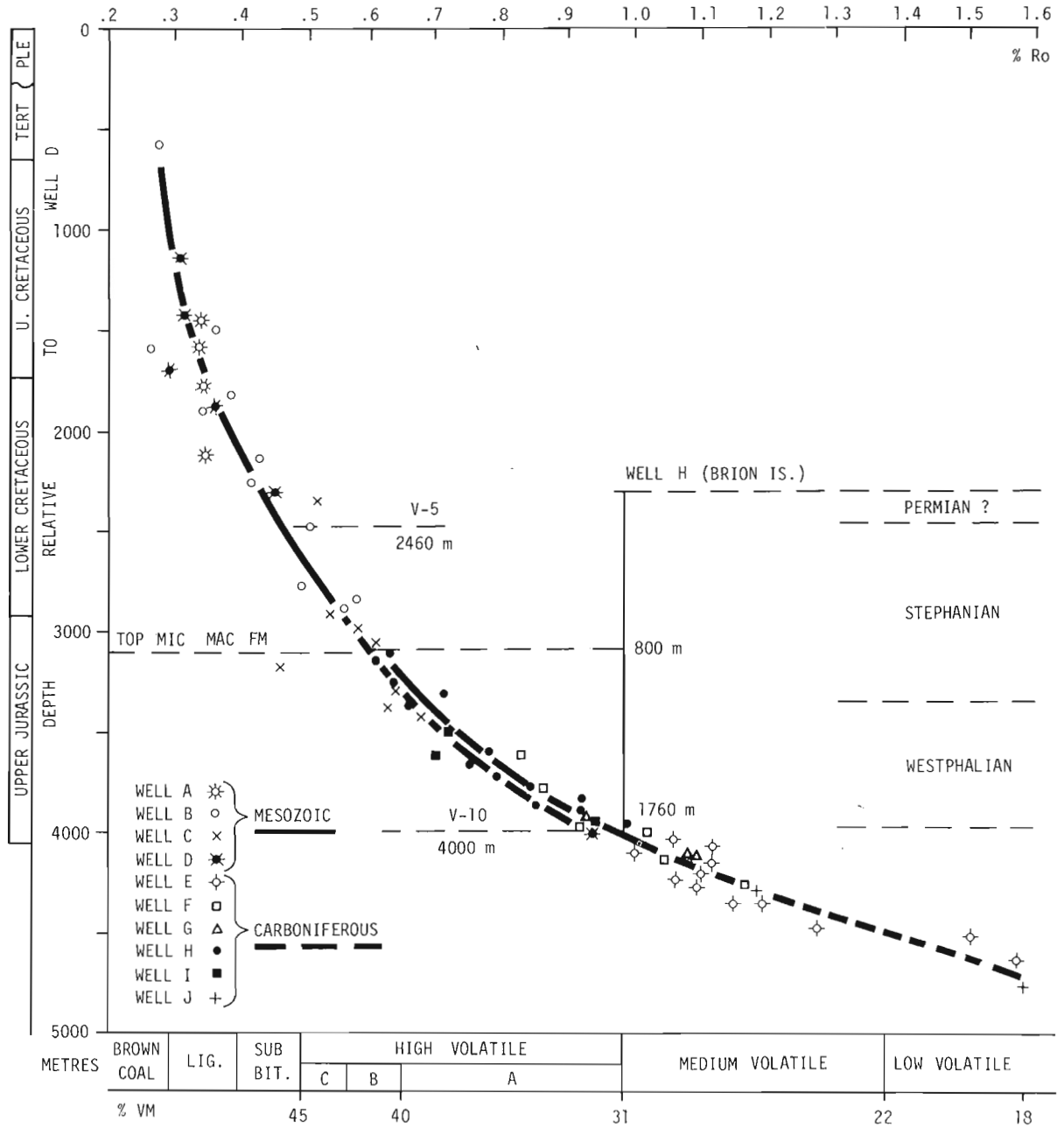

Figure 1. Composite coalification curve of Mesozoic and Carboniferous coal sequences in the Maritime region.

drilled on the Scotian Shelf, about 50 miles northeast of Sable Island. The curve shows a normal increase in rank with depth over some 4,000 metres. Over this distance the reflectance changed from 0.28 per cent at 445 metres in well B, to 0.95 per cent at 3,977 metres in well D. However, in the low-rank range, represented by the upper part of the curve, there is a considerable scatter of the data. This is not surprising, because in the lignites and sub-bituminous coals the vitrinite reflectance is not a very sensitive rank parameter. The curve shows that in these coals the per cent Ro changes only two V-types (from .3 to .5%) over a depth of 1,400 metres, whereas in the high volatile bituminous coals it changes four V-types over 1,400 metres. These figures correspond to coalification gradients that are, respectively, 0.012/100 metres and 0.033/100 metres.

The Mesozoic and Tertiary stratigraphy of the Scotian Shelf has been described by McIver (1972). He showed that a fairly complete succession, with only minor discontinuities, is represented from the Upper Jurassic to the Lower Tertiary. Only the latest Tertiary is missing; it was probably removed by subaerial erosion at the outset of glaciation, and the thickness so removed was likely not very great. From this it is concluded that the present depth of the coals as plotted on the ordinate in Figure 1 is close to the maximum overburden that ever existed.

The rank-depth relationships of 39 Carboniferous coals are plotted in the dashed curve on the right in Figure 1. It is a composite curve derived from six wells drilled at various onshore locations in the Maritimes (Hacquebard and Donaldson, 1970), except for E which is an offshore well in the Gulf of St. Lawrence.

The curve was constructed by using well H (located at Brion Island, in the Gulf of St. Lawrence) for the upper part, which was then extended downward by using overlapping rank data of the other wells. The vertical scale should be read against the depth positions of well H, and not against the depth scale of well D at the left of the diagram. Therefore, the uppermost coal lies at 800 metres and the lowermost coal (in well H) at 1,760 metres below the surface.

The Carboniferous curve covers a depth interval of 1,650 metres with a progressive change in rank from 0.63 to 1.60 per cent Ro. The coalification gradient in the range of the high volatile coals is 0.033/100 metres. This is caused by the nature of the coal samples obtained from well E. These samples, like nearly all others used in Figure 1, are from well cuttings. Those of well E showed more mixing of coals due to caving than was encountered in the other wells.

Upon completion of the Carboniferous curve, which was plotted separately from the Mesozoic curve, it was found that the two overlap in the rank range from 0.63 to 0.95 per cent Ro. Surprisingly, it was also noted that the two curves in this interval have practically the same slope, with coalification gradients of 0.033 and 0.036/100 metres. It was felt that this similarity had more significance than just being a mere coincidence. In order to obtain curves with identical progressions, similar depths of overburden likely are required, unless the duration of the coalification process would effect this.

There is little doubt that time has a significant influence on the maturation of coal. Considerable difference of opinion, however, exists regarding the true relationship. Karweil (1956) considered that the time factor is an ongoing process and that longer heating at the same temperature would produce a coal of higher rank. In contrast, Li-Ping Tan (1956) has advanced the view that a stage of equilibrium is reached in the coalification process, after which a change in rank will occur only with an increase in temperature. By comparing depth of burial of coals of identical rank but of different age, Li-Ping Tan was able to show that after about 65 million years the time factor is no longer of much significance.

As the coals used in this study are considerably older than 65 m.y. (namely 150 m.y. for the Mesozoic and 300 m.y. for the Carboniferous coals) the two curves in Figure 1 have been joined along the overlapping part, and are considered here as one representative coalification curve for the Maritime region. This procedure is considered valid because in coals older than 65 m.y. curves with equal progressions indicate equal temperatures, caused by comparable depth of burial.

The composite curve not only gives the maximum overburden required for the various rank stages of the Mesozoic coals, but also for the Carboniferous coals, because by joining the two curves one depth scale can now be employed. This means, however, that in the Maritime region the same overburden was required to obtain the same rank of coal, regardless of its age. The diagram shows that a depth of burial of 3,620 metres is required to form a high volatile "A" bituminous coal with a reflectance of 0.80 per cent, regardless of whether this coal is Late Jurassic or Carboniferous in age.

The composite coalification curve can be used to obtain, from the rank of surface coals, the thickness of strata that have been removed by erosion. On Brion Island, for instance, the position of well H in relation to the curve, indicates that 2,240 metres of strata have been eroded.

The curve is also of much value for delineating the most favourable interval of organic metamorphism for the occurrence of oil or gas in exploration wells. Recent studies on this subject show that the most promising interval for the formation of oil lies between 0.5 and 1.0 per cent Ro. When the Ro is less than 0.5 per cent, only biogenic methane occurs, and when more than 1 per cent gas will be formed; first wet gas and at about 2 per cent dry gas (CH_4). Beyond 3 per cent reflectance, gas becomes rare and seems to disappear (Robert, in press).

When this information is used in Figure 1, then it becomes apparent that in the Maritime region the favourable zone for oil formation lies at a depth of burial between 2,450 and 4,000 metres. In wells A to D, drilled on the Scotian Shelf, this depth is close to the present subsurface position. However, in well H the fact that 2,240 metres of overburden has been removed by erosion needs to be considered. Consequently, the favourable "oil" zone in this well occurs between 210 and 1,760 metres below the surface.

The composite coalification curve can be used also to delineate the "oil" interval in a well from only a few reliable rank determinations. If, for example, a rank of 0.6 per cent Ro is found at a depth of 2,000 metres, then the 0.5 per cent position according to the curve lies 480 metres above it, and the 1.0 per cent position occurs 1,070 metres below it; the "oil" zone would then lie between 1,520 and 3,070 metres below the surface.

References

Hacquebard, P.A., and Donaldson, J.R.
1970: Coal metamorphism and hydrocarbon potential in the Upper Paleozoic of the Atlantic Provinces, Canada; Can. J. Earth Sci., v. 7, p. 1139-1163.

Karweil, J.
1956: Die Metamorphose der Kohlen vom Standpunkt der physikalischen Chemie; Zeitschr. Deut. Geol. Ges., v. 107, p. 132-139.

Li-Ping Tan
1965: The metamorphism of Taiwan Miocene coals; Bull. Geol. Surv. Taiwan, no. 16, 44 p.

McIver, N.L.
1972: Cenozoic and Mesozoic stratigraphy of the Nova Scotia Shelf; Can. J. Earth Sci., v. 9, p. 54-70.

Robert, P.
Analyse microscopique des charbons et des bitumes dispersés dans les roches et mesure de leur pouvoir reflecteur; Comptes rendus, 6eme Congrès International de Géochimie Organique; Institut Français du Petrole, Rueil-Malmaison, Sept. 18-21, 1973. (in press)

13. LITHOSTRATIGRAPHY AND COAL REFLECTANCE OF A LOWER CRETACEOUS DELTAIC SUCCESSION IN THE GULF-MOBIL PARSONS F-09 BOREHOLE, N.W.T.

Project Nos. 710036, 740032

D.W. Myhr and P.R. Gunther
Institute of Sedimentary and Petroleum Geology, Calgary

Introduction

The Gulf-Mobil Parsons F-09 well is located near Parsons Lake, 24 miles northeast of the East Channel in the modern Mackenzie Delta (Fig. 1), Northwest Territories (lat. 68°54'34"N, long. 133°31'33"W). Present status is a gas well (DIAND, 1970-1972), and proven hydrocarbon occurrence is from Lower Cretaceous sandstones. Helpful comments and suggestions were made by C.J. Yarath, P.A. Hacquebard and L.R. Snowdon. The paper was critically reviewed by F.G. Young and A.R. Cameron.

Samples and cores were examined from a part of the well (8,845'-9,900') in order to determine gross lithologic units and age, identify coal-bearing intervals, interpret depositional environment, and to relate these geological parameters to the occurrence of hydrocarbons (gas and condensate) in the reservoir rocks. Three lithologic rock-units were defined based on well cuttings, two cored intervals, and the gamma-ray log response (Fig. 2). The age of the units is no older than Hauterivian or Barremian as determined from dinoflagellates in core no. 2 (Brideaux, W.W., pers. comm.). The oldest lithologic unit "C" is correlative in a rock-stratigraphic sense with the bluish grey shale division (Jeletzky, 1961), but is younger, hence the unit is diachronous. Lithologic unit "B" is correlative with the coal-bearing division as defined by Jeletzky (1960, 1961) and the overlying lithologic unit "C" is correlative with the upper shale-siltstone division of Jeletzky (1958, 1960).

Lithology and Environmental Interpretations

The following is a brief descriptive summary of the three lithologic rock-units of the Gulf-Mobil Parsons F-09 borehole (8,845'-9,900'). Lithologic unit "A" (8,845'-9,275' = 430', Fig. 2) is identified by the first occurrence of sandstone at 8,845' and consists of argillaceous siltstone (medium grey-brown) interbedded with slightly argillaceous sandstone that is grey-brown, very fine- to fine-grained, and cemented with silica. Accessory lithologies include light brown limestone and dolomitic claystone (?concretionary). The unit contains minor amounts of pyrite and coal and rare foraminifera. Contacts appear to be gradational with the underlying and overlying rock-units.

Lithologic unit "B" (9,275'-9,780' = 505', Fig. 2) consists of an interstratified succession of non-argillaceous (clean) sandstone, argillaceous sandstone, and minor amounts of coal and argillaceous siltstone. The clean sandstone is white, fine- to coarse-grained with silica cement and visible quartz overgrowths on the coarse grains. The sandstone units are 20 to 80 feet thick (gamma-ray log, Fig. 2), and appear to be in abrupt contact with underlying argillaceous arenites. The argillaceous sandstone is grey-brown, very fine- to fine-grained with traces of light green clay (?glauconite) and coaly detritus. Coal, sandy coal and coaly shale occur throughout this interval. Core no. 1 (9,337'-9,397' = 60') consists of sandstone interstratified with minor amounts of shale and a 2-foot seam of interbedded coaly shale and coal near the base of the cored interval. The argillaceous sandstone is fine- to very fine-grained and, in places, medium-grained interbedded with minor amounts of shale, arenaceous shale and siltstone. A 2-foot-thick unit of coal and dark brown coaly shale was encountered between 9,395 and 9,397 feet and is in abrupt contact with the overlying arenites. Sedimentary structures include crosslaminations (wedge-shaped and tangential), wavy microlaminations, low-angle, climbing ripple-drift laminations with complete preservation of laminae, minor bioturbation structures and a few thin fining-upward sequences. Minor constituents include pyrite and carbonaceous clasts. The environment of deposition of the cored interval is interpreted as a nonmarine deposit of a delta plain environment where marsh and fluvial flood basin sedimentary deposits accumulated. The thick, clean, quartz-sandstone units may represent fluvial deposits interpreted from well cuttings and mechanical log response (Fisher et al., 1969, Fig. 98(3)). The base of unit "B" is in abrupt contact with the underlying unit.

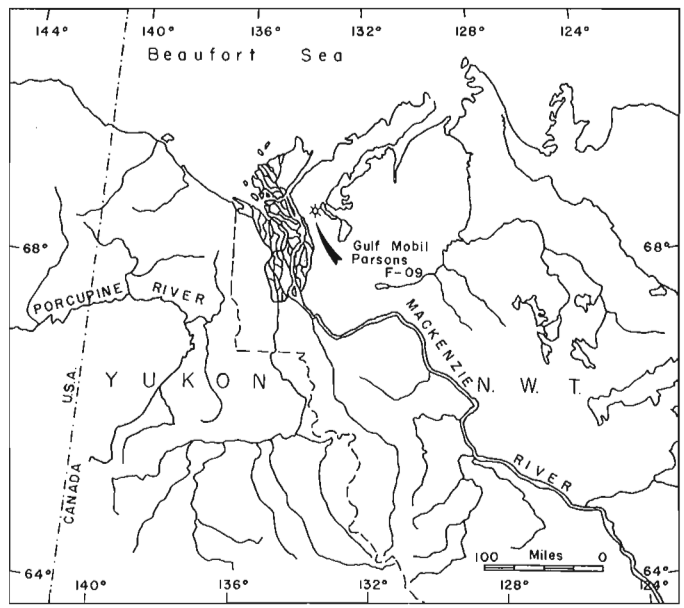

Figure 1. Location map for the Gulf-Mobil Parsons F-09 Borehole.

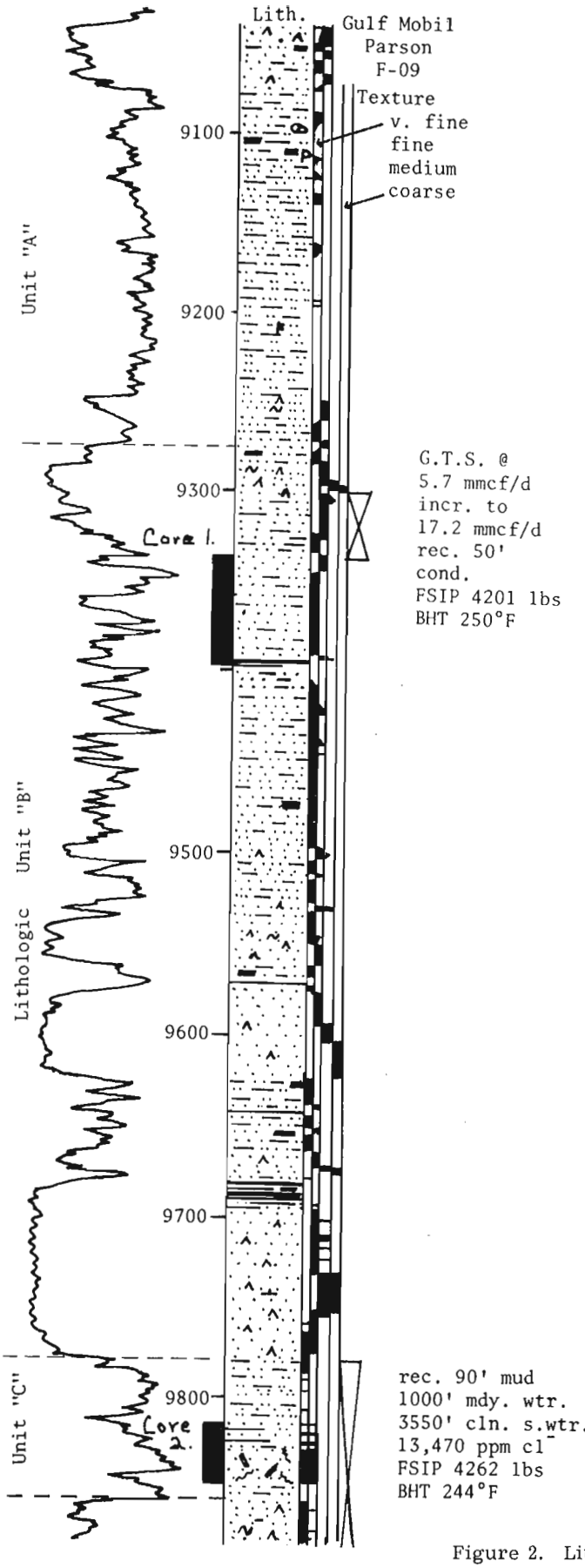

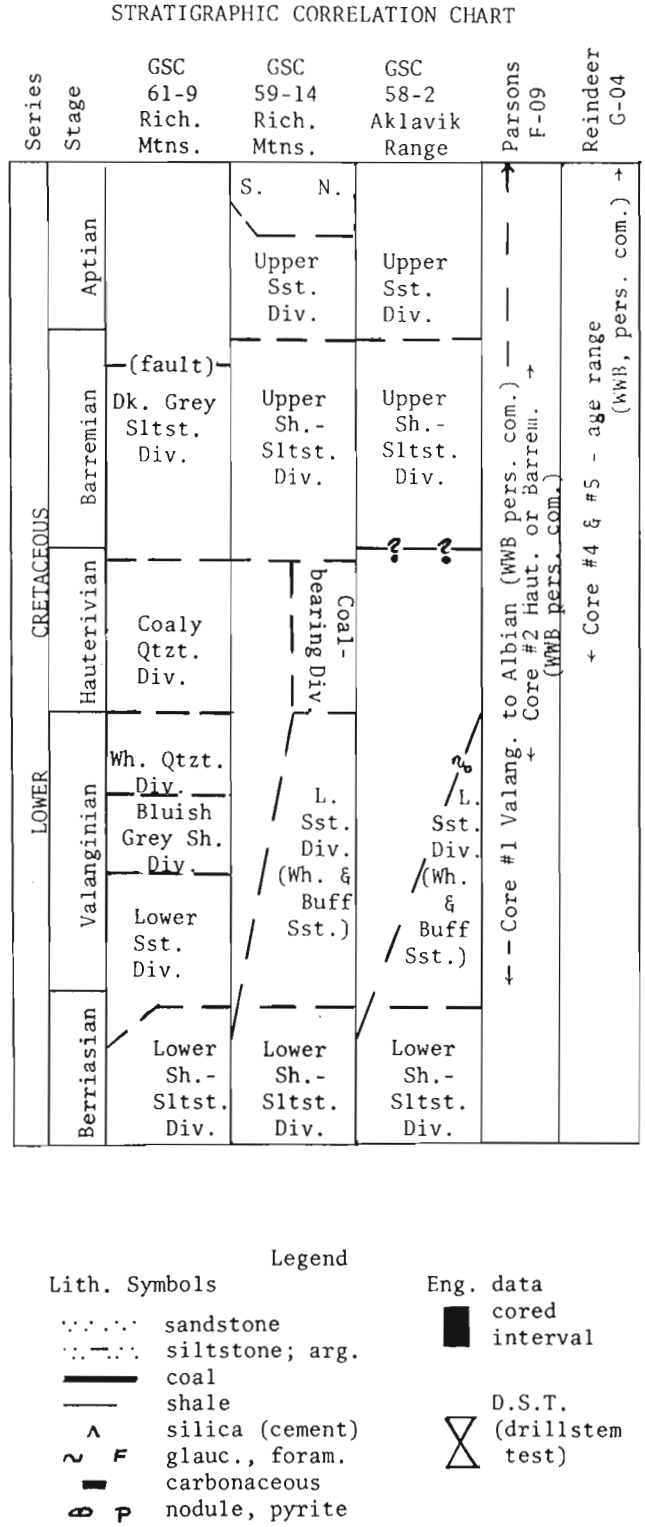

Legend

Lith. Symbols

- sandstone
- siltstone; arg.
- coal
- shale
- silica (cement)
- F glauc., foram.
- carbonaceous
- nodule, pyrite

Eng. data

- cored interval

D.S.T. (drillstem test)

Figure 2. Lithology and stratigraphy, Gulf-Mobil Parsons F-09 borehole.

Lithologic unit "C" (9,780'-9,860') is 80 feet thick of which 34 feet has been cored (core no. 2, 9,814'-9,848'). The cored interval consists of a heterolithic unit (9,814'-32' = 18') of evenly bedded, interstratified shale, siltstone and minor sandstone. Bedding character is horizontal, very thin to microlaminated with a few crosslaminated units. Also noted were scattered patches of finely disseminated pyrite, a few burrows and bioturbated zones and one load structure. The colour of the arenaceous units is grey; the shaly beds are dark brown possibly depicting a high organic content. The underlying unit (9,832'-9,848') is gradational with the unit above and consists of argillaceous sandstone; brownish grey and fine- to coarse-grained (poorly sorted), with minor amounts of pyrite and calcite cement. Bioturbate texture imparted by extensive burrowing has virtually destroyed any evidence of primary sedimentary structures. Very fine-grained sandstones that are argillaceous, silty and glauconitic, underlie the cored succession (9,858'). The sandstones are cemented with silica.

The sedimentary deposits of core no. 2 have been interpreted from base upwards as a coastal, bay or lagoonal deposit (bioturbated sandstone); the evenly bedded, heterolithic unit may represent distributary over-bank flood deposits or splays. Oomkens (1970) has interpreted similar lithologies as sand washed over a coastal shore face barrier-bar into a lagoon. The sedimentary deposits lack carbonaceous detritus, a common constituent of distributary deposits, therefore the latter interpretation is more appropriate.

Stratigraphy

The stratigraphic correlation chart of Figure 2 illustrates the age range of the cored intervals determined by Brideaux (1974, 1973 and pers. comm.) for the boreholes Gulf-Mobil Parsons F-09 and Gulf-Mobil East Reindeer G-04. Lithostratigraphic units measured and described by Jeletzky (1958, 1960, 1961) from the northern Richardson Mountains are, in part, correlative with the lithologic rock-units of the Gulf-Mobil Parsons F-09 borehole.

Core no. 2 yielded a palynomorph assemblage dominated by bisaccate pollen grains and associated trilete spores and rare dinoflagellates of late Neocomian (Hauterivian) or Barremian age (an assemblage typical of lower coastal plain depositional environments). The age determination suggests a correlation with time stratigraphic units of Jeletzky (1960) for the coal-bearing and upper shale-siltstone divisions of the northern Richardson Mountains (Fig. 2). The underlying lower sandstone division (Valanginian) of the Aklavik Range contains a persistent shaly unit (Jeletzky, 1958 and 1972) that is time-correlative with the marine, bluish-grey shale division of mid-Valanginian age (Jeletzky, 1961 and 1972), on the west flank of the Richardson Mountains in the Yukon Territory. The bluish-grey shale division and shale equivalents of the Aklavik Range (eastern flank of Richardson Mountains) are older than strata of core no. 2, but the lithology (shale and argillaceous arenites), interpreted environment of deposition (transitional) and stratigraphic position tentatively suggest that the shaly interval of the Parsons F-09 borehole (9,780'-9,858') is correlative with the lithologic unit of the bluish-grey shale division (Jeletzky, 1961), but of a diachronous nature.

Core no. 1 yielded abundant carbonized plant debris, derived Devono-Carboniferous spores, trilete spores, bisaccate pollen, and rare dinoflagellates indicating a Valanginian to Albian age (Brideaux, 1973, and pers. comm.). Based on lithology, environmental interpretations, lithostratigraphic relationships of the encompassing rock-units, and age relationships of cores no. 1 and no. 2, lithologic unit "B" is correlative in a rock-stratigraphic sense with the coal-bearing division as defined by Jeletzky (1960) in the northern Richardson Mountains.

Lithologic unit "A" can be correlated with a rock-unit in the Gulf-Mobil East Reindeer G-04 well (9,210'-9,825') interpreted by Myhr (this publication) to be equivalent to the upper shale-siltstone division of Jeletzky (1958, 1960). A cored interval within this unit has been dated by Brideaux (1974, pers. comm.) as Hauterivian to Aptian in age (Fig. 2).

Coal Reflectance

One core sample and five samples of well cuttings were examined for reflectance values in the interval under study. The reflectance results are tabulated in Table I.

TABLE I

Footage	Reflectance %(Ro)	Comments
9,190	.60 ± .08	Histogram suggests reworking; lower peak at .54 Ro
9,395 (core)	.81 ± .03	Milky vitrinite; erroneous reflectance
9,430	.55 ± .03	Abundant coal
9,660	.68 ± .05	Poor vitrinite recovery; possibly erroneous reflectance
9,720	.65 ± .05	Abundant coal
9,750	.60 ± .06	Abundant coal

In terms of rank, these reflectance values indicate high volatile bituminous coals which, in turn, suggest a degree of organic metamorphism compatible with hydrocarbon occurrences. Hydrocarbon occurrences are thought to lie approximately between reflectance values of 0.5 per cent and 1.2 per cent if the hydrocarbons have been produced in situ (Alpern, 1973; Hacquebard, P.A., pers. comm.).

With the scant data available (the above reflectances and the reservoir temperature from drillstem test data), a "burial model" is proposed following Bostick's (1973) method. The method attempts to trace the thermal history of carbonaceous material taking into account the geological events (sediment deposition and/or erosion) that influenced the depth of bur-

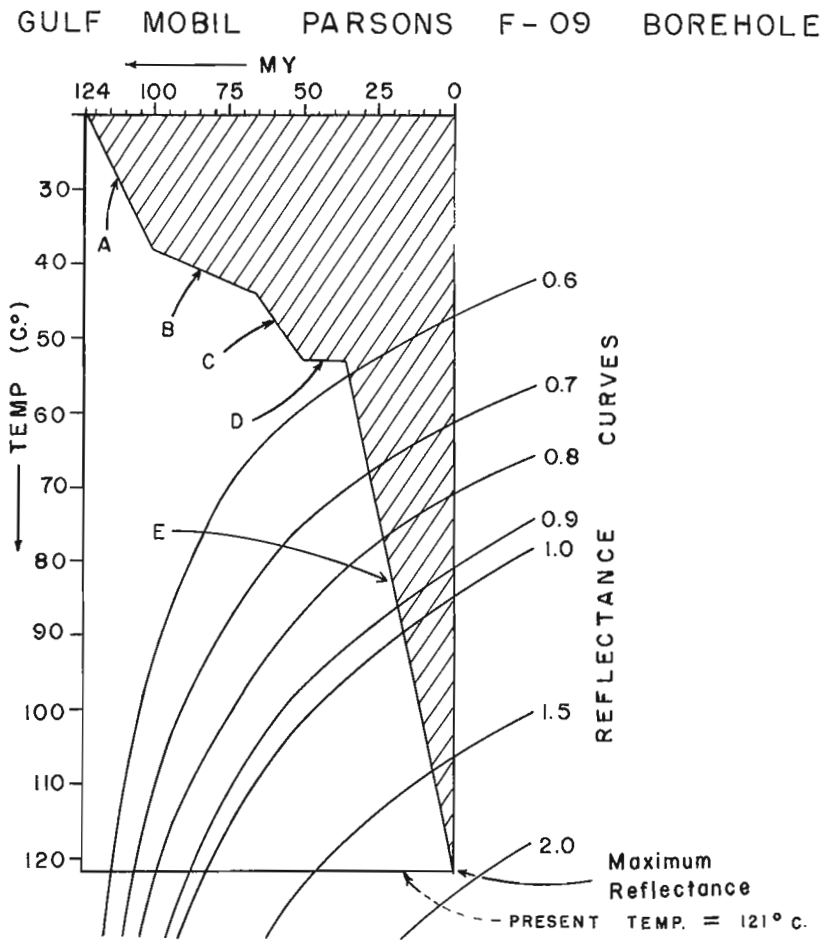

B A

TOTAL AREA (of rect.)	AREA ABOVE CURVE ▨	RATIO A/B	REFLECTANCE % MAXIMUM	EXPECTED	ACTUAL
1252.4	421.9	0.337	1.84	0.62	0.61

Figure 3. Time-temperature "burial model" for approximately 9,400 feet.

ial over the time-span of burial. On the basis of such a model it is possible to predict the rank that a given sample of carbonaceous material may have attained. These predicted values can be compared with those actually obtained by reflectance and may help to explain anomalous results. The reflectance values of Teichmüller and Teichmüller (1968) and the coalification graph of Karweil (1956) are used in the Bostick method to account for the time-temperature relationships. The proposed model for the samples available from the study interval of the Parsons F-09 well is graphically represented in Figure 3. The time-temperature relationships (Fig. 3, at A, B, and C) between 124 m.y. and 50 m.y. (late Neocomian to Early Eocene?) are assumed from temperature gradients calculated from coal reflectances of the IOE Ellice 0-14 borehole. The time-temperature relationships (Fig. 3, at D and E) between 50 m.y. and the present, are plotted in order to account for the present reservoir temperature from drillstem test data and the actual reflectance value found at a depth of 9,400 feet (reflectance value from plot of footage vs. reflectance, Table I). Line segments D and E of the model were developed by a trial-and-error method in which a determined "expected" value is equated to the actual value of reflectance. The expected value is determined as follows. The total area above the curve of thermal history (A, the cross-hatched area) is divided by the total area of the rectangle (B) which yields a dimensionless ratio (A/B). This ratio then is multiplied by the maximum reflectance per cent which gives the expected reflectance per cent. The maximum reflectance per cent represents the reflectance value that would be expected if a coal was exposed to a constant maximum temperature for its complete geologic age. The maximum reflectance per cent in this case is the value of the lower right-hand corner of the rectangle with respect to the reflectance curves. When the expected reflectance per cent approximates the actual reflectance per cent the model is assumed to be reasonable.

The model suggests that only moderate maximum temperatures (about 53°C) influenced the carbonaceous material up to 35 m.y. ago. From that point in time (Oligocene) to the present, the model suggests a rapid temperature increase. The geological causes for this actual or apparent temperature increase can only be speculated upon.

A further observation which can be taken from Figure 3 is that the maximum temperature corresponds with present reservoir temperature, that being 121°C (250°F). Since the "oil window" is considered to be between 60°C and 150°C (Alpern, 1973; L. Snowdon, pers. comm.), one would expect to find liquid hydrocarbons depending upon other favourable geologic conditions. It could be suggested also that oil generation started approximately 30 m.y. ago, and that the hydrocarbons in the Lower Cretaceous reservoir probably are in a state of degeneration since 105°C is the midpoint of the "oil window" temperature range and the reservoir is now beyond this temperature (i.e. 121°C). The types of hydrocarbons encountered tend to confirm this observation (sweet gas and condensate at 39.6° API at 60/60°F).

References

Alpern, B.
1973: Chairman Alpern's summary statements on the colloquium entitled "Dispersed organic matter in sediments, in relation to oil and gas potential", held at the Meeting of the International Commission for Coal Petrology, Paris, September, 1973.

Bostick, N.H.
1973: Time as a factor in thermal metamorphism of phytoclasts (coaly particles); Septième Congrès international de Stratigraphie et de Géologie du Carbonifère, Krefeld, 1971, v. 2, p. 183-192.

Brideaux, W.W.
1972: Geol. Surv. Can. Internal Paleont. Report No. K-8-WWB.

1973: Geol. Surv. Can. Internal Paleont. Report No. K-3-WWB.

Brideaux, W.W., Barnes, C.R., Chamney, T.P., Clowser, D.R., Dunay, R.E., Fisher, M.J., Fritz, W.H., Hopkins, W.S., Jr., Jeletzky, J.A., McGregor, D.C., Norford, B.S., Norris, A.W., Pedder, A.E.H., Rauwerda, P.J., Sherrington, P.F., Sliter, W.V., Tozer, E.T., Uyeno, T.T., and Waterhouse, J.B.
1974: Biostratigraphic determinations of fossils from the subsurface of the Northwest and Yukon Territories; Geol. Surv. Can., Paper 74-11.

Fisher, W.L., Brown, L.F., Jr., Scott, A.J., and McGowen, J.H.
1969: Delta systems in the exploration for Oil and Gas; Bureau of Economic Geology, Austin, Texas.

Jeletzky, J.A.
1958: Uppermost Jurassic and Cretaceous rocks of Aklavik Range, Northeastern Richardson Mountains, Northwest Territories; Geol. Surv. Can., Paper 58-2.

1960: Uppermost Jurassic and Cretaceous rocks, east flank of Richardson Mountains between Stony Creek and lower Donna River, Northwest Territories; Geol. Surv. Can., Paper 59-14,

Jeletzky, J.A. (cont'd)
1961: Upper Jurassic and Lower Cretaceous rocks, west flank of Richardson Mountains between the headwaters of Blow River and Bell River, Yukon Territory; Geol. Surv. Can., Paper 61-9.

1972: Stratigraphy, facies and paleogeography of Mesozoic and Tertiary rocks of northern Yukon and Northwest Mackenzie District, N.W.T. (NTS-107B, 106M, 117A, 116O (N-1/2), 116I, 116H, 116J, 116K (E-1/2)); Geol. Surv. Can., Open File Report No. 82.

Karweil, J.
1956: Die Metamorphose der Kohlen vom Standpunkt der physikalischen Chemie; Deut. Geol. Ges., Z., v. 107, p. 132-139.

Oomkens, E.
1970: Postglacial Rhône delta complex, in Morgan, J.R. (ed.): Deltaic Sedimentation Modern and Ancient - Soc. Econ. Paleontol. Mineral., Spec. Publ., No. 15, p. 204-207.

Teichmuller, M., and Teichmuller, R.
1968: Geological aspects of coal metamorphism; in Coal and coal-bearing strata, D. Murchison and T.S. Westoll, ed., Inter-Univ. 135th Geol. Congr., Edinburgh, p. 233-267.

Schedule of Wells
Northwest Territories and Yukon Territory; Northern Econ. Dev. Br., Canada, Dept. Indian and Northern Affairs. (1970-72)

14. THE TAKLA GROUP NEAR DEWAR PEAK, McCONNELL CREEK MAP-AREA (94D), BRITISH COLUMBIA

Project 720041

J.W.H. Monger
Regional and Economic Geology Division, Vancouver, B.C.

This note, intended to expand upon the previously published brief description of the Takla Group near Dewar Peak (Monger and Paterson, 1974, p. 20), contains (1) the distribution of lithological units near Dewar Peak (Fig. 1); (2) new faunal information, confirming the suggestion of Lord (1948, p. 27) that the lower division of the Takla Group is Upper Triassic, and (3) an interpretation of the environment of deposition of part of the Takla Group near Dewar Peak.

Rocks ranging in age from Lower Permian to Lower Jurassic form a series of fault blocks near Dewar Peak. The orientation and form of minor folds and faults near major faults, and the juxtaposition of rock-units across major faults, suggests that at least some are high-angle reverse faults. The contacts between the Permian and Triassic, and the Triassic and Jurassic rocks are faults. The former may be a sheared stratigraphic contact as basal Triassic argillites are everywhere in contact with the Permian strata. Although no fault block contains all of the Triassic stratigraphic units, the combination of partial sections from the various blocks provides a complete, composite stratigraphic section, that can be divided into three main assemblages. The lowest is dark grey argillite and siltstone (unit 2: 1, Fig. 1). This grades upwards and laterally through grey-green thin-bedded, graded, 'banded' crystal lithic tuff (unit 2: 2) into dominant dark grey, locally green, pillowed augite porphyry flows (unit 2: 4) and massive volcanic breccia containing much augite porphyry detritus (2: 3). Green to brown, coarse-grained, tabular feldspar porphyry pillowed flows (unit 2: 5) are a minor element that contributes conspicuous detritus to the breccias. Upwards, as noted by Lord (1948, p. 16), the breccias (unit 2: 6) contain numerous, maroon, very fine grained feldspar porphyry clasts in addition to their normal components. These clasts are probably precursors of the overlying unit (3), that lies with sharp and conformable contact on unit 2: 6, and consists of maroon well-bedded breccia and tuff containing maroon feldspar porphyry fragments. Units 2: 1 to 2: 6 were mapped by Lord (1948) as belonging to his lower division of the Takla, and unit 3 to the upper division.

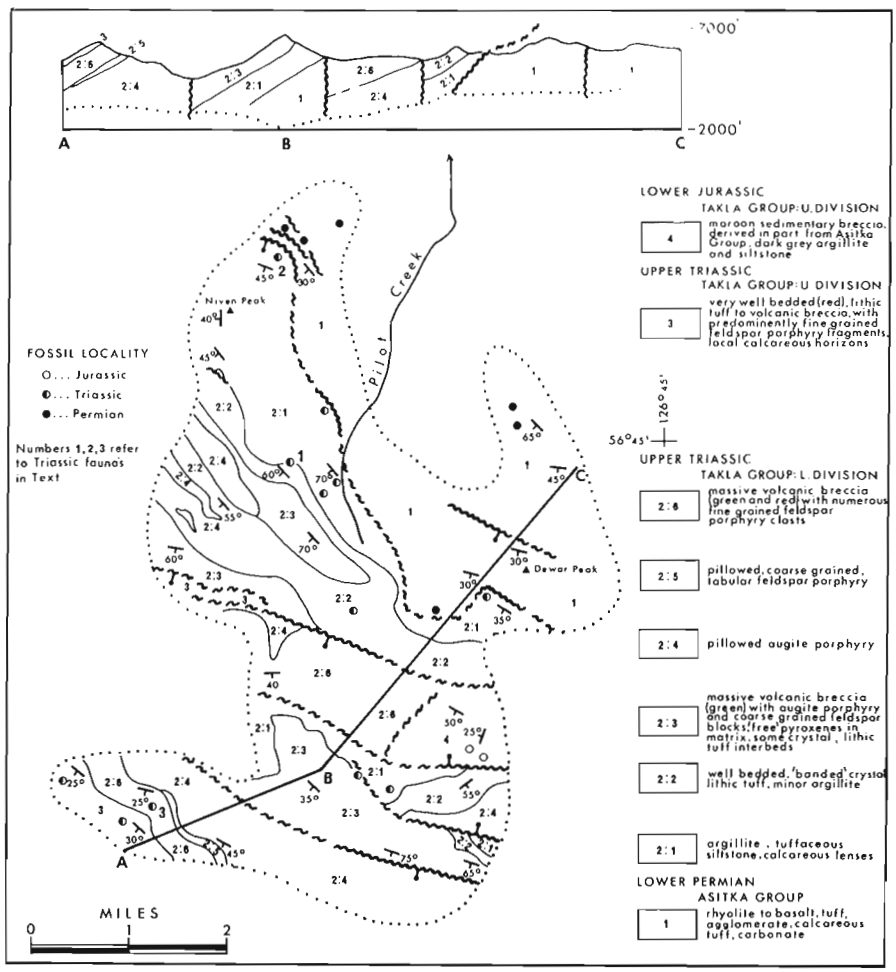

Figure 1. Sketch map of Upper Paleozoic and lower Mesozoic rocks near Dewar Peak, north-central McConnell Creek map-area (94D), British Columbia.

All of these rocks (units 2: 1 to 2: 6 and unit 3) are Upper Triassic. Fossils were identified by E. T. Tozer, and although only three collections from this area are more diagnostic than "Upper Triassic", they suffice to show that these rocks were deposited in a relatively short time interval, from the upper Karnian to the lower Norian. Fossils from locality 1, in the basal part of unit 2: 2, probably belong to the lowest, Dilleri, zone of the upper Karnian. Those from locality 2, in unit 2: 1, are possibly from the uppermost, Macrolobatus zone of the upper Karnian. Although the fossils indicate that unit 2: 1 is younger than 2: 2, there is

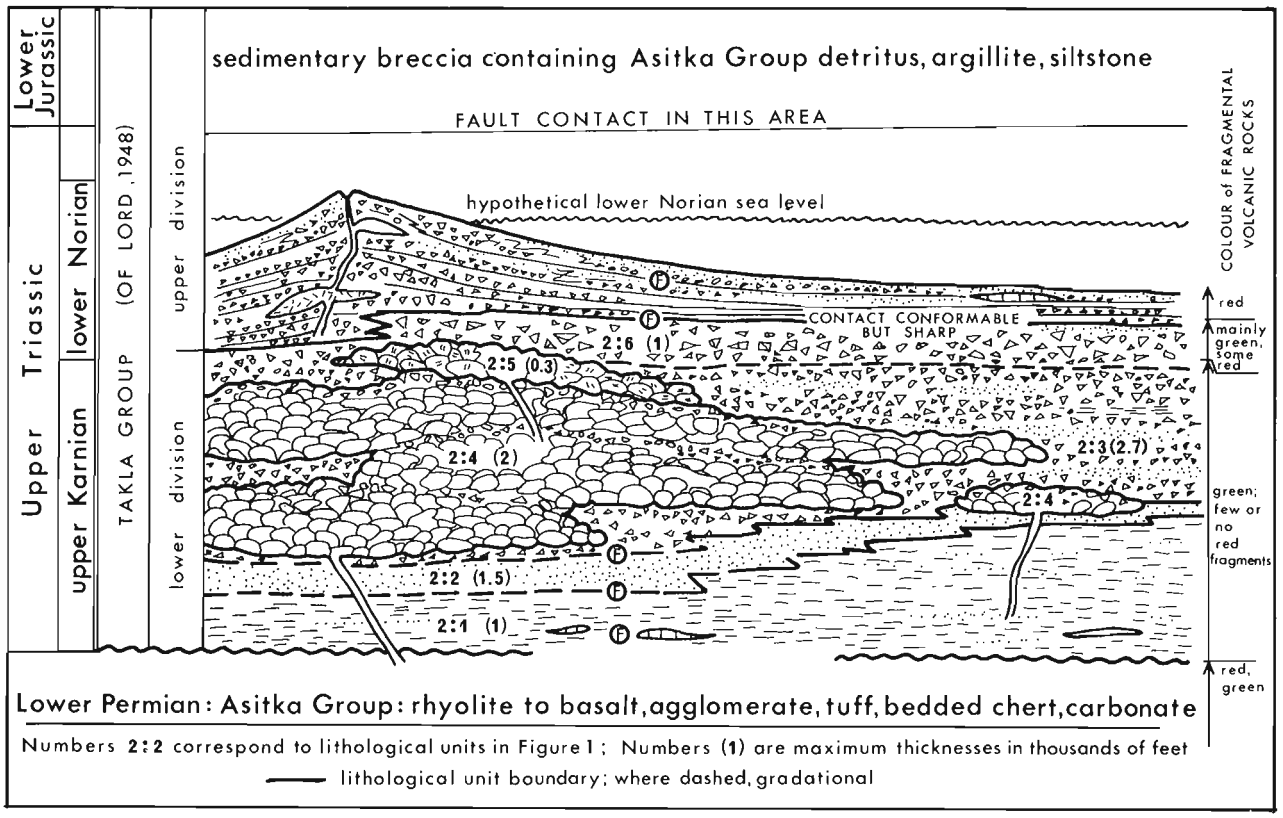

Figure 2. Schematic diagram showing probable relationships between units of the Triassic part of the Takla Group near Dewar Peak.

no doubt that at locality 1, unit 2:2 overlies unit 2:1, and thus these differences are due to facies changes. Finally fossils from locality 3, at the boundary between units 2:6 and 3, originally thought to be of Lower Jurrasic age (Monger and Paterson, 1974), have proven to be from the lowest zone of the lower Norian (Kerri zone).

The significance of these fossils is that they show that the whole of the lower division of the Takla Group in this area is within the Triassic and so are some rocks (unit 3) that were previously mapped as upper division, thought by Lord (1948, p. 28) to range from early Lower Jurassic to middle Upper Jurassic. The stratigraphic relationship between the red, Norian rocks and the Lower Jurassic rocks in this area is not known. The latter form a fault block and comprise dark grey argillite, siltstone, and maroon breccia consisting in large part of detritus from the Lower Permian Asitka Group.

The environment of deposition of these rocks is 'cartooned' in Figure 2. Rocks of the lower division (units 2:1 to 2:6) appear to be entirely submarine, with pillow lavas, related breccias perhaps spalled-off the submarine flows and finer tuffs that are distal parts of the breccias. These rocks were laid down on, and are at least in part coeval with, the argillites and siltstones of unit 2:1. Rocks of unit 3, deposited largely by gravity flows and slides, appear to be entirely submarine in this area, as evidenced by the included fossils. However, possibly equivalent rocks elsewhere, such as in the Sustut Peak area, may be subaerial (B.C. Church, British Columbia Dept. of Mines, pers. comm.). It may be conjectured that the basic rocks of the lower division formed low shield type volcanoes that remained largely submarine, whereas the more acidic andesites of unit 3 built up volcanic cones above sea level. Detritus slumped from the flanks of the cones formed the rocks of unit 3 near Dewar Peak.

References

Lord, C.S.
1948: McConnell Creek map-area, Cassiar District, British Columbia; Geol. Surv. Can., Mem. 251.

Monger, J.W.H., and Paterson, I.A.
1974: Upper Paleozoic and Lower Mesozoic rocks of the Omineca Mountains; in Report of Activities, April to October, 1973, Geol. Surv. Can., Paper 74-1, Pt. A, p. 19-20.

15. GEOLOGY OF CACHE CREEK GROUP AND MESOZOIC ROCKS
AT THE NORTHERN END OF THE STUART LAKE BELT, CENTRAL BRITISH COLUMBIA

Project 720041

Ian A. Paterson*
Regional and Economic Geology Division

Introduction

This study is part of a long term investigation of upper Paleozoic rocks of the Canadian Cordillera being carried out by J.W.H. Monger of the Geological Survey. The area mapped is at the northern end of the Stuart Lake Belt of Cache Creek rocks, approximately 100 miles northwest of Fort St. James in central British Columbia (Fig. 1). The results demonstrate the lithology and structure of the upper Paleozoic rocks and their relationships with continguous lithological assemblages that previously were included in the Cache Creek Group as described by Armstrong (1949).

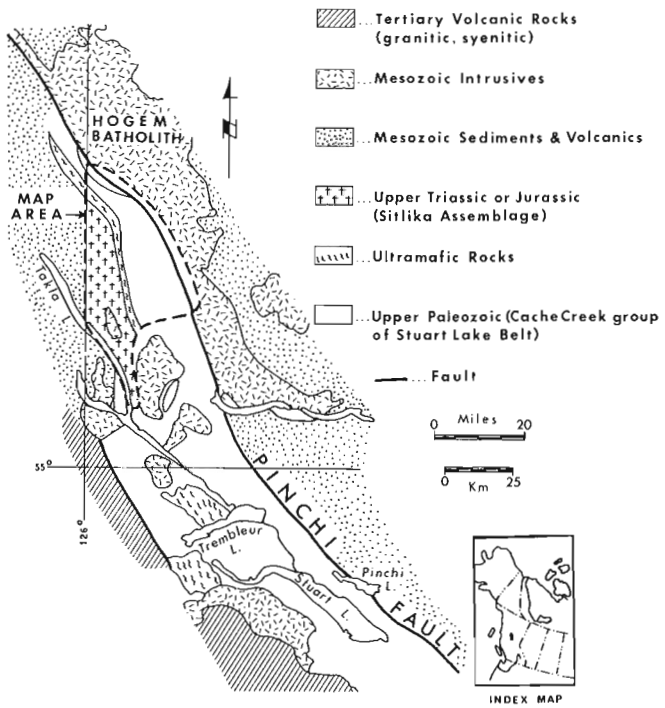

Figure 1. Location of map-area and regional geology.

Several mineral deposits in the area have been or are of economic interest. Placer gold production occurred intermittently between 1869 and the 1950's, and cinnabar was mined in 1943 at Bralorne Takla mercury mine (Armstrong, 1949). Currently, nephrite is mined in the Mount Ogden area.

Two conclusions of this report are possibly of economic interest. The ultramafic belt, which contains nephrite jade boulders in the Mount Ogden area, extends north into the Axelgold Range and south into the Vital Mountains and forms the western boundary of the Cache Creek Group. The extensions of this belt are favourable areas for jade prospecting. Secondly, rocks west of this, in the part of the area previously mapped by Armstrong (1949) as underlain by Cache Creek Group, possibly belong to the Upper Triassic Takla Group. Farther north in the McConnell Creek map-area, Upper Triassic rocks contain copper minerals.

General Geology

The area lies between two major fault zones, the Pinchi Fault to the east and the Takla Fault to the west (Fig. 2). A summary of the rock-units is contained in the Table of Formations. Within the area, the oldest and most extensive rocks belong to the upper Paleozoic Cache Creek Group, an assemblage of predominantly highly deformed chert and phyllite with local greywacke, that contains discontinuous bodies of carbonate and metavolcanic rocks. These rocks are bounded on the west by an east-dipping fault zone up to 3 miles wide that contains a serpentinite-greenstone melange (Fig. 3). This melange in turn, is adjacent to possible Triassic metamorphosed pyroclastic rock, basalt, rhyolite, greywacke and argillite comprising the Sitlika Assemblage. For much of its length, the eastern boundary of the Cache Creek Group is the Pinchi Fault, which for the most part separates upper Paleozoic rocks from the Jurassic Hogem Batholith. However, at the north end of the map-area, an east-dipping fault separates the Cache Creek Group from an early Mesozoic unit made up of chert-pebble conglomerate, argillite, sandstone and tuff, which in turn is separated from the Hogem Batholith by the Pinchi Fault.

Cache Creek Group

It has not been possible to determine the detailed stratigraphy of the Cache Creek Group because of the complex structure and lack of paleontological control. The dominant lithologies in the Cache Creek Group are chert grading to phyllite, carbonaceous phyllite and argillite (Unit 1b, Fig. 2). Chert layers are white, grey or black, and range from a few millimetres to 10 centimetres in thickness. Locally, chert may be massively bedded but generally it possesses phyllitic interlayers less than 5 millimetres thick. In areas where chert is a minor constituent, pelitic rocks lack a phyllitic lustre and are termed argillites. They may be calcareous, carbonaceous, siliceous or chloritic.

Greywacke (Unit 1d, Fig. 2), with interbedded black laminated siltstone and green tuff, outcrops 3 miles west of the Pinchi Fault and forms a remarkably continuous belt up to 3/4 mile wide traceable for 10 miles along strike. The rocks is massive or thick

*Cominco Ltd., 200 Granville Sq., Vancouver, B.C.

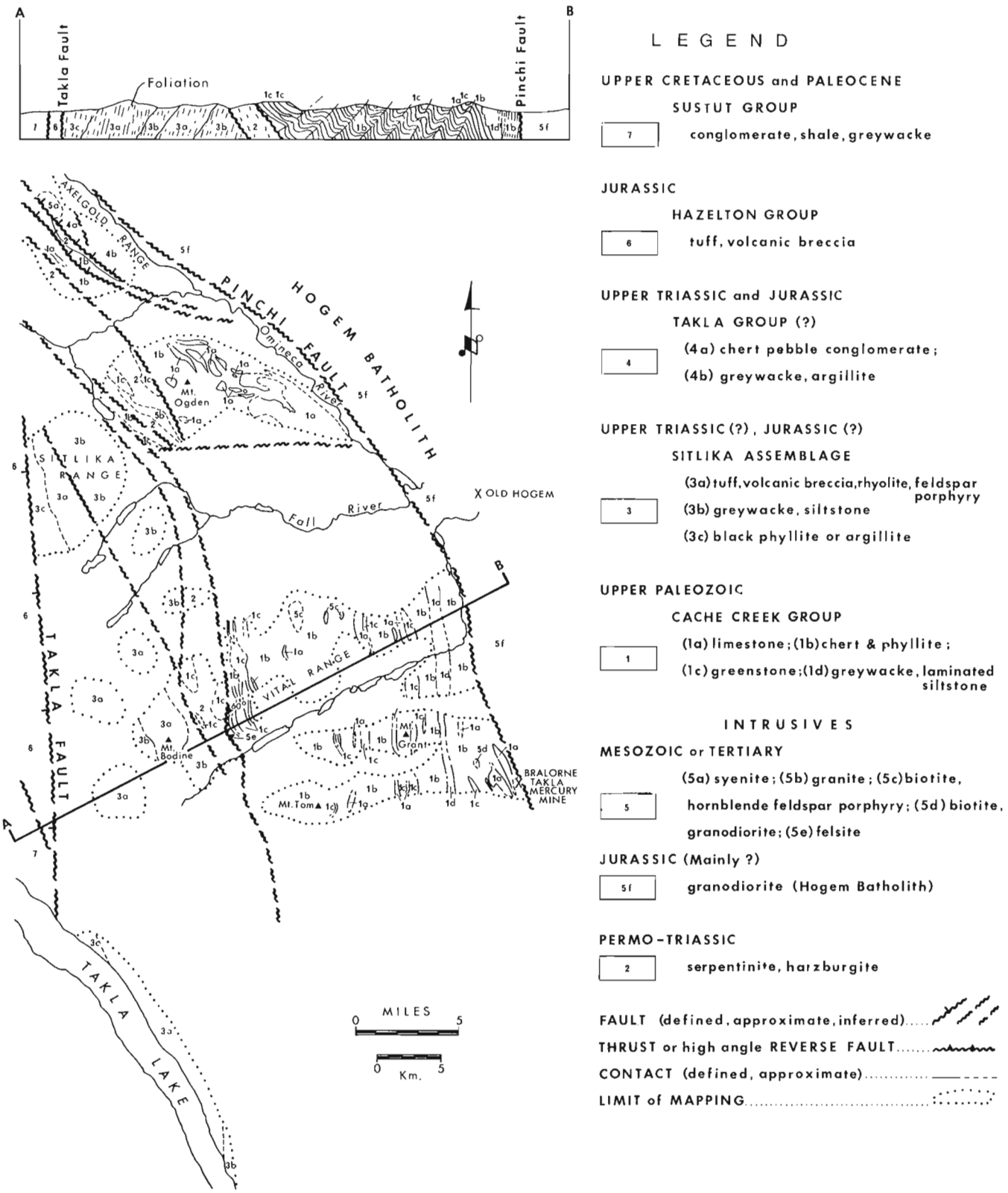

Figure 2. Geological map of Cache Creek Group and Mesozoic rocks at the northern end of the Stuart Lake Belt, central British Columbia.

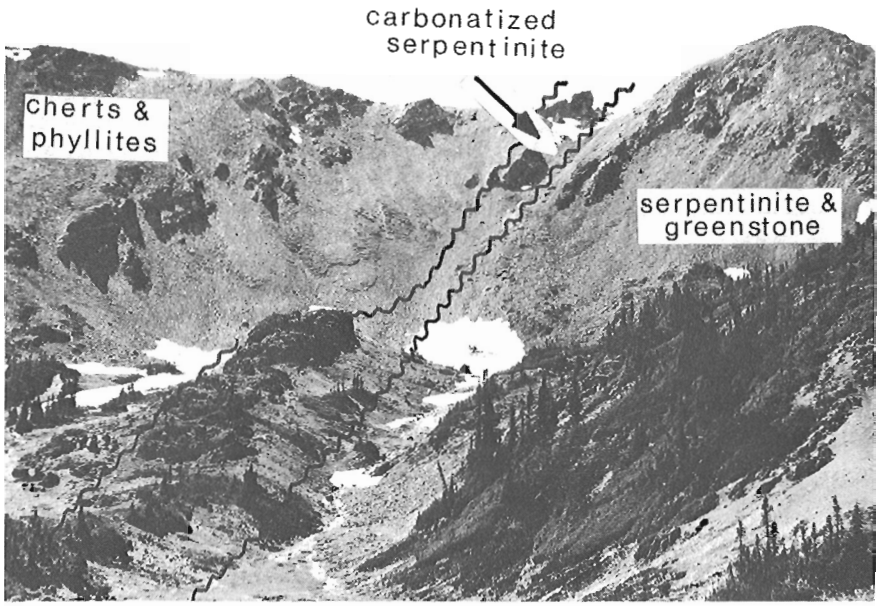

Figure 3. Faulted contact between cherts and phyllites of the Cache Creek Group, and serpentinite - greenstone melange. Photograph is taken looking southwards in Vital Range.

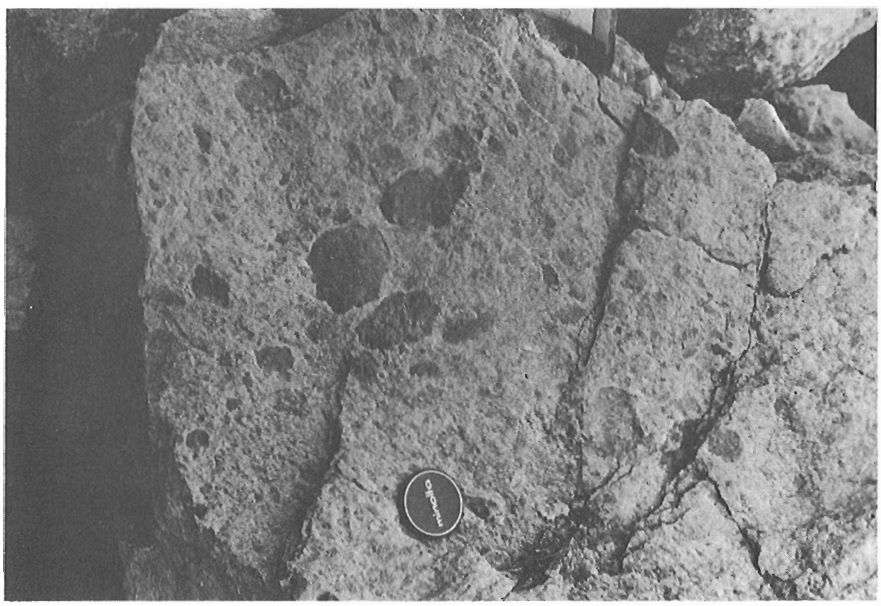

Figure 4. "Bleb" rock from the volcanics in the Sitlika assemblage on the shore of Takla Lake. Blebs are composed of biotite ± tremolite. The rock may originally have been an augite porphyry.

bedded, weathers brown and has a conspicuous blocky jointing. Fresh surfaces are fine grained, grey or green, and reveal relict feldspar or siltstone clasts flattened in the plane of the foliation. Contacts with phyllite and argillite are gradational.

Carbonate (Unit 1a, Fig. 2) forms lenses in the cherty phyllite ranging from bodies 6 miles long and a few miles wide to hand specimen size. It is grey or white, massive recrystallized limestone with some dolomitic limestone that rarely contains recognizable bedding surfaces. Locally preserved primary textures range from laminated aphanitic carbonate to coarse calcarenite and breccia made up of bioclastic debris. Foliated zones occur mainly in thin limestone units and possess a distinctive texture imposed by acicular calcite crystals perpendicular to the foliation. Contacts with chert and greenstone are generally sharp and are either concordant or discordant with the foliation. In places, cherty phyllite and greenstone contain interfoliated lenses of limestone adjacent to concordant contacts with large carbonate bodies. Some limestone units less than 25 feet thick may be interbedded with chert layers.

Faunal collections from limestones in the Mount Ogden area yielded poorly preserved crinoids, horn corals, bryozoans and fusulinids. Neoschwagerine fusulinids (*Yabeina*?) found in three limestone lenses indicate an early Late Permain age (J.W.H. Monger, pers. comm.). Similar fossils were collected by Armstrong (1949) in the southern part of the Stuart Lake Belt.

Greenstone bodies (Unit 1c, Fig. 2) occur as lenses distributed throughout the area in chert, cherty phyllite and limestone. Generally, they are less than 1/2 mile wide and 2 miles long. Massive varieties are green or brown weathering, fine grained, equigranular and dark green. In some flows, relict calcite-filled amygdules and feldspar or augite phenocrysts can be seen. Mineral assemblages, characteristic of the lower greenschist facies, are discussed in the section on metamorphism. Well-preserved pillows and pillow breccias with intercalated recrystallized limestone are found at two localities. The pillows show radial fractures and possess dark green cores which contrast with the pale green (chilled) margins.

The relative age of the chert, phyllite and greenstone with respect to the limestone is uncertain because of the dearth of fossils and complex deformation.

Trembleur Ultramafic Rocks

Rocks correlated with the Trembleur Intrusion (Unit 2, Fig. 2) of Armstrong (1949, p. 79) occupy a north-south trending zone up to 3 miles wide between the Cache Creek Group and the Sitlika Assemblage to the west. These rocks also form lenses along northeast

dipping faults in the Axelgold Range at the northern extremity of the area.

The dominant lithologies consist of blocks of serpentinized harzburgite in a schistose serpentinite matrix. Orange or white weathering talc-carbonate or quartz-carbonate rocks occur commonly as alteration zones. This unit is best described as a melange because of the variable serpentinite lithology and presence of large blocks of amphibolite, greenstone and, in the Mount Ogden area, nephrite jade.

The presence of detrital chromite, derived from ultramafic rocks, in Upper Triassic sediments in the Pinchi Lake area implies that the ultramafic rocks in the Cache Creek Group were emplaced during Early or Middle Triassic tectonism (Freeze, 1942; Armstrong, 1949).

Sitlika Assemblage

Rocks belonging to the informally named Sitlika Assemblage are well exposed in the Sitlika Range and lie between the belt of Trembleur serpentinite west of the Cache Creek Group and the Takla Fault. The assemblage consists of three units, whose dominant lithologies are argillite, volcanic rock and greywacke.

Argillite (Unit 3c, Fig. 2) forms a narrow belt approximately 2 miles in maximum width, east of the Takla Fault in the Sitlika Range, and along the shore of Takla Lake. The unit consists dominantly of argillite which is locally carbonaceous, phyllitic or pyritic but also contains carbonate, pyroclastic rock and greenstone. A penetrative cleavage cross-cuts bedding. The contact with the volcanic unit is sharp.

The volcanic unit (Unit 3a, Fig. 2) is well exposed in the Mount Bodine area, the Sitlika Range, and in the railway cuts along the banks of Takla Lake. The sequence is composed entirely of metamorphosed pyroclastic and flow rock. Foliation is of variable intensity and primary textures are preserved in many places. Many of these rocks could be described as cataclasites because of the common occurrence of augen and mortar textures. Basic volcanics, originally basalt or andesite, are fine grained, equigranular and dark green. Some rocks contain green biotite aggregates (8 mm max.) which are pseudomorphous after augite. Well foliated varieties may contain dark green biotite-rich blebs (Fig. 4), flattened in the plane of the foliation. Flows of feldspar porphyry are common; feldspars are albitized plagioclase, up to 1 cm in diameter, pale green colour and set in a fine-grained epidote-rich matrix. Pink, grey and white leucocratic fine-grained volcanics are common in the Bodine area and in the Sitlika Range and are termed dacite or rhyolite depending on the presence of quartz eyes in the latter. These rocks usually contain feldspar phenocrysts and stilpnomelane porphyroblasts, the latter occurring in veins or as disseminated radiating sprays up to 5 mm in diameter. Some rocks contain relict primary biotite which appears ragged and altered in thin section. The volcanic rocks are in fault contact with greywackes in the Sitlika Range. The same relationship on Takla Lake is marked by a bleached shear zone, 6 feet wide.

The greywacke sequence (Unit 3b, Fig. 2) is best exposed in a fault-bounded block in the Sitlika Range and is also found on the slopes of Mount Bodine and along the shore of Takla Lake and east of the Sitlika volcanic rocks. The dominant lithology is a grey or green weathering, massive to thick-bedded greywacke which commonly contains black siltstone or feldspar porphyroclasts. White or grey weathering laminated siltstone forms interbeds up to one foot thick between greywacke layers. Both greywacke and siltstone are locally very calcareous. All rocks possess a penetrative closely spaced (3 mm) cleavage which cuts across bedding. Along the shore of Takla Lake, a marble member 25 feet thick is interbedded with green chlorite-biotite schist and black lustrous carbonaceous phyllite. This grades into greywacke and laminated siltstone with interbedded conglomerate containing siltstone and quartzitic pebbles.

The age of the Sitlika Assemblage is problematical. Perhaps the most reasonable correlation on lithological grounds is with the Upper Triassic and Jurassic rocks exposed in the McConnell Creek area. There, the Upper Triassic-Jurassic rocks belong to the Takla Group and consist of a basal unit of argillite with minor siltstone, limestone and tuff overlain by lithic crystal tuffs, massive volcanic breccia, augite porphyry, feldspar porphyry and breccia (Monger and Paterson, 1974). The argillaceous and volcanic units can possibly be correlated with the argillite and volcanic sequences in the Sitlika Range. Grounds for correlation include the lithologic similarity of the basal Upper Triassic unit in the McConnell Creek area and the Sitlika argillite. Distinctive feldspar and augite porphyry flows are found in both areas. The Sitlika greywacke could possibly correlate with rocks described by Lord (1948) in the Jurassic "Upper" division of the Takla Group. However, the rocks in the two areas differ significantly with regard to metamorphism and deformation. Sitlika Assemblage rocks have undergone dynamic metamorphism, whereas the Takla Group rocks in the McConnell Creek area commonly have undergone only a burial type metamorphism.

Takla (?) Group

A dominantly sedimentary sequence assigned to the Takla Group as defined by Lord (1948) is exposed on the northeast flanks of the Axelgold Range, southwest of the Omineca Valley (Unit 4, Fig. 2). The sequence can be subdivided into two units consisting of a) feldspathic greywacke, siltstone and tuff with a minimum thickness of 1, 250 feet, and b) conglomerate with a minimum thickness of 3, 000 feet. The arkosic greywacke is green or buff weathering, fine to coarse grained, massively bedded, and locally contains beds of chert-siltstone conglomerate. The siltstone is grey, green or black weathering and in near faults possesses a pronounced fissility parallel with bedding lamination. Green crystal tuff is sporadically interbedded with the siltstone. The conglomerate unit is orange weathering, massively bedded and consists of poorly sorted, subangular pebbles or cobbles of grey and black chert, siltstone, ankeritized siltstone and basalt in a matrix of

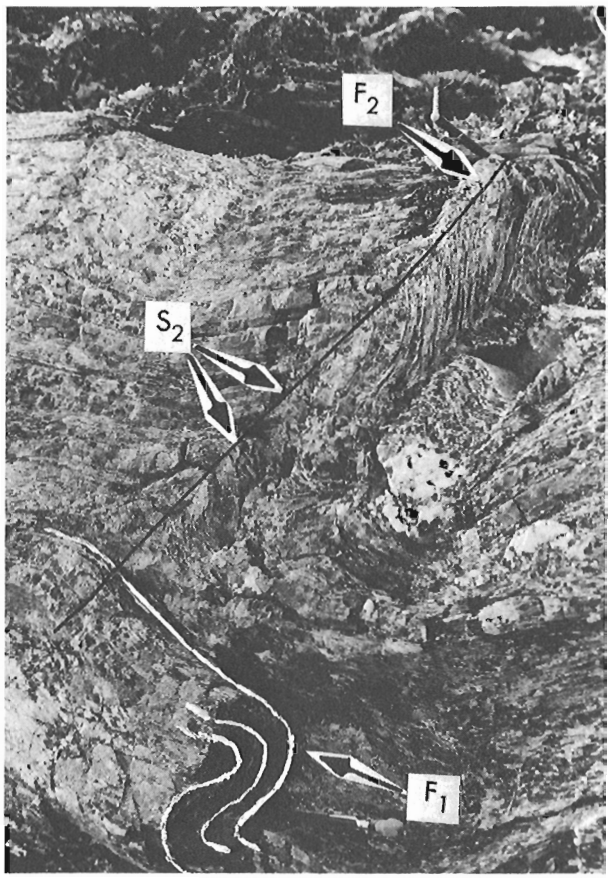

Figure 5a. F_1 fold (in bedded chert) is deformed by F_2 with west dipping S_2 axial surface (Mount Tom).

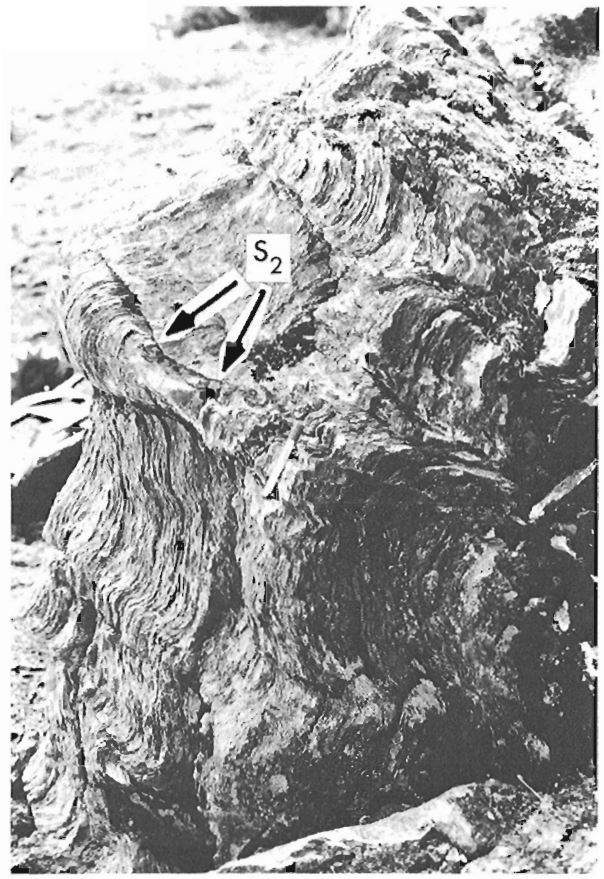

Figure 5b. West dipping S_2 fracture cleavage in cherty phyllite (from approx. 7 miles west of Bralorne Takla Mercury Mine).

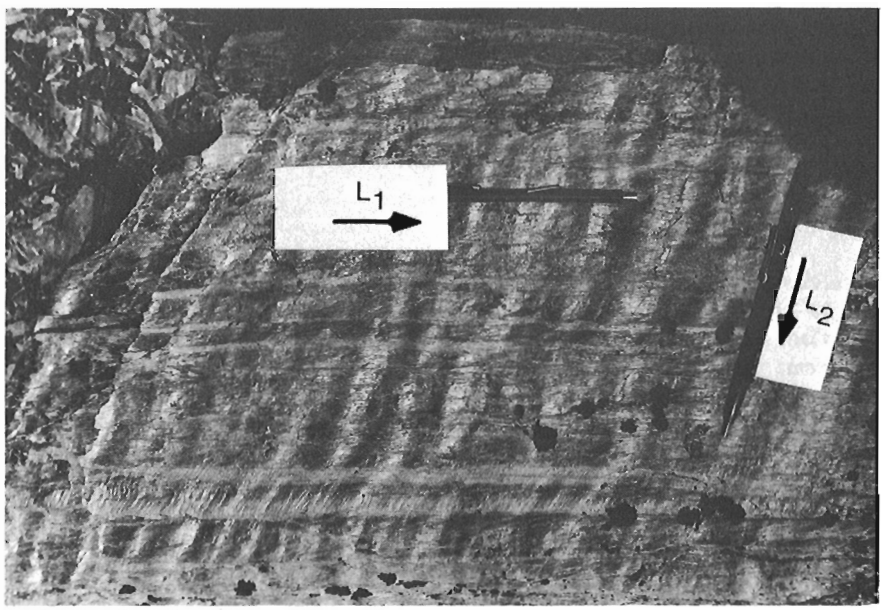

Figure 5c. Streaky L_1 deformed by L_2 crenulations in phyllite (from Mount Grant).

anderite and cryptocrystalline quartz. The relationship between the conglomerate unit and the arkosic greywacke is not clear. In places, the contact is faulted but locally, conglomerate (equivalent to the conglomerate unit?) interdigitates with the greywacke, suggesting that the two units are facies variants of the same sedimentary assemblage.

The conglomerate, greywacke and siltstone are bounded on the west by a narrow belt of schistose serpentinite containing lenses of limestone, contorted chert, brecciated greenstone and siltstone. This zone dips to the northeast at approximately 60 degrees parallel with bedding in the overlying sediments. Conglomerates are flattened and rodded in a foliation plane which parallels the fault zone. The northeastern contact of this unit follows the Omineca Valley where it is commonly faulted against the Hogem Batholith.

The age of the sequence is not known with certainty. On lithological grounds, the best correlation is with rocks of Jurassic age belonging to the upper division of the Takla Group in the McConnell Creek map-area.

Granitic Intrusive Rocks

A body of leucocratic syenite (Unit 5a, Fig. 2), approximately one mile in diameter intrudes Takla (?) Group rocks in the Axelgold Range. It is highly altered, particularly near a fault contact with serpentinite, and contains widespread disseminated pyrite, giving rise to a large gossan. Syenitic rocks are also found intruding the Axelgold layered gabbro which lies 10 km to the northwest (Irvine, 1974).

In the Mount Ogden area, a northwest-trending lenticular body of coarse-grained biotite-muscovite granite (Unit 5b, Fig. 2) measuring 4 miles by 1/2 mile intrudes serpentinized harzburgite. The thermal aureole in the serpentinites is approximately 300 feet wide. Near the serpentinite contact at the southeast end of the intrusion, the granite grades into a peculiar phase composed of spheroidal aggregates of biotite and quartz comprising up to 50 per cent of the rock. In thin section, the biotite in the aggregates is kinked, and adjacent plagioclase lamellae are bent. Strain lamellae are common in quartz grains. It appears that the aggregates formed during late magmatic flow and were deformed and kinked during a post-consolidation episode of deformation.

The remaining intrusives are of limited extent. Three stocks of hornblende-biotite feldspar porphyry (Unit 5c, Fig. 2) intrude Cache Creek Group cherts 11 miles southwest of Old Hogem. A biotite-granodiorite (Unit 5d, Fig. 2) with associated feldspar porphyry and felsite dykes intrudes Cache Creek Group phyllites, cherts and limestones 2 miles northwest of Bralorne Takla Mercury Mine. This stock contains widespread disseminated pyrite. The northerly trending felsite dykes sporadically distributed throughout the Cache Creek Group are possibly related to the large granitic pluton in the Mitchell Mountains. In the Vital Range, felsite sills intrude cherts that form the hanging-wall of an easterly dipping fault at the western boundary of the Cache Creek Group.

Figure 6. Map showing structural domains and distribution of metamorphic minerals.

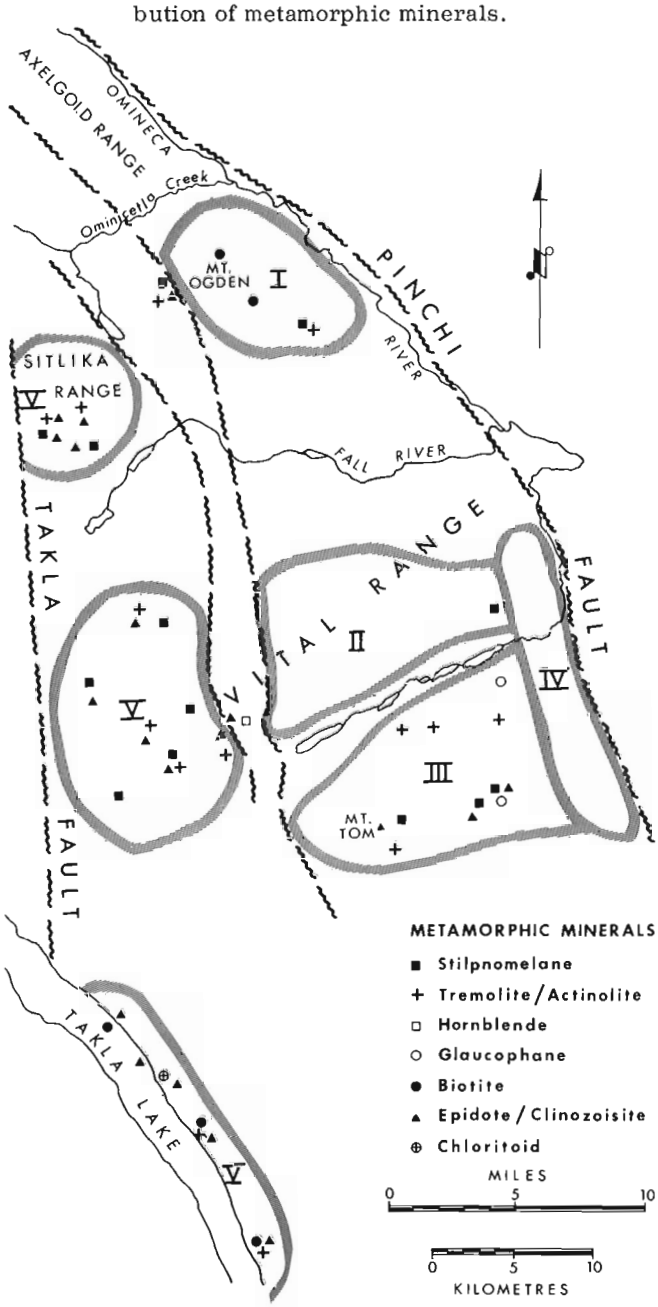

Structural Geology

Foliations, lineations, fold axes and axial surfaces were measured in rocks of the Cache Creek Group and Sitlika Assemblage. The earliest foliation (usually bedding) is named S_0, and subsequent foliations or axial surfaces S_1, S_2, etc. Different generations of lineations and fold axes are termed respectively L_1, L_2 and F_1, F_2 and F_3 from oldest to youngest. Data in the structural domains outlined in Figure 6 were plotted on equal area stereographic projections (Fig. 7) and contoured after the method of Kamb (1959). Observed point densities with the 2σ or 4σ contours are considered statistically significant.

Structures in the Cache Creek Group

There is clear evidence for two generations of minor structures in the Cache Creek Group. Evidence also exists for a third generation which is best developed adjacent to the Pinchi Fault.

The most obvious first generation structure is a foliation (S_1) commonly nearly parallel with the compositional layering but cutting across it in the hinge zones of F_1 golds. The S_1 foliation is defined by the parallel growth of chlorite and actinolite in metabasic rocks and micaceous minerals in phyllites. Metagreywackes contain an S_1 foliation characterized by flattening and elongation of clastic grains. The intersection of S_1 and S_0 gives rise to compositional streaks (L_1) on S_1 surfaces (Fig. 5c), which parallel the axes of F_1 folds. Most F_1 folds are of the recumbent isoclinal type with axial planes parallel with S_1. Some F_1 folds in cherts are fairly open with only minor hinge thickening (Fig. 5a).

Major structures related to the isoclinal minor folds have not been recognized. At least in part, this is because the limestone and volcanic units, obvious marker horizons, are lenticular. The lensing is attributed to initial stratigraphic complexity and extreme transposition parallel with S_1 during formation of first generation structures.

The orientation of first generation structural elements in domains I, II and III is variable mainly because of the effects of northerly trending second generation folds. There is some suggestion from projections Ib, IIb and IIIb that F_1 fold axes are transected by the Pinchi Fault. For instance, projection Ib, (Fig. 7) contains a single maximum indicating a northeasterly trend for F_1 and the Pinchi Fault in this area has northwesterly strike. Farther south, plots IIb and IIIb also show trends discordant with the strike of the Pinchi Fault.

Minor structures associated with second generation folding are especially well developed in cherts, phyllites and foliated greenstones. The folds (F_2) are commonly of flexural slip type with local chevron folds and are generally asymmetrical and overturned towards the east (Fig. 5a, 5b). Thickening of hinge zones in folded chert layers is variable (measured perpendicular to layering) and ranges from zero in some layers up to two or three times limb thickness in others. A crenulation lineation (L_2) is well developed on most S_1 surfaces (Fig. 5c) and parallels F_2 fold axes. The S_2 fracture cleavage has a spacing ranging from 1 cm to 20 cm and lies approximately parallel to the axial surfaces of minor folds. This cleavage is commonly refracted at lithological boundaries and conjugate fracture sets are well developed at some localities.

Second generation folds have near horizontal axes and trend sub-parallel to the Pinchi Fault. Within domains II and III (Fig. 7) folding of S_1 results in well defined girdles, but in the Ogden area (1), S_1 shows a single maximum indicating a northeasterly dip. Plots of the S_2 fracture cleavage show a single maximum depicting a uniform westerly dip in II and III and a vertical dip in I.

Evidence for later deformation in domains I, II and III is poor. Late kink folds are sporadically developed but never common. The change in orientation of F_2 and L_2 structures in domains I and II suggests that the Mount Ogden region was rotated 40 to 60 degrees anticlockwise with respect to the rest of the Cache Creek Group.

There is some evidence for a third period of deformation in domain IV, adjacent to the Pinchi Fault. The orientations of structural elements in this region differ markedly from those in domains II and III. The S_1 foliation possesses a consistent westerly dip and typical F_1 and F_2 folds are absent. Folds where developed are of small amplitude (less than 40 cms), of flexural-slip style and may indicate a third episode of deformation as they deform a crenulation lineation similar to L_2. In the western part of domain IV, these folds are essentially coaxial with the F_2 in domains II and III, but towards the Pinchi Fault the plunge increases considerably. A northerly dipping crenulation cleavage was measured at a number of localities but it was uncertain whether the cleavage was associated with F_2 or F_3 (?) folds. The sense of short limb rotation of the F_3 (?) folds is variable but the majority are right lateral.

In summary, the Cache Creek Group has undergone two episodes of penetrative deformation followed by later less well defined periods of deformation adjacent to the Pinchi Fault, kinking and faulting. The first deformation gave rise to a penetrative foliation and recumbent isoclinal folds. Minor folds and ranges from zero in some layers, up to two or three times limb thickness in others. A crenulation lineation (L_2, Fig. 6c) is widespread on S_1 surfaces and parallels F_2 axes. The fracture cleavage (S_2) is approximately parallel with the axial surfaces of F_2 folds and cleavage spacing ranges from 0.5 inch to 8 inches.

Second generation folds have near horizontal axes and trend parallel with the Pinchi Fault. Folding of the S_1 foliation results in the well-defined girdles shown in plots IIa and IIIa (Fig. 7). Within these domains the S_2 foliations show a single maximum depicting a uniform westerly dip (IId, IIId). One exception to this is the Mount Ogden area (Domain I), where S_1 foliations show a single maximum indicating a northeasterly dip and S_2 foliations dip vertically. These relationships are similar in some respects to those in Domain IV, also adjacent to the Pinchi Fault.

Assuming that the trends of first and second generation structures originally showed a fair degree of regional homogeneity, it would appear that structures in the Mount Ogden area (Domain I) have been rotated 40 to 60 degrees with respect to those in Domains II, III and IV.

A possible third deformational event is shown by structures in Domain IV which are in sharp contrast with those in Domains II and III. The S_1 foliation possesses a consistent steep westerly dip and typical F_1 and F_2 folds are absent. Folds, where developed, are of small amplitude (less than 16 inches), of flexural slip type and deform a crenulation lineation similar to L_2. In the western half of Domain IV, these folds are essentially coaxial with the F_2 folds in Domains II and III but near the

DOMAIN I

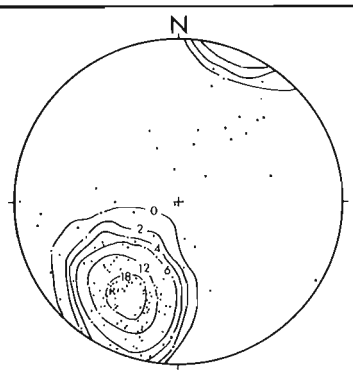

a) Poles to S_1

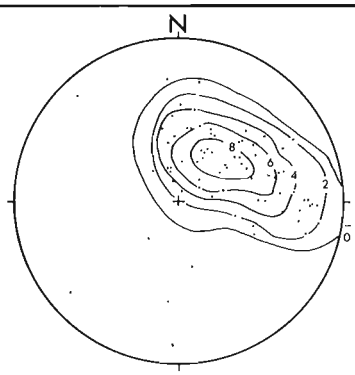

b) F_1, L_1

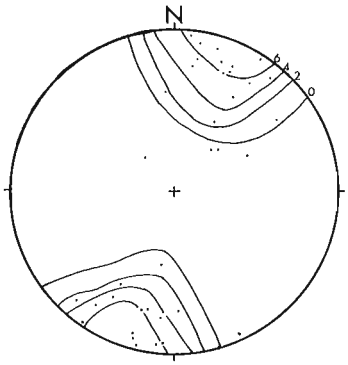

c) Poles to S_2

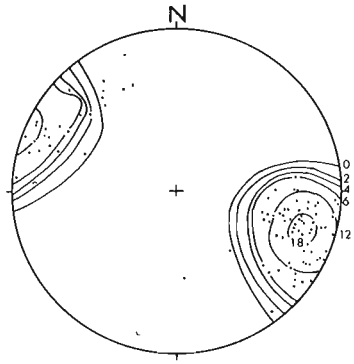

d) F_2, L_2

DOMAIN II

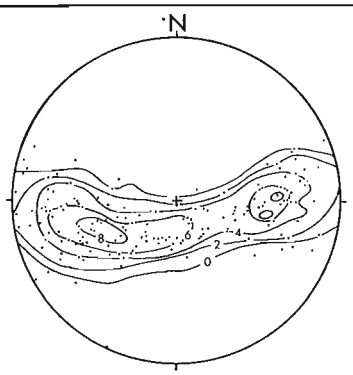

a) Poles to S_1

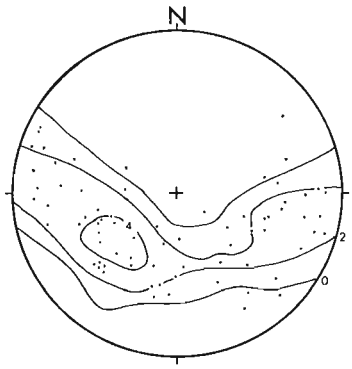

b) F_1, L_1

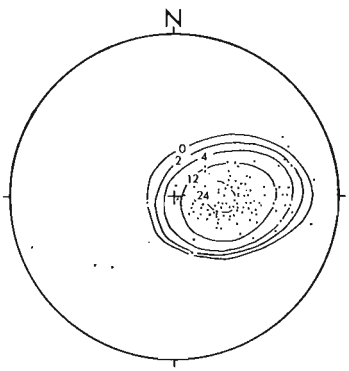

c) Poles to S_2

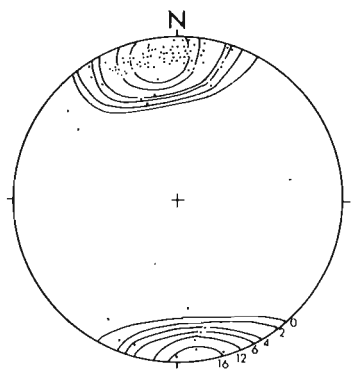

d) F_2, L_2

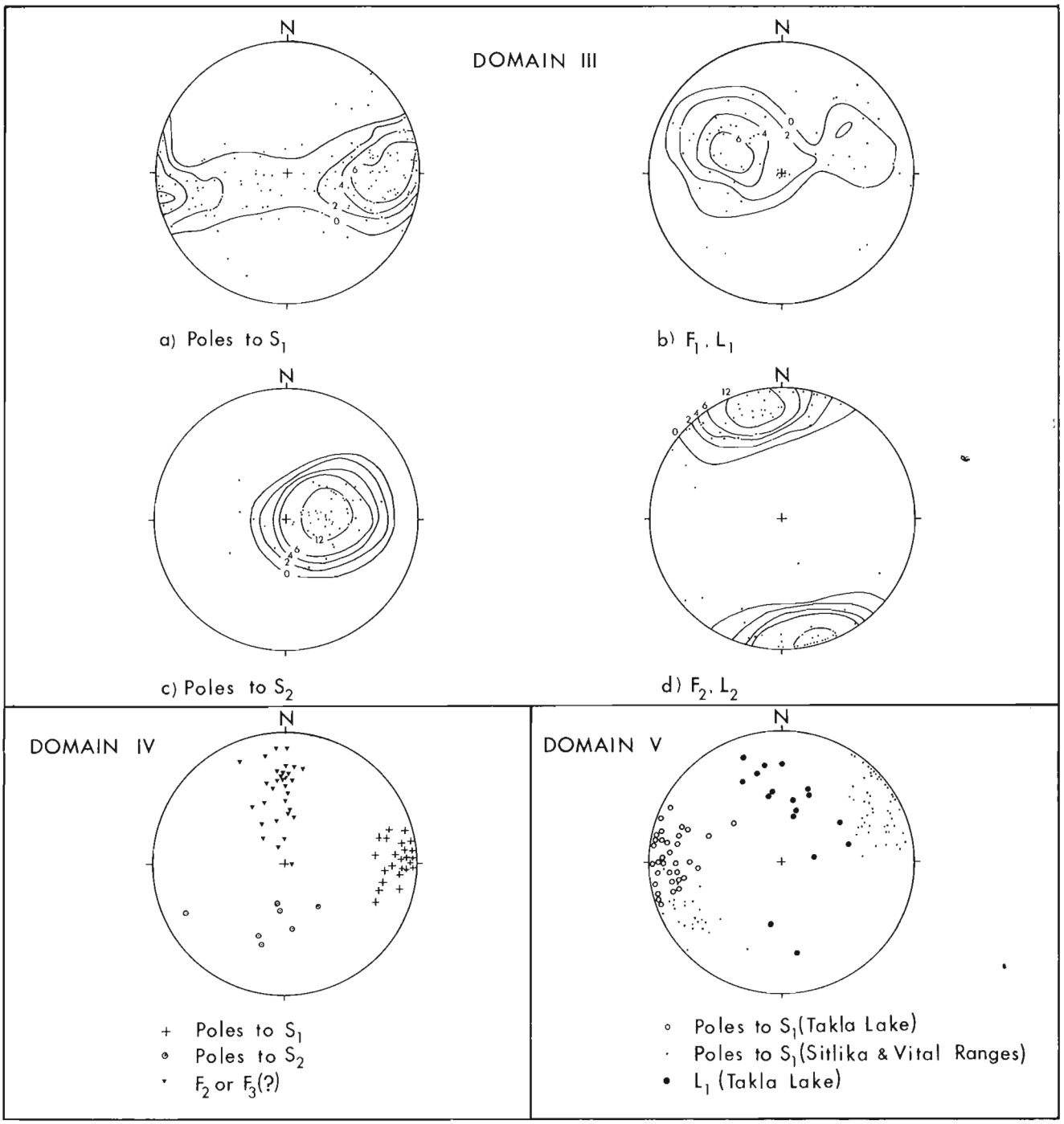

Figure 7. Stereographic projections illustrating orientation of structural elements within the domains shown in Figure 6. Contours are drawn after the method of Kamb (1959) at intervals of 0, 2σ, 4σ, 6σ etc. The zero contour represents the expected number of points if they were randomly distributed over the plot. Observed point densities within the 2σ or 4σ contours are considered statistically significant.

Pinchi Fault, the plunge increases considerably. The sense of short limb rotation of the F_3 (?) folds is variable but the majority are right lateral. A northerly dipping crenulation cleavage is present in some argillites and is interpreted as being the rotated or tilted equivalent of the S_2 foliation in Domains II and III.

In summary, the Cache Creek rocks have undergone two phases of penetrative deformation followed by later poorly defined episodes of deformation adjacent to the Pinchi Fault, kink banding and regional warping. The first phase involved extreme transposition and possibly caused formation of lenticular lithologic units.

Minor folds trend east or northeast, approximately perpendicular to the strike of the Pinchi Fault. The second deformation gave rise to northerly trending sub-horizontal asymmetrical flexural slip folds with westerly dipping axial surfaces. Near the Pinchi Fault there is a marked change in the structural style. Typical F_1 and F_2 folds are absent and the S_1 foliation has a consistent steep westerly dip. In places, minor folds (F_3?) with steep northerly plunge parallel the Pinchi Fault. Finally, the Mount Ogden region was apparently rotated 40 to 60 degrees anticlockwise with respect to the rest of the Cache Creek Group.

Structures in the Sitlika Assemblage

Only one penetrative deformation has effected the Sitlika Group. This deformation was accompanied by metamorphism and appears to have occurred after the first and second deformations of the Cache Creek Group. Structural elements in the Sitlika Assemblage differ in both style and orientation from those in the Cache Creek Group.

The dominant mesoscopic structural element is a penetrative foliation (S_1). In volcanic rocks, the foliation is commonly associated with the development of such cataclastic textures as broken or rounded feldspar phenocrysts that form augen in a microcrystalline foliated matrix. Lineation (L_1) in the volcanic rock is defined by elongation of mafic pseudomorphs and pyroclastic fragments in the plane of the foliation. In argillites, bedding/cleavage intersection defines a streaky lineation (L_1) parallel with the axes of rare isoclinal folds. Limestone boudins in these argillites are elongated parallel with the lineation. Greywackes contain a closely spaced fracture cleavage which parallels the axial surface of open folds.

The orientation of the foliation (S_1) is fairly consistent throughout the area (Fig. 7, Domain V). Steep easterly dips on Takla Lake change northwards to steep southwesterly dips in the Sitlika Range. The L_1 lineation, along Takla Lake has a moderate northerly plunge. The foliation is locally deformed by steeply plunging kink folds.

Metamorphism

Cache Creek Group

Metamorphic basic volcanic rocks within the Cache Creek Group contain the mineral assemblage: tremolite+albite+chlorite+sphene±epidote±glaucophane±stilpnomelane±calcite±dolomite±white mica. Green biotite occurs locally in calcareous phyllites in the Mount Ogden area. The distribution of metamorphic minerals is shown in Figure 6. These assemblages indicate that (1) the rocks were metamorphosed in the lower greenschist facies and (2) there is no metamorphic zonation with respect to the Pinchi Fault. The presence of glaucophane in a few specimens suggests that metamorphic conditions were locally transitional with the lawsonite-glaucophane facies. Crenulations (L_2) on the S_1 foliation bend glaucophane crystals indicating that the second deformation occurred after the main metamorphic episode. Chlorite and stilpnomelane appear undeformed and may have crystallized after the formation of second generation structures.

Sitlika Assemblage

Within the Sitlika Assemblage, the metamorphic grade increases southwards. In the north, the following metamorphic assemblages were recorded:

(i) metabasaltic rock: epidote+albite+chlorite+sphene+tremolite+stilpnomelane
(ii) metarhyolite: albite+stilpnomelane+quartz+white mica+sphene
(iii) meta-impure limestone: calcite+tremolite.

In the southern regions, increase in grade is indicated by the widespread presence of green biotite and the common assemblage in metamorphosed basic rocks is chlorite+green biotite+albite+tremolite+epidote+sphene ±calcite±chloritoid±white mica±quartz. Calcareous pelitic schists contain albite+quartz+white mica+dolomite +calcite. These assemblages indicate metamorphism similar to that of the Cache Creek Group, namely the lower greenschist facies.

Microscopic textures suggest that deformation followed the main metamorphic episode. Disc-shaped blebs (Fig. 4) in metabasic rocks are oriented parallel with the foliation and contain aggregates of kinked and frayed biotite with minor tremolite. The blebs are set in a fine-grained foliated equigranular matrix and are believed to have originated as augite phenocrysts because of their morphological resemblance to augite crystals in some unfoliated rocks. It appears that the biotite replaced augite phenocrysts during static metamorphism, and a later phase of dynamic metamorphism caused flattening and deformation of pseudomorphs.

Timing of Metamorphism and Deformation

Cache Creek Group

Armstrong (1949) believed that metamorphism and deformation of the Cache Creek Group occurred before the deposition of the Upper Triassic. He came to this conclusion largely because of the intense folding and higher grade of metamorphism of the Cache Creek Group compared with the Upper Triassic Takla Group.

The maximum age of deformation and metamorphism of the Cache Creek Group is limited by the occurrence of Late Permian fusulinids in limestones. Together with associated cherts, phyllites and volcanics, the limestones have undergone a lower greenschist facies metamorphism locally transitional to blueschist facies and two penetrative deformations followed by late kinking and warping. In the Pinchi Lake area 100 miles to the south, blueschist facies rocks assigned to the Cache Creek Group have undergone a similar metamorphic and deformational history (Paterson, 1973). There, the first deformation is considered to have been contemporaneous with blueschist metamorphism because of pre-

ferred orientation of glacuophane crystals. K-Ar dates from muscovites in the blueschist (211, 214, 216, 218±7 m.y.) date the end of the second deformation because the micas are severely buckled by second generation folds and have presumably lost argon. By analogy with the Pinchi area, it would appear that the region under consideration has also undergone an early Triassic deformation closely followed by a second deformation which ended in the Middle or Late Triassic.

Sitlika Assemblage

No clear cut evidence is present for the age of deformation and metamorphism of the Sitlika Assemblage. Provided the rocks are of early Mesozoic age as indicated by the lithologies, then it is likely that the main deformation and metamorphism occurred either during the late Middle Jurassic or during the Eocene. Evidence for tectonism during these epochs is substantiated by K-Ar dating (Douglas et al., 1970) and the presence of regional unconformities. However, unmetamorphosed Sustut Group rocks of late Cretaceous or Paleocene age are found immediately west of the Takla Fault near Takla Landing and show no signs of the penetrative deformation undergone by the Sitlika Assemblage to the east of the fault. This suggests that the most probable age for metamorphism and deformation of the Sitlika Assemblage is late Middle Jurassic.

The tectonic setting on the western margin of the Stuart Lake Belt of Cache Creek Group rocks can be compared with that on the southwest margin of the Atlin Terrane in northern British Columbia. The Atlin Terrane, also composed of Cache Creek Group rocks, is faulted on the southwest (Nahlin Fault) against a belt of lower Mesozoic rocks which are involved in a number of northeasterly dipping faults, considered by Souther and Armstrong (1966) to be of Middle Jurassic age. More recently, Monger (in preparation) suggested that the lower Mesozoic rocks have underthrust the Cache Creek Group. On the west margin of the Stuart Lake Belt, foliations in the Sitlika Assemblage are steep and there is no evidence for a series of northeasterly dipping faults which might imply underthrusting. However, the fault which forms the western margin of the Cache Creek Group dips to the northeast at 55 degrees and possibly represents the hanging-wall of a zone of underthrusting which may well be the southerly equivalent of the Nahlin Fault.

Conclusions

1. Rocks hitherto mapped as Cache Creek Group have been divided into three units comprising a) the Upper Triassic - Jurassic (?) Sitlika Assemblage, b) the Cache Creek Group and c) a small area correlated with the upper division of the Takla Group.

2. These units are separated by easterly or northeasterly dipping serpentinite-bearing fault zones.

3. Rocks of Cache Creek Group underwent two phases of penetrative deformation during the Triassic. The first phase involved extreme transposition and possibly formation of lenticular lithological units. Minor folds and lineations have easterly trend. The second phase gave rise to northerly trending subhorizontal asymmetric flexural-slip folds with westerly dipping axial surfaces.

4. Near the Pinchi Fault, there is a marked change in the structural style of the Cache Creek Group. Typical F_1 and F_2 folds are absent and the S_1 foliation has a consistent steep westerly dip. In places, minor folds (F_3 ?) with steep northerly plunge parallel the Pinchi Fault. Other late deformations caused formation of kink bands and possible rotation of the Mount Ogden area from 40 to 60 degrees.

5. Cache Creek Group rocks have been metamorphosed in the lower greenschist facies with biotite and glaucophane occurring locally. There is no evidence for increase in grade towards the bounding faults. The metamorphism occurred during the first Triassic deformation.

6. The Sitlika Assemblage is considered to be correlative with the Upper Triassic and Lower Jurassic Takla Group of the McConnell Creek map-area.

7. The Sitlika Assemblage has undergone one phase of penetrative deformation best dated as late Middle Jurassic. The style and orientation of minor structures is dissimilar to both first and second deformation structures in the Cache Creek Group.

Acknowledgments

The author is indebted to G. Burrowes and P. Gallow for able assistance in the field and to E. Bronlund and A. Leggatt for courtesies extended during the summer.

References

Armstrong, J.E.
1949: Fort St. James map-area, Cassiar and Coast districts, British Columbia; Geol. Surv. Can., Mem. 252.

Douglas, R.J.W., Gabrielse, H., Wheeler, J.O., Stott, D.F., and Belyea, H.R.
1970: Geology of Western Canada; in Geology and Economic Mineral Deposits of Canada, Geol. Surv. Can., Econ. Geol. Rept. 1, 366 p.

Freeze, A.C.
1942: Geology of Pinchi Lake, B.C.; Univ. of Princeton, unpubl. Ph.D. thesis.

Irvine, T.N.
1974: Ultramafic and gabbroic rocks in the Aitken Lake and McConnell Creek map-areas, British Columbia; in Report of Activities, April to October, 1973, Geol. Surv. Can., Paper 74-1, Pt. A, p. 149-152.

Kamb, W. B.
1959: Appendix to "Ice petrofabric observations from Blue Glacier, Washington in relation to theory and experiment"; J. Geophys. Res., v. 64, no. 11, p. 1891-1909.

Lord, C. S.
1948: McConnell Creek map-area, Cassair District, British Columbia; Geol. Surv. Can., Mem. 251.

Monger, J. W. H.
Upper Paleozoic rocks of the Atlin Terrane, northwestern British Columbia and south-central Yukon; Geol. Surv. Can., Paper. (In preparation.)

Monger, J. W. H., and Paterson, I. A.
1974: Upper Paleozoic and lower Mesozoic rocks of the Omineca Mountains; in Report of Activities, April to October, 1973, Geol. Surv. Can., Paper 74-1, Pt. A, p. 19-20.

Paterson, I. A.
1973: The Geology of the Pinchi Lake area, central British Columbia; unpubl. Ph. D. thesis, Univ. British Columbia, 260 p.

Souther, J. G., and Armstrong, J. E.
1966: North-central belt of the Cordillera of British Columbia; in Tectonic History and Mineral Deposits of the Western Cordillera, Can. Inst. Mining Met., Spec. Vol. 8, 171 p.

16. METAL CONTENTS OF LAKE SEDIMENT CORES FROM ESTABLISHED MINING AREAS: AN INTERFACE OF EXPLORATION AND ENVIRONMENTAL GEOCHEMISTRY

Project No. 730002

R. J. Allan
Resource Geophysics and Geochemistry Division

INTRODUCTION

Exploration geochemistry is dependent on the detection of naturally occurring metal levels in various media. Areas of unusually high metal concentrations are often target areas for mineral deposit prospecting. Environmental geochemistry, in particular environmental protection, also requires knowledge of naturally occurring metal levels usually for comparison with higher concentrations suspected to be related to human activity. Both the exploration and environmental geochemist can be looking for the same type of areas, those with high metal concentrations, but obviously from a different motivation.

In the Canadian Shield, mining is one of the activities of man, often associated with increasing metal levels in the environment. However, mines are often to be found in areas which have naturally occurring, higher metal concentrations in surficial materials, such as soils, waters, glacial overburden and drainage sediments. For the exploration geochemist working in such an area, high metal levels in certain easily collected materials may simply reflect mining activity. He must arrive at naturally occurring levels for genuine comparison with exploration geochemical anomalies located in virgin areas. For the environmental geochemist, the problem is the opposite. He asks, whether the higher levels are related to mining activity or (if he is aware of the possibility) just naturally high because the region is geochemically anomalous in certain metals.

In the southern Shield, mining towns have usually only the one industry, ore extraction, and have been established purely for this purpose. However, true wilderness may be found only a few miles from even the largest centres such as Sudbury. Moreover, even the oldest mines such as at Sudbury, have only been in operation for about 80 years. The gold mines at Red Lake have been in operation for about 40 years and the copper mines at Chibougamau for about 20 years. Thus, human activity has been relatively recent compared with the several thousand years that have passed since the areas were deglaciated.

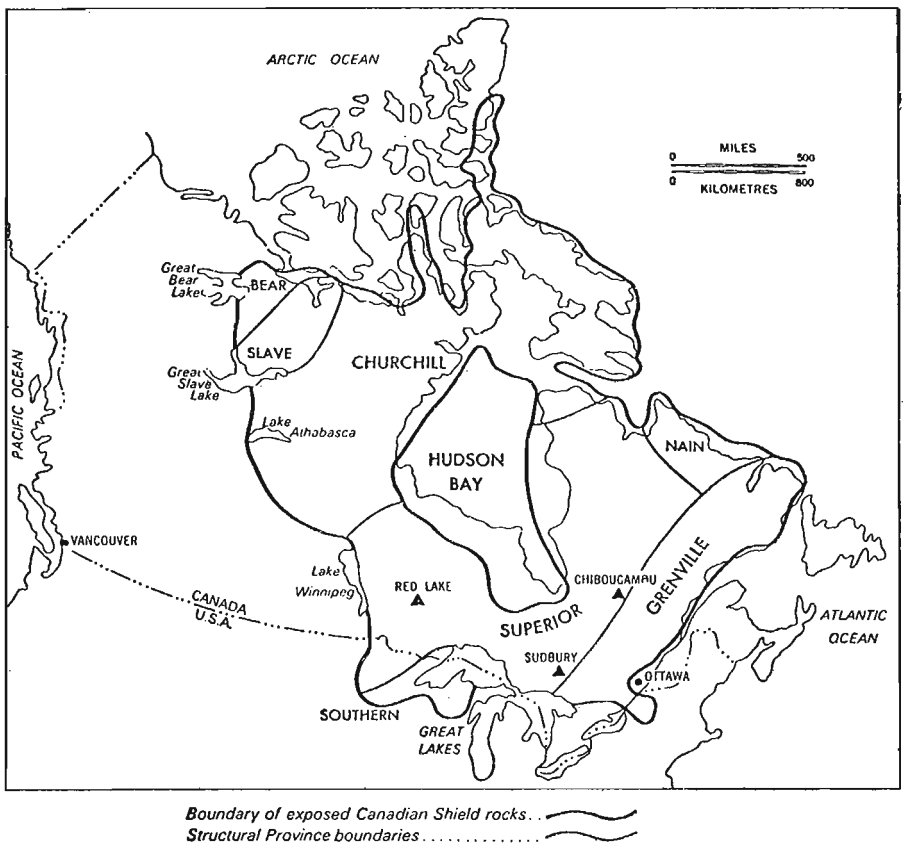

Figure 1. Location of study sites in the southern Canadian Shield

The Advantages of using Lake Sediment Cores as a Sample Medium

As outlined above, knowledge of two metal levels is required: (1) the natural level; and (2) the level since mining activity began. If there is contamination of the area, the difference between (1) and (2) will likely be an indicator of the degree of pollution.

Environment contamination by mining operations is likely to occur in four main ways: (1) tailings introduced as solids into drainage systems; (2) leachates from onshore tailing piles; (3) effluents from mines or mining plants; and (4) airborne particulates from

crushers and smelters. The area affected can vary considerably. If tailings are introduced into a lake with no obvious outflow, the effect is likely to be limited to the lake. In areas with tall smelter stacks, the effect may be very widespread. The examples discussed here are from areas where all of the above cases apply in varying degrees.

Bedrock cannot be significantly contaminated by mining operations and is thus not a sample material reflecting such operations. The types of geological materials available for exploration-environmental studies are thus limited to surficial media: (1) glacial deposits; (2) soils; (3) drainage sediments; and (4) waters. There are of course, biological media such as vegetation or fish. In normal cases, glacial deposits will be shielded from contamination by soils and vegetation. Stream and lake waters are likely to reflect only very recent pollution. Soils, although they may have accumulated the effects of contamination, cannot provide at the same location, two distinct samples, one representing pre-mining metal levels and one post-mining levels. Rivers in the Shield are either disorganized or are large sediment transport systems such as the Ottawa River. By collecting cores of sediment from lake bottoms, it is possible to select levels (samples) in the cores that have been deposited at different times in the past. Lake sediment cores are thus proposed to be an ideal sample media for environmental geochemical studies in the southern Canadian Shield. Also, in developed mining areas, the deeper levels of the cores can be used for exploration geochemical investigations.

In many lakes, large thicknesses of inorganic and organic sediments have accumulated since deglaciation. Most lakes, at least at the latitudes of the three study areas described here, have accumulated less than 10 cm of sediment in the last hundred years (R. Mott. pers. comm., Geol. Surv. Can.). Thus samples of sediment core taken from below this depth should reflect the natural levels which occurred in the sediments prior to mining activity. These are the concentrations that are relevant to the use of lake sediments as an exploration tool in developed mining regions. Samples taken above the 10 cm level reflect a change in concentrations which may be related to mining operations. At Chibougamau, the natural sediment accumulation in the last 20 years since mining began in the area, is probably in the range of 2 to 3 cms.

However, in using such cores, other factors must be considered: (1) diagenesis of the sediments with upward or downward metal movements; (2) biota effects in distributing sediments; (3) the ability of the sample device to collect a continuous core; and (4) bacterial activity which may remobilize metals within the sediments.

Sample Areas and Methods

To test the above basis for an exploration-environmental geochemistry overlap, about 150 cores of lake sediment were collected from sites in and around three widely separated, major mining areas of the Superior Province of the southern Shield. These were at Red Lake, Sudbury and Chibougamau. Geology and mineralization is somewhat unique at each area. Red Lake is a classic Archean greenstone belt of volcanic-sedimentary rocks, surrounded by granites. It is presently a gold mining area, but has a potential for discovery of massive sulphides. The gold is associated with arsenopyrite. The Sudbury area consists of a Proterozoic, norite intrusion surrounded by Archean granites. The intrusion, referred to as the nickel-irruptive contains many Ni-Cu sulphide ore deposits. At Chibougamau, the deposits are mined for Cu. They occur around the periphery of Lac Dore, which is underlain by an anorthositic intrusion. A major fracture, the Lac Dore fault passes beneath the lake of the same name. Because of the different rock types and different ore metals, each area can be used with reservations, as a background area for the other two, at least in the case of the environmental aspect of this study.

The sample sites were reached by boat or small fixed-wing aircraft. The sample device used was an adapted Phleger Corer. The cores were taken from the centres of lakes as these most likely reflect the overall variation within the lake in relation to man's activities. The metal variations in deeper parts of these cores are discussed below in terms of geochemical exploration anomalies. At Red Lake, many of the samples were collected using an Ekman dredge. This sample device tends to collect only surface material. In effect the two jaws scrape the surface layer of sediment. Results for As using this device are compared with core samples from Red Lake itself.

Analyses

The cores were air-dried. All samples were silts, clays, or organic oozes and required no sieving. They were ball-milled to less than 200 mesh and analyzed for Ni, Cu, Co, Zn, Pb, Ag, Hg, Cd, As, Sb, Mo, Mn and Fe by spectrophotometric and colorimetric techniques. Loss on ignition, a measure of organic content was determined on each sample. Only examples for specific metals, As at Red Lake, Ni at Sudbury, and Cu at Chibougamau are given below. A report on the complete results is in progress. Some results for mercury in all three areas have been presented elsewhere (Allan et al., 1974). For Ni and Cu, a weighed sample was digested at 90°C for 1.5 hours with 6 ml of 4N HNO_3 plus two drops of concentrated HCl. The extract was shaken, allowed to settle, then analyzed by atomic absorption spectrophotometry. For As, a weighed sample was leached with 6M HCl at 90° for 1.5 hours. The test solution was centrifuged and an aliquot was then removed for As determination, wherein As is reduced to the trivalent state with KI and $SnCl_2$, and then evolved as AsH_3 upon reaction with nascent hydrogen generated by addition of granulated Zn metal to the test solution. The arsine was scrubbed from the hydrogen stream into a solution of silver diethyldithiocarbamate. The colour intensity of the arsenic complex so formed was determined at 520_{μ} using a colorimeter. The detection limit for As is about 1 ppm.

Results

Analyses of the sediment cores show that in many cases there is a distinct increase in metal levels in the surface few centimetres as compared to the concentration found at depth. This effect is particularly noticeable for nickel in the Sudbury Basin (Table 1, Figs. 2 and 3), the oldest of the three mining areas. In many lakes, the difference in metal content between the surface layers and deeper samples can be used to assess recent metal input into the lakes. At Red Lake, the levels of arsenic in core samples (Fig. 4) show only minor variations with depth. However, much higher concentrations were obtained when the dredge sampler was used (Fig. 5) probably because this sample represented only the surface few centimetres of sediment. Copper changes with depth were minimal in cores from Lac Dore (Fig. 6) which is the most recently developed mining area of the three. Part of Lac Dore has been dammed off as a tailings pond but this does not appear to have affected copper levels in other parts of the lake.

Element concentrations of the levels found in the deeper parts of the cores from all three areas are often less than can be found in similar materials from wilderness areas of northern Canada. Comparison can only be made for silty sediments at this time. At other sites, especially at Sudbury, the metal concentrations of the surface few centimetres of sediment can rise to very high levels.

The deeper strata in the sediment cores could be used for exploration purposes. However, the results, at least in relation to absolute metal concentrations are inconclusive. The presence of major deposits of nickel, gold and copper had apparently little effect on lake sediment metal concentrations. Lake sediments from wilderness areas have been found with higher levels of all these metals than the majority of samples taken from these three mining areas. This could be partly due to the predominantly glacial origin of the lake sediments. For example, Red Lake itself, the larger lakes in the Sudbury Basin, and Lac Dore may all be remnants of much larger glacial lakes. There are significantly large areas of glaciolacustrine deposits in the Sudbury Basin (Burwasser, 1972). If the silty bottom sediments found at the deeper levels in some of the cores are glaciolacustrine in origin, there is slight chance that they will reflect the metal contents of adjacent mineralized outcrops. Also, much of the glacial drift in the three areas is glaciofluvial in origin. Such material when transported to lakes, will bear little mineralogical relationship to the immediately surrounding bedrock. Another possibility, in this case for organic sediments, is that elements moved chemically into such sediment may be so diluted throughout the deep gyttja gels as to result in undetectable concentration changes relative to concentrations in non-mineralized areas. This discussion is limited to comparison of absolute metal concentrations and to the main ore deposit elements for the three areas. Combined element anomalies, element ratios, or specific extraction techniques could result in the detection of characteristic geochemical anomalies for the three areas. This aspect is being looked into further.

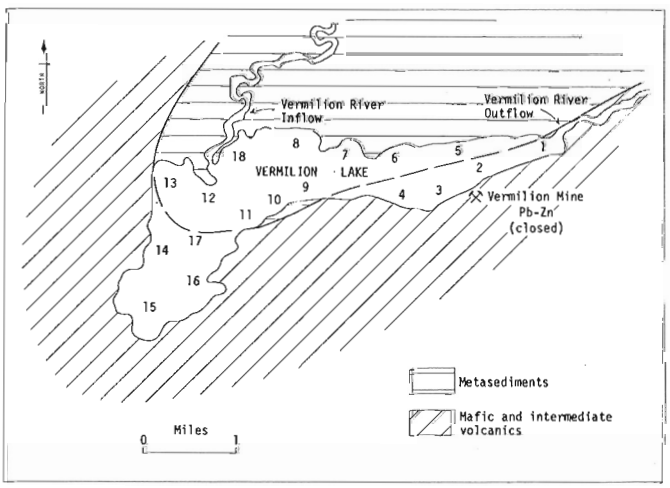

Figure 2. Location of sample sites and geology, Vermilion Lake, Sudbury Basin.

Nickel at Sudbury

The nickel distribution down sediment cores (Fig. 2) from one of the lakes sampled in detail in the Sudbury Basin, is given in Table 1. All samples were inorganic silts. No areas were sampled where the dredge brought up organic samples. The cores are most likely continuous. It appears that the Vermilion River has recently deposited sediment of high nickel content. However, the effect is usually limited to the surface two inches. Normal levels for this lake are close to 30 ppm Ni.

Figure 3 shows the distribution of nickel down lake sediment cores from lakes in and around the Sudbury Basin. These can be compared with nickel levels attributed to airborne pollution from smelters, in the surface two inches of soils around Coniston (Costescu and Hutchinson, 1972). In considering these soil values it should be remembered that natural concentration of metals in soil surface organic horizons is a well documented process and has been put to use in geochemical exploration (Boyle and Dass, 1967). Concentrations in the soils dropped rapidly with depth, for example from 2161 ppm in the 0-2 inch level, to 649 ppm at the 4-5 inch level, at a distance of 1.2 miles downwind from the Coniston smelter. These total analyses were made on extracts from the less than 2 mm fraction, following an HF digestion. The method of analyses used on the lake sediments gives close to a total analysis in most cases. At 5.5 miles from Coppercliff, the surface 2 inches of MacFarlane Lake and Raft Lake contain 871 and 625 ppm Ni respectively. Soils at 2.4 and 6.5 miles from Coniston contain 831 and 356 ppm Ni respectively. The surface 2 inches of a core from Whitefish Lake, about 8.5 miles from Coppercliff con-

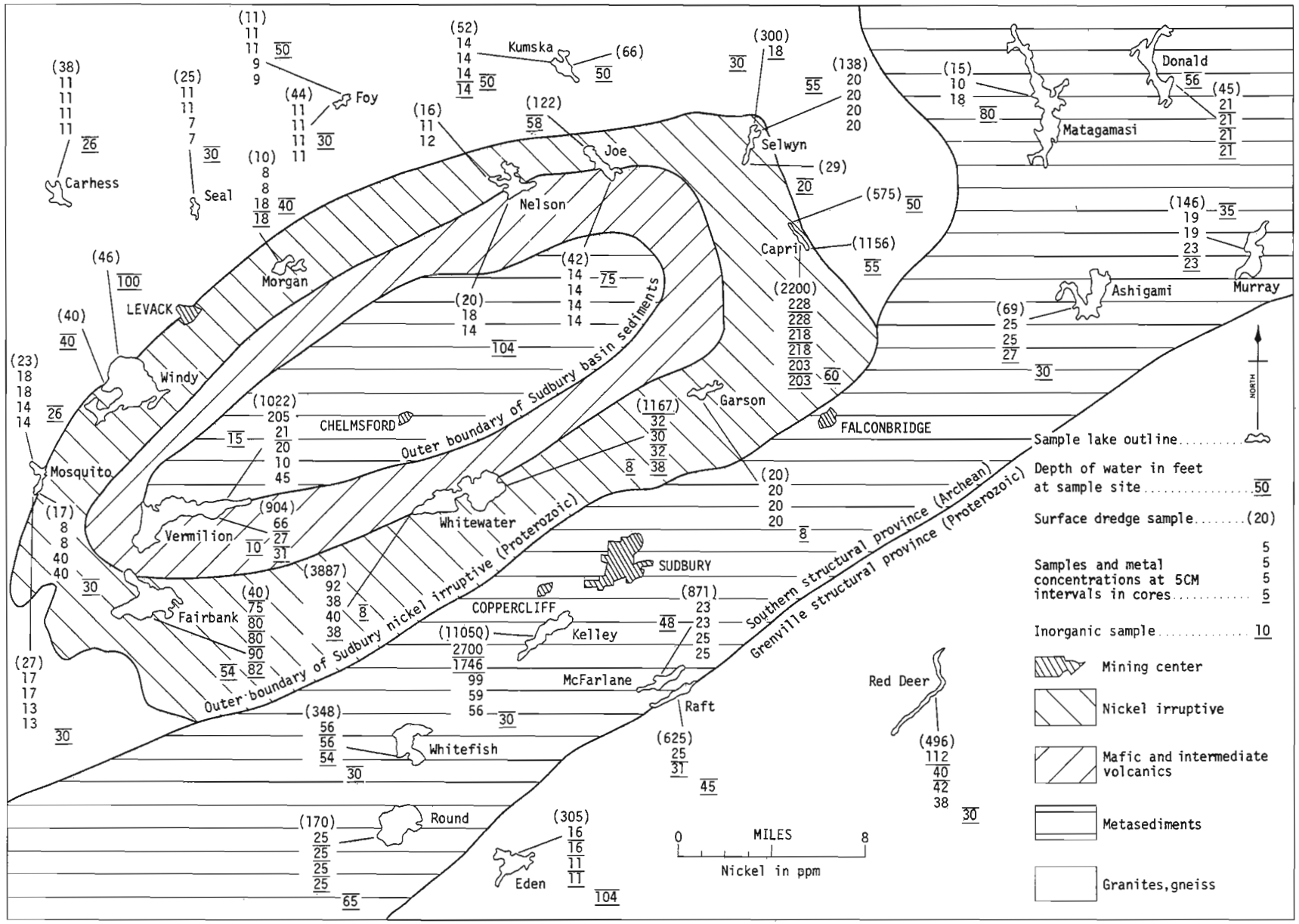

Figure 3. Nickel (ppm) in lake sediment core samples, Sudbury Basin area.

Table 1. Nickel (ppm) distribution in sediment cores from Vermillion Lake, Sudbury Basin

Sample[1] Depth in cms.	Sample Site[2] Number (water depth in feet)																		
	1(15)	2(16)	3(20)[3]	4(10)	9(10)	10(10)	11(18)	16(24)	15(20)	14(26)	13(36)	17(38)	12(36)	18(16)	8(16)	7(10)	6(18)	5(15)	mean[4]
0 - 5	-	42	941	66	423	397	208	139	146	153	252	170	172	337	610	118	146	205	252
5 - 10	-	29	-	27	45	149	279	27	29	25	20	31	23	103	262	17	23	21	68
10 - 15	-	-	-	31	-	141	46	33	31	27	20	-	21	23	21	-	21	30	37
15 - 20	-	-	-	-	-	-	-	31	-	25	12	-	-	-	-	-	25	10	21
20 - 25	-	-	-	-	-	-	-	-	-	21	-	-	-	-	-	-	25	45	30
25 - 30	-	-	-	-	-	-	-	-	-	-	-	-	-	-	-	-	25	-	25

[1]All samples were silty clay in composition.

[2]The sites compose two traverses in an east-west direction across the east-west elongated lake. From 1 to 15 is east to west and from 5 is west to east. Sites opposite the mouth of the Vermilion River are 10, 11, 17, 12, 18 and 8. Sites near the exit of the Vermillion River are 5, 3, 2 and 1.

[3]Site closest to the now closed Vermillion Lake Zn mine.

[4]Means at 10 to 15 cm using 3 samples are: 27, 24, 29, 29, 23, 26, 30, 29.

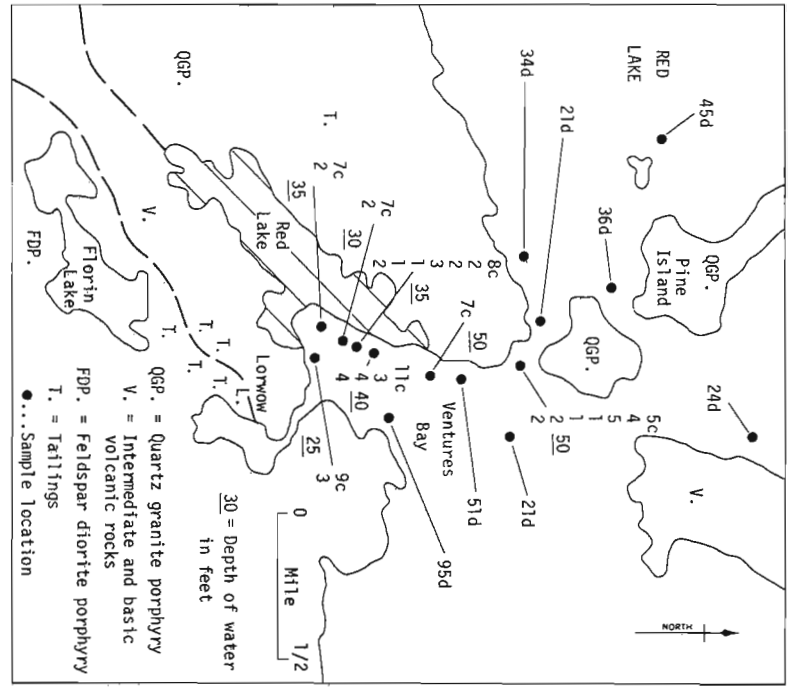

Figure 4. Arsenic concentrations in the Ventures Bay of Red Lake. Sites marked "c" are core samples; marked "d" dredge samples.

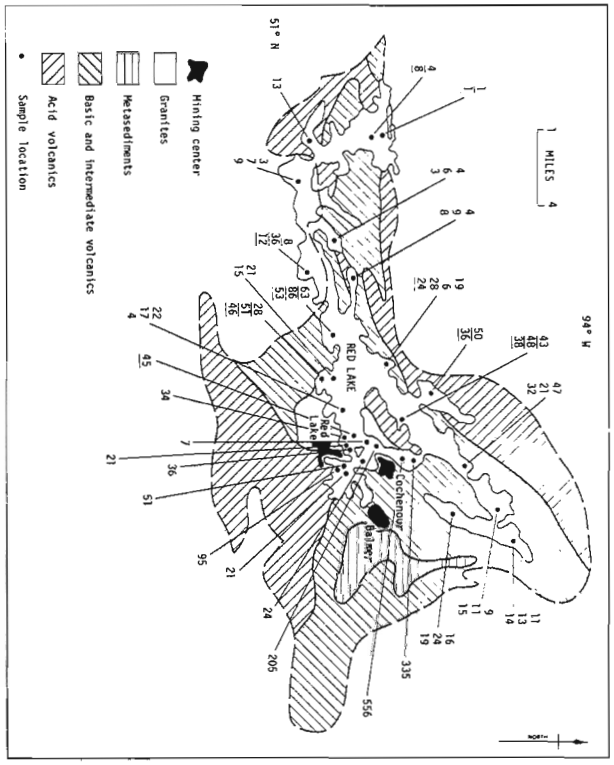

Figure 5. Arsenic concentrations in surface dredge samples. Underlined samples have manganese concentrations exceeding 1,000 ppm.

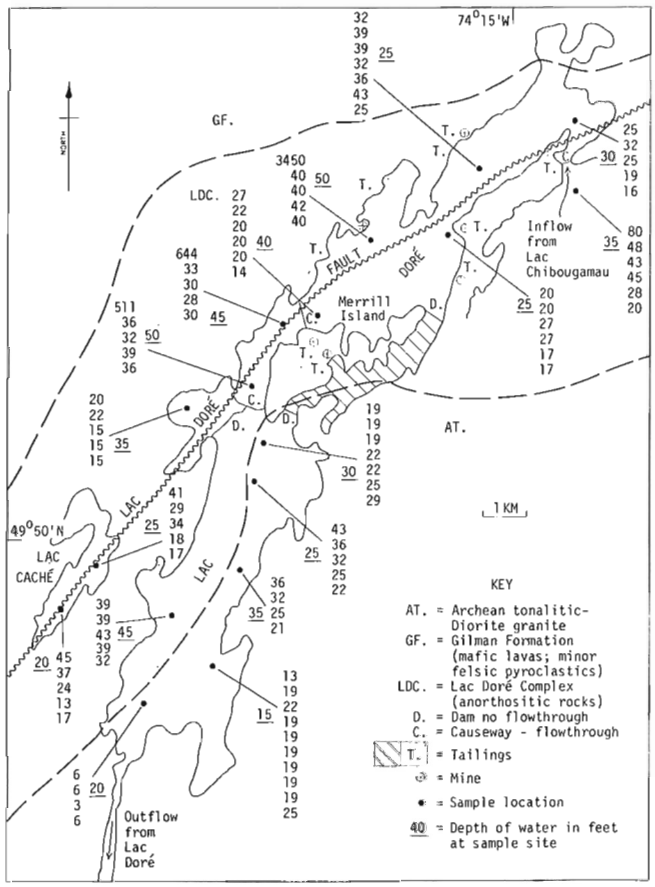

Figure 6. Copper distributions in lake sediment cores from Lac Dore, Chibougamau Area.

tains 348 ppm Ni. A soil at a similar distance downwind from Conistan contains 282 ppm Ni. It is interesting that the total concentrations are so similar. Study of Figure 2, quickly reveals the lakes with unusually high surface nickel concentrations. However, in many cases, it is only the sample collected by the surface dredge that is anomalous. An example is Whitewater Lake. Nickel levels in the cores of most lakes do not change significantly with depth. No distinct trend with depth is visible. Also, organic samples and inorganic samples from the same lake often have similar concentrations; for example, Kumska, Ashigami and Murray lakes. In most lakes, cores were either entirely organic or inorganic. The high contents in the dredge samples indicate that contamination is limited to only the surface few centimetres. The sediments are often thixotropic organic gyttjas, and the dredge settles into this gelatinous ooze. In organic lakes, the corer may well penetrate to some depth before taking a core (R.J. Mott, pers. comm., Geol. Surv. Can.). Thus the cores normally represent premining activity.

A depth of 10 to 15 cm in the cores can be safely taken as representing natural levels. The nickel concentrations in lakes inside the Sudbury Basin are not consistently higher than those from lakes outside the nickel irruptive. Most concentrations at 10-15 cm are between 10 and 40 ppm Ni, for example 40 ppm from Whitewater Lake which was the closest sample site to the Clarabelle open pit. Concentrations of nickel, much higher than these are found in inorganic, silty lake sediments from the Ungava ultramafic belt (Allan, 1971). The implication is that absolute nickel levels do not reflect the proximity of the Sudbury irruptive and nickel ores.

Arsenic at Red Lake

Red Lake is a major gold mining centre. The gold is associated with arsenopyrite in veins and fractures. There are numerous roasters in the area especially at Cochenour and Balmer at the southeast end of Red Lake. Because of the As-Au association, one would expect As levels in lake sediments to be naturally high. Cores (Fig. 4) from Ventures Bay show that this is not the case. At core depths greater than 2 inch, concentrations are typically in the 1 to 3 ppm range. Arsenic levels in lake sediments near similar gold deposits at Yellowknife are usually in the 15 to 60 ppm range (Nickerson, 1972). Higher concentrations in the surface 2 inches of some cores are possibly related to contamination from tailing piles; for example via Lorwow Lake.

It is of interest that, as for nickel at Sudbury, the dredge sampler collected samples of high As content. The reason has been proposed above. Five- to ten-fold differences can be seen between adjacent surface core and dredge sites (Fig. 4). Samples from other parts of Red Lake were collected by dredge. Considering the relationship shown in Figure 4, anomalous concentrations (Fig. 5) are probable effects contamination in the lake, rather than variations due to Au-As occurrences. Except for 3 sites near Cochenour, concentrations are low in comparison with those found in lake sediments from the Yellowknife area (Nickerson, 1972). In Figure 5, samples with very high manganese contents are underlined. The high arsenic levels in these samples are probably due to preferential accumulation of the element in ferromanganese nodules.

Copper at Chibougamau

The location of the copper mines around Lac Dore is shown in Figure 6. Copper concentrations in this lake are relatively low, considering the numerous copper mines around its shores. Lac Dore was found to have a predominantly silty bottom sediment in the section southwest of Merrill Island. Sediments to the north of the southern causeway to Merrill Island were mainly organic gels. Most concentration at depths of 10 to 15 cm are in the range of 20 to 40 ppm for both types of material. Concentrations are uniform with depth and no obvious trend is observed. The only samples which show evidence of Cu contamination come from the surface 2 inches at: (1) two sites between the causeways to Merrill Island, probably sediment deposited during causeway construction; and

(2) one site containing 3,450 ppm Cu in the northwest, probably related to slumping from an adjacent tailing pile. This lake is in the most recently developed of the three mining areas and on the basis of these results is largely unaffected by the Cu mines, at least in terms of Cu pollution. Even the levels of 511 and 644 ppm Cu near Merrill Island are less than found in several lakes from wilderness areas (Allan et al., 1972) of northern Canada. There seems to be a slight correlation between copper concentrations and depth of water at sample sites but the pattern is not consistent.

Conclusions

Sediments from lakes in all three mining areas show the effects of pollution. Contaminated surface samples are more prevalent in the order Sudbury, Red Lake, Chibougamau, where mining operations began approximately 80, 40 and 10 years ago respectively.

Samples of cores generally show the variation between the original pre-mining metal concentrations and the present-day concentrations. At specific locations, the difference between concentrations in the surface 5 cm of core compared to those at 10-15 cm below the surface, show changes that may be partly attributable to mining activity.

However, even at Sudbury, where airborne particulate fallout has caused higher metal levels in the surface of soils (Costescu and Hutchinson, 1972) and presumably also in lake bottom sediments, the effect appears to be limited to the surface few centimetres. Kelley Lake, adjacent to the Coppercliff smelters is as expected, the most striking case. Even here however, concentrations of nickel reached acceptable levels at a depth of 15 cm in the one sediment core collected. Also, in view of the high metal content of this lake it may prove economically feasible to reclaim this or other lakes for their metal content.

The areas sampled represent three of Canada's major mining camps, for gold, nickel and copper. At each area there are numerous large deposits. Often, deposits were adjacent to lakes sampled. Yet, the absolute concentrations of As, Ni and Cu in the lake sediments from the three areas are low and do not reflect the ore occurrences. Various data treatments such as combinations of metals, or metal ratios may however show the areas to be geochemically distinct.

The variations in metal concentrations between samples collected by a dredging as opposed to a coring device is significant, and emphasizes the need for standardization of sampling devices and techniques when metal concentrations are to be compared between different areas. This is particularly important in environmental geochemical studies but also relevant to exploration geochemical surveys.

Acknowledgments

The following helped with sampling operations in the three areas: Mr. R. Lindsay at Sudbury, Dr. M.H. Timperley at Red Lake, and Mr. J. Gasper at all three areas. A detailed report covering several toxic elements is in preparation in conjunction with Dr. Timperley and Mr. Lindsay.

References

Allan, R.J.
1973: Surficial dispersion of trace metals in Arctic Canada: A nickel deposit, Raglan area, Cape Smith-Wakeham Bay belt, Ungava; in Report of Activities, November 1972 to March 1973, Geol. Surv. Can., Paper 73-1B, p. 9-19.

Allan, R.J., Cameron, E.M., and Jonasson, I.R.
Mercury and arsenic levels in lake sediments from the Canadian Shield; Proc. First Internat. Mercury Cong., Barcelona, Spain. in prep.

Allan, R.J. and (in part), Lynch, J.J., and Lund, N.G.
1972: Regional geochemical exploration in the Coppermine River area, District of Mackenzie; A feasibility study in permafrost terrain; Geol. Surv. Can., Paper 71-33, 52p.

Boyle, R.W., and Dass, A.S.
1967: Geochemical prospecting - use of the A horizon in soil surveys; Econ. Geol., v. 62, p. 274-276: discussions v. 62, p. 1102-1103; v. 63, p. 423, 572.

Burwasser, G.J.
1972: Quaternary geology and Industrial Mineral Resources of the Sudbury area (western part) District of Sudbury, Ont.; Ont. Dept. Mines, Prelim. Map P. 751, Geol. Ser., scale 1:50,000.

Costescu, L.M., and Hutchinson, T.C.
1972: The ecological consequences of soil pollution by metallic dust from the Sudbury smelters; Inst. Envir. Science Proc., v. 18, p. 540-545.

Nickerson, D.
1972: An account of a lake sediment geochemical survey conducted over certain volcanic belts within the Slave Structural Province of the Northwest Territories during 1972; Dept. I.A.N.D.; Geol. Surv. Can., Open File 129, 22 p. and maps.

17. TRACE METAL DISPERSION IN AN ARCTIC DESERT LANDSCAPE: A Pb-Zn DEPOSIT ON LITTLE CORNWALLIS ISLAND, DISTRICT OF FRANKLIN

Project No. 700046

R. J. Allan
Resource Geophysics and Geochemistry Division

Introduction

The purpose of this report is to provide information on (1) the concentrations of metals in various surficial materials in the vicinity of, and (2) the relative dispersion of various metals from, a Mississippi Valley type Pb-Zn deposit located in a cold-desert landscape.

The Arctic Desert zone of Canada lies north of the tundra zone. This desert landscape is found in most of the Arctic Islands excluding Baffin Island. Geochemical exploration methods using surface, frost boil soil samples for detailed geochemical prospecting and stream sediment surveys for reconnaissance geochemical mapping, has gone on here for several years. Most of the surveys were carried out in the late sixties by two organizations, Cominco Ltd., and J. C. Sproule and Associates. The areas surveyed included Cornwallis and Little Cornwallis islands, and the northern part of Somerset Island. The primary ore targets sought were Pb-Zn deposits of Mississippi Valley type.

However, in spite of these extensive programs, generally available information on geochemical dispersion in this cold desert landscape is minimal. Nearly all of the information derived from these operations is held in confidential company assessment reports. In fact, many exploration geochemists outside Canada, may be unaware that conventional geochemical exploration techniques can be applied successfully in these far northern latitudes.

In terms of geochemical landscape, i.e., climate lack of vegetation, soil types, deep permafrost, lack of ice cap cover, the Canadian Arctic Archipelago is somewhat unique. Only three land masses of equal area occur at these latitudes, Greenland and Antarctica covered by ice caps; and the Taimyr Peninsula, a tundra vegetated area of the U. S. S. R.

To date, the only major mineral deposit located in the archipelago is the Mississippi Valley type, Polaris Pb-Zn deposit on Little Cornwallis Island. The results described here are from a sampling program carried out in 1971 around the Eclipse ore zone on the same island (Fig. 1)

Since 1971, the mineral exploration situation in the High Arctic has changed. By extensive underground operations and drilling, it has become apparent that the Polaris deposit is one of the major Pb-Zn deposits of the world (Sangster, 1974). Its value is now estimated at $1.5 billion. Plans for the extraction of this ore are now in progress. This would make it the farthest north operating mine in the world. Such a discovery has changed the "mineral potential" of this part of the Arctic Islands. Also, case histories on geochemical prospecting in the High Arctic have not appeared in print. An exception was the sampling of waters and sediments from the mouths of seven rivers flowing into Lancaster Sound from southern Devon Island (Dyck, 1973). This was part of a wider program to promote the use of icebreakers as a base for sampling river estuaries. Thus, the presentation of the complete data from the 1971 Eclipse ore zone study area, is considered pertinent.

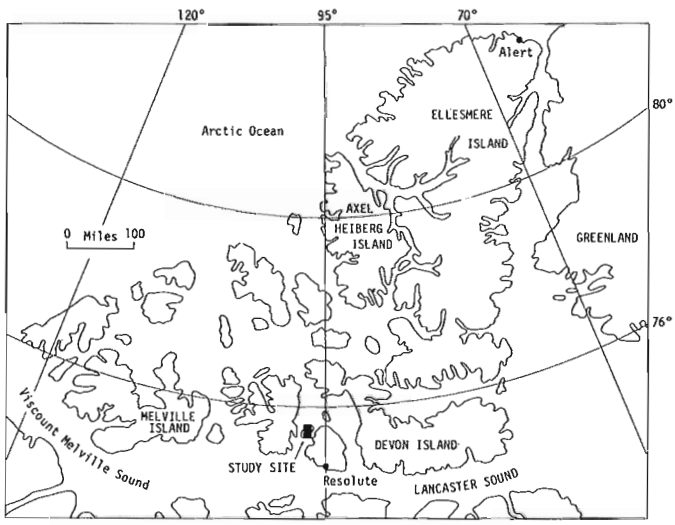

Figure 1. Location of Little Cornwallis study site: Canadian Arctic Archipelago.

Geology and Ore Deposits of Little Cornwallis Island

The geology of the island has been described in detail by Thorsteinsson and Kerr (1968). This geology has been generalized as a base for Figure 2.

The geology of Little Cornwallis Island consists of a succession of shales and dolomitic limestones. The mineralization at the Eclipse zone is approximately 1M tons, 12% Zn, 2.18% Pb. This smaller ore zone is at the east end of Little Cornwallis Island. The much larger Polaris ore zone (now called Arvik Mines) is at the western edge of the island. The ore mineralogy of the two deposits has been described by Sangster (1971; 1974). The Eclipse deposit occurs in the dolomite of the late to middle Ordovician Thumb Mountain Formation. The Polaris deposit occurs at the top of the Thumb Mountain Formation, below a disconformity separating the Thumb Mountain-Irene Bay shale and the overlying Silurian-Devonian Cape Phillips shale. Sangster (1971, 1974) considers both deposits to be Mississippi Valley type, controlled by karst solution caves. Low grade mineralization is in the form of veins, high grade as massive to botryoidal sphalerite and crystalline galena.

Sampling and Analytical Procedures

The eastern part of Little Cornwallis Island is separated from the western part by a narrow neck of land. This eastern part is divided into north and south sections by a broad valley filled with glacial debris, mainly of marine origin, and large lakes. The southern section rises on all sides to a plateau-like area, underlain by the Thumb Mountain dolomite and with the Eclipse ore zone near the height of land (Fig. 2). Several streams drain this higher point. Other than the completely barren, desert landscape of the island, the most distinctive physiographic features are the omnipresent, gravelly, beach ridges formed during isostatic readjustment of the area. The Polaris ore zone outcrops on the coastline at the western edge of the island. Because of this geomorphic setting, the Eclipse ore zone which is located in the centre of the island, was considered to be the more favourable for a metal dispersion study. Samples were collected of gossan soils, frost boils, stream and lake sediments, and stream and lake waters. The sampling was conducted in early August. There were occasional snowfalls which raidly melted. Water flow in streams is related to this early winter snowfall. The lake sediments were taken, where feasible, from the estuaries of inflowing streams. Sample sites were reached by a two-wheel, oversized-tire, motorcycle.

Samples of gossan soils, frost boils, stream and lake sediments were sieved to minus 80 mesh and the metals extracted by digesting 200 mg of sample at 90°C for 1.5 hours with 6 ml of 4N HNO_3 plus two drops of concentrated HCl. The extract was shaken, allowed to settle, then analyzed by atomic absorption spectrophotometry.

Gossan Soils at the Ore Zone

The Eclipse ore zone is marked by an extensive red-brown gossan zone, visible from the air for many miles. However, many rocks in this part of the Arctic Islands weather to similar colours and the presence of the red-brown area is by no means diagnostic as representing an underlying deposit. The metal contents (Table 1) of soil samples (Fig. 2) from gossans in this area are, however, very diagnostic. Concentrations of 4% Zn were found in 56% of the samples collected from depths of up to 45 cm directly over the ore zone. Lead concentrations exceeded 1% in 61% of the samples. Silver concentrations were not particularly high, seldom exceeding 10 ppm. Copper, nickel and cobalt levels were monotonously low and in most samples were close to background values (Table 2) obtained in frost boils located (Fig. 2) over dolomitic limestone some distance from the ore zone. Weathering is intense and soils developed on the shales and limestones are often a water-saturated, thixotropic mud. Although the island was ice-covered and much of the present topography is related to beach ridges, the geological boundaries as shown by colour changes of frost boils appear to be in situ. Glacial transport as affecting geochemical anomalies does not seem to be significant. There was

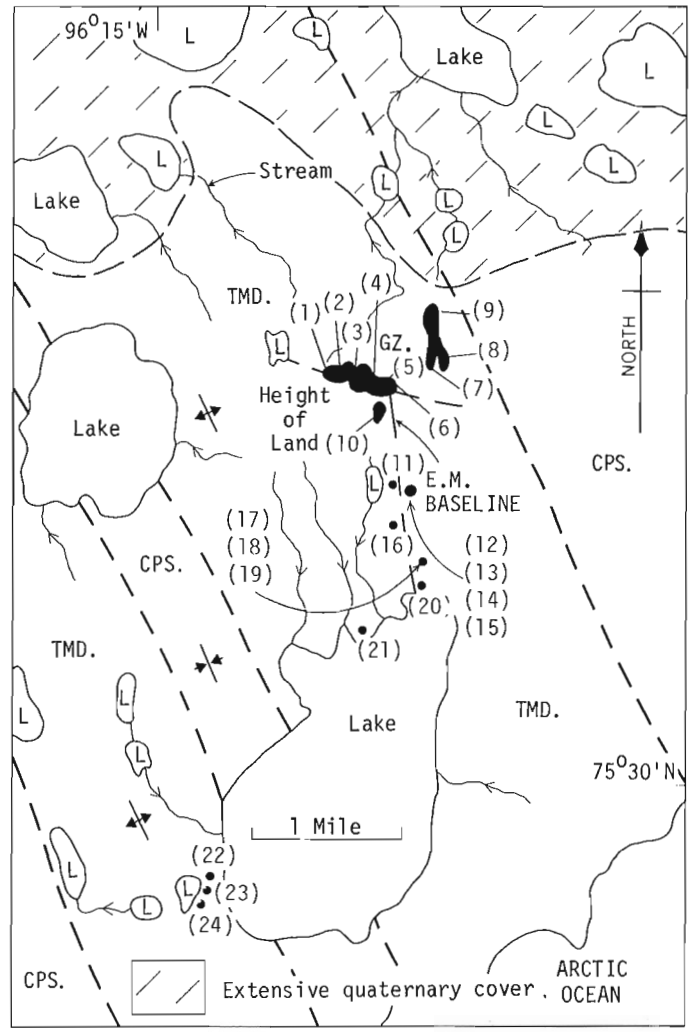

TMD. = Thumb Mountain dolomite and limestone
CPS. = Cape Phillips shale
GZ. = Gossan zone
(10) = Frost boil sample location

Figure 2. Drainage pattern, geology, and frost boil sample locations and numbers.

no consistent variation with depth in metal concentrations of the soils.

Levels of zinc and lead were much lower (Table 1) in samples from a transported gossan to the northeast of the main gossan zone (Fig. 2). This gossan material was probably moved downslope by solifuction processes or by wave action during isostatic readjustment. This latter mode of displaacement implies that a gossan was developed prior to the last glaciation, perhaps during an interglacial period. Relatively low zinc and lead concentrations were also found at a gossan site south of the main ore zone.

Surface Frost Boil Samples

Soil samples from the surface of frost boils were taken at two other (Fig. 2) locations: (1) along a geophysical baseline and mineralized zone extending south

Table 1

Element concentration in the Gossan Frost Boils (Soils): Eclipse Ore Zone, Little Cornwallis Island

DEPTH	SAMPLE SITE (1)	(2)	(3)	(4)	(5)	(6)	(7)	(8)	(9)	(10)
cms	% ZINC									
0-15	0.7	3.4	5.2	3.7	7.7	3.6	0.4	0.5	0.2	0.5
15-30	0.9	4.0	5.4	4.0	7.2	5.1	0.4	0.6	0.2	1.0
30-45	0.7	4.8	4.9	4.2	6.8	6.0	0.4	0.6	0.2	1.0
	% LEAD									
0-15	2.0	0.1	0.8	2.5	1.8	1.2	0.02	0.06	0.03	0.02
15-30	0.7	0.1	0.8	2.5	1.7	2.1	0.02	0.07	0.02	0.03
30-45	2.4	0.1	0.8	2.7	1.8	2.3	0.02	0.06	0.02	0.03
	ppm SILVER									
0-15	11.9	3.0	6.1	4.1	5.2	11.6	2.1	2.5	3.1	1.8
15-30	2.2	3.3	5.7	3.7	5.7	15.1	2.1	2.5	3.0	2.5
30-45	5.5	3.2	5.1	3.6	5.9	17.1	2.1	2.5	3.0	2.5
	ppm COPPER									
0-15	55	13	37	40	30	18	18	24	15	15
15-30	33	13	32	29	27	21	21	29	15	14
30-45	79	13	68	22	31	19	18	31	17	15
	ppm NICKEL									
0-15	13	19	16	18	20	15	41	29	19	36
15-30	13	18	16	16	18	11	47	34	19	23
30-45	14	16	18	20	19	12	42	38	20	24
	ppm COBALT									
0-15	5	7	8	9	12	11	11	16	16	13
15-30	10	9	6	9	12	15	11	19	15	8
30-45	6	8	10	12	12	13	10	21	14	10

1. Samples 1 to 6 from above main ore zone; 7 to 9 from transported gossan anomaly; 10 from possible extension of main ore zone.

2. Locations of sample sites shown on Figure 2. Interval between sites is 185 m.

of the ore zone and; (2) a background location in the southwest of the study area. The results (Table 2) show that high concentrations of zinc and lead only occur at locations where sphalerite and galena are visible. The three background samples show consistent, low metal levels. One unique sample (Table 2, No. 21) comes from a frost boil located purely by chance but with evidence of malachite staining. Copper occurrences are not unknown in the Devonian bedrock of this part of the Arctic Islands.

Table 2

Element concentration in Surface Frost Boil Samples, Little Cornwallis Island

Sample[1] Number	Element ZINC	LEAD	SILVER	COPPER	NICKEL	COBALT
(11)	220	75	2.4	7	7	8
(12)[2]	94,538	25,417	9.8	60	10	8
(13)[2]	88,655	57,111	11.8	66	8	4
(14)[2]	5,065	2,679	3.2	12	9	10
(15)[2]	3,247	1,719	3.2	12	8	8
(16)	97	63	2.8	7	8	7
(17)[3]	165	43	2.8	8	18	7
(18)[3]	113	32	2.8	7	16	10
(19)[3]	142	41	2.6	6	16	11
(20)	513	77	2.5	13	20	8
(21)[4]	14,828	1,563	5.9	2,778	406	68
(22)[5]	75	29	3.0	12	21	10
(23)[5]	75	32	2.7	11	17	10
(24)[5]	79	38	2.4	14	17	10

[1] Sample site location shown on Figure 2.

[2] Four samples taken at a galena showing.

[3] Three samples near a supposed galena showing.

[4] Sample of a boil in an area of Devonian bedrock. Boil was partly stained with malachite.

[5] Three background samples.

Stream and Lake Sediments

Active stream sediments were collected from three streams (Fig. 2) which appeared to drain the area containing the gossans. Only that draining to the north could unambiguously be said to drain the ore zone. Lake sediments come from the estuaries of these streams or others draining the height of land formed by this

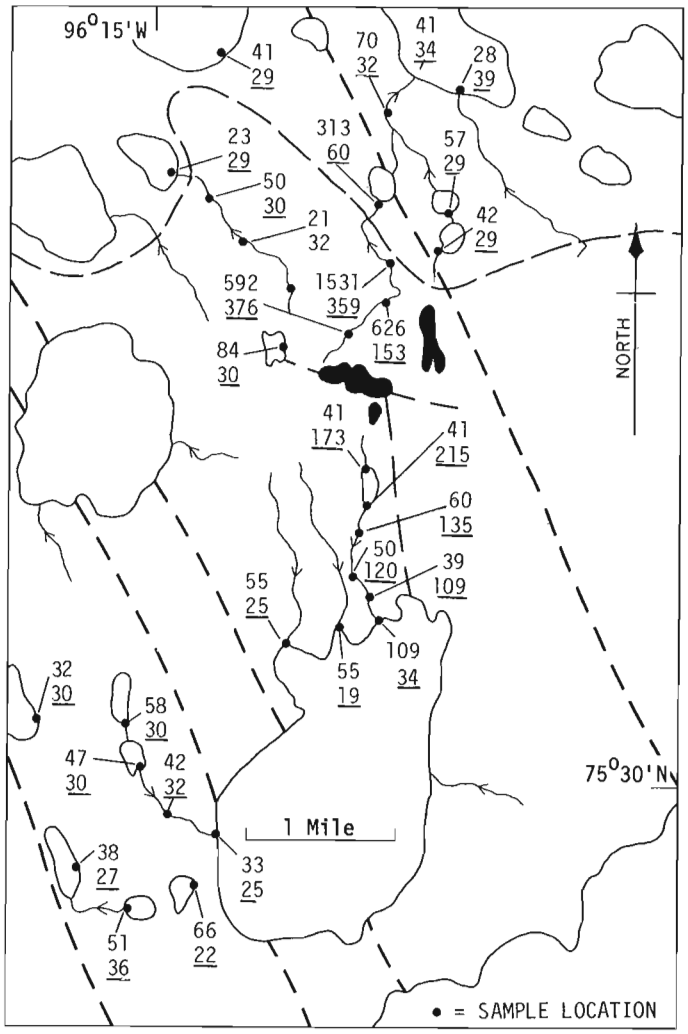

52 = Zinc concentration in ppm

10 = Lead concentration in ppm

Figure 3. Zinc (ppm) and lead (ppm) in stream and lake sediments.

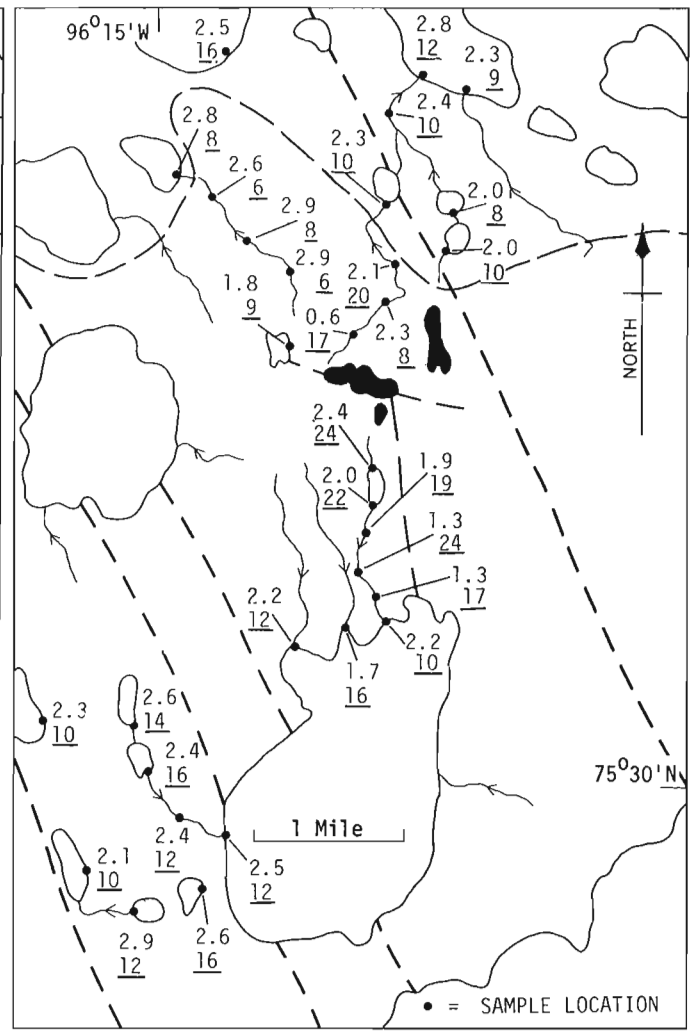

1.5 = silver concentration in ppm

50 = copper concentration in ppm

Figure 4. Silver (ppm) and copper (ppm) in stream and lake sediments.

anticline in the Thumb Mountain Formation. Samples of backgound stream and lake sediments were taken from sites located on a second height of land to the southwest (Fig. 2). As for the Eclipse ore zone site, this area is an anticline formed by the dolomitic-limestone of the Thumb Mountain Formation. At the background sites, concentrations of zinc and perhaps lead appear to be higher in the axis of the anticline (Fig. 3). Levels of zinc increase from 32, 33 and 38 ppm at the edge of the outcrop, through 42 and 47 ppm, to 51, 58 and 66 ppm at sites near the axis of the anticline. This change may be significant when considering the karst, solution cave genesis of Pb-Zn deposits in this area. The variation for zinc is also evident in the water results (Fig. 6).

Metal dispersion from the ore zone seems to be mostly via the stream draining to the north, and to a lesser degree, that to the south. The latter is possibly influenced more by the galena showings to the east, along the geophysical baseline. Levels of zinc in the southern stream sediments are 2 to 3 times background and in the northern stream, 6 to 30 times background concentrations noted for streams in the southwest area. For the southern stream, a concentration of about twice the background level is found in the lake about 1.5 miles south of the ore zone. To the north, concentrations of zinc drop drastically as the stream leaves the dominantly residual soil area on the anticline, and enters the low-lying valley area of marine sediment cover. In areas of nonmarine overlap, dispersion of zinc should reflect mineralization for over 1.5 miles from its source. The stream draining to the northwest appears to be unaffected by the nearby presence of the ore zone. This stream is in fact separated from the ore zone gossan by a slight ridge. Because of the low metal tenor of this stream, dispersion from the ore zone is apparently a surface rather than a groundwater (talik zone) phenomenon.

Dispersion of Pb, as would be expected with a less mobile element, is considerably less. Background

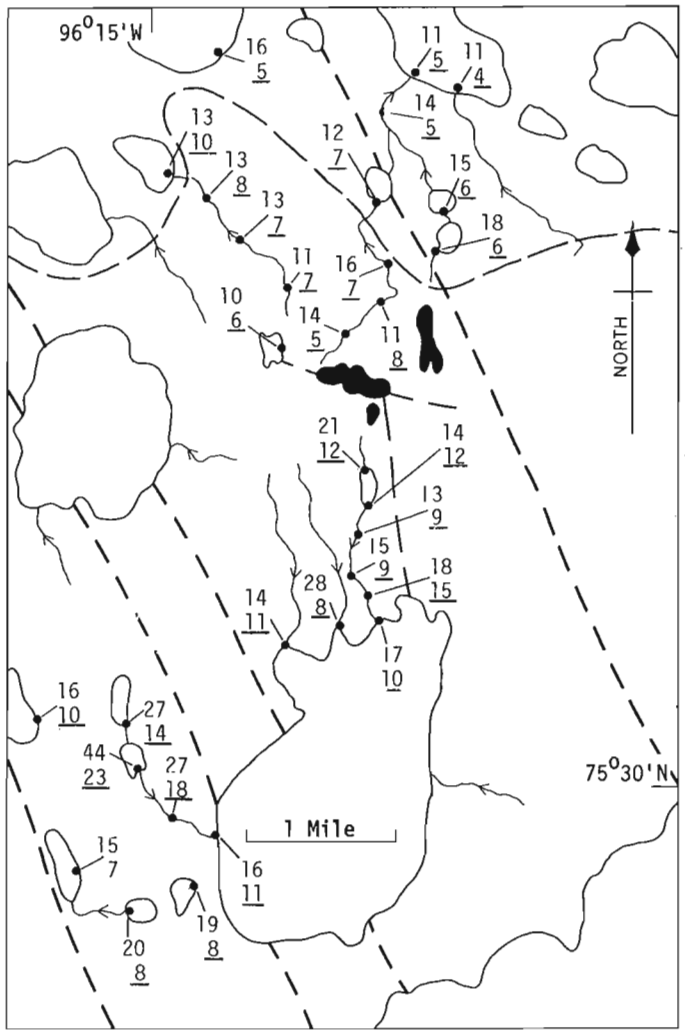

• = Sample Location
20 = Nickel concentration in ppm
10 = Cobalt concentration in ppm

Figure 5. Nickel (ppm) and cobalt (ppm) in stream and lake sediments.

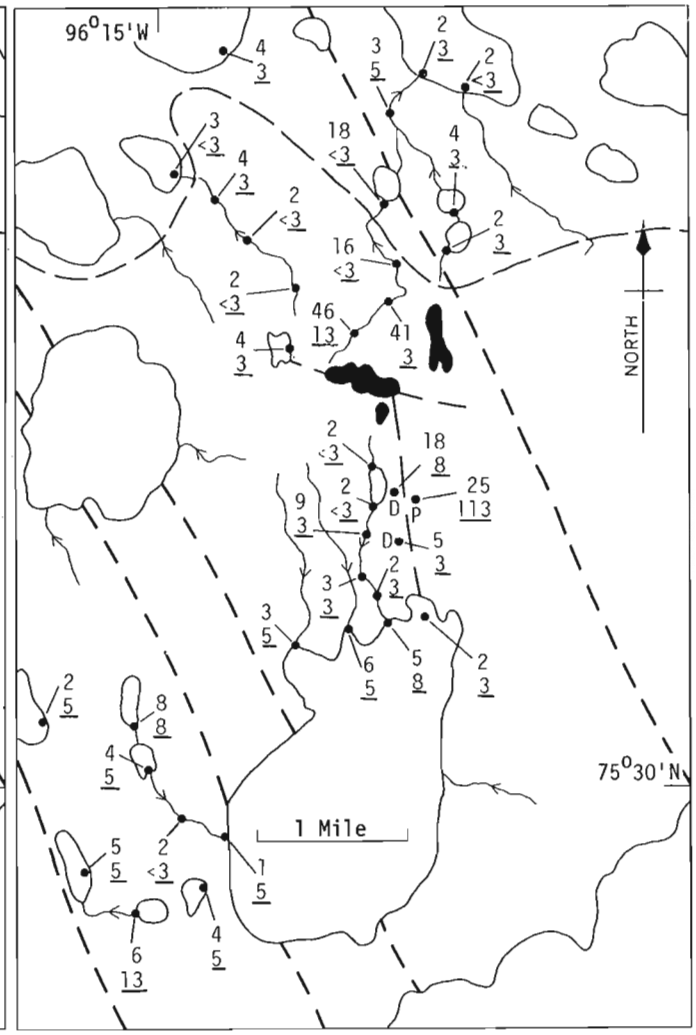

• = Sample Location
5 = Zinc concentration in ppb
3 = Lead Concentration in ppb
D = Small Depression
P = Pit in Galena Showing

Figure 6. Zinc (ppb) and lead (ppb) in stream and lake waters.

levels are reached in the southern stream only 1 mile from the ore zone and in the northern stream are again cut off by marine sediment overlap.

Diagrams are also presented to show the levels of Ag-Cu (Fig. 4) and Ni-Co (Fig. 5) at the stream and lake sediment sample sites. Silver levels are consistently in the range of 2 to 3 ppm. Such levels are similar to those found in the gossan soils (Table 1) and also the background frost boil samples (Table 2). These occur over an area of 20 square miles and are high relative to those found in lake sediments sampled in the tundra zone of the northern Canadian Shield (Allan et al., 1972). This may indicate the presence of the ore zone as part of a regional geochemical silver anomaly. Little Cornwallis Island may have been detected by reconnaissance geochemical mapping, using low sample site densities, as a silver anomaly. The only exceptions to the 2 to 3 ppm Ag range are the samples closest to the ore zone (0.6 and 1.8 ppm Ag respectively). Again, this may be significant in relation to the solution cavity orgin of the ore deposit.

Copper, cobalt and nickel concentrations are monotonously low and are presented: (1) as a contrast to the Zn and Pb dispersion; and (2) as evidence of consistent background levels of such metals both adjacent to the ore zone and in other anomalous samples for zinc and lead. However, it should be noted that the only concentrations of copper greater than 20 ppm are to be found in the stream south of the ore zone. This stream is in the same general area as the Cu-rich (Table 2) frost boil located in Figure 2.

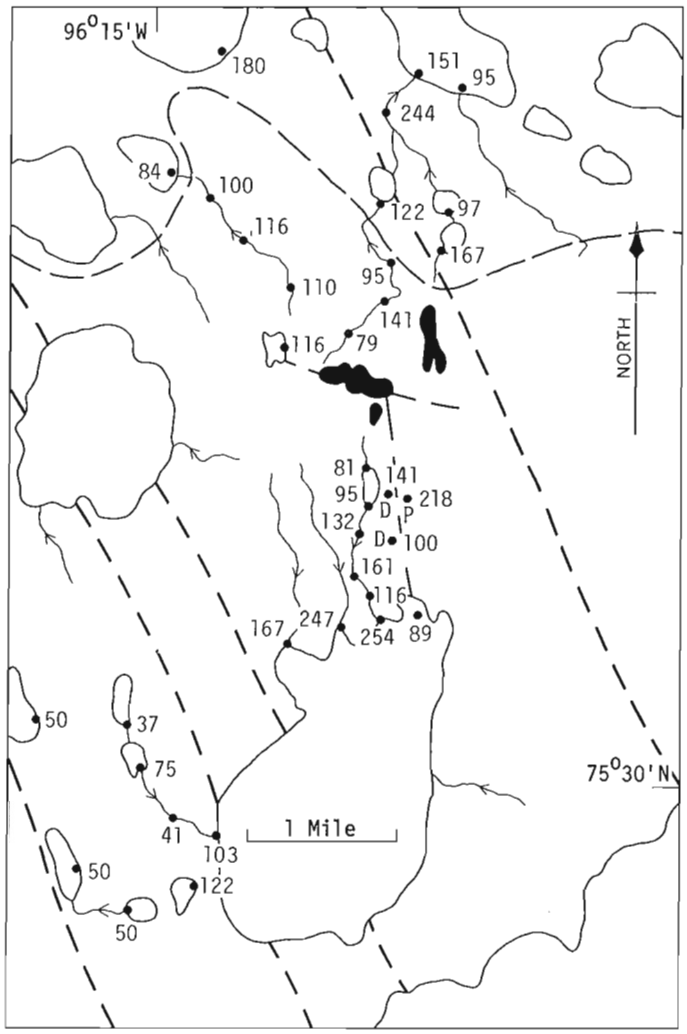

• Sample Location
84: Mercury Concentration in ppt

Figure 7. Mercury (ppt) in stream and lake waters.

Stream and Lake Waters

Stream waters were possibly related to freshly fallen snow, which melted quickly, oversaturating the already poorly drained soils of the area, and thus replenishing the streams with mineralized soil waters. Lake waters were collected from nearshore sites.

Zinc and lead concentrations (Fig. 6) were only above background levels in the stream draining to the north of the ore zone. Again, concentrations dropped drastically (18 to 3 ppb Zn) as the stream entered the area of marine sediment overlap. A concentration of 13 ppb Pb was detected in the background area to the southwest. This was equal to the highest lead value obtained near the ore zone. Lead does not appear to be moved into the drainage system in solution. However, the element does get into solution in this environment, as 113 ppb Pb was found in the water filling a pit in a galena showing.

Mercury is a metal that can often be used as a pathfinder for sphalerite-rich ore bodies. Mercury in drainage water (Fig. 7) shows that concentrations are higher in the Thumb Mountain dolomite area associated with the deposit. Levels here are normally greater than 100 ppt Hg and often over 150 ppt, whereas in the background Thumb Mountain dolomite to the southwest, they are usually less than 100 ppt Hg. A dispersion pattern of Hg from the ore zone itself is not apparent.

Conclusions

The basic conclusion from the company work in the area and from the above results, is that weathering and dispersion of trace metals from anomalous sources, does occur in the Arctic Desert landscape. Exploration geochemistry is a valid tool for mineral prospecting in this somewhat unique area of Canada.

More specifically, if the major targets are Mississippi Valley type, Pb-Zn ores, the following seems to apply. Based on the results given above, and using reconnaissance sample densities, analysis of waters for zinc and mercury, and of drainage sediments for zinc and silver may locate anomalous zones several square miles in area. At more detailed sample densities, zinc and lead in stream sediments is more diagnostic. Gossan samples and drainage sediment samples suspected to be derived from a very close source, should be analyzed for lead and zinc. Anomalous lead levels are more likely to reflect underlying mineralization.

Acknowledgments

The samples were collected during a two-week stay on Little Cornwallis Island. Mr. N.G. Lund assisted with the sample collection.

References

Allan, R.J., Cameron, E.M., and Durham, C.C.
1973: Lake geochemistry, a low sample density technique for reconnaissance geochemical exploration of the Canadian Shield; Proc. 4th Int. Geochem. Symp. Exploration, 1972, p. 131-160.

Dyck, W.
1973: Feasibility study of geochemical sampling of Arctic coastal streams by helicopter based on a Department of Transport icebreaker; Geol. Surv. Can., Paper 72-42, 13 p.

Sangster, D.F.
1971: Geology of lead and zinc deposits in Canada; in Report of Activities, April to October 1970, Geol. Surv. Can., Paper 71-1A, p. 91-94.

1974: Geology of Canadian lead and zinc deposits; in Report of Activities, April to October 1973, Geol. Surv. Can., Paper 74-1A, p. 141.

Thorsteinsson, R., and Kerr, J. Wm.
1968: Cornwallis Island and adjacent smaller islands, Arctic Archipelago; Geol. Surv. Can., Paper 67-64, 16 p.

Project 720067

Willy Dyck
Resource Geophysics and Geochemistry Division

In an effort to determine the source of H_2 in the drillhole water samples near the air-water interface, several drillholes at the New Insco copper sulphide deposit near Duparquet, Quebec were resampled in greater detail before freeze-up. Samples were taken in such a way that at least three came from within the steel casing, the overburden interval between surface and bedrock, and at least three from below the casing in bedrock, alteration zone or ore. The main purpose of this test was to determine whether the H_2 had entered the drillholes at the overburden-bedrock interface and hence could be the result of decay of organic matter in soils. Means of analytical results of the two samplings are given in Table 1. Of the total number of holes, ten were sampled on both occasions. The concentrations of H_2, H_2S, CH_4, O_2, CO_2, and He are expressed as volume fractions of the total dissolved gas content of the water samples. The Rn content is given in picocuries per cubic centimetre of dissolved gas, and the total amount of dissolved gas is expressed in cc (STP) per litre of water. From the results it is clear that CO_2 and N_2 make-up the bulk of the total dissolved gas, but in order to conserve space N_2 along with Ne and Ar are not tabled. A rather marked decrease in the total amount of dissolved gas content due largely to a decrease in the amount of CO_2 is evident in the October samples but the reason for this is not obvious.

Two typical drillhole profiles of dissolved gases from the second sampling are shown in Figure 1. These results show clearly that H_2 does not enter the casing at the overburden-bedrock interface and hence is not due to the decay of organic matter in soils, but rather that it is being generated at a rapid rate in some holes within the first few metres of the water table inside the steel casing. The grouping of results in Table 1 was meant to accentuate the presence of H_2 and the absence of H_2S and CO_2 in the topmost samples compared to lower samples. However, since not all holes had H_2 in the topmost sample and one hole from the October suite contained large amounts of H_2 in the top two samples (47% and 56%, respectively) and another 2.7% H_2S and very little H_2 in the topmost sample, the 'normal' profile illustrated by holes 9 and 27 in Figure 1 is not so clearly evident when averaged over a large number of holes.

Considering all the evidence collected to date the following mechanism is postulated as the one most likely responsible for the production of H_2; it is simply the reaction of the iron in the casing with water thus,

$$Fe + H_2O = FeO + H_2$$

The fact that it occurs only near the air-water interface suggests that the reaction

$$H_2S + 2O_2 = H_2SO_4 \text{ and } H_2SO_4 + Fe = FeSO_4 + H_2$$

also play an important part in this process. Hence the lack of H_2S when H_2 is present. The presence of small amounts of O_2 in all the samples is most likely due to contamination during the handling of the samples in atmospheric air. Tests suggest that on the average close to 1% O_2 in O_2-free samples is picked up during handling. So that in fact the true O_2 level is closer to 0.0% or 0.1% in subsurface samples and about 0.5% to 2% in the topmost samples. By comparison, air dissolved in water in equilibrium with atmospheric air contains about 35% O_2.

A pH of close to 9 in the H_2-rich samples is difficult to explain on the basis of the above mechanism. However, the H_2-rich samples contained virtually no CO_2 (<1%) which appears to be instrumental in lowering the pH in the other water samples in the drillholes. Presumably the CO_2 in the topmost samples is being

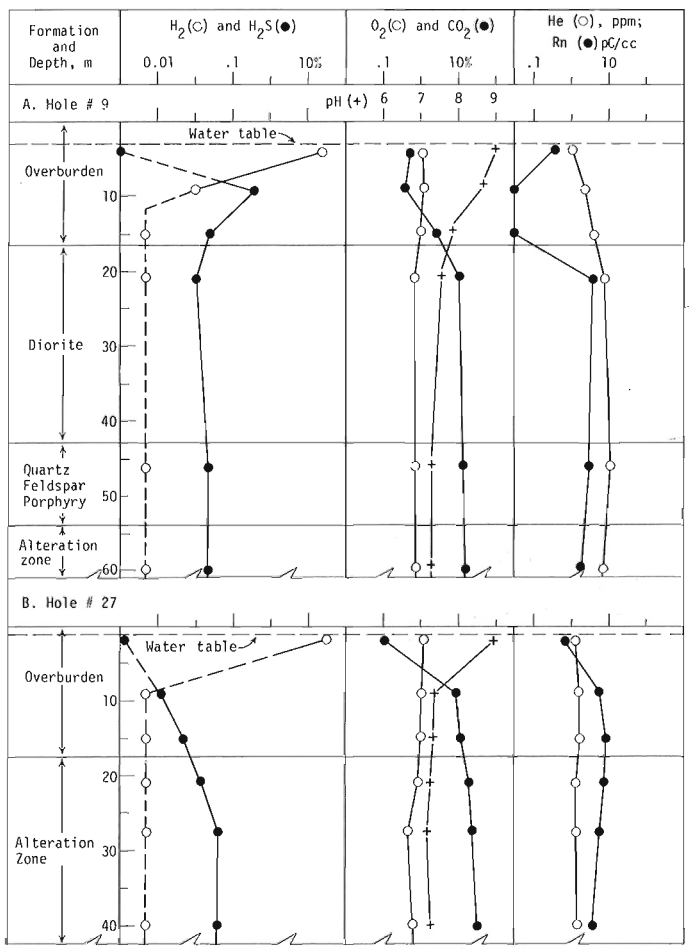

Figure 1. Dissolved gas composition profiles in two drillholes at the New Insco copper sulphide deposit near Duparquet, Que.

Table 1. Arithmetic means, standard deviations, and ranges of dissolved gas constituents from drill hole waters at the New Insco copper deposit in Duparquet, Quebec

Constituent	All but topmost samples				Topmost samples only			
	No. An.*	Mean	S.D.	Range	No. An.*	Mean	S.D.	Range
A. 57 samples from 12 holes collected June, 1973								
H_2, %	18	.44	.75	.01 - 3.09	8	10.17	10.11	.02 - 28.66
H_2S, %	22	.21	.42	.001 - 1.94	8	.01	.02	.001 - .06
CH_4, %	7	.01	.01	.01 - .03	6	.03	.02	.01 - .07
O_2, %	44	1.7	2.1	.1 - 8.7	12	1.2	1.1	.06 - 4.3
CO_2, %	45	48.0	17.4	14.7 - 80.6	12	22.4	18.5	.3 - 51.4
He, ppm	42	2.9	2.6	1.0 - 11.0	11	2.2	.8	1.0 - 3.0
Rn, pC/cc	43	5.4	3.4	1.0 - 16.1	8	3.3	3.3	.5 - 8.6
Gas, cc/l	45	77.3	39.7	32.3 - 193.3	12	52.6	43.0	22.8 -177.3
pH	45	6.91	.44	5.11 - 7.35	12	6.88	1.07	4.58 - 8.68
B. 68 samples from 14 holes collected October, 1973								
H_2, %	8	7.0	19.7	.01 - 55.7	10	14.5	15.4	.01 - 46.6
H_2S, %	50	.13	.35	.001 - 1.6	6	.49	1.10	.001 - 2.7
CH_4, %	13	.02	.02	.01 - .06	7	.03	.03	.01 - .07
O_2, %	52	1.0	.5	.2 - 3.1	14	1.6	1.8	.1 - 7.7
CO_2, %	52	24.4	14.8	.3 - 69.8	14	10.1	14.3	.1 - 36.7
He, ppm	52	4.8	6.6	1.0 - 36.0	14	2.1	.8	1.0 - 3.0
Rn, pC/cc	49	6.1	4.9	.1 - 19.5	14	1.8	1.5	.3 - 4.9
Gas cc/l	54	47.4	18.0	14.7 - 116.0	14	32.4	12.8	22.7 - 67.3
pH	54	7.34	.43	6.45 - 8.72	14	8.18	.89	6.40 - 9.26

* No. An. - Number of analyses above the detection limit.

displaced or expelled by the H_2. While the mere absence of CO_2 still does not explain the high pH, the presence of basic minerals such as dacite and sericite and carbonate materials in the alteration zone could account for the basic character of the water in the absence of CO_2.

A second mechanism, electrolysis of water, could also explain the high pH and H_2 if one can envisage a galvanic cell in which the water-air interface acts as the cathode. Self-potentials of several hundred millivolts, and in one case 1300 mv have indeed been observed over sulphide deposits. Researchers in the field of self-potentials invoke oxidation-reduction reactions to explain self-potentials. However, no self-potential measurements were carried out over the New Insco deposit. While it is difficult to envisage an electrolytic cell in this particular situation, self-potential measurements are needed to help identify the mechanism of production of H_2 in the drillholes.

Aerobic H_2 and NH_3 producing bacteria could also account for the observed H_2 and pH in the water samples. But it is difficult to conceive of a source of nutrients to sustain active colonies of bacteria in more or less stagnant columns of water unless these bacteria can live on CO_2, H_2O and N_2.

The He and Rn values given in Table 1 and Figure 1 were included for comparison with He and Rn values observed in a radioactive drillhole near Gooderham, Ontario and listed in Table 2. Although the U in the Gooderham core did not exceed 200 ppm, the Rn levels in the water were the highest detected to date by the author anywhere, including water from an Elliot Lake uranium mine. A very rough comparison between the Gooderham and Duparquet values gives a U ratio in the rocks of about 100, and He and Rn ratios in the waters of 10 and 3000, respectively. Actually most of the dissolved gas samples from Duparquet contained about 2 ppm He, the normal background level in surface and

Table 2. Concentration of dissolved gases based on the total amount of dissolved gas from a drill hole in radioactive rock near Gooderham, Ontario.

Depth, m	H_2 %	H_2S ppm	O_2 %	CO_2 %	He ppm	Rn pC/cc	cc gas / l H_2O (STP)
A. Samples collected September 25, 1973							
30	<.01	470	1.1	10.9	39	16,100	27.9
60	.5	<10	2.9	8.3	38	19,100	29.9
90	.4	<10	1.2	11.7	31	15,500	26.7
120	<.01	110	3.1	10.7	39	20,600	24.0
150	<.01	<10	1.1	10.8	42	16,000	25.6
B. Samples collected November 16, 1973							
29	.5	<10	1.1	29.0	12	10,100	29.6
40	.3	<10	1.0	18.1	26	15,700	28.4
52	.2	<10	1.2	15.6	29	14,400	28.4
61	.2	<10	1.8	12.0	32	15,300	29.3
92	.1	<10	2.8	14.9	30	13,200	31.9
107	.1	<10	0.9	14.0	34	15,200	27.2
122	.2	<10	1.1	12.4	34	14,600	26.4
137	.3	<10	0.8	19.3	18	12,500	28.9
157	.1	<10	4.1	14.3	30	15,900	26.8

near surface groundwaters. In one hole the He level rose smoothly with depth to about 36 ppm at a depth of 30 m with a similar weak increase in Rn, suggesting some form of communication with U-bearing strata. The relationship between U, He, and Rn in rocks and groundwaters is obviously not a simple one. Factors such as rock porosity, chemical potentials and rate of flow of groundwaters, type of U-mineral structure and dispersion all influence the concentration of He and Rn in groundwaters.

Although the study of dissolved gases in groundwaters gives meaningful results in terms of geochemical processes, a great deal of research is indicated to determine the usefulness of gases for mineral exploration.

Project 720036

E. H. Hornbrook and P. H. Davenport[1]
Resource Geophysics and Geochemistry Division

The purpose of the program was to outline areas in Newfoundland with good potential in metallic mineral resources, in order to facilitate discovery by exploration companies and thus contribute to the economic and social development.

The 1972 pilot studies in the Daniel's Harbour area of the Northern Peninsula where zinc mineralization is associated with the St. George and Table Head Group carbonate rocks have been briefly discussed in Hornbrook (1973) and Hornbrook and Davenport (1973). Essentially, regional organic lake sediment exploration has effectively defined known areas of mineralization and indicated others, some of which were associated with the St. George-Table Head disconformity. A complete discussion of the pilot studies will be published soon in Hornbrook et al. (1974).

Thus, in 1973 a regional organic lake sediment survey was carried out of the total belt of lower Paleozoic carbonate rocks in western Newfoundland. The data are briefly described in Hornbrook and Davenport (1974) and Davenport et al. (1974a). The single element contour maps for Zn, Pb, Mn and Fe and the weight loss on ignition contour maps have been released on open file (Davenport et al., 1974b). The data have outlined several areas throughout the belt of anomalous zinc values comparable to those associated with the zinc deposits at Daniel's Harbour. However, the data have also poorly outlined other areas, whose significance in relation to their zinc potential is difficult to assess. For example, high background zinc values were found south of Hare Bay, in an area predominantly underlain by allochthonous clastic rocks which contain black shale units, Smyth (1973).

All of the data are undergoing statistical analysis to determine primarily the correlation of zinc with features of the surficial environment such as: coprecipitation with iron and manganese oxides and hydroxides; sorption by organic matter; topographic relief and sample lake area and depth. Findings to date have revealed that zinc correlated significantly with iron and loss on ignition (estimate of organic content). Thus, multilinear regression analysis was carried out in order to remove the influence of iron and loss on ignition and obtain the residual zinc values. Further computer processing of the data is in progress and present findings were described in Davenport et al. (1974c). The distribution of residual zinc values resulting from the regression analysis has improved the delineation of zones of known zinc mineralization relative to the distribution of untreated zinc values. Further, referring to the example given above, the high background zinc values in the area of marginal interest south of Hare Bay has been reduced to background residual zinc values through regression suggesting the high background, untreated zinc values are not related to mineralization.

Thus, the residual zinc distribution is believed to be a more reliable indicator than the untreated zinc distribution of new areas of potential zinc mineralization. In the vicinity of known zinc mineralizaiton, residual zinc distribution has also indicated adjacent target areas for further development work.

[1]Province of Newfoundland and Labrador Mineral Development Division.

References

Hornbrook, E. H. W.
1973: In Report of Activities, April to October, 1972; Geol. Surv. Can., Paper 73-1, Pt. A, p. 56.

Hornbrook, E. H. W., and Davenport, P. H.
1973 : In Report of Activities, November 1972 to March 1973; Geol. Surv. Can. Paper 73-1, Pt. B, p. 25-27.

1974 : In Report of Activities, April to October, 1973; Geol. Surv. Can., Paper 74-1, Pt. A, p. 65.

Hornbrook, E. H. W., Davenport, P. H., and Grant, D. R.
1974: Regional and detailed geochemical exploration studies in glaciated terrain in Newfoundland; Newfoundland Dept. Mines Energy, Paper 74-3.

Davenport, P. H., Hornbrook, E. H. W., and Butler, A. J.
1974a: In Province of Newfoundland, Dept. of Mines, Energy, Mineral Development Division, Report of Activities, 1973.

1974b: Geochemical lake sediment survey for Zn and Pb mineralization over Cambro-Ordovician carbonate rocks of western Newfoundland; Newfoundland Dept. Mines Energy, Open File Release, February 15, 1974.

1974c: Regional Lake sediment geochemical survey for zinc mineralization in western Newfoundland; Paper presented at 5th Int. Geochem. Explor. Symp., Vancouver, B. C., April 4, 1974.

Smyth, W. R.
1973: Stratigraphy and structure of the southern part of the Hare Bay allochthon, northwestern Newfoundland; unpubl Ph. D. thesis, Memorial University, St. John's, Newfoundland.

20. SOME STUDIES OF GEOCHEMICAL DISPERSION ABOUT A SMALL URANIUM SHOWING, MARCH TOWNSHIP, ONTARIO

I.R. Jonasson and W.Dyck
Resource Geophysics and Geochemistry Division

Introduction

A preliminary study of the geochemical dispersion of uranium, radon, zinc, copper, lead, nickel and molybdenum has been made over a small area of March Township, eastern Ontario.

The specific location of a uranium occurrence in the study area is described by Grasty et al. (1973) who first discovered it as an anomaly in a series of gamma-ray spectrometer profiles flown over the area in 1972. Steacy et al. (1973) have described the mineralogy of the occurrence which consists largely of discrete radioactive grains associated with hydrocarbon material, a little chalcopyrite and some pyrite in dolomite-sandstone host rock of the Ordovician March Formation.

A series of hydrogeochemical surveys covering 45 square miles (115 km^2) in the vicinity of the occurrence were undertaken to establish the extent of geochemical dispersion of uranium, and to ascertain the effectiveness of various geochemical indicators in locating this and perhaps other similar occurrences.

Results

Table 1 presents summary information on the abundance of several metals in samples from the occurrence (X) and from a pegmatite vein in some nearby Precambrian rocks (Y). It is interesting to note that whilst both locations show a uranium enrichment, the relative abundances of some ancillary metals, viz, Zn, Cu, Mo change markedly between occurrences, an observation which suggests that the material at (X) is probably not derived from occurrences similar to (Y).

Table 2 presents information on the contents of some trace metals in soils near (X) and from soils some distance from (X). The soils clearly reflect the presence of U and Cu in the mineralization beneath, but Mo is not particularly impressive as an indicator element. Contrary to expectations Zn seems to be slightly enriched in the mineralized zone.

Table 3 data indicate that of the elements tested only Pb shows an enrichment in snow cover above the mineralization. U and Cu are notable by their absence. In other areas where snow has been used as a prospecting aid, Cu is usually quite useful in defining zones of mineralization (Jonasson, unpublished data), but to date U has not been found in any significant quantity in snow cover over mineralization. The reasons for this are not yet fully understood.

Figure 1 is a map of radon distribution in stream waters over the whole map-area studied. It can be seen quite readily that the mineralization at (X) is clearly defined as a high Rn anomaly and that the anomalous zone covers about 4 square miles (10 km^2). Two other lesser anomalous zones also appear; the significance of which remains uninvestigated.

Figure 2 presents data for the uranium distribution in stream sediments at the same sample sites from which waters were collected for Rn determination. The mineralization at (X) is again clearly defined although the U contents measured are quite low over most of the area. Nevertheless the U and Rn anomalies are reasonably superimposable.

The lesser anomalies detected by Rn measurement do not reproduce in Figure 2. Rather, several different locations appear to be slightly anomalous. One in particular at the east end of the study area shows a clear dispersion train down a single stream from a point source. This one should be checked further. All of the U anomalous zones are also anomalous in Zn ($\geq$ 85 ppm, b.g., 45 ppm) and perhaps in Cu ($\geq$ 25 ppm, b.g., 12 ppm). Zn is by far the best indicator

Table 1

Analyses of some U-bearing materials (ppm)

a) Interbedded dolomite-sandstone: March Formation (X)						
U	Zn	Cu	Ni	Mo	Pb	Se
60	6	1500	21	100	30	<0.1
b) Biotite from a pegmatite vein: Precambrian (Y)						
575	531	6	<3	0.5	41	-

Table 2

Some trace metals in soils near the uranium occurrence (X) and distant from it (ppm)

a) near (X)				
U	Zn	Cu	Ni	Mo
8.5	133	90	6	2
12.0	76	143	19	3
0.5	47	22	9	3
1.6	80	98	19	3
0.0	82	26	13	1
7.6	37	269	16	-
7.2	35	217	15	-
11.2	43	145	24	-
15.0	52	110	19	-
b) distant				
0.0	61	15	19	1
0.1	71	13	16	3
0.0	61	8	13	2
0.0	62	7	5	2
0.0	37	7	13	2
0.0	44	2	13	1

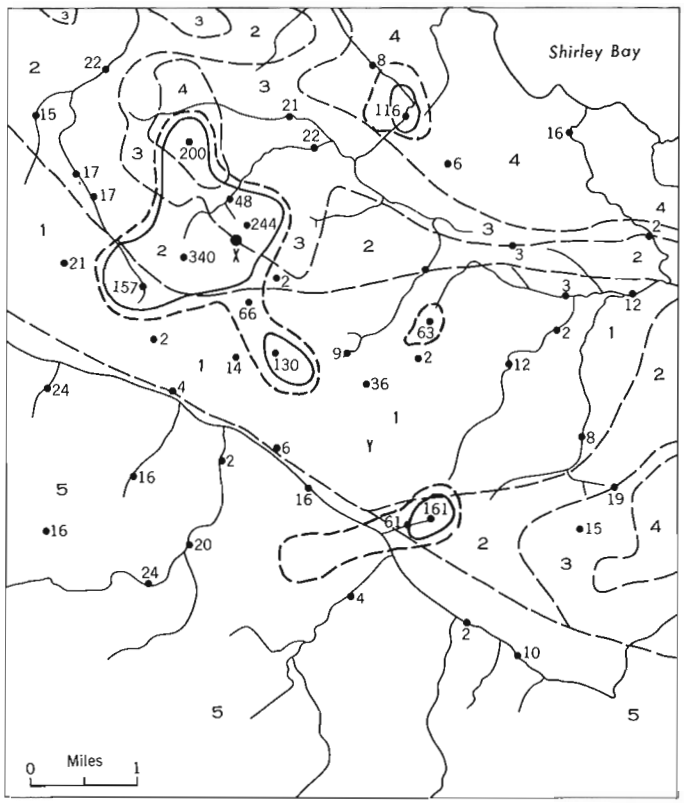

> 100
50–100
Uranium showing
Geological contact
Streams

Precambrian
1 Granite, gneiss etc.
Paleozoic
2 Nepean sandstone (Cambrian)
3 March dolomite · sandstone (Ordovician)
4 Oxford limestone · dolomite (Ordovician)
Cenozoic
5 Recent alluvium and Pleistocene glacial deposits

Figure 1. Radon in stream waters, pc/1. Geology from G.S.C. Map 414A.

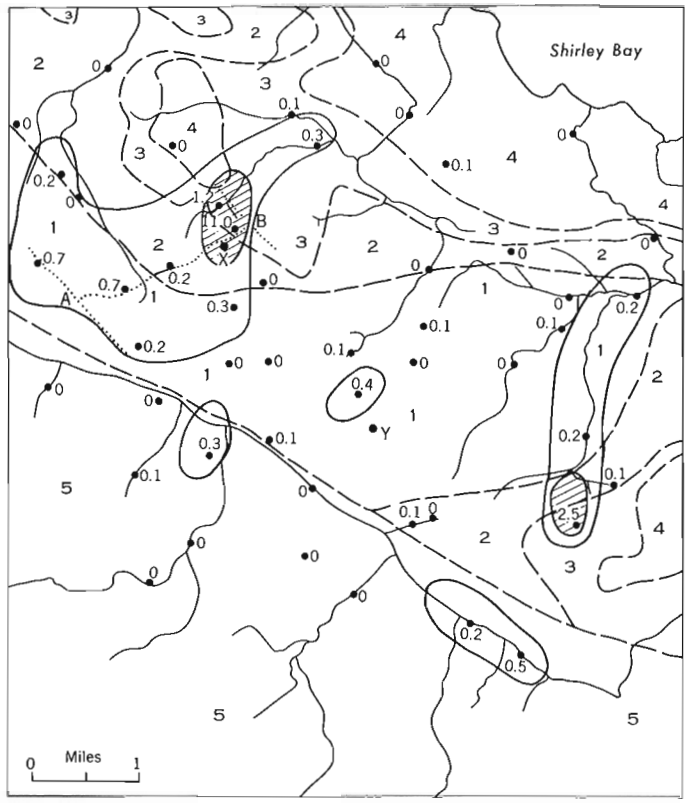

> 1.0
> 0.2
A···B Soil traverse
Uranium showing (X, Y)
Geological contact
Streams

Precambrian
1 Granite, gneiss etc.
Paleozoic
2 Nepean sandstone (Cambrian)
3 March dolomite · sandstone (Ordovician)
4 Oxford limestone · dolomite (Ordovician)
Cenozoic
5 Recent alluvium and Pleistocene glacial deposits

Figure 2. Uranium stream sediments, ppm. Geology from G.S.C. Map 414A.

Note: In Figures 1 and 2 some sample points appear not to be on streams as drawn. These points are an intermittent extensions of the streams shown.

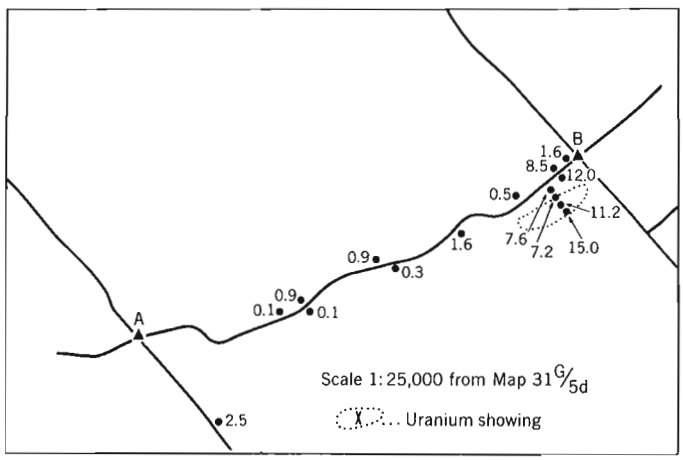

Figure 3. Soil traverse for Uranium, ppm.

Table 3

Snow samples collected above the U showing (X)

Zn	Cu	Pb	U	(ppb)
34	6	19	nd	
11	3	24	nd	
18	4	22	nd	
8	4	24	nd	
16	6	13	nd	
Background				
4	2	8	nd	
30	6	4	nd	
9	2	9	nd	

Table 4

Nature of dissolved gases in stream and run-off waters

Location	total dissolved gas (cc/l) (d.g.)	Rn pc/cc dissolved gas	H_2 % d.g.	CH_4 % d.g.	O_2 % d.g.
Snow-melt	40	2.8	0	0	12.8
at (X)	41	2.0	0	0	21.7
Snow-melt	39	55.1	0	0	25.8
downstream	39	21.2	0	0	16.7
from (X)					
Stream water at B (Fig. 3)	52	3.3	0	2.47	5.5

water temp: 0°C; air temp: 4°C; H_2S detected by odour only at Site B.

element for U in stream sediments in the streams which drain the (X) zone as defined in Figures 1 and 2, where some values reach 250 ppm in sediments and 400 ppm in soils. Further work is required to ascertain the reasons for this strong correlation.

Figure 3 represents an expanded section of a soil traverse, A-B, noted on Figure 2. Traverse distance is about 2 miles (3.2 km). Humic-rich A horizon soils only were collected. The uranium occurrence at (X) is again clearly defined (Table 2) relative to the surrounding area.

Preliminary studies have begun (Spring, 1974) on detailed studies of dissolved gases in stream and snow-melt waters at selected sites across the study area. Table 4 displays some early data. Elevated levels of Rn are found downstream from the occurrence at (X) whereas little is detectable in water overlying the mineralization.

The stream water at B is unusual for its methane (CH_4) content which is matched by a depleted oxygen content and an odour of H_2S. The interpretation at present is that stagnant groundwater is moving into this stream as the water-table in the area rises.

Fuller details of this work and of the movement of dissolved metals in run-off waters will be presented at a later date.

Discussion

The results of this work indicate that the occurrence of uranium mineralization is perhaps more widespread than was apparent from the work of Grasty et al. (1973).

Hydrogeochemical studies of U dispersion and Rn dispersion probably are effective in outlining areas of interest where follow-up soil traverses may be deployed usefully. Analyses of uranium enriched rocks allow a realistic choice of geochemical indicator elements to be made and which can also be sought in soil, sediment and water samples. In this case, Cu and Zn may prove effective as prospecting aids; Mo may yet prove to be useful.

At present the usefulness of snow samples is very limited, but preliminary data indicate that snow-melt-waters may be sampled advantageously for Rn which is flushed from soils and groundwaters of mineralized zones.

References

Grasty, R.L., Charbonneau, B.W., and Steacy, H.R.
1973: A uranium occurrence in Paleozoic rocks west of Ottawa; in Report of Activities, April to October 1972, Geol. Surv. Can., Paper 73-1A, p. 286-289.

Steacy, H.R., Boyle, R.W., Charbonneau, B.W., and Grasty, R.L.
1973: Mineralogical notes on the uranium occurrence at South March and Eldorado, Ontario; in Report of Activities, November 1972 to March 1973, Geol. Surv. Can., Paper 73-1B, p. 103-106.

21. PRELIMINARY RESULTS OF A SHIPBORNE MAGNETIC SURVEY IN AMUNDSEN GULF, DISTRICT OF FRANKLIN

Project 710049

R. G. Currie and D. L. Tiffin
Regional and Economic Geology Division, Vancouver, B. C.

A Natural Resource charting survey of part of Amundsen Gulf (Fig. 1) was carried out during August and September, 1973. The survey was conducted jointly from the Canadian Hydrographic ship *Parizeau* with the Canadian Hydrographic Service, Victoria, B. C., the Earth Physics Branch, Ottawa and the Geological Survey of Canada, Vancouver, B. C.

The instrumentation used included a Barringer OC104 Proton Precession magnetometer which recorded in analogue and digital mode. Navigation, to hydrographic standards, was provided by Polar Continental Shelf Project's Decca Lambda system. Magnetic base stations monitored diurnal variations and magnetic storms at the Decca station on Pearce Point and at Sachs Harbour, Banks Island. Approximately 16,000 kilometres of track line were surveyed with sample intervals of 6 seconds (approximately 40 metres) and line spacing, following Decca lanes, that varied from 1 kilometre to 10 kilometres. Tie lines were run every 15 kilometres. Data collection was ably done by the ship's hydrographers under the supervision of the hydrographer-in-charge (Sandilands and Clarke, 1973).

Because of the high magnetic latitude of the survey, magnetic storms were intense and frequent. Therefore,

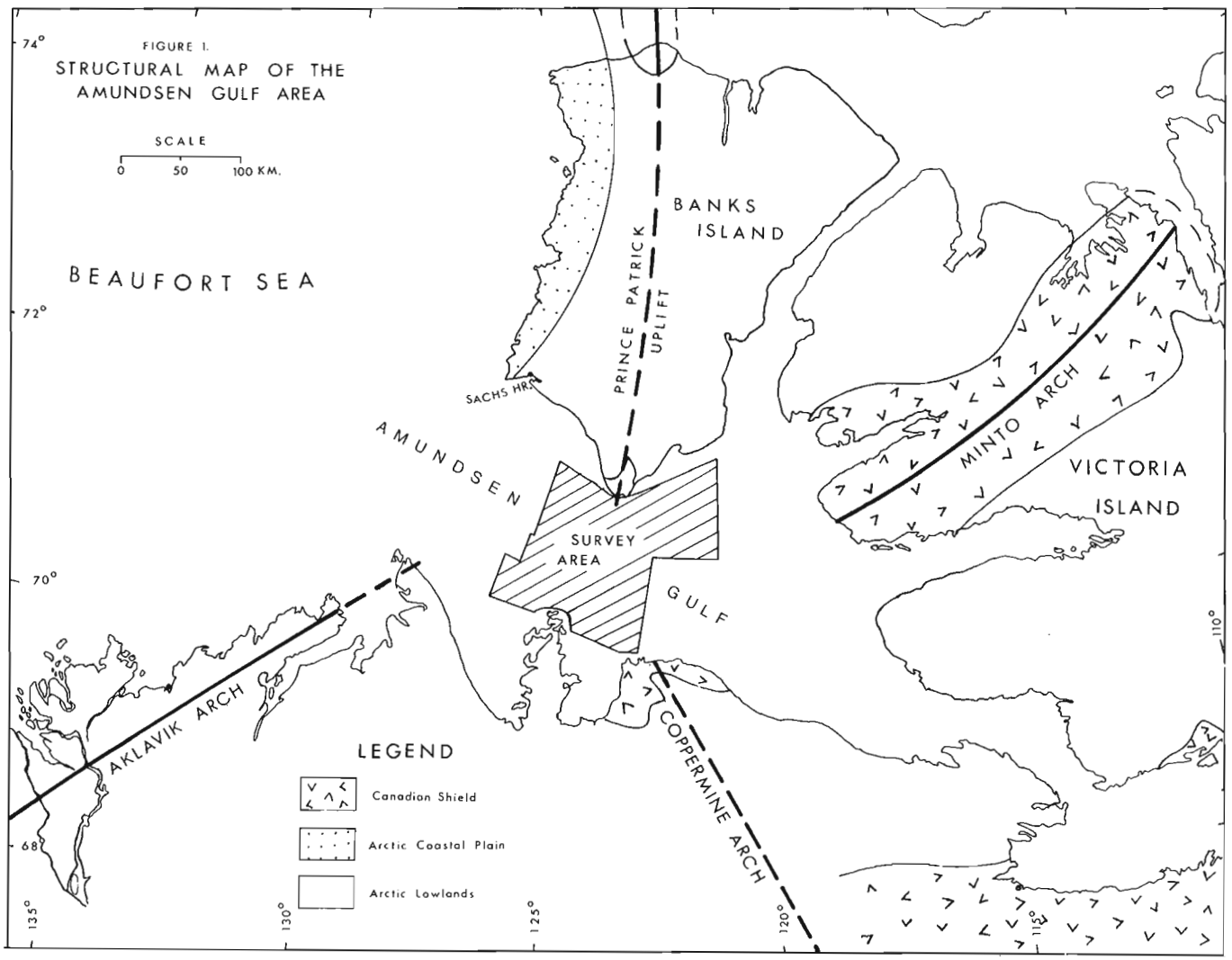

Figure 1. Survey location and structural map of the Amundsen Gulf area (after Thorsteinsson and Tozer, 1960).

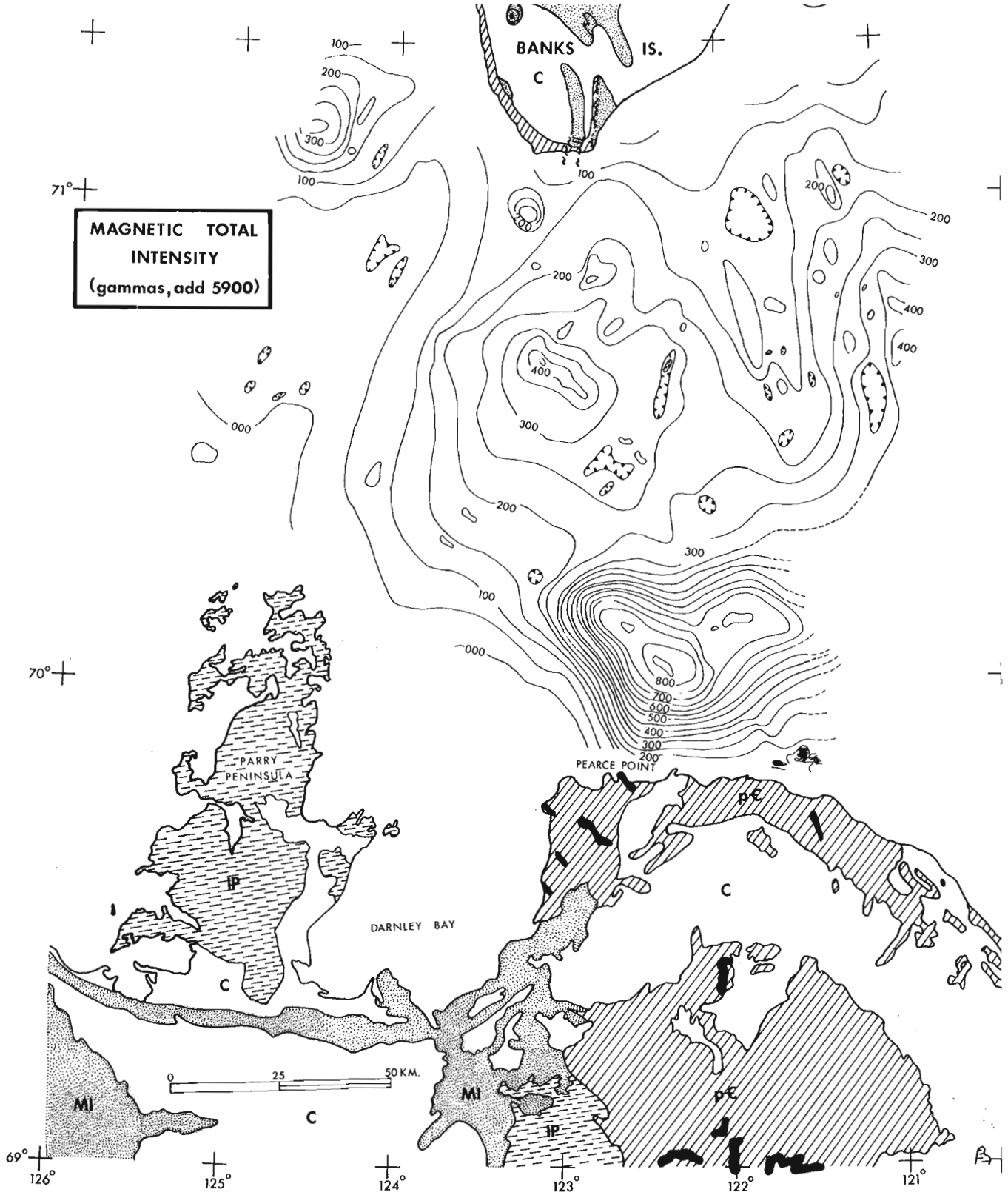

Figure 2. Magnetic total intensity map and local geology (after Thorsteinsson and Tozer, 1962; Yorath et al., 1969). Sedimentary units divided by age: PC - Precambrian, IP - Paleozoic, MI - Mesozoic, and C - Cenozoic. Precambrian diabase gabbro dykes solid black.

in the preliminary processing and mapping, only data collected during magnetically quiet intervals was used. This represented approximately 50 per cent of the total trackline.

An examination of crossovers at the tie lines provided a check on the internal consistency of the data which was found to be good for this survey. Data collected during magnetically distributed periods will be corrected using the base station information and added to the map. This additional data is not expected to significantly alter the character of the preliminary map (Fig. 2).

The regional geology of the Arctic Archipelago consists of relatively shallow, ill-defined remanent basins comprising lower Paleozoic sedimentary rocks lying on the edge of the Canadian Shield and separated by broad basement arches. The survey area is at the junction of a number of these structural and tectonic elements in the western Arctic (Fig. 1). The Minto Arch, Aklavik Arch and Coppermine Arch meet near Amundsen Gulf with the Prince Patrick Uplift of northern Banks Island possibly continuing into the area (Thorsteinsson and Tozer, 1960).

In the areas adjacent to Amundsen Gulf, the exposure consists of sediments and alluvium of Precambrian, Paleozoic, Mesozoic and Cenozoic age plus diabase-gabbro dykes and sills of late Precambrian age (Yorath et al., 1969; Christie, 1964; Thorsteinsson and Tozer, 1962).

Inspection of the preliminary total field map (Fig. 2) indicates a number of magnetic features of geological significance. The northern two-thirds of the map is characterized by anomalies of relatively low amplitude, maximum 350 gammas, and low gradient, 15 gammas per kilometre. These anomalies are most likely associated with extensions of the cratonic arches into the area. The Minto Arch, from the northeast, appears to extend to at least long. 122° W. The Coppermine Arch, from the southeast, appears to extend across Amundsen Gulf.

The dominant feature in the survey area is a rectangular shaped anomaly centred at 70.1°N and 122.4°W, the Pearce Point anomaly. It has an amplitude of 800 gammas, a gradient of 50 gammas per kilometre and a calculated depth to source ranging from 5 to 7 kilometres. This anomaly, somewhat similar to the Darnley Bay anomaly (Riddihough and Haines, 1972) about 100 kilometres to the southwest, may be the magnetic expression of a major diabase intrusive.

A third type of feature of interest occurs in the extreme southeast corner of the survey area. The anomalies characteristic of this area do not show up well at this scale as they have wavelengths of about 1 kilometre, amplitudes to 4600 gammas and calculated depths to source of 0.5 kilometre. It is proposed that the source of these anomalies is a system of diabase dykes that can be seen in outcrop on adjacent land areas. However, the trend of these anomalies differs considerably from the trend of the subaerial exposures suggesting that other interpretations are possible.

References

Christie, R.L.
1964: Diabase-gabbro sills and related rocks of Banks Island and Victoria Islands, Arctic Archipelago; Geol. Surv. Can., Bull. 105.

Riddihough, R.P., and Haines, G.V.
1972: Magnetic measurements over Darnley Bay, N.W.T; Can. J. Earth Sci., v. 9, p. 972-978.

Sandilands, R.W., and Clarke, E.B.
1973: Final field report - C.S.S. Parizeau - Queen Charlotte Sound, British Columbia and Amundsen Gulf, Northwest Territories; C.H.S.. Marine Sciences Branch, D.O.E., Ottawa.

Thorsteinsson, R., and Tozer, E.T.
1960: Summary account of structural history of the Canadian Arctic Archipelago since Precambrian times; Geol. Surv. Can., Paper 60-7.

1962: Banks, Victoria and Stefansson Islands, Arctic Archipelago; Geol. Surv. Can., Mem. 330.

Yorath, C.J., Balkwill, H.R., and Klassen, R.W.
1969: Geology of the eastern part of the Northern Interior and Arctic Coastal Plains, Northwest Territories; Geol. Surv. Can., Paper 68-27.

MARINE SEISMIC REFRACTION SURVEY
POKIAK LAKE, TUKTOYAKTUK, DISTRICT OF MACKENZIE

Project 730006

R. L. Good and J. A. Hunter
Resource Geophysics and Geochemistry Division

At the request of the hamlet council of Tuktoyaktuk, a refraction seismic survey was carried out on Pokiak Lake in an attempt to map the presence of permafrost beneath the lake bottom. This lake, which constitutes the southwest perimeter of the hamlet, is being considered as a site for land reclamation, and the occurrence of permafrost beneath it is of interest to the engineering study.

The lake consists of two "lobes" as shown in Figure 1 with a narrow (15 m) connecting channel. A narrow gravel bar on the northwest side of the lake, separates it from Kugmallet Bay.

Seven single ended profiles were shot across the lake from two shot point positions using an in-line hydrophone array. For the profiles shot in the north "lobe" a 16-metre spacing between hydrophones was used, while for shots in the south lobe an 8-metre spacing was used. Travel times of first arrival seismic waves were plotted vs. distance from the shot to the hydrophones. Average velocities of seismic waves, interpreted to be travelling through the lake bottom, were computed from the plots for each profile. The results are as follows:

PROFILE	AVERAGE VELOCITY (M/S)	RECORD QUALITY
1	1610	Fair
2	1420	Good
3	1330	Good
4	1440	Poor
5	2440	Poor
6	2300	Good
7	2980	Good

The low seismic velocities observed on profiles 1 to 4 are indicative of unfrozen sands and silt. Gravel deposits have also been occasionally observed to give such low velocities but in general, velocities of unfrozen water-saturated gravel should be in the range of 1600-2000 m/s. The velocities given on profiles 5, 6 and 7 correlate well with velocities of frozen silts observed in adjacent areas of Tuktoyaktuk (Wyder, Hunter and Rampton, Geol. Surv. Can. Open File 128).

The results of the seismic survey can be interpreted to indicate the presence of permafrost immediately beneath the bottom of the south "lobe" of Pokiak Lake. Absence of high velocities in the north "lobe" may result from any of the following:

1. The occurrence of frozen clays in the temperature range 0 to -2°C. In this range, frozen clays exhibit velocities close to that of the unfrozen state and definitive interpretation by seismic refraction is not possible.
2. Depression of the top of permafrost to a depth beyond the range of detection by the seismic method (approximately 30 m for the array used).
3. The absence of permafrost beneath the lake.

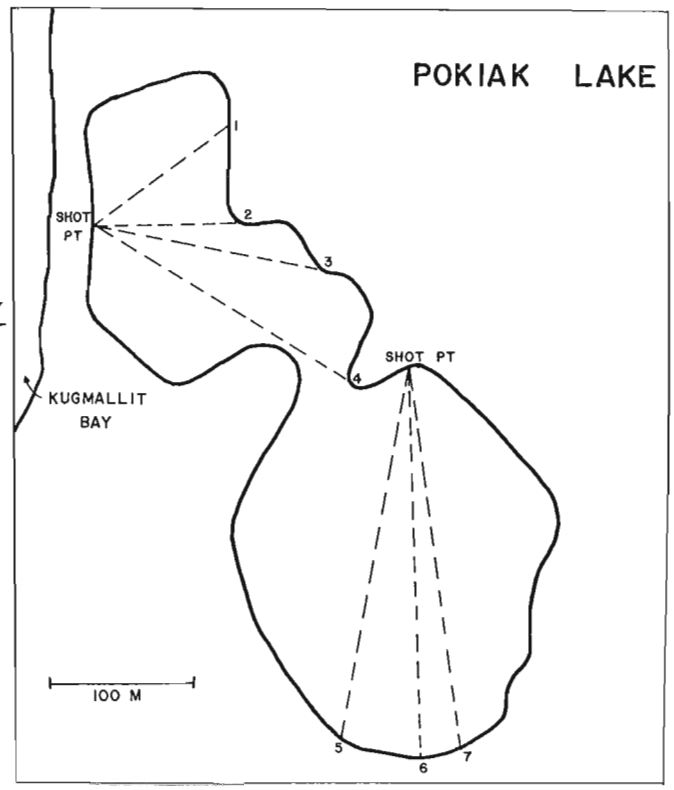

Figure 1. Location of seismic profiles on Pokiak Lake, Tuktoyaktuk area.

23. GAMMA-RAY SPECTROMETER CALIBRATION FACILITIES

Project 720084

R. L. Grasty and B. W. Charbonneau
Resource Geophysics and Geochemistry Division

Two test strips and five calibration pads are presently used by the Geological Survey of Canada for calibrating airborne gamma-ray spectrometers. The locations of these facilities which are close to Ottawa are shown in Figures 1 and 2. The Breckenridge test strip overlaps the original test strip used by Charbonneau and Darnley (1970).

The calibration pads located at Uplands airport Ottawa are 25-foot by 25-foot by 18-inch-thick concrete slabs and are used to obtain spectrum stripping information for ground and airborne spectrometers. Table 1 shows the potassium, uranium and thorium concentration of core samples from the five pads. Potassium was obtained by X-ray fluorescence and uranium and

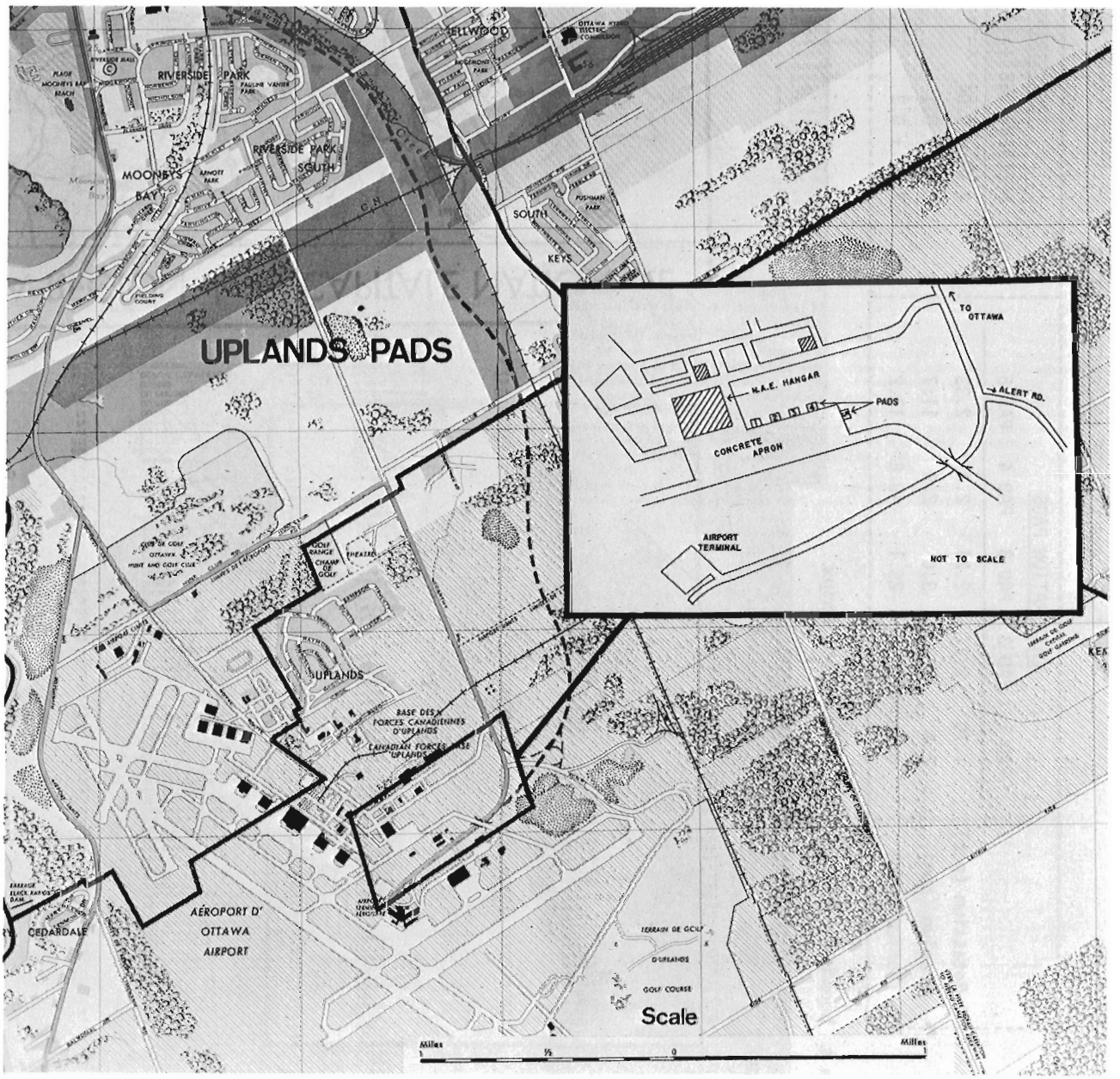

Figure 1. Location of calibration pads.

TABLE I

ANALYSIS OF CALIBRATION SITES

	CALIBRATION PADS					TEST STRIPS	
	PAD 1	PAD 2	PAD 3	PAD 4	PAD 5	BRECKENRIDGE	CARP
Potassium (pct)	1.70	2.27	2.21	2.21	2.33	2.03 ± 0.04	2.1
Uranium (ppm)	2.4	7.3	3.0	2.9	11.7	0.9 ± 0.1	1.6
Thorium (ppm)	8.9	12.6	26.1	40.8	13.2	7.7 ± 0.3	8.0

Figure 2. Location of Breckenridge and Carp test strips.

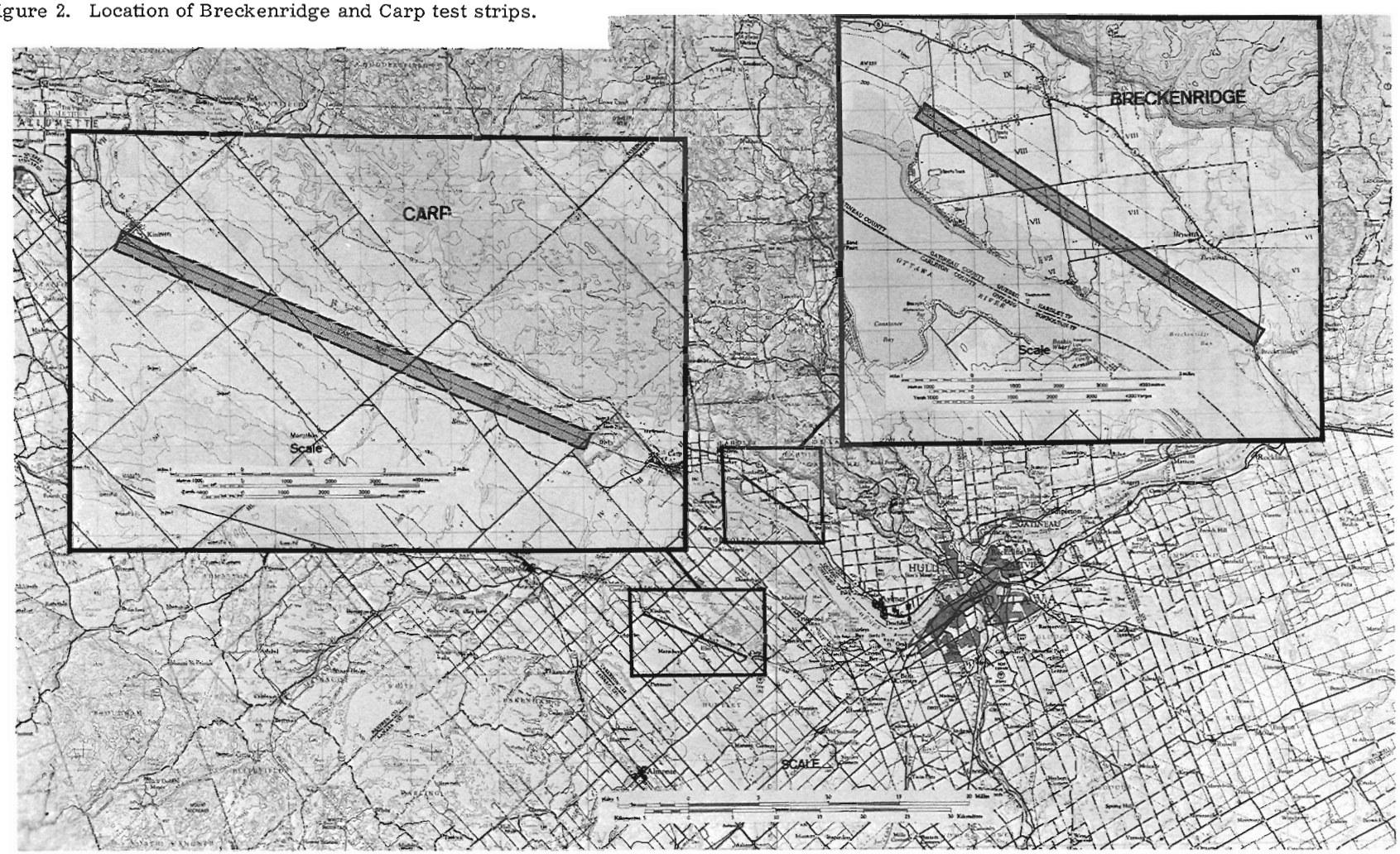

thorium by laboratory gamma-ray analysis. Details of the technique used to obtain stripping ratio information is given in Grasty and Darnley (1971).

In the summer of 1973, 70 field samples were taken at depths up to 10 inches along the Breckenridge test strip and analyzed in the laboratory. This calibration strip was found to be homogeneous along its length and no variation of radioactivity with depth was found. These results are presented in Table 1. The Breckenridge test strip has an abnormally low uranium-to-thorium ratio of 0.11. The second test strip, north of the town of Carp, has a uranium-to-thorium ratio closer to the average crustal value, and provisional radioelement concentrations from field spectrometer measurements along the Carp test strip are also listed in Table 1.

References

Grasty, R.L., and Darnley, A.G.
1971: The calibration of gamma-ray spectrometers for ground and airborne use; Geol. Surv. Can., Paper 71-17.

Charbonneau, B.W., and Darnley, A.G.
1969: A test strip for calibration of airborne gamma-ray spectrometers; in Report of Activities, November 1972 to March 1973, Geol. Surv. Can., Paper 73-1B, p. 17-32.

Project 720084

R. L. Grasty and P. B. Holman
Resource Geophysics and Geochemistry Division

An important consideration in the cost of any airborne survey operation is the size of the sodium iodide detectors. The crystal dimensions should therefore be chosen to give a maximum count rate for a particular volume. Laboratory experiments to investigate detector characteristics were carried out using seven cylindrical crystals of different sizes that are readily available commercially and currently flown by survey companies. Details of these crystals are shown in Table 1.

Two pounds of thorium oxide were placed six feet from the centre of each crystal and spectra recorded, using a 512 channel analyzer, in ten degree steps starting at the axis of the detector. The detector sensitivity was calculated as counts per unit volume using an energy window of 2.41 Mev to 2.81 Mev centred on the 2.62 Mev peak of thallium-208 in the thorium decay series. The uranium stripping ratio, the ratio of counts in the uranium window (1.66 Mev to 1.86 Mev) from a thorium source to those in the thorium window, was also determined for each crystal. Figure 1 shows the relative sensitivity of each detector for different source positions, compared to that of the 11.5- x 4-inch crystal. In Figure 2, the sensitivities of each crystal are normalized to that of the 11.5- x 4-inch crystal in order that the variation of detector response with angle can be more easily compared. Results of the stripping ratio variation with source position for each crystal is illustrated in Figure 3.

For a source on the axis of the detector, it would be expected for the same thickness of crystal, that the larger diameter detector would be most efficient, since fewer gamma-ray photons would be scattered from the sides of the crystal. This was consistent with the results for the 11.5- x 4-inch, the 8- x 4-inch and the 5- x 4-inch crystal as illustrated in Figure 1. The 9- x 4-inch crystal did not fit this pattern and appeared to be related to the poor resolution of this particular crystal, as can be seen in Figure 4. The spectrum from the 5- x 5-inch crystal is also shown in Figure 4 for comparison. The spectra are normalized to the same 2.62 Mev peak height. A second 9- x 4-inch crystal with good resolution was found to have a sensitivity intermediate between that of the 8- x 4-inch and 11.5- x 4-inch crystal and this result is shown in Figure 1. It therefore appears that good resolution is important. The 6- x 4-inch crystal was significantly lower in sensitivity than all the other 4-inch-thick crystals that were measured, even though its resolution was good. This was also found for a second 6- x 4-inch crystal, however the sensitivity of the two 6- x 4-inch crystals were quite different as can be seen in Figure 1. The reason for this is not yet clear, but it should be noted that these crystals are equipped with a light pipe.

For a source on the axis of the detector, the 5- x 5-inch crystal was only slightly lower in sensitivity than the 5- x 4-inch crystal, suggesting that in this case the 4-inch crystal is only marginally better than the 5-inch-thick crystal. It is quite apparent that a 3-inch-thick crystal has a much reduced sensitivity compared to both the 4- and 5-inch-thick crystal.

An airborne detector receives radiation from all angles. At ground level fifty per cent of the unscattered radiation can be shown to lie within a cone of

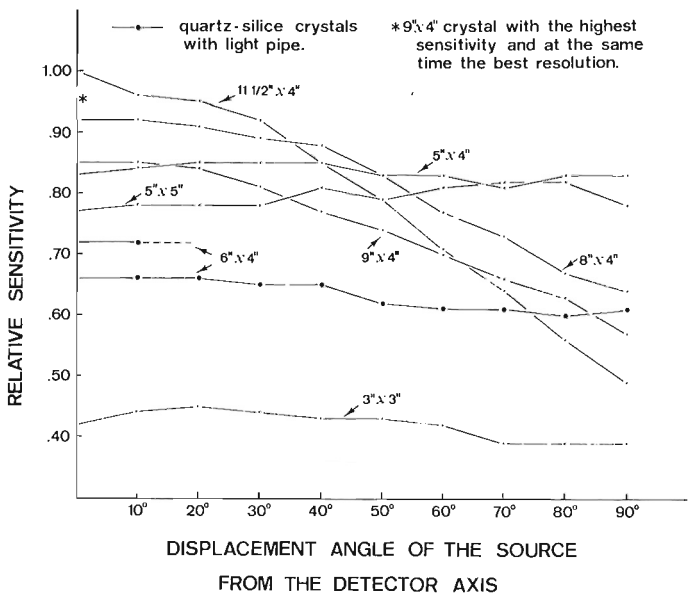

Figure 1. Variation of detector sensitivity with source position.

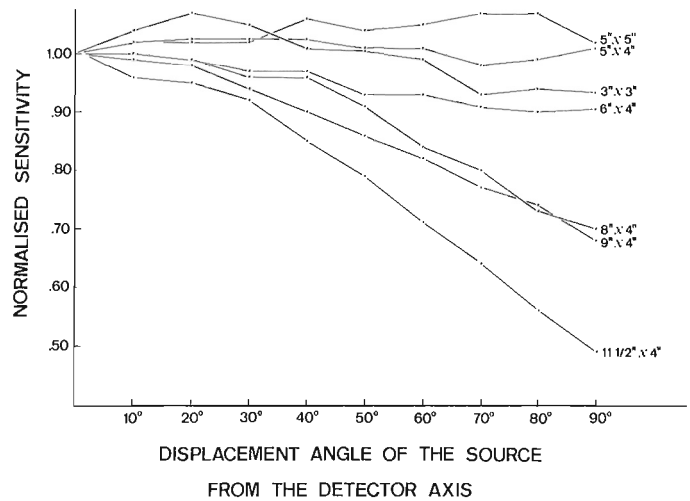

Figure 2. Variation of detector sensitivity with source position, normalized to the 11.5- x 4-inch crystal.

TABLE I

DETECTOR INFORMATION

CRYSTAL SIZE DIAMETER x HEIGHT (Inches)	VOLUME (Cubic Inches)	NUMBER OF PHOTOMULTIPLIER TUBES	COMMENTS
3 x 3	21.2	1	
5 x 4	78.5	1	
5 x 5	98.2	1	
6 x 4	113.1	1	Quartz-Silice crystal with light pipe
8 x 4	201.1	3	
9 x 4	254.5	4	No separate gain for photomultiplier tubes
11.5 x 4	415.5	7	

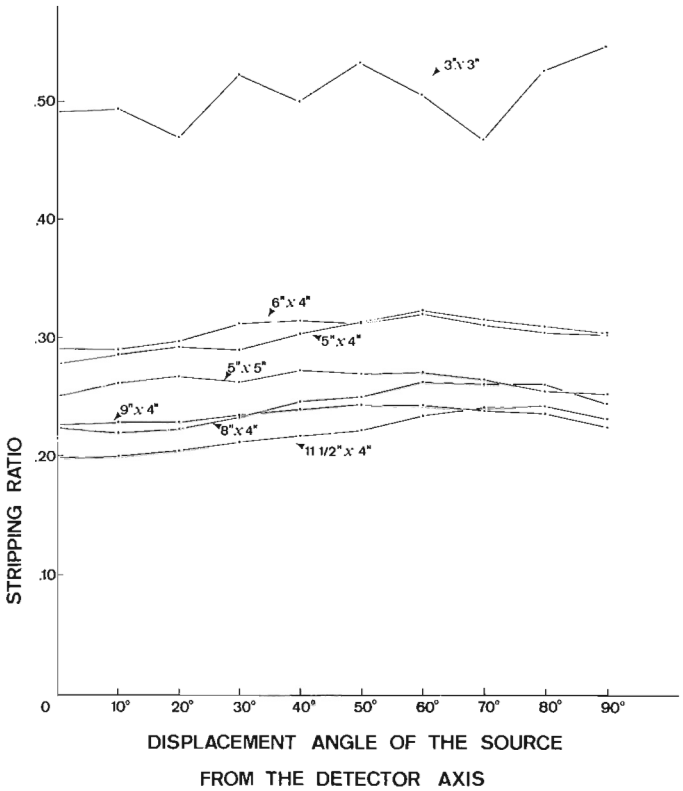

Figure 3. Point source stripping ratio variation with source position.

half-angle 60 degrees. This angle decreases to approximately 45 degrees at 500 feet. At 45 degrees it can be seen from Figure 1 that the 11.5- x 4-inch and 5- x 4-inch crystal have similar sensitivities. At the larger angle of 60 degrees, the 5- x 4-inch crystal is approximately 20 per cent more efficient due to self-shielding effects in the larger crystal. The results therefore suggest that at 500 feet, all 4-inch-thick crystals between 4 and 11.5 inches in diameter will have similar sensitivities in terms of counts per unit volume, but for surveys closer to the ground the smaller diameter crystal will be slightly more efficient.

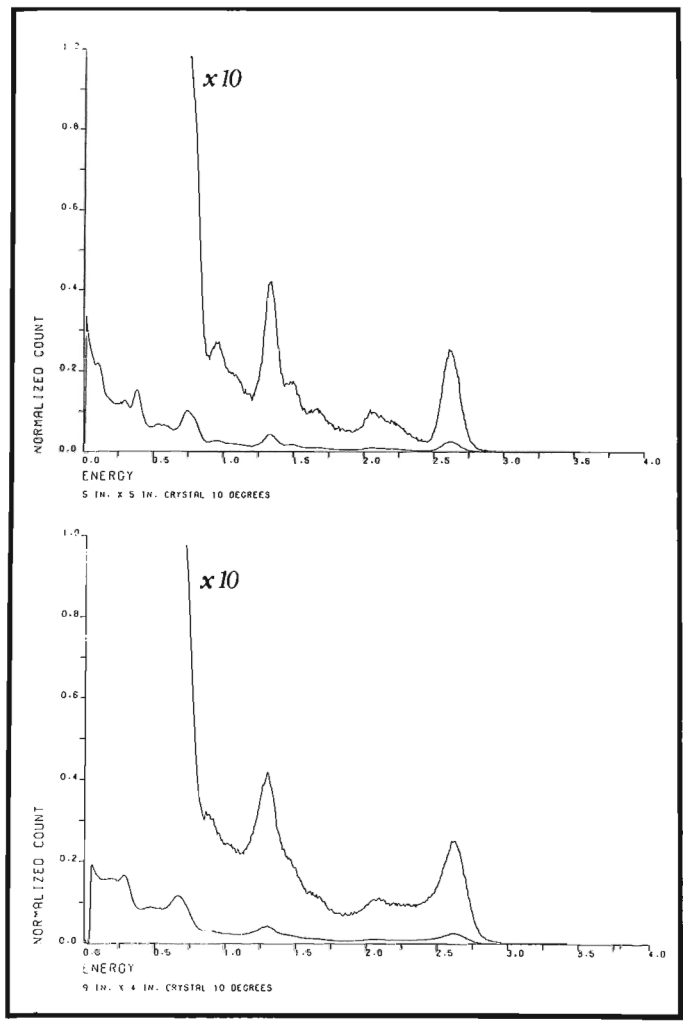

Figure 4. Comparison of the spectra from the 9- x 4-inch and 5- x 5-inch crystal.

The stripping ratios for all crystals show little variation with source position. It should be emphasized that these values are for point sources. For normal survey operation, the stripping ratio would be significantly increased due to scattering in the ground and in the air, as has been shown by Grasty (1973).

We are particularly grateful to Don MacFadyen and Harry Chance of Northway Survey Corporation, George Sander and Ralph Peters of Sander Geophysics; Terry Peacock and Grant Mervin of Geoterrex; and Chris Pomroy of the Radiation Protection Laboratories who kindly loaned their crystals. Thanks are also due to Barbara Elliott for all computer programming and to Scintrex Ltd. for supplying the thorium oxide source.

Reference

Grasty, R. L.
1973: The measurement of uranium by airborne gamma-ray spectrometry. Paper presented at the 43rd Annual SEG meeting, Mexico City, 1973; Abstract in Geophysics, v. 38, no. 6, p. 1202.

25. SEISMIC SURVEY OF THE WELLINGTON BAY-MOUTH BAR, PRINCE EDWARD COUNTY, ONTARIO

Project 680037

G. D. Hobson and E. Mirynech*
Resource Geophysics and Geochemistry Division

A hammer seismic refraction survey was conducted along the southwest side of the bay-mouth bar that separates Wellington Bay and Yeo Lake (West) immediately southeast of the village of Wellington in Prince Edward County, Ontario. The survey area is approximately 10 miles southwest of the town of Picton (Fig. 1). No roads traverse the bar, access being attained by boat out of Wellington.

A Huntec model FS-2 portable hammer seismograph was used to record all seismic data. A 16-pound sledge hammer struck against a steel plate on the ground provided seismic energy for detection by two detectors.

Twenty-one unreversed refraction profiles were run along the beach adjacent to Wellington Bay. Seismic stations were established generally 1, 320 feet apart. All stations are at the elevation of Lake Ontario, that is, 245 feet above sea level.

The bay-mouth bar varies in width from a few tens of feet at the Wellington or northern end to approximately one half a mile at Owen Point or the southerly end. The sand beach adjacent to Lake Ontario is 100 feet wide in some places. Seismic stations were set as far back from the water's edge as required to eliminate confusion or disturbance on the seismic record due to "wave-noise" but not at a higher elevation up on the sandy slopes so that any increased depth of sand might rapidly attenuate the seismic energy. Seismic stations could not be located near Yeo Lake because this lake has no distinct shoreline, there being only a gradual change from sand dunes to grassy marshes. The central part of the bay-mouth bar is covered by sand dunes 25 or 30 feet high that make seismic surveying difficult.

At both extremities of the sand bar, for example at Owen Point, flat-lying, rubbly weathered claystone outcrops, with interbeds up to 12 inches thick of resistant material. Liberty (1960) discussed the bedrock geology of the area, identifying exposures at both ends of the seismic profile as the upper member of the Cobourg Formation of Middle Ordovician age. Liberty also indicated that the bedrock of the islands in Yeo Lake is probably of the same age.

No description of the Pleistocene geology of the area has been published to date.

All observed seismic velocities are plotted against frequency of occurrence in the histogram of Figure 2.

Figure 1 includes a cross-section based upon observed velocities and depths computed from seismic data. Velocities less than 2, 900 feet per second probably are associated with the dry to moist surficial deposits of sand and gravel whereas velocities between 3, 000 and 4, 200 feet per second probably are associated with water-saturated sands and/or gravels. The remaining unconsolidated material, velocity range 4, 900 to 8, 900 feet per second, is probably a till although the lower velocities of 4, 900 to 5, 900 feet per second underlying locations 3 to 8 are more representative of clay beds. Since these velocities were observed on unreversed profiles the range of velocities is not excessive for a clay overburden. Clays probably overlie till, or bedrock directly, in the depressions. Clay is exposed around much of the Yeo Lake basin. These clays were deposited either during the Iroquois lake-stage before emergence of Prince Edward County or, more likely, after Lake Iroquois fell to levels lower than the higher parts of the county. Much of the clay under the bay-mouth bar may be masked or hidden from the "seismic eye" by the overlying sand. Till is also locally very thin and therefore not detectably by seismic methods.

The material designated as clay and till may be weathered limestone but this seems improbable because of its considerable thickness, a relevant point because it is believed that bedrock could only have been exposed locally for a very short time. It is unlikely that exposure of bedrock to subaerial weathering occurred immediately prior to the development of Lake Iroquois rather it was more probable after Lake Iroquois fell to the low Admiralty level. Water levels, even if they fell low enough, started to rise soon after the Admiralty lake-stage was initiated consequently there was little time for the intensive weathering that would be necessary to produce the thickness of decayed rock which might be inferred from the seismic data collected. Furthermore, it is believed that any decayed rock that was formed prior to the last advance of glacier ice through the Lake Ontario basin would have been removed during the final glaciation leaving only fresh rock surfaces. Till or clay deposited on them would preserve their freshness and would retard weathering. It is probable therefore that the "seismic eye" was looking at clay and till rather than decayed limestone.

The form of the bedrock surface shown in profile in Figure 1 is believed to be accurate except perhaps beneath stations 19, 20 and 21. At these stations bedrock may either underlie a thick sand layer or it may be considerably deeper if clay and till are both present. If clay and till occur here, as the data suggest, the till is probably thicker than the clay. Bedrock beneath these stations was not observed as a first cycle seismic arrival of energy but as a second cycle, thereby accounting for the low bedrock velocities. The near-surface materials at these stations highly attenuated the seismic energy from the hammer source suggesting that explosives should have been used as an energy source. Bedrock therefore may be deeper in this part of the section than shown.

*Present address: Brock University, St. Catharines, Ontario.

Figure 1.

Seismic cross section, bathymetry and location map, Wellington Bay area, Prince Edward County, Ontario.

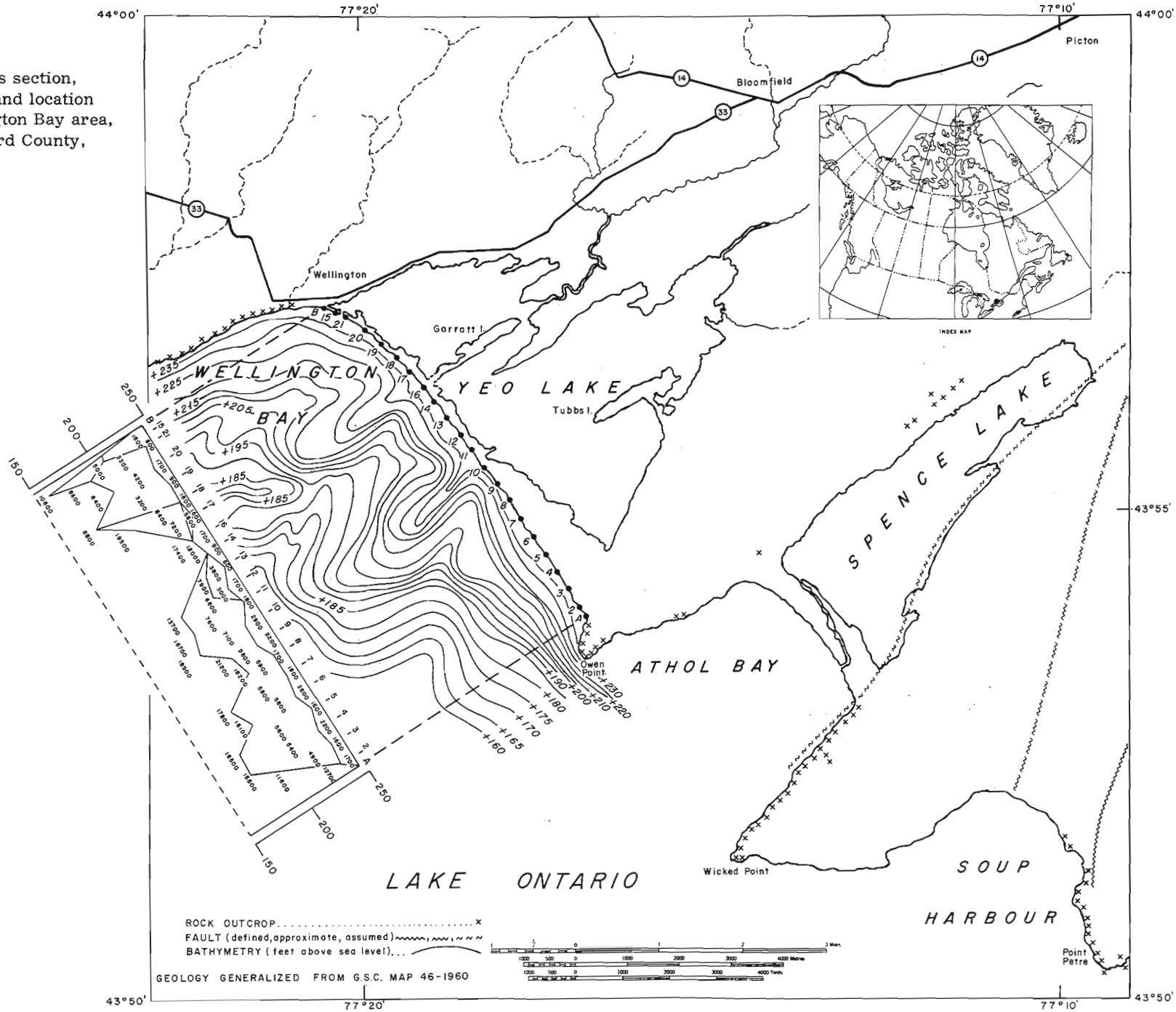

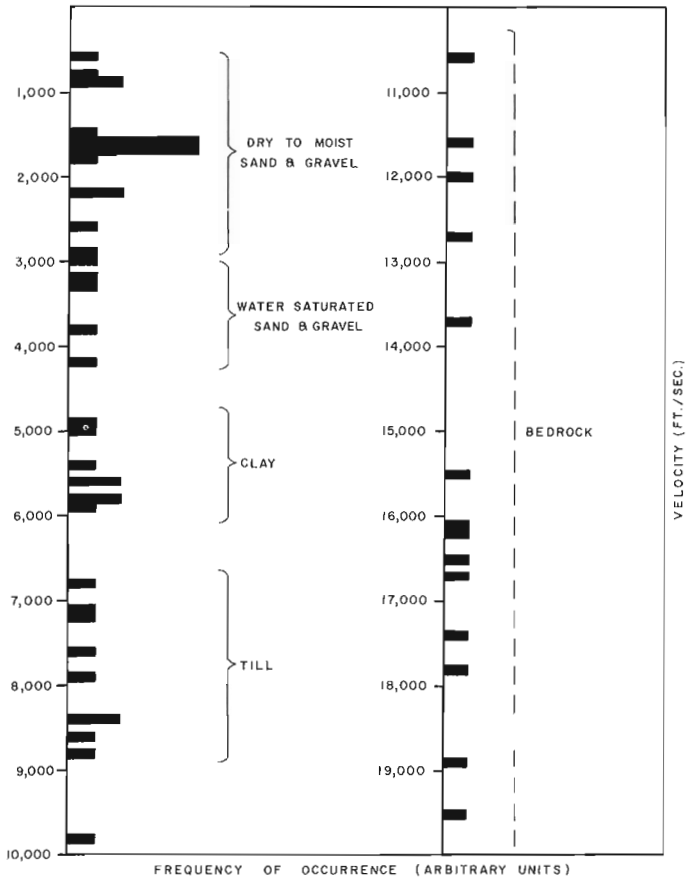

Figure 2. Histogram of observed velocities, Wellington Bay area, Prince Edward County, Ontario, with suggested geological interpretation of seismic velocities.

Some interesting deductions can be made from this seismic survey when it is combined with study of the topographic map, the seismic cross-section and the portion of the bathymetry of Wellington Bay shown in Figure 1. Submerged ridges and emergent topographic forms are definitely aligned in and adjacent to Yeo Lake. This alignment is directly associated with glaciation, particularly with the direction of ice flow. Garratt and Tubbs islands are both drumlins; and most of the linear peninsulas extending southwestwardly into Yeo Lake have a drumlin near their extremity. The drumlins consist of till and are generally quite long and narrow. They may or may not be associated with bedrock highs.

Two subsurface topographic highs that can be aligned with other topographic features are apparent, one centred under seismic stations 14 and 16, and the other under stations 8 and 9. Both of these submerged ridges may be bedrock features although the southerly one may be a drumlin astride a bedrock ridge. It is doubtful that there is any relationship between this submerged feature and Tubbs Island but the bedrock ridge may indeed extend in modified form to the vicinity of that island, or even beyond it to the Mainland. This explanation may help to account for the tiny promentory on the northern side of the bar near station 10 which extends northeastwardly into Yeo Lake, and the bathymetric ridge feature extending southwest from station 10 into Wellington Bay.

The second subsurface high feature, that identified beneath stations 16 and 14, is essentially bedrock. The seismic profile apparently does not detect the southerly end of the drumlin which forms Garratt Island perhaps because the till would be thin there. Also, there is almost certainly a submerged drumlin with an axis between stations 16 and 17. It would probably terminate at the + 220 contour level on top of flat limestone as is suggested by the increased spacing between the + 220 and + 215 contours. This submerged drumlin is separate from that exposed on Garratt Island. It is interesting to note that both seismically detected "high" features are displaced one station interval to the southeast from the bathymetric "highs". Notice also the asymmetry of the ridges; they are distinctly steeper on their southern than on their northern flanks.

If the "highs" representing bedrock ridges are interesting so too are the "lows" in respect to bedrock topography. Three fairly broad bedrock valleys are apparent each partly subdivided into lesser units by smaller bedrock ridges. The more ragged bedrock topography on the west is probably the result of increased glacial plucking along the margin of the bedrock upland situated between the Bay of Quinte and the main part of Lake Ontario.

Reference

Liberty, B. A.
1960: Belleville and Wellington map-areas, Ontario; Geol. Surv. Can., Paper 60-31.

THE AEROMAGNETIC DATA AUTOMATIC MAPPING (ADAM) SYSTEM

Project 680140

M. T. Holroyd
Resource Geophysics and Geochemistry Division

Introduction

The manual compilation process of aeromagnetic map making mainly entails the re-arrangement and combination of large analogue data sets. It is a well established process but includes many of those human capabilities difficult to simulate efficiently with the computer e.g. hand-eye co-ordination and immediate recognition of a deviant region within an otherwise orderly pattern. It is, however, basically a sequence of sort-merge operations interspersed with numerically definable processes and is therefore also related to well established computer practices.

The hoped for advantages of computer compilation systems are increased objectivity and accuracy and decreased time and cost. These advantages can be achieved even if the data is recorded in an analogue mode and is subsequently digitized, but are easier to achieve if the airborne data is digitally recorded.

About six years ago, the Geological Survey began to acquire digitally recorded high sensitivity aeromagnetic data; at first from contracted surveys, then later from their own airborne equipment.

The high sensitivity magnetometer is an instrument capable of absolute measurements to a precision of 10^{-3} gamma (10^{-8} gauss) over a range exceeding 10,000 gammas. Full exploitation of such a capability places great demands upon the recording and processing systems to be employed and it was obvious that conventional analogue recording and manual compilation techniques were inadequate. Consequently inflight digital recording was used and work began on computer software systems to automate the data compilation.

After testing alternative approaches, the nucleus of a system emerged and by early 1972 the first maps were produced by what would later be called the ADAM System.

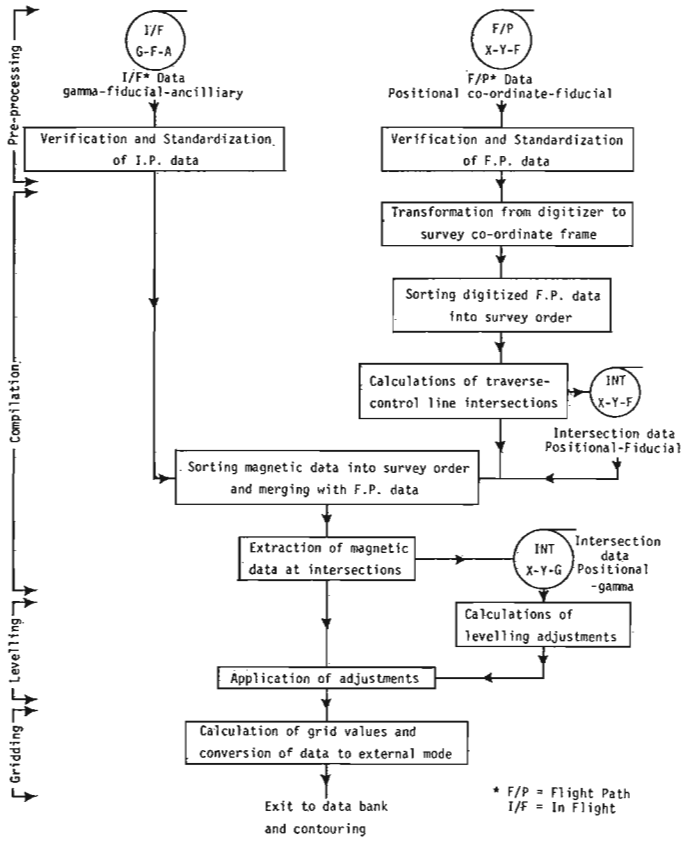

Figure 1. General flow chart of the ADAM System

Source Data Characteristics and Specifications

In addition to the magnetic field measurement, such data as time, radar and/or barometric altitude and along- and across-track Doppler are usually recorded in flight.

Due to various reasons including cost, reliability, accuracy and load capacity of the aircraft, a navigation system capable of providing digital geographical co-ordinates in flight is not employed in the Geological Survey system. Instead, the pilot attempts to fly straight lines as marked on a photo mosaic "Navigation strip" and a 35 mm camera takes a continuous sequence of vertically-downward photographs. The flight path is later recovered by plotting the position of these in-flight photographs on a photo mosaic map, and converted to digital form on a digitizer.

The size, shape and scale of the mosaic maps on which the F/P* was recovered, the orientation and scale of the digitization axes with respect to the geographical axes of the map, and the projection of the map (provided its projection equations are known), are all irrelevant to the system. (N.B. other considerations beyond the system requirements place practical limits on these factors.)

The mandatory conditions are that there must be some slight overlap between adjacent maps, or during the plotting of F/P points, some points must be plotted beyond the mosaic proper in the position they would occupy on an overlap.

*I/F = in-flight, F/P = flight path.

At least four control points of known latitude and longitude must be digitized from the map boundary and the same points must appear on and be digitized from all maps contiguous in the region of the point. The end points of a F/P line segment on a map must extend into the overlap region unless such an end point is a termination within the map or on a survey boundary.

For co-ordinate transformation, the only strict requirement is that at least two latitude-longitude points appear somewhere within a map of known projection; overlaps between adjacent maps are not required. The system requirements as specified in excess of this basic minimum are included to enable the system to detect and rectify errors of displacement or distortion present in the mosaic. If such errors are of greater magnitude than the limits of applicability of the correction algorithm, the system indicates the fact so that alternative means can be applied.

System Structure

The system is subdivided into separate program modules so as to provide greater flexibility of use and also to minimize core requirements without significantly increasing running time. Because of the massive data sets involved* and the nature of the processes applied data are passed through a process to temporary disc residence then re-passed through the next process etc. The natural hiatus between processes allows the use of interchangeable program modules to vary the system operations according to user requirements. The user's task simply involves attaching the permanent files containing the required programs, specifying their execution in the correct order and supplying the control parameter cards required by the programs used. Many programs are used in concatenate groups. Theoretically, for error free data, the whole system of approximately 10,000 FORTRAN statements could be concatenated into a single deck and run as one job.

Input/Output Options

The initial data sets and all subsequent intermediate data are output in binary mode by unformatted FORTRAN write statements. The choice of data code for the final output is a user option.

As all key stages in the system involve intermediate disc storage of the data, the user may:

i) allow the disc resident data to be a transient product which will be overwritten by a more advanced data set by assigning the same file name to the advanced data set.

ii) between the excution of consecutive program modules, insert commands to dump the disc data to tape.

iii) define a file so that the data are written directly to tape rather than disc.

iv) with fiendishly cunning control language commands, execute a job containing a stack of program modules in such a way that if any program aborts the immediately preceding data sets are dumped to tape thus allowing acceptable stages to be by-passed when re-starting the job after the trouble has been traced.

v) employ any combination of the above to achieve user requirements.

System Operations (See Fig. 1)

Pre-Processing F/P and I/F data

The coding and order of the source data sets are both tailored to the requirements of the acquisition environment. The first task of the system is to convert the data to a form more suitable to the processing environment, and to detect and remove data errors. This phase is named pre-processing and is regarded as external to the system proper as the program content is largely dependent on the in-flight recording and digitizer hardware and thus not generally applicable. The output from this phase is in the form of large buffers of binary data but with the general order of the data unchanged from the order of acquisition.

Compilation

Flight path data is digitized from a photo mosaic base map or planimetric map. Many such maps are usually required to cover a survey area and as the survey is not flown by map-sheet the F/P data is therefore acquired in a radically different order from the complementary I/F data.

The first stage of compilation is to transform the co-ordinates on each map in turn from their existing arbitrary units and reference frame to standard units and defined survey frame. During this process the digitized points of known latitude and longitude are used to detect the presence of distortions in the mosaic. Differences in scale between the X and Y axial directions and a change in X and/or Y scale across the map are assessed and magnitude of such distortions listed. X and Y scale factors are then calculated so as to eliminate or reduce distortion.

The second stage is to sort the line segments from map order to total survey order and merge the separate segments from adjacent maps into continuous lines. At this time the overlap of segments into adjacent maps is used to detect erronious shifts between sheets due to the mispositioning of latitude-longitude points and if possible to resolve the shifts.

The data are now in good order and all positional co-ordinates refer to the same reference frame. The third stage is to calculate all possible intersections between traverses and control lines and to establish a separate data set containing the positional co-ordinates and fiducials of the lines at the intersection points.

The fourth stage sees the re-entrance of the I/F data

---

* (The system is designed to deal with up to 500,000 line miles of data as a single throughput = (approx.) 50 million words of data.)

which is sorted into survey order and merged with the F/P data. During this stage the intersection data set is also briefly re-introduced and the magnetic data at the intersection added to it.

Compilation is now complete and all data exists in the desired order and form for Phase 3 of the system.

Levelling

The levelling process is similar to those used in gravity surveys and topographic mapping. Differences along measurement "legs" forming a closed loop have a non-zero sum. The problem is to adjust each difference so as to distribute the error evenly and bring about a zero sum. Many solution methods exist. The one chosen for the ADAM system depends on flying double, overlapping control lines but all require an intersection data set of some form and alternative program modules with different solution methods could be substituted at this point. Let it suffice to say that from the levelling program emerges a set of adjustments to be applied to the data at control line traverse intersection points.

The adjustment to be applied to a data value not falling on an intersection must be interpolated from the two intersections which bracket it. No extrapolation is permitted. A choice of interpolation functions is allowed, once again by the substitution of program modules.

Gridding

Many approaches exist to the interpolation of a regular grid over irregularly spaced data. For the ADAM system one well-suited to the nature of aeromagnetic data was chosen. A set of closely spaced parallel lines are run approximately perpendicularly to the traverse direction. The values at the points where these TDS (traverse data section) intersect the traverses, are extracted and values interpolated along the TDS by a cubic spline method. The grid lattice major axes are parallel to the survey axes, but as the traverse direction may not be parallel to one or other of the survey axes, and the TDS should be close to perpendicular to the traverses, the TDS need not be along the major axes of the grid. Eight different directions are permitted for the TDS with respect to the survey X axis. They are (for those familiar with crystalographic notation) 1:0, 2:1, 1:1, 1:2, 0:1, -1:2, -1:1, -2:1. Thus a gridding direction can be chosen to lie within approximately 12 degrees from the perpendicular to the traverse. The grid size was chosen so that contours produced by short linear interpolations across the cells would be satisfactorily smooth but still economic to produce. A grid cell size of approximately 0.1" is a fair compromise between these two opposing objectives. An exact figure of 10.16 grid cells/inch (4 grid cells/cm) was chosen to fit in with metric publication scales. At the usual scale of 1:25,000 this results in a ground distance of 62.5 metres/cell. Hence super grids can be extracted at 125, 250, 500M, 1 km etc. and contoured still at 4/cm to produce maps at scales of 1:50,000, 1:1:000,000, etc.

Conversion to External Mode

Due to the redundancy of the 60 bit CDC cm word compared to the precision required in many processing phases, "packing" routines were designed into the system. In various stages of the work 2, 3 and 4 binary data values may be packed into one cm word. This is a user option, obtainable by program module substitution. The advantage of word packing is a significant reduction in central core memory requirement at the expense of some increase in central processor time. Such packed words mean little, however, if on transfer from the system the recipient software is unaware of the coding. Hence program modules exist to decode such data into more common form.

Contouring

The existence of many excellent contouring programs outside the Computer Science Centre and (at the time of development of the system) the absence of a flat bed plotter, led to the decision to "go outside" for final contouring of maps for publication. The attached example (produced by Survair Ltd. of Ottawa) is a special map originally drawn at a scale of 1:25,000. The maps so far published (all contoured by Dataplotting Services of Toronto) were contoured at 5 gamma intervals to prevent overcrowding in the many high gradient areas. To show the fine detail in a low gradient area of the Abitibi survey, the area was contoured at both 1 and 2 gamma intervals. Figure 2 is the 2 gamma version.

Data Bank

In my opinion, the high resolution and precision of the original data and the objectivity and accuracy of the processing system have relegated the contour map to the status of a by-product and index, rather than the end product, of digitally recorded and processed high resolution aeromagnetic survey. For more information than can be displayed on a contour map exists in the digital data bank. Furthermore, digital data allow re-processing into any of the various "derived" maps that are of specific use to the interpreter of aeromagnetic data. A system is being developed whereby a potential user may acquire the digital data of any surveyed region in a form suited to his processing software, or if so required a user can obtain "one off" specially processed maps of a region of interest. Such special processes include bank, high and low pass filtering to separate the magnetic effects of different depth horizons, downward continuation or vertical derivative maps to emphasize low amplitude features, and special contour effects or grey-shade mapping to delineate texture.

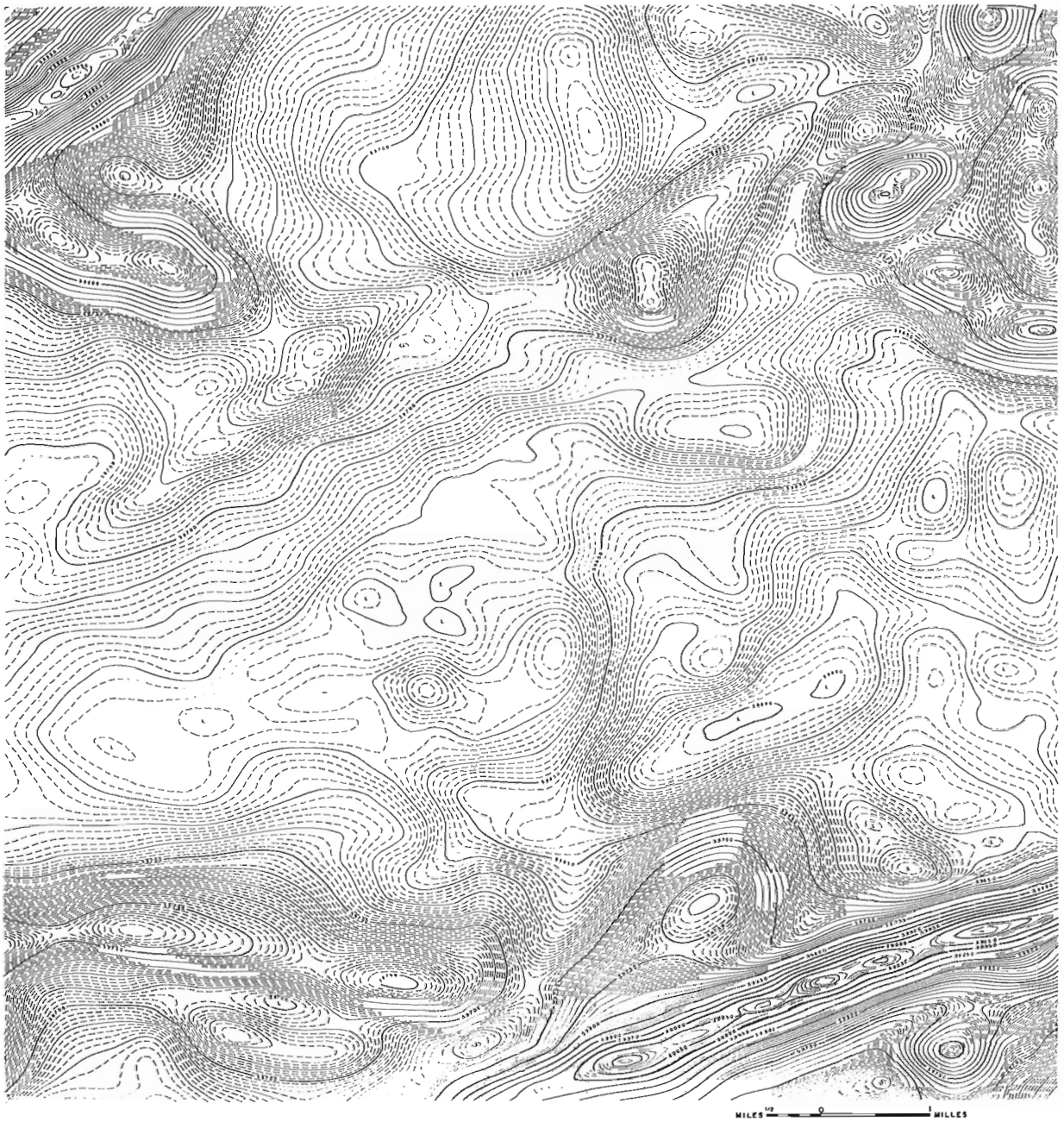

Figure 2. Contour map of high resolution aeromagnetic data compiled by the ADAM System. Range = 530 gamma, contour interval = 2 gamma.

Conclusion

The results of the application of the ADAM system have demonstrated that the potential advantages offered by such an automatic compilation system are attainable. Distinct increases in objectivities and accuracy have emerged along with definite decreases in time and cost. Caution is, however, called for. Once manually prepared data are exposed to the pedantic attention of the computer, hitherto undetected or disregarded flaws become critically apparent. The standards of quality of base mosaics for flight path recovery have regularly been found inadequate. The high potential of high resolution aeromagnetic data should not be degraded by poor quality ancilliary data. The most fitting conclusion is to hope for the advent of an in-flight, digitally recording navigation system whose cost, reliability, weight and precision are commensurate with the same factors within the aeromagnetic measuring-recording system.

27. SEISMIC UP-HOLE WAVEFRONT EXPERIMENTS IN PERMAFROST, SCHEFFERVILLE, QUEBEC

Project 730006

J.A. Hunter
Resource Geophysics and Geochemistry Division

Experimental up-hole wavefront targeting techniques were tested in permafrost rocks at the Iron Ore Company of Canada properties at Schefferville, Quebec, during the week of October 15, 1973. Two four-inch diameter boreholes, approximately 40 metres deep made available by the company for the test, were located in the Fleming 3 pit, in continuous permafrost (as determined by temperature cables installed in adjacent holes by I.O.C.). The objectives of the test were to determine the seismic velocity section circumjacent to the boreholes and to relate these velocities with existing geology and temperature information.

The up-hole wavefront method has been described by Meissner (1961) and has been tested in frozen unconsolidated materials by Wyder et al. (1972). By measuring the travel times of a first arrival compressional wave at geophones situated in a linear array away from the borehole (Fig. 1) for small explosives detonated at known depths in this borehole, a contoured wavefront section can be obtained which under certain assumptions, describes the velocity structure beneath the geophone array. The basic assumption is: all velocity structure beneath the geophone array must be either vertical or horizontal; any departure from these conditions may result in erroneous displacement of interpretive boundaries. Lines A and B in Figure 1 show seismic ray paths for two cases where velocity discontinuities exist along the rays. Ray paths C and D identical in travel time to rays A and B can be constructed from an imaginary shot on surface at the borehole to an imaginary detector at depth below the geophone array position. If travel times are plotted at the depths of these "detectors", the contained wavefront section can be obtained as though for a surface shot. The reader is referred to Meissner (1961) for excellent examples of various types of velocity structure which can be interpreted from such sections.

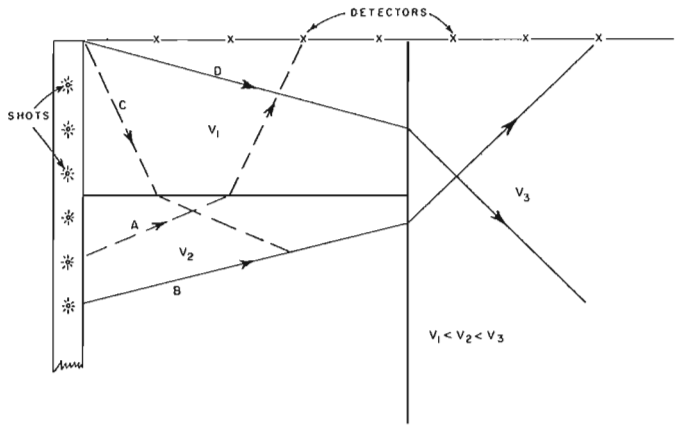

Figure 1. Shots and detector arrays for up-hole wavefront mapping techniques.

Since the technique employs explosives and, in most cases, destroys the borehole, an initial attempt was made on the I.O.C. property to utilize a downhole geophone and a multiple source array on surface. A 16-pound sledge hammer striking an 8-inch x 8-inch x 1-inch steel plate was used as the seismic source. A 20-foot source spacing was used out from the borehole. A Mark Products L-21 downhole geophone was used. Noise levels on the downhole geophone were high. As a result the interpretation error on the records is high, and in some cases no usable data were obtained. The source of the noise on the downhole geophone could not readily be explained; in some instances, however, increased noise levels could be correlated with increased mining activity at the pit face, 300 metres away. Since only one downhole geophone was used, the method was much slower than the conventional reverse method using an array on surface. The wavefront section obtained from hole 424 is shown in Figure 2 in comparison with the borehole geology. Three major low velocities zones can be seen; the first is on surface and extends to a depth of approximately 10 feet; the second zone between 70 feet and 90 feet, and a third zone begins at approximately 100 feet in depth and whose lower limit is not defined. It must be stressed here again that any zones that are not continuous horizontally or vertically across the section cannot accurately be defined. And at best their occurrence is only indicated by the wavefront plot.

Hole 424 was reshot using the conventional geophone array on surface with explosive charges in the hole. As well, hole 426, two hundred feet west of 424, was surveyed. Although both holes had been initially open to a depth of 130 feet, hole 424 became blocked at 62 feet after the first detonation at 130 feet, and hole 426 was blocked at 70 feet. As a result, the wavefront sections from the data are somewhat incomplete and are confined to definition of near-surface structure only.

The up-hole wavefront section for 426 shows a thin, low velocity upper layer on surface extending to a depth of 10 to 15 feet, an intermediate high velocity layer between 15 feet and 60 feet, and a low velocity layer beneath this, whose lower boundary is beyond the detection range. To the side of the borehole, a small low velocity zone has been interpreted to lie between the depth of 15 feet and 35 feet, out to a distance of 50 feet from the borehole. It should be pointed out here that as the borehole-geophone distance increased, the sensitivity of the method to detect minor structure is decreased.

The wavefront diagram for hole 424 shows three layers, a surface low velocity layer 10 feet in thickness, an intermediate velocity zone 10 feet to 40 feet in depth, and a high velocity zone whose lower boundary is not determined. A thin low velocity zone has been outlined between 25 feet and 35 feet in depth extending laterally

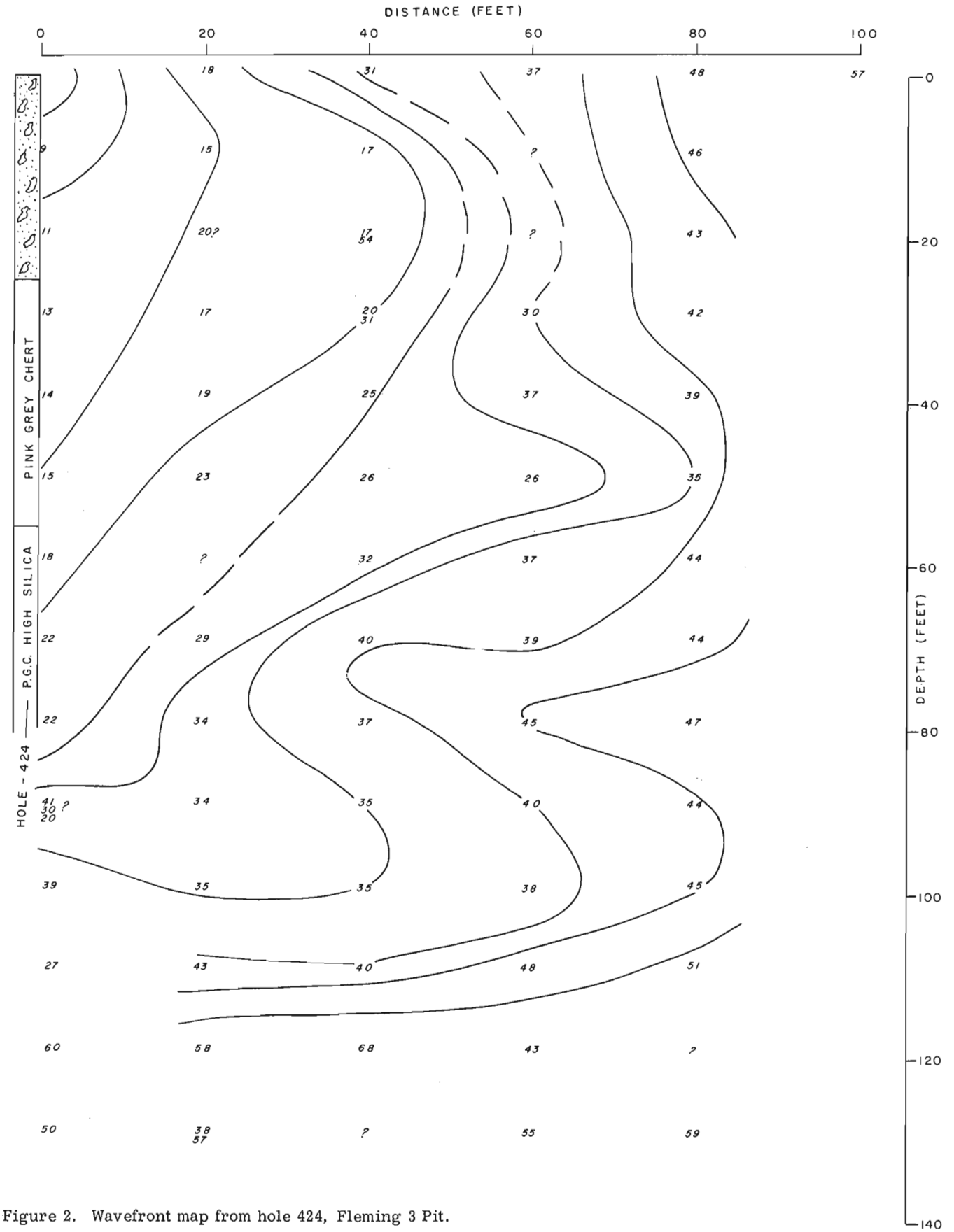

Figure 2. Wavefront map from hole 424, Fleming 3 Pit.

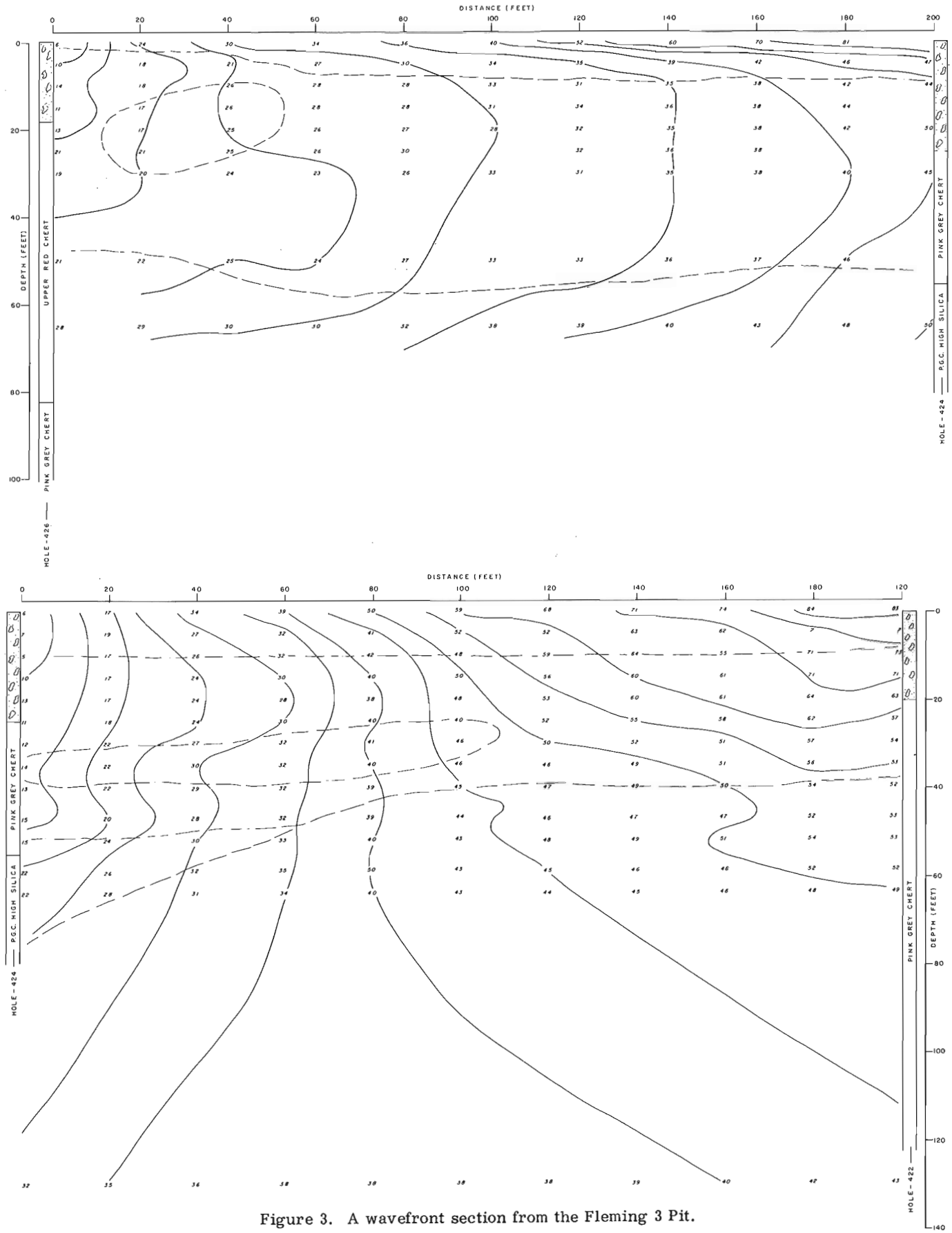

Figure 3. A wavefront section from the Fleming 3 Pit.

to a distance of 100 feet from the borehole. An apparent discrepancy between velocities observed in hole 426 and hole 424 can be seen in the vicinity of hole 424. The apparent velocities observed under geophones at 160 feet, 180 feet and 200 feet from hole 426 apparently do not agree with velocities observed under the geophones at 0 feet and 20 feet from hole 424. That is, wavefront lines appear to be more closely spaced from the 424 up-hole shooting. This is partly a result of the curvature of the wavefronts near the hypothetical surface shot. If one looks at wavefront normals between the 10 and 15 millisecond wavefronts on borehole 424, the high velocity intermediate layer is still in evidence. Farther out from the borehole (under geophones at 6,200 feet) the velocity of the intermediate layer decreases substantially. At larger distances from the borehole, the wavefronts derived from the travel times are averaged over the entire section with little angular difference in travel paths between the upper and lower shots, hence velocities shown beneath far geophone locations are only approximate (i. e. at a distance of 160-180 feet from hole 426).

Little correlation exists between wavefront anomalies and the geology as determined from the boreholes. There appears to be no contrast between overburden and rock. From hole 424 there is some correlation with the high silica zone in the pink grey chert with the low velocity region in both the sections produced by the downhole geophone (Fig. 2) and that produced by the conventional method (Fig. 3).

It is suggested that the velocity anomalies (if real) are a result of temperature variations in the rock around 0^{o}C. Velocity change by freezing of iron-formation is quite large (Garg, 1973). A thermistor cable installed by I.O.C. in hole 422, showed the top of permafrost to be at approximately 40 feet. This corresponds well with the boundary between intermediate and high velocities mapped by the wavefront method.

Since not all pore water is frozen at 0^{o}C, and since seismic velocities increase with the amount of pore water frozen, low velocity zones mapped within permafrost reflect either warm areas within permafrost or unfrozen talik zones. In either case from Garg (1973) it is suggested that the elastic constants of the ore are substantially different in the low velocity zones, a factor which may be of importance in planning the mining procedures for the pit.

References

Garg, O.P.
1973: In situ physicomechanical properties of permafrost using geophysical techniques; In Proc. IInd Int. Conference on Permafrost, North American Contribution; Yakutsk, USSR.

Meissner, R.
1961: Wavefront diagrams from up-hole shooting; Geophys. Prospecting, v. 9, p. 533-543.

Wyder, J.A., Hunter, J.M., and V. Rampton
1972: Geophysical investigations of surficial deposits at Tuktoyaktuk, N.W.T.; Geol. Surv. Can., Open File 127.

Project 730006

J.A. Hunter
Resource Geophysics and Geochemistry Division

A shallow seismic program was undertaken to detect the presence of sub-seabottom permafrost in the presence of a thick ice cover.

An ice layer approximately 2 metres thick, with a seismic velocity of 3,200 m/sec. should act as a masking layer in seismic surveying for the measurement of the thickness of unfrozen seabottom materials and the detection of sub-seabottom permafrost velocities. In designing the experiment it was thought that:

1) the refracted wave in the ice would attenuate rapidly since the ice is a thin layer, hence the refracted compressional wave from the permafrost layer would be the prominent early event at greater distances;

2) the refracted compressional wave from the top of permafrost may be identified as a prominent later event;

3) the reflected compressional wave from the top of permafrost may be identified as a prominent later event on the records.

Sites were occupied on Kugamllit Bay where the previous marine refraction work done by Hunter (1973), and Hunter and Hobson (1974) showed that permafrost with velocities in the range of 3,000 m/sec. was present at depth less than 50 metres from the sea surface in water depths of less than ten feet. Figure 1 shows an RS-4 12-channel seismogram obtained with a 400-metre cable spread with take outs at 30-metre intervals. Contrary to expectations, the refracted wave through the ice did not attenuate as rapidly as expected. Figure 2 shows a plot of amplitude versus distance for the ice arrival. Attenuation of arrivals at geophones beyond 200 metres is much less than that occurring at the near geophones.

Low amplitude events following the ice "break" on the seismogram probably result from multiple reflected events (both compressional and shear) within the ice layer. These events mask possible refracted compressional events from the permafrost layer. No prominent refracted events having velocities of permafrost were identified as later events on the records.

An attempt to observe reflected events from the top of permafrost was made using a short 100-metre cable with geophone take outs every 7.5 metres. Figure 3 shows an RS-4 reflection records. Large amplitude low frequency events are the prominent major later arrivals which have been interpreted to be surface wave events through the ice layer. Only one high frequency event, superimposed on the low frequency

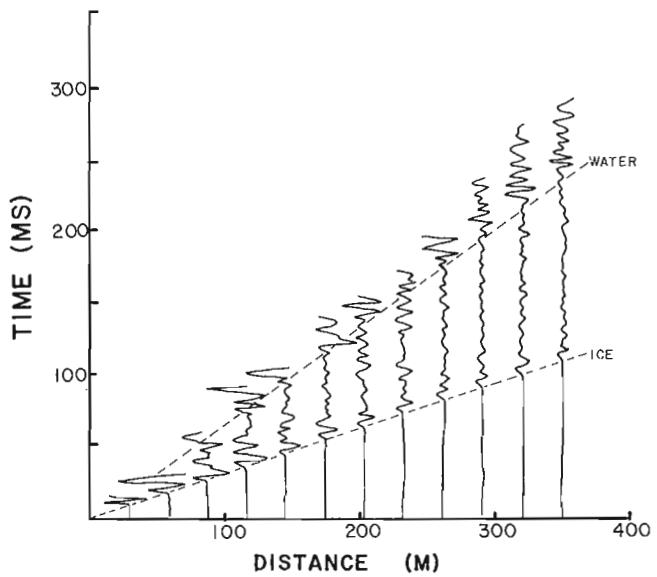

Figure 1. Twelve-channel refraction seismogram shot on the ice in Kugamallit Bay.

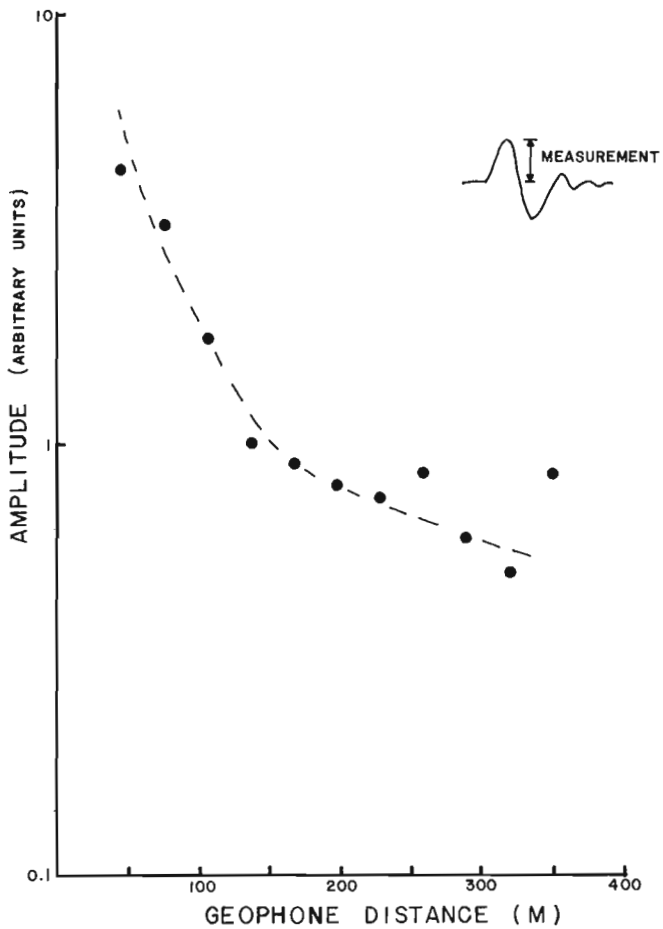

Figure 2. Amplitude attenuation of the first arrival through ice.

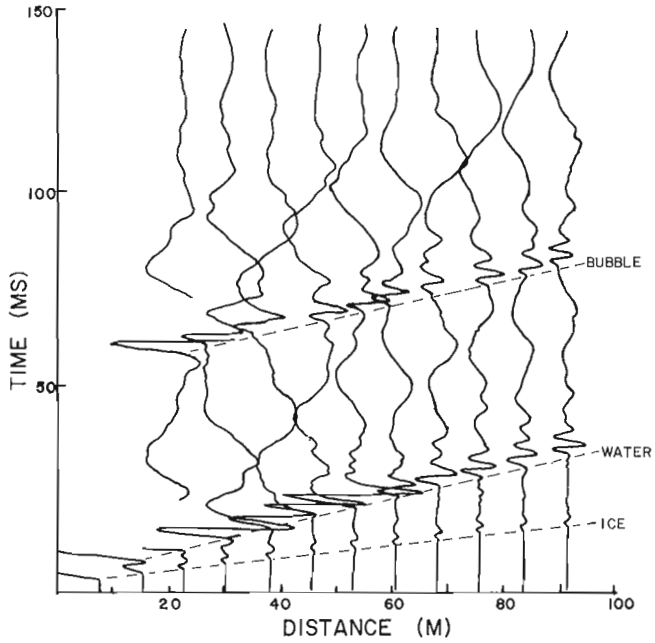

Figure 3. An interpretation of later events on a typical refraction record shot on ice.

surface wave events, can be identified with ease. This event has a centre frequency close to that of the water wave although the pulse shape differs in that it probably has been phase shifted. By reshooting with various charge sizes, it was found that this event shifted in time. The arrival time varied directly with the charge size. As a result the event has been interpreted to be a bubble pulse. No large amplitude reflected events could be identified on the record which were clearly reflections from the top of permafrost. Wide angle reflections from the top of permafrost have been observed on marine refraction records shot in the area during the summer operations. It can be concluded that for records shot on ice, reflected events are being overridden by large amplitude surface wave events within the ice cover. Since the RS-4 seismograph contains no filter setting it was not possible to improve the record quality by band-pass filtering.

References

Hunter, J.A.
1973: Shallow marine refraction surveying in the Mackenzie Delta and Beaufort Sea; in Report of Activities, November 1972 to March 1973, Geol. Surv. Can., Paper 73-1, pt. B, p. 59-66.

Hunter, J.A. and G.D. Hobson
1974: A refraction method to detect sub-seabottom permafrost; Proc. Symposium on Beaufort Sea Coastal and Shelf Research, San Francisco, Jan. 1974; Arctic Institute of North America.

29. SEISMIC VELOCITY MEASUREMENTS IN PERMAFROST, FOX TUNNEL, FAIRBANKS, ALASKA

Project 730006

J.A. Hunter
Resource Geophysics and Geochemistry Division

Introduction

During a recent visit to the U.S. Army Cold Regions Research and Engineering Laboratories facilities at Fairbanks, Alaska, in April 1973, seismic measurements were carried out in the Fox Tunnel by Geological Survey of Canada personnel.

The Fox Tunnel, located approximately 12 kilometres north of Fairbanks in the Glen Creek Valley, was excavated during the winters of 1963-1966 in perennially frozen silts and gravels of Pleistocene age and metamorphic rocks of Precambrian age. The tunnel, measuring 120 m in length, 6 m in width and approximately 2-3 m high, provides unique exposures of ground ice.

In general, the geology exposed in the tunnel consists of a basal gravel (approximately 5 m thick) overlying schistose bedrock. The gravel in other parts of the valley is gold-bearing and has been extensively mined. A thick sequence of silts forms the uppermost unit.

Ice has been observed as intergranular cementing material in the gravel. In the silts, however, ice is observed both as lenses produced by ice-segmentation (referred to as "hair-ice" - several sizes of lenses were observed) and as massive ice wedges, often as wide as 2 m and continuous across the tunnel walls and ceiling. The volume percentage of ice in the silts was relatively high with variations between 40 and 80 per cent.

TABLE I

SITE	SEDIMENT TYPE	COMPRESSIONAL VELOCITY		SEISMIC RECORD QUALITY	ICE CONTENT BY VOLUME	
		Measurement	Average		Measurement	Average
1	Silt	3.20 km/sec 3.05 3.13 3.29 3.02	3.14 km/sec	Good	68% 76	72%
2	Ice wedge	3.45 2.97 2.53 3.05	3.00	Fair	100	100
3	Ice wedge (clear ice)	3.40 2.45 3.81	3.22	Fair	100	100
4	Silt	2.98 2.67	2.83	Fair	57 68	62.5
5	Silt	3.20 3.13	3.17	Good	71 72	71.5
6	Silt	2.96 3.05	3.01	Good	59	59
7	Silt	3.02	3.02	Fair	63	63
	Gravel	--	--	No record	8.9 - 10.0	
Bedrock	Schist	3.20	3.20	Poor	6.5 - 19.9	

Note: Temperature of tunnel walls at time of experiment -4.2°C.

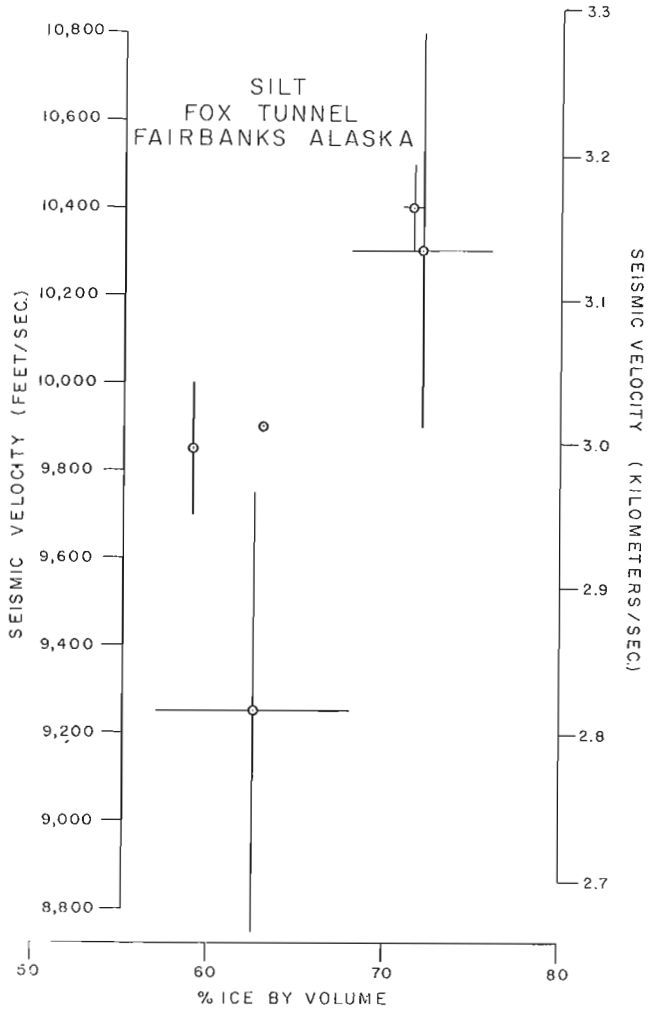

Figure 1. Plot of seismic compressional velocity vs. per cent ice in frozen silt, Fox Tunnel, Fairbanks.

Seismic Measurements

Several sites along the tunnel walls were selected for short range seismic measurements where previous sample borings for ice contents had been taken by CRREL personnel (Delaney et al., 1972). It was hoped that a correlation could be found between ice content and seismic velocities within the silt unit; however, it was noted both visually and from the samples, that large variations in ice content occurs on a small scale.

Measurements of first arrival times of compressional waves at each site were made with a Micro-Seismic Timer built by Dynametrics Ltd. A hammer-type seismic impulse source was used on traverses at 100-m intervals out to 1 metre from the detector. For such close source-detector distances the dominant frequency of the recorded pulse is in the range of 10 kilohertz. A summary of the seismic velocities obtained as well as the sample ice contents is given in Table I.

A qualitative estimate of the seismic records was assigned to each site, based on the relative scatter of arrival time measurements at each hammer location along the traverses. Propagation of seismic waves in ice and ice-saturated silts was relatively good; however, poor records were obtained on frozen ground and bedrock. No reliable estimate of velocity could be made for the gravel sites selected.

A plot of seismic velocity of frozen silt versus ice content by volume is shown in Figure 1. Error bars assigned to the plot show maximum deviations from the arithmetic mean of each variable. Despite the limited number of measurements and the large statistical error associated with them, a trend towards higher seismic velocities with increasing ice content in silts is evident.

Reference

Delaney, A., Hoekstra, P., and Sellmann, P. 1972: Resistivity measurements near Fairbanks, Alaska; U.S. Army, C.R.R.L. internal report.

30. MAPPING THE OCCURRENCE OF SUB-SEABOTTOM PERMAFROST IN THE BEAUFORT SEA BY SHALLOW REFRACTION TECHNIQUES

Project 730006

J.A. Hunter, R.L. Good and G.D. Hobson
Resource Geophysics and Geochemistry Division

Introduction

In recent years, the existence of permafrost underlying part of the Arctic Continental Shelf has been confirmed from offshore drilling operations in the Mackenzie Delta-Tuk Peninsula area by the Arctic Petroleum Operators Association (APOA).

In the summer of 1970, the Geological Survey of Canada cored into freshwater ice lenses about 20 miles north of Cape Bathurst. There is no doubt, therefore, that permafrost is present in the southern Beaufort Sea.

McDonald et al. (1973) discuss shot hole data from a seismic program along the northwest coast of the Tuktoyaktuk Peninsula which give lithologic information and the elevation of the top of the permafrost in the nearshore zone. Bathymetry appears to be a primary control on the depth to the permafrost. Where the sea is frozen to the bottom in winter, permafrost almost always lies within 5 metres of the sea bed. The presence of even a small amount of water beneath the sea ice can have a considerable effect on the permafrost; less than a metre of water beneath the ice can drive the top of the permafrost to a depth of 10 metres.

Mackay et al. (1972) presented evidence to indicate that permafrost, which was originally formed during the Pleistocene, is preserved in frozen sediments along the Arctic Coastal Plain of northwestern Canada. The Pleistocene sediments are now frozen to a considerable depth as permafrost probably exceeds a thickness of 450 metres in some localities. Relic permafrost arising from coastal recession should be common and would be covered by reworked sediments.

Seismic Velocities within Frozen Unconsolidated Material

If the temperature of unconsolidated materials is below the freezing point of water, the difference in seismic velocity from that of the unfrozen state can be fairly abrupt. For water-saturated coarse-grained materials, the change in velocity at the freezing point of water is almost a step discontinuity from approximately 1.48 km/sec to 4 km/sec. For marginally frozen clay at -1°C, the velocity change is relatively small from 1.48 km/sec to approximately 2 km/sec.

In the Mackenzie Delta and Beaufort Sea areas the majority of the sediments offshore are thought to be coarse grained. Hence the velocity contrast between the frozen and the unfrozen state should be large. In some places there is a thin veneer of marine clays, Shearer (1973).

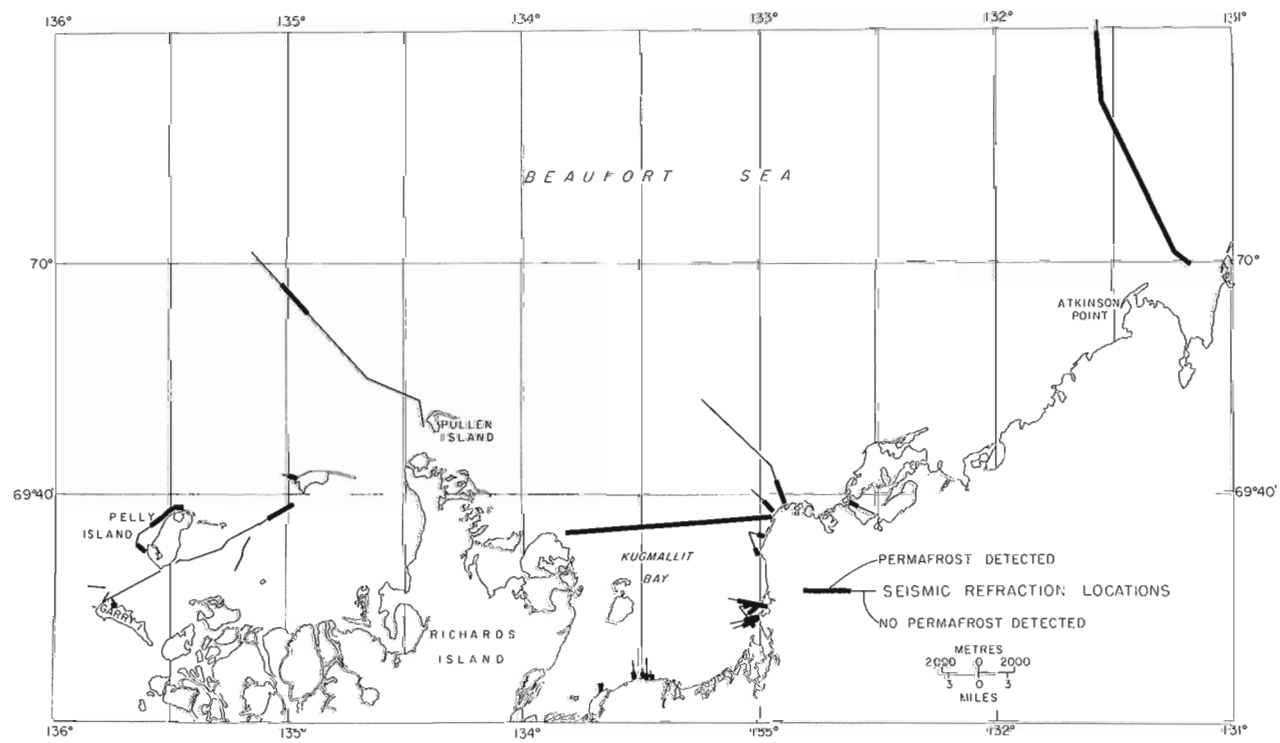

Figure 1. Location of seismic refraction profiles for the 1972 and 1973 field seasons.

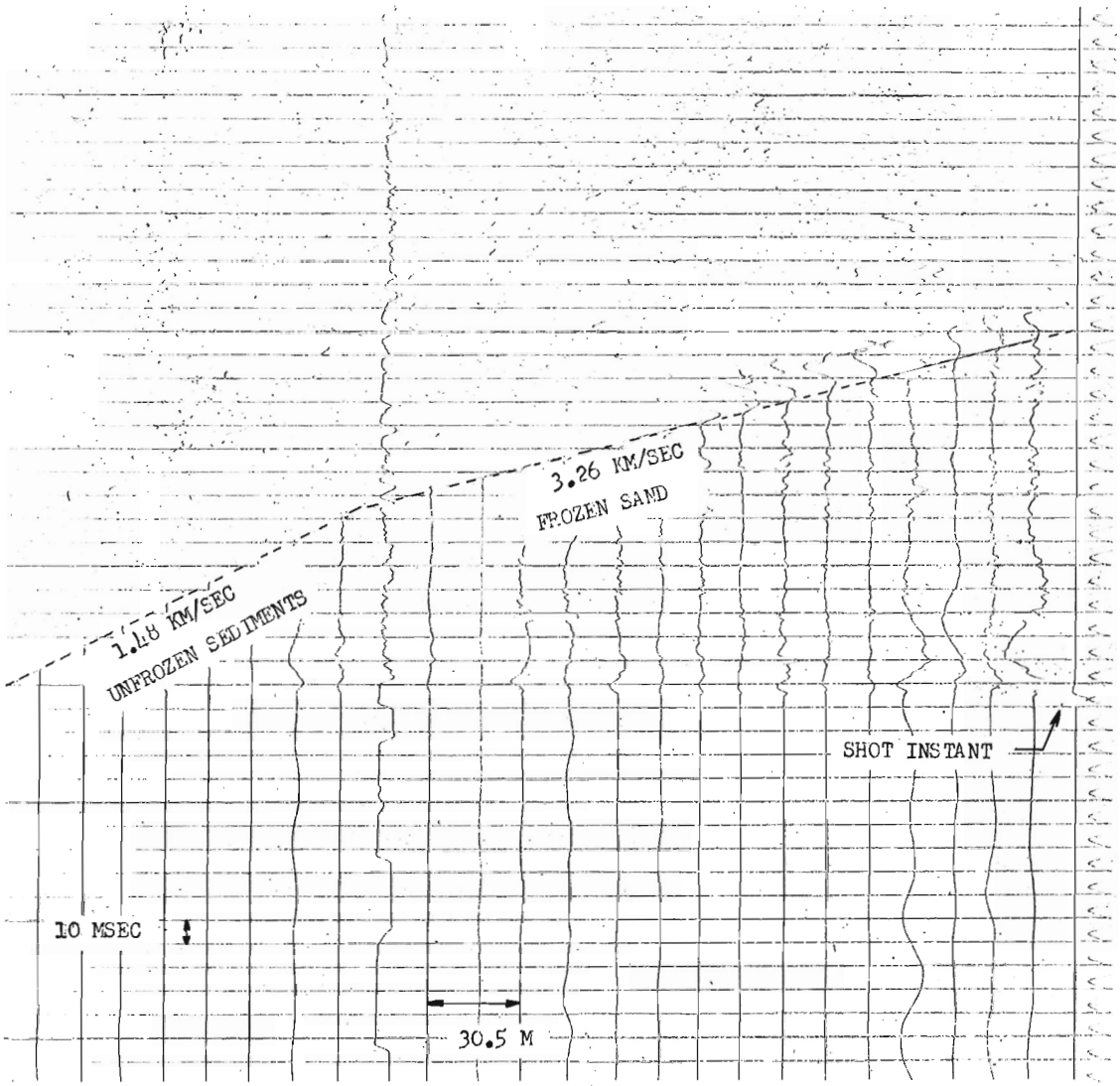

Figure 2. Typical marine refraction record in permafrost.

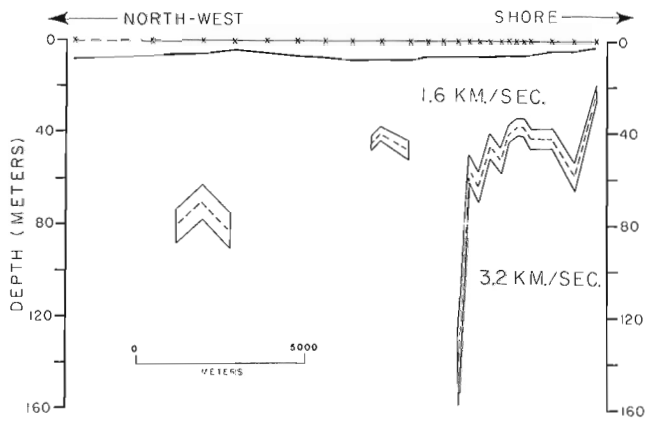

Figure 3. Seismic refraction section northwest from Toker Point.

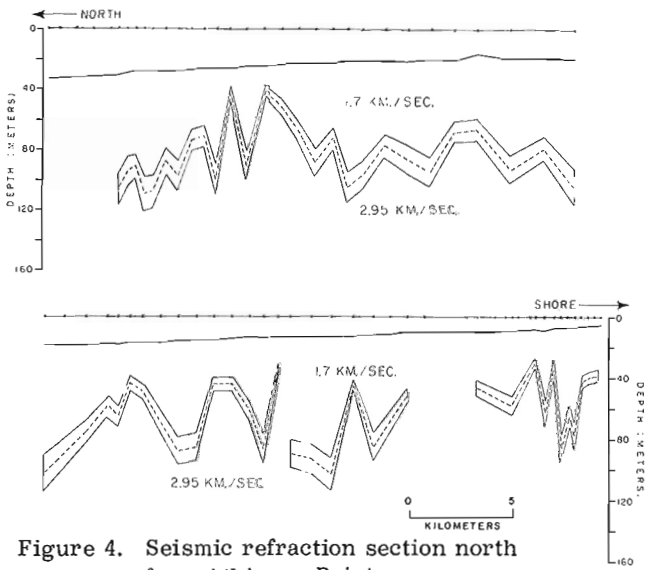

Figure 4. Seismic refraction section north from Atkinson Point.

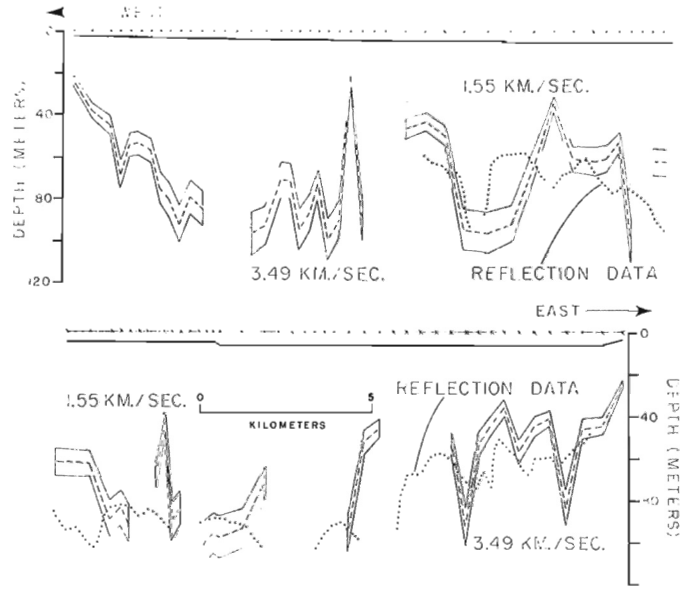

Figure 5. Seismic refraction and reflection sections across Kugmallit Bay.

Location of Seismic Profiles

Figure 1 shows the locations of the seismic lines surveyed in the field seasons of 1972 and 1973. The surveys were concentrated in the Mackenzie Bay area, north of Pullen Island, in Kugmallit Bay, north of Toker Point and as far east as Atkinson Point. This shot point location map also serves to show the areas of interpreted permafrost and no permafrost.

Field Equipment and Techniques

It is assumed that the reader is either conversant with the seismic refraction method or can familiarize himself through such commonly available textbooks as Dobrin (1970).

A 17-metre (55 feet) long, 2-metre draft, diesel-powered, converted fishing vessel, the North Star of Hershel, acted as both instrument and shooting ship. The vessel was equipped with radar, Doppler distance and speed log, gyrocompass, depth sounder, ship-to-shore radio, diesel generator (110 Volts AC). To this support equipment was added a Raytheon DE-719-RTT fathometer depth recorder in conjunction with a Raytheon PTR sub-bottom profiler.

A 24-takeout 381-metre (1,250 feet) Mark Products buoyed marine seismic cable with 15.25 metre (50 feet) takeout intervals was towed directly from the stern of the vessel. Electrotech E.V.P. 7 hydrophones were suspended by "pigtail" takeouts to a depth of 2 metres below the water's surface. The cable was reinforced by taping polypropylene ½" rope to it, allowing for stretch in the rope due to loading.

From a boom over the vessel's side an explosive charge was trailed in the water approximately 15 metres off-line and approximately 15 metres offset from the first hydrophone. The shot was suspended from a float at a depth of 2 metres.

A Texas Instrument 8000 series reflection-refraction seismograph was used in conjunction with a dry-write electrostatic SIE Dresser ERC-10, 24-channel camera and SIE Dresser PMR-20 tape recorder. Explosive charges of ½ to 1 pound of geogel were used. For each shot the ship's engine was stopped to minimize noise and the decreased forward speed allowed the hydrophones to stabilize. A typical refraction record is shown in Figure 2.

During two days of shooting, a Fish and Game officer was on board to observe the effect of the blasts; he reported a minimal fish kill.

All shot-to-detector distances were determined by use of water velocity and travel time to the first two takeouts.

Within 20 miles of shore the boat was positioned by radar, and at greater ranges, gyro compass bearings and a Doppler speed and distance logs were used. Along the profile lines, bottom soundings were fiducialed every 300 metres or 5 minutes.

Two 6-metre aluminum boats, powered by 50 H.P. outboard motors, were used for inshore marine surveys. The shallow draught of these vessels limited their use to conditions of good weather, although they are capable of safely handling a 1-metre chop and a much larger swell. The cable, 198 metres long, was a polypropylene rope reinforced, 12-channel marine cable with takeout intervals of 12.2 metres.

Results

Northwest from Toker Point

Figure 3 shows the interpretation of the seismic data northwest from Toker Point to a point approximately 15 miles distant offshore. The solid line indicating the topography of the sea bottom drops off gradually from the shoreline. The rise on the bottom to the northwest is known as the James Shoal which may have been an ancient island in the delta. The average velocity observed immediately below the sea bottom is 1.6 km/sec. A high velocity refractor is detected close to the shore with an average velocity of 3.2 km/sec. The depth to the top of this refractor varies from 20 metres close to shore to a depth of 140 metres approximately 4 miles offshore and is continuous within this region. Farther offshore the refractor is detected in only a few locations — one about midway in the profile and another which may be associated with the James Shoal, although somewhat offset to the northwest. It is believed that this high velocity refractor is the boundary between unfrozen and frozen (permafrost) coarse-grained materials.

North from Atkinson Point

Figure 4 shows seismic data north from Atkinson Point for approximately 30 miles into water depths of 35 metres. Near the shoreline, the high velocity re-

fractor (permafrost) is detected at depths of 40 metres with an average velocity of approximately 2.95 km/sec. The average velocity of unfrozen material overlying this refractor is 1.7 km/sec. Approximately 4 miles offshore, sub-sea permafrost becomes discontinuous, while farther offshore it is continuous and drops to a depth of 100 metres. Towards the north end of the profile, the refractor rises to approximately 60 metres below sea surface and then drops abruptly to 100 metres.

Permafrost was not detected as far as the seismic line was surveyed; the seismic line was terminated at the edge of the ice pack. The lack of continuous permafrost in some areas along this profile may result from presence of large lakes which were subsequently inundated by the sea. These large lakes with water depths greater than 6 feet probably had unfrozen talik zones beneath them. But these talik zones do not show on the sea bottom as karst depressions on the echograms. The topography of the sea bottom may not reflect an old lake bottom if in subsequent inundation by the sea substantial thawing has occurred circumjacent to the lake and the shores have been reworked by wave action.

The sea bottom demonstrates a gradual slope to seaward; i.e. water depths gradually increase seaward. The topography on the refractor on the other hand is rugged. It must be pointed out, however, that there is considerable vertical exaggeration on this section and the undulations are not as severe as they appear. If one draws an average line through the depth to the refractor from the shoreline to the farthest point of detection one finds that the gradient of the refractor is greater than that of the sea bottom. The anomaly at the north end of this line in which the permafrost surface approaches the sea bottom is real in that the records are of good quality; however, no explanation is offered.

Kugmallit Bay

Figure 5 is the section across Kugmallit Bay from Toker Point to Crumbling Point on Summer Island just east of Richards Island. The top of permafrost detected near the shoreline at a depth of 20 metres drops off sharply to the westward to depths averaging about 60 metres. Farther westward the high velocity refractor becomes intermittent over extensive areas and is again observed rising from a depth of 90 metres on the west side of the profile to a depth of 20 metres close to the shoreline. The dotted line is an interpretation of seismic reflection data (Shearer, 1973). The depth to the top of a good reflector, interpreted to be the top of permafrost, was computed using an average velocity of 1,500 m/sec., which approximates that observed from the refraction profiling. Although the two survey lines (refraction and reflection) are separated by approximately one mile, there seem to be correlations between the presence and absence of permafrost along the line. Wherever the high velocity refractor becomes deep so is the reflector picked as a deep event. Unfortunately, no reflection data are available for the west side of this section. The Shearer (1973) data are unpublished to date.

Conclusion

Large seismic velocity contrasts exist at shallow depths below the sea bottom in the Mackenzie Delta — Beaufort Sea area which are interpreted to denote the top of permafrost. From these few reconnaissance profiles there is a widespread occurrence of permafrost offshore but the detailed areal extent is unknown.

References

Dobrin, M.B.
1970: Geophysical prospecting for oil; McGraw-Hill, New York.

Mackay, J.R., Rampton, V.N., and Fyles, J.G.
1972: Relic Pleistocene permafrost, western Arctic, Canada; Science, v. 176, p. 1321-1323.

McDonald, B.C., Edwards, R.E., and Rampton, V.N.
1973: Position of frost table in the near-shore zone, Tuktoyaktuk Peninsula; Geol. Surv. Can., in Report of Activities, November 1972 to March 1973, Geol. Surv. Can., Paper 73-1, Pt. B, p. 165-168.

Shearer, J.M.
1973: Surficial geology and geomorphology, Mackenzie Bay — Continental Shelf; in Report of Activities, April to October 1972, Geol. Surv. Can., Paper 73-1, Pt. A, p. 242.

31. COMPUTER MODEL STUDIES OF SEISMIC REFLECTION COEFFICIENTS FOR THE BASE OF THE PERMAFROST LAYER

Project 730006

J.A. Hunter and R.F. Mereu*
Resource Geophysics and Geochemistry Division

The variability of permafrost thickness in the Mackenzie Delta and Arctic Islands areas can be a problem in the interpretation of seismic reflection records in oil and gas exploration. Since the velocity difference between frozen and unfrozen materials can be as large as 2:1, a variation in the thickness of the permafrost layer along a seismic record section may be misinterpreted, in some cases, as structural anomalies. Indirect methods of estimating the thickness of permafrost have been evolved (Boulware, 1961). There has been little success in the direct determination of permafrost thickness by reflection methods. It has been suggested that the lack of good reflection data results from the velocity gradient nature of the lower permafrost boundary which yields a small reflection coefficient.

The Geological Survey in co-operation with the University of Western Ontario has undertaken a computer model study of the seismic reflection properties of the bottom of permafrost to determine the relative effects of various physical parameters on reflection coefficients.

Initial work on the problem was done by Hunter (1972) for a permafrost boundary given by a sharp velocity discontinuity. The present computer program written by one of us (RFM), involves the Thompson-Haskell matrix formulation for a gradient boundary consisting of 21 discrete velocity layers. An incident monochromatic plane wave is assumed and, for the present study, all densities are assumed to be 2.0 gm/cm^2 and Poisson's ratio to be 0.25. Reflection coefficients are computed for angles of incidence from 0^o to 90^o in 1^o increments. No provision is made for geometric wavelet spreading or frequency attenuation of the material.

Typical results are shown in Figure 1 for two types of unconsolidated material, sand (Fig. 1(a)) and clay (Fig. 1(b)) based on velocity-temperature relationships given by Nakano et al. (1971) and a typical temperature gradient for permafrost of 0.06^o/m (pers. comm. A.S. Judge, Earth Physics Branch, EMR). Reflection coefficients are low (but significant) for angles of incidence up to 60^o; P-SV converted wave coefficients become prominent in the intermediate range of incident angles; the positions of the peaks and troughs on the plots are dependent on the particular model. Further studies (not shown here) have demonstrated that the details of the curve shapes are strongly frequency dependent and that impulse response frequency spectra display sharp "resonance" peaks which are dependent on the incident angle.

A detailed publication of our results for permafrost models consisting of unconsolidated materials for typical temperature gradients is in preparation. Future studies are planned for models consisting of various rock types.

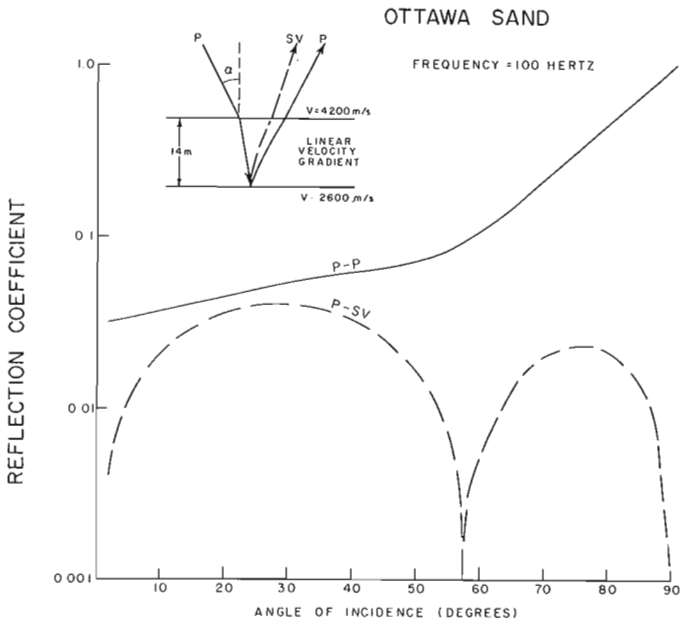

Figure 1a. Plot of reflection coefficient vs. angle of incidence for a gradient boundary in Ottawa sand.

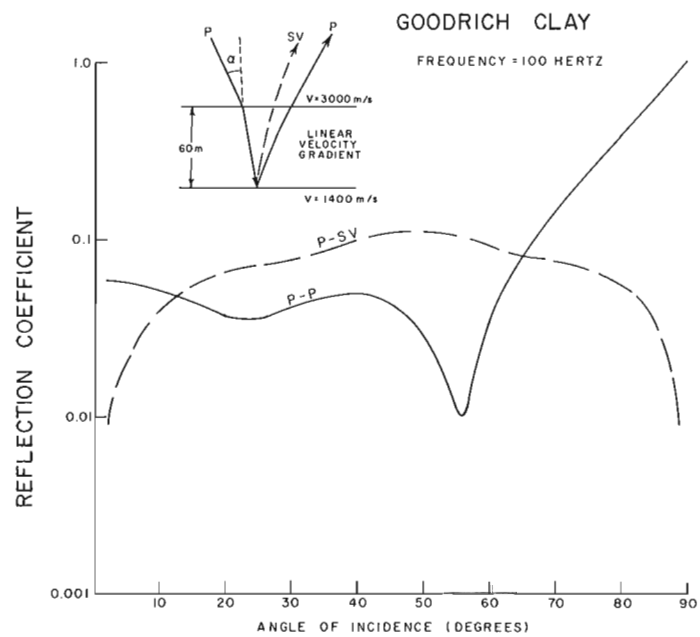

Figure 1b. Plot of reflection coefficient vs. angle of incidence for the same temperature gradient in Goodrich clay.

* University of Western Ontario.

Reference

Boulware, R. A.
1961: How to Analyse Reflection Data; World Oil, April, p. 80-84.

Hunter, J. A.
1972: A model study of reflected seismic waves from the bottom of the permafrost layer; in Report of Activities, November 1971 to March 1972, Geol. Surv. Can., Paper 72-1B, Pt. B., p. 44-46.

Nakano, Y., Smith, M., Martin, R., Stevens, H. and Knuth, K.
1971: Determination of the acoustic properties of frozen soils; U.S. Army Cold Regions Research and Engineering Laboratory Report.

Project 630049

T.J. Katsube
Resource Geophysics and Geochemistry Division

Introduction

It is necessary to know the resistivity and dielectric constant of moist rocks and soils when calculating the depth of penetration for EM waves. At frequencies below the critical frequency (usually 10^5 - 10^7 Hz for most moist rocks and soils), measurement of only resistivity at one frequency will usually provide fairly good data for calculation of the depth of penetration vs. frequency spectrum. This is because the resistivity is usually constant with frequency, and the effect of the dielectric constant is small at frequencies below the critical frequency. However, at frequencies above the critical frequency it is necessary to know both the dielectric constant and resistivity to estimate the depth of penetration. The dielectric constant is usually constant or varies little with frequency at frequencies above the critical frequency, but the resistivity varies unpredictably with frequency to a great extent. Therefore, values of dielectric constant measured at a single frequency can be representative for a wide frequency range. But it is not possible to estimate the depth of penetration vs. frequency spectrum with sufficient accuracy, unless the resistivity is measured at multiple frequencies in the spectrum.

It has been noticed by Katsube and Collett (1972) that the dry rock resistivity affects the moist rock resistivity at frequencies above the critical frequency. From existing data on various types of rocks, it seems that the dry rock resistivity vs. frequency spectrum can be expressed by a relatively simple equation that can simplify the depth of penetration calculations.

In this paper, the effect of dry rock resistivity on moist rock resistivity is discussed in detail. A set of equations are introduced for calculating the depth of penetration vs. frequency spectrum, which requires resistivity measurements at only very limited frequencies.

Depth of Penetration Theory

The rate at which the intensity of the electrical field (E) of electromagnetic waves attenuates when propagating through lossy material is expressed by,

$$E = E_0 e^{-\alpha\chi} \quad \text{- - - - - - - - - - - - - - - (1)}$$

where E^0 is the electrical intensity at the origin, χ is the distance from the origin to the point of observation and α is the attenuation factor. The distance of χ at which E attenuates to 1/e times the value of E^0 is defined as the depth of penetration (δ). That is when $\alpha\chi = 1$, therefore

$$\delta = \chi = \frac{1}{\alpha} \quad \text{- - - - - - - - - - - - - - - (2)}$$

From almost any textbook on electromagnetic waves (Jordan, 1950) the relationship between α can be expressed in terms of electrical parameters by:

$$\frac{1}{\delta} = \alpha = \omega\sqrt{\frac{\mu\varepsilon}{2}\left(\sqrt{1 + \frac{1}{(\omega\,\varepsilon\,\rho_p)^2}} - 1\right)} \quad \text{- - - - - (3)}$$

where

ω : angular frequency ($\omega = 2\pi f$, f = frequency)
μ : permeability ($4\pi \times 10^{-7}$ henrys/m)
ε : permittivity
ρ_p : parallel resistivity

The dissipation factor (D) is expressed by:

$$D = \frac{1}{\omega\varepsilon\rho_p} \quad \text{- - - - - - - - - - - - - - - (4)}$$

Using Eqs. (2), (3) and (4), the depth of penetration can be expressed by:

$$\delta = \left[\omega\sqrt{\frac{\mu\varepsilon}{2}\left(\sqrt{1 + D^2} - 1\right)}\right]^{-1} \quad \text{- - - - - - - - - (5)}$$

Frequency Spectrum of Electrical Parameters

The frequency spectrum of complex resistivity (ρ^*), parallel resistivity (ρ_p) and dissipation factor (D) for

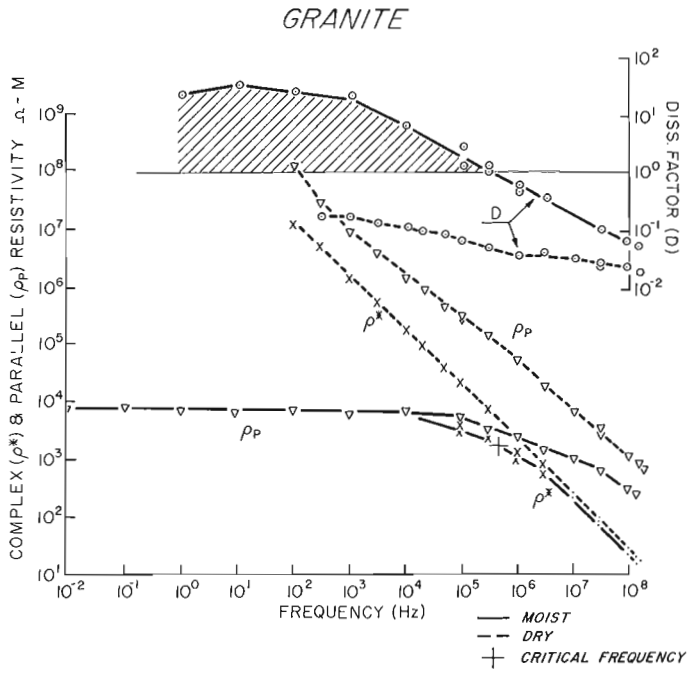

Figure 1. Frequency spectrum of complex resistivity (ρ^*), parallel resistivity (ρ_p) and dissipation factor (D) for a moist and a dry granite sample.

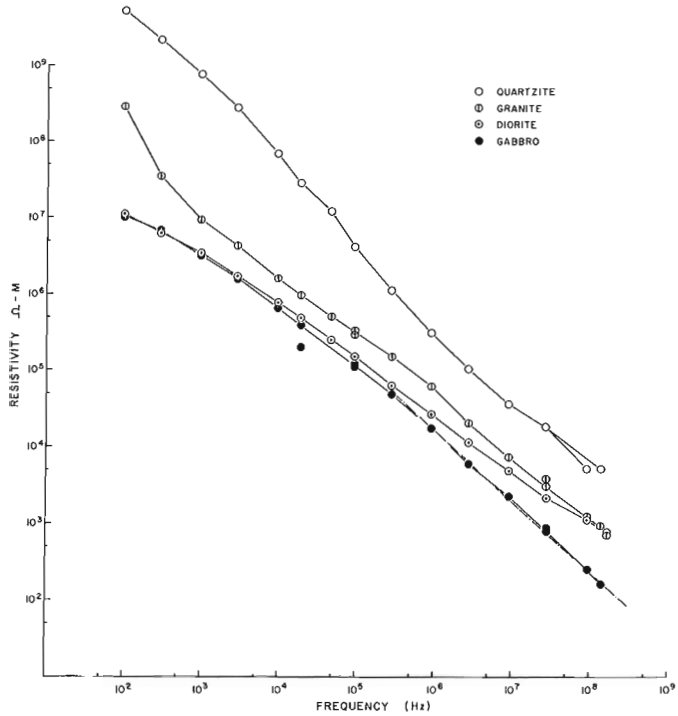

Figure 2. Parallel resistivity (ρ_p) of dry terrestrial rocks.

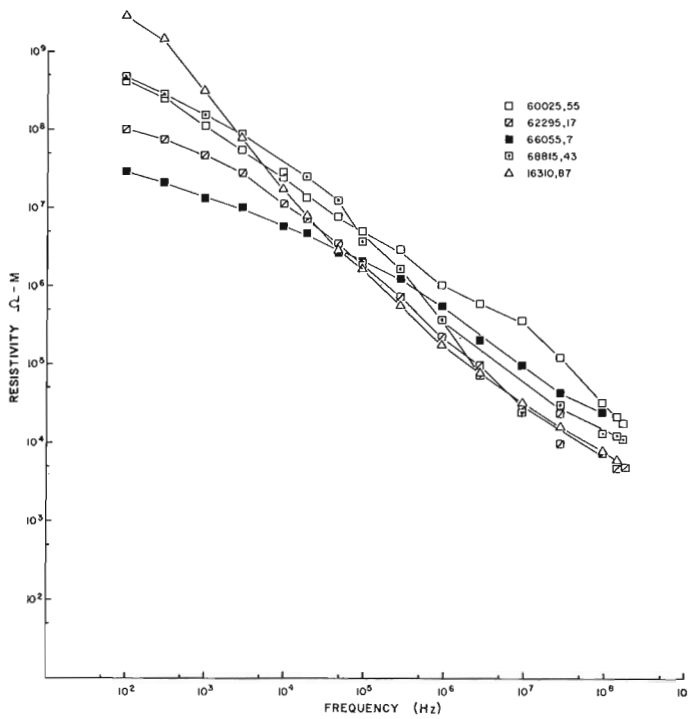

Figure 3. Parallel resistivity (ρ_p) of lunar rocks.

a granite specimen in both dry and moist state are shown in Figure 1. The relationship between ρ^* and the other parameters is

$$\rho^* = \left[\sqrt{\left(\frac{1}{\rho_p}\right)^2 + (\omega\varepsilon)^2}\right]^{-1} \quad - - - \quad (6)$$

From Figure 1 it can be seen that ρ^* of the moist rock specimen is more or less independent of frequency until the applied frequency reaches the critical frequency (f_{cr}). The critical frequency is the frequency at which $D = 1$, or $\omega\varepsilon\rho_p = 1$. Above the critical frequency ρ^* decreases linearly with frequency. Below the critical frequency, the effect of permittivity (ε) in Eq. 6 is small compared to that of ρ_p, so that $\rho_p \simeq \rho^*$, as can be seen in Figure 1 for the moist specimen. Therefore ρ_p is also more or less independent of frequency until the applied frequency reaches f_{cr}. Above f_{cr}, ρ_p gradually decreases with frequency, but not at the same rate as ρ^*.

ρ^* and ρ_p of the dry specimen decrease with frequency as can be seen in Figure 1. ρ^* decreases linearly with frequency, and ρ_p decreases with frequency at a smaller rate than that of ρ^*. These trends are similar to those shown in the paper by Katsube and Collett (1972, 1973).

If a moist rock specimen could be simulated by a RC parallel circuit, it would be expected that ρ_p is constant with frequency above f_{cr}. Actually this is not the case as can be seen in Figure 2. ρ_p of the dry rock apparently affects ρ_p of the rock when moist. For this reason it is essential to investigate the ρ_p vs. frequency characteristics of dry rocks.

Trends of Dry Rock Resistivity

Parallel resistivity (ρ_p) curves for several dry terrestrial and lunar rocks are shown in Figures 2 and 3. If the rock consists of several minerals with different values of ρ_p, it would be expected that ρ_p of the rock would decrease in the form of steps as shown in the paper by Katsube and Collett (1973), and not in a continuous form as seen in these Figures 2 and 3. In some cases the decrease of ρ_p in a step form can be seen to a certain extent, but generally ρ_p decreases in the form shown in these figures. The reason for ρ_p to show a continuous decrease in this form is, perhaps, due to the rock consisting of various minerals with various resistivities, grain size and shape.

From Figures 2 and 3, it can be seen that above 10^6 Hz ρ_p decreases with a more or less constant gradient for each rock type. Therefore frequencies above 10^6 Hz, ρ_p can be expressed by the following empirical equation:

$$\rho_p = \rho_6 \, (f/10^6)^{-n} \quad - - - - - - - - \quad (7)$$

where ρ_6 is the parallel resistivity at 10_6 Hz, n is a constant which determines the decay rate at which ρ_p decreases with frequency, and f is the applied frequency. For terrestrial and lunar rocks in Figures 2 and 3, n varies between 0.64 to 0.92 as shown in Table A.

Averaged curves for ρ_p of terrestrial and lunar rocks can be determined by taking the averages of ρ_p for all rocks at each frequency. The averages (ρ) for ρ_p can be calculated from

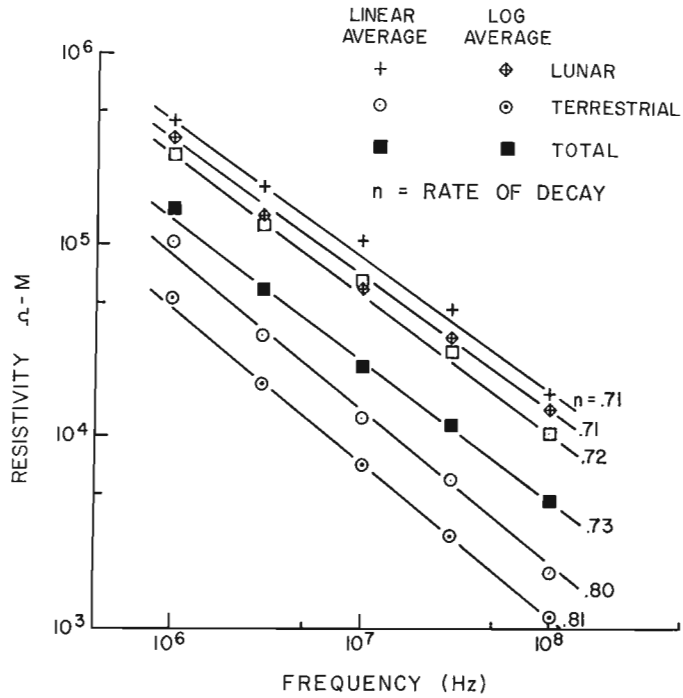

Figure 4. Mean curves of ρ_p for dry terrestrial and lunar rocks.

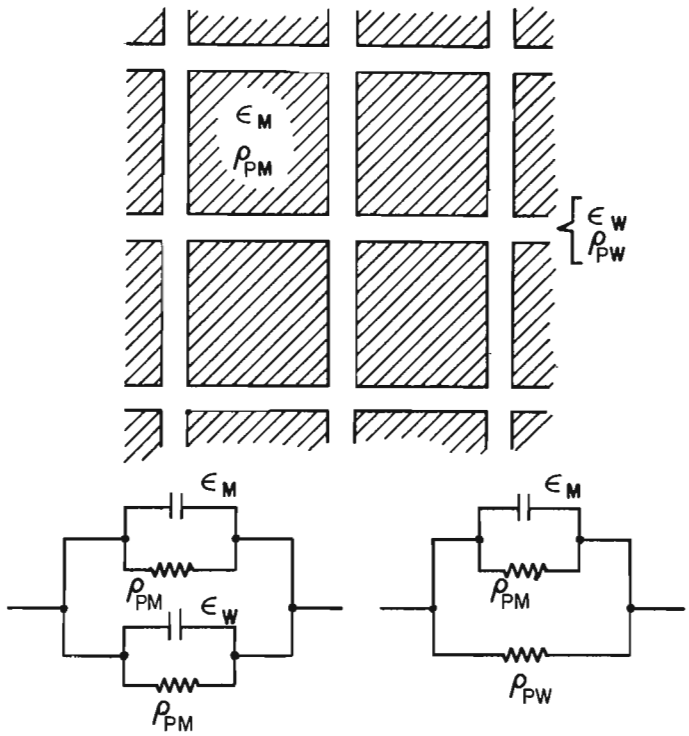

Figure 5. Model for mineral grains and pores in rocks.

$$\text{or} \quad \bar{\rho} = \sum_{i=1}^{N} \rho_{p_i} / N \qquad \text{- - - - - - - - - - - (8)}$$

$$\bar{\rho} = \exp \left(\sum_{i=1}^{N} \ell n \rho_{p_i} / N \right) \qquad \text{- - - - - - - - - (9)}$$

where N is the number of rock samples used for the averaging. The rate of decay, n, is determined from the curves that were obtained from Eq. 8 and Eq. 9 is expressed by the linear average of n (n_{LIN}) and the logarithmic average of n (n_{LOG}) respectively (see Fig. 4). Eq. 9 is thought to be a superior method for calculating averages since the weight of each value of ρ_p in Eq. 9 is the same. In Eq. 8, the weight on larger values of ρ_p tends to be larger than those on smaller values of ρ_p. n_{LOG} for this set of terrestrial and lunar rocks is 0.732. Others values for ρ_p, n, n_{LOG} and n_{LIN} are shown in Table A.

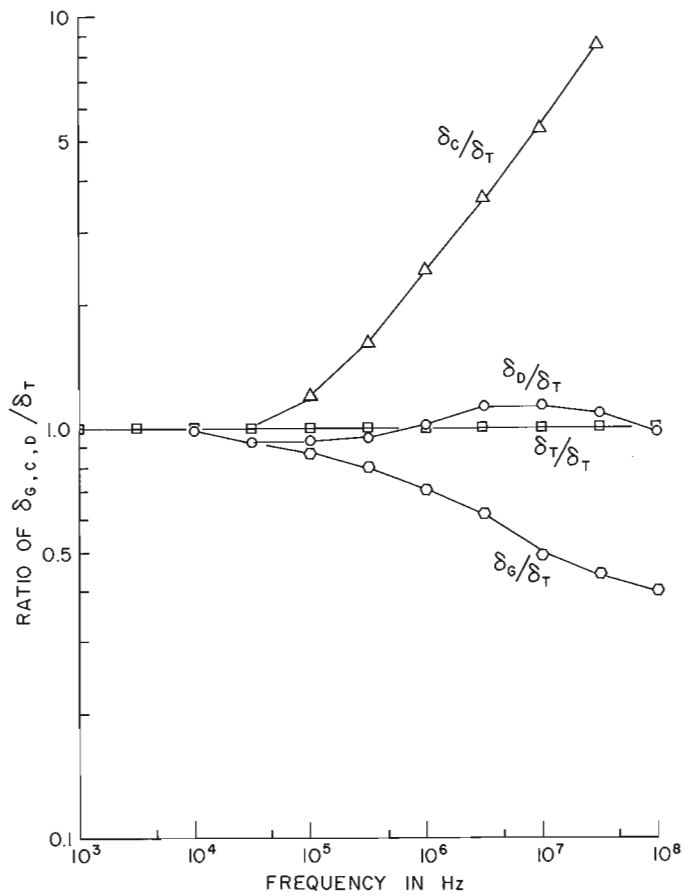

Figure 6. Comparison of normalized depth of penetration calculations using various methods referred to δ_T (Eq. 5).

Effect of Dry Rock Resistivity on Moist Rocks

Parallel resistivity (ρ_p) of the moist rock at the lower frequencies (below f_{cr} in this case) is mainly determined by the structure of the connecting pores (Katsube and Collett, 1973). This resistivity shall be expressed by the ρ_{pw} which is not expected to vary with frequency for moist rocks.

Dry rock ρ_p at the higher frequencies (above f_{cr}) is mainly determined by the mineral composition of the grains that are separated by the pores. Grain boundaries affect ρ_p of the dry rock at the lower frequencies (below f_{cr}) but is not significant in this case. Therefore, only the values of ρ_p determined by the mineral grains are discussed here, and expressed by ρ_{pm}. Actually ρ_{pm}

for dry rocks is equivalent to ρ_p in Eq. 7, therefore,

$$\rho_{pm} = \rho_6 \quad (f/10^6)^{-n} \qquad \text{- - - - - - - - - - - (7a)}$$

ρ_{pm} decreases with frequency as can be seen in Figures 2 and 3, and above a certain frequency it becomes smaller than ρ_{pw}. ρ_p of a moist rock is dependent on both ρ_{pw} and ρ_{pm}. This is the reason that ρ_p of a moist rock is more or less constant with frequency below f_{cr}, and shows a decrease with frequency above f_{cr}. The relationship between ρ_p, ρ_{pw} and ρ_{pm} is set up by using the model and equivalent circuit in Figure 5. From this model,

$$\frac{1}{\rho_p} = \frac{1}{\rho_{pw}} + \frac{1}{\rho_{pm}}$$

therefore

$$\rho_p = \frac{\rho_{pw} \times \rho_{pm}}{\rho_{pw} + \rho_{pm}} \qquad \text{- - - - - - - - (10)}$$

This discussion is an extension of that in the paper by Katsube and Collett (1972).

Equation for Depth of Penetration Calculations

For generalization ρ_{pm} for dry rocks measured at a frequency f_i is expressed by ρ_i and inserted into Eq. 7a:

$$\rho_{pm} = \rho_i \, (f/f_i)^{-n} \qquad \text{- - - - - - - - - - (11)}$$

Substituting Eq. 11 in Eq. 10,

$$\rho_p = \frac{\rho_{pw} \times \rho_i}{(f/f_i)^n \rho_{pw} + \rho_i} \qquad \text{- - - - - - - (12)}$$

Substituting Eq. 12 in Eq. 4

$$D = \frac{1}{\omega\varepsilon}\left[\left(\frac{f}{f_i}\right)^n \frac{1}{\rho_i} + \frac{1}{\rho_{pw}} \right] \qquad \text{- - - (13)}$$

Therefore, from Eq. 5 the depth of penetration from,

$$\delta = \left[\omega \sqrt{\frac{\mu\varepsilon}{2}} \left\{ \sqrt{1 + \frac{1}{(\omega\varepsilon)^2} \left[\left(\frac{f}{f_i}\right)^n \frac{1}{\rho_i} + \frac{1}{\rho_{pw}} \right]^2} - 1 \right\} \right]^{-1} \qquad \text{- (14)}$$

where

f_i : frequency at which dry rock resistivity is measured

μ : magnetic permeability (4×10^{-7} henrys/m)

ε : permittivity of the rock in F/m

ρ_i : dry rock resistivity (ρ_{pm} of dry rock) measured at f_i

ρ_{pw}: bulk moist rock resistivity below f_{cr}.

Actually, from experience an introduction of two additional coefficients A, and B, into Eq. 14 produce more realistic results:

$$\delta = \left[\omega \sqrt{\frac{\mu\varepsilon}{2B}} \left\{ \sqrt{1 + \frac{B^2}{(\omega\varepsilon)^2} \left[\left(\frac{f}{f_i}\right)^n \frac{A}{\rho_i} + \frac{1}{\rho_{pw}} \right]^2} - 1 \right\} \right]^{-1} \qquad \text{- - (15)}$$

where A = 2 and B = 5. These two values for A and B are based on measurements of terrestrial rocks. When the rock is moist, ε of the rock should be measured at frequencies above f_{cr}, and should be larger than that measured when the rock is dry (Katsube and Collett, 1973).

Eq. 15 is advantageous to use when only limited measured values are available, e.g. ρ_{pw} at low frequency, ρ_i at a higher frequency (f_i), for example 1 M Hz, and a value for ε. Eq. 15 is the best calculation for depth of penetration, however, measured values of ρ_p and ε are required over the entire frequency range.

Comparison of Depth of Penetration Calculations

Geophysicists use a simplified form of Eq. 3 for calculating depth of penetration in which ε cancels out of the equation and only the value of ρ_{pw} is considered at low frequencies. The equation for δ reduces to:

$$\delta = \sqrt{\frac{2\rho_{pw}}{\omega\mu}} \qquad \text{- - - - - - - - - - (16)}$$

Communication engineers use Eq. 3 for depth of penetration calculation. Actually they use the low frequency value of resistivity, ρ_{pw}, and a value for ε:

$$\delta = \left[\omega \sqrt{\frac{\mu\varepsilon}{2}} \sqrt{1 + \left(\frac{1}{\omega\varepsilon\rho_{pw}}\right)^2} - 1 \right]^{-1} \qquad \text{- - - (17)}$$

A comparison is made in Figure 6 for quartzite of depths of penetration calculated using Eq. 15 (δ_D), Eq. 16 (δ_G) and Eq. 17 (δ_C) for frequency range from 10^3 to 10^8 Hz. The curves are normalized to δ calculated using Eq. 5 (δ_T) which is the best equation to use since it uses each value of ρ_p and ε at each discrete frequency. For comparison δ_T is set to equal 1 for all frequencies. In calculating δ_D, δ_G and δ_C, the various parameter values used for quartzite are:

$\varepsilon = 5.6$

$\rho_i = 2.3 \times 10^5$ Ω m at $f_i = 10^6$ Hz

$\mu = 4\pi \times 10^{-7}$ H/m

$\rho_{pw} = 1.8 \times 10^4$ Ω m

In calculating δ_D (Eq. 15), an average value for n was used. For Table A, the logarithmic average value is:

$$n = \bar{n}_{LOG} = 0.732 \qquad \text{- - - - - - - - - - - - - - - (18)}$$

From Figure 6, it is noted that the use of Eq. 15 (δ_D), ratio δ_D/δ_T is a very good approximation to the more elaborate calculation using Eq. 5 (δ_T). Below 10^4 Hz, there is no dispersion in depth of penetration. Therefore, the most simplified formula used by the geophysicists (Eq. 16) and communication engineers (Eq. 17) are valid. Above this frequently the depth of penetration, Eq. 16, is too shallow. The formula (Eq. 15) used by the communication engineers

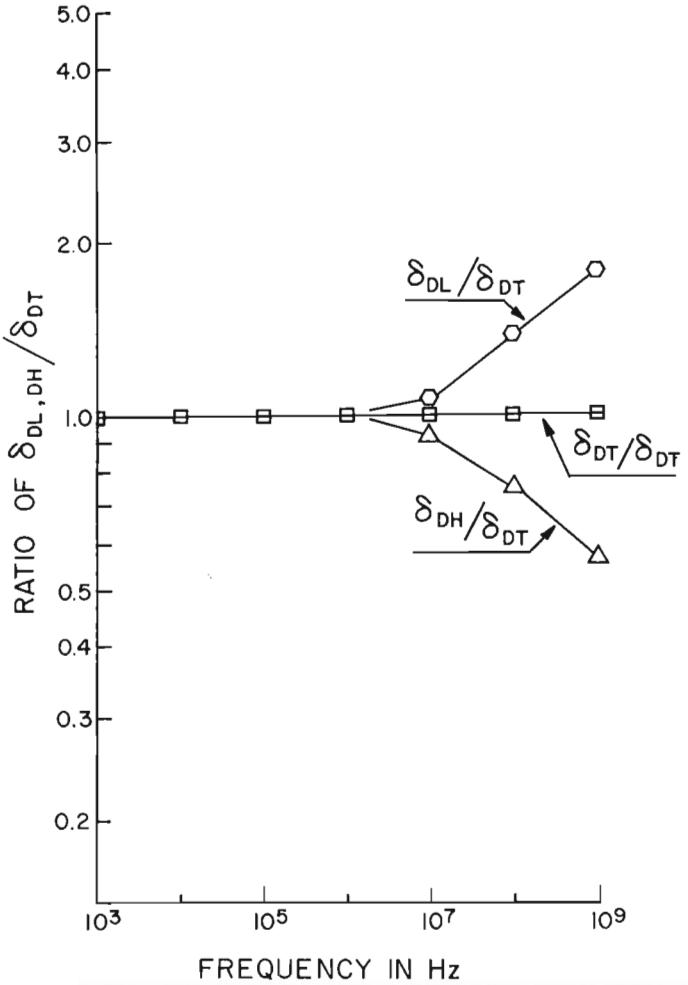

Figure 7. Effect of the choice of n on the depth of penetration calculations using Eq. 15. δ_{DT}, δ_{DH} and δ_{DL} are the depths of penetration when n = 0.73, 0.92 and 0.64, respectively.

gives a depth of penetration that is greater than the real depth.

In using the formula (Eq. 15), errors can be introduced by improper choice of the appropriate value of the rate of decay, n. For various rocks, n can vary from 0.64 to 0.92 as shown in Table A. Fig. 7 shows normalized plots of δ_{DT}/δ_{DT}, δ_{DH}/δ_{DT} and δ_{DL}/δ_{DT} when δ_{DT} is calculated using the average value of n = 0.732, δ_{DH} uses n=0.92 and δ_{DL} uses n = 0.64. When the choice of the average value of n (0.732) is lower than the actual value (0.92), the curve of δ_{DH}/δ_{DT} decreases with frequency, in other words, the calculated depth of penetration is greater than it actually should be. On the other hand, when the choice of the average value of n (0.732) is greater than the actual value (0.64) the curve of δ_{DL}/δ_{DT} increases with frequency, in other words, the calculated depth of penetration is lower than actually it should be.

Discussion

Little difference of n can be seen between the average value of $\bar{n}$ calculated for terrestrial and lunar rocks

TABLE A

VALUES FOR DRY ROCK RESISTIVITY PARAMETERS

ROCK TYPE		RESISTIVITY COEFFICIENT ρ_6 (AT 10^6 Hz)	n
TERRESTRIAL			
QUARTZITE		2.3×10^5	0.76
GRANITE		4.3×10^4	0.79
DIORITE		2.3×10^4	0.64
GABBRO		1.6×10^4	0.92
LUNAR			
14310,87		1.4×10^5	0.64
60025,17		1.0×10^5	0.72
62295,17		1.9×10^5	0.73
66055,7		9.7×10^5	0.67
68815,43		3.3×10^5	0.69
AVERAGES			
TERRESTRIAL	($\bar{n}_{LIN}$)	8.9×10^4	0.80
"	($\bar{n}_{LOG}$)	4.7×10^4	0.81
LUNAR	($\bar{n}_{LIN}$)	4.4×10^5	0.71
"	($\bar{n}_{LOG}$)	3.5×10^5	0.71
TOTAL	($\bar{n}_{LIN}$)	3.0×10^5	0.72
"	($\bar{n}_{LOG}$)	1.4×10^5	0.73

$$\rho_p = \rho_6 \left(\frac{f}{10^6}\right)^{-n}$$

(Fig. 4 and Table A) even though the pores of terrestrial rocks have been exposed to moisture and geological processes. This fact together with the discussions in the paper by Katsube and Collett (1973) suggest that the values of n are characteristic of the mineral grains and show little or no effect of the pores at the higher frequencies.

From the measurements on various materials by Von Hippel (1954), ρ_p decreases with frequency similar to the measurements shown in this paper. Therefore, it is suggested that n and ρ_p should be determined for a wide range of rocks, soils, ice and other materials. No doubt ρ_p measured at multiple frequencies will produce the best results for depth of penetration calculations (Eq. 5). However, by a judicious choice of n and a measured value of ρ_i at f_i a good depth of penetration can be derived by using Eq. 15.

A = 2 and B = 5 in Eq. 15 produce the best results for the set of rocks. Whether these values are applicable to any rock type is a subject that is still under investigation.

Conclusion

This paper discusses the limitations of equations used for depth of penetration calculations at frequencies greater than the critical frequency. The usual depth formulae (Eqs. 16 and 17) introduce errors when the value of resistivity, ρp, at the higher frequencies is not taken into account. This fact has been brought to the authors' attention from having studied the resistivities of dry rocks (lunar) over a broad frequency range. The general equation (Eq. 5) for depth of penetration is valid since the values of ρ_p and ε are measured at each frequency over the whole frequency

range. A modified depth of penetration equation, Eq. 15, has been formulated and expressed as an empirical equation which includes a new parameter, n, the rate of decay for the rock type and a measured value of ρ_{pm} at a single frequency above the critical frequency. The advantage of using this formula reduces the amount of measured data required and is accurate to the extent of the choice of n. Therefore, compilation of a table of values for n and resistivity, at for example 10^6 Hz, would be beneficial.

Acknowledgments

The author is very grateful to Mr. L.S. Collett for his suggestions and aid throughout this study.

References

Jordan, E.C.
1950: Electromagnetic waves and radiating systems; Prentice-Hall, p. 128-131.

Katsube, T.J. and Collett, L.S.
1972: Electrical and EM propagation characteristics of igneous rocks. Presented at 42nd Annual International Meeting of Society of Exploration Geophysicists, Anaheim, California; submitted to Geophysics, Feb. 22, 1974.

1973: Electrical characteristics of rocks and their application to planetary and terrestrial EM Sounding; Proc. of Fourth Lunar Sci. Conference, Supplement 4, Geochim. Cosmochim. Acta, Pergamon Press, v. 3, p. 3111-3131.

Von Hippel, A.R.
1954: Dielectric material and applications; J. Wiley and Sons, Inc., New York.

33.

AN EXPERIMENTAL HIGH RESOLUTION AEROMAGNETIC SURVEY IN THE KAMLOOPS AREA, BRITISH COLUMBIA

Projects 680081 and 720080

P.H. McGrath, M.T. Holroyd and P.J. Hood
Resource Geophysics and Geochemistry Division

With the introduction of the first high resolution airborne magnetometers in the early 1960's, a revolution in the aeromagnetic surveying technique began. It became necessary to record high resolution data on magnetic tape in digital format because of a dynamic range problem, whereas previously analog charts were employed. This permitted the map compilation to be computerized, and resulted in a significant reduction in time and cost required to compile a survey. Having the data in digital form also provided a means of rapidly producing a variety of derived maps, e.g. vertical derivative, which could be tailored to the needs of the user.

Between May 17-21, 1973, an experimental high resolution aeromagnetic survey was flown over mountainous terrain in the Kamloops area of British Columbia (Sawatzky et al., 1974) using the Geological Survey's Beechcraft B80 aircraft. Approximately 790 line miles were obtained at a flying height of 6,500 feet above sea level, the mountain peaks in the area reaching 6,000 feet. Analysis of the data indicates that topographic effects are of less importance than magnetization contrasts within the underlying rocks in controlling the resultant aeromagnetic anomaly patterns (Hood and Holroyd, 1973). In addition to topographic patterns, the 1973 high resolution data were compared with fluxgate survey data which was drape flown in 1967 in the same area of British Columbia at a 1,000-foot mean terrain clearance. Figure 1 is a magnetic map of part of the 1967 fluxgate survey which was manually compiled using a 10 gamma intercept. The flight line spacing was one-half mile. A geology map (Cockfield, 1947) shows the geology to be relatively simple. The map-area is equally divided into essentially two main rock-types separated by a north-south contact zone. On the eastern side of the contact the rocks are chiefly Triassic andesites with minor amounts of basaltic and sedimentary rocks. The western half of the map is underlain by the Coast Intrusions of Jurassic and later (?) age. The rocks are mostly medium- to coarse-grained granodiorites or quartz diorites but locally include more acidic and basic types. Copper deposits have been discovered at many places within this unit. The magnetic anomaly pattern over both of these major rock units suggests that the geology is much more complex than this simplified description would indicate. Only a minor amount of this complexity can be due to topographic effects.

Figure 2 is a map of the 1973 high resolution data which covers the same area shown in Figure 1. Because of the larger flight line spacing (approximately 1 mile), and in general the larger elevation above ground level, the magnetic anomaly pattern shown in Figure 2 is less complex than that seen in Figure 1. In spite of the differences in sampling however, the correspondence between the two surveys is excellent.

Figure 3 is a computed vertical derivative map which was obtained by convolving the 1973 high resolution data shown in Figure 2 with a one-dimensional, forty-one point filter operator. Note the enhancement of the more regional information. The vertical derivative operator brings into focus variations in the data which are more closely allied to variations in the near surface geology, the effects of deeper sources being suppressed by the operator. Comparison of Figures 1 and 3, although not entirely valid because of different sampling densities, suggests that Figure 3 is a superior product for use as a mapping aid by the field geologist.

The vertical derivative operator which was used to produce the map shown in Figure 3 was calculated using five hundred terms of a finite Fourier series (Hamming, 1962, p. 67). The Fourier coefficients were obtained by digitizing in the frequency domain, the theoretical filter response, $\kappa(\mu)$, of a vertical derivative operator, where

$$\kappa(\mu) = 2\pi\mu \qquad (1)$$

and μ = wave number along the flight line direction.

In summary, the clear implication of this experimental survey is that high resolution aeromagnetic surveys at constant barometric elevation are useful in areas of rugged terrain. It is also clear because of the low noise level in the high resolution data, that digital filters can be used effectively to improve the resolution of near surface sources. Our experience with low sensitivity data indicates that the geological information obtained by the process of derivation is often masked by the larger noise level in this type of magnetic data. This is especially true for the higher derivatives. Hence high resolution surveys using fixed winged aircraft at constant barometric elevations supply a viable alternative in mountainous regions to aeromagnetic surveying with helicopters.

References

Cockfield, W.E.
1947: Nicola map-sheet; Geol. Surv. Can., Map 886A.

Hamming, R.W.
1962: Numerical methods for scientists and engineers; McGraw-Hill Book Company, Inc., Toronto.

Hood, P.J., and Holroyd, M.
1973: Results of GSC experiments indicate high resolution aeromagnetic surveys have potential for more development; The Northern Miner, November 29th.

Sawatzky, P., et al.
1974: Experimental high-resolution aeromagnetic surveys: 1973; in Report of Activities, April to October 1973, Geol. Surv. Can., Paper 74-1, Pt. A, p. 95-98.

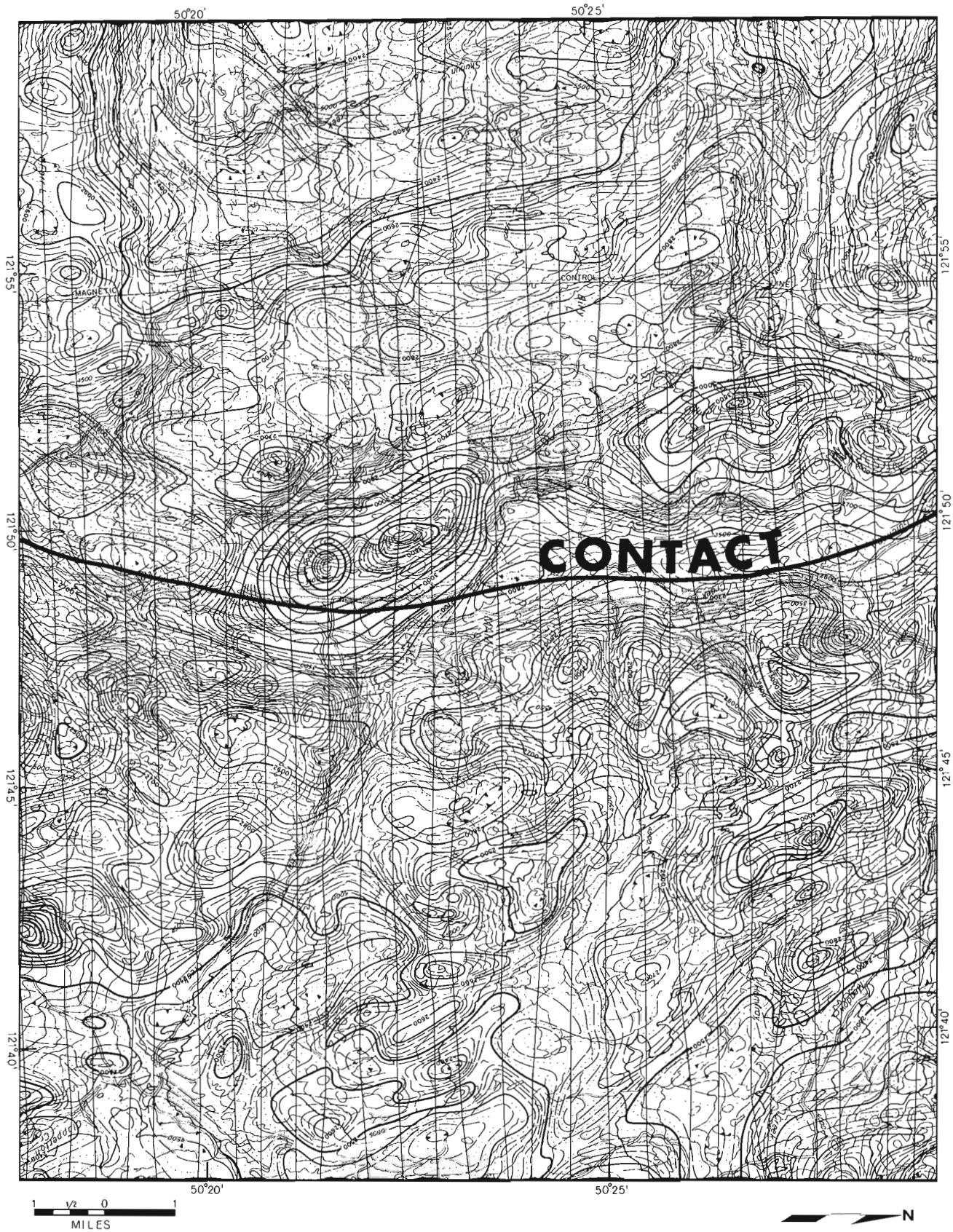

Figure 1. Standard Resolution Aeromagnetic Map; Drape flown at 1,000' above ground level, ½ mile traverse spacing.

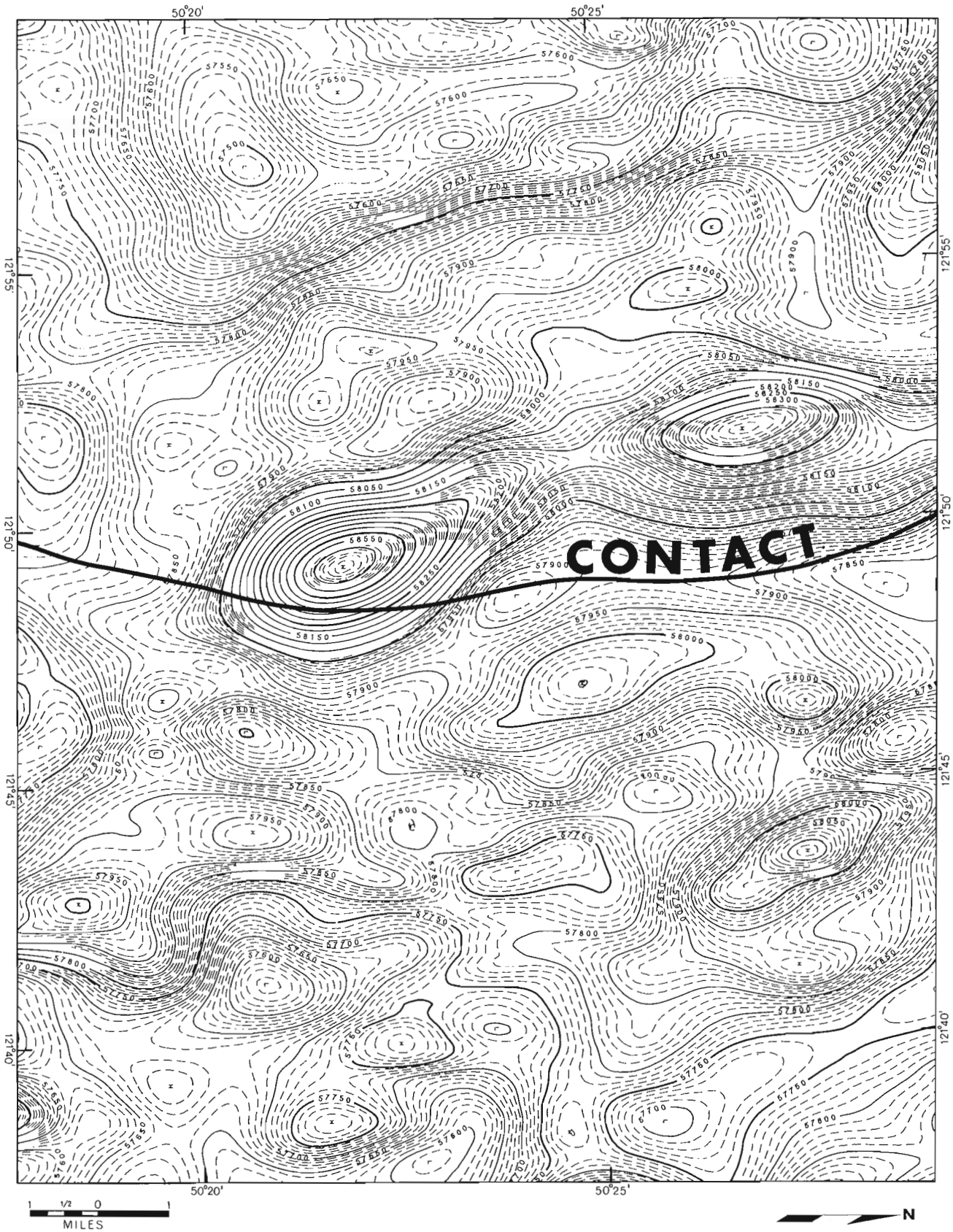

Figure 2. High Resolution Aeromagnetic Map, constant barometric altitude at 6,500' 1 mile traverse spacing.

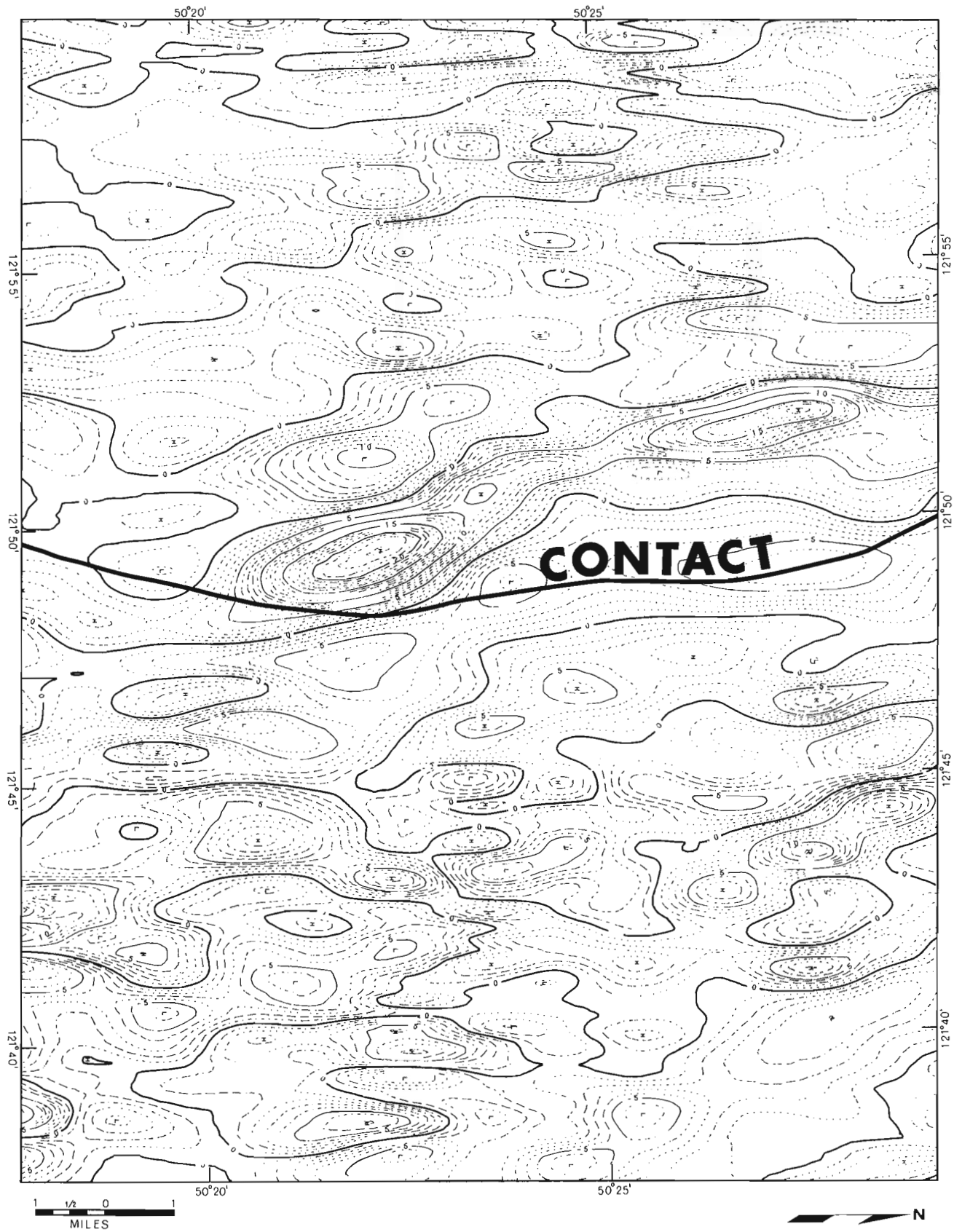

Figure 3. First vertical derivative map produced by digital filtering of high resolution data.

34. AEROMAGNETIC ANOMALIES RELATED TO PYRRHOTITE OCCURRENCES IN THE CANADIAN APPALACHIAN REGION

Project 700054

E.J. Schwarz and P.H. McGrath
Regional and Economic Geology Division

The aeromagnetic maps (Geological Survey of Canada, Maps 7031G, 7034G, 7035G, 7036G and others) show extensive positive linear magnetic anomalies (300 gammas) over the Halifax Formation in Nova Scotia (Fig. 1). These anomalies are elongated in the direction of the Appalachian trend northeast-southwest. They possess steep lateral gradients suggesting that the causative bodies are situated at or near the earth's surface.

The Halifax Formation of Ordovician or earlier age, consists mainly of slates, some of which are pyritiferous Oriented samples were collected across the anomalous zones for laboratory analysis. The remanence directions determined from the oriented samples have a very large scatter and consequently yield no useful information. However, these results do indicate that remanent intensity and low-field susceptibility increase strongly towards the centres of the anomalous zones.

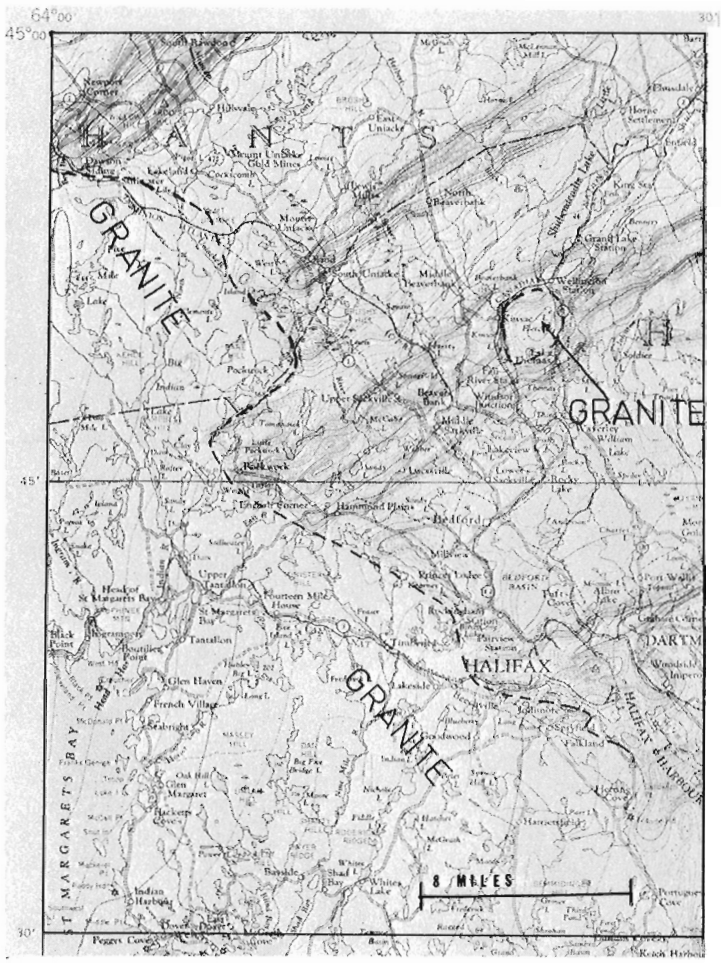

Figure 1. Ne-Sw trending aeromagnetic anomalies near Halifax due to Fe_7S_8 truncated by granite intrusions.

Thermomagnetic experiments were carried out to determine the cause for the high values of remanence and susceptibility of samples from the anomalous zones. The change of the high-field (8000 oe) magnetization with temperature indicated the presence of only one ferromagnetic mineral in the samples with a Curie temperature of 315°C. In a few samples, small peaks are superposed on these simple thermomagnetic curves reminiscent of the pyrrhotite Fe_9S_{10} which is non-magnetic in nature (Schwarz, 1968). The magnetic mineral with a Curie point of 315°C is probably the magnetic pyrrhotite Fe_7S_8 (Schwarz, 1972). This is in accordance with the macroscopically visible pyrrhotite in samples collected from the centres of the anomalous zones. Figure 2 illustrates the increase in Fe_7S_8 con-

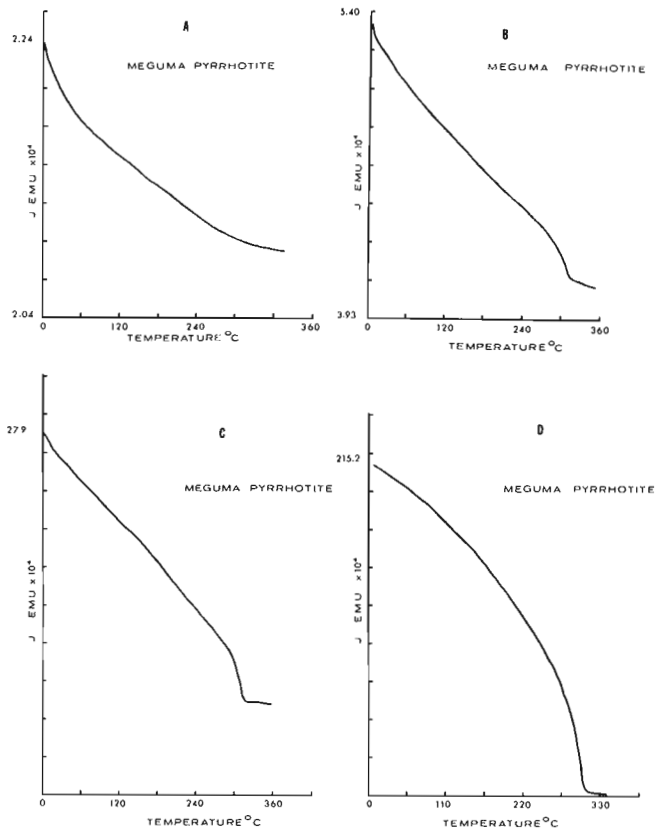

Figure 2. The decrease of the magnetization (J) acquired in magnetic field of 5350 oe for a sample well outside a magnetic anomaly zone (A), samples near the boundary of the concomitant anomaly (B and C), and a sample from the central part of the magnetic zone (D).

tent of four samples collected over about 150 metres going from the low-background area into one of the anomalous zones. The curves also yield the abundance of the Fe_7S_8 pyrrhotite (Schwarz, 1968): 0 weight per cent in Figure 2A, and 2 per cent in Figure 2D. In the centres of the zones, the Fe_7S_8 abundance is 4 to 5 per cent. Fe_9S_{10} occurs in very small amounts in a few samples only.

The Fe_7S_8 occurs as elongated grains parallel to the near-vertical schistosity which strikes northeast or southwest. The maximum susceptibility direction in these grains should lie in the schistosity plane and be almost parallel to the local geomagnetic field direction (Declination: 23°W; inclination: 72°). Consequently, the orientation of the grains probably enhances the induced magnetization resulting in a positive anomaly.

It is suggested here that the pyrrhotite may have originated by the thermal decomposition of pyrite which occurs commonly in the quartzites, shales and slates of the Halifax Formation. The decomposition may be due either to mild heating (Coates and Bright, 1965) during the low-grade metamorphism resulting in exposure of pyrrhotite containing lower layers in the cores of anticlines or to temperature and pressure conditions at or near faults. The pyrrhotite anomalies are truncated by the circular magnetic effects due to intrusive granites containing some magnetite. Thus Fe_7S_8 may be responsible for the generation of many more aeromagnetic anomalies in other areas which in the past have been attributed to magnetite.

References

Coats, A.W., and Bright, N.F.H.
1965: The thermal decomposition of pyrite; Dept. Energy, Mines Resources, Mines Br. Res. Rept., R. 173.

Geological Survey of Canada, Aeromagnetic Maps 7031G, 7034G, 7035G, 7036G.

Schwarz, E.J.
1968: Magnetic phases in natural pyrrhotite; J. Geomag. Geoelec., v. 20, p. 67-74.

1972: Magnetic properties of pyrrhotite and their use in applied geology and geophysics; Can. Mining J., no. 4.

Project 730004

A. K. Sinha
Resource Geophysics and Geochemistry Division

In the last two years, some attempts have been made to obtain the electrical constants of the ground (conductivity and dielectric constant) by the measurement of the mutual coupling of two small horizontal loops placed over the ground (Wait and Spies, 1972). However, the limited results published so far suffer from three disadvantages, (a) the results are available for only one coil configuration and hence it is difficult to judge whether the two horizontal coil configuration is the most suitable for our purpose, (b) the finite height of the coil systems over the earth is neglected, and (c) the mutual impedance Z_o used in the normalization of the final formula has the quasi-static (low-frequency) value rather than the general value. A fourth shortcoming of the published results is the small range of resistivity values considered. This statement becomes clear when we consider the range of resistivity variations that are encountered in the permafrost terrains of northern Canada.

A study was therefore initiated to consider the applicability of using the mutual coupling ratios of loops energized by harmonic currents for the determination of the electrical parameters of the ground in the permafrost zones. The computer program needed to calculate the mutual coupling of two coils in five coil configurations was completely general in the sense that the number of layers of the earth section could be arbitrary, the resistivity and dielectric constant of the layers could assume any value, the elevation of the coils as well as the thicknesses of the layers could be arbitrary and the frequency could assume any value. It was noted that in the general case, it was difficult to achieve high accuracy in computation if the coils were placed on the surface of the ground (Sinha, 1974), since the infinite integrals converged very slowly.

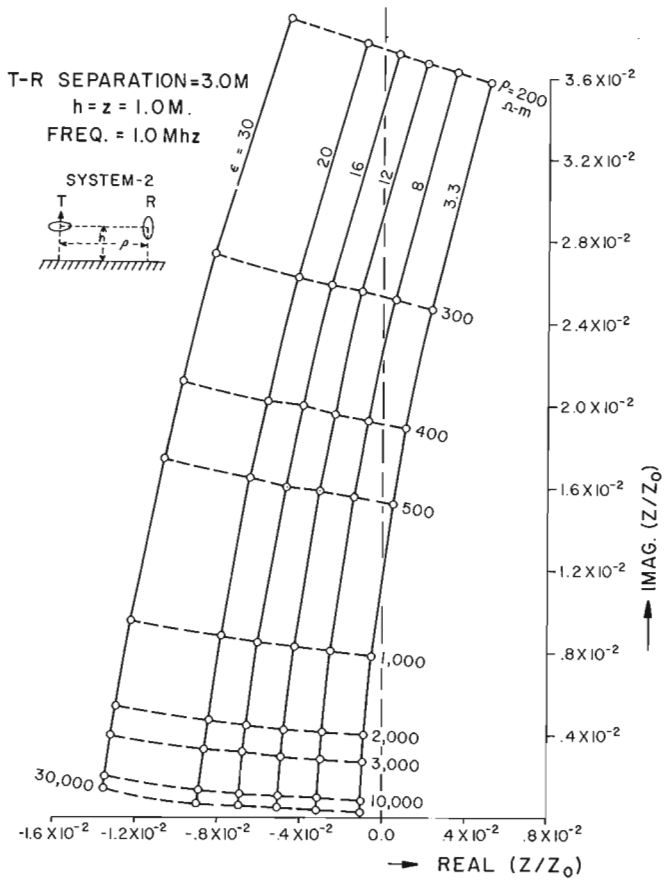

Figure 1. Argand diagram for System 2 at 1 Mhz for a coil separation of 3 metres and elevation of 1 metre for different resistivity and dielectric constant values.

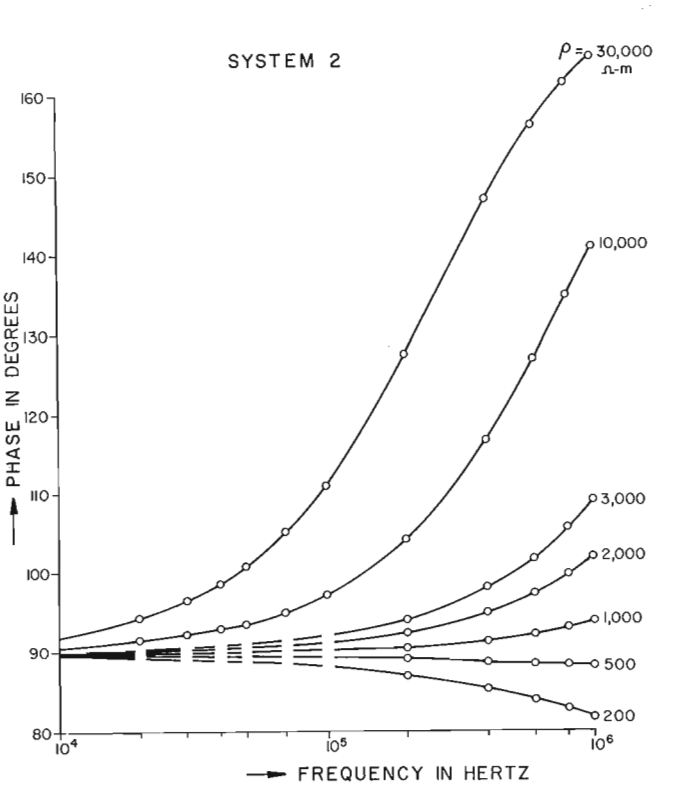

Figure 2. Plot of the phase of the secondary field against frequency for System 2 for a dielectric constant of 3.3 and different resistivity values.

However, the convergence of the integrals improved significantly if finite elevations of the coils were assumed.

Permafrost zones are usually complex structures, but in many cases the situation may be represented as a two-layer case and, in winter, even as a homogeneous case to a first approximation. Therefore our first model was a homogeneous lossy dielectric with relatively high resistivity and moderate value of dielectric constant. The purpose of our study was to compare the response in all five coil systems and decide which one will serve our purpose best for determining the electrical characteristics of the permafrost zone. The other purpose was to find a way of determining the electrical constants from the mutual coupling ratios measured at several frequencies. Since the permafrost is normally highly resistive the choice of frequency was from 10 Khz to 1 Mhz, an order of two decades so that the twin purposes of reasonable depth penetration and adequate resolutions would be met.

It was concluded from our theoretical study that System 2 (one coil horizontal, the other vertical) is the best for our purpose. Figure 1 shows the argand plot for that system at a frequency of 1 Mhz with the elevations of the transmitter and the receiver coils assumed to be 1 metre and their horizontal separations to be 3 metres. The resistivity values range from 200 ohm-m to 30,000 ohm-m while the relative dielectric constants range from 30 H/m to 3.3 H/m. If the real and imaginary components of (Z/Z_o) measured in the field at 1 Mhz with a system of the given dimensions are plotted in the argand diagram, the resultant point immediately provides the apparent resistivity and apparent dielectric constant of the medium for a layered medium and true resistivity and true dielectric constant for a homogeneous medium at 1 Mhz. Similar curves may be plotted for other frequency values so that the electrical parameters at different frequencies may be obtained.

The resolution however deteriorates when higher resistivity values are encountered. For example, the difference between 10,000 and 30,000 ohm-m lines is quite small and interpolations between them will likely produce errors. To overcome this problem, another set of curves would be needed. Figure 2 shows the plot of the phase of the secondary field in degrees against frequency in hertz for a dielectric constant of 3.3. The procedure for interpretation is therefore to determine the dielectric constant of the medium from Figure 1 and then choose the appropriate phase vs. frequency curve for that dielectric constant. The phase value in the field can easily be determined from the real and imaginary components of (Z/Z_o). Therefore a point may be plotted on Figure 2 appropriate to the frequency and phase. By interpolation, the resistivity is therefore determined. It should be noted that the resolution is fairly good even at 30,000 ohm-m (10 degrees). Hence for interpretation purposes, we need a set of similar curves with different dielectric constant values. It should be noted that these diagrams are valid only for the system dimensions discussed above. When either the coil separation or the coil elevations change, new sets of master curves will be needed. The big advantage of this approach is that in addition to determining the electrical parameters of the ground, we can also study the dispersion of these properties (change with frequency) at the same time.

This null-coupled E.M. system could be mounted on a non-conductive sled or trailer and towed by a powered vehicle across the terrain. This system would be useful for mapping the geological parameters of frozen ground, for determining sea-ice thickness and generally mapping ground for engineering purposes in a non-frozen environment.

References

Wait, J.R. and Spies, K.P.
1972: Note on determining electrical ground constants from the mutual impedance of small coplanar loops; J. Appl. Phys., v. 43, no. 3, p. 890-891.

Sinha, A.K.
1974: Theoretical studies to aid EM interpretation; in Report of Activities, April to October 1973, Geol. Surv. Can., Paper 74-1, Pt. A, p. 101.

Project 730004

A.K. Sinha
Resource Geophysics and Geochemistry Division

Several attempts have been made in the last few years to design a technique for determination of sea-ice thickness by geophysical means (Adey, 1970; Christoffersen, 1970; McNeill and Hoekstra, 1973). With development work in the northern part of Canada (Arctic Islands and the sea) gathering momentum every day, this problem has assumed greater importance lately especially in transporting heavy equipment across the ice between the Arctic Islands. Some experiments have been made to use radar sounding or measurement of the wave tilt to accomplish the task. However, for a fast reconnaissance technique, it would be desirable to have an inexpensive, portable system which could be operated by one man and provide a reasonably accurate result right in situ. The two above mentioned techniques hardly meet that criteria. As a result, several alternative approaches are being tried by a few firms with the aim of bringing out a portable sea-ice thickness detecting instrument to the market within a short time.

With this background in mind, it was considered useful to study theoretically the response of two commercially available electromagnetic prospecting instruments to a typical northern situation, so that an idea about their usefulness for determining sea-ice thickness may be obtained. For that purpose, a two-layer situation was assumed where the top layer was sea-ice of a given resistivity and variable thickness. The bottom layer was seawater of another given resistivity. The two instruments considered were the Geonics EM-15 and the Apex double dipole e.m. system. In a way, these two systems are somewhat similar in that they employ the same coil configuration (both coil axes at 54.7° from the horizontal) which produces a minimum

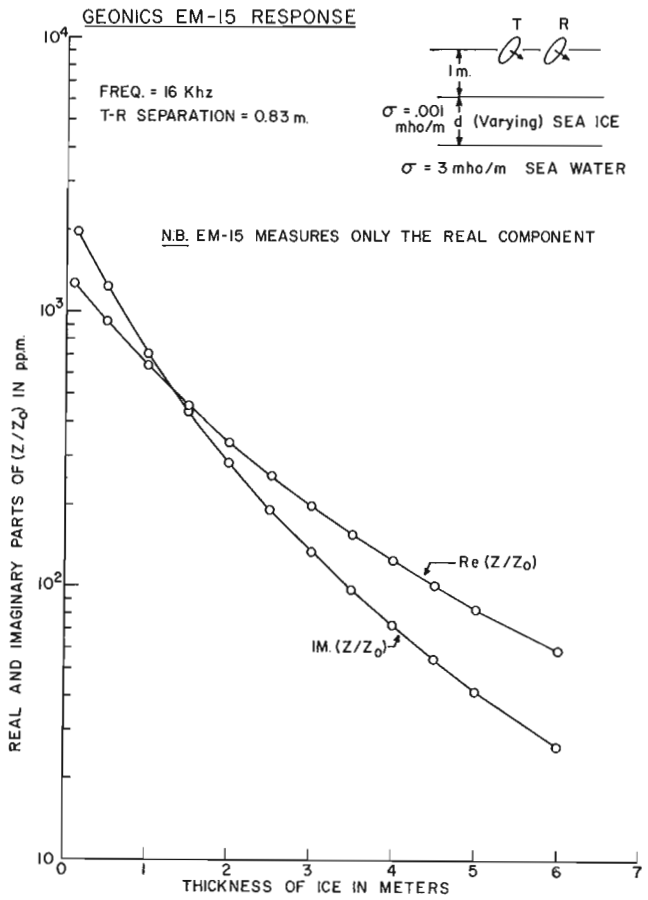

Figure 1. Variation of the real and imaginary parts of (Z/Z_O) against the thickness of sea-ice for the Geonics EM-15 instrument.

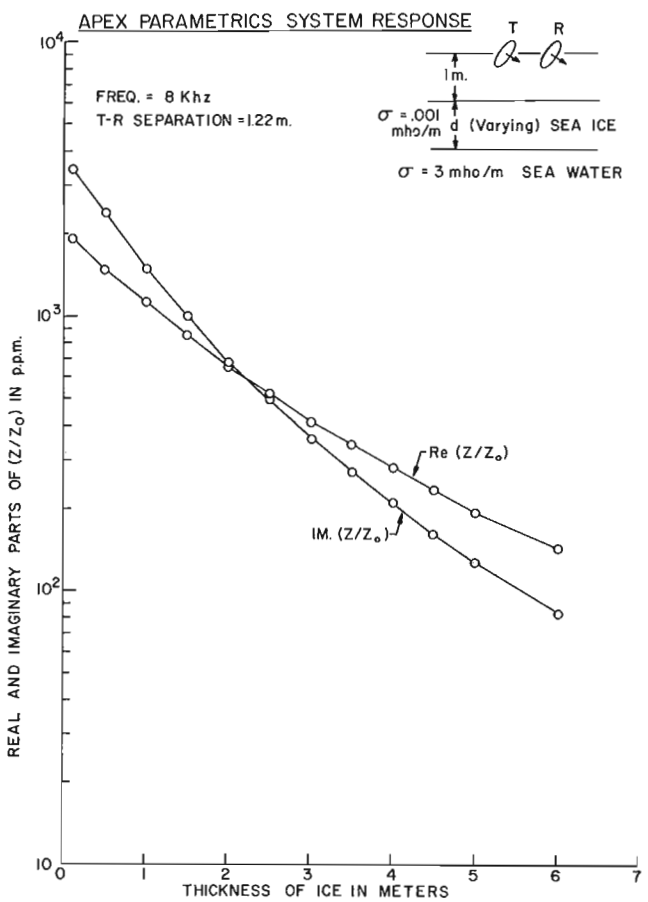

Figure 2. Variation of the real and imaginary parts of (Z/Z_O) against the thickness of sea-ice for the APEX double dipole system

coupled system (Sinha and Collett, 1973). The coil separations and the frequencies in the two systems are 0.83 m. and 16 Khz for the EM-15 and 1.22 m. and 8 Khz for the Apex system. The relatively high frequencies of the two systems are important for this purpose since this results in sharper resolution of the fairly highly resistive ice layer. Each instrument can be operated by one man and it is assumed that the height of the coils over the ice is 1 metre, which would be more or less true when the instrument is carried by the operator.

Figure 1 indicates the variation of the real and the imaginary parts of the mutual coupling ratio (Z/Z_o) in parts per million against the thickness of ice in metres for the EM-15 instrument. The geometry of the system and the layerings are shown at the top of the figure. The imaginary parts of (Z/Z_o) have also been plotted here although, in practice, EM-15 measures only the in-phase component. The trend of the variation of both components with thickness is the same, although imaginary component shows a steeper gradient and hence may be more useful. The quadrature component is also less affected by any slight change in the current in the transmitter coil. From Figure 1, it is clear that the EM-15 may be used advantageously for sea-ice thickness determination up to 5 metres.

Figure 2 indicates the response of the real and imaginary parts of (Z/Z_o) against sea-ice thickness for the Apex system. Qualitatively, the response is similar to that for the EM-15. However, the magnitude of the anomalies are much greater in this case. Hence a greater thickness of ice may be detected by this system than in the previous system. In fact, even when the thickness is 6-7 metres, the anomaly is of the order of 100 parts per million. Furthermore, since both components are measured in this system two independent estimates of thickness may be obtained. However, the imaginary component, because of its greater slope will have higher resolution. It is apparent from these two diagrams that these two portable existing e.m. systems are capable of sea-ice thickness determination up to 6-7 metres at a reasonable cost.

References

Adey, A.W.
1970: A survey of sea-ice thickness measuring techniques; Report 71-14, Communications Research Centre, Department of Communications, Ottawa, Ontario, p. 1-28.

Christoffersen, P.D.
1970: Recent radar soundings of fresh water ice and sea-ice; Proc. Int. Conf. Radioglacialogy, Lyngby, Denmark, p. 149-153.

McNeill, D. and Hoekstra, P.
1973: In-situ measurements on the conductivity and surface impedance of sea-ice at VLF; Radio Science, v. 8 no. 1, p. 23-30.

Sinha, A.K. and Collett, L.S.
1973: Electromagnetic fields of oscillating magnetic dipoles placed over a multi-layer conducting earth; Geol. Surv. Can., Paper 73-25, 48 p.

37. OVERHAUSER MAGNETIC RESONANCE MAGNETOMETER

Project 690035

S. Washkurak
Resource Geophysics and Geochemistry Division

Ever since the main magnetic field of the earth was discovered as early as the eleventh century in China, man has been fascinated by the fact that the earth is a magnet. The search for the cause of the earth's field stimulated the early researches of such men as Wm. Gilbert and Edmund Halley. The direction of the field has remained a most useful tool for navigation. The application of measurement of the earth's field to prospecting and geological mapping had its beginning in Sweden in 1921. The fluxgate magnetometer developed in 1941 by Gulf Research, Bell Labs and Airborne Instrument Laboratory of the U.S. was quickly adapted to antisubmarine purposes in World War II. The U.S. Geological Survey modified this instrument to measuring geomagnetic effects of geological structures and flew the first airborne surveys over potential oil-bearing territory in Alaska in 1945. Gulf Oil, having obtained a worldwide patent on the instrument and initially charging a royalty of $10.00 per line mile, began private aeromagnetic surveys of northern Ontario in 1947 detecting a huge iron deposit in Boston Township which was brought into production in 1964. The Geological Survey of Canada began an aeromagnetic program in 1946 and in co-operation with the National Research Council obtained a magnetometer from the U.S. Navy and installed the modified fluxgate magnetometer in an Anson aircraft and subsequently into a PBY Canso. Aeromagnetic surveys of several million miles have since been completed jointly by the Geological Survey and provincial mining departments since 1948. The need of a new or alternate magnetometer soon became apparent due to the problems experienced with the maintenance of electronic instrumentation, high royalty charges and the advent of digital computer methods. The following report is a summary of the successful development of a royalty-free, continuous reading magnetic resonance proton precession magnetometer with an absolute digital accuracy of 0.03 gamma.

The fundamental discovery of nuclear magnetic resonance (NMR) was made simultaneously in 1946 by independent groups at Stanford and Harvard Universities. This was recognized by a joint award of the Nobel Prize in Physics to Professors Block of Stanford and Purcell of Harvard in 1952. The fundamental NMR equation relating the electromagnetic frequency (Larmor frequency) W to the magnetic field strength H is $W = \gamma H$. The constant γ is commonly called the gyromagnetic ratio. It is a fundamental constant of nature given to atomic nuclear relating its magnetic moment to its nuclear spin. The effect being observed is an extremely minute one relating Boltzman's statistical distribution of energy levels in a static magnetic field. These atoms which absorb a proton of energy in flipping the orientation of spinning nuclei produce a detectable signal of only several microvolts. It wasn't until 1954 that Packard and Varian first observed the free precession of protons in water in the earth's magnetic field.

The working cycle of a nuclear magnetometer includes two successive physical processes: The polarization of the working hydrogenated substance (water or ethanol) and the measurement of the frequency of the nuclear induction signal. Packard and Varian polarized their samples to enhance the detection of the precessing proton by applying a large DC magnetic field (100 Gauss) at right angles to the earth's field. When the polarizing field is removed, the protons precess in phase coherence about the total earth's field direction producing a detectable signal in analogy similar to the affect a stop light would have on the speeding traffic of a freeway. When the light turns green the traffic initially moves in a group. With an intermittent polarize read cycle of one second the magnetic field can be measured to an absolute accuracy of one gamma.

In 1957 Dr. H. Wesemeyer joined the Geological Survey and applied for a Canadian patent (Wesemeyer, 1965) on a continuous reading proton precession magnetometer based on the Overhauser effect first described by Overhauser (1953) and improved on by Abragam (1955). The use of the phenomena of dynamic nuclear polarization (Overhauser effect) in a paramagnetic solution (free radical) has enabled nuclear magnetometers to be substantially improved. Simultaneously, it has been possible to synchronize the processes of polarization and measurement and thus to construct a fast acting continous reading instrument. In liquid solutions the effect can be produced by saturating (applying a radio frequency electromagnetic field) to the electron resonance of a dissolved free radical or paramagnetic ion whilst simultaneously observing the solvent proton magnetic resonance. A free radical is an atom or molecule which contains one or more unpaired electrons. The first authenticated free radical, triphenylmethyl was discovered by Gomberg in 1900. The stability of organic-free radicals depends on the chemical circumstances. The majority are highly reactive and have lifetimes measurable in micro or milliseconds unless stabilized by trapping in some inert matrix. The initial major problem was to synthesize an organic stable free radical soluble in water that exhibited a single narrow resonance line easily saturated to maximize dynamic nuclear polarization. Initially fremy salt (potassium nitro-sodisulfonate) was the only working free radical available which exhibited these properties; unfortunately, it decomposed in tens of minutes even with stabilizing substances such as K_2CO In the early sixties, highly stable nitroxyl radicals possessing properties analogous to those of fremy salt were synthesized. K. Hoffman of the American Cyanamid

Corp. described the synthesis of di-t-butyl nitroxide in the Journal of the American Chemical Society and Neiman and Rozontzev (1962) described another nitroxyl radical tetra methyl piperidine oxyl (TEMPO). Dr. L.C. Leitch of the Organic Synthesis Division of the National Research Council first synthesized TEMPO in Canada. These free radicals are stable indefinitely and are now available off the shelf from Frinton Laboratories, N.J.

An emission type maser magnetometer using TEMPO was successfully completed by the Geological Survey in 1968 with a resolution of 0.05 gamma. To reduce Larmor frequency pulling, electromagnetically decoupled "Block coils" were used. These are two coils with perpendicular axis. One set of coils is used for the precession frequency pickup and the other for decoupled feedback. A coaxial cavity was used for saturation of the electron resonance line at 69 megahertz. A homogeneous electromagnetic field of two watts of radio frequency power is required to saturate the electron resonance line. Unfortunately, a simple solenoid of a few turns does not produce a homogeneous field and also heats both the high dielectric sample of water due to eddy currents. Cavities are commonly used at higher frequencies for electron spin studies but for wavelengths of a few metres it would appear that the size of cavity required would be too large. This is not the case, in fact, a cavity shorted at one end and less than 1/10 wavelength in length has the added feature of having little electric field component to heat the sample and of course no field outside the cavity to heat the Larmor pickup coils.

Scintrex of Toronto, Ontario, have been licensed through Canadian Patents and Development to produce a commercial magnetometer based on the Wesemeyer patent. Dr. Ivan Hrvoic the Scintrex project engineer did an excellent design of the commercial MRM-1 multiple resonance magnetometer that has a resolution of 0.03 gamma at a sampling rate of 1 second. Two major design improvements were incorporated in the instrument for which Scintrex have submitted a patent application that does not affect the royalty-free status of the Geological Survey. The dispersion component of the NMR signal to stabilize the frequency of a voltage controlled oscillator is used which offers an improvement on the signal to noise ratio and the synthesis of an alternate nitroxyl free radical tetra methyl piperidone oxylidine has been found.

The objective of producing a royalty free continous reading Overhauser nuclear magnetic resonance digital magnetometer with a resolution of 0.03 gamma has been realized.

References

Abragam, A.
1955: Dynamic nuclear polarization of non-metals; Phys. Rev., v. 98, no. 84, p. 642-643.

Neiman, P. and Rozontzev, I.
1962: Synthesis of Nitroxyl, Free Radical; Nature, v. 89, no. 6, p. 711-712

Overhauser, A.W.
1953: Dynamic nuclear polarization; Phys. Rev., v. 92, no. 62, p. 411.

Wesemeyer, H.H.
1965: Nuclear magnetic resonance magnetometer; Can. Patent No. 706, 520, issued March 23.

A. Environmental Marine Geology

38. ENVIRONMENTAL MARINE GEOLOGY OF A COASTAL INLET

Project No. 730070

Dale E. Buckley
Atlantic Geoscience Centre, Dartmouth

A Summary of Results of the Impact of Man on the Marine Environment of Canso Strait and Chedabucto Bay

In 1954, a causeway was completed linking the Nova Scotia mainland to Cape Breton Island across the Strait of Canso. Upon its completion, the tidal circulation (previously about the equivalent of one-half of the daily discharge of the St. Lawrence River) and ice transport through the strait between the Gulf of St. Lawrence and the Atlantic Ocean ceased. The causeway has inadvertently created an excellent, year-round, deep-water harbour in the area southeast of the causeway. Nearby communities swelled as a result of industrial development encouraged by the potential of the harbour facilities. The industries established, such as a pulp and paper mill, oil refinery, and heavy-water plant, are affecting not only the economy but the environment as well.

In 1973, an integrated multidisciplinary team of scientists and technicians from the Atlantic Geoscience Centre carried out a research evaluation of the marine area (Buckley, 1973) to establish: (1) the effects of the causeway on the marine environment, especially on the distribution of sediments and benthonic ecosystems; (2) the urban and industrial impact as measured by environmental quality surveys including chemical, biological, and sedimentological parameters and a comparison of paleoenvironmental and present-day indicators; (3) the degree of restoration of the beach and nearshore environments of Chedabucto Bay from the ARROW oil spill of 1970; and (4) the geotechnical properties of bottom sediments in the strait for use in planning future development.

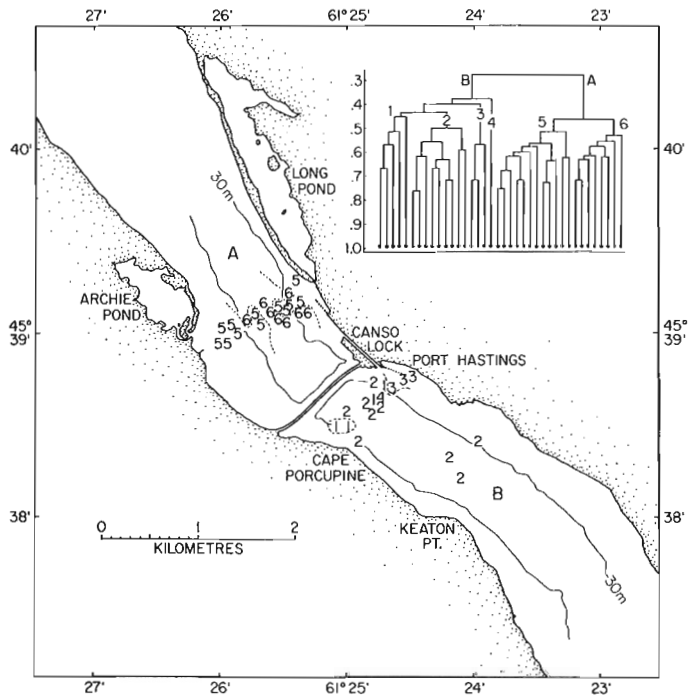

Figure 1. Foraminiferal associations defined by cluster analysis in the vicinity of the causeway. Numbers designate clusters formed between the significance levels 0.4 and 0.5. The letters A and B designate major clusters which differentiate the north and south portions of the strait while the numbers designate minor differences associated with substrate and bathymetric controls.

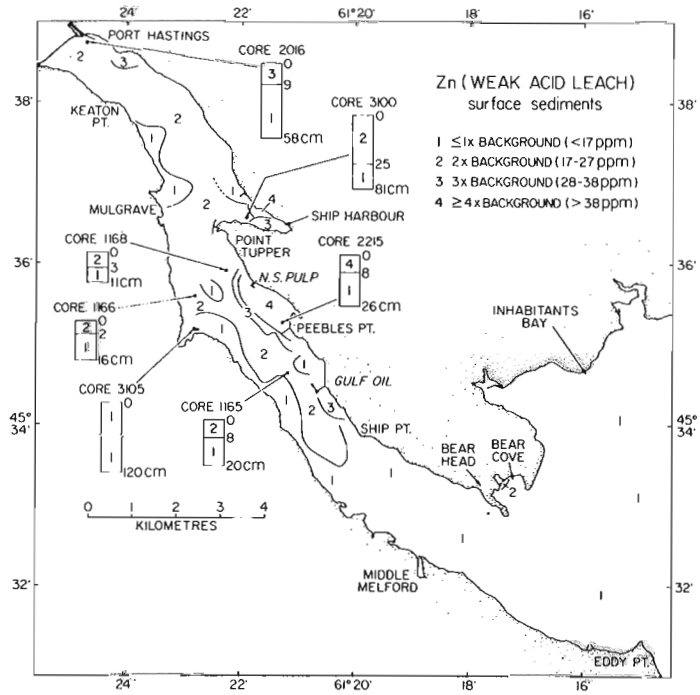

Figure 2. Turbidity of surface waters in the Strait of Canso as measured by optical attenuance of white light. Turbidity maximum occurs slightly northwest of major industrial effluent, under the influence of southeasterly winds.

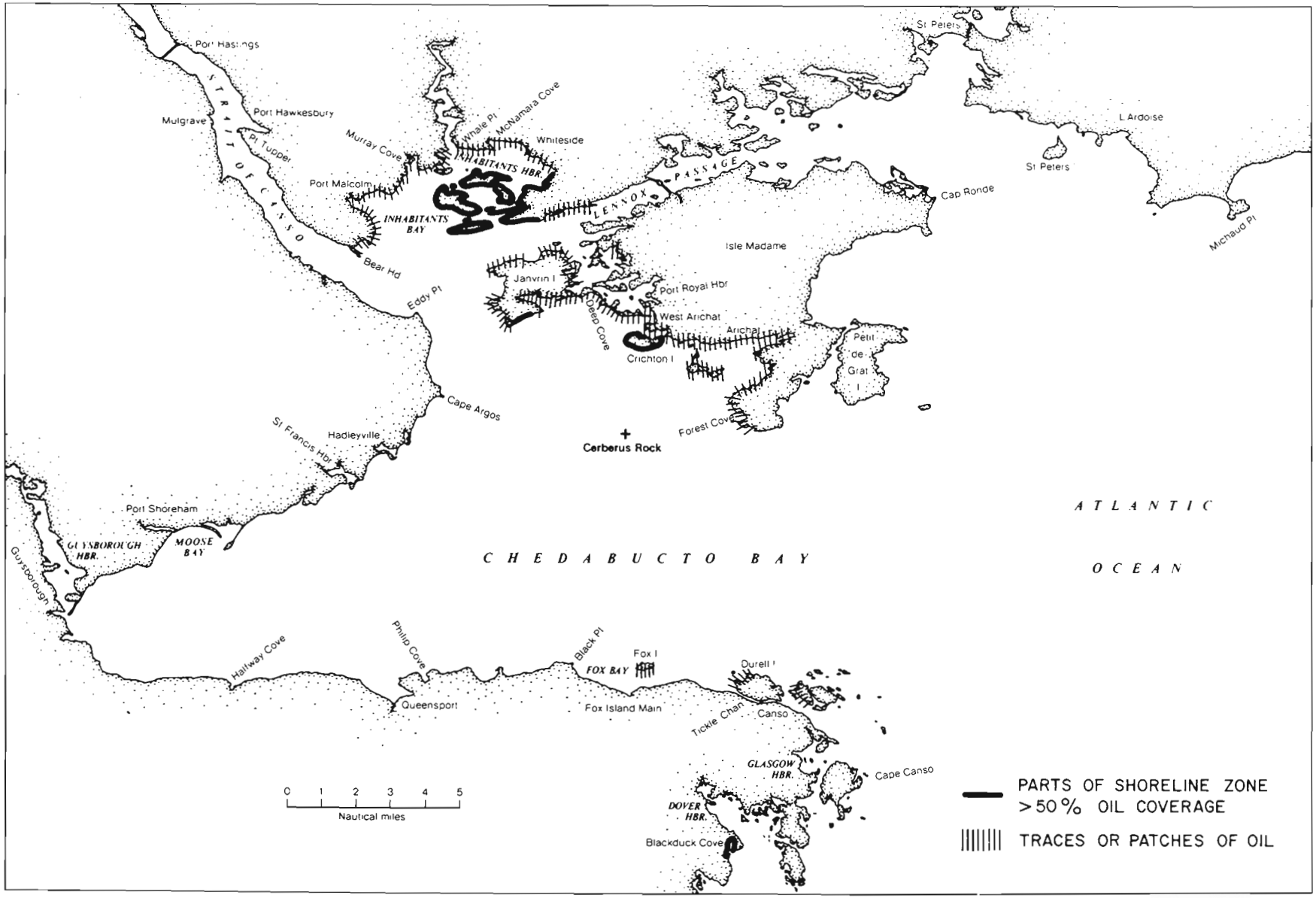

Figure 3. Distribution of oil contaminated beaches in Chedabucto Bay, September 1973.

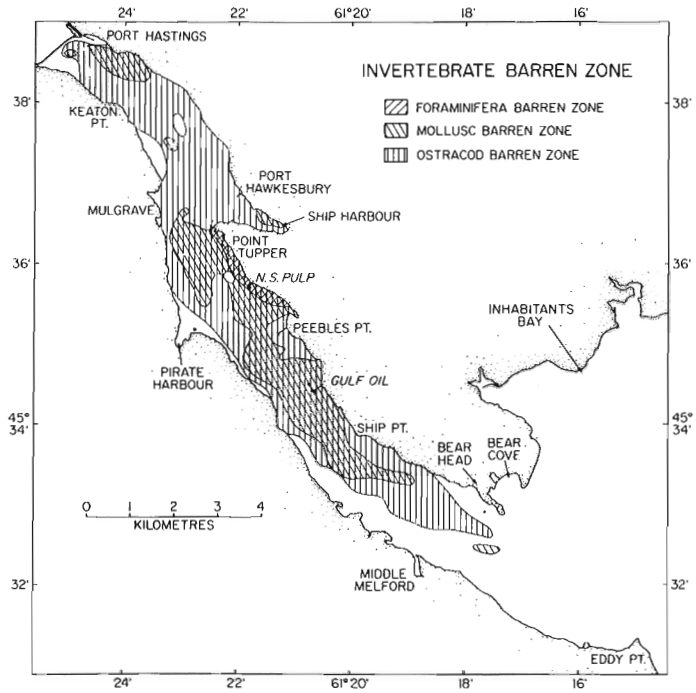

Figure 4. Aerial relationships of foraminifera, mollusc and ostracod barren zones in the Strait of Canso. Location and extent of barren zones appear to be related to proximity of industrial and urban centres.

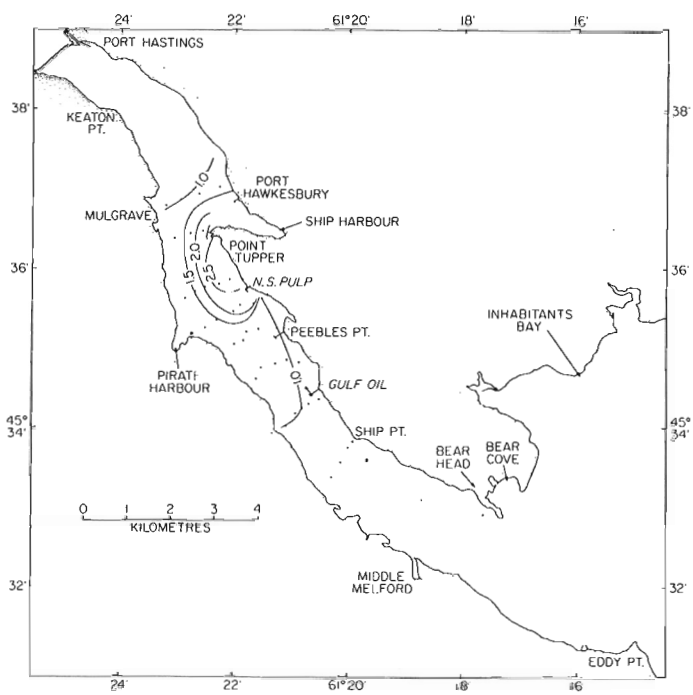

Figure 5. Distribution of leachable (weak acid) zinc in surface sediments and cores from the Strait of Canso. Note that highest leachable metal was found adjacent to urban and industrial centres and in upper portions of cored samples.

Since the causeway, circulation in the strait has changed from vigorous exchange and mixing between the Atlantic and Gulf of St. Lawrence areas to a system of separated bays within which wind-driven circulation dominates over tidal influences. Each segment of the strait now has different water-mass characteristics during much of the year and different sources and quantities of sediment. The quality and distribution of suspended particulate matter on either side of the causeway differ significantly during the summer months, with more organically-rich particulate matter south of the causeway.

Existing benthonic ecological differences between the south and north sections of the strait can be characterized by the different species assemblages of foraminifera (Fig. 1) and molluscs in surface sediments. Bathymetric and sedimentological substrate variations within the strait have only secondary influence on the distribution of foraminifera and molluscs. Paleoecological studies of sediment cores show that there is only a subtle difference in foraminiferal assemblages at a depth of 1 to 2 cm in some cores. By contrast, a distinct change in the molluscan assemblages with depth indicated a post-causeway influence could be recognized in the upper 5 cm of the sediment. Calculated rates of sedimentation deduced from analyses of pollen in sediment cores indicate that a minimum of 1.6 to 3.8 cm of sediment were deposited north of the causeway since its construction and that similarly 1.8 to 2.9 cm of sediment were deposited south of the causeway.

The contemporary environment of the marine area of the Strait of Canso south of the causeway is being affected by the presence of urban and industrial centres along the shores, mainly by the addition of anthropogenic substances to the marine waters of the strait. The major concentration of waste materials emanates from the industrial effluent of the Nova Scotia Forest Industries pulp plant located on the eastern shore of the strait near Point Tupper. These waste materials, including high concentrations of organically-rich suspended solids, are dispersed through the surface waters of the strait and carried in the direction of the prevailing winds (Fig. 2). From these processes significant quantities of such wastes are being deposited in the bottom sediments adjacent to, and south of, the industrialized area.

The ecological impact of the environmental stress induced by the industrial effluents is indicated by the biotopes mapped on the basis of three types of benthonic invertebrate fauna. Foraminiferal species appear to be relatively more tolerant to environmental stress, but even these forms cannot inhabit the bottom immediately adjacent to the outfall areas from the pulp mill and the heavy water plant. The coincidence of low populations of foraminifera with the absence of living molluscs in the central channel areas adjacent to the industrialized shore south of Point Tupper indicate that the polluted environment extends to the middle of the strait and south of the Gulf Oil Company ocean terminal. Ostracod species appear to have been most sensitive to the "subnormal" environment of the strait and are not rep-

resented by living specimens in 66 per cent of the bottom sediments of the strait (Fig. 4).

Geochemical and ecological indicators determined from sediment cores taken in the polluted and subnormal areas of the strait show that the environment has changed during the periods of most recent sediment deposition. This environmental change has resulted in a decrease in the foraminiferal species diversity and the displacement of biotopes that previously occurred in the presently polluted areas. Molluscan species also occur in subsurface sediments in areas now barren. The correlation of these ecological changes with changes in the concentration of the indicator metal, Zn (Fig. 5), strongly suggests that the advent of urban and industrial growth has induced significant biological responses.

The diverse shoreline environments of Chedabucto Bay are somewhat characteristic of the variety of inlets found along much of the coast of eastern Nova Scotia. Many of the beaches in Chedabucto Bay are in a delicate state of equilibrium with the hydrodynamic environment of the littoral zone, and the rising sea level. Only in the northern sections of the bay is there an available source of erosional products to supply sediments to the beaches. The removal of sediments from beaches to reduce the effects of oil contamination due to the spill from the tanker ARROW had an immediate effect on all beaches, but the lasting effects were most pronounced on the beaches where the resupply of sediments from along shore or the littoral zone is limited.

Although the coastline appears to be essentially free of large oil concentrations, residues are still present in varying amounts on nearly all previously contaminated beaches (Fig. 3). These residues are most prevalent in low-energy environments or on sections of beaches above the normal high-water mark. The chemical composition of oil residues indicates that in low-energy environments the rate of degradation is very slow and that these areas will remain polluted for many years. In high-energy environments the oil is being degraded by normal weathering processes and by bacterial degradation with the result that the highly viscous resins and non-hydrocarbon compounds adhere to rock and pebble substrates.

The nearshore marine sediments from Chedabucto Bay and from the northern and southern portions of the Strait of Canso are unique because of their low bulk densities but are otherwise characteristic of these type of sediments found in similar depositional environments. Clayey silts and silty clays found most frequently below coarser-textured sediments in small bays and in the central portion of the strait exhibit two geotechnical characteristics that differ from those expected for recently deposited marine sediments. These sediments exhibited a reserve resistance to stresses applied in excess of the in situ stresses. The second unusual characteristic of these sediments is their capacity to be compressed to a degree greater than would have been predicted from accepted empirical relationships. The most probable cause of these unusual properties is the alteration of the sediments by rheological processes and the high content of organic matter.

The profound regional and stratigraphic variability of sediment types and their geotechnical properties in the Strait of Canso area precludes the extrapolation of both in situ and laboratory data to a regional assessment of engineering implications. If, however, the few samples studied are representative of the range of possible characteristics that might be expected in a coastal inlet of this type, it is clearly indicated that detailed survey techniques will be required to evaluate the potential use of the natural sediments in future industrial developments.

References

Buckley, D.E.

1973: Environmental Marine Geology of the Strait of Canso and Chedabucto Bay, Port Hawkesbury, Nova Scotia. Field Report No. 73-022, Bedford Institute of Oceanography, Dartmouth, N.S.

1974: Environmental Marine Geology of a Coastal Inlet; in Report of Activities, April to October, 1973, Geol. Surv. Can., Paper 74-1, Pt. A, p. 111-112.

39. GEOCHEMICAL INTERACTION BETWEEN NATURAL WATERS AND PARTICULATE SOLIDS IN THE MARINE ENVIRONMENT

Project No. 730089

R.E. Cranston
Atlantic Geoscience Centre, Dartmouth

Introduction

Steady state equilibrium theories have been proposed in the past to account for the amount of major ions added to and removed from the marine environment in the process of forming present day oceans. However, analyses of natural systems have not been adequate to confirm the specific reaction schemes that have been used in the steady state theories or to answer basic questions concerning total salt content, constancy of major ion composition, the importance of solid-liquid equilibrium and the controls of oceanic pH.

Part of the purpose of this project was to document the effect on cation composition and pH of water by storing natural suspended matter in natural water and in deionized water. A river-estuary system was selected as an environment that would produce varying degrees of oceanic conditions as well as relatively freshly weathered suspended matter. A second environment was chosen, containing samples from a marine bay with high concentrations of natural suspended matter that were from a different geological setting and had been in contact with sea water for a longer time than had been the freshly weathered material in the river-estuary system.

Results

When concentrated amounts of natural suspended matter are stored in their natural water for a short period of time, significant changes in water chemistry result for pH, dissolved silicon and dissolved calcium. When the same suspended matter is stored in deionized water, significant changes in the water chemistry with respect to natural water result for pH, Mg, Ca, K and Sr. No indication of cation exchange was detected. It is suggested that the short storage time and an insufficient amount of suspended matter account for the lack of exchange.

Significant interrelationships result between (a) suspended matter concentration and pH; (b) suspended matter and dissolved Si; (c) Si and pH; (d) salt content and pH and (e) dissolution of particulate Ca and pH. The control of pH in natural water results from the concentrations of total salt, particulate and dissolved silicon and the carbonate — CO^2 cycle.

The actual control of pH in nearshore saline water is a result of carbonate equilibrium, however the activities of the species involved in this equilibrium are controlled by the total ionic strength of the water. Silicate control of pH is significant in natural low chlorinity water (<0.1% Cl) containing high concentrations of suspended matter (>100 mg/ℓ).

40. GEOCHEMICAL ANALYSIS OF HYDROCARBONS OF SAMPLES FROM EASTERN OFFSHORE OIL WELLS — GASEOUS HYDROCARBONS AS A MEASURE OF OIL AND GAS POTENTIAL

Project No. 730086

J.D. Leonard and M.A. Rashid
Atlantic Geoscience Centre

The main objective of these investigations is to provide basic geochemical information for the estimation of oil and gas potentials of the offshore exploratory oil wells being drilled off the Atlantic coast. These studies involve: (1) an estimation of the gaseous hydrocarbon content (C_1-C_4) of the cuttings of the exploratory oil wells; (2) organic richness based on organic carbon content of the sedimentary strata penetrated during coring; (3) degree of wetness of gaseous hydrocarbons and (4) evaluation of the maturity of organic facies under different lithological conditions.

During the report period, a total of 1,874 canned core cuttings from nine exploratory oil wells were analyzed for organic carbon and gaseous hydrocarbons (C_1-C_4).

AN INVESTIGATION OF ICE IN THE LITTORAL ZONE AT RICHIBUCTO, NORTHEAST NEW BRUNSWICK

Project No. 730088

E.H. Owens
Atlantic Geoscience Centre, Dartmouth

Introduction

A barrier beach near Richibucto Head, N.B. (46°40'30"N; 64°43'00"W) was monitored at regular intervals from mid-December 1973 to mid-April 1974 to record the effects of ice in the littoral zone. Few data are available on the formation and decay of ice or on the transport of sediment by ice in the shore zone of the southern Gulf of St. Lawrence. As ice is present on these beaches for up to four months each year, further data are required to identify the role of ice in littoral processes and sediment transport. Beach profiles were surveyed at approximately a two-week interval from December 12th to April 10th along a 250 m section. Nearshore profiles were obtained by echo-sounding before freeze-up of the sea-ice (January 3rd) and at the first occurrence of open water (March 20th). To determine the volume and nature of sediment incorporated in the ice during freeze-up, trenches were cut in the beach-ice and the shorefast-ice. The results of this investigation represent the effects of ice in a relatively sheltered micro-tidal (mean range < 1 m) environment in the southern Gulf of St. Lawrence.

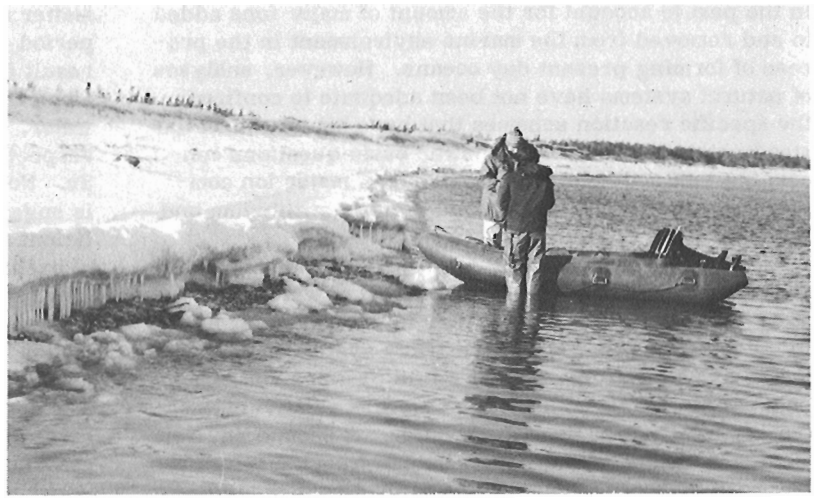

Figure 1. Intertidal zone January 15, 1974, two hours after high tide. An ice-foot has developed at the high water mark (mean tidal range 0.7 m) and is being enlarged by the freezing of swash and wave spray. The ice-foot contained only small amounts of sediment. The intertidal zone is frozen and covered by a thin (5-10 cm) veneer of ice.

Freeze-up

Ice began to form at the mean high water mark during the first week of January following the passage of a storm centre through the region on December 30-31. By January 15th the ice foot was up to 1 m in height and the entire supratidal zone was covered with ice and/or consolidated snow (Fig. 1). Ice formed a nearly continuous cover in the intertidal and subtidal zones. It was not possible to determine the seaward extent of this ice but a minimum distance was 6 m seaward of the low-tide swash line.

The freeze-up cycle was complete by early February at which time three distinct zones of ice could be identified: the ice foot; the hinge zone; and the sea-ice. The hinge zone is that part of sea-ice adjacent to the ice foot which is grounded at low tide and which is characterized by a series of cracks parallel to the shore

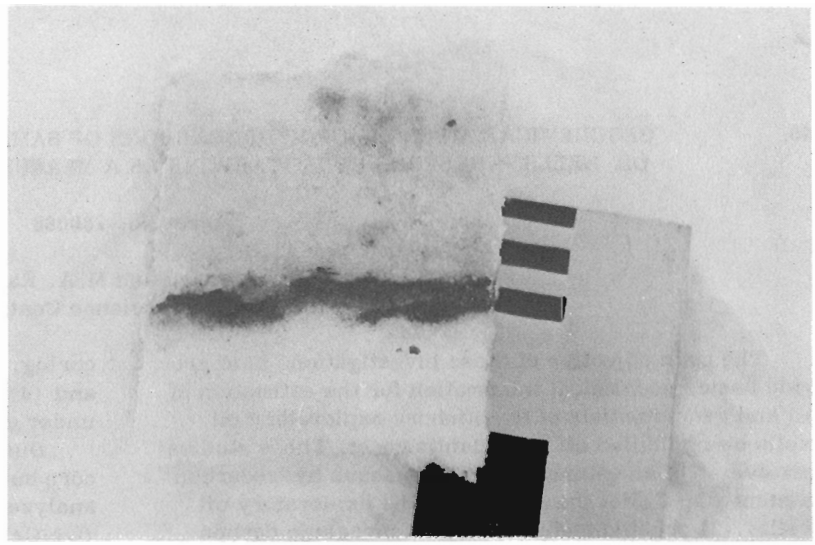

Figure 2. Section cut from the base of hinge zone ice. Sediment froze to the ice when it was grounded and with a higher tidal or sea level new (cleaner) ice formed as the floe was lifted off the bottom. Each of the three black bars on the scale is 1 cm wide (January 29, 1974).

that permit independant movement of floes. At this location the width of the hinge zone varied between 5 and 20 m, depending on the beach gradient. The sea-ice grounds occasionally, such as at spring low tides or on the nearshore bar, but is usually floating and does not have the maze of cracks which characterizes the hinge zone.

Trench sections in all three ice zones indicated that only small amounts of sediment were incorporated within the ice. Sediment was present as a result of (1) wave action during freeze-up, (2) aeolian transportation from the backshore, and (3) translocation of sediments frozen to the base of grounded ice in the hinge zone (Fig. 2). This latter process is discussed in more detail by Medcof and Thomas (in press).

Break-up and Ice Decay

The nearshore sea-ice had moved by the second week in March and open water conditions with varying fetches remained until the end of the observation period in mid-April. Once the sea-ice went the ice-foot decayed rapidly and by April 10th only traces of ice remained in the littoral zone. Beach profiles surveyed on April 10th show that on some sections of the study site the beach had eroded to a level lower than that surveyed before freeze-up. Thus all the effects of ice in these sections had been removed within one month of break-up.

Although this investigation terminated in April the influence of ice continues into May by limiting fetches and by the presence of floes. During studies undertaken in 1972 (Owens and Harper, 1972), remnants of ice-push ridges similar to those described in arctic regions (Owens and McCann, 1970), were observed on the beaches of northeast New Brunswick during June. These were not visible in August and the sediments had been redistributed by wave action.

Discussion

The winter of 1973/74 was relatively mild in this area, with mean daily minimum and maximum temperatures often near or above the long-term averages. The nearshore zone was frozen over for a 10-week period and an ice-foot was present for a 12- to 13-week period. No major storms occurred during freeze-up and only small amounts of sediment were disturbed in the littoral zone by the effects of ice. Small amounts of sediment were incorporated within the shorefast ice and little material was lost from the shore zone by ice-rafting. Ice-decay features were rapidly destroyed by storm waves. The most important effects of ice in this region are in limiting littoral zone processes for three to four months and in the formation of ice-push ridges above the high water mark.

References

Medcof, J.C. and Thomas, M.L.H.
Surfacing on ice of frozen-in marine bottom materials; J.Fish. Res. Bd. Can. (in press).

Owens, E.H. and Harper, J.R.
1972: The coastal geomorphology of the southern Gulf of St. Lawrence: A reconnaissance; Marit. Sediments, v. 8, no. 2, p. 61-64.

Owens, E.H. and McCann, S.B.
1970: The role of ice in the arctic beach environment with special reference to Cape Ricketts, southwest Devon Island, N.W.T., Canada; Am. J. Sci., v. 268, no. 5, p. 397-414.

42. INFLUENCE OF MARINE ORGANIC MATTER ON THE ENGINEERING PROPERTIES OF SEDIMENTS AND UNDERWATER STRUCTURES.

Project No. 730087

M.A. Rashid, Atlantic Geoscience Centre
J. Brown, Nova Scotia Technical College, Halifax

A careful evaluation of the geotechnical properties of sediments is highly essential to avoid high performance risks of all onshore, nearshore and underwater structures that are increasing in use with increased ocean exploration. The geotechnical properties of sediments depend upon a number of factors; one of the most significant being the inherent organic matter content. Organic matter in sediments exerts an influence on the physical and chemical properties of sediments even at concentrations of a few per cent by weight.

The results of laboratory investigations suggest the following modifications in the engineering properties of sediments with various organic content.

Atterberg limits	Per cent organic matter			
	0	2	3	4
Liquid limit	28.6	40.3	46.2	49.8
Plastic limit	19.1	21.9	25.5	28.0
Plasticity index	9.5	18.4	20.7	21.8

The tests indicate an increase for all Atterberg limits with increasing organic content.

The results also suggest that for a given water content the remoulded shear strength increased with increasing organic matter. The organic sediments containing 2-4 per cent organic matter were found nearly twice as compressible as the inorganic sediments. In the presence of organic matter the sediments exhibit much greater creep tendencies and would consolidate under load at about one-seventh of the rate of the inorganic sediments.

The organic compounds (humic acid, fulvic acid, amino acids, etc.) present in soils, sediments and water columns are known to exert solubilizing effects on normally insoluble salts, rock forming minerals and clay minerals, etc. (Rashid and Leonard, 1973; Baker, 1973; Kodama and Schnitzer, 1973). It was therefore, considered pertinent to ascertain the possible effect of marine organic compounds on cement-concrete structures that are being used extensively in ocean exploration. The experimental work of this project is not yet completed. The preliminary observations of the laboratory investigations tend to suggest that 10-40 pp concentrations of organic compounds in sodium chloride solutions release certain cations from the cement-concrete blocks.

References

Baker, W.E.
1973: The role of humic acids from Tasmania podzolic soils in mineral degradation and metal mobilization; Geochim. Cosmochim. Act. 37: 269-281.

Kodama, H. and Schnitzer, M.
1973: Dissolution of chlorite minerals by fulvic acid; Can. J. Soil Sci. 53: 240-243.

Rashid, M.A. and Leonard, J.D.
1973: Modifications in the solubility and precipitation behavior of various metals as a result of their interaction with sedimentary humic acid; Chem. Geol., v. 11, p. 89-91.

43. GEOCHEMICAL ANALYSIS OF HYDROCARBONS OF EASTERN OFFSHORE OIL WELL SAMPLES — HEAVY HYDROCARBONS AS SOURCE AND MATURITY INDICATORS

Project No. 730098

M.A. Rashid and J.D. Leonard
Atlantic Geoscience Centre

The research conducted in this project is designed to evaluate the hydrocarbon potentials of the sedimentary basins of offshore areas of the East Coast. Qualitative and quantitative assessment, are made of the geochemical alterations of organic matter entrapped in different geological structures sampled during exploratory well drilling operations. The soluble extracts, of high molecular weight organic compounds from the core cuttings of different wells, are being analyzed in detail by column chromatography, gas chromatography and a wide variety of other instrumental techniques to ascertain differences in composition of organic matter relative to stratigraphic position. Special emphasis is given to the distribution of organic carbon, nature and amounts of n-alkanes, odd-even carbon number predominance of the alkanes and relative amounts of various hydrocarbon and non-hydrocarbon structures to ascertain the extent of thermal maturation, degree of conversion of organic matter to petroleum and quality of source rock. The geochemical data obtained on the nature and distribution of C_{15+} fractions are being correlated with the data of gaseous hydrocarbon (Project 730086).

These studies were initiated very recently and during the report period a total of 172 core cuttings from several wells were extracted of which 110 samples were fractionated into various components for further investigations.

Project 730092

C.T. Schafer and F.E. Frape
Atlantic Geoscience Centre, Dartmouth

During 1973 surface sediment samples collected in Chaleur Bay were analyzed to determine their grain size distributions as well as the number and relative abundance of the included species of benthonic foraminifera (Fig. 1). The biologic data were processed using a cluster analysis method described by Parks (1970) which objectively classifies related samples into groups which can usually be mapped. The clustering technique used here is based on a sample-by-sample (Q mode) comparison of the similarity of species occurrence and relative abundance using the simple distance function (D) where

$$D_{1,2} = \left[\sum_{i=1}^{M} (X_{i1} - X_{i2})^2 / M\right]^{\frac{1}{2}}$$

M is the number of species or phi classes and X equals the normalized (transformed to range from 0 to 1) value of the relative abundance of each species. The resulting matrix of D values will range from 0.0 (shortest distance equals closest similarity) to 1.0 (longest distance equals greatest dissimilarity). Clusters of related samples are determined from this matrix using the Unweighted Pair-Group method (for details see Parks, 1966; 1970) and the resulting groups are represented in an easily interpreted dendrogram. This graphical representation is simply a two-dimensional hierarchical diagram on which the "natural breaks" between groups can usually be easily discerned. How-

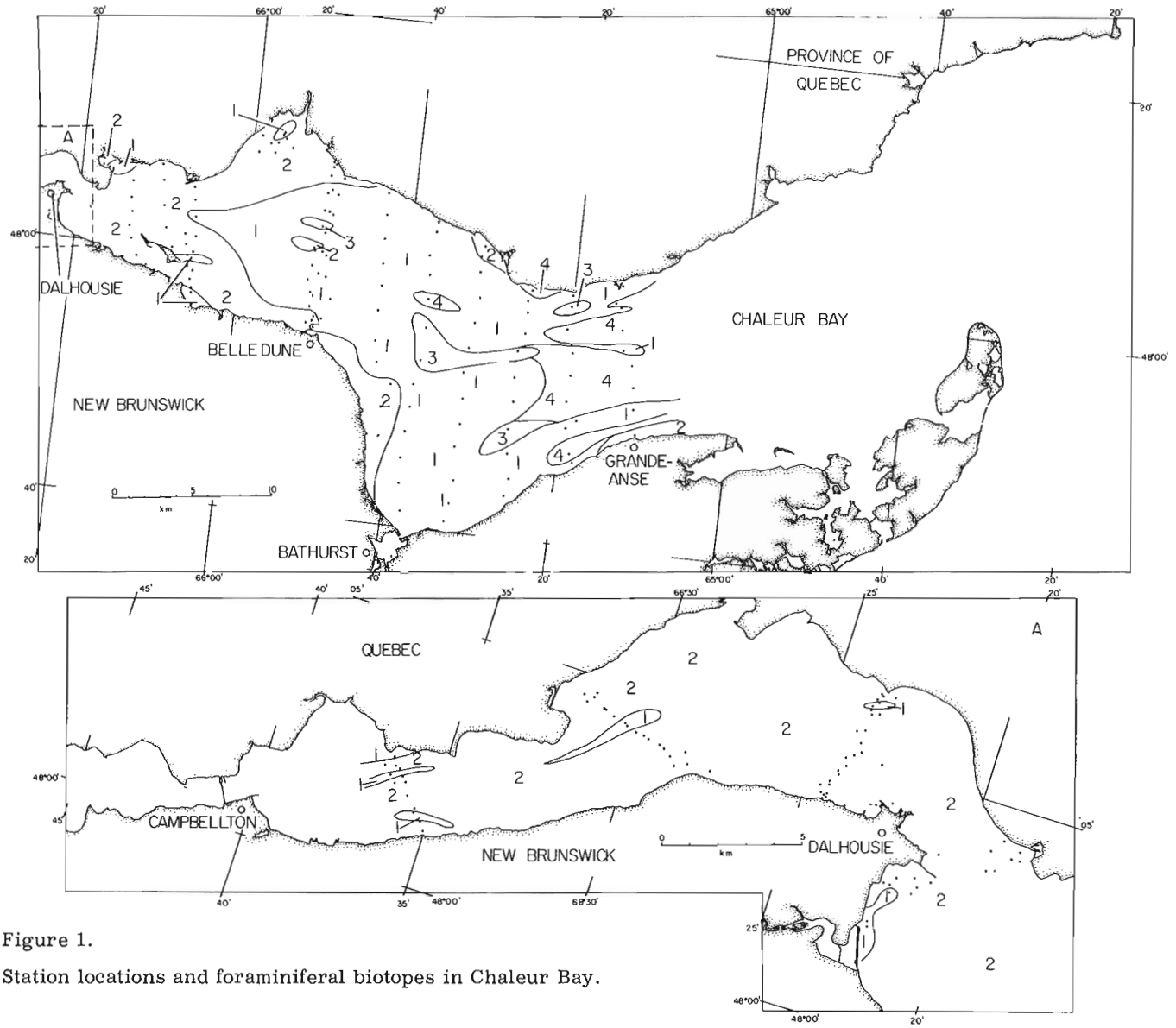

Figure 1.

Station locations and foraminiferal biotopes in Chaleur Bay.

Table 1. Biogeographic fidelity and constancy of Chaleur Bay Foraminifera

SPECIES	CLUSTER GROUPS			
	1 84 stns. BF (c)	2 104 stns. BF (c)	3 6 stns. BF (c)	4 11 stns. BF (c)
Ammodiscus catinus	3(50)	2(30)	3(50)	3(55)
Ammotium cassis	3(74)	3(79)	2(50)	2(55)
Buccella frigida	3(95)	2(68)	3(100)	3(100)
Buliminella elegantissima	2(12)	2(11)	3(17)	3(18)
Cibicides lobatulus	2(13)	1(7)	3(17)	4(27)
Cribrostomoides jeffreysi	4(35)	2(13)	2(17)	2(18)
Eggerella advena	2(96)	2(91)	3(100)	3(100)
Elphidium frigidum	2(25)	3(30)	3(33)	2(18)
E. incertum/clavatum group	3(99)	2(95)	3(100)	3(100)
E. margaritaceum	3(21)	3(27)	2(17)	2(18)
E. subarcticum	2(32)	1(18)	2(33)	2(36)
Miliammina fusca	4(50)	7(86)	4(50)	2(27)
Protelphidium orbiculare	3(83)	2(60)	3(83)	3(82)
Bigenerina arctica (≡Reophaxarctica)	2(70)	1(43)	3(100)	3(91)
Trochammina lobata	3(31)	2(18)	2(17)	3(27)
Ammobaculites salsus	3(55)	1(9)	5(83)	2(36)
Cassidella complanata	3(62)	1(8)	3(67)	3(73)
Cribrostomoides crassimargo	2(39)	1(1)	4(83)	4(73)
Cyclogyra involvens	2(13)	1(3)	4(33)	4(36)
Fissurina marginata	1(7)	1(1)	7(33)	2(9)
Hemisphaerammina sp.	2(35)	4(63)	2(33)	2(27)
Hippocrepina indivisa	2(30)	1(11)	3(50)	4(63)
Islandiella islandica	1(29)	1(2)	3(67)	5(100)
I. norcrossi	3(35)	1(3)	3(33)	4(45)
I. teretis	2(44)	1(3)	5(100)	3(73)
Lagena semilineata	1(7)	1(2)	3(17)	5(27)
Nonionella atlantica	2(20)	1(2)	4(50)	4(55)
Nonionellina labradorica	2(62)	1(8)	4(100)	3(82)
Pateoris hauerinoides	3(23)	1(10)	4(83)	1(9)
Quinqueloculina seminulum	2(19)	1(9)	3(100)	5(45)
Recurvoides turbinatus	2(26)	1(2)	3(17)	4(73)
Reophax fusiformis	2(70)	1(24)	2(17)	3(91)
R. nana	2(59)	1(7)	4(83)	4(91)
R. scottii	3(79)	1(34)	3(100)	3(91)
Rosalina floridana	2(13)	1(2)	3(17)	5(27)
Saccammina atlantica	4(31)	1(11)	2(17)	3(27)
Spiroplectammina biformis	3(76)	1(33)	3(83)	3(91)
Textularia torquata	3(65)	1(14)	3(67)	4(82)
Trochammina ochracea	2(36)	1(19)	4(67)	2(27)
Adercotryma glomeratum	2(32)	-	4(67)	4(64)
Astrononion stellatum	1(6)	-	4(17)	4(18)
Bolivina pseudopunctata	2(29)	-	5(83)	3(55)
Dentalina frobisherensis	1(1)	-	8(33)	2(9)
Globobulimina auriculata form.	1(4)	-	4(17)	6(27)
Hyperammina subnodosa	1(12)	-	6(50)	1(18)
Reophax cf. nodulosus	1(6)	-	7(33)	2(9)
Robertinoides charlottensis	1(6)	-	4(33)	5(45)
Trifarina fluens	2(10)	-	3(17)	6(36)
Gordiospira arctica	5(10)	1(2)	-	4(9)
Quinqueloculina agglutinata	5(17)	2(5)	-	3(9)
Trochammina macrescens	3(15)	5(21)	-	2(9)
T. squamata	3(20)	3(16)	-	4(27)
Elphidium bartletti	3(7)	1(3)	6(17)	-
Fissurina lucida	3(7)	1(4)	6(17)	-
Reophax nodulosus	3(10)	3(10)	5(17)	-
R. pilulifera	2(6)	2(5)	4(17)	-
Ammobaculites dilitatus	3(5)	7(13)	-	-
Ammomarginulina fluvialis	3(11)	7(31)	-	-
Buccella inusitata	6(5)	4(4)	-	-
Cibicides pseudoungerianus	6(7)	4(4)	-	-

Table 1 (cont'd)

SPECIES	CLUSTER GROUPS			
	1 84 stns. BF (c)	2 104 stns. BF (c)	3 6 stns. BF (c)	4 11 stns. BF (c)
Dentalina ittai	6(7)	4(4)	-	-
Difflugia capreolata	5(6)	5(7)	-	-
D. oblonga	5(7)	5(7)	-	-
Elphidium excavatum	6(7)	4(5)	-	-
Lagena gracillima	7(5)	3(2)	-	-
PLANKTONICS	8(4)	2(1)	-	-
Pontigulasia compressa	3(4)	7(8)	-	-
Protoschista findens	6(4)	4(2)	-	-
Saccammina sphaerica	6(1)	4(1)	-	-
Scutuloris tegminis	8(4)	2(1)	-	-
Trochammina inflata	4(17)	6(26)	-	-
Dentalina baggi	3(5)	-	-	7(9)
Esosyrinx curta	3(4)	-	-	7(9)
Lagena laevis	1(1)	-	-	9(9)
Oolina borealis	1(1)	-	-	9(18)
Parafissurina himatiostoma	2(6)	-	-	8(18)
Patellina corrugata	3(10)	-	-	7(18)
Pseudopolymorphina novangliae	1(2)	-	-	9(18)
Spirillina vivipara	2(2)	-	-	8(9)
Nodosaria emphysaocyta	-	-	5(17)	5(18)
Pyrgo williamsoni	1(2)	-	9(17)	-
Astacolus crepidulus	-	-	-	10(9)
Bulimina marginata	-	-	-	10(18)
Lagena mollis	-	-	-	10(9)
Oolina caudigera	-	-	-	10(18)
O. melo	-	-	-	10(9)
Quinqueloculina stalkeri	-	-	-	10(18)
Triloculina trihedra	-	-	10(17)	-
Textularia earlandi	10(1)	-	-	-
Eoepondiella pulchella	10(1)	-	-	-
Glabratella wrightii	10(1)	-	-	-
Lagena nebulosa	10(2)	-	-	-
Reophax gracilis	10(2)	-	-	-
Ammonia beccarii	Present only in inshore areas			

ever, some caution must be used in its interpretation because the dendrogram forces samples into hierarchical groups even though these groups may not really exist in nature. Previous studies have demonstrated that among the various clustering techniques the Unweighted Pair-Group method gives the highest fidelity between dendrogram representations and the original pair-wise similarity matrix, both analytically and empirically (Brooks, 1973).

Four biotopes were distinguished in Chaleur Bay (D = 0.15) by clustering the relative abundance and frequency of occurrence of 93 species of benthonic foraminifera identified in one or more of 205 samples (Fig. 1). Biotope 2 includes upper estuarine and (or) relatively dynamic nearshore environments while biotope 4 delimits deeper, relatively open marine conditions which are first encountered just to the east of Bathurst, New Brunswick. Biotopes 1 and 3 appear to be transitional and will require further study in order to define the dominant conditions controlling the occurrence of the observed foraminiferal species in this part of the Bay. The total foraminiferal populations observed in biotopes 1 and 2 are characterized by a relatively large proportion of arenaceous species compared to the biotope 4 assemblage. For example, of the 71 sediment samples associated with biotope 2, 72 per cent contain foraminiferal populations in which arenaceous specimens comprise more than 75 per cent of the total. Conversely, in biotope 4, only 30 per cent contain arenaceous forms which account for more than 75 per cent of the total number of specimens. Variations in the proportion of arenaceous specimens in cores may therefore be a useful indicator of river flow variations, the post-glacial rise in sea level or glacial rebound along this portion of the coast.

The relationship between the compound diversity (H) of the total foraminiferal population ($H = \Sigma\, p_i \log_2 p_i$ where p_i is the proportion of specimens belonging to the ith species; see Margalef, 1968) and the established biotopes indicates that foraminiferal compound

diversities greater than 1.0 are confined to biotopes 1, 3 and 4. There is also a bathymetric diversity pattern emerging which suggests that substrates characterized by H values less than 0.75 are confined to shallow nearshore environments less than 25 metres deep in a central section of the Bay between Belledune and Grand Anse, New Brunswick. Because of the gradual westward decrease in water depth, foraminiferal compound diversities less than 0.75 predominate west of Belledune (i.e. longitude 65°50'W).

Important members of the foraminiferal assemblages associated with each of the four biotopes were determined using the Biostratigraphic Fidelity (BF) relationship noted by Hazel (1970) where

$$BF_{j,i} = \frac{Pi}{\sum_{i=1}^{p} Pi} = 10$$

In this equation j is the species (j = a, b, c...n), and Pi is the percentage of occurrences of a species in a biogeographic unit (or biotope) i (i = 1, 2, 3...p). The BF of a species for a particular biotope is determined by dividing the percentage occurrences of a species in a biotope by the sum of the percent occurrences of that species in all other biotopes within the limits of the problem. Table 1 is a summary of BF and Constancy values all the species occurring in one or more of the Chaleur Bay biotopes. Constancy (C) is defined as the percentage of all samples within a biotope in which the species occurs and is thus indicative of the extent of its aerial distribution. Species with high BF and C values are used for the primary identification of the biotope. Hazel (1970) notes that the method can be considered as a quantified form of the guide-fossil concept used in stratigraphy. In Table 1 the important species in each biotope are underlined. The biogeographic distribution and the relative abundance distribution of these species comprise the important elements of the assemblage model that will be used to interpret the paleoecologic record of Holocene cores. Important diagnostic forms ($C \geq 10\%$) include *Cribrostomoides jeffreysi*, *Saccammina atlantica*, *Quinqueloculina agglutinata*, and *Gordiospira arctica* in biotope 1; *Trochammina inflata*, *T. macrescens*, *Ammomarginulina fluvialis*, *Ammobaculities dilitatus*, and *Miliammina fusca* in biotope 2; *Triloculina trihedra*, *Pyrgo williamsoni*, *Rephox* cf. *nodulosus*, *Dentalina frobisherensis* and *Fissurina marginata* in biotope 3; finally, calcareous forms such as *Quinqueloculina stalkeri*, *Oolina caudigera*, *O. borealis*, *Bulimina marginata*, and *Pseudopolymorphina novangliae* in biotope 4. It is also evident from Table 1 that presence-absence relationships of certain species may also be potentially useful in interpreting the within-Bay paleoecologic record.

References

Brooks, W.W.
1973: Distribution of Recent Foraminifera from the Southern Coast of Puerto Rico; Micropaleontology, v. 19, p. 385-416.

Hazel, J.E.
1970: Binary Coefficients and Clustering in Biostratigraphy; Geol. Soc. Am. Bull., v. 81, p. 3237-3252.

Margalef, R.
1966: Cluster Analysis applied to Multivariate Geologic Problems; J. Geol., v. 74, p. 703-715.

1968: Perspectives in Ecological Theory. Univ. Chicago Press, Chicago, 111 p.

Parks, J.M.
1970: Fortram IV Program for q-mode cluster analysis on distance function with printed dendrogram; Kansas Geol. Surv. Computer Contr. 46, 32 p.

45. FORAMINIFERAL, MOLLUSCAN AND LITHOLOGIC STUDY OF SEDIMENT CORES FROM THE BEAUFORT SEA AND NORTHWEST PASSAGE

Project 720115

Gustavs Vilks
Atlantic Geoscience Centre, Dartmouth

Foraminifera in Sediment Cores of the Northwest Passage, Canadian Arctic Archipelago

Foraminifera were identified and counted from ten sediment cores collected during HUDSON '70 (Fig. 1). Sediments older than Pleistocene were not recovered. The dominant foraminiferal genera in these Upper Pleistocene-Holocene sediments are *Islandiella* and *Elphidium*, which are useful indicators of changes in paleoenvironment. In general, *Islandiella teretis* is dominant throughout the cores collected in the Viscount Melville Sound and Barrow Strait, but *Elphidium incertum* dominates the sediment at the southwestern end of Prince of Wales Strait. The former species is generally found in deeper waters of the Canadiaan Arctic Archipelago and the latter in the shallow localities of areas influenced by estuarine waters.

Two stratified cores in terms of foraminifera were recovered at the northeastern end of Prince of Wales Strait (Stations 450 and 451). In both cores three layers can be recognized on the basis of *E. incertum*, *I. teretis* and the planktonic species *Globorotalia pachyderma* (see Fig. 2). In comparison to the sediment layers below, the surface layer contains higher fractions of *E. incertum*, but lower percentages of *I. teretis* and *G. pachyderma*. In the middle layer both the latter species occur in high percentages, but decrease again towards the bottom of the cores.

The fluctuations in the occurrence of the three species can be used for paleo-oceanographic synthesis. The bottom layer was deposited during the time when relative sea level was lower than at present. The middle layer represents time when the waters locally were deeper in combination with a more open access to the Arctic Ocean. The latter conjecture is based on the higher number of *G. pachyderma* preserved in the sediment of the lower middle layer. The circulation of water through the Prince of Wales Strait during that time was dominated by a southwesterly flow, as indicated by the

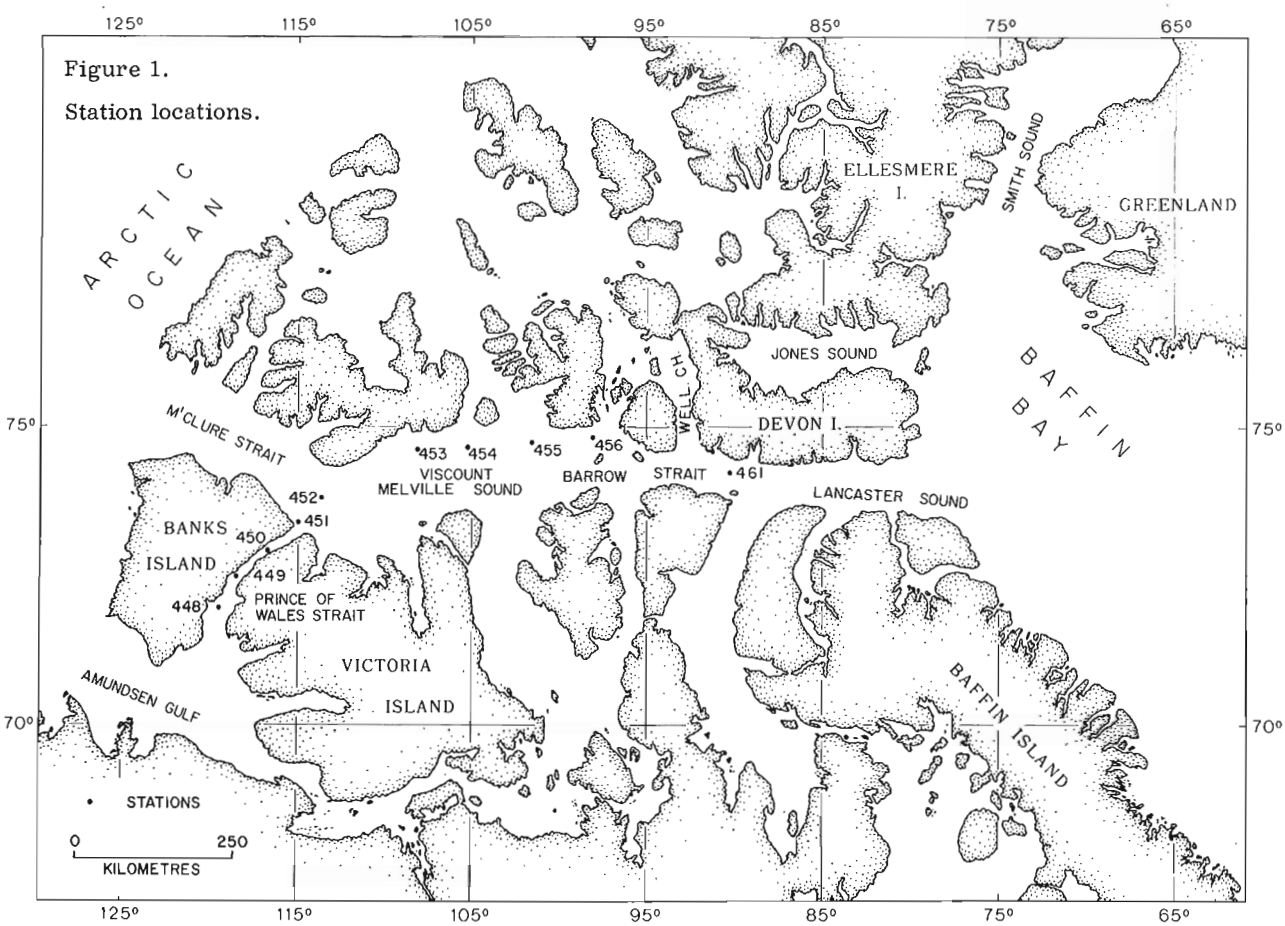

Figure 1.

Station locations.

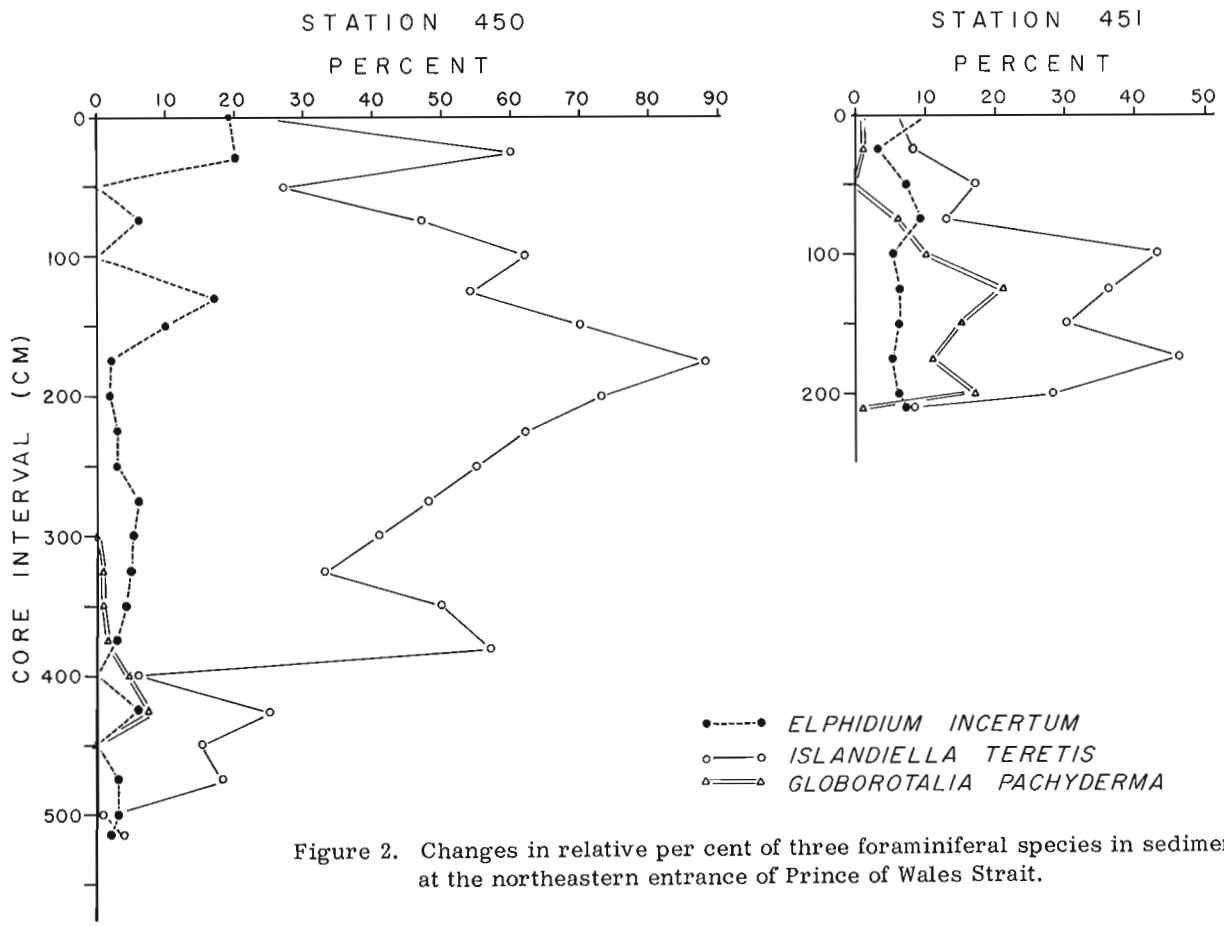

Figure 2. Changes in relative per cent of three foraminiferal species in sediment cores at the northeastern entrance of Prince of Wales Strait.

high percentage of *I. teretis*. The recent isostatic rebound of the islands is reflected in the two cores by the lower percentages of *I. teretis* towards the surface. The higher percentages of *E. incertum* in the surface sediments indicate an increasing influence of waters originating in the Mackenzie River delta area and a dominant northeasterly flow of water through the strait.

46. MICROPALEONTOLOGY OF UNCONSOLIDATED SEDIMENTS ON THE LABRADOR CONTINENTAL SHELF

Project 730091

Gustavs Vilks
Atlantic Geoscience Centre, Dartmouth

Between November 22 and October 5, 1973, thirty-six sediment cores were collected on the Labrador continental shelf and slope within an area between latitudes 53°00'N and 55°15'N and longitude 56°30'W and 52°30'W (Fig. 1). The sampling program was designed to: 1) provide information on sedimentary environment during glacial-post glacial periods in two enclosed basins on the continental shelf and 2) to seek for possible Mesozoic-Tertiary outcrops that could be reached with a 400-pound gravity corer.

For the first part, two areas were selected showing a reasonable thickness of acoustically semi-permeable surface layer on the ship's precision depth recorder. In these localities five stations were occupied on a grid pattern not more than two miles apart. At each station a piston core was taken using a 1,400 pound core head and 40 feet of barrel containing plastic liners. In most instances the entire corer penetrated the sediment, with a core recovery ranging between 30-39 feet.

For the second part, localities were selected on the continental slope showing steepest regional slopes and on the continental shelf showing acoustically opaque surfaces and cuestas. At most of these stations a 400-pound gravity corer was used with a 6-foot barrel, but

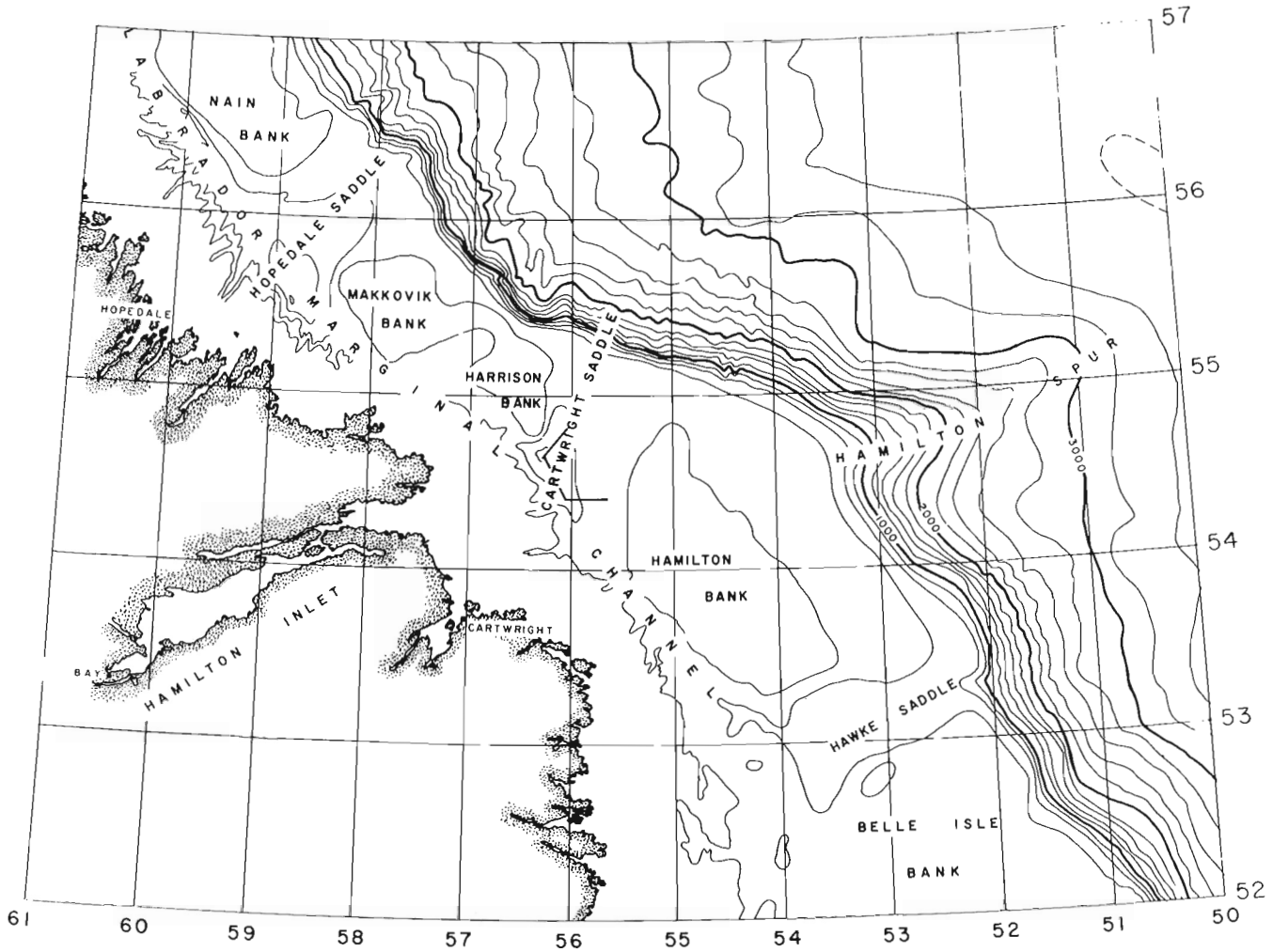

Figure 1. Sampling locality.

at a few stations the 1,400-pound piston corer was used as well. As expected, the corer recovery at these localities was poor, where the corer was stopped by either a large pebble or a tough layer of silty clay. Upon recovery the sediment within each core cutter was washed through an 80-micron sieve and the residue inspected under a microscope.

The preliminary inspection indicates that sediments older than Pleistocene were not recovered. All samples contained only species of planktonic foraminifera; the sinistral *Globorotalia pachyderma* with a few *Globigerina bulloides* and only a small percentage of the dextral *G. pachyderma*. The benthonic foraminifera consists of species living in the area at the present time ranging from nearshore to offshore marine environment. However, in a number of localities specimens were recovered that may have been redeposited from sediments older than the Holocene. The exact age of these species has not been determined yet.

In each of the sedimentary basins the sediments are very fine and about 99 per cent of the material washed through the sieve. In these sediments the state of preservation of the fossils was excellent. The sediments contained a large amount of authigenic pyrite and about 30 per cent of the tests were replaced by this mineral. In addition to foraminifera, a number of ostracods and shells of pteropods were found. The sediments also contained a large amount of chitinous fragments that could be identified as inner linings of worm tubes.

Within minutes of extraction from the core, the sediment collected in both basins began to release gas that formed transverse fissures in the core. These fissures gradually increased in size forcing the sediment out through the ends of the plastic liner. As a result of the released gas the volume increase of the sediment was about 5 per cent. The gas was identified to be pure methane; gas was not found in sediments of the upper 10 feet of the cores.

The preliminary investigation indicates that the fine sediments were received in the basins at a rapid rate in addition to a large amount of organic material from the surface waters. The rapid burial enhanced the preservation of the skeletal material of foraminifera and the partly oxidized matter. After burial anaerobic decomposition continued, which explains the presence of pyrite and the gas. At the present time fine sedi-

ments are still delivered to the basin, but at a slower rate, allowing for a more complete decomposition of the organic matter. These fine sediments are relatively impermeable, thus preventing the escape of the gas accumulating below.

Detailed analysis of one core in terms of organic geochemistry and foraminifera was carried out and a manuscript submitted, Vilks et al. (1974).

Reference

Vilks, G., Rashid, M.A., and van der Linden, W.J. Methane in Recent Sediments of the Labrador Shelf; Can. J. Earth Sci. in press.

47. BENTHONIC FORAMINIFERIDA AND MOLLUSCA IN THE BEAUFORT SEA

Project 720115

F.J.E. Wagner
Atlantic Geoscience Centre, Dartmouth

Benthonic Foraminiferida and Mollusca were collected from Beaufort Sea between longitude 128°19'W and 140°37'W and from the coast north to latitude 71° 43.3'N. Foraminiferal distribution analysis is based on 198 stations (C.S.S. Hudson, 1970; M.V. Richardson, 1970; helicopter operation, 1971), and mollusc distribution on samples from 657 stations (C.S.S. Parizeau, 1970, 1971 and 1972, in addition to the foregoing). One hundred and forty-five foraminiferal species and 85 molluscan species have been identified.

Foraminiferal distribution pattern shows the calcareous species to be predominant at shallower depths. These are replaced on the outer shelf and down the slope by arenaceous species. This situation is the reverse of that noted farther north (Vilks, 1964; Marlowe and Vilks, 1963; Wagner, 1962 and 1964) where arenaceous forms were most common at depths of less than 200 metres, and calcareous forms were characteristic of the deeper waters.

Molluscs were found primarily on the shelf with few living specimens being collected from depths greater than about 100 metres. Samples from the slope were generally barren. Numerous areas on the shelf that were found to be barren of molluscs or that yielded only reworked specimens may be indicative of the scouring action of ice.

A few molluscs were observed when the Hudson '70 cores were logged and these have been identified. Two samples were radiocarbon dated. The cores are now being processed systematically for additional molluscs and for foraminifera. Fossils were obtained also from upraised marine deposits on Herschel Island and the Yukon mainland coast.

General distribution maps and maps showing the areal distribution of certain key species of both foraminifera and molluscs currently are being readied for publication in the Beaufort Sea Atlas. Preliminary observations on the molluscan faunas and on estimated changes in sea level during the past 3,500 years were presented at the 24th International Geological Congress (Wagner, 1972). A future report will cover, in detail, the ecological significance of the present-day benthonic foraminifera and molluscs, and an interpretation of late Pleistocene history based on comparison of the assemblages from the cores with the living faunas.

References

Marlowe, J.I. and Vilks, Gustavs
1963: Marine Geology, Eastern Part of Prince Gustaf Adolf Sea, District of Franklin; Geol. Surv. Can., Paper 63-22.

Vilks, Gustavs
1964: Foraminiferal study of East Bay, Mackenzie King Island, District of Franklin; Geol. Surv. Can., Paper 64-53.

Wagner, F.J.E.
1962: Faunal Report, Submarine Geology Program, Isachsen, District of Franklin; Geol. Surv. Can., Paper 61-27.

1964: Faunal Report - II, Marine Geology Program, Polar Continental Shelf Project, Isachsen, District of Franklin; Report B.I.O. 64-1.

1972: Molluscan Faunas as Indicators of Late Pleistocene History, southern Beaufort Sea; 24th Int. Geol. Cong., sect. 8, p. 142-153.

48. TEST SURFACE ULTRASTRUCTURE OF BENTHONIC FORAMINIFERA AND APPLICATIONS OF SCANNING ELECTRON MICROSCOPY

Project No. 730093

D.A. Walker
Atlantic Geoscience Centre, Dartmouth

Morphogenesis of Some Littoral Foraminifera

Investigation of wall cross-sections in *Cibicides lobabulus* has revealed a multilamellar structure. As each new chamber is added a complete calcite layer covers previously formed chambers, resulting in the last-formed chamber being monolamellar. Winter populations tended toward construction of thicker walled tests. Porosity was calculated for *C. lobabulus*. Results showed high levels (10-20%) for the summer population relative to the generation produced during late summer - early fall (4%). These figures show a positive correlation to water temperature.

Reproductive cycles of the following species were investigated from tide-pool habitats: *Rosalina floridana, Spirillina vivipara, Quinqueloculina seminulum, Pateoris hauerinoides* and *Eggerella advena*. Preliminary data analysis suggests that only the asexual phase of the life cycle occurs in the tide pool habitat, and the sexual phase in deeper subtidal waters. Data extracted from the tide pool investigation reveal a single major reproductive period for *R. floridana*, namely in late summer - early fall, occurring simultaneously with the highest productivity of *C. lobabulus*. The same holds for *S. vivipara, Q. seminulum* and *P. hauerinoides*. Although *E. advena* had a reproductive period during late summer - early fall, its major peak occurred during mid-winter.

49. SUDAN BLACK B: A STAIN FOR QUANTITATIVE DETERMINATION OF LIVING FORAMINIFERA

Project No. 730092

D.A. Walker and C.T. Schafer
Atlantic Geoscience Centre, Dartmouth

Quantitative evaluation of the living fraction of a foraminiferal population is possible by using either heated acetylated or heated saturated Sudan Black B as alternative stains to the conventional rose Bengal. In the experiments conducted using heated acetylated Sudan Black B, 96.8% of the specimens stained a vivid blue-black; 95.1% of the specimens stained with heated saturated Sudan Black B; and 70.3% of the specimens treated with rose Bengal stained to some degree. Washing and heating prior to staining aided in removing algal detritus adhering to the tests that would otherwise obscure internally stained protoplasm. Results of staining experiments on empty tests showed only 4.0% of the tests stained with heated acetylated Sudan Black B, 5.5% with heated saturated Sudan Black B, compared with 28.1% with rose Bengal. Although there is a slight loss in accuracy in using the saturated over the acetylated version, the time saved in preparation of the former is sufficient compensation if large numbers of samples are to be processed routinely.

50. BIOSTRATIGRAPHIC ZONATION (FORAMINIFERA AND OSTRACODA) OF THE MESOZOIC AND CENOZOIC ROCKS OF THE ATLANTIC SHELF

Project 710065

P. Ascoli
Atlantic Geoscience Centre, Dartmouth

Biostratigraphy

The study of the foraminifera and ostracoda from the offshore wells: Shell Cree E-35, Shell Mohawk B-93, Shell Naskapi N-30, Shell Onondaga E-84, and Mobil Sable Island C-67 (Scotian Shelf) and Amoco IOE Puffin B-90 (Grand Banks off Newfoundland) has provided broad biostratigraphic control of the Jurassic and Early Cretaceous and detailed zonation of the Late Cretaceous and Cenozoic. The preliminary zonations presented herein are based primarily on well sample cuttings. Supporting data have also been obtained from three conventional cores of the Sable Island C-67 well and from sidewall cores from each of the above wells. Consequently, the necessity for relying on cuttings for zonation and correlation means that both foraminiferal and ostracod zones are based on the "top" or youngest or highest occurrence of a species, unless they are "peak zones". In the latter, the species after which the zone is named attains its maximum abundance in that zone.

A preliminary biostratigraphic foraminiferal and ostracod zonation of the Mesozoic-Cenozoic sediments of the Scotian Shelf and western Grand Banks, based on the wells examined as listed above, is illustrated in Table 1.

The Jurassic-Early Cretaceous sediments on the Scotian Shelf are characterized by a paucity of planktonic foraminifera, necessitating the extensive use of benthonic foraminifera - most of which have previously been described from European sections - and ostracods for biostratigraphic control. Of particular importance are the species *Buccicrenata italica, Epistomina caracolla* and *Epistomina uhligi,* each of which characterizes a "peak zone" and a "top zone" respectively.

Recognition of the Barremian and Aptian stages and particularly of the Barremian-Aptian boundary does not appear to be possible in the reported wells utilizing foraminifera and ostracoda only. Sediments of this age are therefore tentatively included in the "*Epistomina caracolla* zone" (which should approximately correspond to the Barremian) and in the "*Gavelinella barremiana-Choffatella decipiens* zone", which more or less corresponds to the Aptian.

From the Late Cretaceous to Miocene the zonation is based on the most abundant planktonic foraminifera, which permit world wide correlation. Unfortunately, however, only eight of the zones proposed by Bolli for the Late Cretaceous-Cenozoic planktonic foraminifera zonation could be utilized since many of his zones are delineated by the "base" or oldest occurrence of a species. The Late Eocene, Late Oligocene and Middle to Late Miocene have not been dated with precision due to the absence of zonal markers in the reported wells.

The ostracods permit a good zonation of the Jurassic and Cretaceous periods and are the best fossils for establishing the Jurassic-Cretaceous boundary. The zonation of the Late Cretaceous based on ostracods utilizes several species which have been already used for biostratigraphic purposes in the Gulf Coast area and eastern United States. As yet, they have not been used for biostratigraphic control in the Cenozoic due to their paucity in this part of the geological column. In the Middle-Late Jurassic and Early Cretaceous the ostracod faunas show several species in common with the European faunas; consequently, mostly European ostracod species have been selected for the biozonation of this interval.

Comparing the stratigraphic ranges of our ostracod and foraminiferal species with the ranges of the same species as reported in Europe, we see that several of our ostracod species seem to range stratigraphically higher than in the European sections where they were originally described, while most of the benthonic foraminifera show approximately the same range on the Scotian Shelf and in Europe, although some of the species range either higher or lower than in Europe.

Both ostracods and foraminifera exhibit marked provincial affinities throughout the Mesozoic and Cenozoic. In the Jurassic and Early Cretaceous several of the species have previously been recorded from European sections. In the Late Cretaceous and Paleogene, benthonic foraminifera and ostracod species are predominant species also present in North America but rare or absent in Europe. This provincialism becomes even more marked in the foraminiferal assemblages of the Neogene, which implies a "North Atlantic" affinity, related to cool climatic conditions.

Paleoecology

The oldest sediments dated so far in the Scotian Shelf belong to the lower part of the Middle Jurassic (Mohawk Formation), which was deposited in a mostly continental, occasional littoral marine environment, characterized by extremely scarce foraminiferal and ostracod faunas and by abundant evidence of continental origin. Some sporadic continental episodes might still be found in the upper part of the Middle Jurassic and in the Late Jurassic, where the environment mostly varies from littoral marine (Abenaki Formation) to inner neritic (Mic Mac Formation and Verrill Canyon Formation), being characterized by abundant arenaceous foraminifera and often by abundant ostracoda.

TABLE 1

Foraminiferal and Ostracod biozonation of the Scotian Shelf

	AGES	FORAMINIFERAL ZONES	OSTRACOD ZONES
TERTIARY	LATE-MIDDLE MIOCENE	*Globorotalia praemenardii*	
	EARLY MIOCENE	*Globigerinita dissimilis*	
	LATE-MIDDLE OLIGOCENE	*Globorotalia opima opima*	
	EARLY OLIGOCENE	*Globigerina ampliapertura*	
	LATE-MIDDLE EOCENE	*Globorotalia centralis* *Globorotalia bullbrooki*	
	EARLY EOCENE	*Globorotalia formosa* *Globorotalia rex*	
	PALEOCENE	*Globorotalia velascoensis* *Globig. triloculinoides*	
CRETACEOUS	MAASTRICHTIAN	*Globotruncana contusa* *Globotruncana arca*	*Veenia arachoides*
	CAMPANIAN	*Globotruncana ventricosa* *Globotr. globigerinoides*	*Brachycyth. rhomboidalis* *Amphicytherura distincta*
	SANTONIAN	*Globotruncana coronata*	*Protocythere triebeli*
	CONIACIAN	*Globotruncana renzi*	*Orthonotacythere hannai*
	TURONIAN	*Globotruncana helvetica* *Praeglobotruncana stephani*	*Cythereis* sp. 2
	LATE CENOMANIAN	*Rotalipora cushmani*	*Cythereis roanokensis*
	EARLY CENOMANIAN	*Hedbergella washitensis*	
	ALBIAN	*Epistomina reticulata* *Lenticulina gaultina*	*Schuleridea jonesiana*
	APTIAN	*Choffatella decipiens* *Gavelinella barremiana*	(Not yet defined)
	BARREMIAN	*Epistomina caracolla* (top) *Epistomina ornata*	
	HAUTERIVIAN	*Planularia crepidularis* *Epistomina caracolla* (peak)	*Paracypris* ex gr. *acuta*
	VALANGINIAN-BERRIASIAN	*Buccicrenata italica* (top) *Ammobaculites alaskensis*	
JURASSIC	TITHONIAN	*Buccicrenata italica* (peak) / *Anchispiroc lusitanica*	*Schuleridea* aff. *triebeli oblonga*
	KIMMERIDGIAN	*Epistomina uhligi* (top)	*Orthonotacythere?* sp. 1
	(? EARLY KIMMERIDGIAN) OXFORDIAN	*Pseudocyclammina jaccardi* *Epistomina soldanii*	*Cytherella index*
	MIDDLE JURASSIC	*Epistomina uhligi* (peak) *Epistomina regularis*	*Lophocythere* spp. *Oligocythereis* spp.

The Jurassic-Cretaceous boundary generally does not correspond to any major change in environment, which persists from littoral to inner neritic in the Berriasian, Valanginian and Hauterivian (top of Mic Mac Formation or Verrill Canyon Formation, lower part of Mississauga Formation), where the foraminiferal and ostracod faunas may be abundant and represented also by frequent calcareous foraminifera.

In the Barremian, Aptian and Early Albian (upper part of Mississauga Formation, Naskapi Formation) the microfaunas generally are very scarce or totally absent, indicating a prevailing continental environment with some shallow marine episodes. Above the Albian, the environment generally appears marine, varying from littoral to inner neritic until the top of Turonian (Logan Canyon Formation and Dawson Canyon Formation). Abundant arenaceous coarse foraminifera are often found in the Albian, Cenomanian and Early Turonian, indicating a nearshore environment.

The first planktonic foraminifera (with the exception of very few specimens observed in the Neocomian) are recognized in the Albian, but only very exceptionally in the Cenomanian and Turonian are they so abundant as to indicate an outer neritic environment.

In the basal Coniacian the environment still is inner neritic and the microfaunas are characterized by the latest Mesozoic coarse arenaceous foraminifera (Dawson Canyon Formation). From the Middle-Late Coniacian to the Late Maastrichtian (Wyandot Formation and Banquereau Formation) the foraminiferal faunas show a progressive increase in the percentage of planktonic and deep water species, suggesting mostly deep marine, outer neritic and even epibathyal environments which clearly indicate the top of the Cretaceous.

In the Tertiary (Banquereau Formation) the Paleocene and Early Eocene may have been deposited either in an outer neritic or in an epibathyal environment, the first being generally characterized by abundant arenaceous foraminifera, the second by abundant planktonic foraminifera and/or radiolaria.

The Middle-Late Eocene abundant planktonic foraminiferal faunas suggest an even deeper environment, probably epibathyal.

The Paleocene and Eocene foraminiferal faunas of the Western Grand Banks differ considerably from those of the Scotian Shelf, showing a marked reduction in the number of planktonics and a much higher quantity of arenaceous benthonics. These combined features indicate a typical "boreal" environment. Such an assemblage has not been observed in the same interval on the Scotian Shelf, where "temperate" and perhaps "warm" foraminiferal faunas, close to the coeval assemblages from the Gulf Coast area, have been found.

In the Oligocene and Early Miocene the environment of deposition still is deep (outer neritic), but less deep than in the Middle-Late Eocene. The Oligocene-Early Miocene benthonic foraminiferal faunas are extremely rich, well developed and diversified. The latest relatively deep water microfaunas have been observed in the Late Miocene-Early Plio-Pleistocene, which have been deposited in an outer neritic environment tending to inner neritic towards top.

Sediments of Plio-Pleistocene age (Banquereau Formation) have been recognized only in the Sable Island C-67 well, where they show a progressive trend to shallower waters from bottom to top. The environment is in fact outer neritic tending to inner neritic in the Early Plio-Pleistocene and inner neritic tending to littoral in the Late Plio-Pleistocene, which is characterized by a typical shallow water foraminiferal assemblage.

Paleogeographic Implications Suggested by Micropaleontological Data

Direct comparisons between the Cenozoic and Mesozoic foraminiferal and ostracod faunas from the Scotian Shelf and the coeval faunas from United States, Caribbean area and Central-Western Europe (Germany, England, France, Spain, Portugal, etc.) have been made.

The affinities of the Scotian Shelf-Grand Banks foraminferal and ostracod assemblages to their European and North American counterparts exhibit significant changes in the Mesozoic-Cenozoic. Throughout the Jurassic and Early Cretaceous the foraminifera and ostracods show closer affinity with the coeval assemblages from western and central Europe than from the North American continent.

In the Albian the Scotian Shelf ostracods show a marked inversion of affinity, so that post-Albian assemblages most closely resemble time equivalent ostracod faunas from the Late Cretaceous of the eastern United States. The cosmopolitan Late Cretaceous planktonic foraminiferal zones can be readily recognized in the Scotian Shelf and Grand Banks sediments, although there are indications of North American provincialism.

In the Cenozoic, the Scotian Shelf and Grand Banks foraminifera show affinity with the United States Gulf Coast and East Coast, and the northwest European assemblages.

The close similarity between Eastern Canada and European microfossil assemblages in the Jurassic to Early Cretaceous suggests that during this time the Eastern Canada margin was within a "European" biogeographical province. Our post-Early Cretaceous assemblages tend to fit more in a Mid-North Atlantic province.

Increasing provincialism in the Neogene presumably reflects climatic cooling which probably began during the Miocene, when for the first time our planktonic assemblages show a sharp difference from the United States East and Gulf Coast - Caribbean faunas. This difference mainly consists in remarkable scarcity of the genus *Globorotalia* and in the absence of the genus *Orbulina*, both typical temperate to warm water indicators.

The changes of faunal affinity may relate to opening of the North Atlantic in the Mesozoic or merely reflect changes in environment or oceanic current patterns, or be coincidental. Present data suggest that the opening of the Atlantic was the controlling factor.

Selected Bibliography

Bartlett, G.A. and Hamdam, A.R.A.
1972: The Canadian Atlantic continental margin - biostratigraphy, paleoecology and paleo-oceanography from Cretaceous to Recent; 24th Int. Geol. Cong., sect. 8, 15 p.

Bartlett, G.A. and Smith, L.
1971: Mesozoic and Cenozoic history of the Grand Banks of Newfoundland; Can. J. Earth Sci., v. 8, p. 65-84.

King, L.H., MacLean, B., Bartlett, G.A., Jeletzky, J.A. and Hopkins, W.S., Jr.
1970: Cretaceous strata on the Scotian Shelf; Can. J. Earth Sci., v. 7, p. 145-155.

McIver, N.A.
1972: Cenozoic and Mesozoic stratigraphy of the Nova Scotia Shelf; Can. J. Earth Sci., v. 9, p. 54-70.

51. PALYNOLOGICAL ZONATION OF THE CARBONIFEROUS AND PERMIAN ROCKS OF THE ATLANTIC PROVINCES

Project 680109

M.S. Barss
Atlantic Geoscience Centre, Dartmouth

Palynological studies in the Atlantic Provinces have established twenty assemblage zones, ranging in age from Middle Devonian to Lower Permian. These have allowed accurate correlation of many outcrop sections and wells throughout the Atlantic area, and with exploration extended to the offshore, have proved extremely useful in dating the rocks encountered in wells drilled in the Gulf of St. Lawrence and on the Grand Banks.

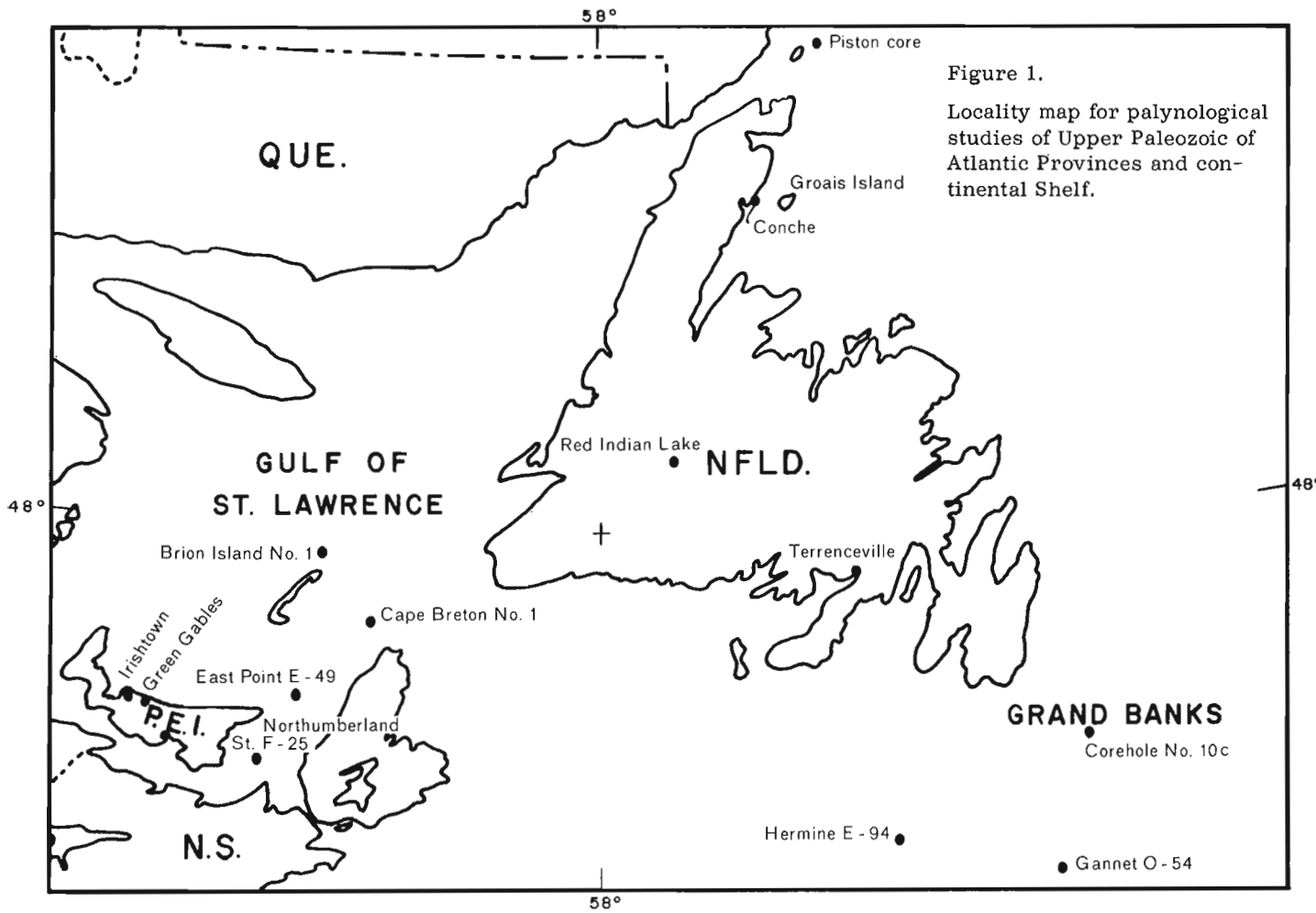

Figure 1.

Locality map for palynological studies of Upper Paleozoic of Atlantic Provinces and continental Shelf.

Five wells, Sarep HQ Brion Island, HB Fina Northumberland Strait F-25, HB Fina East Point E-49, HB Fina Green Gables, HB Fina Irishtown, and one shallow core hole, Pan-Am Cape Breton No. 1 have been examined from the Gulf of St. Lawrence. Athough not all are "offshore", these wells have provided valuable information to the understanding of the geology in the gulf.

Age of the rocks encountered in these wells ranges from possible Permain to Viséan. The thickness and age of the sediments in these wells has been drastically affected by the presence or absence of Windsor Group salt of Viséan age.

On the Grand Banks, two wells, Elf Hermine E-94 and Amoco-IOE Gannet O-59, and one shallow core hole, Pan-Am Grand banks 10C, have been examined. The two revealed an unconformity between the Cretaceous and Carboniferous. In the Hermine well the first Paleozoic rocks are Westphalian B age, bottoming in Viséan age. In the Gannet well, the Paleozoic consists of possible Namurian to Frasnian age, bottoming in metamorphosed rocks of uncertain age. Shallow core hole 10C and a sample obtained from a piston core taken in a tillite, offshore from Belle Isle, Newfoundland, proved most interesting in that they contained fossils that indicated ages from Mississippian to Ordovician and Pennsylvanian to Ordovician respectively.

Recent examination of samples from the Terrenceville area of Newfoundland, dated previously as Devonian, yielded a spore assemblage similar to those from the Conche-Groais Island and Red Indian Lake areas of Newfoundland. Those assemblages have been correlated with the type Horton Group of Nova Scotia of Late Tournaisian age.

The results of the above studies are incorporated in a forthcoming Geological Survey of Canada paper containing a series of isopach maps of the upper Paleozoic rock units of the Atlantic Provinces, and continental shelf.

52. DEPOSITIONAL HISTORY AND FACIES DISTRIBUTION OF THE TERTIARY SYSTEM ON THE SCOTIAN SHELF

Project 730084

Iris A. Hardy
Atlantic Geoscience Centre, Dartmouth

The Scotian Shelf of offshore Eastern Canada is underlain by sedimentary strata in excess of 10-km thick, which McIver (1972) divided into a succession of rock-units varying in age from Triassic, through Jurassic, Cretaceous to Tertiary. The object of the present investigation is to redefine the stratigraphy and sedimentology of McIver's youngest unit, the Banquereau Formation, a rock-stratigraphic sequence that was initiated in the Late Cretaceous and continued uninterrupted into the Tertiary period. The investigation is carried out by the microscopic study of sample cuttings and cores from wells drilled in exploration for oil and gas on the Scotian Shelf, in addition to geophysical data in the form of high resolution and deep reflection seismic profiles.

From a regional viewpoint, the Banquereau Formation has been observed to underlie an area of some 35,000 square miles (89,600 km^2) of the Scotian Shelf and occupies a volume of 36,000 cubic miles (147,456 km^3). The formation thickens rapidly in a southeast direction across the shelf from its erosional edge to 6,000 feet (1,830 m) near the shelf edge forming a simple wedge-shaped geometrical configuration. Parallel to the shelf, the formation is lenticular and its thickness thus parallels the topographical configuration of the underlying basement rocks, which gradually rise to form the La Have Platform at the western extremity of the shelf and the Canso Ridge to the east respectively (Wade, 1973 - unpublished data).

From the detailed microscopic examination of sample cuttings and cores from 11 wells drilled on the Scotian Shelf (Fig. 1) the writer has subdivided the Banquereau Formation into four informal but relatively consistent lithostratigraphic units in ascending order of sequence as follows (Fig. 2): (i) Maskonomet beds; (ii) Nashwauk beds; (iii) Manhasset beds; and (iv) Esperanto beds.

The Maskonomet beds of Maastrichtian to Campanian age are composed primarily of argillaceous mudstone which attains a maximum thickness of 1,675 feet (511 m) in Shell Oneida O-25 (43°14'N, 61°33'W). They form the basal unit of the Banquereau Formation and usually overlie chalks of the Wyandot Formation with abrupt contact. The succeeding Nashwauk beds of Paleocene and Eocene ages attain a maximum thickness of 740 feet (226 m) in Mobil Tetco Esperanto K-78 (44°47'N, 58°11'W) and consist of argillaceous and glauconitic sandstone at the base, overlain by calcaerous and gluconitic mudstone. The unit is well defined in most of the wells examined and is a good marker unit for defining the Cretaceous-Tertiary boundary on the Scotian Shelf. The Manhasset beds of Oligocene age overlies the Nashwauk and consist of coarse-grained, argillaceous and conglomeratic sandstone which attains a maximum thickness of 750

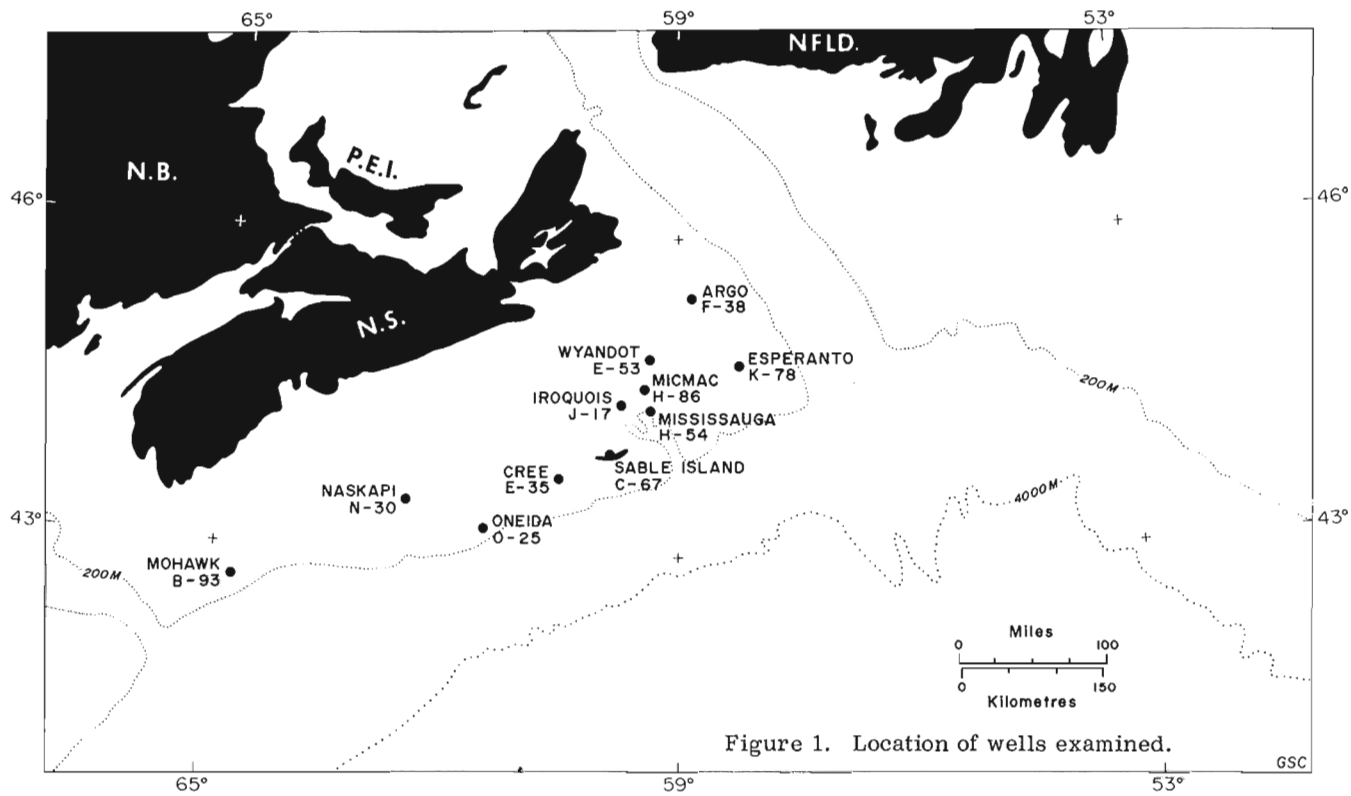

Figure 1. Location of wells examined.

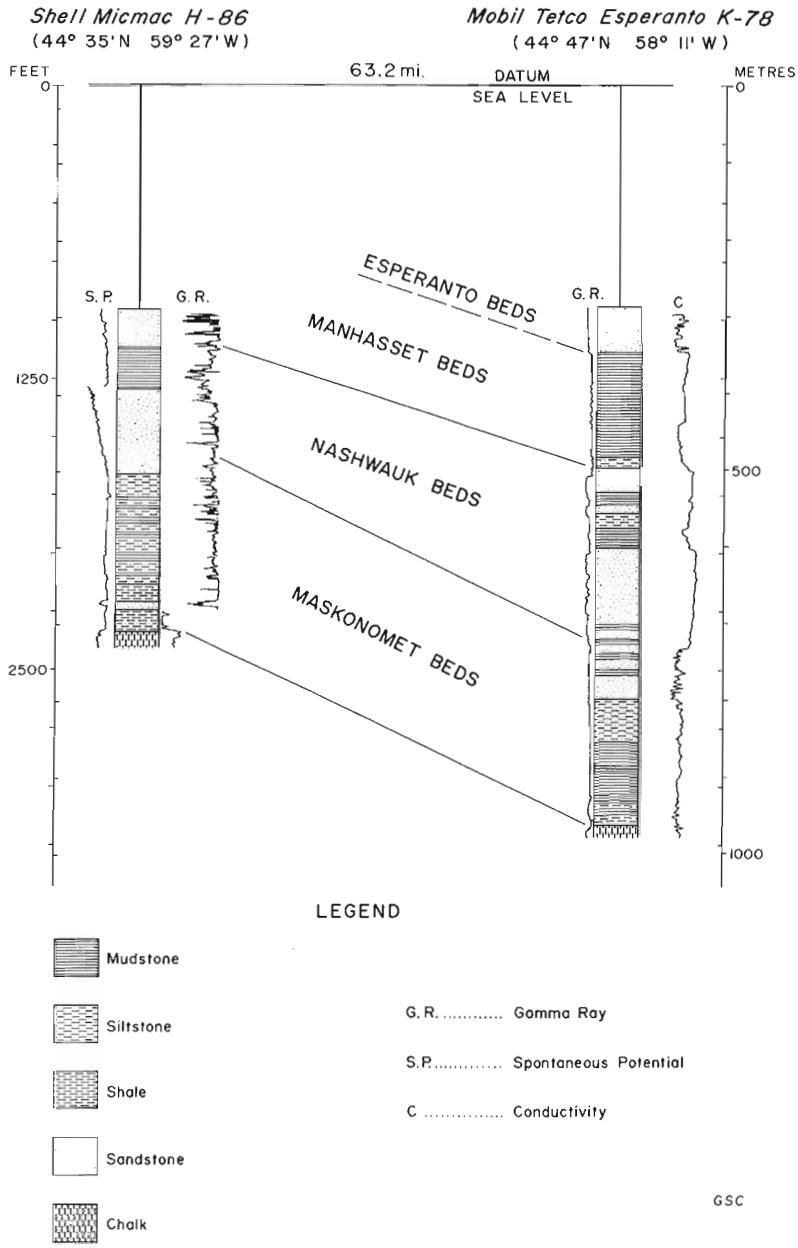

Figure 2. Lithostratigraphic zonation of the Banquereau Formation on the Scotian Shelf.

feet (229 m) in Mobil Sable Island No. 1 (C-67) (43°56'N, 59°55'W). The youngest unit of the Banquereau Formation is the Esperanto beds of Miocene and possible Pliocene age and are comprised of unconsolidated medium- to coarse-grained sandstone which attains a maximum thickness of 720 feet (220 m) or more in Shell Oneida O-25.

Sample cuttings are generally not recovered from above -850 feet (-259 m) in wells drilled on the Scotian Shelf and consequently the stratigraphic relationships of Tertiary and Pleistocene sediments cannot be directly observed in subsurface. One exception is the Mobil Sable Island No. 1 (C-67) Well, where the upper limit of the Banquereau Formation is clearly defined at a depth of 875 feet (267 m). The contact is placed where sandy, glauconitic and calcareous claystone and glauconitic sand are abruptly and unconformably succeeded by coarse-grained sand of Pleistocene age. The Tertiary-Pleistocene contact is an unconformity of wide regional proportions on the Scotian Shelf that is well defined on high resolution seismic profiles.

Detailed lithostratigraphic studies of the Banquereau Formation are continuing on the Scotian Shelf and these will gradually be projected into the Grand Banks and ultimately to Northeast Newfoundland and Labrador Shelves.

Reference

McIver, N.L.
1972: Cenozoic and Mesozoic stratigraphy of the Nova Scotia Shelf; Can. J. Earth Sci., v. 9, p. 54-70.

53. COMPILATION OF GEOSCIENTIFIC DATA IN THE PALEOZOIC BASINS OF EASTERN CANADA

Project 710061

R.D. Howie
Atlantic Geoscience Centre, Dartmouth

The upper Paleozoic sediments in the Atlantic Provinces, Gulf of St. Lawrence and the continental shelf adjacent to Newfoundland, range in age from Middle Devonian to Early Permian. These rocks have been subdivided into four major lithologic divisions (Groups) as illustrated in Table 1 (Howie and Barss in preparation) and mapped in the subsurface on a broad regional scale throughout the Atlantic Provinces and adjacent offshore regions.

Post-Acadian Horton Group sediments represent the first infilling of the uneven surface of the Acadian orogenic belt. In a measured section, Horton Group rocks range in thickness up to 10,795 feet (3,291 m) (Kelley, 1967). From eastern Prince Edward Island to the Magdalen Islands, the area is predicted to contain 12,000-14,000 feet (3,659-4,268 m) of Horton Group rocks, shallowing to less than 10,000 feet (3,049 m) in the central part of the basin beneath the Magdalen Islands. Ten thousand feet (3,049 m) of strata is estimated for the Moncton Basin, western Newfoundland and western Cape Breton Island. Eight thousand feet (2,439 m) of Horton Group rocks are estimated for the Cumberland Basin, and 4,000 feet (1,220 m) for a large part of the Minas Basin, Nova Scotia; and the White Bay area of northwestern Newfoundland. At least 2,000 feet (610 m) of Horton Group rocks estimated for the Sydney Basin, and on the continental shelf south and east of Newfoundland is based on spores from a section at Terrenceville, Newfoundland (Barss, 1974a) and in the Amoco-IOE Gannet O-59 exploratory well (Barss, 1974c) (Fig. 1).

In the type area the marine Windsor Group is composed of clastics, carbonates and evaporites of not less than 1,550 feet (473 m). In areas somewhat removed from the shoreline, a rapid increase in the thickness of Windsor Group rocks can be attributed to accumulations of evaporites, mainly salt. The thickest accumulation of Windsor Group rocks occurs in the Cumberland Basin, where up to 20,000 feet (6,098 m) of sediment is postulated. Up to 18,000 feet (5,488 m) of Windsor Group strata is estimated for the central and eastern part of the Magdalen Basin. Several smaller structures in the Gulf of St. Lawrence, Prince Edward Island and eastern New Brunswick have been estimated to contain 10,000-12,000 feet (3,049-3,659 m) of Windsor rocks. In the Sydney Basin and on the continental shelf south and southeast of Newfoundland, 2,000 feet (610 m) of Windsor Group sediment is postulated, based on data from Amoco-IOE Gannet O-59 and Elf Hermine E-94 wells (Barss, 1974b).

Regional uplift resulted in withdrawal of the Windsor sea and the deposition of the Canso Group fine clastics and the Riversdale Group clastics and coal. The areal distribution of the Canso-Riversdale groups is not as widespread as the underlying Windsor and Horton groups, and have fewer thick accumulations. The

AGE		GROUP
PERMIAN	LOWER	
CARBONIFEROUS	STEPHANIAN	PICTOU
	WESTPHALIAN D	
	WESTPHALIAN C	
	WESTPHALIAN B	CUMBERLAND
	WESTPHALIAN A	
	NAMURIAN	RIVERSDALE
		CANSO
	VISEAN	WINDSOR
	TOURNAISIAN	HORTON
DEVONIAN	LATE	
	MIDDLE	

TABLE 1. STRATIGRAPHIC SUBDIVISIONS AND AGES OF UPPER PALEOZOIC ROCKS OF EASTERN CANADA.

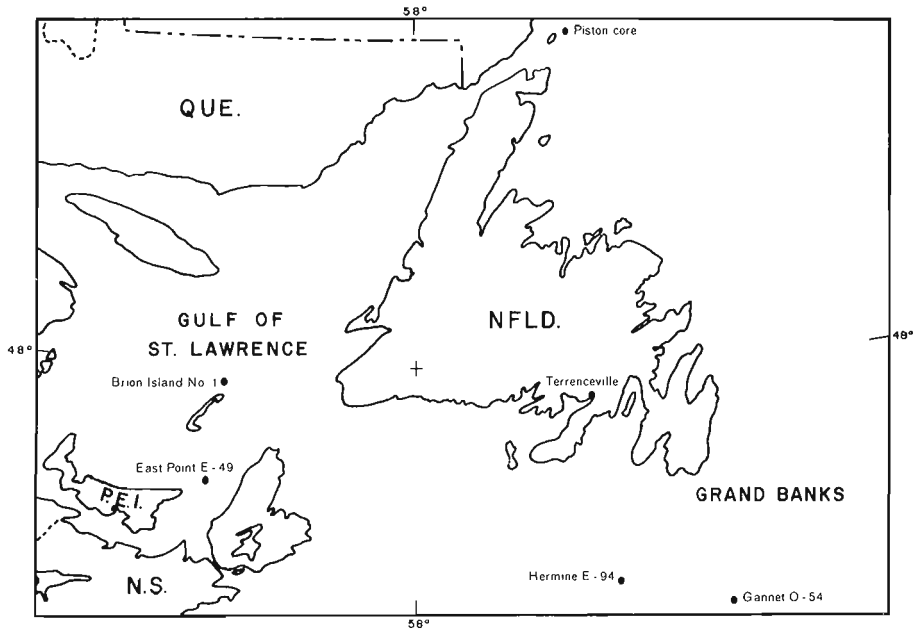

George Bay area of Nova Scotia contains an estimated 8,000 feet (2,439 m) of clastics. In the Pictou area and in the western part of the Cumberland Basin, Nova Scotia; St. George's Bay, Newfoundland; eastern Prince Edward Island and in several locations in southern Cape Breton Island sections have been estimated to contain 6,000 feet (1,829 m) of sediments. In the Magdalen Islands area, less than 2,000 feet (610 m) of strata have been postulated due to the migration of Windsor salt. In the Sydney Basin and the area to the east, at least 2,000 feet (610 m) of clastics have been postulated over a wide area. The Elf Hermine E-94 well contains 2,445 feet (745 m) of Canso-Riversdale rocks. Northeast of the Long Range Mountains of Newfoundland the occurrence of some Canso-Riversdale rocks has been postulated based on palynomorphs from piston core samples taken east of Belle Isle (Barss, 1974d) (Harris and Jollymore, 1974).

The greatest accumulation of Cumberland-Pictou Group rocks occurs in the Cumberland Basin and in eastern Prince Edward Island where in excess of 12,000 feet (3,659 m) of sediment are indicated. In the Gulf of St. Lawrence, northeast of Magdalen Islands, there is at least 10,000 feet (3,049 m) of Cumberland-Pictou Group rocks. Ten thousand feet (3,049 m) of mainly coal bearing strata occurs in the Stellarton Gap area of Nova Scotia. In the Magdalen Islands area and other parts of the Gulf of St. Lawrence less than 2,000 feet (610 m) of Cumberland-Pictou sediments is attributed to the movement of Windsor Group evaporites. Eight thousand feet (2,439 m) of strata is postulated for the Sydney Basin. Up to 2,000 feet (610 m) of Cumberland-Pictou rocks have been extended east of the Sydney Basin based on 225 feet (69 m) of Westphalian B-age rocks in the Elf Hermine E-94 well.

Five gas shows have been reported from Pictou Group sands in the HB Fina East Point E-49 well. One gas show and a little oil stain has also been reported from the Pictou Group in the Sarep HQ Brion Island No. 1 well. Present information on the Gulf of St. Lawrence indicates the migration of evaporites may have produced a variety of stratigraphic traps in post-Windsor sediments suitable for the accumulation of oil and gas. Additional geophysical surveys and considerable drilling are necessary to properly evaluate the area.

References

Barss, M.S.

1974a: Report on palynomorph assemblage from Terrenceville, Newfoundland; Geol. Surv. Can., Internal report, EPGS-Pal. 3-74 MSB.

1974b: Report on Paleozoic palynomorphs from Elf-Hermine E-94; Geol. Surv. Can., Internal report, EPGS-Pal. 4-74 MSB.

1974c: Report on Paleozoic palynomorphs from Amoco-IOE Gannet O-59; Geol. Surv. Can., Internal report, EPGS-Pal. 5-74 MSB.

1974d: Report on palynomorphs from piston core east of Belle Isle, Newfoundland; Geol. Surv. Can., Internal report, EPGS-Pal. 6-74 MSB.

Harris, I.M. and Jollymore, P.G.

1974: Iceberg furrow marks on the continental shelf northeast of Belle Isle, Newfoundland; Can. J. Earth Sci., v. 11, no. 1, p. 43-52.

Howie, R.D. and Barss, M.S.

Upper Paleozoic rocks of the Atlantic Provinces, Gulf of St. Lawrence and continental shelf adjacent to Newfoundland; Geol. Surv. Can. Paper 74-30, v. 2. (in preparation)

Kelley, D.G.

1967: Baddeck and Whycocomagh map-areas with emphasis on Mississippian stratigraphy on central Cape Breton Island, Nova Scotia (11K/2 and 11F/14); Geol. Surv. Can., Mem. 351, 65 p.

54. STRATIGRAPHY AND SEDIMENTOLOGY OF THE MESOZOIC AND TERTIARY ROCKS OF THE ATLANTIC SHELF

Project 710059

L.F. Jansa
Atlantic Geoscience Centre, Dartmouth

The objective of this project is to provide a lithostratigraphic and sedimentological framework of the Mesozoic and Tertiary sedimentary sequences of the Atlantic continental margin of Eastern Canada.

In 1973 this study was carried out mainly in the Grand Banks region where four wells (Elf Hermine E-94, Amoco-Imperial Puffin B-90, Eider M-75, and Murre G-67) were studied in detail (Fig. 1).

From a regional point of view the Grand Banks can be sudbivided into two major structural provinces. The southern structural province located at the western edge of the Grand Banks represents the eastern extremity of the Scotian Basin, in which the same lithostratigraphic units, as defined in the Scotian Basin, have been identified in the Puffin well. The thickness of the Cenozoic and Cretaceous sediments exceeds 15,500 feet. The northern province is located over the central part of the Grand Banks and contains a stratigraphic sequence that differs significantly with that of the Scotian Basin. The most striking structural feature of the latter area is a major angular unconformity that occurs at the base of the Cretaceous sequence. Above the unconformity, the Cretaceous and Cenozoic sedimentary wedge is uniformly thin and relatively flat lying. Beneath the unconformity, the structural attitude of the strata is markedly different. Jurassic and older formations are gently folded and are preserved in subbasins locally bounded by basement block-faulted structures, which according to Ayrton et al. (1974) appear to be of an extension origin with some evidence of strike slip movement.

The continental shelf of the Grand Banks would appear to represent a portion of the foundered continental crust that is overlain by Paleozoic, Mesozoic and Cenozoic sedimentary sequences. Paleozoic "basement" rocks that were encountered in the Murre well are composed of slightly metamorphosed metasediments of a phylitic appearance, which were dated by Jenkins (1974) as Devonian. The unmetamorphosed Paleozoic clastics and evaporites, Devonian to Mississippian age, were encountered in the Gannet well (Ayrton et al., 1974) and in Elf Hermine well (Fig. 1), where the Carboniferous sediments are over 5,000 feet thick and the well bottomed in the Windsor salt. The above wells thus indicate that Carboniferous rocks of the Sydney Basin are present over broad regions of the western Grand Banks. During the Permian phase of the Variscan Orogeny the Grand Banks area was uplifted and exposed to denudation. In the Triassic, a new depositional cycle was initiated as might be indicated by the some 700 feet of soft reddish shale which overlies the Devonian rocks and underlies evaporites of Early Jurassic age, as encountered in the Murre well. This red shale unit has not been paleontologically dated and its age can only be tentatively interpreted from the stratigraphic position of the unit, which could in part be correlative with the Eurydice Formation of the Scotian Basin.

The marine inundation of the Grand Banks occurred in the Early Jurassic during which a 1,400-foot-thick evaporite sequence was deposited in a shallow semi-restricted sea. The unit is composed of microcrystalline dolomite, anhydrite, dolomitized oolitic and peloid limestone and thin beds of salt associated with the lower part of the unit. Near the top of the unit skeletal calcarenites and oolitic grainstones are dated as Pleisbachian (Murre G-67 Amoco Well History Report, 1971) and the underlying dolomitic sequence is considered to be Hettangian-Sinemurian in age. The unit has a similar lithological composition to the Iroquois Formation on the Scotian Shelf and these units are considered to be coeval. With the progressing Lower Jurassic transgression, the water depth deepened and consequently, dark grey calcareous shale, enclosing occasional siltstone beds, coalified plant fragments, foraminifera and molluscs were deposited in a shallow epicontinental sea. Toward the end of the Lower Jurassic and during early Middle Jurassic, 400 feet of limestone composed of light grey oolitic and skeletal grainstone and wackestone (Murre well) were deposited, and these grade laterally southwestward to biomicrites with rare peloid wackestone in the vicinity of the Eider well. The presence of oolites suggest deposition in a shallow marine environment and indicate a lowering of the sea level during this period. However, marine deposition in the Grand Banks area does not appear to have been interrupted.

Depositional condition, similar to those at the late Lower Jurassic, were re-established in the late Middle Jurassic over the Grand Banks and deposition of calcareous shale continued. In the Upper Jurassic the light grey shale grades into brownish grey and reddish brown shale which is interbedded with 10- to 20-foot-thick limestone beds composed of superficial oolitic packstone and grainstone, peloid and skeletal wackestone, with foraminifera, molluscs, echinoderms, bryozoan and algae fossils and thin beds of fine-grained protoquarzitic sandstone. Sandstone became the dominant lithology in the upper part of the Upper Jurassic. The presence of superficial oolite and oolitic limestone and their association with protoquarzitic sandstone, occurrence of coalified plant fragments and the scarcity of foraminifera indicate a very shallow nearshore marine environment, with water depth not exceeding 10 feet during deposition of oolites. Presence of thin coal seams, lack of dinoflagellates (G. Williams, pers. comm.) and the presence of palynomorph assemblages in parts of the sequence suggest that the depositional environment during Late Jurassic time was occasionally brackish

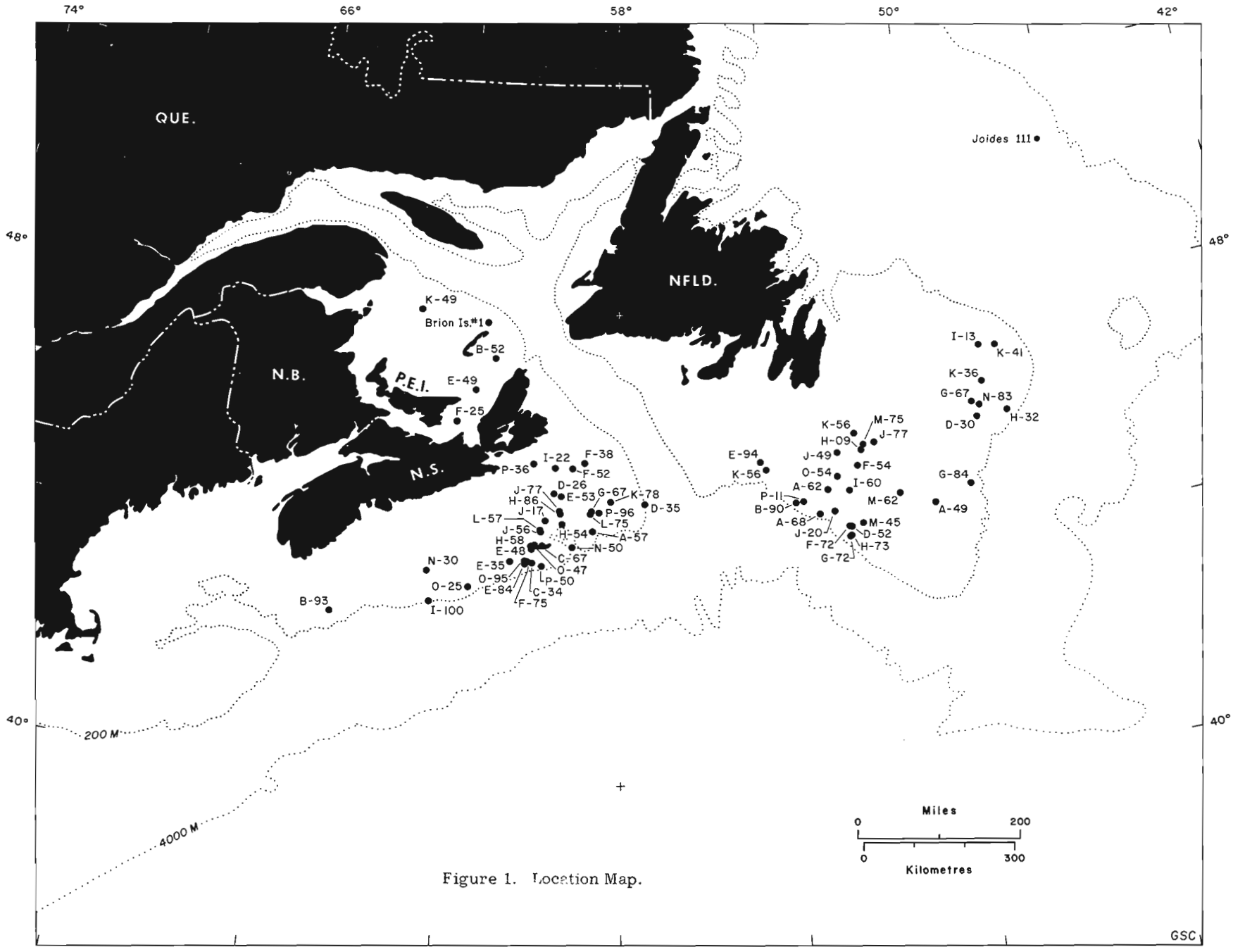

Figure 1. Location Map.

or even nonmarine. The lithological composition of the Upper Jurassic rocks from the Grand Banks is very similar to the Mic Mac Formation of the Scotian Basin, which indicates uniformity of depositional conditions from La Have Platform up to the East Newfoundland Basin at this time. Type of sediments, lithofacies pattern, and microfauna of the Jurassic period indicate deposition in an epicontinental seaway, covered by a shallow sea which extended northeast across the Grand Banks into the Scotian Basin at the south, and was interconnected to the northwest with the North European Jurassic sea. Thickness of the Jurassic sediments in the Grand Banks, as confirmed by studied wells, is about 10,000 feet - although thickness in excess of 20,000 feet is interpreted from deep seismic reflection profiling (Ayrton et al., 1974).

In the Early Cretaceous time the central part of the Grand Banks was epirogenetically uplifted and fragmented, which led to the formation of grabens and half grabens that preserved Jurassic sediments across the northern portion of the Avalon Uplift. The central part of the Grand Banks was, at this time, subaerially exposed and subjected to erosion; consequently, the Lower Cretaceous and parts of the Upper Jurassic were in places not deposited and/or were removed. The angular unconformity is strongest at the Eider well, where the Cenomanian overlies the Tithonian-Kimmeridgian rocks. The unconformity diminishes rapidly southward and northward to the deeper basins where it is finally lost in conformable beds. Age of the unconformity is reported to be Late Albian, although the vertical movement started probably in the Upper Jurassic.

The first transgression over the Lower Cretaceous unconformity resulted in deposition of a marginal to shallow marine sand-shale sequence, which is 400 feet thick at the Eider well. The sandstone of this unit displays an excellent porosity, but no hydrocarbons were reported in these wells. Age of the unit is Cenomanian-Late Albian and it is correlated with the upper part of the Logan Canyon Formation on the Scotian Shelf. The argillaceous siltstone, mudstone, thin limestone and chalk overlying the Logan Canyon Formation equivalent were deposited in a middle neritic to epibathyal environment as the transgression continued, and the depositional environment deepened during the Upper Cretaceous. The limestone at 2,230 feet at Eider well and at 8,610 feet at Puffin well was named Petrel by Amoco Geological Staff (Ayrton et al., 1974) and is composed of foraminiferal-skeletal packstone to wackestone. The Petrel limestone is Turonian in age and can be correlated with the "G" marker (McIver, 1972) on the Scotian Shelf. Two beds of chalk were encountered by Puffin well. The lower chalk (7,418 feet), about 100 feet thick, is composed mainly of cocoliths and marks the culmination of the Upper Cretaceous transgression. At the time of chalk deposition the depositional environment in the vicinity of Puffin well was outer neritic to epibathyal. The age of the lower chalk is, according to D. Clark (pers. comm.), Early Maastrichtian to Late Campanian and the chalk is correlated with the Wyandot Chalk on the Scotian Shelf. The upper chalk at the Puffin well (7,280 feet) is about 90 feet thick and was dated as Late Paleocene. The upper chalk is underlain by a pale reddish and greenish grey marl, indicating a diastem at the pre-Late Paleocene time in the vicinity of the well. Similarity in the composition of both chalks suggests similarity of the depositional environments of the Tertiary and Upper Cretaceous chalks.

During the Tertiary brownish grey and olive grey glauconitic mudstones and medium- to coarse-grained sandstones were deposited in several offlapping regressive sequences over the Grand Banks. The thickest Tertiary section was penetrated by Puffin well where it is 7,400 feet thick.

Fourteen days field work was carried out in the Essaouira Basin in Morocco in collaboration with geologists of the Lamont-Doherty Geological Observatory and South Carolina University. Work was directed particularly to the Jurassic stratigraphy and fauna in the coastal area, extending from Essaouria to Agadir. The results will form part of a wider study aimed at: 1) lithostratigraphic study aiming to establish the sedimentological trends and tectonic relations as relevant to the theories concerning the relative position of continental plates during Mesozoic and to the sea-floor spreading theory; 2) assessing the distribution and affinities of microfauna in Mesozoic circum-Atlantic coastal basins; and 3) studying the outcrop sections for source rock and reservoir rocks to properly evaluate the subsurface Mesozoic section of the Atlantic continental margin for the hydrocarbon evaluation program, applying the continental drift theory.

The preliminary lithostratigraphic comparison of the Late Triassic and Jurassic of the Essaouira Basin with the time synchronous Mesozoic section on the Canadian Atlantic continental margin show an exteme similarity to the Scotian Basin, but significant difference with the Mesozoic of the Grand Banks.

References

Amoco Canada Petroleum Company Ltd.
1971: Well History Report Amoco-IOE A-1 Murre G-67; Amoco Canada Petroleum Company Ltd., Calgary.

Ayrton, W.G., Birnie, D.E., and Swift, J.H.
1974: Grand Banks - future marine theater?; Oil Gas J., Jan. 14, 1974, p. 77-79.

Jansa, L.F.
1973: Stratigraphy and sedimentology of the Mesozoic and Tertiary rocks of the Atlantic Shelf; in Report of Activities, November 1972 to March 1973, Geol. Surv. Can., Paper 73-1B, p. 81-83.

Jenkins, W.A.M.
1974: Age determinations in the interval 10,000' to 10,949' (T.D.) of Amoco IOE A-1 Murre G-67 well, Grand Banks, Newfoundland; Geol. Surv. Can., Internal Report EPGS-Pal. 8-74, 2 p.

McIver, N.L.
1972: Cenozoic and Mesozoic stratigraphy of the Nova Scotia Shelf; Can. J. Earth Sci., v. 9, no. 54, p. 54-70.

PALEOZOIC GEOLOGY OF THE HUDSON BAY REGION

Project 710066

Bruce V. Sanford
Atlantic Geoscience Centre, Dartmouth

The Hudson Platform embraces an area of some 460,000 square miles, nearly half of which is submerged beneath Hudson and James bays, Hudson Strait, Foxe Channel and Foxe Basin. Two well known sedimentary basins occur within the Hudson Platform: the Moose River Basin in the south, mainly in Ontario and extending beneath western James Bay; and the Hudson Bay Basin lying mainly offshore but extending into Manitoba and Ontario in the south and into Mansel, Coats and Southampton islands in the north. These basins are defined, one from the other, by a northeast-trending basement high, the Cape Henrietta Maria Arch. The Paleozoic rocks preserved in graben structures beneath Hudson Strait, Foxe Channel and Foxe Basin, as well as beneath Frobisher Bay and Cumberland Sound are now merely remnants of a much broader cratonic cover that probably at one time mantled the entire Canadian Shield.

Geological mapping has been carried out on a broad reconnaissance scale in the Hudson Platform by officers of the Geological Survey and the generalized results of this work are illustrated in Figure 1. In the onshore areas, air supported surveys have been carried out in the Hudson Bay Lowlands (1950-51) by S.J. Nelson and (1967) by A.W. Norris, B.S. Norford, B.V. Sanford, L.M. Cumming and H.H. Bostock; on Southampton, Coats and Mansel islands (1968-69-70) by B.V. Sanford, W.W. Heywood and W.L. Davison; and in the Foxe Basin area by R.G. Blackadar and H.P. Trettin in 1965 and 1968 respectively. Reconnaissance mapping of the offshore areas of Hudson Platform were carried out by B.V. Sanford and C.F.M. Lewis in 1971 and by A.C. Grant in 1965, 1966 and 1971.

The stratigraphic framework that has emerged as a result of this work is illustrated in Table 1. There is some question as to whether the stratigraphic nomenclature used herein should be extended into Foxe Basin, but because the writer has recognized a similarity of some of the Ordovician and Silurian units in that area to those in the southern areas of the Hudson Platform, a uniform nomenclature for the entire region is tentatively adopted. Studies in progress by H.P. Trettin will provide a stratigraphic nomenclature for the Foxe Basin consistent with his previous investigations of the Arctic Platform.

Considerable assistance and advice in the construction of a time-stratigraphic framework for the Hudson Platform has been forthcoming from T.E. Bolton, T.T. Uyeno and D.C. McGregor of the Geological Survey of Canada, and C.R. Barnes of the University of Waterloo.

Rocks of Ordovician, Silurian and Devonian age are represented in various parts of the Hudson Platform. In the Moose River Basin these have a combined thickness of about 2,000 feet whereas in Hudson Bay Basin the three systems probably exceed 8,000 feet. So far as is known, only Ordovician and Silurian Systems and minor remnants of Devonian are preserved beneath Hudson Strait, Foxe Channel and Foxe Basin, where they are believed to be 3,000 and 1,700 feet thick respectively.

For the most part, the Ordovician, Silurian and Devonian sequences are composed of limestones and dolostones with minor shales, siltstones, sandstones and evaporites that reflect a variety of depositional environments. Extensive reef development occurs in Upper Ordovician (Red Head Rapids), Middle Silurian (Attawapiskat) and Middle Devonian (Kwataboahegan) rocks. Evaporite deposits are widespread in the form of anhydrite/ gypsum and halite in Middle and Upper Ordovician (Bad Cache Rapids and Red Head Rapids), Upper Silurian (Kenogami River) and Middle Devonian (Moose River) strata.

Sandstone facies are poorly developed but intertongue sporadically with carbonate rocks bordering areas of local uplift of Precambrian basement rocks. Coarse clastics are confined mainly to the basal few feet of the Bad Cache Rapids, and as interbeds of the Red Head Rapids, Kenogami River and Sextant formations. A basal Paleozoic coarse clastic facies is well developed in Foxe Basin and beneath Hudson Strait in the Ship Point-Admiralty succession and may also be present in the subsurface in the lower part of the Hudson Bay Basin.

Although the Paleozoic rocks of the Hudson Platform are for the most part relatively flat lying, local deformation has occurred as a result of basement block faulting. Faulting is known to have taken place during a number of intervals from Ordovician to Mesozoic and possible Cenozoic time. Probably the most intensive recorded epeirogeny was during the Early Devonian (Siegenian) period. Faults of this age are well known and have been mapped both at surface and in subsurface. One significant feature of widespread proportions is a horst structure some 250 miles long that extends in a northwest direction across central Hudson Bay where it is concealed beneath rocks of Middle and Late Devonian age. This structure was tested in 1969 by a well that was drilled to the Middle Silurian Severn River Formation and suspended at a depth of 3,926 feet.

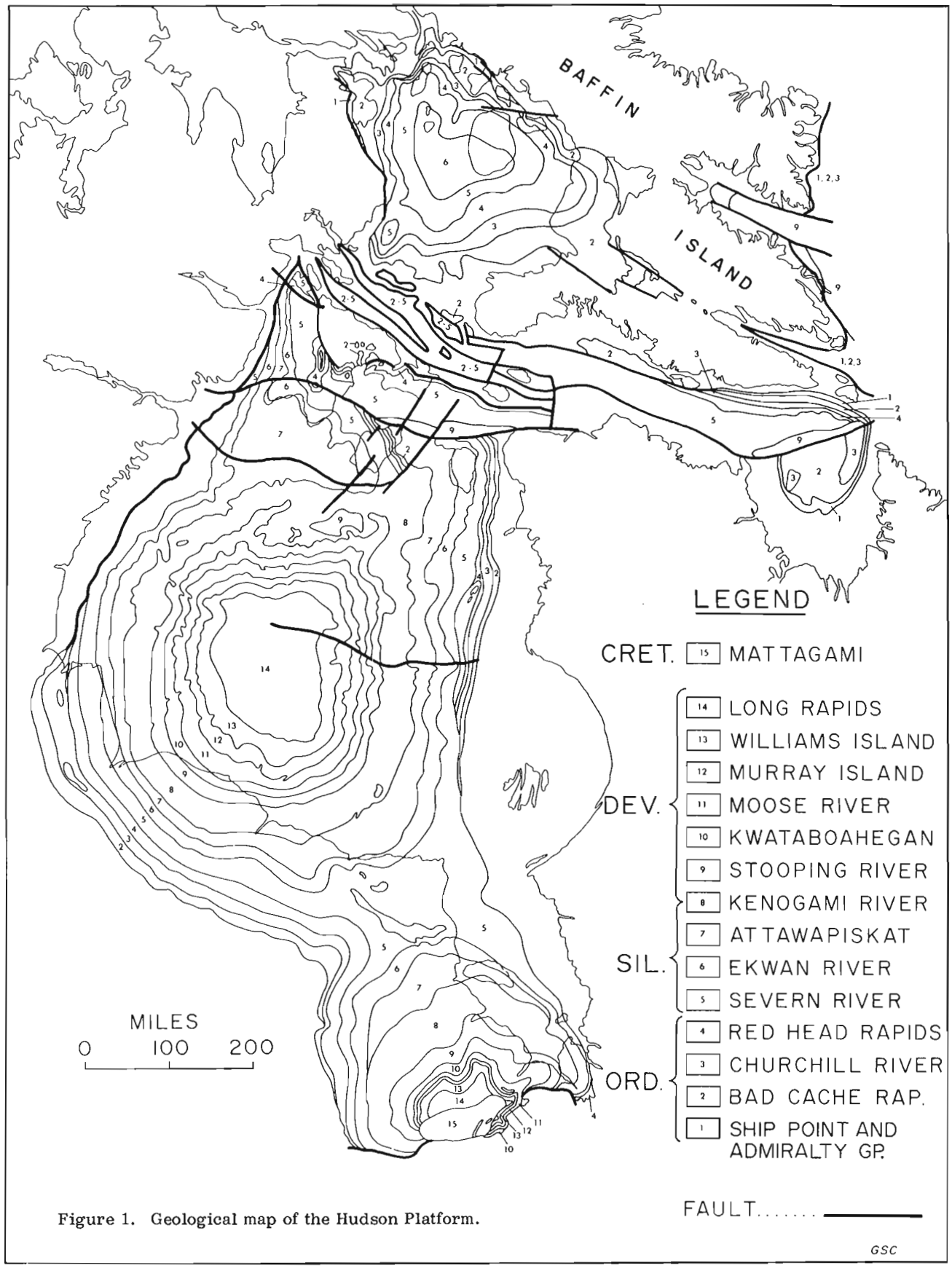

Figure 1. Geological map of the Hudson Platform.

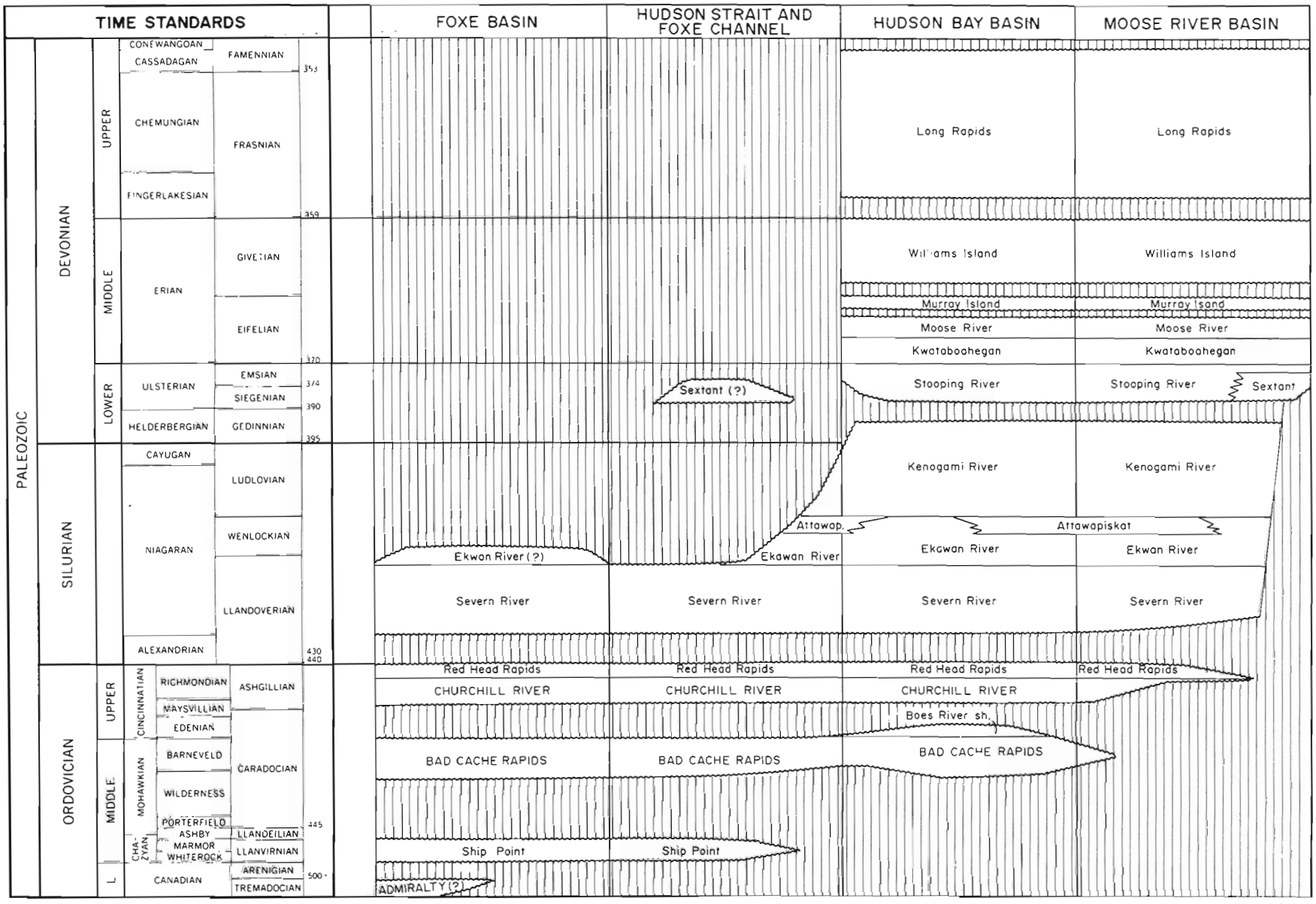

TABLE 1. STRATIGRAPHIC FRAMEWORK - HUDSON PLATFORM

56. REGIONAL GEOLOGY OF THE MESOZOIC-CENOZOIC SEDIMENTS OFF NOVA SCOTIA AND NEWFOUNDLAND

Project 720104

John A. Wade
Atlantic Geoscience Centre, Dartmouth

Ongoing studies of exploratory well data and participation seismic profiles purchased by the Department, have resulted in further delineation of structural elements of the Atlantic continental margin of Canada (Fig. 1). Three major depocentres are recognized and designated the Scotian Basin, East Newfoundland Basin and Flemish Basin. The Scotian and East Newfoundland basins were connected through Late Jurassic time by means of a seaway across the northern Grand Banks. The Flemish Basin appears to have developed during a period of Early Cretaceous tectonism.

The sub-basins within the Scotian Basin received maximum sedimentation from Late Triassic to Late Tertiary and probably contain in excess of 10 kilometres of sediments.

The La Have Platform and Canso Ridge, which form the northwest margin of the Scotian Basin were positive until late Early Jurassic and were slowly transgressed during Middle and Upper Jurassic time. The South Bank High appears to have been positive throughout Jurassic time.

A disturbance which commenced in latest Jurassic and continued through the late Early Cretaceous elevated the Avalon Uplift province and deformed the Jurassic and older sediments. Remnants, separated by basement ridges, are preserved in the Whale, Horseshoe and Carson subbasins of the Avalon Uplift and the Jeanne d'Arc subbasin of the East Newfoundland Basin. This disturbance is thought to be related to the Early Cretaceous separation of the Iberian Peninsula from the eastern side of the Grand Banks and the formation of the Flemish Basin. Seismic profiles across the west flank of this basin indicate sediment thickness from less than 2 km near the top of the slope to more than 6 km at the base of the rise. From seismic correlation, these sediments are interpreted to be mainly post-Early Cretaceous in age. No salt diapirs have been seen in this basin.

The La Have Platform was stable to mildly positive during the Early Cretaceous and sedimentation was concentrated in the actively subsiding Scotian Basin with the development of a thick deltaic complex. Sedimentation continued into the Late Cretaceous with deposition of a paralic sequence which transgressed the entire area. During the Cretaceous, numerous halokinetic structures developed in the Abenaki, Sable and South Whale subbasins and a series of growth faults were formed along the southeastern edge of the Scotian Shelf. Beneath the Scotian Slope a large number of salt and/or shale diapirs were emplaced (Fig. 2). These are outlined as the Sedimentary Ridge Province (Fig. 1).

Diapirs within the ridge province rise as much as 7 km into the overlying sediments. The height and width of the individual piercements varies and their third dimension is unknown. That is, it is not known whether they are circular, elliptical or elongate. However, since the number of structures seen on each profile crossing the area is approximately the same, they may be elongate or ridge-like features. Emplacement may have been caused by sediment load on overpressured shales or salt beneath the shelf edge resulting in slight seaward movement of the shelf-edge sediment pile and intrusion of diapiric material into the sediments beneath the slope.

Without exception, the most southerly structure on each of the control lines is in sharp vertical contact with the sequence of layered sediments beyond. In a number of instances the diapirs appear to cut oceanic Layer 2 indicating the diapiric material may be derived from below Layer 2 and that Layer 2 is a flow or an intrusion into sedimentary material. It further indicates that sediments and even continental crust may lie beneath the so called "oceanic basement" in this region.

South of the Sedimentary Ridge Province, the Layer 2 event exhibits considerable relief with ridges(?) rising several thousand feet above the general level of the event. In the southeastern corner of the Scotian Basin, off the South Bank High, the nature of the basement is changed and a number of prominent, relatively circular basement highs are identified from seismic profiles. These appear to be ancient seamounts which, because of their proximity to the Avalon Uplift, have been buried by sediments.

The Tertiary system beneath the Scotian Shelf and Grand Banks is represented by a regressive clastic sequence which, in latest Tertiary time, shows rapid progradation in response to eustatic lowering of sea level. Although up to 2 km of Tertiary sediments occur along the shelf edge in the Scotian Basin, up to twice this thickness may occur beneath the continental slope. Some of the diapirs beneath both the shelf and slope continued to grow during the Tertiary period. Pleistocene sediments beneath the Scotian Shelf and Grand Banks are generally thin; however, on the lower slope and upper rise they may reach a thickness in excess of 2 km.

Reference

Ayrton, W.G. et al
1973: Regional Geology of the Grand Banks: presented at joint CSPG-CSEG meeting in Calgary, April 18, 1973. Reported in Daily Oil Bulletin, April 23, 1973; Oilweek, April 23, 1973, and Oil and Gas Journal, Jan. 14, 1974.

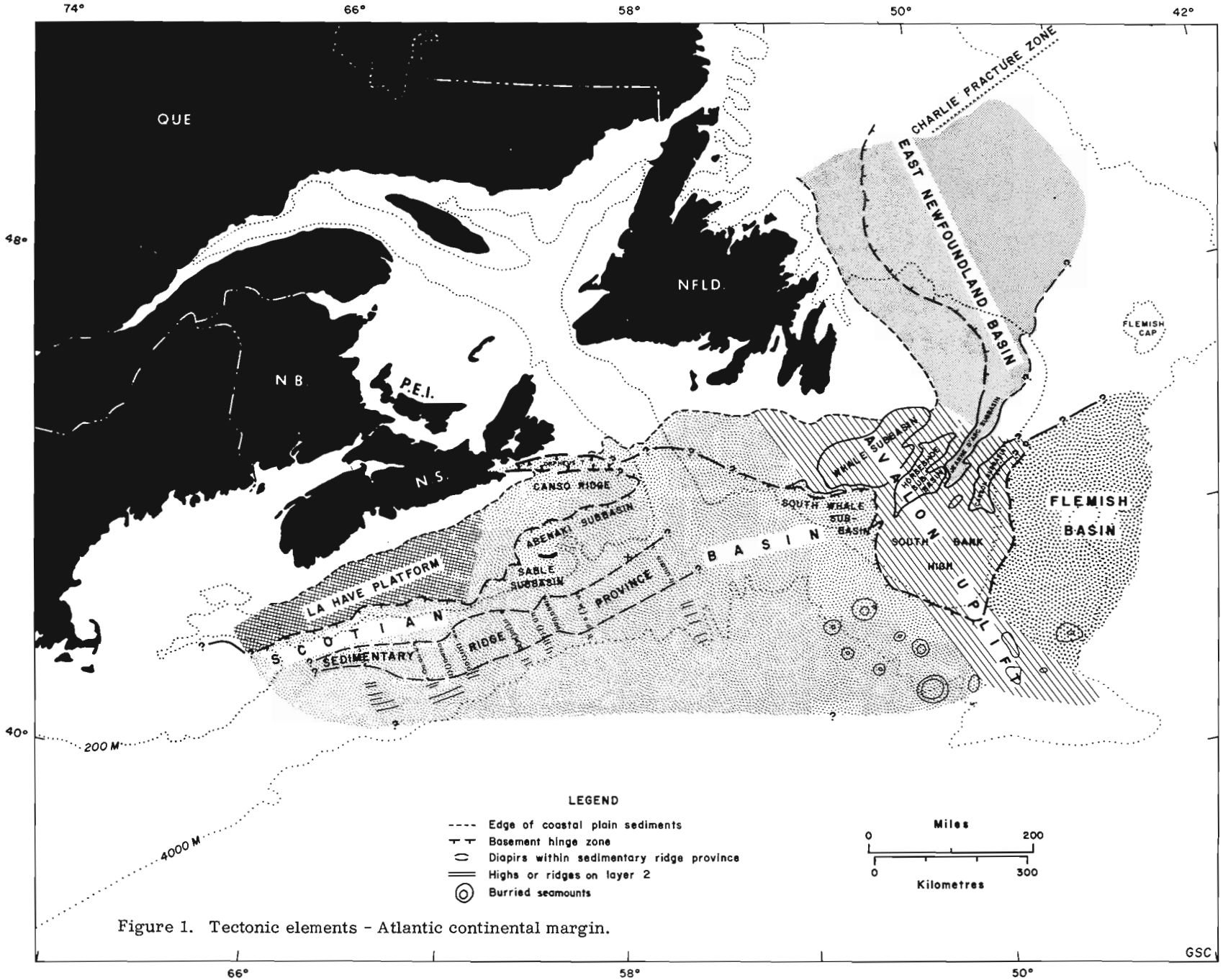

Figure 1. Tectonic elements - Atlantic continental margin.

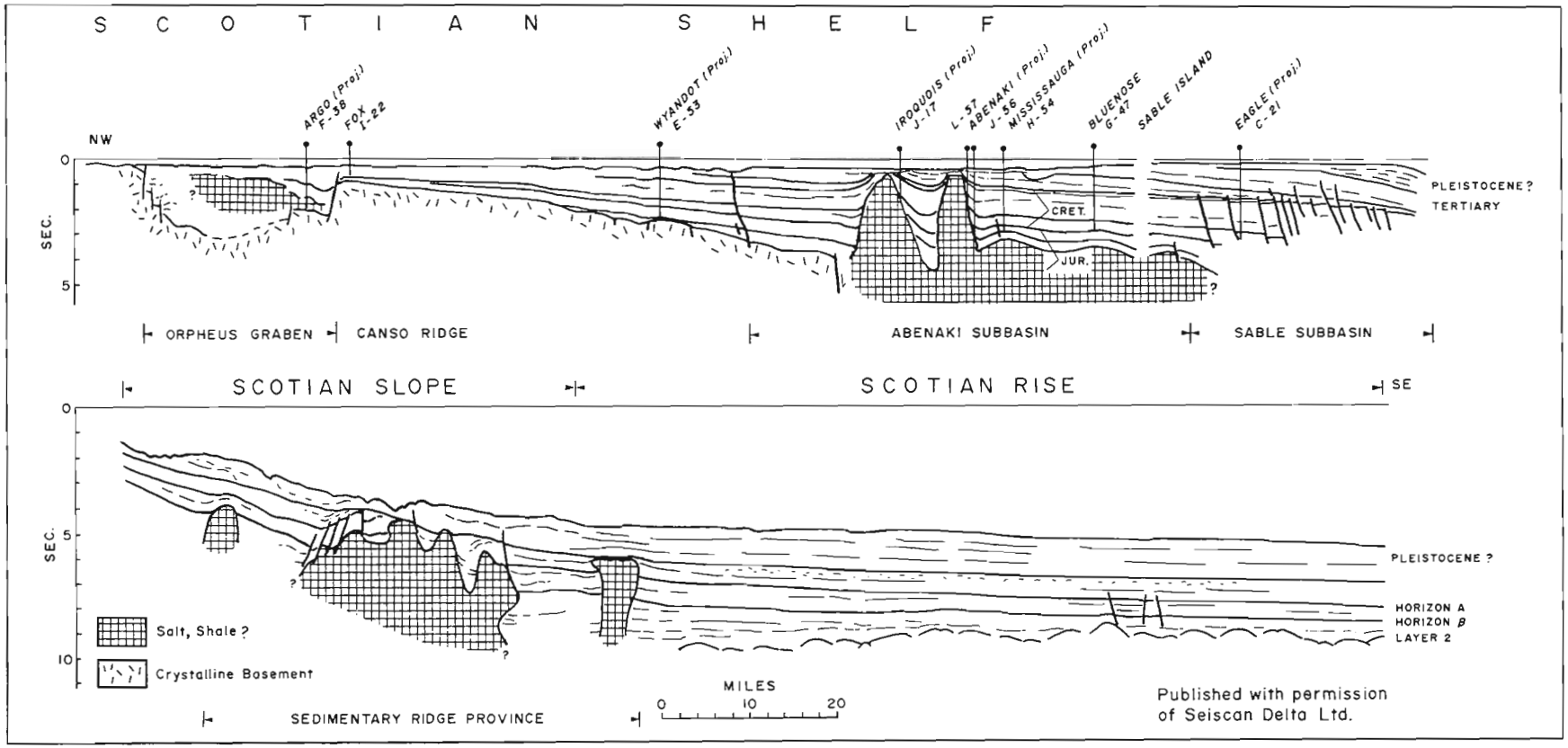

Figure 2. Composite seismic profile across the Scotian Shelf, slope and rise.

57. BIOSTRATIGRAPHY AND PALEOECOLOGY OF THE MESOZOIC AND CENOZOIC ROCKS OF THE ATLANTIC SHELF

Project 710062

G. L. Williams
Atlantic Geoscience Centre, Dartmouth

Introduction

The recent exploration for oil and gas on the Scotian Shelf and Grand Banks has resulted in the drilling of over eighty wells in an area exceeding 170,000 square miles. Palynological analyses of cores and cuttings samples from seven of the wells on the Scotian Shelf and two wells plus eight shallow core holes on the Grand Banks are now completed. The dated sediments range from Late Devonian (Barss, pers. comm.) to Plio-Pleistocene. A preliminary zonation of the Mesozoic-Cenozoic utilizing dinoflagellates, spores and pollen permits correlation of the wells with the European type section.

Stratigraphy

Bartlett and Smith (1971) proposed seven formal divisions for the Mesozoic-Cenozoic sections in the Pan American IOE Tors Cove and Pan American IOE Grand Falls wells on the Grand Banks. McIver (1972), based on the examination of twenty well sections, subdivided the Mesozoic-Cenozoic stratigraphy of the Scotian Shelf into three groups, twelve formations and four members. These are Early Jurassic to Pliocene. The present palynological studies have permitted refinement of the age of McIver's formations and revealed their time stratigraphic nature (Fig. 1).

Biostratigraphy

Previous Investigations

Published palynological studies of the Mesozoic-Cenozoic of eastern Canada are few. Terasmae and Scott (in Stevenson, 1959), Stevenson and McGregor (1963) and Lin (1971) described spore and pollen assemblages from onshore nonmarine Lower Cretacous

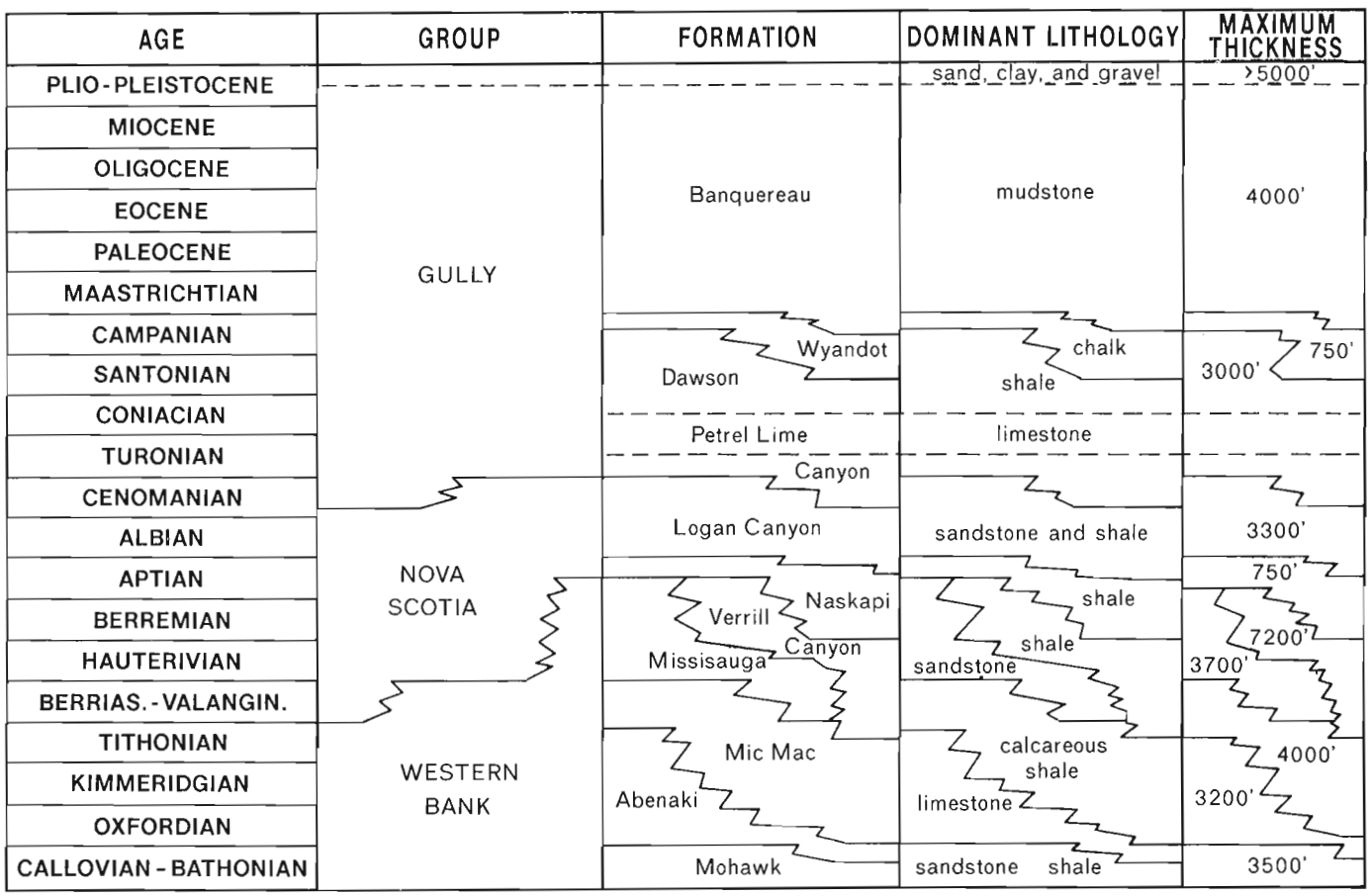

Figure 1. Postulated relationship of biostratigraphy and lithostratigraphy in the Mesozoic-Cenozoic of the Scotian Shelf. (Lithostratigraphy from McIver, 1972, Biostratigraphy based on Palynology).

sediments of Hants and Halifax Counties, Nova Scotia. King et al. (1970) described spores and pollen recovered from dredge hauls on the Scotian Shelf, to which they assigned an Albian age. The parent flora was believed to have lived in a warm, humid temperate to subtropical climate.

Williams and Brideaux (in press) report on the detailed palynological analysis of 104 samples from 8 shallow core holes drilled on the Grand Banks by Pan American Petroleum Corporation and Imperial Oil in 1965. These core holes penetrated sediments ranging from Late Albian to Pleistocene. Williams and Brideaux recognize 19 dinoflagellate divisions, based on 96 species, of Cenomanian-Pleistocene age, and 24 spore and pollen divisions, based on 100 species, extending from the Late Albian to the Pleistocene. The geological history, as determined from the shallow core holes, indicates a period of nonmarine deposition in the Albian. This was succeeded in the Cenomanian-Turonian by a marine transgression. Subsequent deposition through to the Pliocene occurred in a wholly marine environment, although breaks in the record, particularly between the Cretaceous and Tertiary suggest periods of uplift and erosion.

Current Investigations

The palynomorphs present in samples from the nine wells, Shell Mohawk B-93, Shell Naskapi N-30, Shell Mohican I-100, Shell Fox I-22, Shell Oneida O-25, Mobil Sable Island C-67, Mobil Dauntless D-35, Amoco IOE Puffin B-90 and Amoco Eider A-1 and eight shallow core holes, permit correlation of the Mesozoic-Cenozoic sediments of the Scotian Shelf and Grand Banks. Twenty palynomorph zones ranging from the Middle Jurassic to Plio-Pleistocene are recognized. The postulated age of the zones in order of succession is: Lias, Bajocian-Bathonian, Callovian, Oxfordian, Kimmeridgian, Tithonian, Berriasian-Valanginian, Hauterivian, Barremian, Aptian, Albian, Cenomanian, Turonian, Coniacian, Santonian, Campanian, Maastrichtian, Danian, Late Paleocene, Early Eocene, Middle Eocene, Late Eocene, Early Oligocene, Middle-Late Oligocene, Early Miocene, Middle Miocene, Late Miocene and Plio-Pleistocene. The Albian can be further subdivided into Early and Late Albian. Each zone equates with an assemblage zone or peak zone and is characterized by a distinctive palynomorph assemblage.

Shell Mohawk B-93 is at the extreme southwest of the Scotian Shelf and contains sediments dated as Middle Jurassic, Late Jurassic, Neocomian, Aptian, Late Cretaceous, and Paleogene. Shell Naskapi N-30 contains a more or less complete sequence from Middle Jurassic to Late Cretaceous. Shell Mohican I-100 on the southern edge of the Scotian Shelf has a thick Jurassic and Early Cretaceous sequence overlain by thin Cenomanian which in turn is overlain by over 5,000 feet of Miocene-Pleistocene. The nearby Shell Oneida O-25 has penetrated Middle Jurassic-Miocene sediments, with the Eocene being very attenuated. Mobil Sable Island C-67 has a very thick Early Cretaceous sequence overlain by Late Cretaceous and Tertiary rocks. The Middle Eocene appears to be absent. Shell Fox I-22 lies to the north of the Scotian Shelf. In this well the Late Jurassic-Early Cretaceous totals less than 2,000 feet. Mobil Dauntless D-35 is on the southern edge of the Laurentian Channel. It has encountered Oxfordian-Miocene sediments in a more or less continuous sequence. Amoco IOE Puffin B-90 and Amoco IOE Eider A-1 are located on the Grand Banks. Puffin, which can be correlated with Mobil Dauntless D-35, contains Cretaceous-Cenozoic sediments. The Cenozoic is over 7,000 feet thick. In Amoco Eider A-1 the Jurassic is overlain by Upper Cretaceous sediments. The 8 shallow core holes studied have revealed sediments ranging from Albian to Plio-Pleistocene.

Comparison of the Scotian Shelf-Grand Banks palynomorphs with coeval assemblages indicates a change in affinities. In the Jurassic and Early Cretaceous there is a close similarity with the assemblages from the European type sections of England and France. In the Albian and Late Cretaceous the dinoflagellate zones appear to be as cosmopolitan as the equivalent planktonic foraminiferal zones. During the Cenozoic there is increasing provincialism. The Paleogene assemblages of the Scotian Shelf and Grand Banks are initially similar and compare favourably with those described from the JOIDES core holes, offshore Florida. In the Late Eocene-Early Oligocene differences between the Grand Banks and Scotian Shelf begin to emerge and become more pronounced in the Late Oligocene and the Miocene. Correlation of the Neogene, even locally, is extremely difficult; regionally it is hindered by a sparsity of species.

Paleoecology

Paleoecological conclusions are based on benthonic foraminiferal and ostracod data generated by P. Ascoli and dinoflagellate, spore and pollen data. The Mesozoic-Cenozoic depositional history of the Scotian Shelf and Grand Banks, based on the examination of the nine wells listed and the eight shallow core holes, was predominantly marine, with nonmarine intercalations in the Jurassic, Early Cretaceous and Pleistocene. The Jurassic and Cretaceous of Shell Fox I-22 is predominantly nonmarine. In Mohawk B-93, Naskapi N-30 and Oneida O-25 the Middle and Late Jurassic and Early Cretaceous is nonmarine to inner neritic. In Amoco Eider A-1 the Jurassic ranges from nonmarine to neritic.

The Early Cretaceous, where present, is inner neritic to nonmarine. The absence of Early Cretaceous sediments in Amoco Eider A-1 presumably denotes a time of uplift and erosion on the Grand Banks before the marine transgression in the Cenomanian. On the Scotian Shelf there was a widespread marine transgression in the Aptian followed by regression in the Albian.

The Cenomanian of the Scotian Shelf was a time of widespread inner shelf, inner neritic deposition with a few nonmarine episodes. Throughout the remainder of the Late Cretaceous, both on the Scotian Shelf and Grand Banks, the sediments were deposited in a marine, generally middle to outer shelf, environment. Sedimentation appears to be continuous across the Maastrichtian-Danian boundary only in Oneida, Sable and Dauntless.

The Tertiary is predominantly marine with non-sequences in the Early Paleocene, Middle and Late Eocene, Oligocene and Early Miocene. The Pleistocene is nonmarine to inner neritic.

Conclusions

The detailed studies of the palynomorphs of the nine wells and eight shallow core holes has permitted the establishment of a biostratigraphic zonation covering the Middle and Late Jurassic, Cretaceous and Cenozoic. There is a major unconformity on the Grand Banks with marine Cenomanian overlying marine Late Jurassic rocks. On the Scotian Shelf and western Grand Banks this unconformity is not evident, although there are significant non-sequences in the Albian, Maastrichtian, Paleocene and Eocene. Nonmarine to neritic deposition occurs in the Jurassic and Early Cretaceous. In the Late Cretaceous-Tertiary, most of the area was inundated by the sea with environments ranging from inner to outer neritic.

References

Bartlett, G.A. and Smith, Leigh
1971: Mesozoic and Cenozoic history of the Grand Banks of Newfoundland; Can. J. Earth Sci., v. 8, p. 65-84.

King, L.H., MacLean, Brian, Bartlett, G.A., Jeletzky, J.A., and Hopkins, W.S., Jr.
1970: Cretaceous strata on the Scotian Shelf; Can. J. Earth Sci., v. 7, p. 145-155.

Lin Chang, L.
1971: Cretaceous deposits in the Musquodoboit River Valley, Nova Scotia; Can. J. Earth Sci., v. 8, no. 9, p. 1152-1154.

McIver, N.L.
1972: Cenozoic and Mesozoic stratigraphy of the Nova Scotia Shelf; Can. J. Earth Sci., v. 9, p. 54-70.

Stevenson, I.M.
1959: Shubenacadie and Kennetcook map-areas, Colchester, Hants and Halifax Counties, Nova Scotia; Geol. Surv. Can., Mem. 302, 88 p.

Stevenson, I.M. and McGregor, D.C.
1963: Cretaceous sediments in central Nova Scotia, Canada; Geol. Soc. Am. Bull., v. 74, p. 355-356.

Williams, G.L., and Brideaux, W.W.
Palynological analyses of Late Mesozoic-Cenozoic rocks of the Grand Banks of Newfoundland; Geol. Surv. Can., Bull. 236. (in press)

C. Regional Reconnaissance

58. ELASTIC PROPERTIES OF BERMUDA BASALTS

Project No. 730080

D.L. Barrett
Atlantic Geoscience Centre

During the summer of 1972, an 800-m corehole was drilled into the island of Bermuda. The cores include basalt, hydrothermally altered basalt and gabbros with varying degrees of infilling and porosity. Compressional and shear wave velocities were measured in 44 samples at pressures to 2.5 kb. In addition, bulk densities of the samples were determined.

Compressional wave velocities of the massive basalts, typical of the flow lavas, reach an average value of about 6 km/sec at 2 kb, while the microsyenogabbros, typical of the many intrusive sheets, reach a velocity of up to 6.9 km/sec at 2 kb. Hydrothermally altered basalt velocities are somewhat higher than those of the massive basalts while the more porous material exhibits lower velocities in the range of 3 to 4 km/sec.

Elastic constants were calculated from the compressional and shear wave velocities of typical rock types and perhaps the most informative and useful in rock identification in Poisson's ratio because of its independence with pressure. Poisson's ratio for the massive basalts ranges from 0.25 to 0.27, altered basalts and porous gabbros from 0.28 to 0.31 whereas the values for massive gabbros lie between 0.32 and 0.34. The separation is sufficient in the groups of values to identify these oceanic rock types on this elastic criteria. If reliable compressional and shear wave velocities from bottom seismometers were available in the ocean basins, the foregoing results could be compared with the elastic properties of layers 2 and 3.

A chemical analysis of the high velocity gabbros shows a high titanium content which not only gives the material a high mean atomic weight but probably contributes to its high velocity.

A presence of sulphides in the intrusive material of up to 15 per cent by volume in .5-m sections suggests that the volatile constituents of these rocks has not been lost through permeable exposure to the surface. This relatively high concentration of sulphides may well be the mobilizing agent in triggering lava outpours such as those comprising the island of Bermuda.

Projects 730079, 720103, 720104

A.C. Grant and R.F. Macnab
Atlantic Geoscience Centre, Dartmouth

High resolution seismic reflection profiles from the continental shelf northeast of Newfoundland, collected by the M.V. MINNA in September - October, 1973, have been integrated with prior coverage to enable more detailed mapping of bedrock and surficial geology. Previous surveys have shown that the inner shelf northeast of Newfoundland is underlain by a relatively smooth erosional surface, which extends eastward beneath Cretaceous Tertiary coastal plain-type deposits. Off Notre Dame Bay this erosional surface is cut on gently folded sedimentary strata, which are considered to be Carboniferous or post-Carboniferous but pre-Cretaceous in age. It has been observed (Grant, 1972; Harris and Jollymore, 1974) that the axes of folding of these strata tend to lie approximately normal to the general northeast structural trend of the Appalachian system, a result which would seem to bear very importantly upon tracing the seaward extent of the Appalachian system northeast of Newfoundland.

The navigational systems carried by the M.V. MINNA enabled a precise crossing (± 125 m) of two of the seismic lines for the purpose of obtaining a strike and dip measurement within this area of folded strata (Fig. 1). The resultant direction at this point was slightly west of north. A review of all seismic profiles from this area supports a north to northwest direction as the dominant trend of fold axes. However, local departure from this direction and apparent localization of relatively strong fold structures observed on the seismic profiles that some of these features may be domal in form. One interpretation that must be considered for these possible domal structures is that they are salt diapirs.

Data from the MINNA cruise (B173-019) are being prepared for submission to open file.

References

Grant, A.C.
1972: The continental margin off Labrador and eastern Newfoundland-Morphology and Geology; Can. J. Earth Sci., v. 9, p. 1394-1430.

Harris, I.M. and Jollymore, P.G.
1974: Iceberg furrow marks on the continental shelf northeast of Belle Isle, Newfoundland; Can. J. Earth Sci., v. 11, p. 43-52.

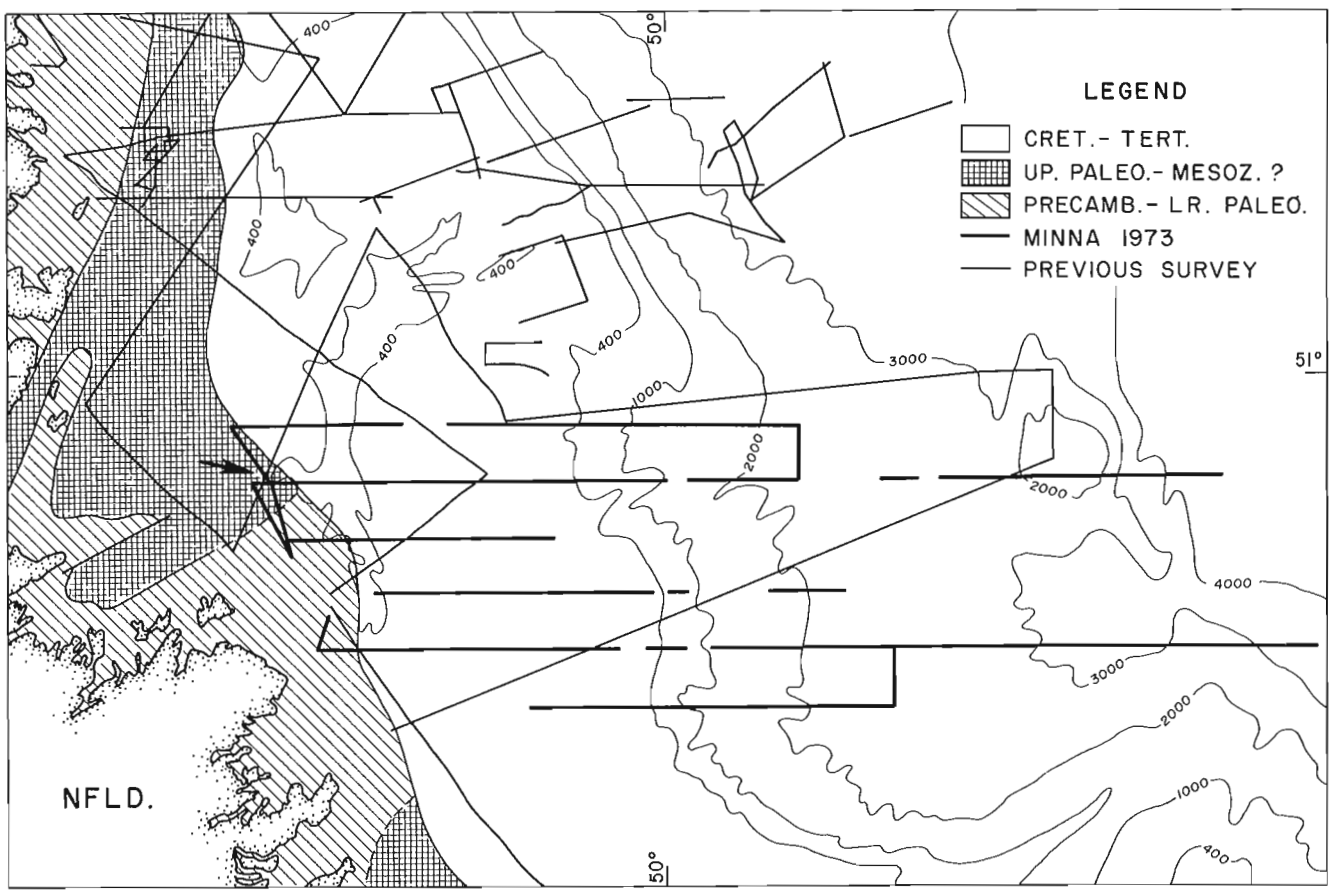

Figure 1. Location of seismic profiles recorded by M.V. MINNA, 1973. Arrow indicates line crossing discussed in text.

MARINE SEISMIC REFLECTION DATA PROCESSING

Project 720112

D. Heffler
Atlantic Geoscience Centre, Dartmouth

A program for the dereverberation of single-channel marine seismic reflection data has been developed for the PDP-11 computer. Some new variations on some old techniques have shown promise in offering significant signal enhancement with a reasonable computational load. This processing is accomplished in real time, and the program may be operated by a watchkeeper with little training. Utility operations, such as filtering and controlling gain, as well as effective displays using a storage cathode ray tube, have been included.

The method used is based on a Backus two-point filter which subtracts from the signal a replica of itself by the two-way travel time and multiplied by the reflection coefficient. Errors in timing of multiples due to the horizontal separation of the sound source and receiver is the major problem. A correction for this has been found which has shown a significant improvement in the effectiveness of the Backus Filter.

The different decay rates of the bottom and pegleg multiples is also a problem. Coupled to this is the complexity introduced by spherical spreading and any gain control used while recording data. A method which calculates a time-varying reflection coefficient along a trace has been included in the program. This has offered further reduction of multiple energy.

Figure 1 shows a seismic section near Jones Sound recorded in 1971. The top section has no processing while the lower one has been dereverberated using the timing correction but not the variable reflection coefficient

The program has been designed for processing deep seismic reflection data, in water over 400 metres. In very deep water where multiples are not a problem, vertical stacking may be used to improve signal noise ratio.

The system will be ready for real-time processing on CSS HUDSON for a cruise to Baffin Bay in 1974. A paper on the processing used and a manual on the use of the program are in preparation.

The advantages of this system are obvious when compared with the same system without processing. However, there are several advantages over the industry standard long array (up to 7,000 feet) and on-shore processing:

1. The processed data is available in real time allowing better monitoring of performance and the ability to base cruise decisions on the data.
2. The system is designed for processing single channel data. This allows the array to be slackened for the listening period improving the signal to noise ratio by up to 20 db.
3. The capital invested in the computer is less than that invested in a long array. It is also safer, as the computer is less subjected to failure and loss.
4. The space and equipment-handling facilities required on the ship are less.
5. The ability to acquire data in ice is improved.
6. The entire cost of land-based processing is saved.

These advantages are gained only at the cost of two disadvantages.

1. No velocity information can be obtained. Expendable sonobuoys provide some assistance in this regard.
2. Many of the assumptions made in developing the programs become invalid in water depths less than 400 metres. The system has not been tested in shallow water and may need different techniques for successful processing.

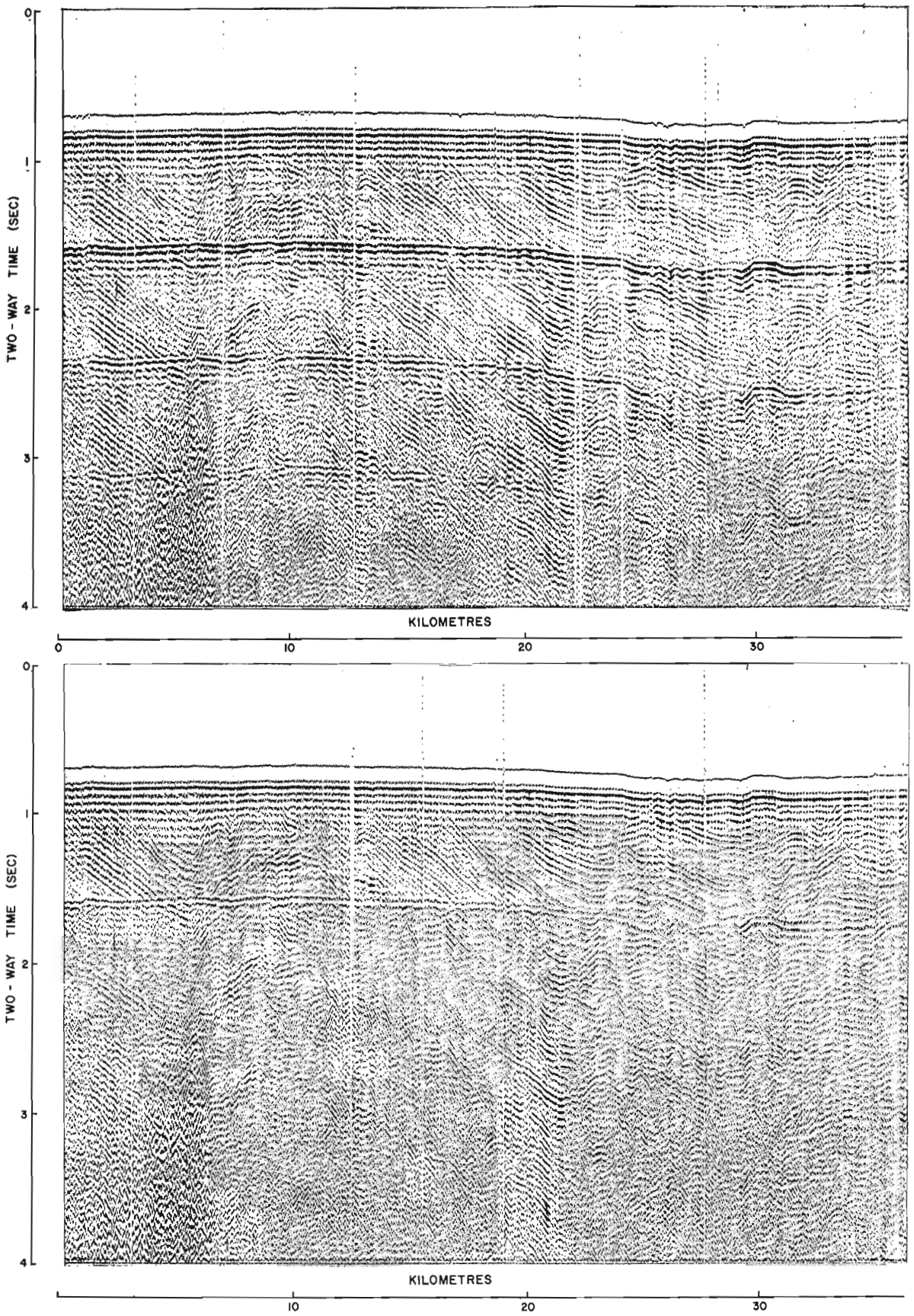

Figure 1. A seismic section near Jones Sound before (upper) and after (lower) processing.

Project 730081

R.F. Macnab
Atlantic Geoscience Centre, Dartmouth

Seventy-six new Natural Resource Maps have been completed or are at an advanced stage of production. As shown in Figure 1, these maps cover a block of nineteen areas in the Natural Resource Series. Four maps have been drawn for each area, portraying free-air gravity anomaly, Bouguer gravity anomaly, total magnetic field, and magnetic anomaly. (Production of the corresponding bathymetric editions is the responsibility of the Bathymetric Research Division of the Canadian Hydrographic Service.)

Thirty-two of these maps contain data derived primarily from a 1972 survey aboard the M/V MINNA: these are complete, and have been turned over to the Canadian Hydrographic Service, which is the printing and publishing agency for the Series. The digital data used in the preparation of these maps was released in December 1973 through Geological Survey of Canada Open File 183.

The remaining forty-four maps contain data collected almost exclusively during the 1973 M/V MINNA survey, described in Geological Survey Paper 74-1, Part A. (Survey coverage is shown in Fig. 2) These maps are being produced under contract by Digitech System Co. Ltd., Calgary.

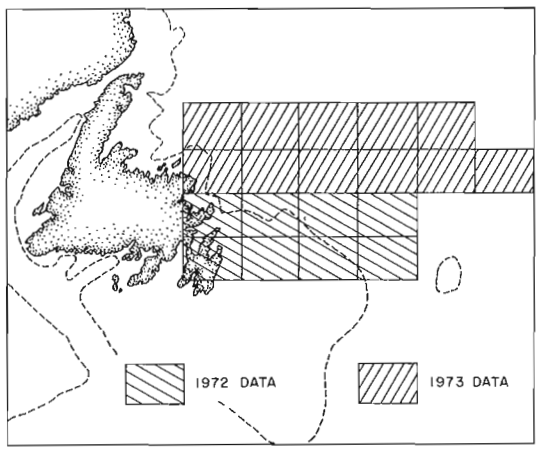

Figure 1. Areas in the Natural Resource Series for which new gravity and magnetic maps have been produced.

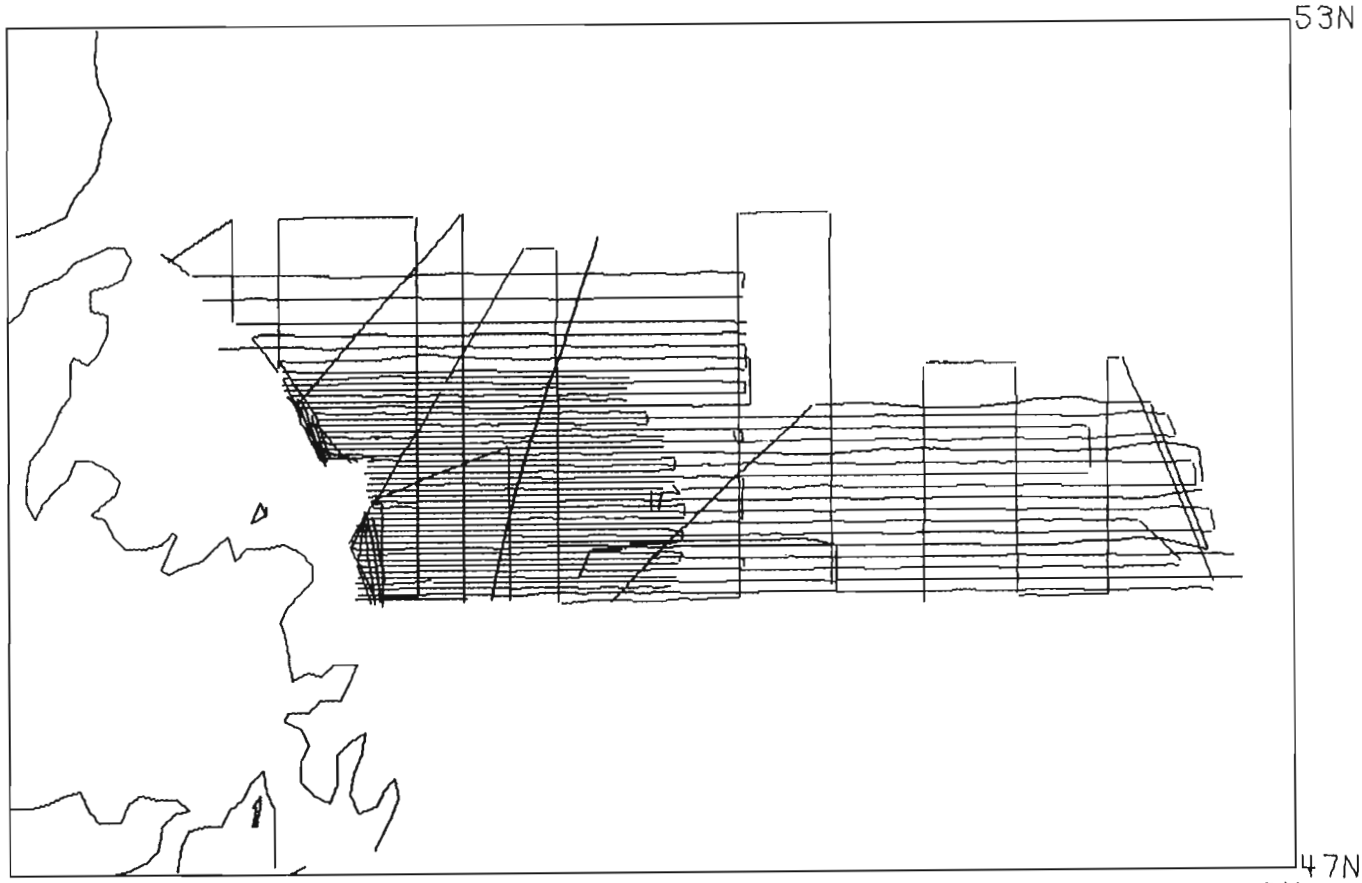

Figure 2. Track chart from the 1973 M/V MINNA survey.

THE SURFICIAL GEOLOGY OF HAMILTON BANK AND PERIPHERY

Project 730076

Willem J.M. van der Linden
Atlantic Geoscience Centre, Dartmouth

During the last decade several expeditions have entered the Labrador Sea to investigate the geological structure stratigraphy and evolution of the NW arm of the Atlantic Ocean and of the adjacent continental margin. The reconnaissance during those years showed that appreciable thicknesses of sediment underlie a wide Labrador shelf and the area therefore logically attracted exploration industries to search for promising structures, indicative of possible accumulations of oil and gas.

The effects of the Pleistocene glaciations on the continental margin and specifically on the shelf evolution are much more pronounced in the Labrador Sea than they are on the Atlantic seaboard in lower latitudes. On the shelf, the wide-spread occurrence of a glacial drift cover, the presence of an ice-enhanced marginal channel, some 50 km offshore, and the incidence of ice movement and scouring provide challenging opportunities for the study of glacial and peri-glacial influences on continental margins. At the same time the economic and environmental interests require at least a first appreciation of the difficulties that exploitation of resources will encounter in those areas. Techniques will have to be developed to drill and plough through thick Pleistocene boulder fields and to cope with the hazards of drift ice, icebergs and subarctic sea conditions.

Hamilton Bank and periphery (Fig. 1) an area about 50,000 km^2 is large enough to be elected representative of the Labrador shelf and is small enough to be tackled in order to resolve the near surface geology within a reasonably short period of time, as appropriate for a GSC project.

88 grab samples, collected by the Earth Physics Branch, E.M.R. in 1972 from the northern Hamilton Bank, while occupying gravimeter stations, gave clues to an at first sight unusual bottom sediment distribution; fine sediments in shallow water and coarse sediments in deep water, towards the periphery of the Bank. Subsequent sampling in 1973 during BIO cruise 73-027, substantiated this pattern and on the basis of an accumulated total of about 250 samples a map could be produced, showing the bottom sediment distribution (Fig. 2).

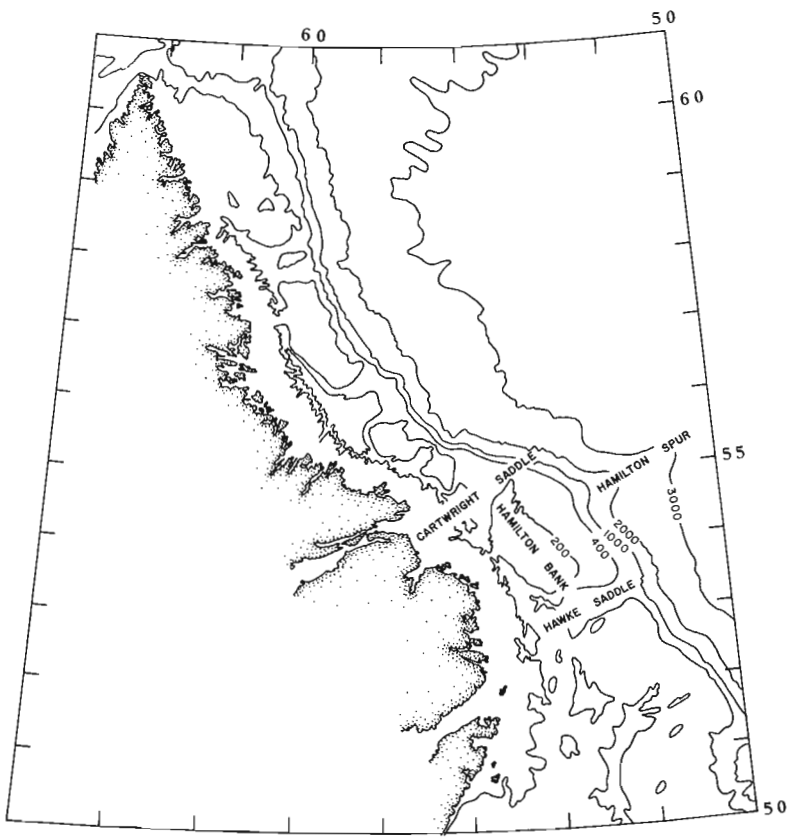

Figure 1. Map of the western Labrador Sea and position of the Hamilton Bank. Depth contours in metres. Note the position of a marginal channel separating a rough inner shelf from the smooth outer shelf bank area.

The pattern that emerges is that of relict glacial sediments that were reworked through repeated cycles of erosion and deposition by ice and water. Medium and fine sands occupy Hamilton Bank in water depths between about 150 and 250 m, with mud, gravel and pebbles as subsidiary fractions. Approaching the periphery of the Bank, both towards the continental slope and near Cartwright and Hawke Saddles the proportion of coarse clastics, gravel and pebble increases. The saddles themselves are floored by well sorted silty clays and fine sediments also become dominant seaward of the gravel and boulder belt, which fringes the upper slope. It is interesting to note that in the cores, taken from the saddles, unusual high concentrations of methane occurred (up to 16,000 ppm at a depth of about 10 m below the sediment-water interface). From the analysis of the cores and the structure and stratigraphy of the enclosed basins it was concluded that the methane was produced in situ under mildly anaerobic conditions (Vilks et al., in press).

From seismic reflection profiles, from a number of cores, up to 12 m in length, and from bottom photographs the impression is gained that the sands of the Bank and the muds of the saddles are relatively thin veneers of sediment which cover poorly sorted glacial drift, which appears ubiquitous underneath the shelf and adjacent slopes. The south flowing Labrador Current, which follows the continental

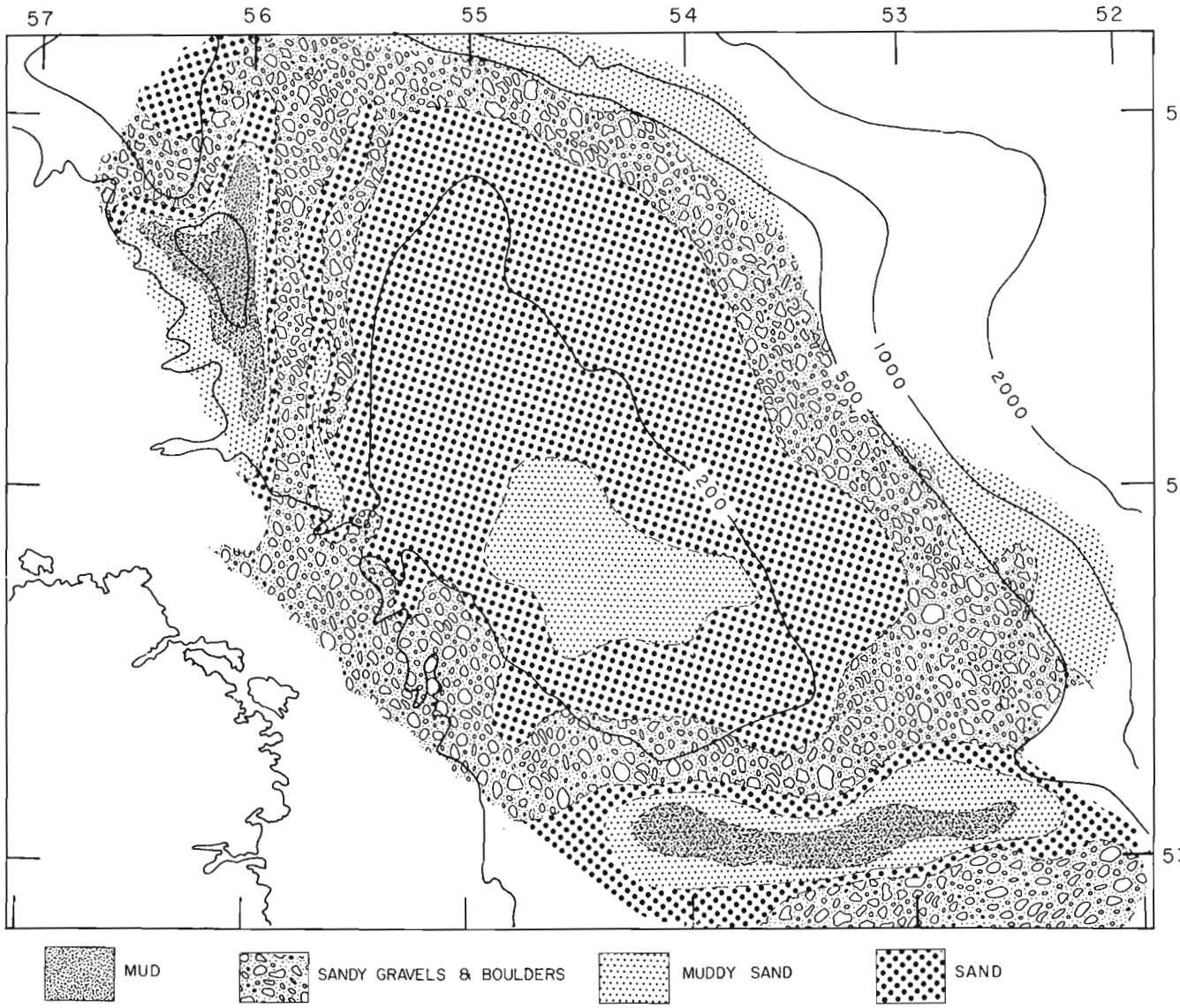

Figure 2. Sediment size distribution over Hamilton Bank and periphery.

slope and branches through the saddles and marginal channel, has winnowed the glacial debris since the Wisconsin, about 15,000 years ago. Current action thus left a relatively better sorted boulder and pebble zone in the Bank's periphery. Fine-grained sediments accumulated in slack water areas on top of the Bank and in the deeper basins at the junctions of the marginal channel and the saddles. The variability in sediment types on the western margin of Hamilton Bank, reflects the occurrence of moraine ramparts, indicative of recessional phases of the Pleistocene ice. Examples of poorly sorted glacial debris, well sorted pebble pavements and thinly covered glacial drift are given in Figure 3. In the same figure a photograph is shown with a rather unusual concentration of apparently reworked worm tubes.

A compilation of 1972 soundings, obtained by CSS HUDSON, revealed an 180 km long sedimentary ridge off central Hamilton Bank, which gently curves in an easterly to north easterly direction from the shelf edge down into the deep basin (Fig. 1). This ridge, Hamilton Spur, appears to have been shaped by deep geostrophic current action, caused by the deviation of the Labrador Current by a buried basement structure, Cartwright Arch.

During the 1973 cruise a deep-towed high resolution system resolved the acoustic stratigraphy of the upper few tens of metres of surficial sediments and in places marked the thickness of the postglacial sediments. A surface-towed airgun-hydrophone combination was useful, particularly in deeper water, in determining the structure thickness and succession of Quaternary, Tertiary and folded older sedimentary sequences.

Along 1,300 km of track side-scan sonar records were obtained over Hamilton Bank in water depths less than 250 m. These records are being analyzed presently

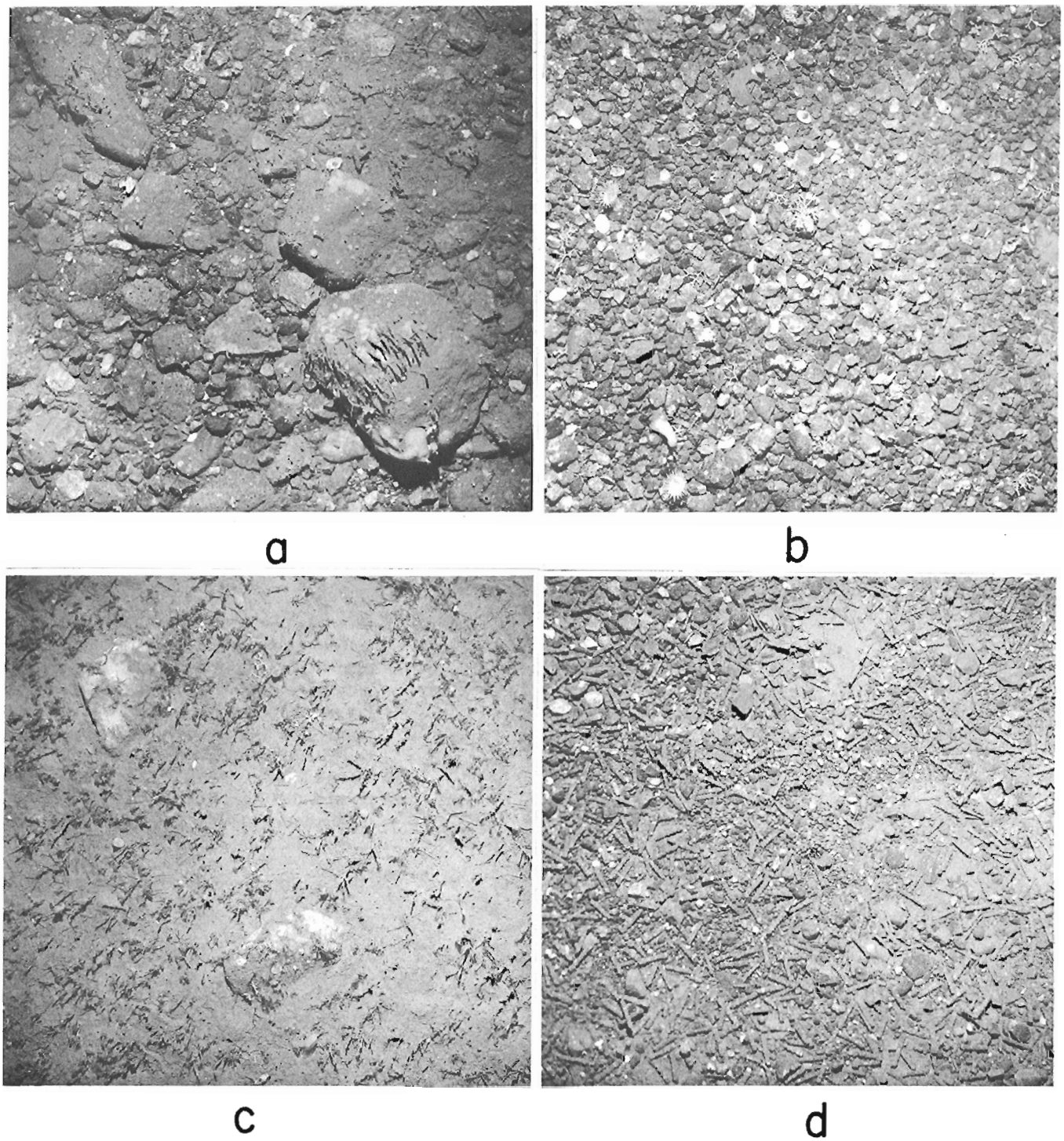

a. "washed" glacial moraine
b. well sorted pebble pavement
c. sand covered boulders with worm tubes in life position
d. sandy gravel with reworked worm tubes

Figure 3. Selected bottom photographs.

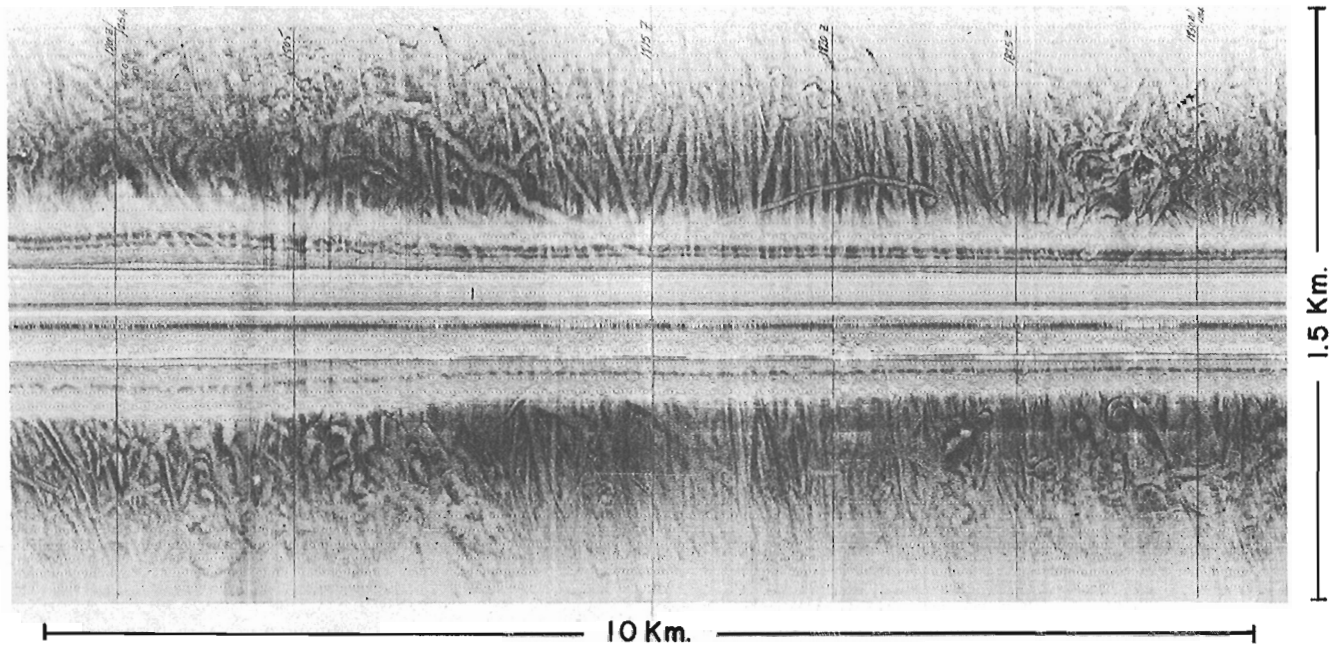

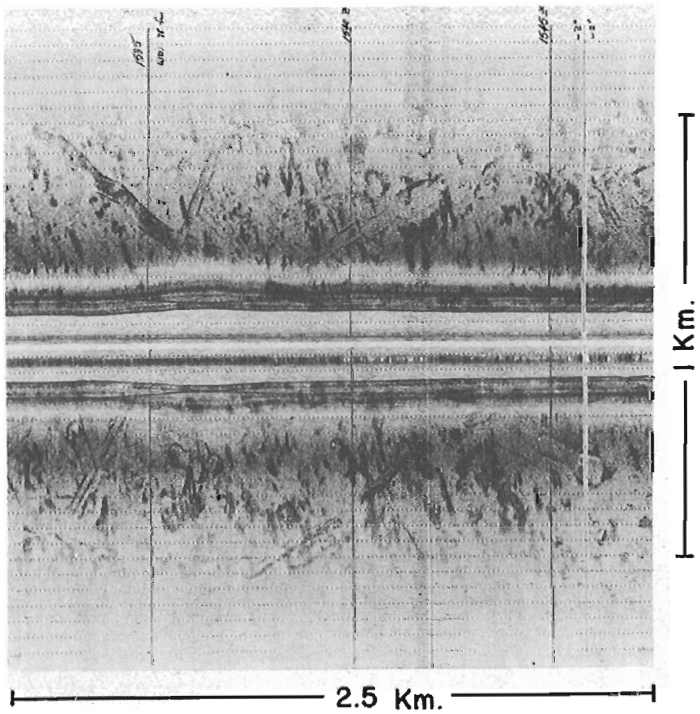

Figure 4. Side scan records from Hamilton Bank, illustrating gouging of the sea floor by icebergs over respectively a sandy gravel and boulder bottom (a) and over a sand bottom (b). The ice scours in frame (a) indicate predominantly NW-SE movement of ice through the marginal channel from Cartwright Saddle to Hawke Saddle. Note the erratic movements of stranded bergs (e.g. near 1827Z) and the formation of kettles at the S. end of scours (near 1803Z and 1810Z) in frame (a).

to obtain a more accurate picture of sediment variability One characteristic of the Labrador Shelf is immediately apparent however and that is the abundance of ice scours, examples of which are given in Figure 4. The age of these features is still a puzzle. Some gouges have a distinct and "fresh", high relief appearance, with well marked levees. Others produce only very vague images and appear either eroded or covered by sediment. A first as yet unqualified impression is that some of the scouring is inherited from the Pleistocene. The incidence of the scours or gouges is variable as might be expected from current born drift ice. The sill between Cartwright and Hawke Saddles, for instance, is a natural trap, grounding bergs entering the marginal channel. Rarely the scouring is directional, mostly it seems rather chaotic. No doubt the slope of the seabed, wind and tidal changes in the current pattern have a marked influence on the apparent erratic movement of ice. In places, see Figure 4, circular and oval depressions occur which might be explained by on the spot melting of a stranded berg (kettle formation) and by current scouring around the obstruction.

Reference

Vilks, G., Rashid, M.A., and van der Linden, W.J.M. 1974: Methane in recent sediments of the Labrador Shelf; (submitted to Can. J. Earth Sci.).

63. A SELF-CONTAINED UNDERWATER TELEVISION SYSTEM

Project 730154

C.A. Godden
Atlantic Geoscience Centre, Bedford Institute of Oceanography

A portable underwater videorecorder system has been developed and constructed offering two modes of operation. It may be used by a free-swimming diver; or in a fixed location, time-lapsed or continuously recording.

The system components include a commercially available Sony Rover II television camera and video recorder originally developed for the home entertainment market. Advantages of this system are compactness and light weight.

The camera and recorder are housed in watertight pressure cases constructed of acrylic plastic and steel respectively with an operating depth of 150 feet (45 m). These housings are almost buoyant when immersed with their respective equipment. In the diver-operated mode the system operates on its own internal battery for a period of 30 minutes. In the fixed mode (Fig. 1), power is supplied from a small, lead-acid battery housed in its own watertight case. The battery also powers the underwater lighting system and electronic programmable timer for time-lapse recording over a period of several days.

The system is unique since it does not require the use of any cables to connect it with a surface vessel or external power source.

For the fixed mode of operation a cradle was constructed of alluminum tubing, designed to house all component parts and yet allow free acess to the rear of the television camera by a diving operator. External controls on the camera allow for image focussing, and aperture controlling using normal urethane diving gloves.

The lighting system is readily adjustable underwater and is made up of two Canadian General Electric "wide flood display", 50 watt, sealed beam lamps. These lamps have their electrical connectors sealed in

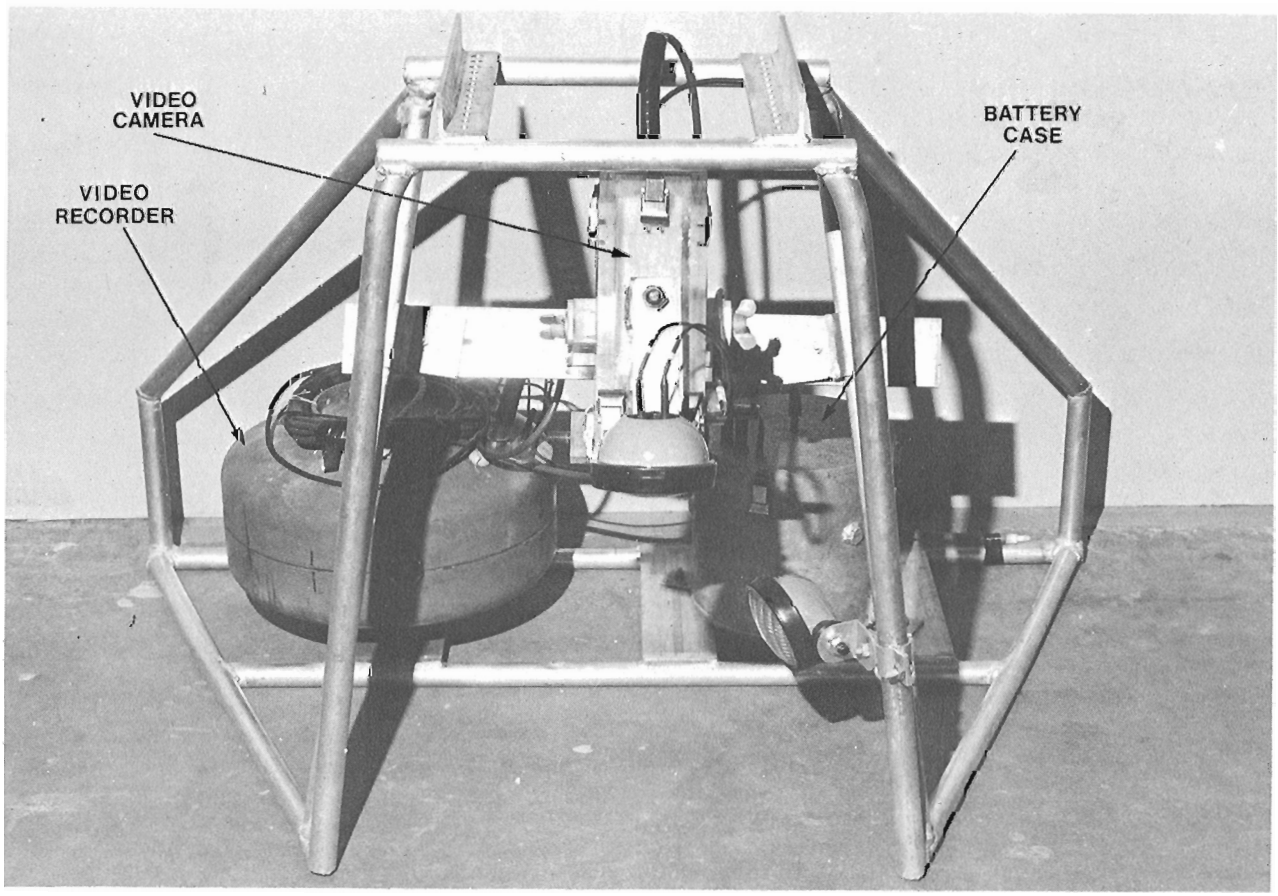

Figure 1. Photograph of self-contained underwater television system.

a polyurethane resin and terminated by suitable submersible connectors.

The lens system which is fitted to the camera is a special super-wide angle of very short focal length. It is fitted with an electro-mechanical focussing and aperture-controlling device. This particular unit utilizes two small flashlight batteries for its source of power. Its focussing range is from 15 cm to 6 m underwater as fitted.

The latest development to the camera system is the integration of a solid optical system which will be fitted to the front of the camera outside of the acrylic housing. Use of this optical system enables a 20X magnification to be utilized, coupled with the very long working distance of over 5 cm. Since the optical system is essentially "solid", a pressure case is not necessary. Further work on this and other solid optical systems for undersea camera systems is continuing.

64. A FEASIBILITY STUDY OF COMPUTER-BASED SUBSURFACE DATA SYSTEMS

Project 740007

K.G. Shih, I.A. Hardy and A.G. Sherin
Atlantic Geoscience Centre, Bedford Institute of Oceanography

With the vast volume of geological data generated by commercial drilling programs and by processing of ocean-bottom unconsolidated sediment core and rock core by government agencies, the need for a computer based subsurface data system for the Eastern Canadian sedimentary basins was recognized by Atlantic Geoscience Centre personnel. This project is being conducted to provide the geologist with a powerful tool with which he may retrieve the wealth of information as desired, easily and quickly.

Initially several established systems were investigated and found inadequate as the required system had to be: (1) useful to the geologist; (2) simple in data file construction; and (3) programmed to permit the exchange of data with other institutions. Since the systems investigated could not entirely meet the cri-

Table 1

Contents of the Index Data File

Parameter Code	Record Type	Contents of Data Information
0101	Label	Well number, confidential code, country code, region code, latitude, longitude, NTS, R.T./ K.B., length unit code, elevation, ground, total depth, PBTD, sample tray number and pool/field.
0102	Region	Region name (20 characters) and country name (16 characters).
0103	Area	Area name (20 characters).
0104	Well name	Well name (48 characters).
0106	Location	Well location name (48 characters).
0107	Survey	Survey system description (48 characters).
0108		Non-operating description (48 characters).
0109	Scientist	Geology by whom and date.
0110	Operator	Operator's name (48 characters).
0302	Performance	Spud date, finished date, completed date, suspended date, abandoned date, rig released date, and date released date.
0303	Contractor	Name of contractor (40 characters).
0304	Class	Classification (40 characters).
0305	Reason	Drilling reason (40 characters).
0306	Status	Status (48 characters).
0402	Initial gas	Interval, natural flow and S. I. Pressure.
0502	Initial oil	Interval, estimated flow, S. I. Pressure.
0602	Water	Interval and flow type.
0701	Logging	
0801	Casing	
0901	Coring	
1001	Results	Final results information (code by yes or no).
1101	Comments	
9999	END	

Table 2

Contents of the Geological Data File

Parameter Code	Record Type	Contents of Data Information
1201	Label	Well number, confidential code, country code, region code, latitude, longitude, NTS, R.T./ K.B., elevation, ground, sea floor, total depth, length unit code and area code.
1202	Section	Well number, length unit code, top, elevation and thickness of the formations, age (106 == 10 million years), geological periods (in numerical code), rock types (15 characters) and geological formations (16 characters).
1203	Comments	
9999	END	

teria listed above a new computer-based subsurface data system was initiated at the Atlantic Geoscience Centre.

This new subsurface data system utilizes subject data files to keep the overall files within a reasonable size, and to facilitate updating and file search. Full geological names are used which eliminates the usage of dictionaries in the transfer of data to coding sheets, the deciphering of retrieved data, and the translation of data for exchange purposes. Where geological periods and mineral names are required, accepted numerical codes and abbreviations have been adopted (Briskin and Ediger, 1967), (Blackadar, 1972).

The system presently contains two subjects data files; (1) the index file containing information on drilling operations and well performance (Table 1); and (2) the geological file containing the name, age and lithology of geological formations encountered (Table 2). Other subject files will be initiated to include data originating from well studies in geochemistry, micropaleontology and palynology, etc.

The system is divided into five sections. The input and display sections utilize routines already established at AGC for other geoscience data systems.

I Input: The input portion of the system consists of coding sheets and software for loading data onto magnetic tape.

II Retrieval: The retrieval section is designed to retrieve information according to given output option and to transfer this information concurrently with labelling information such as latitude, longitude, total depth, etc., to the display portion of the system. Retrieval options for the geologic data file at present include searches by latitude, longitude, area name, geological period, geological formation name and rock type.

III Display: The display portion of the system presents retrieved data in forms identifiable by the geologist, by using routines developed around facilities such as the line printer, Calcomp plotter and EAI flatbed plotter.

IV Update: The update portion of the system will be designed to correct, delete and add data as required.

V Merge: The merge portion of the system will permit the retrieval of data from two or more data files, enabling correlation studies.

The future activities of this project will be directed towards the initiation of an adequate update and merge portion of the system, which will greatly aid the geologist to solve geological problems without the task of editing large volumes of data.

References

Blackadar, R.G.
1972: Guide for the Preparation of Geological Maps and Reports; Geol. Surv. Can., Misc. Report 16, Revised edition 1972, p. 18-20.

Brisbin, W.C. and Ediger, N.M.
1967: (Editors) A National System for the storage and Retrieval of Geological Data in Canada. In: Report by the Ad Hoc Committee on Storage and Retrieval of Geological Data in Canada by the National Advisory Committee on Research in the Geological Sciences; p. 46-47.

65. SPECIFICATIONS FOR A MARINE SEISMIC REFLECTION ARRAY

Project 740006

Bruce D. Vardy
Atlantic Geoscience Centre, Bedford Institute of Oceanography

A large amount of data on all types of commercially available hydrophone arrays has been gathered and a preliminary evaluation carried out. Several major oceanographic institutes and universities have been canvassed in order to find out what type of equipment they have used in the past and what they are presently using. Also, they were asked to give their opinion as to what they thought was the best hydrophone array commercially available today. In the field, hydrophone arrays have been evaluated by streaming them behind a ship using an air gun as an energy source, and attempting to measure their sensitivity and signal-to-noise ratio. In the area of the Bedford Basin, some tests have been carried out to measure array sensitivity while holding constant as many variables as possible. Some of the variables involved with such testing are varying level of ship's noise, changing sea conditions, water temperature and the amount of sea traffic in the area.

Two arrays were rented for evaluation purposes and were tested on the CSS HUDSON. The tests and the data gathered to date have aided greatly in deciding upon an array to purchase for our 1974 field season. Before the coming season begins, each section of each array which we presently own is to be given a serial number for identification purposes. Since all of our arrays will be in use gathering seismic data during the summer, by the fall we shall be able to directly correlate good data with a particular array serial number. This will be accomplished by asking each person who uses an array to record the serial number of the array used along with other pertinent data. Thus, we will be able to determine which is the best of the arrays used during this period. From the testing performed thus far and from that which is yet to be done, the array which performs best under field conditions shall be determined and future purchases of arrays can thus be based on our findings.

66. URANIUM IN STREAM SEDIMENTS, BATHURST-JACQUET RIVER DISTRICT, NEW BRUNSWICK

Project 670029

H.W. Little
Regional and Economic Geology Division

Stream sediment samples collected in Bathurst-Jacquet River district, New Brunswick in 1965 by Boyle et al. (1966) have been stored by the Geological Survey since that time. In 1972 samples from areas that are underlain by Pennsylvanian red beds were selected for analysis for uranium. Where marked anomalies in uranium content occurred, resampling was attempted by the writer, but, as it was a time of high water, and beaver had moved into the country, flooding many streams with their dams, resampling was not possible in several localities. The uranium content of most of the new samples is about half that of the old ones, possibly due to the conditions of high water at the time the resampling was done.

R.W. Boyle (oral comm.) is of the opinion that the flushing action of the high water dissolves some of the uranium, and some is probably carried away in humic material. Govett (1973) has referred to some work done on this problem by Villard (1972), but this reference is not available to the author at the time of writing.

In the area near Bathurst underlain by Bathurst Formation (Fig. 1), the arithmetic mean of the uranium content of the 331 stream sediment samples is only 0.5 ppm. which may be taken as the background. Within the area of Figure 1, only a few samples exceeded the background by more than a factor of four. Two samples were relatively high in uranium, being 13 and 20 times background. At the locality of the first, 3½ miles east southeast of East Bathurst, two new samples were taken but neither contained uranium. The other locality, 5 miles south of South Bathurst, was inaccessible due to a large beaver pond.

Within the area shown in Figure 1 the best anomalies occur in and near Pabineau Indian Reserve, and near East Bathurst.

From areas underlain by the Pennsylvanian Bonaventure Formation northwest of Bathurst, along Chaleur Bay (see Boyle et al., 1966), twenty-eight stream sediment samples were analyzed for uranium. The background of 0.66 ppm U is only slightly higher than for the Bathurst Formation near Bathurst. Of these, only a few are of interest. A value of three times background was obtained from a sample collected one-quarter mile south of Jacquet River post office, and values, from south to north respectively, of 1.1, 1.2, and 4.4 ppm. U were obtained from the three samples collected on Heron Island.

Near Tetagouche Lakes, however (Fig. 2), samples of stream sediments underlain by Bathurst Formation yielded much more encouraging results; background is 4 times that near Bathurst. When it was realized that uranium is fairly abundant beyond the boundaries of the Pennsylvanian rocks, additional samples from near Tetagouche Lakes were analyzed. These showed that background for the surrounding older rocks is about half that for the Bathurst Formation, and double that near Bathurst. Because higher values occur in the Bathurst Formation, these rocks may be the source of the uranium. On the other hand the same formation near Bathurst has a low uranium content. The uranium near Tetagouche Lakes may therefore be genetically related to the major faults. Further sampling of the stream sediments is recommended.

The writer acknowledges with thanks the services of J.J. Lynch for the uranium analyses, A. Boyer for preparation of the maps, and R. Skinner for advice on the legend of Figure 2.

Selected Bibliography

Boyle, R.W., Tupper, W.M., Lynch, J., Friedrich, G., Ziauddin, M., Shafiqullah, M., Carter, M., and Bygrave, K.
1966: Geochemistry of Pb, Zn, Cu, As, Sb, Mo, Sn, W, Ag, Ni, Co, Cr, Ba, and Mn in the waters and stream sediments of the Bathurst-Jacquet River district, New Brunswick; Geol. Surv. Can., Paper 65-42.

Govett, G.J.S.
1973: Exploration Geochemistry, in Geology of New Brunswick, Dept. Geol., Univ. New Brunswick; NEIGG Guidebook, N. Rast, Ed.

Villard, D.J.
1972: Factors affecting the distribution of uranium in stream sediments, Newcastle area, New Brunswick; unpubl. M.Sc. thesis, Univ. New Brunswick.

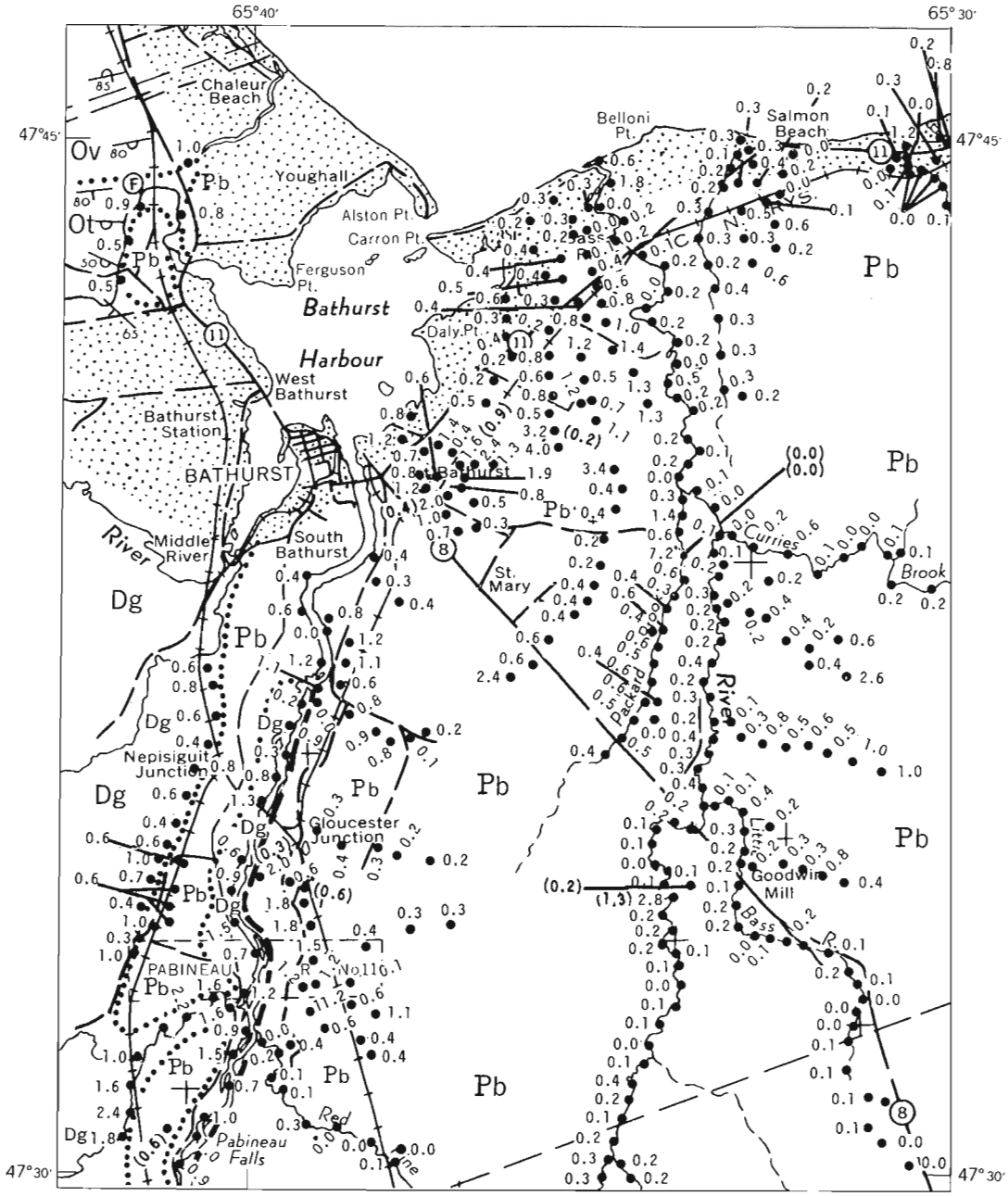

PENNSYLVANIAN

Pb — BATHURST FORMATION: red conglomerate and grit, at base; red sandstone, siltstone, shale

DEVONIAN (?)

Dg — Pink, coarse- to medium-grained biotite granite, granodiorite, granite porphyry

ORDOVICIAN

MIDDLE ORDOVICIAN

TETAGOUCHE GROUP (Ot, Ov)

Ot — Grey, black, green, and red slate, greywacke, conglomerate; graphitic schist; minor limestone, basic volcanic rocks

Ov — Basic volcanic rocks; interbedded slate, graphitic schist; iron formation

Sample location with uranium content in ppm.....0.1 ●

Figures in brackets show uranium content of new samples from the same localities.....(0.6)

Geological contact.....

Geology from GSC Prelim. Map 57-1
(Smith et al., 1957)

Miles

2 0 2

Figure 1. Uranium in stream sediments near Bathurst, New Brunswick.

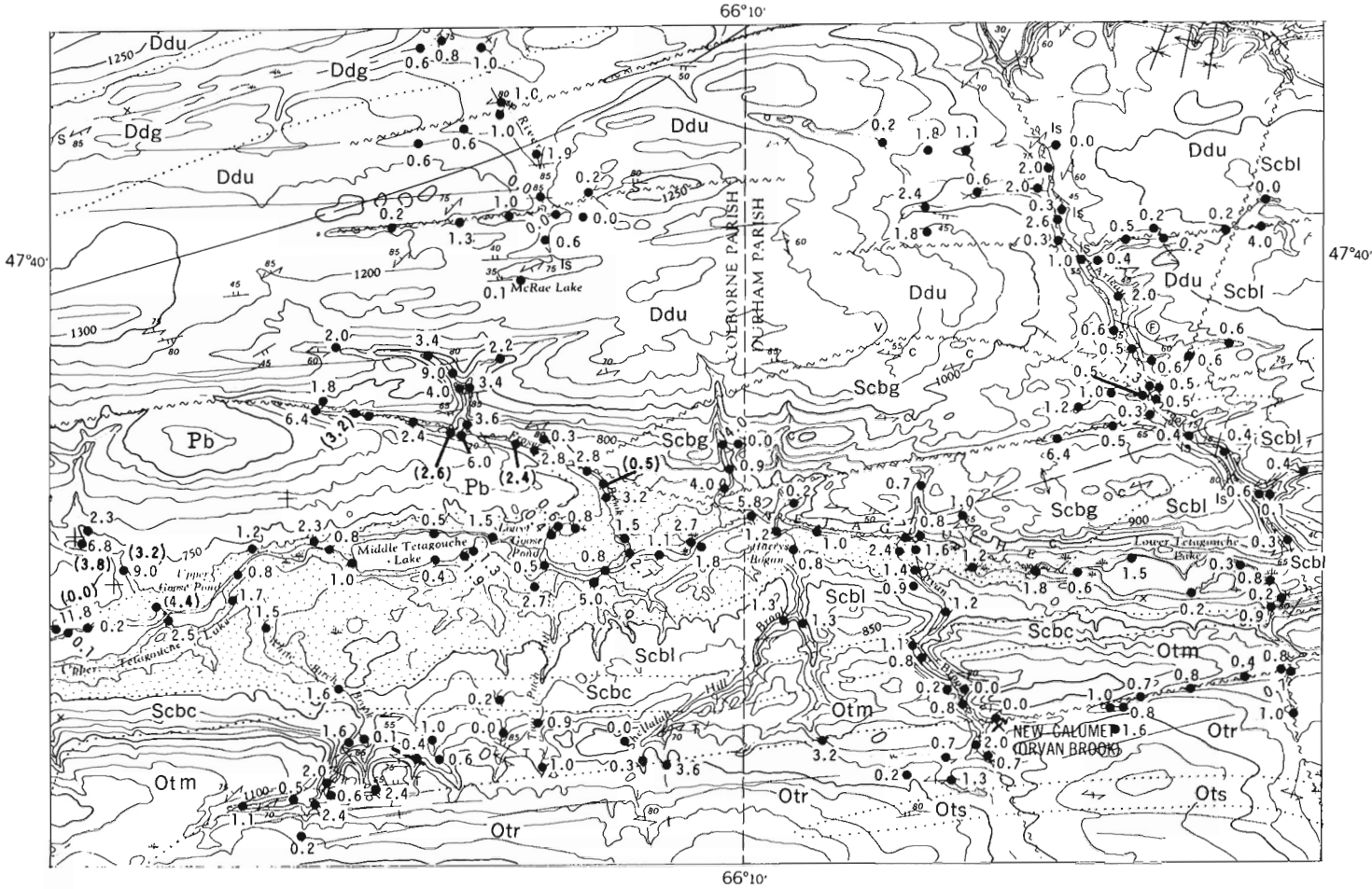

PENNSYLVANIAN

Pb — BATHURST FORMATION: red sandstone, shale, grit, quartz-pebble conglomerate

DEVONIAN

MIDDLE DEVONIAN OR OLDER

Ddg — Diabase, diorite, gabbro

LOWER DEVONIAN

DALHOUSIE GROUP

Ddu — Upper Unit: greenish grey limy quartz greywacke, siltstone, shale, limestone; minor basalt, andesite

SILURIAN

MIDDLE AND UPPER SILURIAN

CHALEURS BAY GROUP

Scbl — Limy sedimentary Unit: greenish grey and red limy slate, shale, shaly limestone

Scbc — Conglomerate Unit: green, grey and red volcanic conglomerate

Scbg — Greywacke Unit: green and red conglomerate, greywacke, slate, limestone; basalt

ORDOVICIAN

MIDDLE ORDOVICIAN

TETAGOUCHE GROUP

Otr — Rhyolitic Unit: grey rhyolite crystal tuff, rhyolite tuff, quartz-sericite schist; phyllite, rhyolite, greenstone

Otm — Metabasalt Unit: greyish green, schistose, and grey laminated greenstone, dark slate, iron-formation; rhyolite tuff

Ots — Sedimentary Unit: grey slate and siltstone

Sample location with uranium content in ppm...0.2

Uranium content of new samples collected.....(0.2)

Geological contact.....

Fault, assumed.....

Mine (zinc-lead-silver-copper).....

Geology from GSC Map 1330A (Skinner et al., 1972)

Miles

1 0 1

Figure 2. Uranium in stream sediments near Tetagouche Lakes, New Brunswick.

67. RELATION OF COMPOSITIONS AND METAL RATIOS OF MASSIVE SULPHIDE DEPOSITS TO GEOLOGICAL ENVIRONMENT

Project 680060

R. I. Thorpe
Regional and Economic Geology Division

In an attempt to investigate the variation of composition of volcanogenic massive sulphide deposits in relation to their age, size and geological setting, data have been compiled in computer-processable form for a large number of Canadian and foreign deposits. In particular it is hoped that the factors controlling the precious metal contents of these deposits can be identified.

For each deposit the chemical abundance, when available, for Cu, Pb, Zn, Ag, Au, S, Fe, SiO_2, Al_2O_3, CaO, MgO, As, Se, Co, Ni, Mn, Sb, $BaSO_4$, Sn, Hg, Bi, Te and Cd has been recorded. From the primary data, values have been calculated for the quantities Au + Ag, $^{Cu}/_{Pb + Zn}$, Ag/Au and Cu/Zn. In addition to these compositional values, data on selected geological features and on age and size of the deposits have been recorded. The geological data recorded include the character (composition, texture, etc.) of associated volcanics and/or sediments, metamorphic grade (high, medium, low), and type of rock alteration. The presence of additional features and components, such as alteration pipe, magnetite, carbon, barite, manganese and iron-formation, has been recorded.

For Canadian deposits a total of 155 records represent 148 separate deposits. In the case of foreign deposits a total of 517 records represent approximately 295 separate orebodies. Published grades representative of entire orebodies are much more readily available for Canadian than for foreign deposits. For foreign deposits the available compositional data may, for example, consist of the analysis of a single sample stated to be "typical" of the deposit, the grade of ore produced during a single year, or the average grades for two to eight different ore types occurring within the deposit. For this reason the collection of strictly comparable data on the basis of individual orebodies is virtually impossible for foreign deposits, and this difficulty explains the great excess of records relative to the number of orebodies. Other problems include the lack of adequate data on age and geological environment of the deposit, especially when the grade data has been obtained from a mining journal. Data on many minor and trace elements in these deposits are often not available, so that for such interesting components as Se, Sb, Bi, Hg, Mn, $BaSO_4$ and Sn it is difficult to obtain sufficient values for meaningful statistical treatment.

First treatment of the data will be to establish what compositional relationships can be found in these deposits. To achieve this a variety of available statistical programs will be employed including correlation analyses based on the raw data and also on logarithmically transformed values. This type of treatment will probably progress to the use of factor analysis. The primary hope, however, is that the chemical correlations and factors that are defined can be related to the geology of the deposits. By the use of the proper techniques of grouping data, statistical analysis, and plotting it should be possible to show which chemical changes in massive sulphide deposits can be expected with an overall change in geological setting and with some more specific changes in geological features of the deposits.

68. X-RAY POWDER DIFFRACTION PATTERN RECOGNITION BY MINICOMPUTER

Project 680023

M. Bonardi
Central Laboratories and Technical Services Division

A Powder Diffraction File of more than 900 patterns of minerals from the reference file of the X-ray laboratory has been completed and stored on Magnetic Tape. A computer program has been written in HP Fortran IV for powder diffraction pattern recognition using a Hewlett-Packard 8K computer. This search program compares the d-spacings of the five strongest lines of the unknown X-ray diffraction pattern with all the entries in the Powder Diffraction File. The program prints out interplanar d-spacings, relative intensities, and mineral names of all possible matches with the standard patterns, within a given tolerance. This program is designed for routine X-ray diffraction pattern recognition to eliminate the time-consuming manual search.

69. EMISSION MICROSPECTROCHEMICAL ANALYSIS OF MINERALS WITH THE LASER MICROPROBE

Project 680023

M. Bonardi
Central Laboratories and Technical Services Division

A recently developed technique employing Laser beam as a microsampling device has been used for spectrochemical analysis of minerals. The instrument consists of a Jarrell-Ash 1.0 metre Czerny-Turner Spectrograph and a Q-switched Neodymium-doped glass laser manufactured by the American Optical Company with a 10 millijoule output in a 25 micrometer target spot size. Spectrochemical analysis with this device involves vaporization of a microamount of matter by the laser beam focused onto a specimen by a specially designed microscope, the excitation of the vapour by an auxiliary spark discharge produced synchronously. A sample area as small as 10μ in diameter can be analyzed and no sample preparation is required. The spectra are recorded on photographic plates and interpreted by means of a computer-controlled Optronics Stripscan digital microdensitometer. Qualitative and semi-quantitative analysis of minerals can be performed for 60 elements from lithium (atomic number 3) to uranium (atomic number 92). A computer search program has been developed to read the emission spectra on photographic plates and record as output the positions and intensities of selected lines of elements corrected for background.

Project 70041

J. L. Jambor and I. D. MacGregor*
Regional and Economic Geology Division

Prior to publication of Part 1 of this study (Jambor, 1964), data had been accumulated for anticipated subsequent papers dealing with aurichalcite and rosasite. As more than a decade has passed and, as it has become apparent that studies of these carbonates will not be resumed, publication of the data accumulated seems worthwhile because little has appeared in the literature during the elapsed interval.

Aurichalcite

Aurichalcite, $(Zn, Cu)_5(CO_3)_2(OH)_6$, and hydrozincite, $Zn_5(CO_3)_2(OH)_6$, are chemically similar but do not form a solid solution series. Ramsdell's (1947) cell dimensions and monoclinic symmetry for hydrozincite were confirmed in the structural study by Ghose (1964), who obtained $\underline{a}$ = 13.62, $\underline{b}$ = 6.30, $\underline{c}$ = 5.37A, b = 95°50', space group C2/m. Aurichalcite is orthorhombic, $\underline{a}$ = 27.2, $\underline{b}$ = 6.41, $\underline{c}$ = 5.29A, space group $B22_12$ (Jambor and Pouliot, 1965). Copper substitution in hydrozincite is known to be negligible; zinc substitution in aurichalcite is well-documented, with Zn/Cu in published analyses ranging from about 3 to 1.3 (Lauro, 1938). Several specimens were examined in the present study in order to establish the effect of cation variations on the refractive indices and x-ray powder diffraction patterns.

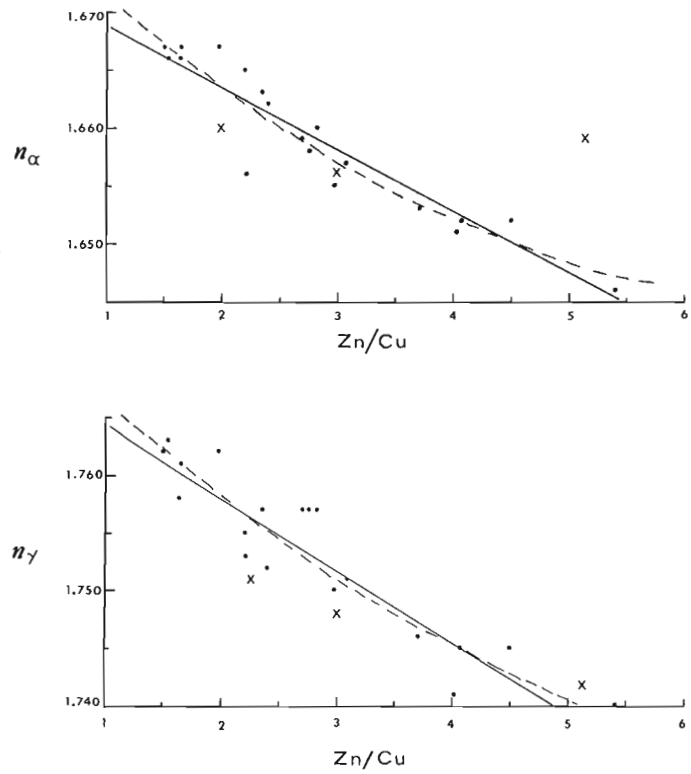

Figure 1. Refractive indices versus atomic Zn/Cu for the aurichalcites listed in Table 1. The solid and dashed lines are, respectively, the linear and quadratic relationships of R.I. and Zn/Cu assuming no error in the latter. Shimazaki's (1957) thesis results are represented by X (sample 4446 at Zn/Cu = 2.26, 5225 at 3.00, and 5224 at 5.12).

Zn/Cu Ratios and Refractive Indices

Copper-zinc ratios were determined by x-ray fluorescence spectrography. In nearly all cases only a few milligrams of material were used as it was found that Zn/Cu varies considerably at different positions in some specimens. The results of the analyses (Table 1) show that Zn/Cu ranges from 1.25 to 5.4. With increasing zinc content the greenish colour typical of most aurichalcites becomes increasingly bluish; the samples with the highest zinc contents are pale blue.

The refractive indices of the aurichalcites studied are listed in Table 1. The estimated error for $n\alpha$ is ± 0.003, and for $n\gamma$ ± 0.005. Both indices systematically increase as the copper content increases (Fig. 1). An assessment of possible bias in the results is limited by the general absence of comparable data in the literature. However, Rozybakieva (1966) reported $n\alpha$ 1.653-1.658 and $n\gamma$ 1.738-1.754 for an aurichalcite with Zn/Cu = 2.17. Only the upper range of $n\gamma$ fits the present data. Three analyses are also available in the unpublished thesis by Shimazaki (1957). Refractive indices for two of the samples (4446 and 5225, Fig. 1) are in reasonable agreement with the present data, but the results for the remaining sample are not. However, our refractive indices and Zn/Cu values obtained from fragments of Shimazaki's samples also differ from his results. This suggests that each of Shimazaki's specimens contains aurichalcites having variable compositions, and that each analytical value reflects the dependency upon the particular area of the specimen that was selected for study.

X-ray Powder Patterns

X-ray powder diffraction patterns are not identical for all aurichalcites. Four examples showing the variations in line intensities are given in Figure 2. On the basis of these intensity variations, the aurichalcites examined in this study were divided into three principal groups. As shown in Figure 3, these groups seem to be correlative with Zn/Cu ratios.

Calculation of the unit cell parameters and cell volumes using a least-squares refinement of the powder diffraction lines 10.1.0, 402, 820, 602, 612, 630, 11.2.1, and 16.0.0 showed relatively little change,

*Present address: Dept. of Geology, University of California, Davis, California 90561

TABLE 1. AURICHALCITES STUDIED

Number	Locality	Source*	Atomic Zn/Cu	$n\alpha$	$n\gamma$
4446	Magdalena, New Mexico	Stanford U.	1.25		
AMNH 18063	Socorro County, New Mexico	AMNH	1.50	1.667	1.762
NMC	Mapimi, Durango, Mexico	GSC	1.54	1.666	1.763
M 18529	New Mexico	ROM	1.64	1.666	1.758
M 13409	Magdalena, New Mexico	ROM	1.65	1.667	1.761
M 16.1.4 A3	Magdalena, New Mexico	UBC	1.90		
M0120(?)	Graphic Mine, Magdalena, N.M.	Queen's U.	1.98	1.667	1.762
NMC	Durango, Mexico	GSC	2.2	1.665	1.755
5225	White Pine County, Arizona	Stanford U.	2.21	1.656	1.753
AMNH 31260	Bisbee, Arizona	AMNH	2.35	1.663	1.757
M 4924	Ophir, Arizona	ROM	2.40	1.662	1.752
--	Magdalena, New Mexico	Mr. G. Thompson	2.4		
M 23310	Mina Ojuela, Mapimi, Mexico	ROM	2.70	1.659	1.757
Ott. U.	Durango, Mexico	Ottawa U.	2.75	1.658	1.757
AMNH 33689	Apex Mine, St. George, Utah	AMNH	2.82	1.660	1.757
M 7707	Fissure Cave, Utah	Queen's U.	2.98	1.655	1.750
M 7712	Tinctic District, Utah	ROM	3.08	1.657	1.751
M 21833	Big Cottonwood District, Salt Lake County, Utah	ROM	3.70	1.653	1.746
5224	West of Ruth, Nevada	Stanford U.	4.02	1.651	1.741
M 16.1.4 A2	Salt Lake County, Utah	UBC	4.07	1.652	1.745
NMC	Laurium, Greece	GSC	4.5	1.652	1.745
A 290-1	Cottonwood, Utah	Queen's U.	5.4	1.646	1.740
10621	San Xavier Mine, Tuscon, Ariz.	ROM	†		
M 14760	Tsumeb, S.W. Africa	ROM	††		
--	Cassiar (?), Yukon	GSC	2.7		

* AMNH = American Museum of Natural History; GSC = Geological Survey of Canada; ROM = Royal Ontario Museum; UBC = University of British Columbia

† fragments shown by x-ray powder diffraction patterns to be aragonite

††labelled as paraurichalcite and found to be predominantly malachite, with adamite, olivenite, and bayldonite; malachite thinly coated with light bluish rosasite.

with cell volumes ranging from 915 to 922A^3, and no correlation of volumes and Cu/Zn ratios. Thus intensity changes in most, but not all, aurichalcite powder diffraction patterns are related to Cu-Zn substitution. Exceptions to the general trend can be attributed to CO_3-OH variations, such as occur in hydrozincite. Although such variations may also account for some of the scatter in the relationship of refractive indices and Cu-Zn ratios, the regularity of this change suggests that anion variations are less pronounced in aurichalcite than in hydrozincite.

Acknowledgments

The writers are grateful to F. Agterberg, R.N. Delabio, G.R. Lachance, and H.R. Steacy of the Geological Survey for assistance in the study. Specimens were kindly loaned or donated by J.A. Mandarino (Royal Ontario Museum), L.G. Berry (Queen's University), Grant Thompson of Ottawa, C.O. Hutton (Stanford University), Brian Mason (American Museum of Natural History), the late R.M. Thompson of the University of British Columbia, and D.D. Hogarth of the University of Ottawa.

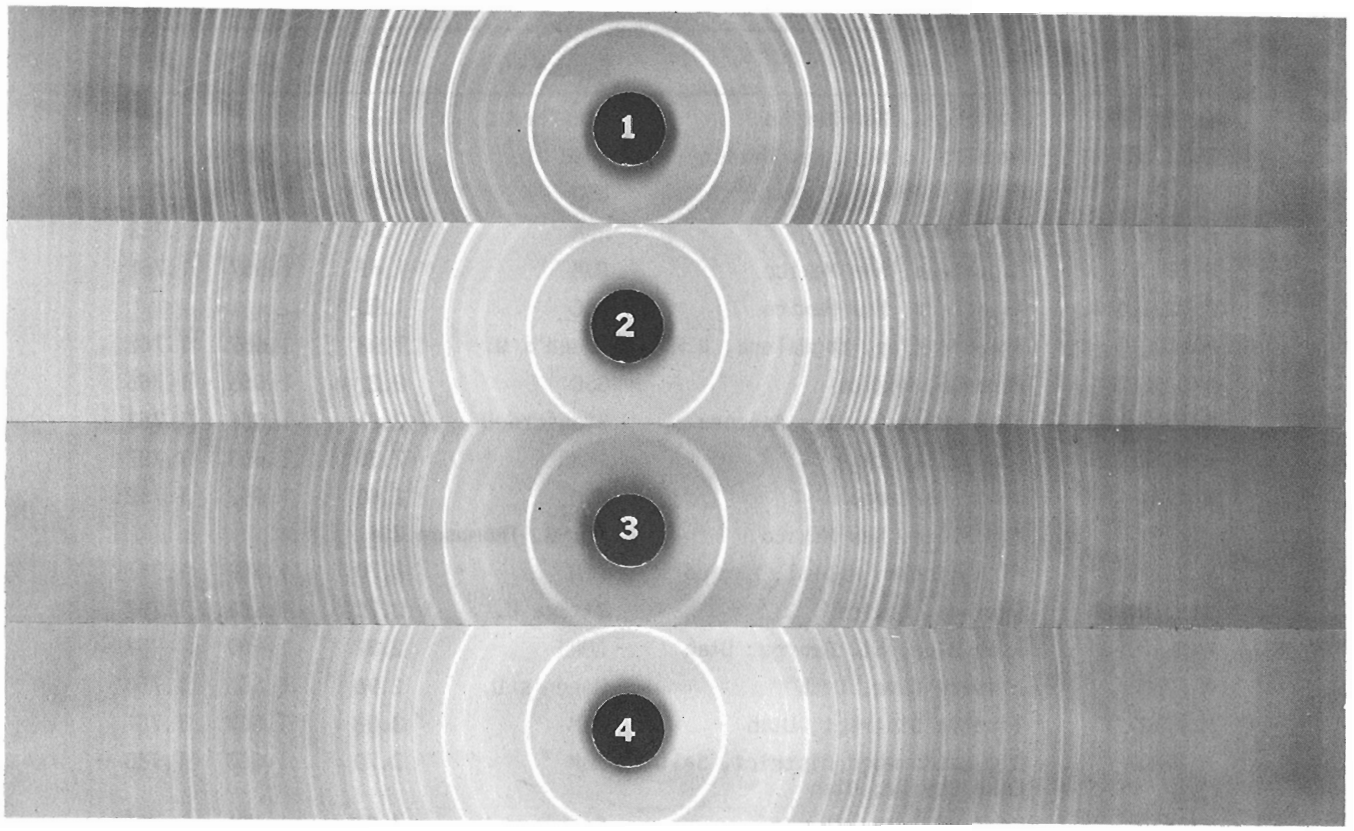

Figure 2. Representative x-ray powder diffraction patterns of aurichalcites (Cu radiation, Ni filter, camera diameter 114.6 mm). Top (1): Zn/Cu = 1.54; (2) Zn/Cu = 2.4; (3) Zn/Cu = 4.07; (4) anomalous pattern from Yukon material, Zn/Cu = 2.7.

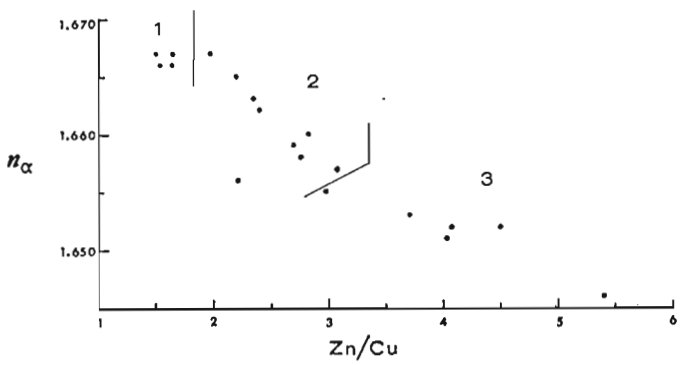

Figure 3. Relationship of Zn/Cu and x-ray powder pattern types as shown in Figure 2.

References

Ghose, Subrata
1964: The crystal structure of hydrozincite, $Zn_5(CO_3)_2(OH)_6$; Acta Cryst., v. 17, p. 1051-1057.

Jambor, J. L.
1964: Studies of basic copper and zinc carbonates: Part 1-synthetic zinc carbonates and their relationship to hydrozincite; Can. Mineral., v. 8, p. 92-108.

Jambor, J. L., and Pouliot, G.
1965: X-ray crystallography of aurichalcite and hydrozincite; Can. Mineral., v. 8, p. 385-389.

Lauro, C.
1938: Su alcuni carbonati basici di rame e zinco naturali; Periodico Mineral., v. 9, p. 105-135.

Ramsdell, L. S.
1947: The composition and unit cell of hydrozincite; Am. Mineral., v. 32, p. 207-208.

Rozybakieva, N. A.
1966: Mineralogy of oxidation zone in the Koksu deposit of the Dzhunger Alatau; Tr. Inst. Geol. Nauk, Akad. Nauk Kaz. SSR, v. 15, p. 134-144 (in Russian).

Shimazaki, Y.
1957: Mineralogy of basic carbonate minerals of copper and zinc; unpubl. Ph.D. thesis, Stanford Univ.

71. NOTES ON THE ASSOCIATION OF BRANNERITE AND NATIVE GOLD AT THE RICHARDSON MINE, SOUTHEASTERN ONTARIO

Project 550101

H. R. Steacy and A. G. Plant
Central Laboratories and Technical Services Division

R. W. Boyle
Resource Geophysics and Geochemistry Division

The association of brannerite and native gold at the Richardson Mine (Steacy et al., 1973) has been studied in detail in the two specimens available. The specimens are composed essentially of crystalline calcite with muscovite, brannerite, tourmaline, pyrite, native gold and uraninite. Brannerite occurs in grains and masses up to 1.2 cm in size, and shows a composition fairly typical for brannerites. Gold replaces both the calcite and brannerite, and is late in the paragenetic sequence. Uraninite occurs within the brannerite in two forms. A high thorium (6% Th) variety fills fractures. A variety free of thorium, which in the classical sense may be classed as pitchblende, occurs as irregular masses which have apparently developed through the alteration of the brannerite.

The identification of the brannerite also afforded the first opportunity to place an upper limit on the age of the gold mineralization in the gold belt of southeastern Ontario. A sample of approximately 45 mg, composed essentially of brannerite with some inseparable native gold and some intimately associated uraninite, was submitted to a commercial laboratory for a lead-uranium age determination. The ages reported were: Pb_{206}/U_{238} 936 ± 28 m.y., Pb_{207}/U_{237} 957 ± 29 m.y. and Pb_{207}/U_{206} 1,001 ± 30 m.y. These may be compared with ages carried out on the Deloro stock (Wanless and Loveridge, 1972). A Rb-Sr whole-rock isochron age gave 1059 ± 46 m.y. K-Ar ages of two riebeckites from the stock gave 875 m.y. and 989 m.y. The aforementioned ages would seem to suggest a contemporaneity of the intrusion of the Deloro stock and the emplacement of the brannerite and further suggest a genetic relationship of the gold deposits with the Deloro stock. The study further supports the fact that the sites and existing specimens of all former gold producers in the area should be checked for radioactivity, as should the entire aureole of skarn rocks bordering the Deloro stock.

References

Steacy, H. R., Boyle, R. W., Charbonneau, B. W., and Grasty, R. L.
1973: Mineralogical notes on the uranium occurrences at South March and Eldorado, Ontario; in Report of Activities, April to October 1972, Geol. Surv. Can., Paper 73-1, Pt. B, p. 103-105.

Wanless, R. K., and Loveridge, W. D.
1972: Rubidium-strontium isochron age studies, Report 1; Geol. Surv. Can., Paper 72-23.

NATIONAL MINERAL COLLECTION

Project 550101

H. R. Steacy and H. G. Ansell
Central Laboratories and Technical Services Division

A basic re-organization of the Systematic Reference Series of the National Mineral Collection was completed during the report period. The Series is the research arm of the National Collection and is the responsibility of the Geological Survey of Canada. In progress for about one year, the re-organization will enable the Series to assist more effectively research programs of government, university and industry.

To improve and extend its representation, and correspondingly its usefulness and research capacity, the Series welcomes gifts of specimen material, particularly that of Canadian origin.

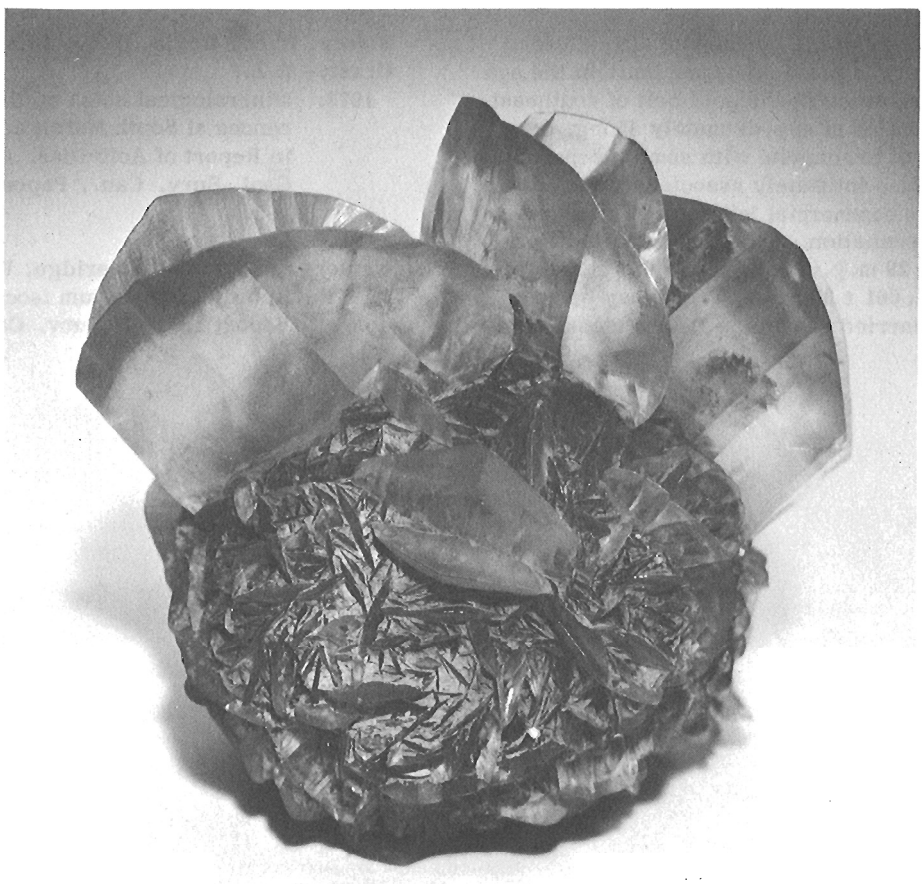

Figure 1. Selenite from the Red River floodway, Winnipeg, Manitoba, obtained by purchase for the Systematic Reference Series, National Mineral Collection, February 1974. About 1½ times natural size.

73.

PALEOMAGNETISM OF THE LOWER JURASSIC TULAMEEN ULTRAMAFIC-GABBRO COMPLEX, BRITISH COLUMBIA

D. T. A. Symons*
Regional and Economic Geology Division

Introduction

The Tulameen ultramafic-gabbro complex is located about 15 miles west of Princeton in south-central British Columbia (Fig. 1). The complex is a zoned pluton about 10 miles in length and from 2 to 4 miles in width. When the sampling was undertaken, the pluton was known to intrude Upper Triassic rocks (Rice, 1947), to give a K-Ar age on biotite of about 186 m.y., and to be cut by the Eagle granodiorite which gives a K-Ar age on biotite of 143 m.y. (Leach et al., 1963; GSC dates 62-55 and 62-56). Several iron prospects (Eastwood, 1960) and the name of its highest peak, the 6,218-foot Lodestone Mountain, reflect the high magnetite content in parts of the complex. Paleomagnetic study of the Tulameen Complex promised two results. If a stable remanence direction could be isolated, it would be of interest to see if individual petrologic phases could be distinguished. Also very few rocks of Jurassic age have given reliable pole positions so that the Tulameen pole if undisturbed would be helpful in constructing the North American polar wander path.

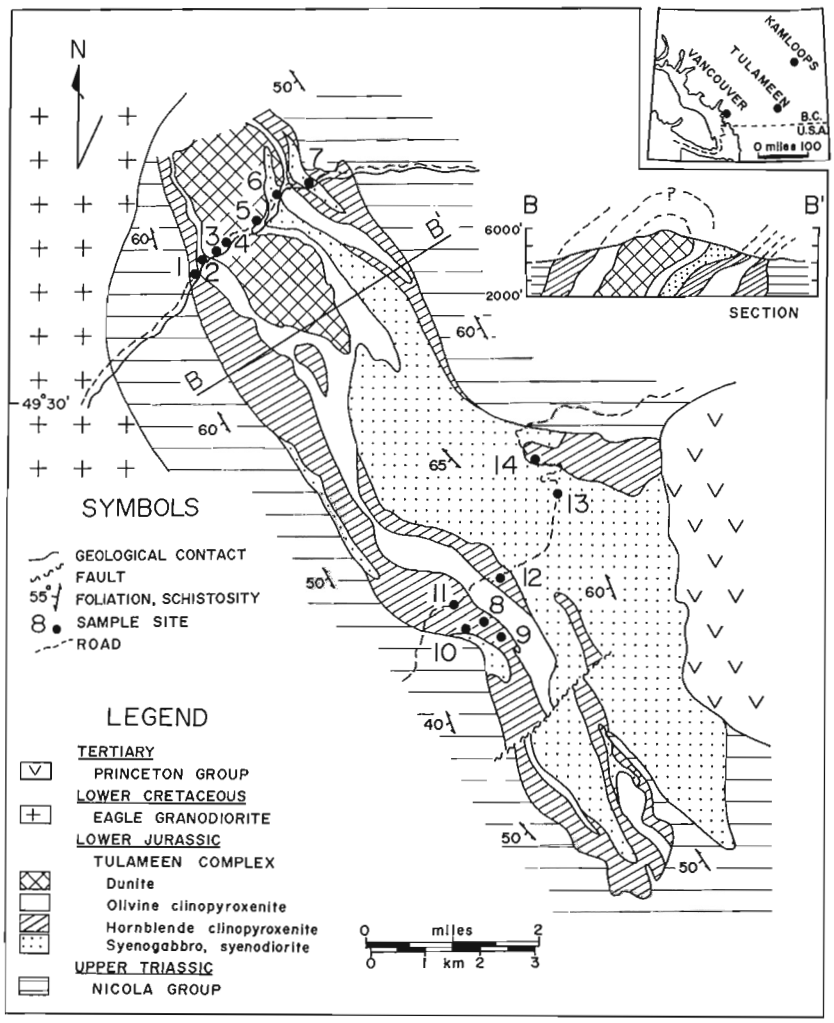

Figure 1. Location, general geology (after Findlay, 1969), and sample site locations.

Geology

Findlay (1969) has described in detail the geology of the Tulameen complex with emphasis on its petrology, geochemistry, and structure (Fig. 1). The complex intrudes deformed metavolcanic and fossiliferous metasediments of the Upper Triassic Nicola Group (Karnian and Norian; Frebold and Tipper, 1969). The Nicola Group has been intruded by rocks as old as the Guichon batholith (30 miles to the north) dated at 198 ± 8 m.y. by K-Ar on biotite and hornblende (White et al., 1967) and at 200 ± 2 m.y. by Rb-Sr isochron (Chrismas et al., 1969).

The Tulameen complex is an ultramafic assemblage consisting of a dunite core, changing outwards through an olivine clinopyroxenite phase, to a hornblende clinopyroxenite phase (Fig. 1).

The Tulameen complex strikes on average ≈N30°W. Its dip is ≈55° ± 5°W which is well established from contact and primary foliation attitudes on both sides of the complex. There is no evidence of internal secondary deformation.

The gabbroic rocks consist of syenogabbro and syenodiorite and are found mainly along the southeastern side and southern end of the complex. Contact relations indicate that the gabbroic rocks were emplaced first. Magnetite, probably with a high chromium content, is the only magnetic mineral reported in the rocks. It occurs as discrete grains and segregations associated with hornblende and to a lesser extent with diopside and olivine. Modal analyses show trace to accessory amounts of magnetite in the diorite and olivine clinopyroxene phases, up

*Present address: Department of Geology, University of Windsor.

Table 1: Sampling and remanance data by sites

Site	Petrologic phase	Location		Step Demagnetization			Number of cores[2]				Mean Remanent Magnetization				
		Longitude West degrees	Latitude North degrees	Mean Coercivity oersteds	Stability Index	AF Cleaning Field Intensity oersteds	N	a	b	n	Resultant Vector R	Declination degrees	Inclination + down degrees	Precision Parameter k	Radius $P_0.05$ degrees
1	Hornblende pyroxenite	120.91	49.52	410	16.9	200	5			5	4.9651	125.4	-35.2	115	7.2
2	Olivine pyroxenite	120.91	49.53	660	17.4	400	5			5	4.9741	137.0	-42.3	154	6.2
3	Dunite	120.90	49.53	460	36.4	200	6			6	5.9150	145.6	-42.8	58.8	8.7
4	"	120.90	49.53	650	18.9	300	5	1		4	3.9863	127.9	-29.8	219	6.2
5	"	120.89	49.53	570	16.3	300, 650	5			5	4.9916	150.4	0.4	476	3.5
6	Syenogabbro	120.89	49.54	240	10.8	100	5		1	4	3.8776	280.0	41.1	24.5	18.7
7	"	120.88	49.54	30	2.3	100, 650	5	1		4	3.9167	352.5	60.8	36.0	15.7
8	Hornblende pyroxenite	120.83	49.54	20	6.0	300, 650	5			5	4.0573	319.6	-27.2	4.2	--[3]
9	" "	120.83	49.46	20	5.5	200, 650	5			5	1.9645	78.7	60.4	1.3	--[3]
10	" "	120.84	49.46	20	6.2	100, 400, 800	5			5	1.7958	353.2	70.3	1.3	--[3]
11	" "	120.85	49.47	20	2.0	400, 800	5	1		4	2.9175	86.4	77.7	2.8	--[3]
12	" "	120.83	49.47	390	11.5	100, 650	5			5	4.9707	136.5	- 2.5	137	6.6
13	Syenogabbro	120.82	49.48	50	16.5	300, 800	4			4	3.9697	147.4	5.4	99.0	9.2
14	Hornblende pyroxenite	120.82	49.49	170	25.5	100, 650	5	1		4	3.9271	36.4	63.5	41.2	14.7
	Mean of Accepted Sites[4]	120.87	49.52							10	8.6253	140.8	-45.9	6.6	22.0

Notes: 1) Underlined cleaning field produced reported remanence data.
2) Each core is the average of two specimens. "N" is the number of cores collected. The number of cores rejected as inhomogenously magnetized (i.e. angle between two specimens $\geq 20^{o}$) and as anomalously directed are listed under "a" and "b". "n" is the number of cores used to calculate the site statistics.
3) Site mean magnetization regarded as inhomogenous.
4) Sites 1 to 7 and 12 to 14 with sites 6, 7 and 14 in their antiparallel position.

Table 2: Paleomagnetic pole positions from North American rock units of Jurassic of Upper Triassic age.

Pole	Unit	Locality	Age million years	Number of sites, samples, and specimens	Pole Position: Longitude East degrees	Pole Position: Latitude North degrees	Axes of oval of 95% confidence, degrees δ_m	Axes of oval of 95% confidence, degrees δ_p	References
1	Chinle red beds	Utah, New Mexico	Upper Triassic	3, 40, 115	93	55			Collinson and Runcorn (1960), Irving (1964)
2	Mistastin Lake volcanics	Labrador	202±13	10, 73, 117	118	86	4	4	Currie and Larochelle (1969)
3	North Mountain basalt	Nova Scotia	200±10	17, 28, 54	113	66	1	5	Larochelle (1967)
4	North Mountain basalt	Nova Scotia	200±10	25, 25, 38	104	73	7	5	Carmichael and Palmer (1968)
5	Guichon batholith	Southcentral B.C.	198± 8	15, 58, 116	13	66	14	9	Symons (1971a)
6	Copper Mountain stocks	Southcentral B.C.	194± 8	17, 81, 162	351	68	10	7	Symons (1973a)
7	Newark Gp - lavas	Massachusetts	≈193	5, 16, 32	88	55	11	6	Irving and Banks (1961)
8	Newark Gp - lavas	Connecticut	193± 6	53,313, 609	87	65	12	7	de Boer (1968)
9	Newark Gp - redbeds, igneous	New Jersey	190	29, 78, 329	108	63	4	3	Opdyke (1961)
10	Newark Gp - diabase	Pennsylvania	≈190	20, 95, 95	105	62	3	2	Beck (1965)
11	Kayenta red beds	Utah	≈190	2, 26, 26	90	59	5	9	Steiner and Helsley (1972)
12	White Mountain batholith	New Hampshire	185± 3	3, 36, 36	169	76	8	12	Opdyke and Wensink (1966) (Sites 6, 7 and 8 only); Foland et al. (1971)
13	Tulameen ultrabasic complex	Southcentral B.C.	176± 3	10, 46, 92	119	46	20	11	this paper
14	Appalchian diabase dikes	Eastern U.S.A.	≈Jurassic	74,121, 223	145	66	3	3	de Boer (1967); McElhinny (1968)
15	Island Intrusions, granodiorite	Vancouver Island, B.C.	159±10	17, 65, 130	240	79	11	10	Symons (1971b)
16	Belknap-Monadnock stocks	Vermont, New Hampshire	158± 4	4, 35, 35	29	89	4	6	Opdyke and Wensink (1966) (Sites 4, 5, 11, 12); Foland et al. (1971)
17	Topley monzonites	Northcentral B.C.	139± 4	13, 57, 114	129	70	14	11	Symons (1973b)
18	Summerville brown sandstone	Utah	≈Upper Jurassic	1, 40, 40	86	70	5	8	Steiner and Helsley (1972)
19	Alaskan diorite & sediments	Southcentral Alaska	≈Upper Jurassic	9,100, 100	303	54	24	17	Packer and Stone (1972); Burk (1965); Richter (1967)
20	Bucks batholith	California	138± 6	9,116, 116	195	58	8	8	Grommé et al. (1967)
21	Guadeloupé Mtn. complex	California	≈136	4, 56, 56	171	43	27	27	Grommé et al. (1967)

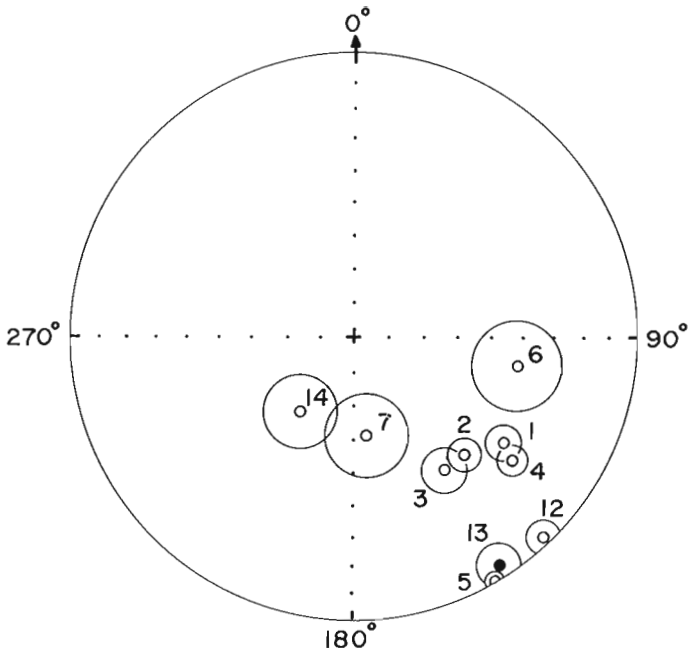

Figure 2. Site mean remanence directions plotted on a Schmidt net. Downward normal (+ ve) inclinations are shown as solid circles and reverse (- ve) inclinations as open circles. Sites 5, 6 and 14 are plotted in their antiparallel position. The means are circumscribed by their cone of 95% confidence.

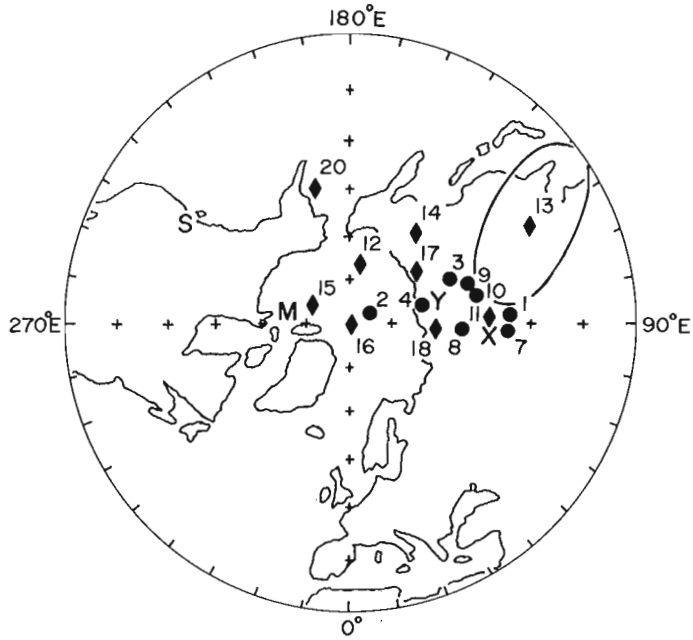

Figure 3. Polar porjection of the northern hemisphere above 30°N latitude. Upper Triassic poles are shown as circles and Jurassic poles as triangles. The pole numbers refer to Table 2. The pole for the Tulameen ultramafic-gabbro complex (no. 13) is circumscribed by its oval of 95% confidence. Correcting this pole's position for ≈35° east-northeast tilt moves it to X, and for the resultant ≈20° east-southeast tilt to Y. The locations of the sampling site S and present magnetic pole M are also shown.

to 7 per cent by weight in the gabbroic and up to 22 per cent in the hornblende clinopyroxene phases (Findlay, 1969). Roddick and Farrar (1971) have done K-Ar age determinations on 4 hornblende separates which give an age of 176 ± 3 m.y., on 4 biotite separates which range up to a minimum age for the complex of 172 ± 3 m.y., and on 2 whole rock samples which average 188 ± 10 m.y.

Quartz veins presumably associated with the Eagle granodiorite cut the Tulameen complex (Camsell, 1913), thereby establishing a minimum age from independent evidence for the complex. The Eagle granodiorite has been dated at 104 ± 5 m.y. by K-Ar on biotite and hornblende pairs (Roddick and Farrar, 1972). The Eagle granodiorite is unconformably overlain by non-marine grits of the Paysaten Group which contain very late Lower Cretaceous (Albian) fossils. The Tulameen complex itself is overlain by flat-lying flood basalts of the Tertiary Princeton Group.

The complex is near the centre of a panel or tectonic block bounded by the north-northwest-striking Hozameen and Otter fault systems (Rice, 1947). The Hozameen system of thrust faults dips westerly and passes about 8 miles (13 km) to the west-southwest of the complex. The Otter system of left lateral faults passes about 4 miles (7 km) to the east-northeast. On proceeding northward both systems merge into the Fraser fault system.

Procedure

At each of 14 sites, 4 to 6 rock cores were drilled and oriented in situ by sun compass. Local magnetic distortions were so great that a magnetic compass could not be used. The natural remanent magnetization (NRM) was measured for 2 specimens from each of 70 cores using a biastatic magnetometer (Larochelle and Christie, 1967). One pilot specimen with an average NRM was demagnetized in an alternating field (AF) (Larochelle and Black, 1965) in 8 steps up to 800 oe. Guided by the pilot specimen's remanence intensity decay curve and stability index (Tarling and Symons, 1967), an optimum AF intensity was chosen to clean the remaining specimens from the site before measuring their remanent magnetization (RM_c). For 9 sites a second AF treatment, and in one case a third treatment, was attempted and the results reported in Table 1 are from the more successful cleaning treatment in terms of producing the best clustering of remanence directions. Four cores were regarded as inhomogeneously magnetized because the remanence directions of their 2 specimens deviated by more than 20°. The mean direction for each core was calculated by averaging the direction of its 2 specimens. One core was rejected because it was found to be anomalously directed

and nearly antiparallel to the remaining 4 core directions for the site. The mean site RM_c directions and statistics were calculated by giving each core unit weight (Table 1).

Remanence Stability

The AF step-demagnetization results indicate two distinct ranges of RM_c stability. The majority of sites (1-6 and 12-14) have high mean coercivities or median destructive fields (m.d.f., i.e. the AF cleaning intensity required to reduce the NRM by one-half), and high stability index values (Table 1). These parameters show that the remanence is very stable both in terms of intensity and direction. All of these sites give well clustered remanence directions as shown by their high precision parameter (k) values and small radii for their cones of 95% confidence ($P_{0.05}$) (Fisher, 1953). Five sites (7-11) have low stability or unstable remanence. This is shown by their m.d.f. values of 30 oe or less, their low stability index values, and, except for site 7, their very low k and high $P_{0.05}$ value. Sites 8 to 11 all come from highly magnetiferous hornblende clinopyroxenite at or near the top of Lodestone Mountain. These sites also give NRM intensities in the 10^{-1} or high 10^{-2} emu/cc range whereas the other sites fall in the lowest 10^{-2} to 10^{-4} range. Therefore it is thought that these 4 sites retain intense randomly-directed lightning-induced anhysteretic remanent magnetization components residing in magnetically soft domains which prevent the isolation of the primary remanence components. Alternatively their instability may reflect intense magnetic interactions between the abundant grains of $(Fe(Cr))_3O_4$.

Pole Position

Of the 10 site mean remanence directions (Fig. 2), sites 1 to 4 form a consistent reversely-polarized cluster. Sites 5, 12 and 13 are scattered about this cluster as are normal sites 6, 7 and 14 when plotted in their antiparallel position. These sites indicate that the earth's magnetic field reversed its polarity at least once about 175 m.y. ago during the Lower Jurrasic. The scatter of the site mean remanence directions combined with their high stability and small cones of 95% confidence shows that the sites are statistically independent. It is obvious that the data is not sufficiently consistent to consider the RM_c of individual petrologic phases. Therefore the site mean remanence directions have simply been combined to get the mean direction for the Tulameen complex of 141°, -34° ($P_{0.05}$ = 17°). The pole position calculated from this RM_c direction is 119°E, 46°N ($P_{0.05}$ = 20°, 11°).

In Table 2 are listed the Upper Triassic to mid-Upper Jurassic pole positions from North American rock units that are based on the remanence data of several samples from several sites. After excluding 4 poles (numbers 5, 6, 19 and 21) for which the original authors cite evidence of significant tectonic rotation, the remainder have been plotted on Figure 3. As can be readily seen, the oval of 95% confidence for the Tulameen pole (no. 13) just reaches to the older Upper Triassic poles (numbers 1-4, 7-11) but not to the equivalent younger Jurassic poles (numbers 12, 14, 18 and 20). Thus there is a finite chance - about 1 in 20 - that the Tulameen pole is consistent with the other poles in Figure 3. Alternatively there are a number of possible tectonic explanations for the discrepancy. These can most easily be considered in terms of correcting the declination and inclination deviations of the mean remanence vector to give a concordant pole position.

The declination deviation could be caused by an ≈20° clockwise rotation of the complex. In view of the consistent N30°W trends found for the complex as a whole, for the foliation planes in the complex, for the adjacent Nicola horizons, and for the regional structures as a whole (Rice, 1947; Findlay, 1969), this is thought to be an unlikely possibility. Alternatively, the declination deviation could be caused by an ≈35° east-northeast tilt of the tectonic block containing the complex. This is an appealing choice for three reasons. First, if, as is likely, the contact attitudes and foliation planes were originally vertical upon emplacement, then an ≈35° east-northeast tilt would rotate them over to their present attitudes. Second, the Hozameen fault system to the west was likely produced by compression towards the east-northeast which would also produce an east-northeast tilt to the tectonic block. Finally, correcting the pole position for this tilt only, brings the pole position (X in Fig. 3) into reasonable agreement with some of the Upper Triassic positions.

Both poles (numbers 13 and X) for Tulameen are somewhat more southerly in latitude than appears reasonable which likely reflects some inclination deviation. The deviation could be corrected by assuming a 25° northward post-emplacement translation of the complex relative to the North American craton. This is thought unlikely for a number of reasons of which the most compelling is the concordant pole (no. 15) found for the Jurassic Island Intrusives. These granitic plutons cut flat-lying strata throughout Vancouver Island in the Insular Fold Belt. They have clearly not been translated northward so that it is also unlikely that the Tulameen complex has been translated. Furthermore, simple translation of the uncorrected Tulameen pole (no. 13) would move the pole onto the Kamchatka Peninsula which would not be an improvement. The alternative possibility is that the tectonic block has been tilted ≈15° south-southeast. Although not unequivocally, two geologic arguments support this possibility. First, within the complex itself, the lower level dunite phase is exposed in the northwestern end and the higher level gabbroic rocks are exposed dominantly in the southeastern end thereby indicating a gentle south-southeast tilt (Fig. 1). Second, although Rice (1949) does not report any attitudes for the overlying Princeton Group in the adjacent Coalmont basin, it is apparent from his map that the strata get younger to the south-southeast and therefore most likely dip gently to the south-southeast.

In summary, it is probable that the discordance in the Tulameen pole position is the product of deformation during the Laramide orogeny. During the deformation the tectonic block containing the Tulameen complex has most likely been tilted ≈20° east-southeast. This tilt is probably the resultant of the combined ≈35° east-northeast tilt associated with thrust faulting and the ≈15° south-southeast tilt as the northerly end of the complex was uplifted relative to the southerly end. This tectonic interpretation assumes that the pole for the Tulameen complex was originally near the middle of the Upper Triassic to mid-Upper Jurassic pole cluster, i.e. near Y in Figure 3.

References

Beck, M.E.
1965: Paleomagnetic and geological investigations of magnetic properties of the Triassic diabase of southeastern Pennsylvania; J. Geophys. Res., v. 70, p. 2845-2856.

Burk, C.A.
1965: Geology of the Alaska peninsula-island arc; Geol. Soc. Am., Mem. 99, 250 p.

Camsell, C.
1913: Geology and mineral deposits of the Tulameen district, B.C.; Geol. Surv. Can., Mem. 26, 186 p.

Carmichael, C.M., and Palmer, H.C.
1968: Paleomagnetism of the Late Triassic North Mountain basalt of Nova Scotia; J. Geophys. Res., v. 73, p. 2811-2822.

Chrismas, L., Baadsgaard, H., Folinsbee, R.C., Fritz, P., Krouse, H.R., and Sasaki, A.
1969: Rb/Sr, S, and O isotopic analyses indicating source and date of contact metasomatic copper deposits, Craigmont, British Columbia, Canada; Econ. Geol., v. 64, p. 479-488.

Collinson, W.W., and Runcorn, S.K.
1960: Polar wandering and continental drift: evidence of paleomagnetic observations in the United States; Bull. Geol. Soc. Am., v. 71, p. 915-958.

Currie, K.L., and Larochelle, A.
1969: A paleomagnetic study of volcanic rocks from Mistastin Lake, Labrador, Canada; Earth Planet. Sci. Lett., v. 6, p. 309-315.

de Boer, J.
1967: Paleomagnetic-tectonic study of Mesozoic dike swarms in the Appalachians; J. Geophys. Res., v. 72, p. 2237-2250.

1968: Paleomagnetic differentiation and correlation of the late Triassic volcanic rocks in the Central Appalachian (with special reference

de Boer, J. (cont'd.)
to the Connecticut Valley); Bull. Geol. Soc. Am., v. 79, p. 600-626.

Eastwood, G.E.P.
1960: Magnetite in Lodestone Mountain stock; Brit. Columbia Dept. Mines, Ann. Rept. 1959, p. 39-53.

Findlay, C.D.
1969: Origin of the Tulameen ultramafic-gabbro complex, southern British Columbia; Can. J. Earth Sci., v. 6, p. 399-425.

Fisher, R.A.
1953: Dispersion on a sphere; Roy. Soc. London, Proc., Ser. A, v. 217, p. 295-305.

Foland, K.A., Quinn, A.W., and Giletti, B.J.
1971: K-Ar and Rb-Sr Jurassic and Cretaceous ages for intrusives of the White Mountain Magma Series, northern New England; Am. J. Sci., v. 270, p. 321-332.

Frebold, H., and Tipper, H.W.
1969: Lower Jurassic rocks and fauna near Ashcroft, British Columbia, and their relation to some granitic plutons; Geol. Surv. Can., Paper 69-23, 20 p.

Grommé, C.S., Merrill, R.T., and Verhoogen, J.
1967: Paleomagnetism of Jurassic and Cretaceous plutonic rocks in the Sierra Nevada, California, and its significance for polar wandering and continental drift; J. Geophys. Res., v. 72, p. 5661-5684.

Irving, E.
1964: Paleomagnetism and its application to geological and geophysical problems; John Wiley and Sons, 399 p.

Irving, E., and Banks, M.R.
1961: Paleomagnetic results from the Upper Triassic lavas of Massachusetts; J. Geophys. Res., v. 60, p. 1935-1939.

Larochelle, A.
1967: Preliminary data on the paleomagnetism of the North Mountain basalt, Nova Scotia; Geol. Surv. Can., Paper 67-30, p. 7-12.

Larochelle, A., and Black, R.F.
1965: The design and testing of an alternating-field demagnetizing apparatus; Can. J. Earth Sci., v. 2, p. 684-696.

Larochelle, A., and Christie, K.W.
1967: An automatic 3-magnet or biastatic magnetometer; Geol. Surv. Can., Paper 67-28, 28 p.

Leech, G.B., Lowdon, J.A., Stockwell, C.H., and Wanless, R.K.
1963: Age determinations and geological studies (including isotopic ages - Report 4); Geol. Surv. Can., Paper 63-17, 140 p.

McElhinny, M.W.
1968: Notes on progress in geophysics: paleomagnetic directions and pole positions - IX; Geophys. J. Roy. Astr. Soc., v. 16, p. 207-224.

Opdyke, N.D.
1961: The paleomagnetism of the New Jersey Triassic: a field study of the inclination error in sediments; J. Geophys. Res., v. 66, p. 1941-1949.

Opdyke, N.D., and Wensink, H.
1966: Paleomagnetism of rocks from the White Mountain plutonic-volcanic series in New Hampshire and Vermont; J. Geophys. Res., v. 71, p. 3045-3051.

Packer, D.R., and Stone, D.B.
1972: An Alaskan Jurassic palaeomagnetic pole and the Alaskan orocline; Nature Phys. Sci., v. 237, p. 25-26.

Rice, H.M.A.
1947: Geology and mineral deposits of the Princeton map-area, British Columbia; Geol. Surv. Can., Mem. 243, 136 p.

Richter, D.H.
1967: Geology of the Upper Slana-Mentasto Pass area, south-central Alaska; Div. Mines Min., Alaska, Geol. Rept. 30, 25 p.

Roddick, J.C., and Farrar, E.
1971: High initial argon ratios in hornblendes; Earth Planet. Sci. Lett., v. 12, p. 208-214.

1972: Potassium-argon ages of the Eagle granodiorite, southern British Columbia; Can. J. Earth Sci., v. 9, p. 596-599.

Steiner, M.B., and Helsey, C.E.
1972: Jurassic polar movement relative to North America; J. Geophys. Res., v. 77, p. 4981-4993.

Stockwell, C.H.
1969: Tectonic map of Canada; Geol. Surv. Can., Map 1251A.

Symons, D.T.A.
1971a: Paleomagnetism of the Triassic Guichon batholith and rotation of the southern Interior Plateau, British Columbia; Can. J. Earth Sci., v. 8, p. 1388-1396.

1971b: Paleomagnetism of the Jurassic Island Intrusions of Vancouver Island, British Columbia; Geol. Surv. Can., Paper 70-63, p. 1-17.

1972: Paleomagnetism of the Triassic Guichon batholith and rotation of the southern Interior Plateau, British Columbia; Reply; Can. J. Earth Sci., v. 9, p. 1343-1347.

1973a: Unit correlations and tectonic rotation from paleomagnetism of the Triassic Copper Mountain intrusions, B.C.; Geol. Surv. Can., Paper 73-19, p. 11-28.

1973b: Paleomagnetic results from the Jurassic Topley intrusions near Endako, British Columbia; Can. J. Earth Sci., v. 10, p. 1099-1108.

Tarling, D.H., and Symons, D.T.A.
1967: A stability index of remanence in paleomagnetism; Geophys. J. Roy. Astr. Soc., v. 12, p. 443-448.

White, W.H., Erickson, G.P., Northcote, D.E., Dirom, G.E., and Harakal, J.E.
1967: Isotopic dating of the Guichon batholith, B.C.; Can. J. Earth Sci., v. 4, p. 677-690.

74. MIDDLE ORDOVICIAN OSTRACODA FROM SOUTHWESTERN DISTRICT OF MACKENZIE

Project 500029

M. J. Copeland
Regional and Economic Geology Division

Fifty-two collections of silicified Middle Ordovician ostracodes from 10 stratigraphic sections near South Nahanni and Root rivers, southwestern District of Mackenzie, were submitted by R. Ludvigsen, University of Western Ontario. Thirty-six ostracode species (9 new) were identified from this 3,000-foot-thick composite section of Sunblood and Whittaker formations and an unnamed intervening stratigraphic unit. This unique western Canadian ostracode succession may be correlated with Mohawkian faunas from widespread occurrences elsewhere in eastern and western North America.

The lower 800 feet of the composite section (Sunblood Formation) contain index ostracodes of the Whiterock Stage previously reported from the upper Pogonip Group of Nevada, lower Table Head Formation of Newfoundland and Oil Creek Formation of Oklahoma. The upper 900 feet of the Sunblood Formation has a variable ostracode fauna, referred, because of its stratigraphic position, to the 'Chazy' Stage. As an unequivocal 'Chazyan' ostracode fauna has not been recorded from eastern North America, no more precise correlation is possible. The 600-foot-thick unnamed unit bears, in its lower two-thirds, the earliest representatives of an ostracode fauna previously known only from the lower, Porterfield part of the Edinburg Formation of Virginia. This well-defined fauna is succeeded by a cosmopolitan Wilderness-type fauna in the upper 200 feet of the unit. Only 700 feet of the lower Whittaker Formation are represented in the composite section. These beds contain the widespread late Wilderness-early Barneveld 'Decorah' fauna of common occurrence throughout the northern part of the continent.

The widespread occurrence throughout North America of this ostracode succession reflects the general transgression of Mohawkian seas, in that restricted older (Whiterock-Porterfield) ostracode faunas occurred along the continental margins and extensive younger (Wilderness-Barneveld) ostracode faunas occupied much of the developing continental platform. The transition between these faunas is marked by the development, in Porterfield-Wilderness time, of new ostracode genera that were prominent throughout the rest of the Ordovician. Also, the biogeographic occurrence of these faunas would seem to support the mid-North American Ordovician paleoequatorial position suggested by previous workers.

Reference

Copeland, M. J.
Middle Ordovician Ostracoda from southwestern District of Mackenzie; Geol. Surv. Can., Bull. (in preparation)

75. MAGNETIC FABRIC OF A RECENT VOLCANIC BOMB

Project 730071

Mikkel Schau
Regional and Economic Geology Division

An eared 12 cm diameter, fusiform (Macdonald, 1967) bomb (Fig. 1) from Heimaey was selected for this magnetic study as it still retains its aerodynamic shape.

The bomb is composed of microphenocrysts of plagioclase and olivine set in a variably vesicularized glass charged with small (1μ or so) grains of homogeneous opaque oxides (Schau and Gasparrini, this publ., rept. 76).

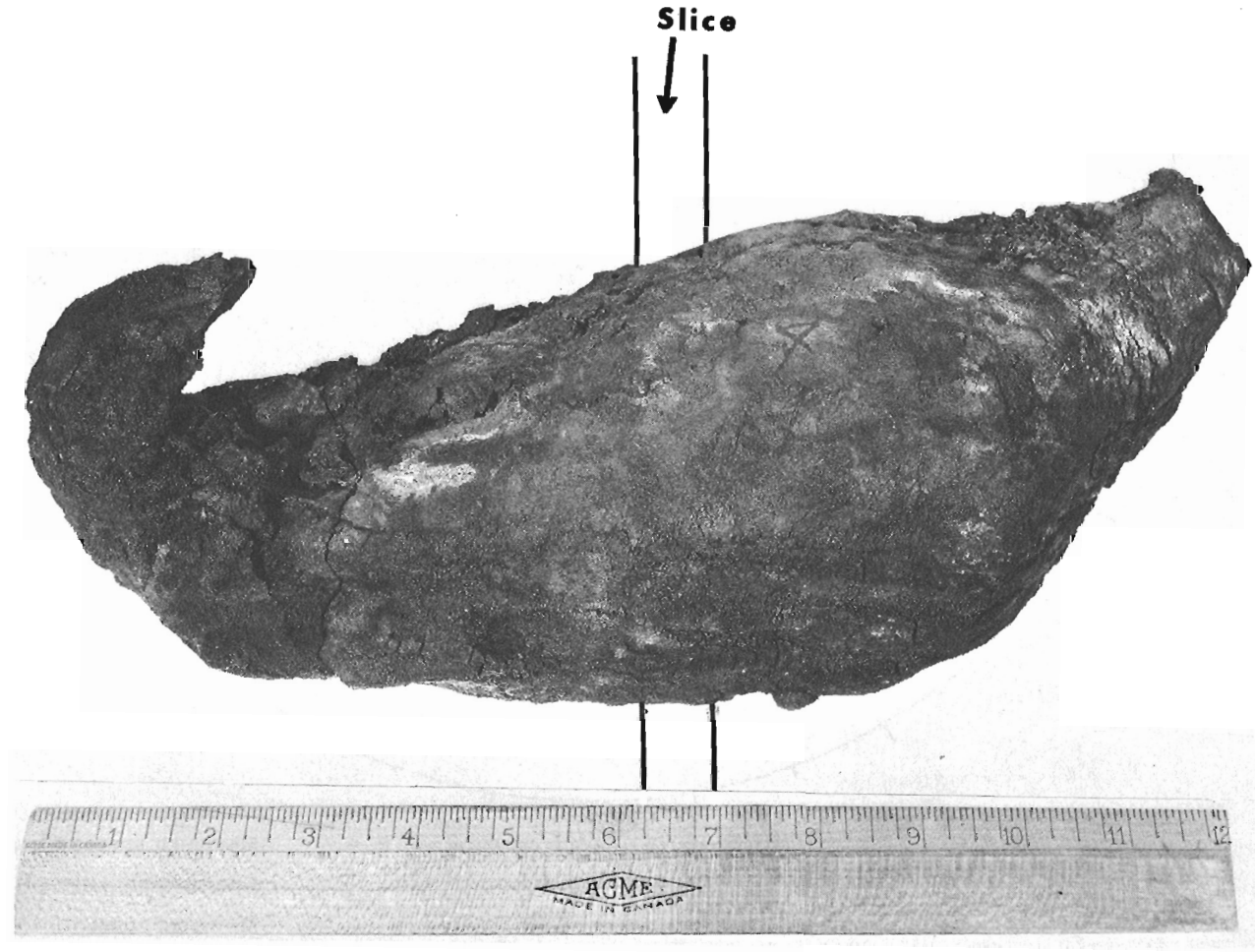

Figure 1. Fusiform bomb from Heimaey showing location of slice from which samples were taken (sample locality No. 5 on Fig. 1 in Schau and Gasparrini, this publ., rept. 76). GSC Photo 202230-B

The Curie point of two samples were measured to estimate the amount and composition of the opaque oxides. A sample from the outside skin contains about 5% of slightly heterogeneous titanomagnetite (mostly near 65% Fe_2TiO_4, 35% Fe_3O_4) as determined from Curie points distributed from 100°C to mainly 180°C. A sample from the inside of the bomb contains about 8% of homogeneous titanomagnetite (70% Fe_2TiO_4, 30% Fe_3O_4) determined from a clear Curie point at 150°C. These results indicate that *surface oxidation* of this fusiform bomb *is not an important process* in contrast to the oxidized subaqueous volcanic bombs reported from Heimaey by Thorarinsson et al. (1973).

The interior of the bomb is variously textured; regions of more vesicular glass are complexly interfolded with dense glass. These textures suggest that flow may have taken place leading to a possible orientation of mineral grains. The degree of magnetic anisot-

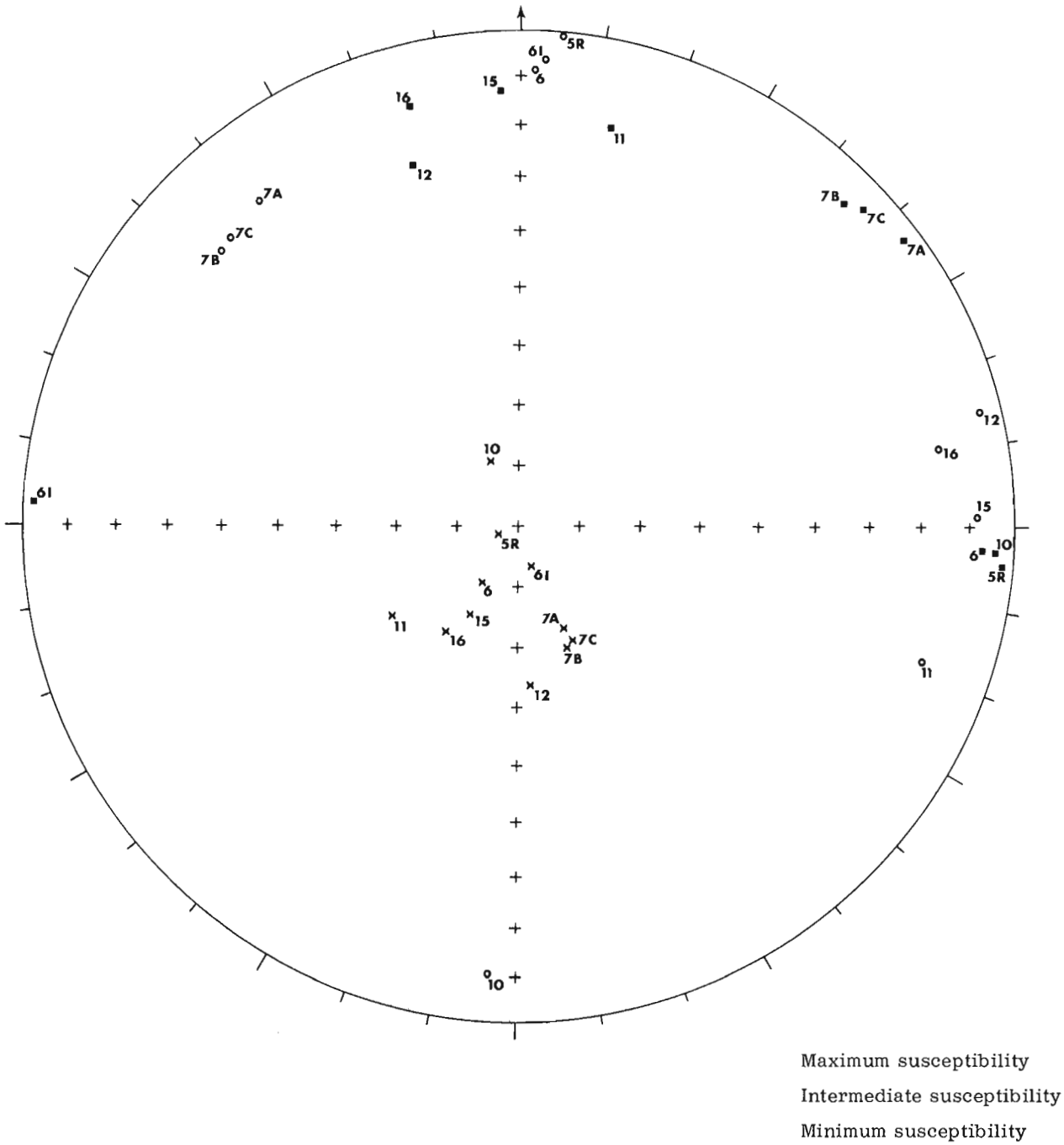

Figure 2. Stereogram showing directions of magnetic anisotropy.

ropy is significant and ranges from 4-8 per cent with the direction of maximum susceptibility oriented along the elongate axis of the bomb. This suggests that the long axes of the mineral grains show preferred orientation parallel to the long axis of the bomb (Fig. 2). The susceptibility varies about 14 per cent about a value of . 4 cgs units. This spread probably reflects variation in the amount of oxides throughout the bomb. There is no obvious correlation with position in bomb or vesicularity.

The intensity of natural remanent magnetism is between . 015 and . 033 cgs emu/cm^3. This variability also reflects the spread in content of titanomagnetite throughout the bomb. The remanent intensity is high and confirms the rather small grain size (single or pseudo-single magnetic domain) of the oxides as the

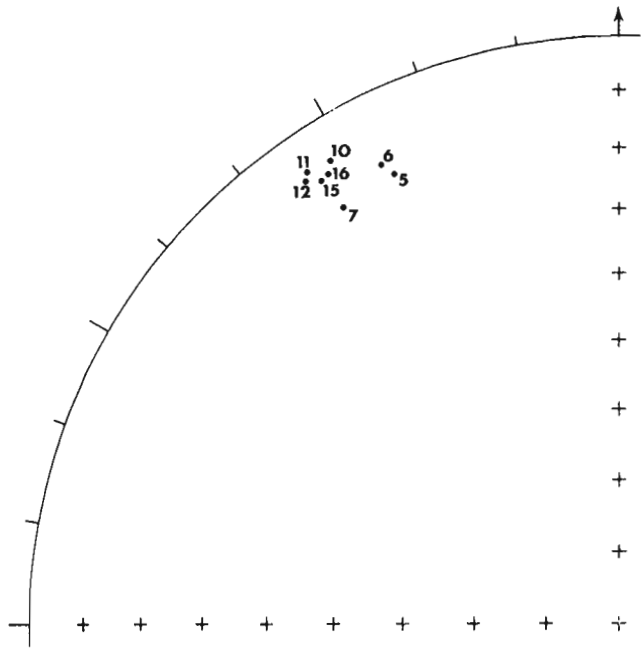

Figure 3. Stereogram showing direction of natural remanent magnetism.

magnetic capacity of titanomagnetite is low. The ratio of remanent and induced (H=0.50e) intensity yields a Q of .11.

The close clustering of natural remanent magnetism directions (Fig. 3), carried by low Curie point titanomagnetite, indicates the *bomb became magnetized after it hit the ground.* These results indicate that a bed of agglomerate would yield a uniformly magnetized unit whereas a slumped or remobilized agglomerate (volcanic breccia) would contain widely dispersed magnetic directions. Stability of remanent magnetization tests would be necessary to distinguish primary from secondary magnetism of an agglomerate unit.

Ken Clark measured the natural remanent magnetism of 8 cubes taken from a slab from the bomb Fig. 1 on an astatic magnetometer. Clark measured the magnetic anistropy of the same specimens on a Kappabridge KLY1. Computer programs by M. Larochelle were used. E. Schwarz measured the Curie points, computed compositions of titanomagnetite and discussed the implications of the data with the author. H. Bostock and W.R.A. Baragar critically read the manuscript. The author is responsible for all errors and omissions.

References

Macdonald, G.A.
1967: Forms and Structures of Extrusive Basaltic Rocks in H.H. Hess (ed.); Basalts, The Poldervaart treatise on rocks of basaltic composition, Vol. 1, p. 1-6, Interscience Pub.

Thorarinsson, S., Steinthorsson, S., Einarsson, Th., Kristmannsdottir, H., and Oskarsson, N.
1973: The eruption of Heimaey, Iceland; Nature, v. 241, p. 372-375.

Project 730071

Mikkel Schau and Elvira Gasparrini
Regional and Economic Geology Division

Major oxide concentrations of igneous rocks are regularly used to infer the nature of igneous processes and to some extent as aids in stratigraphic correlation. Hence it is necessary to have an estimate of the compositional variability of various kinds of igneous rocks (Watkins et al., 1970). Newly erupted tephra from Heimaey, Iceland, collected January 30, 1973 (Lambert et al., 1973) has been analyzed to estimate the variation within a tephra sheet and a bomb deposited at the same time to provide some variance estimates that might be useful in considering ancient tuffs and agglomerates were they to remain isochemical systems through time.

Thorarinsson et al. (1973), and Jakobsson et al. (1973), indicate that the extruded material was mainly gas and molten material with dominant tephra during the early phases of the eruption followed by lava and more volatile gases toward the end. The composition of the solid material slowly changed with time from (Jakobsson et al., 1973) "mugearite" to "hawaitte" and the gas became more "carbon"-rich.

The initial gas pressure was high (Jakobsson et al. 1973) and resulted in fountaining to a height in excess of 1,000 m on rare occasions, indicating a gas pressure well over 1 kb (Maløe, 1973). Large tephra clouds rose to a maximum height of 10 km as a result of earth-shaking explosions of gas-charged magma about every three seconds. The pressure decreased markedly with time, resulting in fewer, smaller fountains. The change in composition of lava was recorded by a change in the mode of advance of the flows. At first, the lava, relatively cool (1030°C or so) advanced by a process analogous to the moving of a caterpillar track. Later, when the lava was 50°C hotter it moved as lava rivers which ran rapidly to the sea.

From these descriptions, and the analyses presented later, it is apparent that considering the entire volcanic edifice as a single event would necessitate lumping together volcanic products with widely different textures and chemistry. Yet from a field geologist's viewpoint deposits like those of Heimaey are not extensive. On a 4-mile map they would constitute only a small local unit consisting of a central small agglomerate lens 100 m thick and 1,000 m length, with some interbedded autobreccia maybe 50 m thick and 700 m long with a core of finely crystalline rock surrounded by widespread but thin beds of lapilli tuff.

It would be of considerable interest to know if a given tuff could be correlated with a given volcanic centre on the basis of chemistry.

A MAC electron microprobe with a Kevex Lithium drifted solid state detector for energy dispersive analysis was used for quantitative analyses of glass, plagioclases and olivines. The operating conditions were: 20 kv accelerating voltage; .3 nano-amps specimen current measured on the glass, 40 seconds counting time; focussed beam. An analyzed kaersutite amphibole was used as a standard for Si, Al, Ti, Fe, Mg, Ca, K and Na, an analyzed biotite for Mn, and an analyzed chromite for Cr.

The very low specimen current required for energy dispersive analysis made it possible to use a focussed beam (~3μ) for the examination of the glass with no loss of alkalies. A defocussed beam, generally used in spectrometer analysis for alkali rich glass, could not have been used in our case as the glass contains up to 10% micron sized magnetite grains.

Computer programs EDS5C (Lachance and Plant, unpubl.) and EMPADR VII (Rucklidge and Gasparrini, 1969) were used for background corrections to the energy spectrum; fluorescence, absorption and atomic number corrections to the net peak intensities; and for the presentation of chemical analyses as oxide weight percentages.

A number of samples of tephra were collected from the new volcano on Heimaey (Fig. 1).

Textures of the tephra and the bomb are variably vesicular with few microphenocrysts of lath-shaped plagioclase and rare skeletal olivine and abundant opaques in a dark brown glassy matrix. A copper-bearing sulphide resembling chalcopyrite occurs as small blebs in olivine.

The microphenocrysts are approximately the same composition throughout the sheet on January 30, 1973 (Tables 4 and 5). Thorarinsson et al. (1973) first reported a variation in the refractive index of the glass in material extruded on January 23. This implies that

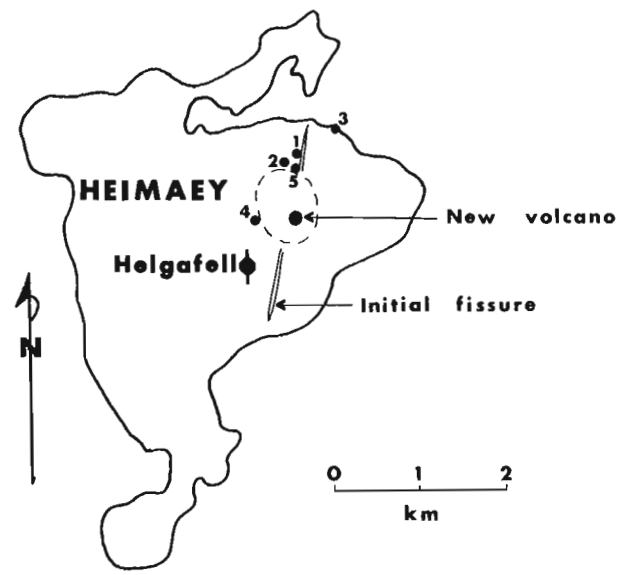

Figure 1. Sketch map of Heimaey showing localities of samples.

Table 1. Chemical composition of glass in tephra; January 30, 1973.

	1*	2	3	4	pooled ±S	5	+S
SiO_2	50.4	50.8	57.45	52.81	1.48	55.3	1.25
Al_2O_3	16.6	15.6	18.66	21.90	2.16	22.8	1.85
TiO_2	2.57	2.99	1.12	1.28	.42	.64	.185
tot FeO	11.7	12.0	5.48	5.47	1.90	2.93	.91
MnO	.24	.23	.17	.14	.07	.08	.03
MgO	2.80	2.97	1.78	1.06	.799	.729	.50
Cr_2O_3	.078	.066	.07	.08	.023	.068	.01
CaO	7.42	7.64	6.02	9.22	1.127	8.028	1.11
K_2O	1.30	1.32	1.53	.69	.33	.847	.37
Na_2O	6.40	6.26	7.49	6.68	.89	7.57	.57
N	5	5	6	5		24	

Sample 1. Tephra 250 metres north of vent.
Sample 2. Tephra from fumarole 250 metres north-northwest of vent.
Sample 3. Average of two sections, coagulated tephra, 750 metres north of vent from top of flow near sea. See Table 2.
Sample 4. Average of two sections of variably vesicularized tephra from 250 metres west of vent in valley between Helgafell and new vent. See Table 2.
Sample 5. Average of 6 sections in large bomb, found 200 metres northwest of vent. See Table 3.

the chemical composition of the glass varies (Tilley, 1922) along the fissure at time of extrusion.

Our results agree with this observation. Table 1 shows the variation in chemical composition of glass in tephra. The standard deviations are noted and are relatively great especially for iron. Table 2 shows the relationship between amount of vesicularity and chemistry. Table 3 shows the variation of chemical composition of glass within a single large fusiform bomb. These analyses demonstrate a considerable variation within the glass which must be considered primary. In Table 6 samples collected from the same fumarolic region a week apart are very similar indicating that short term fumarolic activity probably is not an important agent in changing the chemical composition of the glass.

Chemical variability in volcanic glass is well known (cf. Scott, 1971). The Heimaey example shows that the degree of variability of the chemistry in a single volcanic event at one locality must be well understood before we can properly correlate the event regionally on the basis of its chemistry.

The mechanism whereby the variability is generated is not known. The obvious link between degree of vesicularity and composition may simply reflect the different gas holding capacities of different compositions. Since the lava seems to have changed composition as the eruption progressed (Jakobsson et al., 1973), perhaps magma mixing in the chamber was not efficient, or gabbro xenoliths were variably ingested (Jakobsson et al., 1973), or degassed material flung onto the cone early in the eruption slid back into the vent later on without being mixed. The possibilities are numerous and were not investigated. For whatever reason, glass produced during this single eruption is heterogeneous. Care should be taken therefore in the interpretation of petrochemical "trends" in ancient volcanic examples.

We would like to thank S. Steinthorsson for his kind help during the visits to Iceland. J. B. Henderson and M. B. Lambert critically read the manuscript, however, we are totally responsible for the interpretation and errors.

References

Jakobsson, S.P., Pedersen, A.K., Ronsbo, R.C., and Melchior, Larson L.
1973: Petrology of mugearite - hawaiite, early extrusives in the 1973 Heimaey eruption, Iceland; Lithos, v. 6, p. 203-214.

Lambert, M.B., Baragar, W.R.A., and Schau, M.
1973: The Kirkjafell Eruption, Iceland 1973; in Report of Activities, November 1972 to March 1973, Geol. Surv. Can., Paper 73-1, Pt. B, p. 203-204.

Maloe, S.
1973: Temperature and pressure relations of ascending primary magmas; J. Geophys. Res., v. 78, p. 6877-6886.

Table 2. Chemical composition of glass in fragments with varying vesicularity.

	3A	3B	4A	4B
SiO_2	56.78	58.51	52.66	53.03
Al_2O_3	16.99	21.69	19.82	25.01
TiO_2	1.32	0.70	1.71	0.64
FeO	7.21	2.02	7.49	2.44
MnO	0.23	0.06	0.18	0.07
MgO	2.42	0.50	1.49	0.62
Cr_2O_3	0.07	0.07	0.08	0.08
CaO	6.21	5.56	8.65	10.07
K_2O	1.67	1.93	0.88	0.41
Na_2O	6.97	8.92	6.63	6.74

3A medium dense vesicular part of tephra
3B finely vesicular part of tephra
4A medium dense vesicular part of tephra
4B finely vesicular part of tephra

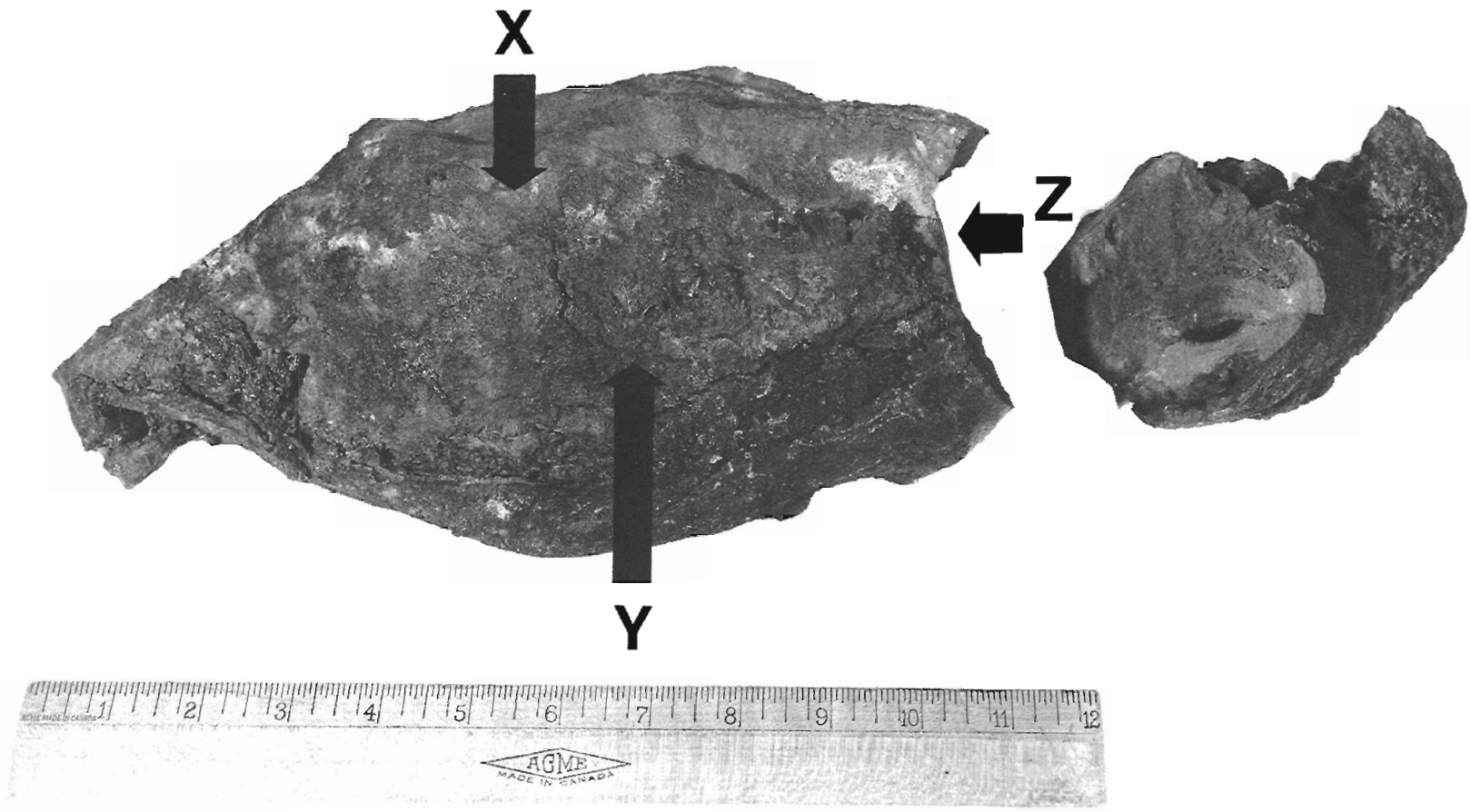

Figure 2. Fusiform bomb from Heimaey. Axes for core samples in Table 3 shown by X, Y, Z. Note internal structure on broken surface of bomb. GSC Photo 202230-A

Table 3. Chemical composition of glass in a large fusiform bomb.

	5a	5b	5c	5d	5e	5f
SiO_2	57.0	55.88	54.53	54.05	56.37	55.0
Al_2O_3	20.8	22.74	21.70	24.99	23.92	24.90
TiO_2	.63	0.59	0.90	0.25	0.50	0.50
FeO	2.87	3.15	3.90	2.02	2.43	2.02
MnO	0.07	0.11	0.11	0.06	0.07	0.06
MgO	1.18	0.73	1.07	0.52	0.27	0.98
Cr_2O_3	0.06	0.06	0.06	0.08	0.07	0.06
CaO	6.74	8.09	8.01	9.47	7.39	8.29
K_2O	1.94	0.89	0.87	0.53	0.89	0.61
Na_2O	7.64	7.09	8.00	6.55	8.04	7.40
N =	3	4	7	4	4	2

5a near centre of bomb (core Z) (8 cm deep)
5b between 5a and 5c (core Z) (5 cm deep)
5c near spindly end (core Z) (1 cm deep)
5d near centre of bomb (core Y) (6 cm deep)
5e in dense material of bomb (core Y) (4 cm deep)
5f near outside edge of bomb (core X) (Z cm deep)

Table 4. Chemical composition of olivine in tephra (1) and bomb (2).

	(1)	(2)	Pooled Standard Deviation
SiO_2	35.79	35.23	.495
Al_2O_3	.20	.18	.258
TiO_2	.145	.092	.102
tot FeO	31.10	29.95	.848
MnO	.559	.565	.101
MgO	32.21	33.23	.812
Cr_2O_3	.069	.065	.014
CaO	.219	.200	.108
K_2O	.03	.03	-
Na_2O	-	-	-
N	14	25	

Table 5. Chemical composition of plagioclase in tephra (1) and bomb (2).

	(1)	(2)	Pooled Standard Deviation
SiO_2	52.67	52.95	.676
Al_2O_3	28.41	28.40	.547
TiO_2	.141	.128	.053
tot FeO	.754	.693	.162
MnO	.060	.061	.004
MgO	.138	.137	.056
Cr_2O_3	.075	.075	.025
CaO	11.233	11.182	.506
K_2O	.184	.184	.046
Na_2O	6.02	5.95	.475
N	34	40	

Table 6. Chemical composition of glass in tephra over a Fumarole.

	2	6
SiO_2	50.8	50.3
Al_2O_3	15.6	15.1
TiO_2	2.99	2.9
tot FeO	12.0	12.8
MnO	.23	.28
MgO	2.97	3.18
Cr_2O_3	.066	.071
CaO	7.64	7.38
K_2O	1.32	1.47
Na_2O	6.26	6.21

2 tephra from fumarole (Jan. 30)
6 tephra from same fumarole (Feb. 6)

Scott, R. B.
1971: Chemical variations in glass shards and interstitial dust of ignimbrite cooling units; Am. J. Sci., v. 270, p. 166-173.

Thorinsson, S., Steinthorsson, S., Einarsson, Th., Kristmansdottir, H., and Oskarsson, N.
1973: The eruption of Heimaey, Iceland; Nature, v. 241, p. 372-375.

Tilley, C. E.
1922: Density, refractivity and composition relations of some natural glasses; Mineral. Mag., v. 19, p. 275-293.

Watkins, N. D., Gunn, B. M., and Coy-yll, R.
1970: Major and trace element variations during the initial cooling of an Icelandic lava; Am. J. Sci., v. 268, p. 29-49.

77. SHALLOW MARINE PLATEAU BASALTS OF THE APHEBIAN HURWITZ GROUP AT LAST LAKE, DISTRICT OF KEEWATIN

Project 700052

R.H. Ridler
Regional and Economic Geology Division

Introduction

Base camp for project 700052, the purposes of which have been described elsewhere (Ridler and Shilts, 1973) was located at Last Lake, District of Keewatin, N.W.T. (Fig. 1) during the field season of 1972. A prominent belt of northeast-trending mafic volcanic rocks which occurs in this vicinity was pointed out to the author by A. Davidson (pers. comm., 1971) who suggested that it might be of Hurwitz Group age. L. Covello and G. Thurlow (senior assistants), R. Bell (visiting geologist) and the author briefly examined these volcanics and their associated sediments. G. Thurlow and L. Tihor (junior assistant) collected all but one of the chip samples along the cross-section (Fig. 1) for which chemical analyses appear in Table 1.

Davidson's suggestion was verified by these investigations (Ridler, 1972) some of the results of which are presented here or have been incorporated by Heywood (1973).

Distribution

Mafic to intermediate volcanic rocks of the Hurwitz Group, of probable upper Aphebian age according to work currently in progress (pers. comm., R.K. Wanless, K.E. Eade), occur in the Kaminak Lake belt 30 miles northwest of Last Lake (Davidson, 1970) and as relatively thin lenses locally as far west as Ameto Lake (Bell, 1970). They are interbedded with the slates and minor stromatolitic dolomites of the Ameto Formation and have been named the Happotiyik member (Bell, 1970). The Ameto Formation overlies the "backbone" of the Hurwitz Group, the widespread Kinga orthoquartzite, a blanket sand of unusually constant thickness and composition (Bell, 1968). Gabbros, probably coeval with the Happotiyik member, intrude the older Hurwitz formations.

Mafic volcanic rocks and minor slate and dolomite overlie orthoquartzite in the Rankin Inlet area (A. Davidson, pers. comm., 1971 and unpublished data; P. Laporte, 1973). Their proximity to the Last Lake area (40 miles) and stratigraphic/lithologic similarity to the Happotiyik member suggest a possible correlation. Thus, the Happotiyik member of the Ameto Formation appears to be more extensive than originally believed, occurring discontinuously within the Hurwitz Group along the trend of the group for at least 200 miles.

The distribution of the Happotiyik member in the Last Lake belt roughly corresponds to the distribution of the Ameto Formation as shown on Figure 1. It clearly overlies the Kinga quartzite (1a on Figs. 1 and 2). In the vicinity of the cross-section (A-B, Fig. 1) the Happotiyik member is approximately 3,000 feet thick (Fig. 2). No volcanics have been found in the adjacent and parallel belt of Hurwitz Group only a few miles to the southeast (Bell, 1968). A simple explanation is that a fault system, operative at the time, prevented extension of the volcanics to the southeast.

Structure

In cross-section (Fig. 2) the Last Lake belt is a relatively simple, asymmetric syncline or trough. The northwest limb rests with marked angular unconformity on a basement of Archean metagranite and metabasalt and dips moderately at 45 degrees to the southeast. Progressing to the southeast the rocks become more foliate (parallel to the long axis of the belt and vertical) and relatively short wavelength folds of relatively shallow plunge (30 degrees to the northeast) appear (Figs. 1 and 2). The dip of the southeast limb varies but tends to be steeper (>65 degrees to the northwest) than that of the opposing limb. The lack of refolding and the presence of mylonitic zones in the basement along strike from and parallel to the belt supports a "semi-graben" interpretation of the structure, consistent with that offered for the Kaminak Belt (Ridler, 1973; Davidson, 1970; Bell, 1968).

Metamorphism

Thin sections of five samples were examined. The metamorphic mineral assemblage is notable for abundant groundmass saussurite, fibrous epidote, plus characteristic coarser-grained epidote porphyroblasts and locally large aggregates of relatively coarse-grained epidote. Chlorite and uralite in the matrix were abundant. Green mica (biotite?) and carbonate were present locally. Stilpnomelane was noted in two cases, extending the zone first noted by Davidson in pre-Hurwitz diabase dykes significantly to the southeast (Davidson, 1970). Relict plagioclase laths and microlites were well preserved in the less foliate specimens. Minor quartz, magnetite and pyrite are present. The metamorphic assemblage is low to middle greenschist and of probable Hudsonian age.

Preservation of primary fabric is good in the non-foliate specimens from the northwest limb of the trough. In the axial and southeastern portions of the structure the rocks have a well-developed foliation. In thin section the foliation is represented by discrete

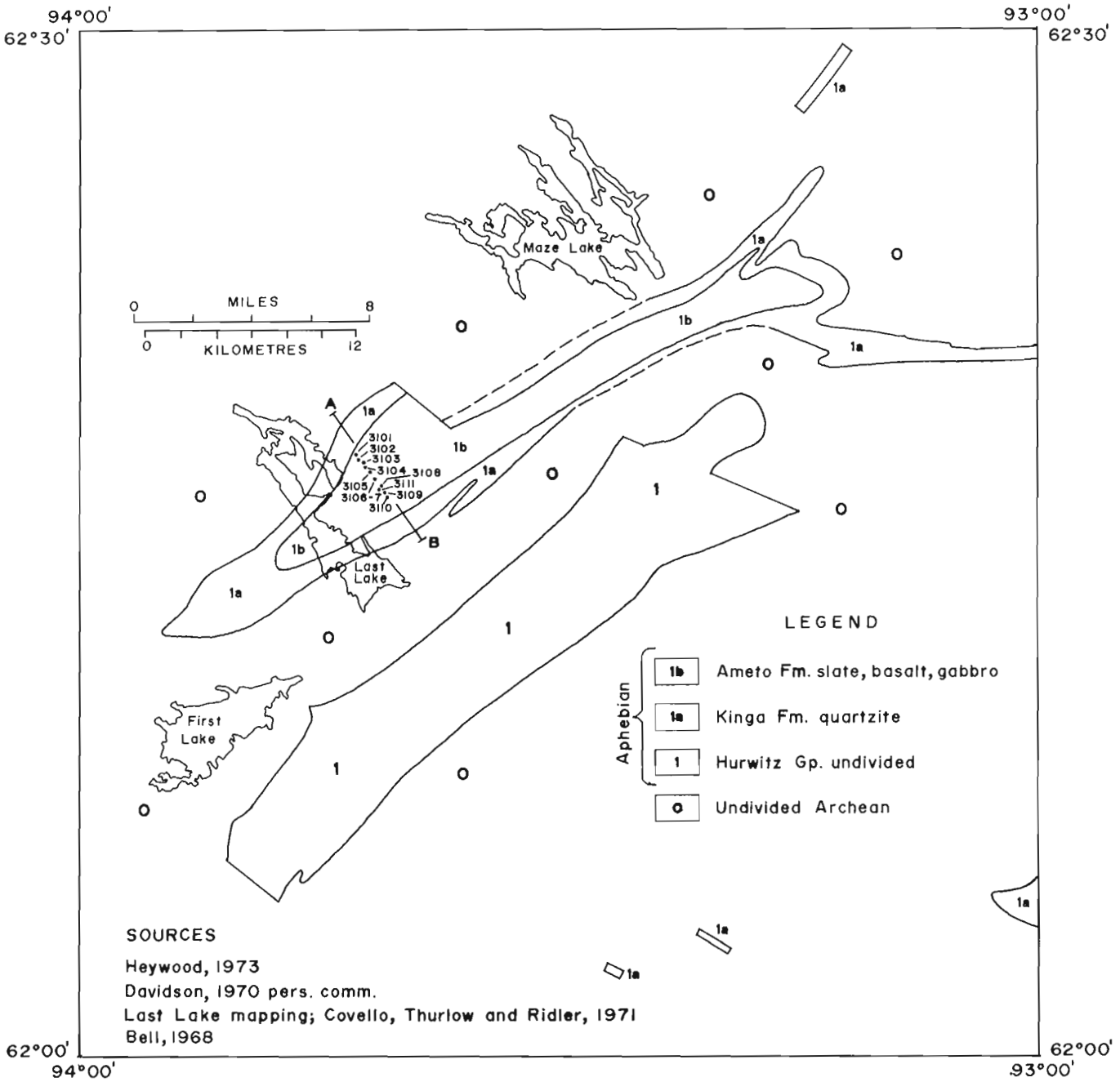

Figure 1. Hurwitz Group, Last Lake area.

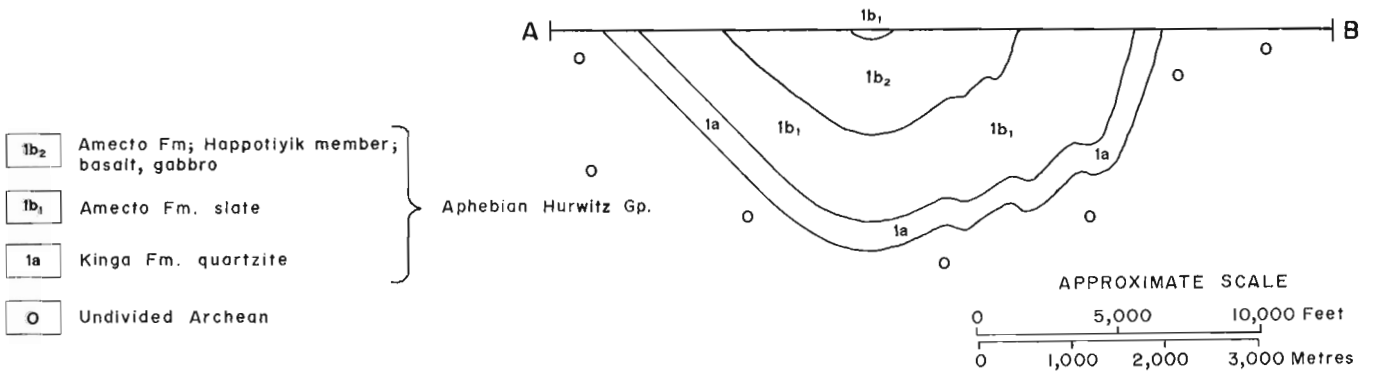

Figure 2. Cross-section A-B in Figure 1.

TABLE 1.

Chemical analyses, Hurwitz Group volcanics, Last Lake area, N.W.T.

No.	MnO	TiO_2	CaO	K_2O	SiO_2	Al_2O_3	MgO	FeO	Fe_2O_3	Na_2O	P_2O_5	CO_2	H_2OT	Lat.	Long.	Rock Type
3100	0.26	0.97	4.5	1.1	52.7	13.3	8.2	8.6	3.0	4.5	0.08	0.1	3.6	62°17'35"	93°42'25"	Pillow lava
3101	0.12	0.92	4.6	1.4	52.0	13.9	7.2	7.8	1.9	4.8	0.08	1.3	3.1	62°17'25"	93°42'20"	Pillow lava
3102	0.17	1.59	3.4	0.5	52.0	12.5	8.1	10.8	3.0	3.1	0.13	0.2	4.9	62°17'25"	93°42'20"	Breccia with tuff matrix
3103	0.21	1.21	11.6	1.0	42.5	10.8	6.6	9.9	3.6	3.0	0.12	5.0	4.2	62°17'20"	93°42'00"	Amygdaloidal breccia and tuff
3104	0.20	1.45	4.3	0.1	48.1	12.3	8.4	11.6	4.3	3.5	0.12	0.1	5.1	62°17'10"	93°41'45"	Massive lava, tuffaceous(?)
3105	0.27	1.15	6.7	<0.05	49.5	12.3	7.2	9.6	3.1	4.6	0.11	1.8	3.8	62°17'05"	93°41'30"	Massive lava, tuffaceous(?)
3106	0.17	1.57	3.0	0.1	44.2	16.6	8.5	12.5	2.4	4.0	0.13	0.1	6.1	62°16'50"	93°41'20"	Coarse breccia, tuff matrix
3107	0.19	1.46	6.7	0.2	48.7	11.4	6.5	10.3	5.0	4.1	0.13	0.7	3.8	62°16'50"	93°41'20"	Massive lava, tuffaceous(?)
3108	0.17	1.20	4.2	<0.05	55.9	12.9	6.4	8.3	1.9	5.6	0.12	0.1	3.2	62°16'40"	93°40'45"	Breccia with tuff matrix
3109	0.22	1.02	8.1	<0.05	52.3	11.5	6.2	9.1	2.5	4.6	0.11	0.5	6.0	62°16'25"	93°40'30"	Breccia with tuff matrix
3110	0.20	0.92	7.4	0.3	51.8	13.3	6.1	7.4	3.2	4.6	0.08	0.1	3.0	62°16'20"	93°40'20"	Breccia with tuff matrix
3111	0.17	1.20	6.2	0.1	52.1	13.9	7.0	8.4	2.5	5.0	0.12	0.6	3.0	62°16'30"	93°41'00"	Pillow lava

parallel slip surfaces within the rock rather than being pervasive. These are occasionally emphasized by the presence of concentrations of opaque minerals. In the more fissile schists the slip surfaces are more closely spaced. Intervening zones display relict primary texture. These textural features are more compatible with low intensity mylonitization than compressive failure, supporting a graben origin for the troughs. "First" foliations in the Archean Kaminak Group, with which the Happotiyik member is often confused, are truly pervasive, while "second" foliations may be similar to the above. Only one foliation has been recognized in the Happotiyik member.

Primary Structures and Fabric

The lower portion of the Happotiyik member in the Last Lake area is characterized by pillowed lava with varying proportions of tuffaceous matrix (submarine tephra?). In the Kaminak Group, pillowed sequences lack volumetrically significant matrix. With a low proportion of matrix the pillows adopt their characteristic bun shape and "top" determination is a simple matter. As matrix increases the individual pillows separate and lose their distinctive downward projection making "top" determination impossible. Much of the upper Happotiyik member is predominantly tuffaceous, with only scattered "pillows" or locally thin pillowed zones. The lower pillowed zone is relatively rich in disseminated magnetite (2-3%) causing a noticeable positive magnetic anomaly which outlines the nose of the major syncline. Amygdaloidal zones were noted at several levels. A pronounced one occurs sporadically in the vicinity of samples 3103 - 3105 (Fig. 1). Individual amygdules have highly irregular shapes. They are lined with a thin, coarsely fibrous layer of quartz occupying less than 5 per cent of the vug and then filled with coarse-grained chlorite plus occasional carbonate and coarse euhedral epidote.

Basaltic texture is reasonably well preserved in the flows although two populations of primary plagioclase may be present; a microlitic matrix phase and a relatively coarser "micro-phenocryst" phase of varying grain size. The matrix pyroxene is entirely replaced by a "saussuritic" felted growth of epidote, uralite and chlorite.

Other than the discrete pillows or as they may be, "bombs", fragmental texture is subtle and bedding largely absent. Lack of pronounced compositional variation and the widespread development of foliation have conspired to destroy either structure.

The pillow structures, amygdules and relatively high proportion of matrix are consistent with a relatively shallow, submarine environment of deposition.

Chemistry

Chemical data for twelve samples are presented in Table 1, located on Figure 1 and illustrated in Figure 3.

Except for one sample rich in volatiles (highly amygdaloidal) the analyses behave as a well-defined cluster on each of the variation diagrams of Figure 3. No attempt was made to adjust the analyses for their volatile content.

On the total alkalis versus silica diagram the cluster straddles the boundary separating the alkaline from the sub-alkaline field. The field of the cluster coincides with that of the Coppermine River basalts (Irvine and Baragar, 1971) and is characteristic of tholeiitic plateau basalt suites.

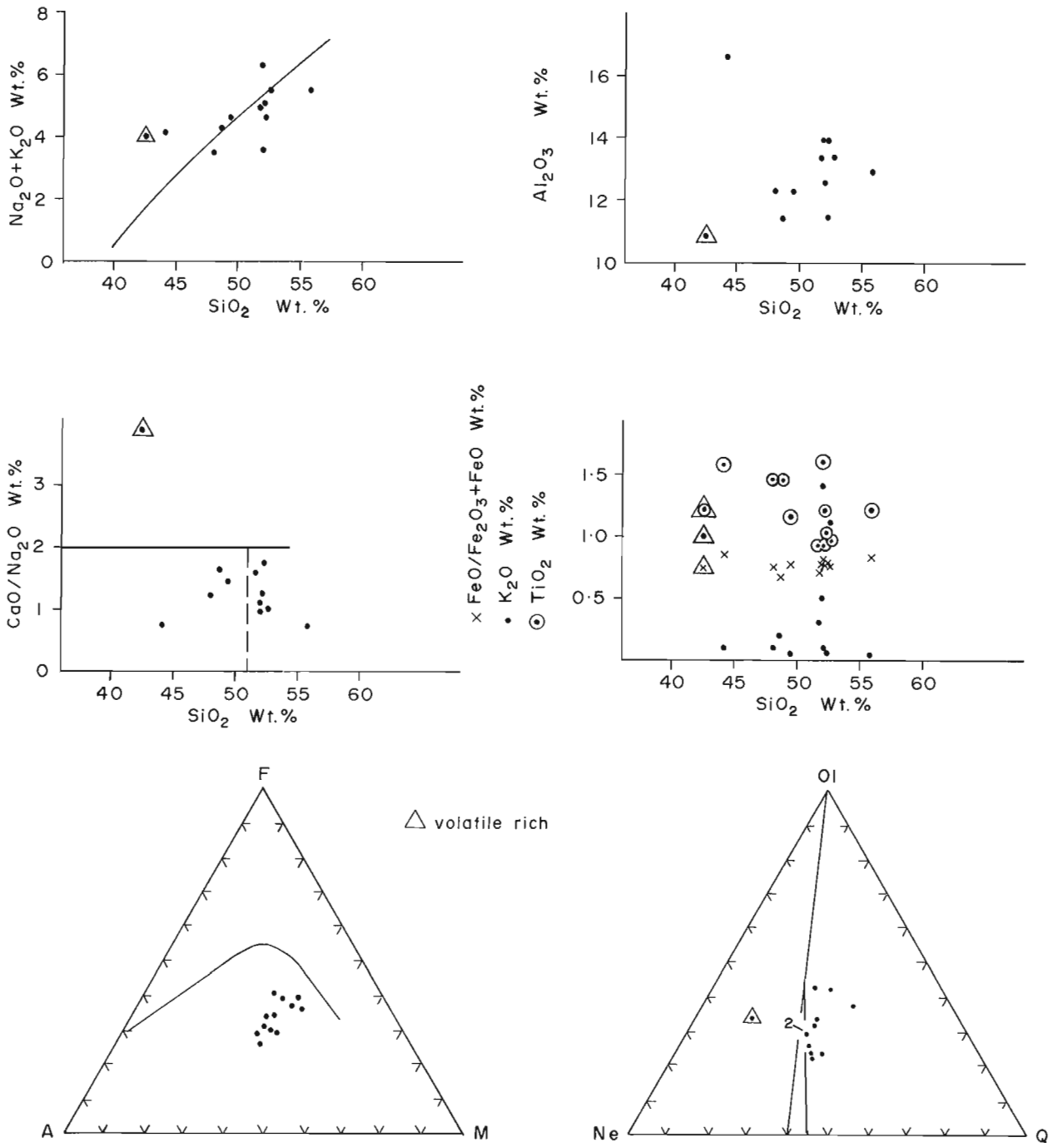

Figure 3. Variation diagrams - Hurwitz volcanics, Last Lake, N.W.T.

The alumina diagram illustrates that the volcanics are alumina normal (with one exception) but, slightly siliceous for normal basalts; overlapping the andesite field.

The lime/soda ratio versus silica diagram illustrates one of the most striking features of the basalts' chemistry; they are rather "spilitic". Reference to Table 1 indicates that the lavas are very lime deficient and only slightly enriched in soda. Their field on this diagram falls entirely below that of the Archean Kaminak Group (Ridler, 1974). As might be expected, the normative plagioclase content of most of the samples is oligoclase or andesine. The Happotiyik member was, because of its textural, metamorphic and gross compositional similarity with the Kaminak Group, originally mapped as Archean. The distinctly different fields of the two suites on the lime/soda diagram would appear to be of important diagnostic value.

The next diagram shows that most of the flows are potash deficient with respect to most continental basalt suites. On the other hand the titania cluster falls within the field of the platform basalts; higher

than their geosynclinal analogues (Baragar, unpublished data). The oxidation state is intermediate; a feature consistent with their submarine rather than subaerial nature.

On the AFM diagram the cluster falls well within the calc-alkaline field, but is more magnesian than most calc-alkaline suites. In addition the twelve samples display no hint of either a calc-alkaline "alkali enrichment" trend or a tholeiitic "iron enrichment" trend. The Ne: Ol: Q plot shows that the cluster is silica saturated and unlike the AFM diagram the field coincides with that of the Coppermine basalts (Irvine and Baragar, op. cit.) and is tholeiitic.

Mineral Deposits

No economically or metallogenetically significant mineralization has been recognized associated with the Happotiyik member in the Last Lake area, but the environment appears favourable for copper.

Conclusions

The Happotiyik member of the Ameto Formation is a rare example of a shallow marine tholeiitic plateau basalt suite. Primary structures within the suite, the intermediate FeO: FeO+Fe_2O_3 ratio and the associated sedimentary facies are consistent with a shallow marine environment. The total alkalis, titania and Ne: Ol: Q diagrams indicate striking similarity with the Coppermine River tholeiitic basalt suite. The calc-alkaline displacement of the cluster on the AFM diagram, and the generally though not uniformly low potash contents, suggest affinities with a continental margin tectonic environment (i.e. thin crust) rather than a continental interior (i.e. thick crust).

In addition to, or in the absence of, the appropriate stratigraphic criteria, the Happotiyik member can be differentiated from its Archean counterpart in the underlying Kaminak Group by its diagnostically lower CaO: Na_2O ratio.

The Happotiyik member is much more extensive than originally believed, and in the Last Lake belt, thicker than its known correlatives. However, additional and much more detailed study than that presented herein must surely be productive of much more tectonic, metallogenic and facies implications.

References

Bell, R. T.
1968: Preliminary notes on the Proterozoic Hurwitz Group, Tavani (55K) and Kaminak Lake (55L) areas, District of Keewatin; Geol. Surv. Can., Paper 68-36, 17 p.

Bell, R. T. (cont'd.)
1970: Preliminary notes on the Hurwitz Group, Padlei map-area, Northwest Territories; Geol. Surv. Can., Paper 69-52, 13 p.

Davidson, A.
1970: Precambrian Geology, Kaminak Lake map-area, District of Keewatin; Geol. Surv. Can., Paper 69-51, 27 p.

Heywood, W.W.
1973: Geology of Tavani map-area, District of Keewatin; Geol. Surv. Can., Paper 72-47, 14 p.

Irvine, T.N., and Baragar, W.R.A.
1971: A guide to the chemical classification of the common volcanic rocks; Can. J. Earth Sci., v. 8, no. 5, p. 523-548.

Laporte, P.J.
1973: Geology, Rankin Inlet, District of Keewatin, Northwest Territories, D.I.A.N.D. Preliminary Edition; Geol. Surv. Can., Open File 179.

Ridler, R.H.
1972: Volcanic stratigraphy and metallogeny of the Kaminak Group; Geol. Surv. Can., Paper 72-1, p. 128-134.

1973: Volcanic stratigraphy and metallogeny of the Rankin Inlet - Ennadai Belt, District of Keewatin; in Report of Activities, April to October 1972, Geol. Surv. Can., Paper 73-1, p. 165-174.

1974: Volcanic stratigraphy and metallogeny of the Rankin Inlet - Ennadai Belt, District of Keewatin, Northwest Territories; Geol. Assoc. Can., Spec. Publication. (in preparation)

Ridler, R.H., and Shilts, W.W.
1973: Exploration for Archean polymetallic sulphide deposits in permafrost terrains: an integrated geological/geochemical technique; Kaminak Lake area, District of Keewatin; Geol. Surv. Can., Paper 73-34.

78. TERRAIN PERFORMANCE, POINTED MOUNTAIN GAS PIPELINE

Project 710077

J.A. Heginbottom
Terrain Sciences Division

In September, 1973, four days were spent examining terrain performance of the pipeline right-of-way and the performance of post-construction rehabilitation measures. This work was a continuation of that done by N.W. Rutter in May and June, 1973 (Rutter, 1974). Initial work with regard to this pipeline had been done by E.B. Owen during the construction phase (Owen, 1971).

The Pointed Mountain pipeline runs from Pointed Mountain, N.W.T., through the southeast corner of Yukon Territory, 34 miles to Beaver River in British Columbia. It is a 20-inch buried line, owned and operated by Westcoast Transmission Co. Ltd. The pipeline was built during the winter of 1971-72, and it was the first natural gas pipeline in the Territories and the first engineering structure to be built under the rules of the Territorial Land Use Regulations (Rowland, 1972).

In general, the pipeline right-of-way was in good condition; most of the land was stable, vegetated and undamaged. There were three sections where conditions were bad, a few places where repair work was needed, and in a number of places minor maintenance work was required. The three bad areas were (i) the steep sand bluff south of the Kotaneelee River, (ii) the steep till slope north of the La Biche River, and (iii) the swamp area west of Fisherman Lake. Westcoast Transmission Co. Ltd. has indicated that they are aware of these problems and planned repair work during the winter of 1973-74. In the case of the Kotaneelee sand bluff, they proposed to regrade the slopes of the cut, to build more extensive check dams, to line the ditches behind the check dams and down the sides of the right-of-way with half-culvert, and finally to fertilize and seed the cut slopes and the right-of-way. A similar procedure was planned for the steep slope north of La Biche River. In the spring of 1973 some repair work was done here from a packed snow pad.

At Fisherman Lake the pipe ditch cut off two large meanders in the main creek flowing into the lake from the west. The creek naturally followed this shorter, steeper route and abandoned its own channel. The pipe shifted and a number of the concrete, swamp (saddle) weights fell off, which allowed the pipe to float. In June and September of 1973, the pipe was exposed above ground level. Westcoast Transmission Co. Ltd.'s proposals for rectifying this were (i) to cut a new, meandering channel for the creek through a series of ponds and hollows to the west of the pipe, (ii) to fill in the old channel of the creek, (iii) to rebury the pipe in a widened ditch using river (ring) weights, and finally (iv) to refill the ditch.

The other problems along the pipeline right-of-way included subsidence of the backfill, gullying along the pipe ditch or alongside it, ponding and minor diversions of cross-cutting streams, and minor slope movements. Some subsidence of the backfill was ubiquitous because the backfill was frozen when placed, and thus resisted adequate consolidation. The backfill material probably contained a significant proportion of snow as well. Gully erosion along the ditch or right-of-way in general was not very extensive and normally not severe. Much of the gully erosion occurred during heavy rains in the fall of 1972 (Rutter, pers. comm.). During the spring of 1973 ponding of water on the right-of-way was widespread; in most cases it was caused by the creek channels being choked by logs and wood debris. The significance of this ponding is not obvious. On most creeks it occurred only during the spring run-off, when the ground surface normally is frozen. In many cases of ponding, the debris damming the creek is older than the pipeline construction. This is particularly true where the pipeline was routed along pre-existing trails and cut-lines. The problem was less severe in areas where the pipeline right-of-way was cut through undisturbed forest. Diversions of pre-existing drainage were few and small and were of low significance. Areas of sediment deposition within the right-of-way were confined largely to stream beds. The few exceptions were of small extent and of low significance. In most cases erosion products had been removed completely from the cut-line. In a few places there was some evidence of downslope soil movement or incipient slope failure. Only one such site appeared to be significant at present. Normal right-of-way maintenance should prevent any serious problems from developing. In one section a rock-cut has been left along the east side of the right-of-way. In this case both the cut slope and the right-of-way surface were stable and in good condition.

Only one problem had developed at the two river crossing sites. The Kotaneelee River had shifted its channel somewhat, exposing a stretch of pipe. The pipe was laid deeply below the main channel of the river, but quite near the surface under an adjacent, active, gravel bar. During the 1973 spring run-off peak, the bar and the channel changed sides - a fairly common occurrence in gravel bed rivers of this type. The pipe was to be reburied at the greater depth for the full width of the active channel.

Close aerial observation was made of both the Kotaneelee and La Biche rivers from some 5 km upstream of the pipeline crossings down to their confluences with the Liard River. No indication of down-

stream disturbance resulting from pipeline construction was seen. Both rivers are high-energy, gravel bed rivers with a high sediment load and a wide annual variation in discharge. Thus any moderate changes in sediment load or discharge due to pipeline construction presumably were insignificant when compared with the natural, annual fluctuations in river conditions.

During construction of the pipeline, a few small patches of permafrost were encountered, totalling less than 3 km in about 55 km of pipeline - about 5 per cent. Evidence of degradation of permafrost was even more limited. In a few areas there are cracks in the ground surface and various irregular, shallow depressions, some containing water. These are presumed to be thermokarst hollows. No severe thermokarst had developed, and it is unlikely that any will develop. No information on changes in the thickness of the active layer was obtained. In no cases could permafrost be reached with a hand auger before encountering a stone or a piece of wood.

In their efforts to prevent erosion of the right-of-way and speed stabilization of the ground surface, the company ordered the construction of diagonal check dams across the cut-line at regular intervals on all slopes. They also spread fertilizer and grass seed during the spring of 1973. The grass seed and fertilizer were spread while there was still some 15 cm of snow on the ground. A commercial grass-seed mixture was used, all the species being exotic to this area. Over much of the area the growth of these grasses has been most impressive, reaching heights of as much as 1.5 m in some places and over 1 m in many sections. Along the west side of the right-of-way, however, the growth is only fair to poor in many sections. This material appears to consist largely of humus, peat and wood debris, which seem to form a poor, acid seedbed. Westcoast Transmission propose to fertilize and seed the cut-line again next spring in an effort to promote grass growth in these spoil areas. No growth of endemic species was noticed, and revegetation by such species presumably will be retarded by the heavy cover of grass. The diagonal check dams were designed to prevent slope wash becoming severe. In most cases they were working quite satisfactorily. The exceptions were (i) in cases where the downslope end of the dam did not reach the edge of the cleared land, when a ditch developed, and (ii) where subsidence of the backfill breached the dam, when water was channelled into the trough over the ditch. In the latter case, normal maintenance work should repair things satisfactorily.

Along some sections of the right-of-way, vehicle track marks could be seen clearly. They were formed presumably during the repair work of spring 1973. They are generally not severe, and in only a couple of cases were they guiding any erosion.

During construction of the pipeline two short trails were cut off the right-of-way to allow vehicles to climb the steep bluffs of the Kotaneelee and La Biche rivers. No attempt was made to rehabilitate these trails after their usefulness had ended. Now fairly severe erosion, gullying and slope collapse is occurring along and beside these trails. Such trails could be rehabilitated and/or maintained along with the pipeline right-of-way in all future pipeline construction operations in the north. These particular trails could still be repaired, though not very easily.

Within the last year a number of new access trails and seismic lines have been cut in this area; several of these have crossed the pipeline. In all cases the pipeline has been crossed by means of a "bridge" made of earth and logs. In a couple of cases these "bridges" have caused water to pond on the upslope side, over the pipeline.

References

Owen, E. B.
1971: Soils along Westcoast Transmission Company's proposed pipeline, Pointed Mountain, N.W.T., to Beaver River, B.C., Canada; Geol. Surv. Can., unpubl. rept., 5 p.

Rowland, L.
1972: Pointed Mountain line completed in record time; Oilweek, v. 23, no. 5, p. 28-34 (20 March, 1972).

Rutter, N.W.
1974: Surficial geology and land classification, Mackenzie Valley transportation corridor; in Report of Activities, Part A, April to October, 1973, Geol. Surv. Can., Paper 74-1, Pt. A, p. 285.

Research Agreement 1135-D13-4-199/72

B.D. Kay*
Terrain Sciences Division

During the course of developing the necessary theory to permit measurement of unfrozen water and ice content of frozen soils using a cylindrical heat source, it has been necessary to predict the specific heats of the various components of frozen soil. The specific heats have been required at various subzero temperatures.

Kersten (1949) has indicated the specific heats of various soils change with temperature; however, the data which he reported shows considerable variability. Consequently the specific heats of a number of soil components have been measured over the temperature range of -70°C to +30°C using a differential scanning calorimeter.

The extent to which the specific heats of some representative components of frozen soil vary with temperature is illustrated in Figure 1. The data for ice is taken from Giauque and Stout (1936). In all cases the specific heats of the components vary substantially with temperature. These data suggest that the specific heats of soil materials which have been determined at room temperature will be 30% to 45% greater than the specific heats of the same materials at, say, -30°C.

Subsequent calculations have shown that the functional dependence of specific heat on temperature becomes important in frozen soil when there is negligible unfrozen water present. In such a case a linear temperature function can be used to predict the required specific heats.

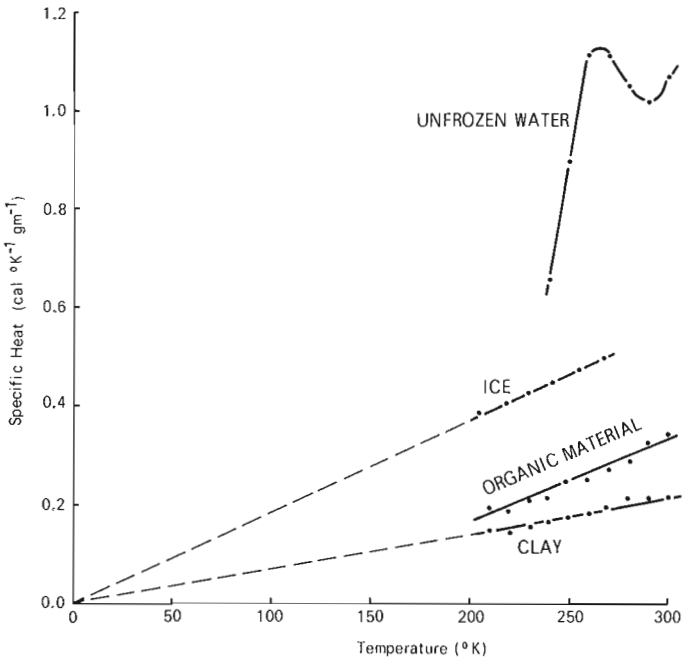

Figure 1. The specific heats of components of frozen soil.

References

Giauque, W.F., and Stout, J.W.
1936: The entropy of water and the third law of thermodynamics. The heat capacity of ice from 15 to 273°K; J. Am. Chem. Soc., v. 58, p. 1144-1150.

Kersten, M.S.
1949: Thermal properties of soils; Univ. Minn. Bull. No. 38.

*Department of Land Resource Science, University of Guelph, Guelph, Ontario.

A STUDY OF SHORELINE EROSION IN WESTERN LAKE ONTARIO

Research Agreement 1135-D13-4-85/73

E.L. Matyas, O.L. White, and B. LeLievre*
Terrain Sciences Division

This study commenced in May, 1972 under a Research Agreement with the Department of Energy, Mines and Resources through the Terrain Sciences Division and with the co-operation and assistance of the Canada Centre for Inland Waters, Department of the Environment, Burlington, Ontario.

The area studied extended from Etobicoke Creek on the western edge of Metropolitan Toronto to the Niagara River for a total distance of 108 kms.

The objectives of the study were (1) to measure the extent of the erosion, (2) to determine the mechanics of shoreline processes related to erosion and to identify the principal factors involved, and (3) to determine whether a relationship existed between the magnitude of the erosion and the geotechnical properties of the soil deposits along the shoreline.

Geology

Most of the north shore of the study area has been mapped by Karrow (1963) and exists largely as low bluffs (up to 7 m high) consisting of shale, till, and a variety of lacustrine deposits. The bedrock consists of grey interbedded shale, siltstone, and limestone of the Georgian Bay Formation or the red shales of the Queenston Formation but is not exposed everywhere along the shoreline. Approximately 40 per cent of this shoreline is protected by seawalls and/or rip rap.

The south shore is much less protected than the north shore and is formed up to 13 m high. Queenston shale forms part of the bluff in the vicinity of Grimsby and outcrops sporadically near Vineland, but in general, the bluffs consist of massive silt and other lacustrine deposits underlain by a grey silt till. For most of the south shore the grey silt till is underlain by an older reddish sandy till. This sandy till was encountered in most boreholes and is exposed intermittently in the bluffs for several miles east of Port Weller.

The south shore geology presently is being mapped and part has already been published (Feenstra, 1972).

Geotechnical Properties

Soil samples were obtained from exposed bluffs, beaches, and boreholes at selected sites. The natural water contents, grain size distribution, Atterberg limits, specific gravity, bulk density, and shear strength were determined for most of the samples. On the basis of the test results and field observations, soil profiles were determined at 17 sites along the shoreline. These were used to construct a longitudinal section for the entire length of the subject shoreline.

*Department of Civil Engineering, University of Waterloo.

Measurements of Erosion

The amount of bluff recession was measured at 98 sites along the shoreline using aerial photographs taken in 1931 and 1969. In addition, the amount of bluff recession for the periods 1931-54, 1954-60, 1960-65, and 1965-69, similarly was measured for several selected sites where other detailed studies were being conducted.

Measurements were made by scaling distances from inland reference points to the edge of the shore bluff. It was recognized that this method of measurement had inherent human and systematic errors; nevertheless, the accuracy of the recession measurements was considered adequate for the purposes of the study.

Erosion rates of up to 3 m per year over the 38-year period covered by the photography were measured. Erosion rates along the south shore were higher than along the north shore. The erosion rates measured from the aerial photographs were in general agreement with rates determined at particular sites by other means and other investigators.

Measurements at ground stations during 1972-73 gave indications of the amount of erosion that could result from a single storm or from several closely spaced storms. Bluff recessions of up to 4.7 m were recorded at particular locations in the late winter/early spring of 1973 and were attributed largely to two severe storms within a four week period.

Hydrodynamic Factors

An analysis was made to determine a relationship between erosion and hydrodynamic factors. Wind data for the period 1955 to 1956 were used in conjunction with wave forecasting techniques to hindcast the deep water wave regime for the study area. A computer program was used to plot wave refraction diagrams and to calculate relative magnitudes and components of wave energy in the nearshore zone.

Wave energy which is dissipated along the shoreline is related primarily to wave height and period. Other factors such as lake levels and offshore topography, however, also have a significant effect on wave energy. Wave direction appears to have a minor effect on wave energy.

Stepwise multiple regression analyses were used to analyze the effect on erosion of 29 variables and the analyses indicated that only 5 of these variables were significant. Of the factors considered, the most significant variable was the number of months that the water level was greater than elevation 246 feet (75 m). On this basis, simple regression analyses were used to analyze the effect of various water levels on the

magnitude of erosion from one time period to another at specific sites. Differences in erosion at a given site during different time periods can be accounted for by fluctuations in water levels.

A qualitative relationship was evident between the magnitude of erosion and the energy per unit time in a breaking wave. Lack of agreement in the erosion-energy relationship can be accounted for by other factors such as bluff height, soil type, presence of bedrock, beaches, protective works, etc. Studies are continuing in an attempt to quantify the apparent energy-erosion relationships and to evaluate the efficiency of methods of shoreline protection.

References

Feenstra, B.H.
1972: Quaternary geology of the Niagara area, southern Ontario; Ont. Div. Mines, Prelim. Map P764, Geol. Ser., scale 1:50,000.

Karrow, P.F.
1963: Pleistocene geology of the Hamilton-Galt area; Ont. Dept. Mines, Geol. Rept. No. 16, Queen's Printer, Toronto.

81. EFFECTS OF THE BURRARD INLET OIL SPILL ON VARIOUS GEOLOGIC INTERTIDAL ENVIRONMENTS

Project 730023

K.E. Ricker
Terrain Sciences Division, Vancouver

Introduction

On September 25, 1973 two freighters collided at 0300 hours (PDT) in the Vancouver outer harbour area of Burrard Inlet. About 240 metric tons of "Redwood No. 975" light bunker oil escaped into the harbour, though nearly one half of this release was effectively confined to the immediate vicinity of the vessels while the remainder quickly fanned into a large tear-shaped configuration 15 to 20 square km in area. A few hours later, despite light sea conditions, the slick parted into smaller masses. While clean-up equipment moved to the site, tidal currents had transported the slicks onto 30 kilometres of varied and rugged coastline comprising the north shore of the inlet (West Vancouver).

The writer began making shoreline observations on an 'opportunity basis' on September 26, after the oil slick already had parted into about 12 smaller discrete masses (30 to 400 m in width by 100 to 1,200 m in length) each fouling some of the north coastline. Clean-up operations were already in progress at some sites upon the writer's arrival. Observations were continued on the following day after overnight re-invasion of oil at some locales that had been treated already. Between three and four days after the spill, a few areas of Stanley Park and the south shore line of the Kitsilano district of Vancouver were invaded to a lesser degree and some iridescent films also were traced into the inner harbour located east of First Narrows (Lions Gate Bridge). At the conclusion of the winter storm cycle all localities that had been previously examined were revisited to assess the degree of disappearance of oil.

Observations

Observations were limited to selected geologic environments on the shoreline of West Vancouver though several of the severely oil-coated islands were bypassed. The field methods involved visual observations supported by photography; digging was limited and because of prior bulldozer operations, the procedure of measuring beach profiles before and after clean-up could not be carried out to yield any meaningful results. Table 1 gives the geologic setting, clean-up status, and observations of each site inspected.

Movements of the individual oil slicks onto a given stretch of coastline were unpredictable because of their tendency to hover off headlands before the final drift on shore. Flood tides during darkness helped to create this uncertainty. At the shore the oil appeared in two forms initially: 1) as a light volatile product which left iridescent films on all types of surfaces, and 2) as a heavy, glistening, and black target-like mass which preferentially adhered to cobbles, angular blocks, logs, and vertical outcrop. Heavy oil bands on the latter were pronounced at the high tide mark and oil dribbled below this level only where heated by the direct radiation of the sun. The light volatile product soaked into porous sands at a few locales but beyond a few centimetres depth there was no odoriferous or visual presence and on succeeding days after intervening surf action, not even their surficial presence could be detected. With the heavy fraction there was no observable penetration of the sands, but on some intertidal sandy areas the globules were covered by subsequent sand deposition which lasted through the

Area	Line Distance west of 1st Narrows (Lions Gate) Bridge	Geologic setting	Status of clean-up before observation	Observation September 1973	Observation Spring 1974
Ambleside Park	1-1.5 km	Beach with a steep upper slope of sand and a lower gradient intertidal zone of sandy gravel and cobbles.	Upper zone had been raked and graded; residual oil left on intertidal zone only; fires of oil-covered driftwood.	Heavy oil globules on pebble and cobble surfaces absorbed by peat moss.	Beach virtually restored except for 'pelletized' oily sand under few cm of intertidal sand; fresh oil on scattered clasts; and a few oil-soaked Tertiary conglomerate fragments.
Dundarave Pier	3.6 km	Beach as above; and of gentle dip slope of Tertiary sandstone.	Upper beach sand had been scraped and contaminants buried; slick lickers operating offshore; removal of driftwood.	Most oil adhered to driftwood. Cobbles oil coated. No oil absorption on sandstone outcrop except in joints, topographic lows.	Some discoloration of rock clasts; only one intertidal cobble with 'fresh' heavy oil. Burial pit not breached by winter storms.
Proctor Park to 31st Ave.	4.6-5.2 km	Cobble pavement low-gradient beach; some sandy re-entrants; granitic outcrop with associated angular blocky "talus".	Partial peat moss treatment; some shoreline fires of oil-covered driftwood.	Cobble pavement oil coated in preference to other surfaces. Oil cover concentrated near high tide level; 15-30 cm oil band on granitic outcrop resisted blow-torch vaporization. One to two cm oil globules on pebbly surface of swash zone.	Thoroughly restored and oil removed except on cobble undersides and on cobble tops in areas of minor sand.
Sandy Cove	7.2 km	Sandy beach abutting against granitic outcrop.	Local oil boom contaminant only.	Vertical granitic outcrop preferentially attracted oil as black trim line.	Oil showings barely discernible.
Caulfeild Cove	8.5 km	Constricted embayment; gravelly low gradient beach strewn with molluscan shells, and driftwood; enclosed entirely by rounded to precipitous granitic outcrop.	Worst affected area; in varying stages of peat moss treatment; driftwood fires; oil boom at entrance and slick licker in operation.	Extensive oil contamination and inundation of all coastal surfaces. Oil scum several cms thick on gravelly sand beach with negligible penetration.	Cove protected from winter storm wave action. Clean-up effective - only thin, grey, discontinuous oil residue seen on outcrops.
Whyte Cove	13.2 km	Sandy beach of moderate gradient with intertidal gravelly bands; cobbles and blocks on tombolo connecting to Whyte Island.	Local but incomplete raking.	30 to 40-cm-wide bands of oil globules left on gravel beach during falling tide. Oil removed by peat moss during subsequent flood tide.	
Whytecliffe Point (West side)	13.5 km	Precipitous granitic outcrop with vertical joints, minor re-entrants and irregular surface microtopography; extensive Mytilus clam fauna.	No treatment.	Heavy tarry oil plastered onto vertical granite outcrop as thick bands to 60 cm wide. Lighter fractions cover extensive beds of Mytilus clams. Frequent wave splash from heavy ship traffic at site.	Oil band transformed into dull black, thin, 'case-hardened' scum. Rock knobs polished clean. Joints, cavities, etc., contain altered residue. Fresh, unaltered oil band remains in shady protected rock.

winter storm cycle at one locale at least. The grain size of a rock surface does not correlate with the presence or absence of the heavy fraction though adjacent joints could be coated while other surfaces would be free of any residue. After meticulous clean-up involving peat moss, water jets and wire brushing of rocky surfaces, and the passing of a winter storm cycle, much of the effects of the oil spill now only are slightly visible. In the spring of 1974, however, untreated sheltered vertical cliffs (shaded from the sun) and non-treated cobble pavements (exposed to the sun) revealed unaltered tarry surfaces. In addition, treated and wave-exposed rocks still exhibit, on close inspection, a mosaic of discontinuous, thin, hardened, dull-black residue which resists removal by scratching with a knife. Several seasonal storm cycles obviously will be required to remove the last vestiges of the spill. Thus, a series of long-term periodic checks should be carried out to determine the length of time of removal.

Conclusions

1. Were it not for the continuous presence of beach driftwood the expense and magnitude of cleaning up the Burrard Inlet oil spill would have been far greater. With the exception of rounded cobble surfaces, logs are the preferred adsorptive substrate of this particular type of fuel oil.

2. Because of complexities of currents and weather, the prediction of the exact zone of invasion of an oil slick is difficult and the problem becomes infinitely more complex as the slick breaks up into smaller discrete bodies. Prevention of oil encroachment onto shore by the use of barriers or artificially produced wind or water currents is difficult and such measures probably will be impossible to use during storm conditions and at times of restricted visibility.

3. The preferred geologic environment of oil adsorption is the rounded boulders and cobble pavements of the upper intertidal zones. However, vertical

outcrops will retain a narrow band of continuous residue because of the repeated pressing action of oil-ridden waves at the high tide level. Sloping outcrop on the other hand, is not conducive to retention of oil products, possibly because of the non-uniform sweeping action of waves on rising surfaces. A high-energy, sandy beach environment will collect heavy oil only if the quantity is sufficient and no other media are present to selectively adsorb it. Grain size of a particular rock surface does not appear to affect selective adherence, though joints, fractures and other depressions, affording preferential protection from erosive processes, are favoured centres of accumulation. Exoskeletal and epidermal tissue of many benthonic organisms attached to bedrock did not retain heavy oil globules because of the almost frictionless nature of their surfaces; oil preferentially could collect on adjacent barren rock.

4. Regardless of the substrate of deposition, peat moss liberally applied before and immediately after oil invasion is a very effective method of removal. Water jetting of rock surfaces in the presence of peat moss is more thorough, but this method causes biological damage. Because of its high ignition point, this type of oil cannot be volatilized satisfactorily using hand-held blow torches though enough heat apparently is generated in big fires of oil-soaked driftwood.

5. A solely geologic agent of oil removal requires a repeated, vigorous, and abrasive process, and in protected areas where this action cannot be possible, years of exposure will be required before the tars or altered residues are removed totally.

6. In spite of the advance of technology, immediate clean-up of a large oil spill will be a formidable if not an impossible task on a rocky coastline. With surficial and moveable materials, restoration can be accomplished by their removal but such methods cannot be employed in a practical manner with heavier boulders and rugged outcrop.

ANALYSIS OF CHARACTERISTICS RELATING TO GROUND SURFACE STABILITY IN A COLD REGION

Research Grant 1135-D-13-4-180/73

M. W. Smith and P. J. Williams*
Terrain Sciences Division

Work was begun in 1973 on two objectives:

(1) To develop an understanding of strength and deformation properties in the temperature range of intensive phase change; and
(2) To determine the types of data required to design operational codes for activity in cold regions.

Variations in ground thermal regime give rise to a sequence of changes in soil properties (Fig. 1). Stability thus is viewed as a function of microclimate and lithology.

Work is proceeding towards the prediction of thermal and hydrologic regimes, using computer models:

(1) Substantial progress has been made in modelling the ground thermal regime, incorporating phase change relations.
(2) Work has been initiated on the hydro-climatological aspects of ground stability. A computer model has been conceived which will synthesize the soil hydrologic regime and produce stability predictions. In this way it is hoped to correlate stability in situ with the frequency and magnitude of climatic events.

Other work is proceeding to provide input data required by such models. This includes:

(1) A technique developed for the determination of apparent heat capacity as a function of temperature, using the suction-moisture test. Further, an experimental examination has been carried out on the effect of using disturbed or undisturbed samples for suction-moisture determinations.
(2) An experiment designed to successfully measure the hydraulic conductivity of freezing/thawing soil, as a function of temperature.

The systematic examination of dominant variables will continue.

FIGURE 1

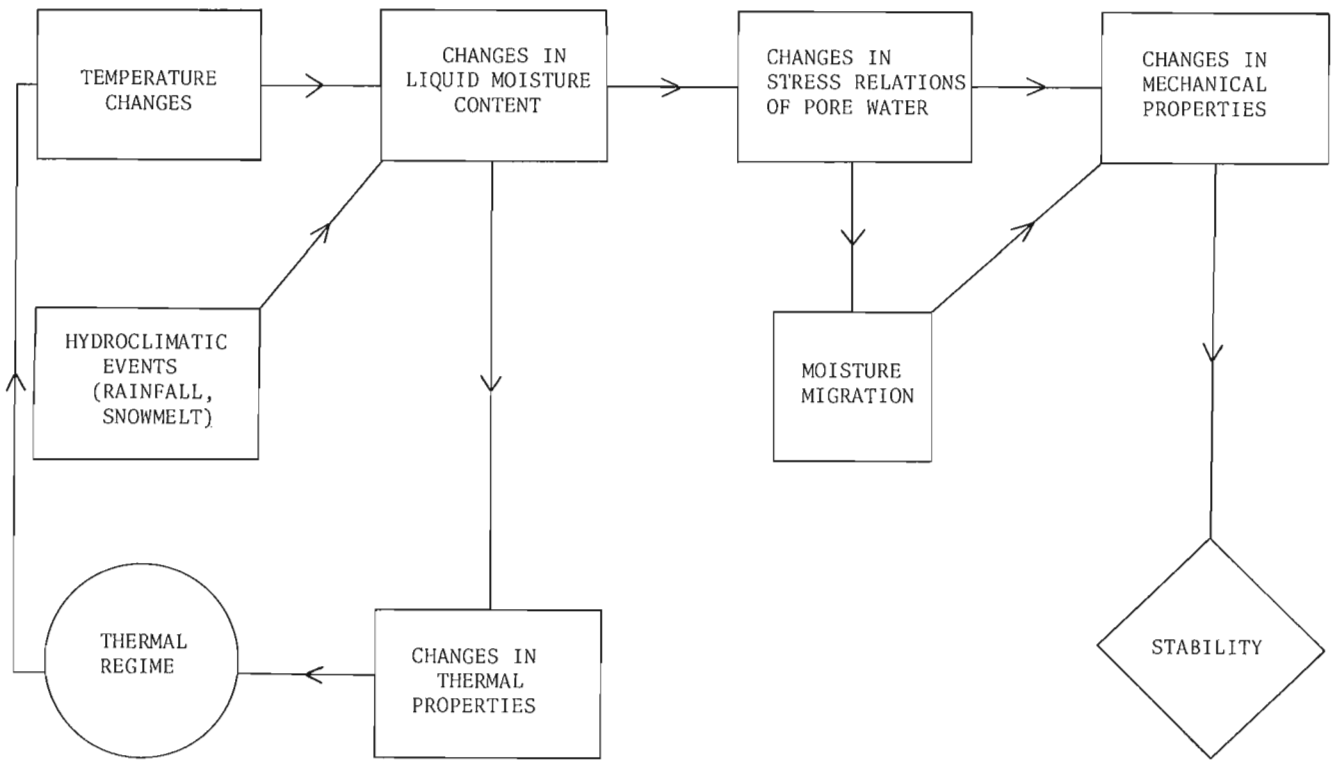

*Geography Department, Carleton University, Ottawa.

83. TERRAIN MAPPING AND QUATERNARY GEOLOGY, SOUTHERN VANCOUVER ISLAND, BRITISH COLUMBIA

Project 720004

N. F. Alley
Terrain Sciences Division, Kelowna, B. C.

Terrain inventory and Quaternary geological investigations were carried out on southern Vancouver Island during the summer of 1973. Areas mapped at 1:50,000 scale include 92C/8, 92C/9 and 92C/15 (east half) map-sheets (Fig. 1). Map-area 92C/10 (east half) was inaccessible and was mapped entirely be aerial photograph interpretation. An attempt was made to check this area by helicopter survey, but forest cover was too dense to allow adequate coverage.

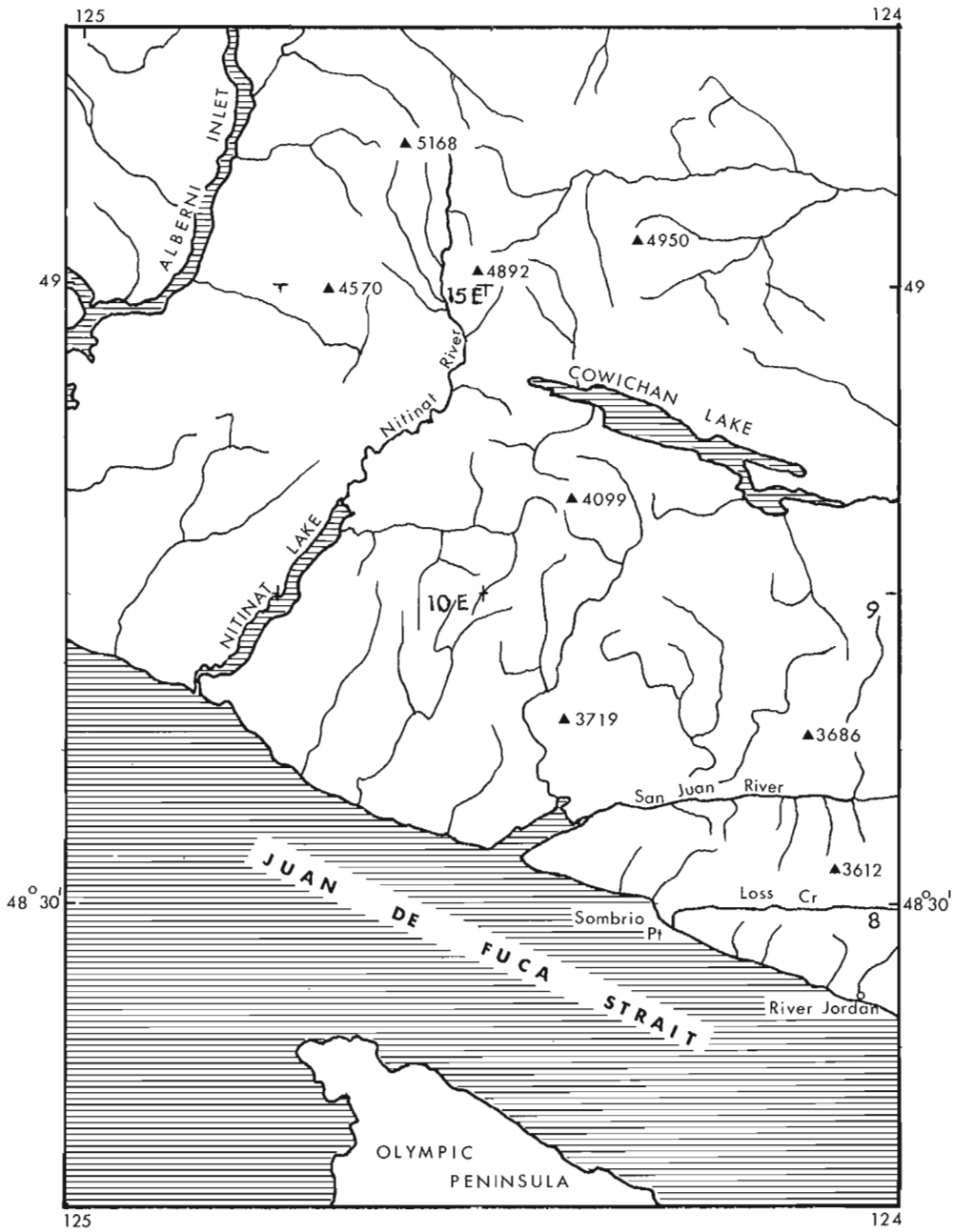

Figure 1. Study area.

Terrain

The area consists of two broad physiographic units. North of the San Juan River the relief is rugged with isolated peaks exceeding 4,000 feet in elevation, whereas south of the river a broad plateau slopes gently southwards to the Juan de Fuca Strait. The pattern of valleys in both areas is closely related to the pattern of major joints and faults in the country rock. Nitinat, San Juan, and Loss Creek valleys are three major valleys which have resulted from erosion along such lineaments.

Quaternary Deposits

Although the entire area was overridden by ice at some stage (or stages) during the Pleistocene, morainal deposits are not ubiquitous. Large areas, particularly of higher relief, are heavily colluviated and only scattered erratics or a very thin veneer of till remains. Thick till is best preserved on the lower parts of valleys, and along the coastal slope east of Sombrio Point. Tills in the uplands and along the Juan de Fuca Strait contain a highly variable pebble lithology. Tills of homogeneous pebble lithologies, however, are more characteristic of glacial valleys extending down from shallow cirques located in areas of higher relief. In the far northern and central parts of the

map-area, lateral and terminal moraines occur a few miles down valley from the cirques.

Ice-contact deposits are not common and, apart from isolated outcrops along the major valley bottoms, almost entirely are confined to the coast east of Sombrio Point along the Juan de Fuca Strait. In the latter area a prominent kame terrace, reaching a maximum thickness of 200 feet, forms a prominent coastal bench stretching from Sombrio Point to just a few miles east of River Jordan township. Unlike the tills on the coastal slope immediately above the terrace, it contains a high proportion of basic and ultrabasic rocks.

Lacustrine and fluviolacustrine deposits occur sporadically in the major valleys attesting to the presence of glacial lakes during deglaciation. Although silts and clays occur in the Nitinat and San Juan River valleys, the greatest thickness of sediments is found in the smaller Loss Creek Valley. Here, glaciolacustrine silts interbedded with large lenses of colluvium extend from approximately 500 feet a. s. l. near the coast to just over 1,800 feet a. s. l. in the headwaters of the creek. A series of dissected deltas below 500 feet a. s. l. stands at the mouth of the valley in the vicinity of the coast. The great thickness of glaciolacustrine silts and the deltas located farther downstream probably are related to a series of levels of an ice-dammed lake formed by gradual thinning of ice standing in the Juan de Fuca Strait.

Erosional Features

Indicators of the direction of regional and local ice movements are common. These consist predominantly of glacial striae and ice-moulded features such as roche moutonneés. Drumlins and grooves are less common although small fields occur in the northeast of the map-area and on the plateau surface between Loss Creek and Juan de Fuca Strait.

At the height of glaciation the movement of ice was in a south-southwest direction across the island. The ice was probably part of the Cordilleran Ice Sheet which formed on the mainland. A second less intense movement of ice is suggested by the pattern of striae and ice-moulded features in the valleys of the higher parts of the area, and along the Juan de Fuca Strait. Not only do the features indicate local ice-flow patterns at high angles to the regional trend, but also in the opposite direction to it in some valleys.

Because the relief amplitude of the map-area is low compared with the central part of the island, large valley glaciers did not develop during the Pleistocene. Shallow cirques and glacial U-shaped valleys, however, occur in areas where ridge tops exceed 3,000 feet a. s. l., but are best developed in the northwestern part of the map-area where ridge tops commonly exceed 4,000 feet.

Glaciated bedrock shoulders occur around the uppermost portions of the highest peaks in the map-area, especially those in the headwaters of the Nitinat River. The lower limit of the shoulders is approximately 4,000 feet a. s. l. Associated with the shoulders is a thin scattering of highly weathered granitic erratics.

Glacial Chronology

The till of the map-area is stratigraphically contiguous with tills in the Alberni Inlet, Cowichan Valley and Victoria area. Other studies have shown that these tills were deposited during the Vashon stage of the Fraser Glaciation (Fyles, 1963; Halstead, 1966) and thus the major advance of ice, which overrode the southern part of the island, is regarded as Vashon (Classical Wisconsin) in age. This advance accounts for the dominant southerly trend of glacially-moulded features in the uplands. At its maximum the ice extended beyond Juan de Fuca Strait into the Pacific Ocean.

During the early stages of deglaciation, ridges and peaks emerged from the ice sheet and separated it into discrete valley glaciers. Stagnation of the remaining ice, however, was interrupted by a minor re-advance of the valley glaciers. This re-advance accounts for the:

1. Pattern of glacial striae along the coast of Juan de Fuca Strait and in the valley bottoms of the major uplands.
2. Occurrence of shallow cirques and glacial U-shaped valleys in uplands which were completely overridden by Vashon ice.
3. Homogeneity of tills in the bottom of the glacial valleys in contrast to a greater variety of pebble lithology of till on the intervening uplands.
4. Position of valley moraines in the northern part of the map-area.
5. Presence of a prominent kame terrace along part of the coast. The abundant basic and ultrabasic rocks contained by the terrace probably were derived from the Sooke area where the rocks outcrop (Cooke, 1919). This would indicate a local movement of ice northwest by west along the strait, a conclusion agreeing with the pattern of striae along the coast.

By virtue of its mass, ice remained longer in Juan de Fuca Strait. It dammed waters flowing out of the Nitinat, San Juan, and Loss Creek valleys, forming glacial lakes. The various stages in the stagnation of the Juan de Fuca Strait lobe of ice probably account for differing levels of deltas in these valleys and the prominent kame terrace along the Strait itself (see above). This interpretation agrees with that proposed to account for a similar distribution of ice-contact and glaciolacustrine deposits along the Juan de Fuca coast to Olympic Peninsula, United States (P. Snavely, U. S. Geol. Surv., pers. comm., 1973).

Although there is no stratigraphic evidence of a glacial advance prior to the Vashon stage, the presence of weathered erratics on glaciated bedrock shoulders in the highest parts of the area suggests that a glacial advance of even greater magnitude preceded the last glaciation. It is not known, however, to which of the earlier glaciations these features are related.

References

Cooke, H. C.
1919: Gabbros of East Sooke and Rocky Point, British Columbia; Geol. Surv. Can., Mus. Bull. 30.

Fyles, J. G.
1963: Surficial geology of the Horne Lake and Parksville map-areas, Vancouver Island, British Columbia; Geol. Surv. Can., Mem. 318.

Halstead, E. C.
1966: Surficial geology of Duncan and Shawnigan map-areas, British Columbia; Geol. Surv. Can., Paper 65-24.

STUDIES ON QUATERNARY SITES AT WELLSCH VALLEY AND LANCER, SASKATCHEWAN, AND HEATHER COULEE, NEAR IRVINE, ALBERTA

Project 650027

C.S. Churcher*
Terrain Sciences Division

The Wellsch Valley Site, near Swift Current, Saskatchewan, is located in the southeast quarter of Section 4, Township 20, Range 14, West of the 3rd Meridian (Fig. 1). It has yielded an extensive vertebrate fauna (Stalker, 1967, 1971, 1972), for which each taxon of larger mammals has been represented by adequate material for identification to genus and often to species (Table 1). The collection of remains of small animals, however, proved inadequate for their identification to species, leaving a hiatus in the possible information. The possibility of obtaining further material was made even more intriguing because the microtine rodent remains found earlier, and tentatively assigned to ?*Pliophenacomys meadensis* in Stalker (1972), had been examined further by Dr. J.E. Guilday and the late Dr. C.W. Hibbard, who suggested that there were three microtine species present, *Pliomys* sp., *Synaptomys* sp., and a *Microtus* near *M. deceitensis*. Since *Pliomys* (*P. deeringensis*) and *M. deceitensis* are known previously only from the Lower Pleistocene (Gunz I?, pre-Late Kansan) deposits at Cape Deceit, Alaska (Guthrie and Matthews, 1972), these tentative identifications suggest an early Pleistocene age for the Wellsch Valley local fauna. *Pliomys*, the Pliocene meadow vole, is an Eurasian genus, with a temporal distribution into the Lower Pleistocene, and is confirmed as present in North America at only Cape Deceit. *M. deceitensis* is a very primitive species of a modern genus of voles and the Wellsch Valley form is apparently more primitive than *M. deceitensis*. Thus, the specific identification of these two forms bears directly on the age assigned to the Wellsch Valley's fossiliferous lag gravel deposit and its associated tills (Stalker and Churcher, 1972).

In addition, three taxa required further investigation based on new materials: the lagomorph provisionally identified as ?*Hypolagus limnetus* (Gazin's marsh rabbit), the pocket gopher identified only as Geomyidae, ?*Geomys* or *Thomomys*, and the ground squirrel provisionally assigned to *Citellus ?meadensis* (Meade ground squirrel).

A further visit therefore was paid to the Wellsch Valley site in 1973 to collect matrix materials from those levels that previously had produced bones and teeth of rodents, lagomorphs, and other small mammals. It was hoped that these samples would yield the elements of small mammals that would allow more detailed identifications of those forms reported previously.

Samples of matrix were taken from three separate levels at the Jaw Face in the Wellsch Valley site: from the coarser, plum-pudding gravel lenses about 6 feet (2 metres) above the base of the cut made in 1969, from coarse, sandy layers about 15 feet (4.5 metres) above the base, and from just above and below the ash band that lies about 25 feet (8 metres) above the base (Stalker and Churcher, 1972). These samples were water washed in wooden boxes with fine, screened bases to remove the silt, and the concentrated matrix with its contained specimens was sent to Toronto for sorting during the winter of 1973-74. Sorting has not been completed at the time of writing, although bones and teeth have been recovered from the concentrate.

Dr. Stalker and the writer visited a sand and gravel pit in the southeast quarter of Section 23, Township 21, Range 21, West of the 3rd Meridian, northeast of Lancer, Saskatchewan (Fig. 1). Fossil mammals are present in the lower half of the sands and in the basal gravels, and remains of mammoth (*Mammuthus* sp.), horse (*Equus* cf. *conversidens*), and camel were obtained. This site was first reported to Dr. Stalker by Dr. Peter David of the Université de Montréal. Other specimens are deposited in the Saskatchewan Provincial Museum of Natural History, Regina. From the fossil evidence, the age of the sands and gravels appears to be Rancholabrean, or Upper Pleistocene.

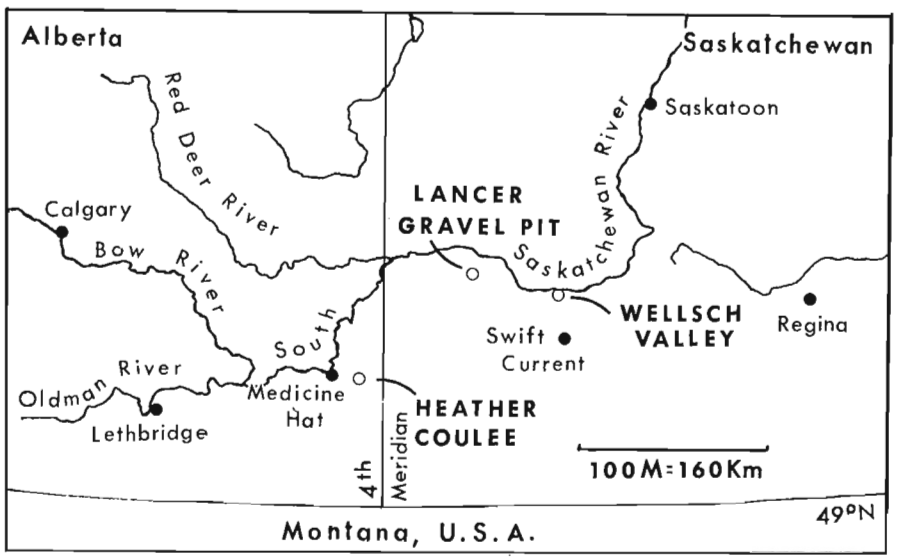

Figure 1. Locations of the Wellsch Valley, Lancer Gravel Pit, and Heather Coulee fossiliferous sites (open circles).

*Department of Zoology, University of Toronto, Ontario.

Table 1. Faunal elements identified from the Wellsch Valley and Heather Coulee sites

TAXON	Wellsch Valley Fauna (Revised from Stalker, 1972)	Heather Coulee Fauna
Xenarthra		
?*Megalonyx* sp. - ground sloth	X	
Lagomorpha		
?*Hypolagus limnetus* - Gazin's marsh rabbit	X	
Rodentia		
Citellus ?meadensis - Meade ground squirrel	X	
Geomydae *indet.* - unidentified pocket gopher	X	
Pliomys sp. - unidentified extinct meadow vole	X	
Synaptomys sp. - unidentified bog lemming	X	
Microtus sp. cf. *M. deceitensis* - extinct, ?Cape Deceit, meadow vole		
Carnivora		
Borophagus diversidens - Cope's bone-eating dog	X	
?Canidae *indet.* - unidentified carnivore		X
Lynx sp. cf. *Lynx rufus* - bobcat	X	
?Felidae *indet.* - unidentified large carnivore		X
Proboscidea		
Mammuthus sp. cf. *M. haroldcooki* - Cook's mammoth	X	
Proboscidea *indet.* - unidentified proboscidean		X
Perissodactyla		
Equus pacificus - extinct Pacific horse	X	
Equus complicatus - extinct eastern horse	X	
Equus sp. - unidentified large horse		X
Artiodactyla		
Platygonus bicalcaratus - Cope's peccary	X	
Camelops sp. - unidentified camel	X	X
Camelidae *indet.* - unidentified ?llama		X
Antilocapridae *indet.* - unidentified prongbuck	X	
Bovidae *indet.* - unidentified bovid	X	

A new site in the hills north of Irvine, Alberta, here named the Heather Coulee site, was reported to the author by Mrs. Hope Johnson of Ralston, Alberta and by the discoverers, Mr. and Mrs. Donald L. Heather of Redcliff, Alberta, after whom the site is named (Fig. 1). It is located in the northwest half of Section 4, Township 12, Range 2, West of the 4th Meridian. This occurrence was impressive to a vertebrate paleontologist as whole and partial bones and fragments of bones were scattered in cascades over the surface of, and down minor gullies in, the Bearpaw shale. Overlying the Bearpaw there appears to be a lag gravel deposit, similar in many respects to that which occurs at Wellsch Valley. The vertebrate remains, presumably derived from this lag gravel, are well mineralized, well preserved, and apparently were undamaged or little worn or weathered at the time of their deposition. Field identifications of the specimens indicate that remains of Proboscidea, Carnivora (two forms, one large and probably felid and one coyote-sized and probably canid), Perissodactyla (*Equus* sp., large size), and Artiodactyla (two forms, a camel, ?*Camelops*, and possibly a llama) are present (Table 1). Because of the presence of *Equus*, the oldest possible age for this fauna would be latest Pliocene or early Pleistocene. Because of the similarities in preservation and mineralization of the bones, and in the stratigraphy, the Heather Coulee site tentatively is considered to correlate with the Wellsch Valley site.

This work was carried out by the author, accompanied by Dr. A. MacS. Stalker of the Department of Energy, Mines and Resources, Ottawa, and by Miss Brenda F. Beebe and Mrs. Rosemary Johnson, graduate students in vertebrate paleontology, University of

Toronto. Dr. T.S. Parsons of the University of Toronto and Dr. Stalker have kindly read and criticized the draft of this report. The project was funded mainly by the Geological Survey of Canada, and the vehicle used was provided by the Department of Vertebrate Palaeontology of the Royal Ontario Museum, Toronto.

The author is most grateful to his friends, the late Dr. C.W. Hibbard of the University of Michigan, Ann Arbor, and Dr. J.E. Guilday of the Carnegie Museum, Pittsburgh, for giving their opinions on the identities of the rodents from Wellsch Valley on inadequate materials.

References

Guthrie, R.D., and Matthews, J.V., Jr.
1972: The Cape Deceit fauna in Early Pleistocene mammalian assemblage from the Alaskan Arctic; Quat. Res., v. 1, no. 4, p. 474-510.

Stalker, A. MacS.
1967: Quaternary studies in the Southwestern Prairies; in Report of Activities, Part A, May to October, 1966, Geol. Surv. Can., Paper 67-1, p. 113-114.

1971: Quaternary studies in the Southwestern Prairies; in Report of Activities, Part A, April to October, 1970, Geol. Surv. Can., Paper 71-1, p. 180-181.

1972: Quaternary studies in the Southwestern Prairies; in Report of Activities, Part A, April to October, 1971, Geol. Surv. Can., Paper 72-1, p. 136.

Stalker, A. MacS., and Churcher, C.S.
1972: Glacial stratigraphy of southwestern Canadian Prairies, the Laurentide Records; Quat. Geol., 24th Int. Geol. Cong., Montreal, Sect. 12, p. 110-119.

85. PROSPECTING IN NEWFOUNDLAND AND THE THEORY OF MULTIPLE SHRINKING ICE CAPS

Project 720028

D. R. Grant
Terrain Sciences Division

An attempt is being made to reconstruct the pattern of ice movement, and the configuration of ice-marginal positions during the disappearance of glacial ice in Newfoundland. Apart from the purely scientific interest in deciphering ice retreat in a maritime climatic area, the knowledge may be used as a reconnaissance tool to infer the direction and extent of glacial dispersal of rock materials prior to actual field testing. These inferences have application primarily to the search for orebodies based on analysis of transported surficial debris (geochemical prospecting).

The deglaciation of this continental marginal island, and the notion of separate ice caps, has been debated in the scientific journals for 150 years. The purpose of this paper is not to trace the evolution of those ideas to their present expression, but merely to present the results of a recently completed examination of air photos throughout the island. In connection with an inventory of gravel and sand deposits (Grant, 1974), all deglacial features were noted. These include mainly glaciofluvial deposits (eskers, kames, outwash) and meltwater channels. On the principle that the meltwater system of an ice sheet follows the hydraulic gradient radially to the ice margin, the trend of eskers and slope of outwash trains can be used indirectly to infer ice margins by constructing othogonals (Fig. 1). As well, series of ice marginal sidehill meltwater channels reveal stages of recession of individual lobes. The coastal ice caps show evidence of sustained active flow during recession, while those in the interior receded mainly by backwasting. Very few end moraines appear to have been formed by any ice masses except the latest cirque glaciers.

The general pattern of recession was toward an ice divide arcing across the island from Port aux Basques to the Avalon Peninsula - as was earlier inferred from the general divergence of fluted till plains shown on the Glacial Map of Canada (Prest et al., 1968). Beyond the ice divide, separate ice caps became isolated on the Burin Peninsula (P), the Avalon Peninsula (L, M, N), the Burlington Peninsula (D), over Sheffield Lake basin (E), north of Grand Falls (F), near Gander (G), and high on the Long Range plateau of the Northern Peninsula (A, B, C). The last centre was probably that at K, that culminated as cirque glaciers along the Codroy Valley.

The present average elevation of the ground surface under the several ice caps varies from 100 to 600 m, and although partly a function of time, as the latest ice masses receded to higher windward sites, the variation of height partly suggests a general lack of topographic control. Persistence in various sites may be attributed to initial accumulation domes on the overall ice sheet, to local climate and sustained accumulation during recession, and partly to random separation. The Burin cap, in particular (like (A) near St. Anthony), merits attention because it appears to have been isolated from the interior domes by circumferential calving judging by the disjunctive marine overlap - Great Miquelon and northern Burin have prominent strandlines and terraces to 20 m whereas St. Pierre Island and southern Burin have unmodified eskers to present sea level. While the separate ice caps are depicted as a static condition, with only a suggestion of successive changes, it is essential to remember that they evolved from one all-embracing ice sheet, perhaps with three separate domes over Avalon Peninsula, Northern Peninsula, and the interior, by a process of shrinkage, separation, and migration. Successive ice-marginal positions can be inferred only after detailed mapping. Relative age or persistence is unknown, but it is thought that southern and western coastal caps were longer lived, because they evidently sustained active radial flow, whereas many others disappeared by disintegration.

The practical significance of this deglacial pattern lies in the fact that most of the prime prospecting areas are heavily drift covered, and have been affected by the changing ice-flow directions associated with shifting ice centres. 1) The Cambro-Ordovician carbonate belt along the west coast between Cape St. George and Strait of Belle Isle, with its zinc-lead potential, is obscured also by thick glaciofluvial and marine deposits and has been glaciated mainly by westward-flowing spatulate piedmont glaciers.
2) The Carboniferous terrane around St. George's Bay, with barite-celestite prospects, is complicated by two till/marine depositional episodes, whereas the related terrane extending southwest from White Bay was the site of late ice disintegration and is covered extensively with glaciofluvial deposits.
3) The Central Mineral Belt, extending southwest from Notre Dame Bay is characterized by base-metal copper-lead-zinc deposits, and has been influenced by divergent flow associated with at least four ice caps (D, E, F, H), the largest of which culminated in Grand Lake basin. 4) The copper/asbestos chromium area in the interior north of Hermitage Bay lies in an extensive area of disintegration moraine related to ice caps I and J, situated near Maelpeg Lakes and Meta Pond respectively. 5) The uranium-fluorine region of southern Burin Peninsula was the site of a persistent radially-flowing late ice mass, that became localized over a fluted till plain lineated by ice that earlier crossed the peninsula from north to south.

The validity of these reconstructions is being substantiated by observations of crossed striations, sequences of lithologically dissimilar tills, and

Figure 1. Approximate location of remnant ice caps during deglaciation of Newfoundland. (Dotted lines mark end moraines and other ice-marginal features; figures are average ground elevation in metres.)

analyses of drift transport. The importance of individual ice centres as agents of metallic mineral dispersal is known to vary considerably, and in a few cases fortunately has been shown to be minimal, but as long as thick tills and migrating ice centres are involved, prospecting will be affected by complications difficult to resolve.

References

Grant, D. R.
1974: Granular resources inventory, Newfoundland; Geol. Surv. Can., Open File 194, scale 1:500,000.

Prest, V. K., Grant, D. R., and Rampton, V. N.
1968: Glacial Map of Canada; Geol. Surv. Can., Map 1253A, scale 1:5,000,000.

86. DÉPÔTS ET FAITS QUATERNAIRES DU BAS SAINT-MAURICE, QUEBEC

Convention de Recherche 1135-d13-4-121/73

Serge Occhietti*
La Division de la science des terrains

Des relevés sur le territoire de Trois-Rivières et l'exploration des régions plus au nord ont permis de préciser la stratigraphie de la fin du Wisconsin. On observe successivement les dépôts de l'interstade de Saint-Pierre, le till de Gentilly, des dépôts glaciomarins et de réavancée glaciaire, des dépôts fluvioglaciaires et juxtaglaciaires, les limons stratifiés ou non de la transgression de la mer de Champlain, les sables et graviers d'émersion et deltaïques, les dépôts alluviaux. La cartographie des dépôts quaternaires a permis de dégager les grandes unités morpholithologiques régionales: les épandages fluvioglaciaires, les deltas perchés, les plaines deltaïques et d'émersion, les plaines argileuses, les terrasses fluviatiles et le complexe morainique de Saint-Narcisse. Cette dernière unité, de structure complexe, semble indiquer une réavancée glaciaire située dans l'écart des datations au C^{14} de 11300-10200 avant le présent. Le sens des stries glaciaires et des fabriques des tills a révélé un mouvement glaciaire vers le SE pour cette réavancée. La lithologie régionale comprend plusieurs types de tills: sans structure, feuilleté, en écailles, à lambeaux de substratum. Des dépôts glaciomarins et des argilotills fossilifères sont fréquents à la base de la moraine de Saint-Narcisse.

Bibliographie

Occhietti, S.

1972: Moraine de poussée Valders (Dryas III) à Saint-Narcisse, Québec. 22e Congrès international de Géographie, Montréal, La Géographie Internationale, T.1, p. 117-119.

1973: Éléments caractéristiques du complexe morainique de Saint-Narcisse, en Maurice et la région de Charlevoix, p. 15-16.

Stratigraphie fini-glaciaire au nord du complexe morainique de Saint-Narcisse, région de Shawinigan, Le Quaternaire du Québec, 2e Colloque, Montréal, résumés des communications, p. 21-22.

*Université du Québec à Trois-Rivières, 3351, boul. des Forges, Trois-Rivières, Québec.

87. SURFICIAL GEOLOGY MAPPING: OTTAWA-HULL AREA (PARTS OF 31 F, G)

Project 700049

S.H. Richard
Terrain Sciences Division

Surficial geology mapping of the Kemptville (31 G/4), the west-half of the Winchester (31 G/3), the east-half of the Carleton Place (31 F/1), the west-half of the Russell (31 G/6), the Ontario part of the west-half of the Thurso (31 G/11) and the southern parts of the east-half of the Quyon (31 F/9) and of the west-half of the Wakefield (31 G/12) map-areas has been completed; the surficial geology maps of the Ottawa (31 G/5) map-area (Gadd, 1963) and of the east-half of the Arnprior (31 F/8) map-area (Minning, 1972) have been updated. This information is being compiled as a single Quaternary geology and geomorphology map of the Ottawa-Hull region at the scale of 1:125,000. In advance of completion of this final map, open file release will be made of the individual map-sheets at a scale of 1:50,000.

In the Quyon, Wakefield, and Ottawa map-areas north of the Ottawa River, the overburden of Quaternary deposits over bedrock is thin and discontinuous in the Precambrian basement upland north of the Eardley fault-line escarpment. Glacial sediments occur only as small disconnected patches of siliceous sandy ground moraine and as small bodies of glaciofluvial deposits that were trapped on the floors of the main valleys by late-melting ice tongues. Postglacial marine sediments, especially marine clay, are widespread in the Ottawa and Gatineau river valleys and in some of the adjacent small rock basins where they have been found up to the elevation of about 198 m (650 ft.) a.s.l. This is at least 100 feet higher than in the area south of the Ottawa River, where the highest marine gravel beach lies at 167-168 m (550-560 ft.) a.s.l. (Prest, 1970).

Subaerial erosion had carved parts of the Ottawa Valley to within 50 to 100 feet of present sea level before postglacial marine transgression. Since the level of the depositional marine clay surface reached an elevation between 350 and 400 feet a.s.l. before emergence, the marine clay is as thick as 250 feet and even reaches 300 feet where the bedrock floor is lowest.

A large amount of this original marine clay has been removed from a narrow belt on either side of the

Table 1

Champlain Sea Radiocarbon dates relating to marine limit in the Ottawa region

Date No.	Date	Locality	Material	Collector	Reference
GSC-842	11,600 ± 150	Meach Lake, Gatineau Park, Quebec	Marine shells in beach gravels at 169 m (557 ft.) a.s.l.	J.T. Buckley	Lowdon and Blake, 1970, p. 59.
GSC-1013	11,800 ± 210	Maitland, Ontario	Marine shells in beach gravels at 103 m (340 ft.) a.s.l.	E.P. Henderson	Lowdon and Blake, 1970, p. 60.
GSC-1772	11,900 ± 160	Martindale, Gatineau County, Quebec	Marine shells in beach gravels at 176 m (578 ft.) a.s.l.	R. Romanelli	Lowdon and Blake, 1973, p. 17.
GSC-936	12,000 ± 230	L'Avenir, Quebec	Marine shells in beach gravels at 400 ft. a.s.l.	B.C. McDonald	Lowdon and Blake, 1970, p. 58.
GSC-1646	12,200 ± 160	Cantley, Gatineau County, Quebec	Marine shells in beach sands at 195 m (640 ft.) a.s.l.	R. Romanelli	Lowdon and Blake, 1973, p. 16-17.
GSC-1859	12,800 ± 220	Clayton, Lanark County, Ontario	Marine shells in beach gravels at 168 m (555 ft.) a.s.l.	S.H. Richard	Unpublished

Ottawa River. The limits of this eroded central belt are well marked in the present landscape by abandoned river bluffs cut in the marine clay. The oldest and highest ones occur at an elevation of about 325 feet and extend down to the present river level. North of the Ottawa River, the remains of the primary marine clay surface extend as a narrow belt at the foot of the Eardley escarpment from Quyon in the west to Angers in the east between the edge of the oldest and uppermost abandoned fluvial bluffs and the Precambrian basement upland. South of the Ottawa River, the primary marine clay surface extends south from the brow of the uppermost of the abandoned fluvial bluffs, forming a clay plain surrounding isolated bedrock uplands. In this area the small uplands that rise above the 325-foot a. s. l. elevation of the clay plain surface escaped marine clay sedimentation but, in addition to their usual patchy modified glacial drift mantle, they exhibit large numbers of fossiliferous marine gravel beaches marking positions of various former shorelines of the Champlain Sea between elevations of 500 to 300 feet a. s. l.

In addition to removing clay and cutting erosional terraces in the Champlain Sea deposits within the narrow central belt described above, the degrading Ottawa River exposed the underlying glacial drift or bedrock. Downstream from the areas of glacial drift or bedrock exposures, the surfaces of erosional clay terraces are usually mantled by a thin cover of alluvial sand derived from the exhumed drift.

Finally, in postglacial times, massive slope failures and mass movements have taken place in the marine clays. The largest of these, as for example the one at Quyon, occur along the uppermost abandoned fluvial bluffs producing aprons and fans of hummocky topography of tilted or slumped clay blocks on abandoned fluvial terraces of the ancestral Ottawa River.

Specimens of fossil marine shells (*Macoma balthica*), recovered from the highest beach found on the south side of the Ottawa River at an elevation of 167-168 m (550-560 ft.) a. s. l. and located 5. 6 km (3. 5 miles) north of Clayton, Ontario, and 9. 6 km (6. 0 miles) west of Almonte, Ontario, in Lanark County, have a radiocarbon age of 12,800±200 years BP (GSC-1859). This is the oldest radiocarbon date obtained so far for Champlain Sea material in the Ottawa area and appears to date the first arrival of marine waters at the western and highest limit of the Champlain Sea between the St. Lawrence and the Ottawa river valleys. This is the oldest date obtained so far for this submergence anywhere in the entire of the Champlain Sea Basin. Table 1 lists radiocarbon dates pertinent to marine limit in the Ottawa region.

References

Gadd, N. R.
1963: Surficial geology of Ottawa map-area, Ontario and Quebec; Geol. Surv. Can., Paper 62-16 and Map 16-1962, 3 p.

Lowdon, J. A., and Blake, W., Jr.
1970: Geological Survey of Canada Radiocarbon Dates IX; Geol. Surv. Can., Paper 70-2, Part B.

1973: Geological Survey of Canada Radiocarbon Dates XIII; Geol. Surv. Can., Paper 73-7.

Minning, G. V.
1972: Preliminary draft of a surficial geology map of the Arnprior map-area (31 F/8) Ontario-Quebec; Geol. Surv. Can., Open File 118, 1: 50,000.

Prest, V. K.
1970: Quaternary geology of Canada; in Geology and Economic Minerals of Canada, ed. R. J. W. Douglas, Geol. Surv. Can., Econ. Geol. Rept. no. 1, 5th ed., Fig. 16i, p. 718.

88. INVENTORY OF MARINE SURFICIAL GEOLOGY, SEDIMENTOLOGY, GEOMORPHOLOGY, QUATERNARY PALEONTOLOGY AND PALEOECOLOGY, GEOCHEMISTRY AND RELATED STUDIES OF THE PACIFIC WATERS OF CANADA

Project 730023

K. E. Ricker
Terrain Sciences Division, Vancouver

Preparations, now under way, for a long-term program of surficial sediment mapping with related studies of the sea bottom and coasts of the Pacific region of Canada include an inventory of all known and relevant reports and sources of data. Information on these matters is being extracted from existing marine and geologic indexes, consultation with many academic and governmental officials, and discussions with consultant firms engaged in coastal work. In addition, the library staff of the Vancouver office has obtained about 50 pertinent theses as well as other unpublished reports, and these items now are catalogued and available at this regional facility of the Geological Survey of Canada.

The initial phase of the compilation has been directed to the collection of most reports and sample site records of the coastal and Continental Shelf region; about 600 items are listed in Open File No. 197. A companion 1:1,000,000 base map shows the locations of these various studies, and accompanying marginal notes describe the various aspects of each study. During 1974, this report will be updated as users provide additional information or editorial comment. A second phase of the project will be released in late 1974 and will include sample sites and Quaternary studies for the region lying beyond the Continental Shelf to about 500 kms west of the Pacific coastline. The latitudinal limits of this second inventory are off the mouth of the Columbia River (46°N) to the southern portions of the Gulf of Alaska (58°N).

To date, the inventory has revealed a record of considerable marine geologic effort with almost every facet of the surficial sediment study being explored on at least a one-attempt basis. In addition to the published sedimentological work, cataloguing of the numerous "dart" cores provided by Shell Canada Ltd. suggests that much of the Vancouver Island Shelf, Queen Charlotte Sound, and Hecate Strait areas have been moderately to well sampled. Hecate Strait is the least studied of all major "inside" waterways in terms of publications and continuous seismic profiling (CSP). The southern Strait of Georgia is the most studied major basin but the Quaternary stratigraphic framework of the Strait of Juan de Fuca may be at a more advanced state of understanding. Dixon Entrance has been the focus of several reconnaissance geoscience investigations by academic institutions while the adjacent Queen Charlotte Island Shelf, by comparison, has had only relatively token efforts to date.

Estuarine geologic studies of the Fraser Delta have been conducted sporadically on the delta-front during the past 55 years and similar studies have now begun on the nearby Squamish Delta. Other deltaic estuaries (including the Skeena and the Nass, and smaller sized ones deemed critical by the Department of the Environment) have been almost totally neglected on a geologic basis. Of the fjords, Saanich Inlet is probably the most geologically-studied body of water in Canada and the international attention it attracts is credited to a unique condition of anoxic bottom waters. Recently, however, Howe Sound and Rupert Inlet have had an increasing number of thorough studies done and Bute and Jervis Inlets (the latter being endowed with manganese nodules) continue to receive periodic attention by the University of British Columbia. There are CSP tracklines in these and a few other fjords with Rupert Inlet having received the most attention. In many other fjords, preliminary analyses have been published at some random spot locales, but inlets within the Queen Charlotte Islands appear to be completely void of any geologic sampling. Despite the extensive influence of industrial and other users, Indian Arm of Burrard Inlet and the Alberni Canal of Barkley Sound, surprisingly, have a dearth of marine geologic information as compared to the vast number of other oceanographic studies performed to date.

Only a few sediment and geomorphic studies of beaches have been carried out on the British Columbia coastline. There have been some student projects near Vancouver and at least one or two by engineering firms using ancillary hydraulic model studies, but there is only one major investigation of the open ocean shoreline - the Long Beach area of Vancouver Island. This study also evaluated the economics of a potential beach placer; similar evaluations of less exhausting scrutiny have been completed for the lengthy beaches of the Queen Charlotte Islands. Sea bottom materials have been dredged for fill at deep superport sites near Vancouver and have been considered for fill at proposed sea-side transportation facilities at Prince Rupert, Squamish, and the Vancouver airport. Sea bottom materials have also been surveyed for the inner harbour areas of a few smaller ports as well. Up to now the sediments have been used for construction only and active mineral exploitation of the sea bed surface has not occurred yet.

For the complex subject concerning the relationships of substrate-benthos-bathymetry, studies of living biota by the Pacific Environment Institute (D. O. E.) and the Department of Biology of the University of Victoria have focused on critical deltaic estuaries, the Strait of Georgia, Rupert Inlet and a few other localities about Vancouver Island. Personnel of the University of Washington have conducted similar studies in international waters off Washington and British Columbia. Foraminiferal research is common, though many studies of the outside Shelf and of the

more northerly major waterways are unpublished. A few investigations have been directed to other fossils at sea-side locales of the southwest portion of British Columbia.

Marine surficial geologic investigations in adjacent areas of the United States are more advanced in some respects. In the Puget Sound and Washington-Oregon Shelf regions there have been several decades of radionuclide sediment studies; tracer studies of any kind are rare off British Columbia. The Shelf, south of 48°30'N has been mapped fully on several parameters while to the north off Canada, the majority of the samples are yet to be processed and existing maps are few. In southeastern Alaska the main emphasis has been on a series of studies on complex chemical changes at the sediment-water interface, and only a few regions have undergone geomorphic and sedimentological mapping. Glacier Bay, Taku Inlet, and Yakutat Bay have been the target of most investigations in southeast Alaska.

89. RADIOMETRIC AGE STUDIES OF SPELEOTHEM

Research Agreement 1135-D13-4-190/73

D.C. Ford and H.P. Schwarcz
Terrain Sciences Division

The age of deposition of calcite speleothem was determined using the $^{230}Th/^{234}U$ method, by alpha-particle spectrometry. Samples were taken from caves in three localities as a part of comprehensive studies of geomorphic evolution and paleotemperature records (via $^{18}O/^{16}O$ measurements) at these sites. Several samples yield $^{230}Th/^{234}U$ ratios equal to or greater than unity, indicating ages greater than 300,000 y., though in some cases excess (allogenic) ^{230}Th appears to have been deposited in the speleothem. This is also indicated by low $^{230}Th/^{232}Th$ ratios (<50).

1) South Nahanni River, N.W.T.

a) Grotte Valerie:

A well-laminated flowstone was found resting on clastic fill in one of the passages of this cave. The base of this flowstone has a $^{230}Th/^{234}U$ of 1.216, which is too great to have formed by closed-system decay although $^{230}Th/^{232}Th = 122$, which argues against incorporation of allogenic ^{230}Th. The top of the flowstone yields an age of 237,700 ± 24,000 y. B.P., compatible with earlier dates on the Major Stalagmite Phase of evolution of this cave, as reported in Ford (1973).

b) Igloo Cave (in the northern part of the S. Nahanni River area):

A sample of finely crystalline speleothem from the base of a stalagmite yielded a $^{230}Th/^{234}U$ of 1.146, which indicates allogenic ^{230}Th incorporation. The top of this specimen is now being dated.

2) Crowsnest Pass Area, Alberta-British Columbia

Gargantua Cave has an entrance at about 8,800 feet elevation. A basal section of a stalactite from the lower level of this cave was dated at 145,300 ± 10,600 y. B.P. This is comparable to a 178,000 ± 10,500 y. date obtained previously on adjacent Yorkshire Pot; both speleothems apparently formed during a pre-Illinoisan interglacial. The new date is consistent with the geomorphic evolution of this region as described in Ford et al. (1971). A new measurement from Middle Cave gave a $^{230}Th/^{234}U$ of 1.051 possibly indicating that this cave existed more than 300,000 y. B.P. Previous dates (in Ford et al., 1971) indicated an older age limit of 275,000 y.

3) Castleguard Cave, Banff National Park:

A loose piece of a pure, white calcite stalagmite was recovered. Its upper layer was dated at 62,400 ± 2,700 y. B.P., indicating that it ceased deposition near the end of the last interglacial. Another stalagmite sampled in situ from a face dissected by corrosive drip waters, yielded a $^{230}Th/^{234}U$ ratio of 1.646, and a rather low $^{230}Th/^{232}Th = 36.0$, indicating gross addition of ^{230}Th.

Some of the dated samples from this study and earlier ones are now being analyzed for oxygen isotope ratios. The Igloo Cave sample was found not to have been deposited in isotopic equilibrium.

References

Ford, D.C., Thompson, P. and Schwarcz, H.P.
1971: Dating cave calcite deposits by the uranium disequilibrium method: Some preliminary results from Crowsnest Pass, Alberta; in Research Methods in Pleistocene Geomorphology, Proc. 2nd Guelph Symp. on Geomorphology, 1971, E. Yatsu and A. Falconer, eds., p. 247-255.

Ford, D.C.
1973: Development of the canyons of the South Nahanni River, N.W.T.; Can. J. Earth Sci., v. 10. p. 366-378.

90. A PRELIMINARY LIST OF FOSSIL PLANTS FROM THE BEAUFORT FORMATION, MEIGHEN ISLAND, DISTRICT OF FRANKLIN

Research Agreement 1135-D13-4-75/73 and Project 730027

L. V. Hills* and J. V. Matthews, Jr.
Terrain Sciences Division

Introduction

The Beaufort Formation on Meighen Island is comprised of about 730 feet of unconsolidated crossbedded, fine to coarse-grained sands and pebbly sands with interbedded wood fragments, lignite, and shale (Thorsteinsson, 1961). Cross-stratification indicates a paleocurrent flow to the northwest. A 10- to 30-foot thick dark grey silty shale, first recognized as a marine unit by Fyles (Caley et al., 1962) has yielded a small foraminiferal assemblage which is being studied by B. E. Cameron. This unit, which is underlain and overlain by cross-stratified sands and gravels typical of the Beaufort Formation, apparently thickens to the north.

Fossils

Kuc (1974) has listed the Hepaticae, Musci, unidentified Coniferae, *Salix*, *Dryas*, *Carex* and Gramineae from the Beaufort Formation on Meighen Island, and Matthews (1974) has provided a preliminary list of fossil insects.

During mid July of 1973 plant macrofossils and samples for palynological study were collected from the lowermost 300 feet of the Beaufort Formation on the southwestern part of the island. A preliminary list of the taxa recovered is presented in Table 1.

Paleoecology

The sediments and sedimentary structures indicate deposition within the floodplain of a river or rivers. The peat and associated plants such as the Musci, *Myrica*, *Ledum*, *Betula*, *Carex*, and *Nuphar*, indicate wet bog or open shallow ponds within the floodplain. Drier habitats were occupied by such species as *Picea banksii*, *Abies* sp., *Betula* cf. *papyrifera* and Gramineae. The co-occurrence of the conifers and bog plants indicates a very open forest with interspersed tundra areas. This interpretation is in agreement with that of Matthews (1974).

Correlation and Age

Precise age correlations within the Beaufort Formation are difficult because of the wide latitudinal range (70°N to 80°N) of its exposures. General trends in the flora, however, can be followed from south to north. The Beaufort Formation in southwestern Banks Island contains the following plant macrofossils: *Picea banksii*, *Pinus* cf. *strobus*, *Pinus* (2 needle types), *Metasequoia*, *Juglans eoceinerea* (Hills et al., 1974), and within the pollen assemblage: *Alnus*, *Carya Tilia* and *Tsuga*. In northwestern Banks Island (Hills and Ogilvie, 1970; Kuc and Hills, 1971; Roy and Hills, 1972) this assemblage is represented only in the lower Beaufort (Hills, 1969) whereas the upper Beaufort is characterized by a dominance of macrofossils of *Picea banksii*, *Pinus* cf. *strobus*, *Larix* sp., and *Tsuga*, as well as an abundance of Ericaceous type pollen. On Prince Patrick, Borden, and Ellef Ringnes Islands, pollen of *Picea*, *Pinus* and Ericaceae plus Bryophyte spores, are dominant, with Ericaceae, *Betula*, *Alnus*, and Bryophytes being relatively better represented than at Beaufort exposures to the south. This trend to greater abundance of tundra elements (*Myrica*, *Betula*, *Ledum*, etc.) apparently continues northward to Meighen Island. Such a progressive change in vegetation, from a deciduous hardwood type in the south to a coniferous forest and ultimately open coniferous forest or tundra vegetation in the north, most probably reflects the latitudinal differences of the Beaufort fossil localities. However, an alternative explanation - that northern Beaufort assemblages differ from those of the south because they are of younger Tertiary age - cannot be ruled out. Elsewhere Hills and Ogilvie (1970), Roy and Hills (1972), Hills et al. (1974) have argued that the Beaufort Formation on Banks Island is most probably Miocene and cannot be younger than Early Pliocene. In northeastern Asia, Biske (1974) records the common occurrence of *Myrica gale L.* in beds equivalent to the late Homerian (late Miocene) and early Clamgulchian (Pliocene). Although the Meighen Island plant assemblage correlates floristically with the Pliocene Clamgulchian stage of Wolfe et al. (1966) and Biske (1974), its high latitude location compared to other Clamgulchian localities may mean that it achieved the Clamgulchian stage of taxonomic diversity earlier than the southern sites, i.e., before the Pliocene.

References

Biske, S. F.
1974: Correlation of Tertiary nonmarine deposits in Alaska and northeastern Asia; in Arctic Geology, ed. Max G. Pitcher; Am. Assoc. Pet. Geol., Mem. 19, p. 39-245.

Caley, J. F., Fortier, Y. O., Morley, L. W., Robinson, S. C., and Weeks, L. J.
1962: Field work, 1961; Geol. Surv. Can., Information Circular no. 5, p. 4-6.

Hills, L. V.
1969: Beaufort Formation, northwestern Banks Island, District of Franklin; in Report of Activities, Part A; April to October 1969, Geol. Surv. Can., Paper 69-1, pt. A, p. 204-207.

*University of Calgary.

Table 1

Plant macrofossils, Beaufort Formation, Meighen Island

PINACEAE	
Picea banksii Hills and Ogilvie	2 cones
Abies sp.	needles
Pinus cf. *albicaulis* Engelm. *	needles
Larix sp.	1 cone
Thuja cf. *occidentalis* L.	leafed twigs
CYPERACEAE	
Eleocharis cf. *palustris* (L.) or *uniglumis* (Link)	seeds
Carex sp.	seeds
SPARGANIACEAE	
Sparganium sp.	seeds and pollen
SALICACEAE	
Salix sp.	leaves, twig fragments
Populus ?	
MYRICACEAE	
Myrica cf. *gale* L.	leaves
BETULACEAE	
Betula cf. *papyrifera* Marsh	samaras, bracts, leaves
Betula cf. *nana* L. or *glandulosa* Michx.	samaras, bracts, leaves
Alnus sp.	samaras and pollen
POLYGONACEAE	
Polygonum spp.	seeds
NYMPHAEACEAE	
Nuphar sp.	1 seed and pollen
ROSACEAE	
Potentilla cf. *palustris* (L.)	seeds
LEGUMINOSAE	
Hedysarum sp.	seed
EMPETRACEAE	
Empetrum sp.	seeds
ERICACEAE	
Ledum cf. *palustre* L.	leaves
Cassiope cf. *tetragona* L.	leafy stem
Vaccinium sp.	leaves
GENTIANACEAE	
Menyanthes trifoliata L.	seeds

*Where detailed comparisons have been possible, it has been found that the fossils are similar to but not identical to extant species; therefore, "cf." has been used to imply relationship.

Hills, L.V., Klovan, J.E., and Sweet, A.R.
1974: *Juglans eocinerea* n. sp., Beaufort Formation (Tertiary) southwestern Banks Island, Arctic Canada; Can. J. Bot., v. 52, no. 1, p. 65-90.

Hills, L.V., and Ogilvie, R.T.
1970: *Picea banksii* n. sp. Beaufort Formation, Banks Island, Arctic Canada; Can. J. Bot., v. 48, no. 3, p. 457-464.

Kuc, M.
1974: Fossil flora of the Beaufort Formation, Meighen Island, Northwest Territories; in Report of Activities, Part A, April to October 1973, Geol. Surv. Can., Paper 74-1, pt. A, p. 193-195.

Kuc, M. and Hills, L.V.
1971: Fossil mosses Beaufort Formation (Tertiary), northwestern Banks Island, Western Canadian Arctic; Can. J. Bot., v. 49, no. 7, p. 1089-1094.

Matthews, J.V., Jr.
1974: A preliminary list of insect fossils from the Beaufort Formation, Meighen Island, District of Franklin; in Report of Activities, Part A, April to October 1973, Geol. Surv. Can., Paper 74-1, pt. A, p. 203-206.

Roy, S.K. and Hills, L.V.
1972: Fossil wood from the Beaufort Formation (Tertiary) northwestern Banks Island, Arctic Canada; Can. J. Bot., v. 50, no. 12, p. 2637-2648.

Thorsteinsson, R.
1961: The history and geology of Meighen Island, Arctic Archipelago; Geol. Surv. Can., Bull. 75, 19 p.

Wolfe, J.A., Hopkins, D.M., and Leopold, E.B.
1966: Tertiary stratigraphy and palaeobotany of the Cook Inlet region, Alaska; U.S. Geol. Surv., Prof. Paper 398-A, p. 1-29.

91. THE INTERGLACIAL FLORA OF WORTH POINT, WESTERN BANKS ISLAND

Project 690044

M. Kuc
Terrain Sciences Division

Introduction

The interglacial deposits exposed in the coastal cliff at Worth Point (Figs. 1, 2), discovered by J. G. Fyles in 1959, were restudied in detail by the author in 1969. They represent two environmental complexes: (1) lacustrine environments represented by a series of sapropels (see e. g. Craig and Fyles, 1960) and (2) forest-Sphagnum bog environments represented by a sequence of woody-peat strata (Fig. 3). Both are covered by organic debris interbedded with silty deposits filling up the narrow, steep-walled valley formed in sandstone of the Eureka Sound Formation (Fig. 2). The second sequence was available for study in 1969 and some of the results are discussed in this report (cf. Kuc, 1970, 1973, 1974).

The full biostratigraphic diagram of the Worth Point interglacial profile, the pictorial documentation of fossils and reconstructions of past environments are deposited with Terrain Sciences Division and fossil samples are in the National Type Fossil Collection, Geological Survey, Ottawa.

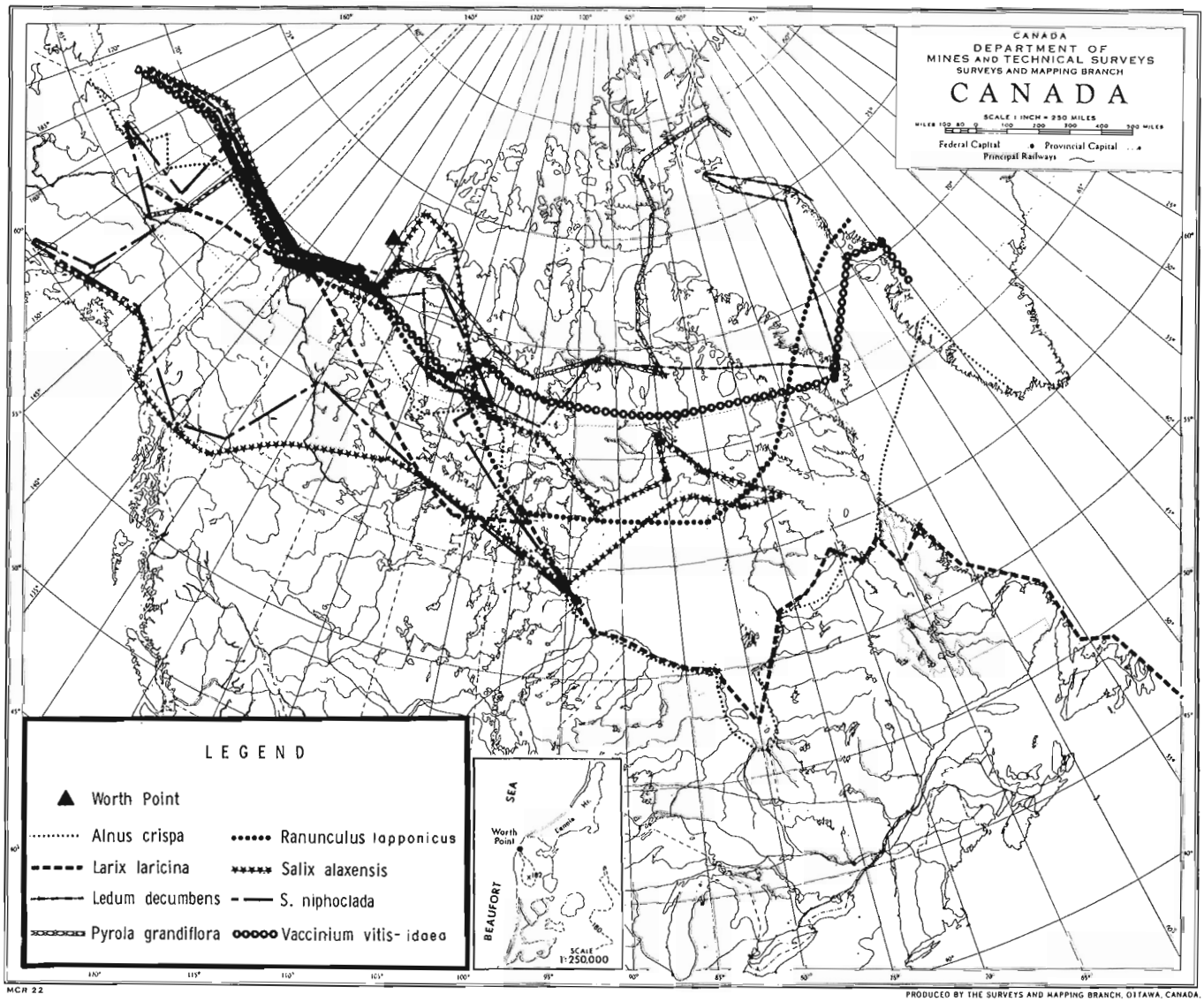

Figure 1. Location of Worth Point and recent northernmost limits of some plants found in Worth Point interglacial deposits.

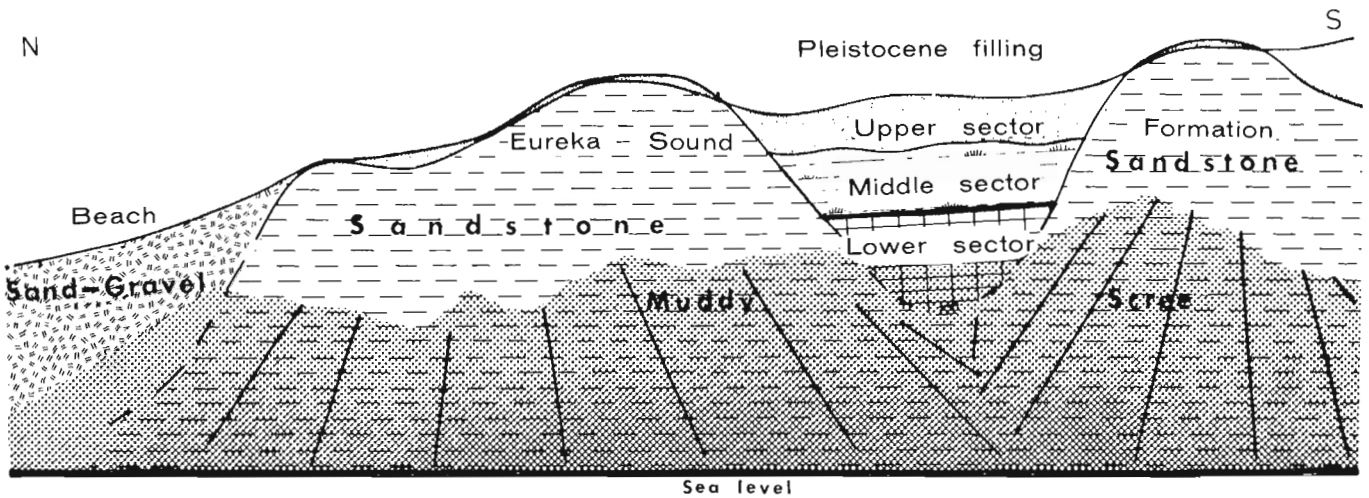

Figure 2. Highly schematicized illustration of stratigraphy position of interglacial deposits exposed on vertical slopes of the coastal Worth Point cliff.

Fossil flora

LICHENES

Peltigeraceae

Peltigera aphthosa (L.) Willd.

Cladoniaceae

Cladonia deformis (L.) Hoffm.

C. sp. [cf. *bellidiflora* (Ach.) Schaer.]

C. rangiferina (L.) Wigg. -s.l.

C. sp.

BRYOPHYTA

Hepaticae

Ptilidiaceae

Ptilidium ciliare (L.) Hampe

Lophoziaceae

Lopozia quadriloba (Lindb.) Evans -s.l.

L. sp.

Anastrophyllum minutum (Schreb.) Schust.

Musci

Sphagnaceae

Sphagnum teres (Schimp.) Aongst.

Polytrichaceae

Polytrichum juniperinum Hedw.

P. strictum Brid.

Ditrichaceae

Ditrichum flexicaule (Schwaegr.) Hampe

Distichium capillaceum (Hedw.) B.S.G.

Dicranaceae

Kiaeria glacialis (Berggr.) I. Hag.

Dicranum leioneuron Kindb.

Bryaceae

Pohlia nutans (Hedw.) Lindb.

Bryum pseudotriquetrum (Hedw.) Gaertn., Meyer & Scherb.

B. neodamense Itzig.

B. ovatum Jur.

B. sp.

Mniaceaea

Mnium affine Bland. - s.l.

Aulacomniaceae

Aulacomnium palustre (Hedw.) Schwaegr.

A.p. var. *polycephalum* (Brid.) Hüb.

A.p. var. *serratum* Warnst.

A.p. var. sp.

A. turgidum (Wahlenb.) Schwaegr.

Meesiaceae

Meesia uliginosa Hedw.

M. triquetra (Richt.) Aongst.

Bartramiaceae

Philonotis tomentella Mol.

P. sp.

Timmiaceae

Timmia norvegica Zett.

Theliaceae

Myurella tenerrima (Brid.) Lindb.

Thuidiaceae

Thuidium abietinum (Hedw.) B.S.G.

Helodium blandowii (Web. & Mohr) Warnst.

Amblystegiaceae

Campylium stellatum (Hedw.) C. Jens.

C. polygamum (B.S.G.) C. Jens.

Amblystegium cf. *kochii* B.S.G.

Drepanocladus exannulatus (B.S.G.) Warnst.

D. revolvens (Sw.) Warnst.

D. uncinatus (Hedw.) Warnst.

Calliergon cordifolium (Hedw.) Kindb.

C. giganteum (Schimp.) Kindb.

C. richardsonii (Mitt.) Kindb.

C. aftonianum Steere

C. stramineum (Brid.) Kindb.

Brachytheciaceae

Tomenthypnum nitens (Hedw.) Loeske

Brachythecium salebrosum (Web. & Mohr) B.S.G.

Eurhynchium pulchellum (Hedw.) Jenn.

E. p. var. sp.

Hypnaceae

Hypnum callichroum Funck

H. hamulosum B.S.G.

H. sp.

Isopterygium pulchellum (Hedw.) Jaeg. & Sauerb.

Rhytidiaceae

Rhytidium rugosum (Hedw.) Kindb.

Hylocomiaceae

Hylocomium splendens (Hedw.) B.S.G.

PTERIDOPHYTA

Equisetaceae

Equisetum arvense L.

SPERMATOPHYTA

Gymnospermae

Abietaceae

Larix laricina (Du Roi) K. Koch

Angiospermae

Dicotyledones

Betulaceae

Betula glandulosa Michx.

Alnus crispa (Ait.) Pursh

Salicaceae

Salix niphoclada Rydb.

S. alaxensis (Anderss.) Cov.

S. sp. cf. *ovalifolia* Trautv.

S. sp.

Caryophyllaceae

? *Arenaria humifusa* Wahlenb.

Ranunculaceae

Ranunculus lapponicus L.

Empetraceae

Empetrum nigrum L. -s.l.

Pyrolaceae

Pyrola grandiflora Radius

Ericaceae

Ledum decumbens (Ait.) Lodd.

Vaccinium uliginosum L. var. *uliginosum*

V. u. subsp. *microphyllum* Lange.

V. u. var. *alpinum* Big.

V. vitis-idaea var. *minus* Lodd.

Monoctyledones

Cyperaceae

Carex. sp.

Gramineae

Indetermined genera.

Paleoecological evidence

The interglacial forest defined by the Worth Point fossils and deposits, was open, subarctic forest-tundra such as is now extensively represented in the northern part of the Boreal Forest Zone. Its tree stratum was fairly discontinuous, mainly composed of *Larix laricina*, which is represented by fossils of crooked shrubby specimens and minor trunks (maximum 26 cm in diameter and only a few meters tall), with very thin and dense annual rings and poorly developed root systems. The trees were abundantly fruiting and produced large amounts of duff preserved as a needle deposit. The shrub stratum was dense, composed of taller shrubs (*Alnus crispa, Betula glandulosa, Salix niphoclada, S.* sp.) and an abundance of low shrubs such as *Empetrum nigrum, Ledum decumbens, Vaccinium uliginosum*. In some places the community was grassy, mesic, or boggy. Based on well preserved specimens, terminal growth seems to have decreased during the life of some individuals. The mossy forest floor was discontinuous. Sciaphiles (*Amblystegium* cf. *kochii, Calliergon cordifolium, Eurhynchium pulchellum, Isoperygium pulchellum*) grew in scattered shaded humic sites, while in wet habitats, peat-formers (*Aulacomnium, Campylium, Lophozia, Hypnum, Sphagnum, Tomenthypnum* etc.) formed a heavy carpet associated

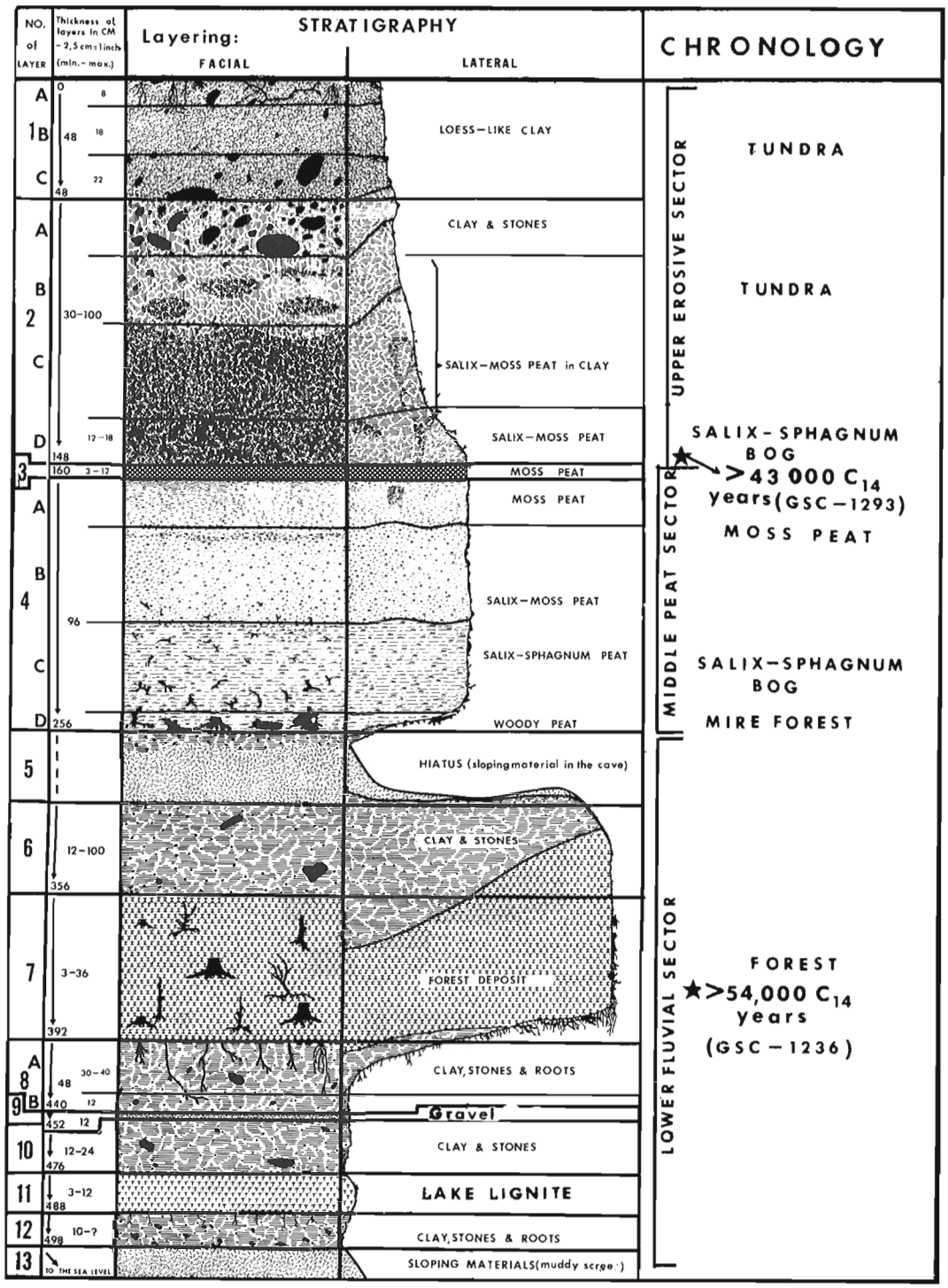

Figure 3. Biostratigraphic diagram of the Worth Point interglacial sequence. Worth Point, Banks Island, 72°15'N - 125°37'W, (Field work, 1969).

with single herbaecous plants (*Carex* sp., *Equisetum arvense, Pyrola grandiflora, Ranunculus lapponicus*). *Ditrichum flexicaule, Drepanocladus uncinatus, Hylocomium splendens* and in some places the lichen *Peltigera aphthosa* grew in mesic habitats. Environments controlled by a water deficit possessed xeric, low, treeless, lichen-moss growth: *Cladonia* species, *Empetrum nigrum* (dwarf specimens), *Polytrichum juniperinum, Rhytidium rugosum, Thuidium abietinum* and *Vaccinium vitis-idaea.*

Structure of tree root systems and the stumps preserved in the moss humic layer indicate presence of a

shallow active zone. Asymmetry of root cross-sections and their very narrow growth rings also indicate subarctic substrate conditions. The stratum of duff and humus is slightly decomposed.

The type of forest that existed at Worth Point certainly extended northward across Banks Island but its existence in the present High Arctic, which at that period probably was within a Low Arctic zone, is doubtful. High Arctic vegetation, if it existed during this time, could have occurred on the northernmost Queen Elizabeth Islands and at higher elevations in mountains.

Present-day northernmost limits of *Larix laricina*, *Ranunculus lapponicus*, *Vaccinium vitis-idaea* and some other bio-climatic indicators are shown in Fig. 1. They give evidence that the growing period on the west coast of Banks Island which is now 72 to 85 days long was distinctly longer during interglacial time.

Higher in the Worth Point profile the disappearance of forest and Sphagnum deposits, the appearance of tundra species and the presence of deposits with erratics, indicate a gradual deterioration of a climate and the post-optimal phase of the Pre-Wisconsin interglacial represented by the Worth Point sequence.

References

Craig, B. G., and Fyles, J. G.
1960: Pleistocene geology of Arctic Canada; Geol. Surv. Can., Paper 60-10, 21 p.

Kuc, M.
1970: Peat deposits and fossil mosses in the Arctic; in Report of Activities, Part A, April to October 1969, Geol. Surv. Can., Paper 70-1, pt. A, p. 161-162.

1973: Fossil statoblasts of *Cristatella mucedo* Cuvier in the Beaufort Formation and in interglacial and postglacial deposits of the Canadian Arctic; Geol. Surv. Can., Paper 72-28, 12 p.

1974: Noteworthy vascular plants collected on the southwestern part of Banks Island; Arctic, v. 27.

Project 690064

R. J. Mott
Terrain Sciences Division

During the summer of 1971, while assisting in a mapping project (690043) in Labrador, R.D. Thomas collected modern surface samples for pollen analysis from several localities in the Churchill River region (Fig. 1). The results of analysis of ten of these samples comprise the following report.

A similar investigation of the modern pollen deposition in the Nichicun Lake area of Quebec, located to the west of the present study area, has been reported by Terasmae and Mott (1965). An early study by Wenner (1947) of pollen diagrams from Labrador included one site, among the otherwise coastal locations, from the Churchill Falls area. Grayson (1956) included analyses of four bogs from Schefferville and areas to the north and south, while Drummond (1965) included two diagrams by Terasmae from the area north of Schefferville. More recently Morrison (1970) studied several sites from the Churchill River area, but his analyses did not always include surface samples and did not include actual counts or the pollen sum used for calculation, a requirement for some statistical analyses.

Physiography

The area is part of the Lake Plateau physiographic region (Hare, 1959), a subdued area of the Canadian Shield covered by thick and profuse drift deposits. Occasionally, the Precambrian bedrock outcrops as low knobs less than 500 feet higher than the surrounding plateau surface, which ranges in elevation from about 1,600 to 2,000 feet above sea level. The disrupted drainage and flooded depressions form a myriad of lakes. The Churchill River drains much of the area and flows from the plateau over the Churchill Falls and associated rapids into a valley about 1,000 feet lower in elevation. Michikamau Lake in the northeastern corner of the area is drained to the east by the Naskaupi River.

Climate

The climate of the area, a humid continental type with cool summers and no dry periods, is severe. (Geographical Branch, 1957; Meteorological Branch, 1960). The mean daily January temperature is -20°F, while the mean daily July temperature is 55- to 60°F, with winter lows as cold as -55°F and summer highs up to 85°F. The frost-free period is less than 80 days, and the growing season is less than 140 days. Average annual precipitation totals 32 inches, with total snowfall averaging about 140 inches. Prevailing winds are from the northwest most of the year, but southeasterly winds are common in June.

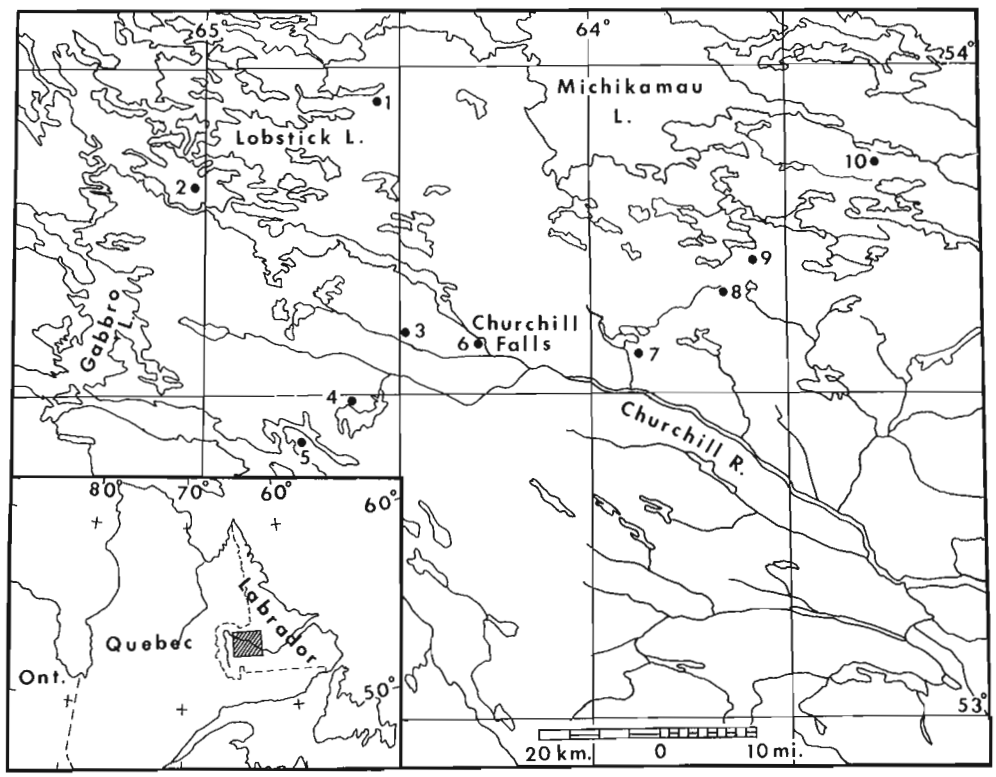

Figure 1. Map showing location of sampling site (•6).

Vegetation

Rowe (1959) includes the area in the Northeastern Transition Section of the Boreal Forest Region in his description of the forest regions of Canada. In a more detailed study of the vegetation, Hare (1959) classifies the area as a woodland or parkland subzone of the Boreal Forest, describing it as a more or less open lichen woodland of black spruce (*Picea mariana*) and a lichen-covered floor of *Cladonia*, with a close lichen woodland occurring sparingly on better sites such as near Churchill Falls where the spray promotes better growth. On the more closed forest sites Labrador tea (*Ledum groenlandicum*) forms a prominent shrub layer. White spruce (*Picea glauca*), balsam fir (*Abies balsamea*), and paper birch (*Betula papyrifera*) also may be present on the

TABLE I

Site Locations

Site No.	N. Lat.	W. Long.	NTS
1	53°57'40"	64°33'45"	23H/15
2	53°49'	65°02'	23H/14
3	53°36'20"	64°27'40"	23H/9
4	53°28'40"	64°38'	23H/7
5	53°25'20"	64°45'	23H/7
6	53°35'30"	64°18'	23H/9
7	53°33'15"	63°52'30"	13E/12
8	53°39'	63°39'	13E/12
9	53°42'30"	63°29'45"	13E/11
10	53°51'	63°16'	13E/14

better sites but generally are not abundant. Tamarack (*Larix laricina*) may fringe wet areas, but such areas often support abundant alder (*Alnus* sp.) thickets. Open areas covered by bogs, fens, or muskeg are abundant. *Sphagnum* and heath plants (Ericaceae) dominate the bogs, while sedges (Cyperaceae), grasses (Gramineae) and various mosses are abundant in the sedge fen and swampy areas. Buckbean (*Menyanthes trifoliata*) is often common in pools.

Sampling Sites

The samples were collected by hand from the bottoms of shallow pools in bogs or fens. Since the pools were in open areas some distance from the trees and shrubs surrounding the wet areas, their contained pollen spectra probably are similar to what would be obtained by sampling the mud/water interface of small lakes. Although the vegetation of the bog or fen itself is represented in the pollen spectra, overrepresentation of this component does not seem to be a problem. The site locations are plotted on a map of the area (Fig. 1), and the exact locations are listed in Table I.

Results

The pollen spectra from the ten sites are listed in Table II. Percentages are calculated on a pollen sum which includes the total number of pollen grains and spores exclusive of aquatics. The pollen sum used for each sample also is shown.

As would be expected, the assemblages are dominated by spruce pollen. Since it is difficult to differentiate reliably between the two spruce species, the percentages shown for each may not be accurate, but the figures do show the preponderance of the black spruce pollen type. Jack pine (*Pinus banksiana*) does not grow in the area, and the few pine grains counted result from long distance transport. The same is true of hemlock (*Tsuga canadensis*). Balsam fir and tamarack pollen are present in small amounts, reflecting their limited occurrence in the area. Birch is the second most abundant pollen taxon outside of some aquatic types, and although present in the area, it probably is not as generally abundant as some of the higher percentages might indicate. Birch may be locally abundant at some sites and lacking at others judging by the range of percentages obtained. Despite the fact that balsam poplar (*Populus balsamifera*) ranges farther north than the Churchill Falls area, it is not present in the area in any significant numbers, and the few pollen grains present probably were blown in from some distance away. Long distance transport must also explain the few temperate hardwood grains present.

Among the shrub, pollen alder is the most abundant as would be expected from its local abundance around wet sites. The absence of willow (*Salix*) pollen is puzzling as it certainly grows in the area, possibly not to the same extent as in the shrub tundra to the north, but still abundant enough to be represented. Sweet gale (*Myrica gale*) must be locally abundant at some sites, as indicated by the various frequencies obtained. The meagre pollen percentages of heath plants show that this family is greatly under-represented in pollen spectra when contrasted with their prevalence on the landscape.

Small percentages of various herbs and spore-bearing plants are characteristic of the assemblages, with grass, composites (Tubuliflorae, Ambrosiea and *Artemisia*), club-mosses (*Lycopodium*), selaginella (*Selaginella selaginoides*), etc., being present in small numbers. It is interesting to note the presence of burnet (*Sanguisorba canadensis*) pollen at almost every site. Sedge and *Sphagnum* are more or less abundant depending on their local abundance at the sites. Buckbean pollen is represented at many sites and is conspicuous in many muskeg pools. Other aquatics are poorly represented in the pollen spectra.

Summary

The Lake Plateau region of Labrador with its spruce woodland vegetation is characterized by modern pollen assemblages dominated by spruce and abundant birch, alder, sedge, and *Sphagnum*, with a variety of other taxa in lesser amounts. Similar assemblages have prevailed in the area over the past 4,000 to 5,000 years, indicating a type of vegetation similar to the present for this time period (Morrison, 1970).

References

Drummond, R.N.
1965: Glacial geomorphology of Cambrian Lake area, Labrador-Ungava; Ph.D. Dissertation, McGill University, Montreal, Que.

Geographical Branch
1957: Atlas of Canada; Can., Dept. Mines Tech. Surv., Ottawa.

Grayson, J.F.
1956: The postglacial history of vegetation and climate in the Labrador-Quebec region as determined by palynology; Ph.D. Dissertation, Univ. Michigan, Ann Arbor, Michigan, 252 p.

TABLE II

Pollen Spectra

Taxa	Site No. 1	2	3	4	5	6	7	8	9	10
Trees										
Picea mariana	46.8	53.2	60.9	49.5	64.2	66.1	67.9	56.1	52.8	61.8
Picea glauca	9.0	6.3	4.4	0.3	1.4	5.4	1.9	7.9	0.5	1.1
Pinus banksiana	2.6	2.2	3.9	4.7	2.5	3.9	1.1	2.3	1.3	1.1
Abies balsamea	1.0	2.2	1.1		0.6	5.7	1.7	1.2	0.5	0.9
Larix laricina	0.7		0.6		0.6					
Tsuga canadensis								0.3		
Betula	21.0	8.8	13.3	24.1	19.1	4.8	12.6	20.8	28.8	18.6
Populus			0.3		0.6					
Ulmus			0.3							
Fraxinus									0.3	
Shrubs										
Alnus	9.7	11.7	11.1	11.1	5.7	6.0	9.3	7.3	8.8	6.3
Elaeagnus commutata									0.3	
Myrica gale	1.9	10.5	0.3	0.8	0.3	0.3	1.7		0.3	0.2
Ericaceae	1.0	0.2	0.8	2.1	0.6	0.9	1.4	1.8	2.8	2.3
Herbs										
Gramineae	1.3	0.5	0.3		0.3		0.8	0.3	0.3	0.9
Tubuliflorae	0.7		0.3		0.3					1.6
Ambrosieae	0.3	0.7	1.4	0.8	1.1					
Artemisia	0.3		0.3		0.3	0.6			1.0	
Chenopodiineae	0.3	0.2		0.3	0.3	0.3				
Sanguisorba canadensis	1.6	0.5		0.3	0.6	0.9		0.3	0.3	1.1
Rubus chamaemorus						0.3				
Potentilla		0.2								
Thalictrum		0.2							0.3	
Saxifragaceae								0.3	0.3	
Epilobium								0.3		
Koenigia islandica										0.9
Selaginella selaginoides	0.3	0.7	0.3	1.0	0.3					1.8
Lycopodium annotinum	0.3	1.0	0.3	1.8	1.4	0.6	0.6		0.5	0.2
L. clavatum				2.1		0.6	0.6		0.3	0.5
L. lucidulum				0.8					0.5	0.5
L. selago		0.2								
Equisetum	0.3									
Pteridophyta			0.3	0.3		0.6	0.6			
Polypodiaceae	0.7	0.2				3.0				
Unidentified N.A.P.	0.3	0.2		0.3	0.3			0.9	0.5	0.2
Pollen Sum (no. of grains)	310	410	361	386	366	333	364	342	396	442
Aquatics										
Cyperaceae	43.6	20.5	70.4	11.1	26.5	14.7	8.8	12.9	8.6	31.0
Sparganium							0.3			
Potamogeton		1.2								0.2
Menyanthes trifoliata		0.2		0.5	0.3		0.6	0.6		0.2
Sphagnum	2.6	1.0		4.7	2.5	2.7	1.7	1.2	5.8	19.5

Percentages are based on total pollen (pollen sum) excluding aquatics.

Hare, F.K.
1959: A photo-reconnaissance survey of Labrador-Ungava; Can. Geograph. Br., Mem. 6, 83 p.

Meteorological Branch
1960: The climate of Canada; Can. Dept. Transport; 74 p.

Morrison, A.
1970: Pollen diagrams from interior Labrador; Can. J. Bot., v. 48, no. 11, p. 1957-1975.

Rowe, J.S.
1959: Forest regions of Canada; Can. Dept. Northern Affairs Nat. Resourc., Forestry Br., Bull. 123, 71 p.

Terasmae, J., and Mott, R.J.
1965: Modern pollen deposition in the Nichicun Lake area, Quebec; Can. J. Bot., v. 43, p. 393-404.

Wenner, C.-G.
1947: Pollen diagrams from Labrador; Geogr. Ann., v. 29, p. 137-374.

93. PERIGLACIAL FEATURES AND LANDSCAPE EVOLUTION, CENTRAL BATHURST ISLAND, DISTRICT OF FRANKLIN

Project 630005

W. Blake, Jr.
Terrain Sciences Division

Introduction

While carrying out a reconnaissance of the surficial geology of Bathurst Island in 1963, a number of observations were made of periglacial features, especially those which occur along the low, central valley which crosses the island. This valley, named Polar Bear Pass by Kerr (1973), passes close to the site where our base camp was located and where the National Museum of Natural Sciences, under the leadership of S. D. MacDonald has had a field station since 1968 (Fig. 1).

Much of the 1963 field season, as well as June 1964, was devoted to collecting samples of terrestrial and marine materials for radiocarbon dating, in order to establish a chronology of events bearing on the glacial history of the island (Blake, 1964, 1974). One result of the accumulation of age determinations is that a time framework is now available within which a variety of periglacial landforms are known to have developed, and the purpose of this report is to describe and illustrate a few of the features which occur in the vicinity of Polar Bear Pass. For a discussion of permafrost conditions in the archipelago as a whole, the reader is referred to the summary paper by Brown (1972).

Bracebridge Inlet

Approximately the western half of the east-west valley, which divides Bathurst Island into two unequal parts, is still below sea level, forming an eastward extension of Bracebridge Inlet. On its south side this inlet is bounded by an elongate ridge developed on steeply south-dipping strata of the Bathurst Island, Stuart Bay, and Eids formations, all of Devonian age (Kerr, 1973). Figure 2 shows this ridge looking toward the east-southeast (Locality 1, Fig. 1). The mantle of till (sand: silt: clay ratios of 39: 48: 13, 42: 43: 15, and 25: 55: 20 were obtained on samples at three different sites along the ridge) which obscures the bedrock is characterized by a well-developed and commonly rectangular network of ice-wedge polygons as well as by the presence of abundant fragments of marine shells; a sample of *Hiatella arctica*, from an elevation of 475 feet (145 m), was dated at $33,100\ ^{+1300}_{-1100}$ years (GSC-212, 20-53% fraction) and $35,900\ ^{+1400}_{-1200}$ years (GSC-212, 54-100% fraction). These shells are interpreted as being erratics, picked up in the inner part of 'Dartmouth Bight' or along Polar Bear Pass by a westward-flowing lobe of ice and plastered onto the ridge. Some of the shells also may have originated in the valley to the southeast of the ridge. Although the somewhat arcuate form of the till mantle suggests that it might represent a position of the ice margin during a stillstand or readvance, it seems more likely that the till is simply restricted to the crest of the ridge; much of the finer material at lower elevations has been reworked or removed by the washing action of the sea in early postglacial time.

Near the headwaters of the drainage line shown in Figure 2, a mound of peat was found adjacent to a pool about 0. 8 m deep. This pool had developed at a junction of the trenches, commonly 2 to 4 m wide and up to 0. 5 m deep, which define the borders of polygons and which have resulted from partial thawing of the underlying ice wedges. The peat mound, at an elevation of 450 feet (130 m), was cored to a depth of over 2. 76 m with a hand-operated, SIPRE type ice-corer (8-cm-diameter core). The core bottomed in greyish brown sand, believed to correspond to the adjacent till, and the basal organic material that could be dated, at a depth of 2. 61 to 2. 64 m, was 9210 ± 170 years old (GSC-180; Blake, 1964, Dyck et al., 1965). A sample at 17 to 21 cm depth, immediately above the level at which the peat was frozen on July 2, 1963, was 7820 ± 140 years old (GSC-233, fraction soluble in NaOH; Dyck et al., 1966).

The age determination on the basal organic material provides a minimum age for deglaciation, and when one considers that a certain amount of time must elapse between disappearance of the ice, the invasion of plants, and the accumulation of sufficient organic material for dating, it would appear that the age is in good agreement with a date of 9780 ± 190 years (GSC-249; Lowdon et al., 1967) obtained on *Hiatella arctica* shells at an elevation of 335 to 350 feet (102 to 107 m) at Schomberg Point, which is close to the westernmost extremity of Bathurst Island and some 95 km west of this hilltop peat site.

Thus, for a period of time approaching 2,000 years, mosses and other vegetation accumulated in this tiny depression. Brassard (pers. comm., 1967) reported *Drepanocladus* sp. in all core increments from 2. 61 to 2. 76 m depth and *Campylium stellatum* at the 2. 64 to 2. 76 m levels (cf. Brassard and Steere, 1968). Kuc (unpublished G. S. C. Bryological Rept. No. 279) found *Drepanocladus revolvens*, *Drepanocladus* sp., and *Scorpidium scorpioides* among other organic remains in the heterogeneous peat at 15 cm depth. All these mosses are characteristic of wet habitats. Deposition of organic material probably ceased as a result of filling of the original depression,

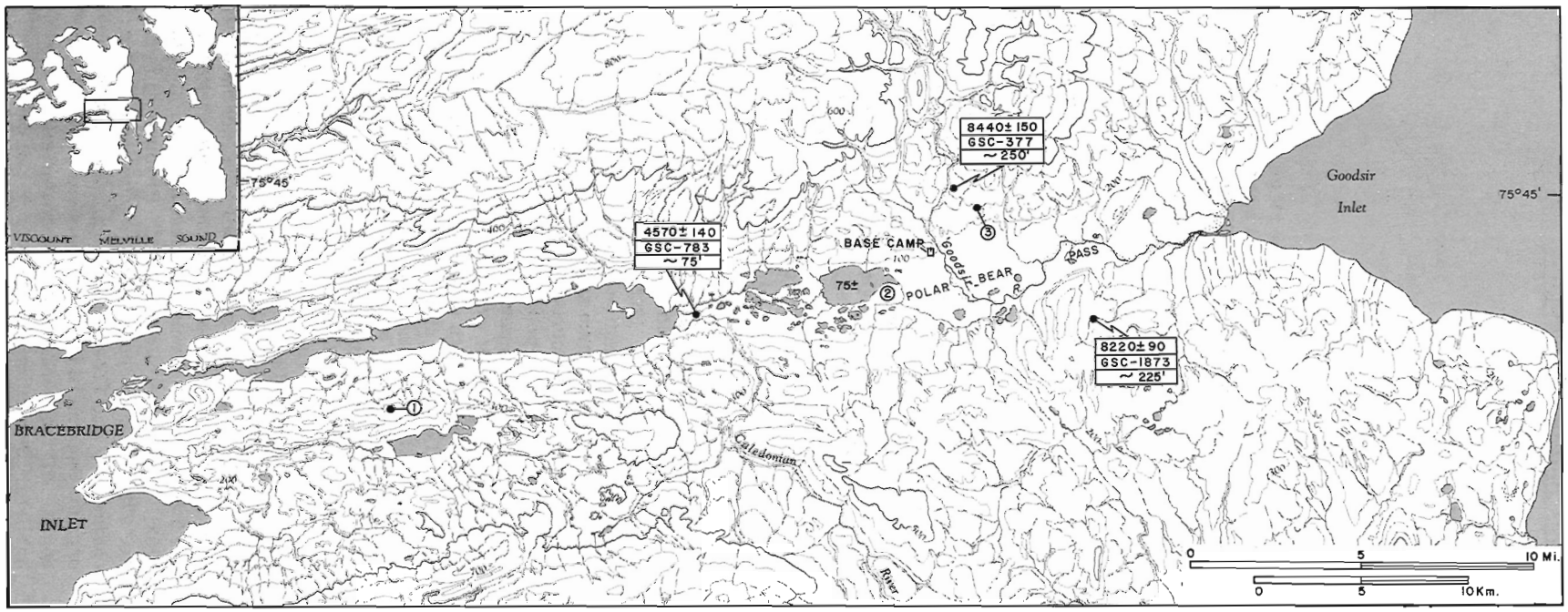

Figure 1.

Location map, central Bathurst Island. Base map is sheet 68H, McDougall Sound (1: 250, 000), Army Survey Establishment, R. C. E., 1965; contour interval, 100 feet. Locality numbers refer to sites described in the text and in the following figures. Radiocarbon age determinations shown are those on marine shells.

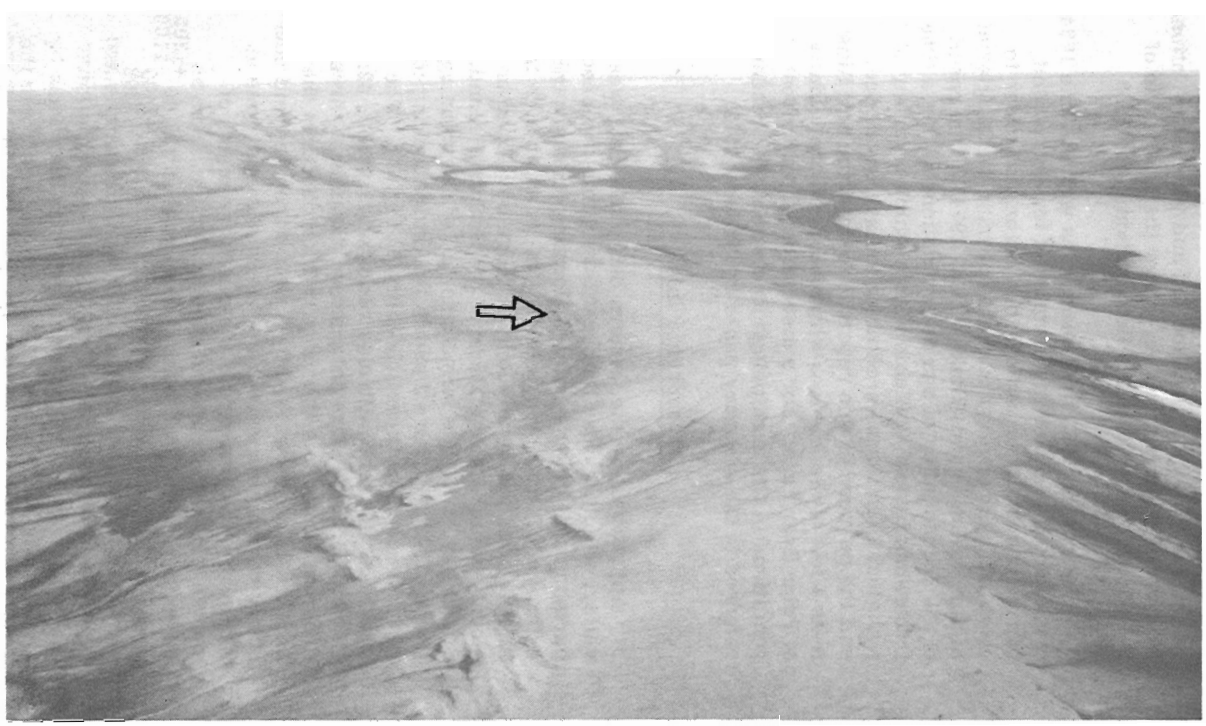

Figure 2.

Oblique air view east-southeast at till-mantled ridge east of Bracebridge Inlet (Loc. 1, Fig. 1). Note pattern of ice-wedge polygons developed in till. Arrow indicates location of peat mound shown in Figure 3. GSC photo 202349-C, from Kodachrome slide, July 1963.

Figure 3. Detail of peat mound on ridge shown in Figure 2. Frozen coring surface was at depth of 21 cm. Open part of core barrel is 35 cm long. Peat at 17-21 cm depth, unfrozen, was 7820 ± 140 years old (GSC-233). July 2, 1963. GSC photo 202566.

and the build-up of ice lenses within the peat ultimately transformed the accumulation basin into a topographic high - the mound that is present today. Temperatures in the hole, as recorded by thermometer, were close to -8°C (17 to 18°F) at depths of 1.8 m (July 2nd) and 2.65 to 2.75 m (July 22nd), respectively.

Polar Bear Pass

Following the deglaciation of the hilltop peat site near Bracebridge Inlet, several hundred years elapsed before Polar Bear Pass became free of glacier ice, presumably in part because there still was a considerable flow into this valley from the plateau areas which reach elevations of over 800 feet to both the north and the south, and in part because after active flow had ceased, it still took time for the dead ice remaining in the valley to melt away. Two age determinations on marine mollusks delimit the time by which Polar Bear Pass had become an arm of the sea: sample GSC-377, 8440 ± 150 years old (Lowdon et al., 1967), composed of fragments of *Hiatella arctica* and *Mya truncata*, was collected in the central part of Polar Bear Pass at an elevation of 240 to 250 feet (73 to 76 m), and sample GSC-1873, 8220 ± 90 years old (Blake, 1974), made up of whole valves of *Mya truncata*, was found at an elevation of ca. 220 to 225 feet (67 to 69 m) at the eastern end of this through valley, southeast of the head of Goodsir Inlet (Fig. 1).

In round figures then, close to 8,500 years ago the sea filled Polar Bear Pass, which now does not exceed 100 feet (30 m) in elevation, to a depth of more than 150 feet (46 m). As the land rose relative to the sea, because of isostatic rebound following removal of the ice load, features such as the beach ridges shown in Figures 4 and 5, were cut at successively lower elevations; the particular ones illustrated, above the 200-foot (60-m) level, are close to 8,000 years old. On the other hand, the uppermost layer of *Mya truncata* shells exposed in a section along the Caledonian River at the western end of Polar Bear Pass is 4750 ± 140 years old (GSC-783; Blake, 1970; Lowdon et al., 1971), and sea level at the time these molluscs were living was an unknown amount above the level at which they now occur, ca. 75 feet (23 m). This is approximately the same elevation as that of the largest lake now occupying Polar Bear Pass (Fig. 1), indicating that this through valley persisted as an arm of the sea until nearly 4,500 years ago.

The various landforms now occupying the central section of Polar Bear Pass are displayed in Figures 4 and 5. During the melt season each year, much of the valley bottom is inundated, and as the pattern of braided channels shows, when in spate one branch of

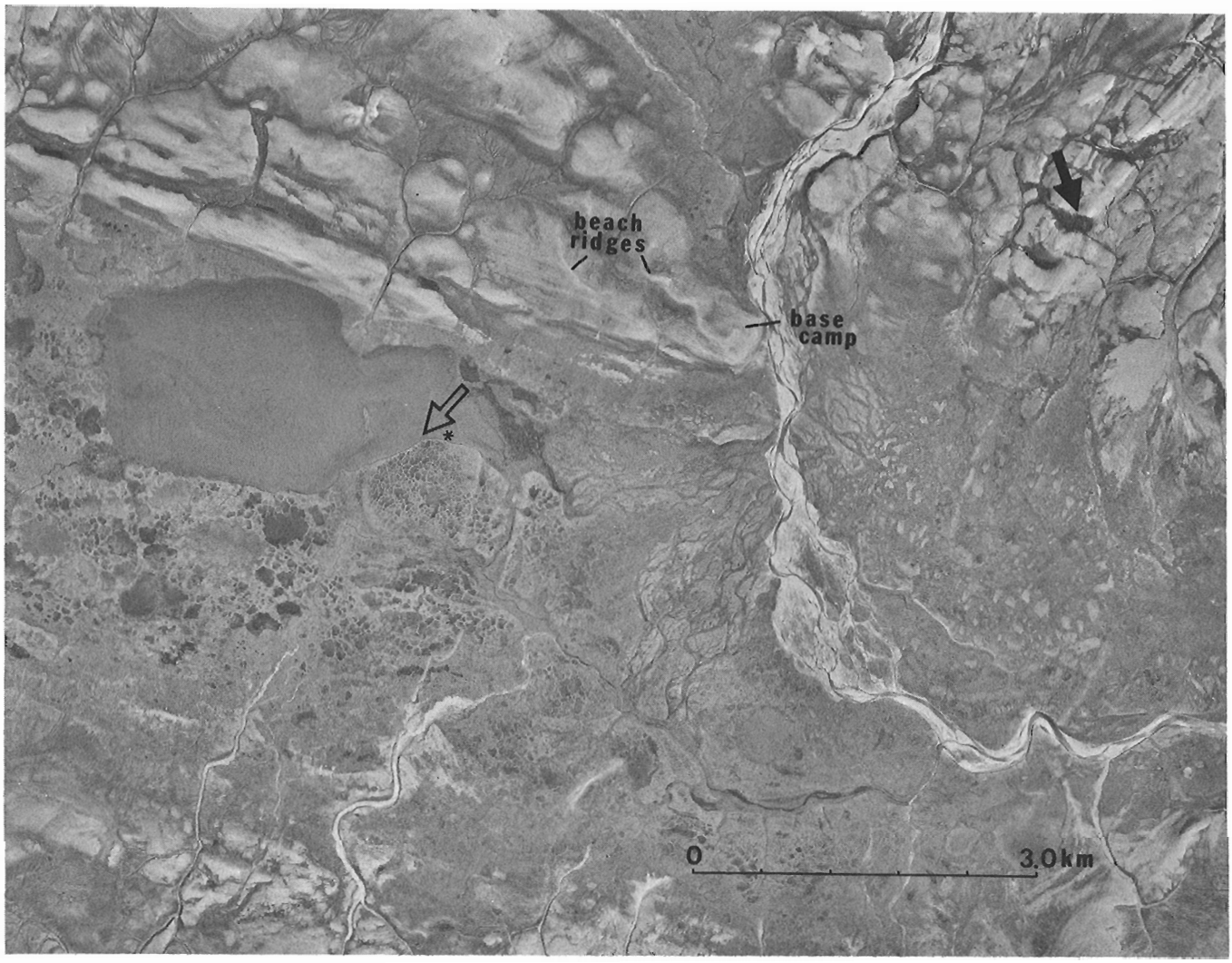

Figure 4. Part of air photograph A16203-66 (National Air Photo Library), taken from an altitude of 30,000 feet (ca. 9100 m), photo scale 1:60,000, July 25, 1958. Open arrow indicates position of Figure 6, Locality 2; asterisk shows location of ground photographs (Figs. 7 and 8); solid arrow shows drainage channel (Figs. 10 and 11, Loc. 3).

'Goodsir River' may flow westward into the large lake in the central part of the valley; otherwise this lake drains eastward to the river via a separate channel (cf. Fig. 1). The periodic inundation results in the deposition of silt on the tundra covering the valley bottom.

Particularly striking is the area of low-centred, non-sorted tundra polygons which characterizes the southeast side of the lake (Loc. 2, Fig. 1). The pattern there is best displayed in Figure 6, taken from a low-flying aircraft in 1963. The bank exposed along the lake shore, usually <2m high, in places was being undercut at lake level and large blocks of silty peat were toppling into the lake (Fig. 7). The dominant process here would appear to be thermoabrasion, defined by Are (1972) as "the destruction of shore zone under the action of mechanical and thermal energy of water". Although this type of erosion presumably is continuing, an examination of the air photographs taken in 1973 shows that it has not resulted in the drainage of any of the major lakes within the polygon area during the last decade (cf. Fig. 5) or in the 15 years since the original vertical air photography was flown (Fig. 4). In some places erosion along the lake shore has exposed ice wedges, such as the one shown in Figure 8, which underlie the ridges of the polygon area. The nature of the material in which the wedges have developed, alternating layers of tundra vegetation and inorganic material that has been washed in, is shown in the close-up photographs. Dominant mosses in the peaty layers at depths of both 45 to 47 cm and 75 to 78 cm are *Drepanocladus revolvens* and *Calliergon giganteum* (G.R. Brassard, pers. comm., 1967), the latter species also being a characteristic moss of a tundra pool area such as this (Kuc, 1973).

Another feature which has developed adjacent to the area of low-centred polygons is beaded drainage, the "beads" (pools) having formed as a result of

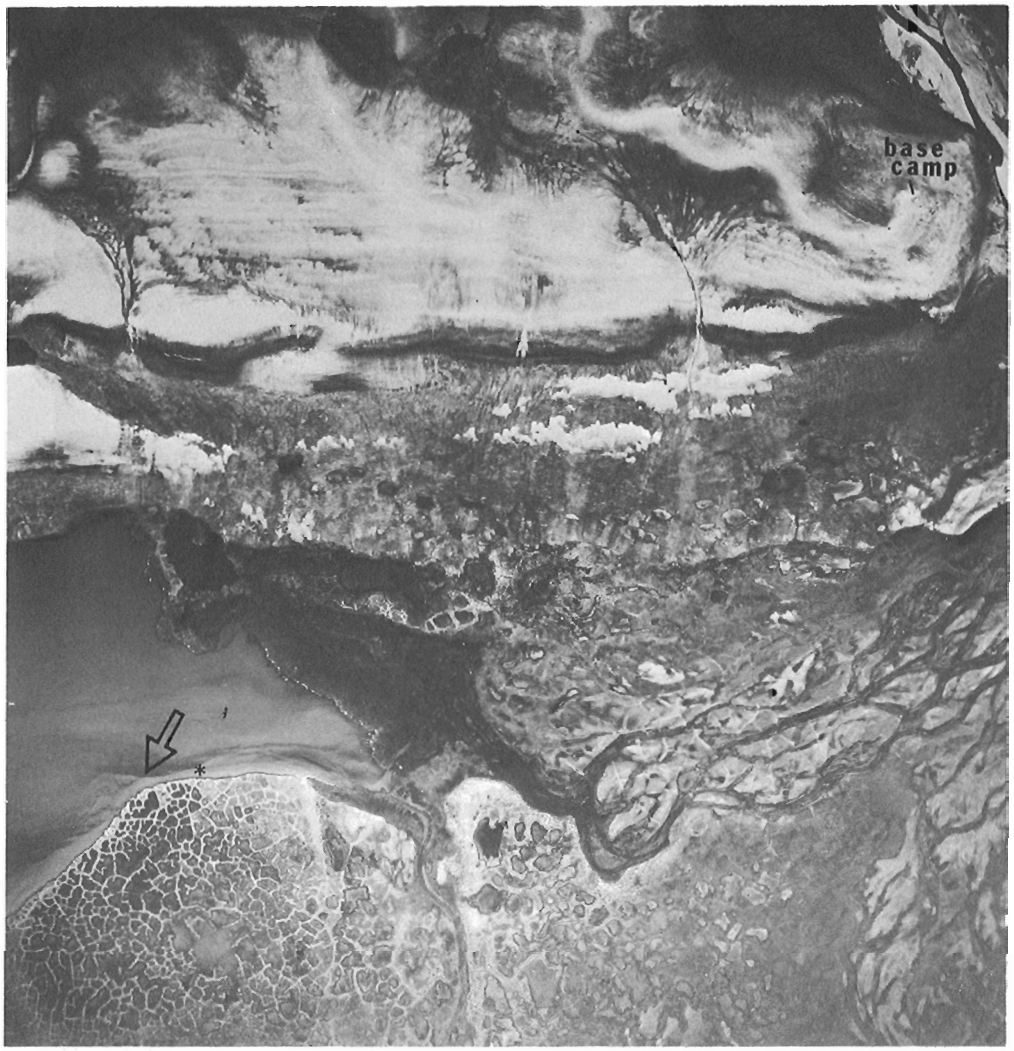

Figure 5.

Black and white print from colour infra-red air photograph A30816-107 (National Air Photo Library), taken from an altitude of 8,000 feet (ca. 2440 m), July 31, 1973. Note buildings of National Museum base camp at end of beach ridge, upper right-hand corner. Other symbols as in Figure 4.

thawing where a stream intersects ice-wedge junctions. The stream illustrated in Figure 9 certainly fits Washburn's (1973) description that "the connecting drainage is commonly along thawing ice wedges and therefore tends to comprise short straight sections separated by angular bends".

About 3.0 km to the northeast of the field station site overlooking 'Goodsir River', on the north side of Polar Bear Pass (Locality 3), a succession of marginal drainage channels have been cut across a prominent north-northeast-trending ridge developed in shale of the Cape Phillips Formation (of Upper Ordovician to Lower Devonian age; Kerr, in press). These channels were excavated by meltwater flowing toward Goodsir Inlet at a time when Polar Bear Pass was still occupied by ice. The largest of the channels is cut approximately 80 feet (24 m) below the ridge crest, and part of its flat bottom is occupied by small ponds for much or all of the summer season. Early in each summer, while the outlet of the channel is still dammed by the winter's accumulation of snow, the water level is higher, as can be seen from the strandline in Figure 10. The elevation of the channel bottom is ca. 295 feet (90 m), 40 feet (12 m) above the highest postglacial marine shells found in Polar Bear Pass.

Near the eastern end of the channel was a peat mount roughly 12 feet (3.5+ m) in diameter and rising ca. 4.5 feet (~1.5 m) above the general level of the channel bottom (Fig. 11). Some open cracks were present around the margin of the mound, and in places a small ridge, a few centimetres high, occurred peripheral to the cracks. On August 11, 1963 the peat was frozen below a depth of 40 cm, and on June 8, 1964, when coring was carried out, the level of frozen material was at a depth of only 13 to 23 cm. Unlike the mound described earlier, this feature consisted for the most part of peat for the first 2.5 m (although ice lenses were present), from 2.59 to 2.73 m ice was estimated to comprise half the core, and then from 2.73 to 2.90 m solid peat was encountered again. Below this level the content of ice increased, and little organic material was noticed below 3.26 m. From this level to 5.00 m the core consisted nearly entirely of ice. Lack of additional extension rods prevented further penetration, but the presence of sand and pebbles in the basal

Figure 6. Oblique air photograph of low-centred polygon area (Locality 2) shown in Figures 4 and 5; view southwestward. July 31, 1963. GSC photo No. 201950.

Figure 7. Detail of effects of thermoabrasion along lake shore. Note interbedded layers of vegetation and silt. August 3, 1963. GSC photo No. 202567.

Figure 8.

Ice wedge exposed under ridge bordering polygons along lake shore. Hammer handle is 22 cm long. August 6, 1963. GSC photo No. 202568.

sections of the core suggested that the bottom of the channel was close at hand. The lowest temperature recorded in the hole by thermometer was -17°C (1°F) at a depth of 3 m on June 9th. This value agrees well with the data presented by Brown (1972), in which the -17.5°C (0.5°F) isotherm for mean annual air temperature crosses north-central Bathurst Island.

This mound is perhaps best described as a miniature pingo, for although in dimensions it resembles a palsa more than a pingo, palsas are usually characterized by ice lenses rather than by a core of solid ice, an exception being those described from the central Yukon by Hughes et al. (1972). Palsas are also more commonly found in the zone of discontinuous permafrost (Lundqvist, 1969; Washburn, 1973). Nor does this miniature pingo correspond to the ice-cored mounds described from western Banks Island by French (1971), as those features were never more than 50 cm high, had only a thin organic cover above the ice core, and for the most part were located within low-centred tundra polygons.

Radiocarbon age determinations were carried out at two levels in the core. The lowest core increment from which enough organic material could be obtained for dating was at a depth of 3.12 to 3.26 m, and the age was 6510 ± 150 years (GSC-253, fraction soluble in NaOH; Lowdon et al., 1967). The uppermost sample dated, solidly frozen peat at 9- to 12-cm depth, was 1170 ± 150 years old (GSC-402, fraction not dissolved in NaOH; Lowdon et al., 1967), and according to M. Kuc the material was composed mainly of roots and rhizomes derived from the abundant growth of grasses and sedges in this boggy area (unpublished G.S.C. Bryological Rept. No. 281).

Thus the initial accumulation of organic material in this drainage channel took place significantly later than the time of deglaciation, as deduced from the age of nearby marine pelecypods. Once the formation of peat started, however, it continued for more than 5,000 years, and perhaps only ceased once the doming-up process started.

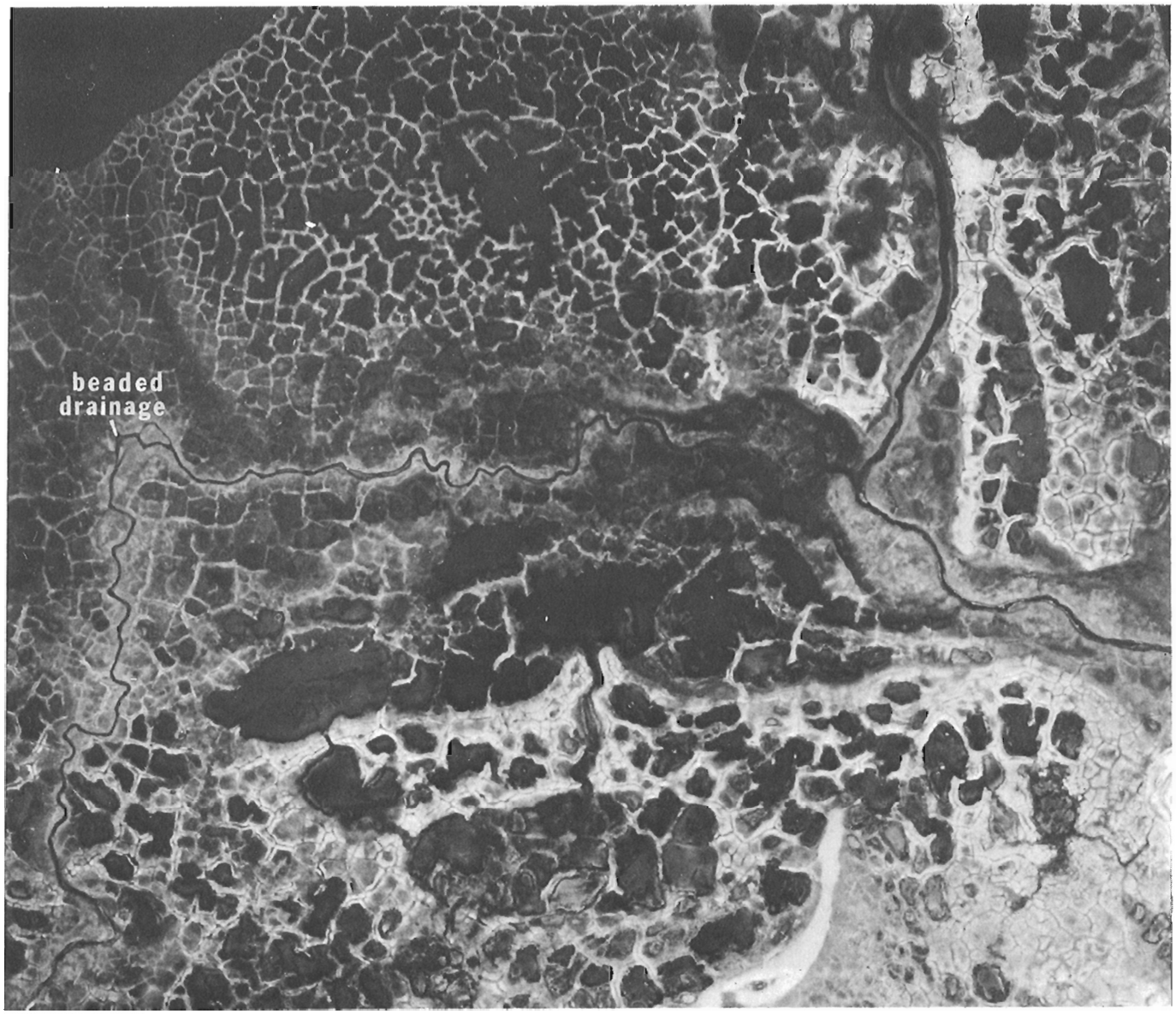

Figure 9. Beaded drainage south of low-centred polygon area (Locality 2) shown in Figure 5. Drainage to right toward 'Goodsir' River. Black and white enlargement from colour infra-red air photograph A30816-129 (National Air Photo Library), taken from an altitude of 8,000 feet (ca. 2,440 m), July 31, 1973.

Acknowledgments

The author is grateful to Dr. J. Wm. Kerr for providing base camp facilities on Bathurst Island, to J.D. Macdougal and D. Seller (1963) and F. Affleck (1964) for assistance with the coring, and to the late R. Warnock, Bradley Air Services, for his excellent work as pilot of our Piper Super-Cub. Drs. G.R. Brassard (now at Memorial University) and M. Kuc identified the mosses in peat samples, and the age determinations were carried out by the staff of the Geological Survey Radiocarbon Dating Laboratory. Dr. D.C. Thomas, Canadian Wildlife Service, kindly made available the colour infra-red air photographs taken for this organization by Survair, Ltd. D.A. Hodgson and Dr. P.J. Kurfurst provided helpful comments on the manuscript.

References

Are, F.E.
1972: The reworking of shores in the permafrost zone; in International Geography 1972 (eds. W.P. Adams and F.M. Helleiner); 22nd Int. Geogr. Cong., Montreal 1972, Univ. Toronto Press, Toronto, v. 1, p. 78-79.

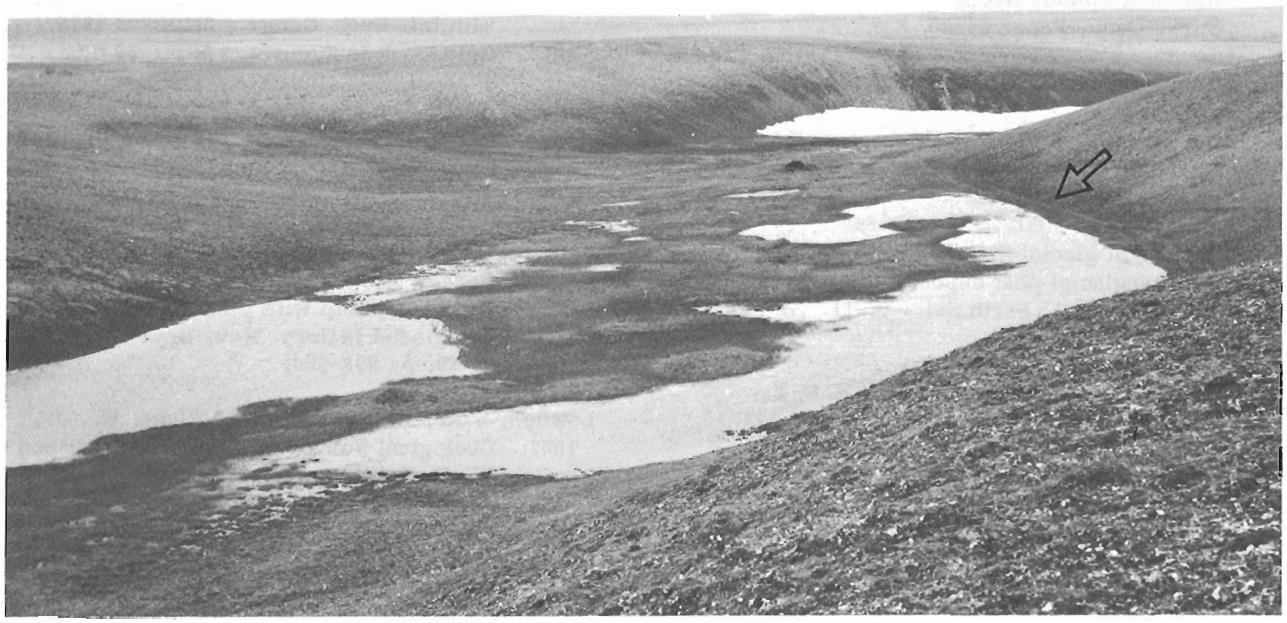

Figure 10. View eastward at miniature pingo in marginal drainage channel on north side of Polar Bear Pass (Locality 3). Note strandline (arrow) indicating higher water level when snow (remnant present in distance) blocks drainage earlier in summer. August 11, 1963. GSC photo 202569.

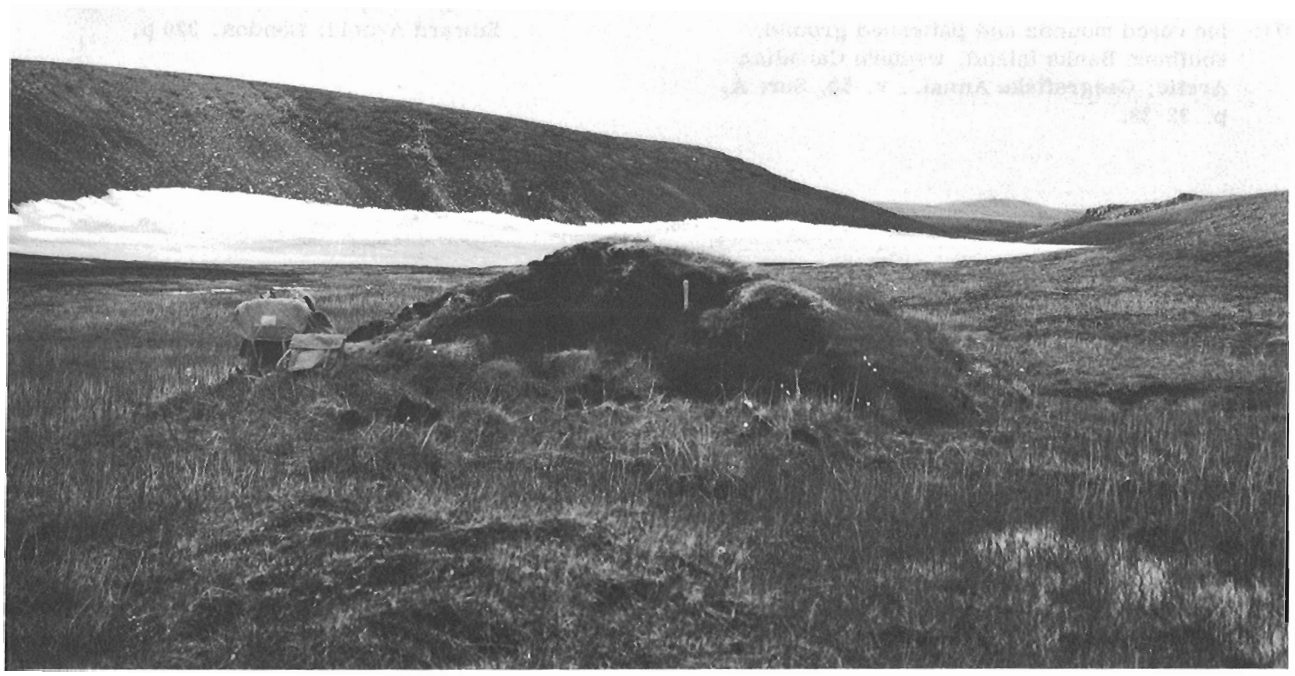

Figure 11. Detail of miniature pingo, shown in Figure 10, which was cored to a depth of 5.0 m. Hammer handle is 22 cm long. Peat at 9-12 cm depth, frozen, was 1170 ± 150 years old (GSC-402). August 11, 1963. GSC photo 202570.

Blake, W., Jr.
1964: Preliminary account of the glacial history of Bathurst Island, Arctic Archipelago; Geol. Surv. Can., Paper 64-30, 8 p.

1970: Studies of glacial history in Arctic Canada. I. Pumice, radiocarbon dates, and differential postglacial uplift in the eastern Queen Elizabeth Islands; Can. J. Earth Sci., v. 7, p. 634-664.

1974: Studies of glacial history in Arctic Canada. II. Interglacial peat deposits on Bathurst Island; Can. J. Earth Sci., v. 11. (in press)

Brassard, G.R., and Steere, W.C.
1968: The mosses of Bathurst Island, N.W.T., Canada; Can. J. Bot., v. 46, p. 377-383.

Brown, R.J.E.
1972: Permafrost in the Canadian Arctic Archipelago; Zeit. fur Geomorph. N.F., Suppl. Bd. 13, p. 102-130.

Dyck, W., Fyles, J.G., and Blake, W., Jr.
1965: Geological Survey of Canada radiocarbon dates V; Radiocarbon, v. 7, p. 24-46.

Dyck, W., Lowdon, J.A., Fyles, J.G., and Blake, W., Jr.
1966: Geological Survey of Canada radiocarbon dates VI; Radiocarbon, v. 8, p. 96-127.

French, H.M.
1971: Ice cored mounds and patterned ground, southern Banks Island, western Canadian Arctic; Geografiska Annal., v. 53, Ser. A, p. 32-38.

Hughes, O.L., Rampton, V.N., and Rutter, N.W.
1972: Quaternary geology and geomorphology, southern and central Yukon (northern Canada); 24th Int. Geol. Congr., Montreal 1972, Guidebook to Excursion A-11, 59 p.

Kerr, J. Wm.
Bathurst Island group and Byam Martin Island; Geol. Surv. Can., Map 1350A. (in press)

Kuc, M.
1973: Addition to the arctic moss flora. VI. Mossflora of Masik River valley (Banks Island) and its relationship with plant formations and the postglacial history; Rev. Bryol. et Lichénol., v. 39, p. 253-264.

Lowdon, J.A., Fyles, J.G., and Blake, W., Jr.
1967: Geological Survey of Canada radiocarbon dates VI; Radiocarbon, v. 9, p. 156-197.

Lowdon, J.A., Robertson, I.M., and Blake, W., Jr.
1971: Geological Survey of Canada radiocarbon dates XI; Radiocarbon, v. 13, p. 255-324.

Lundqvist, J.
1969: Earth and ice mounds: a terminological discussion; in The Periglacial environment (ed. T.L. Péwé); Arctic Institute of North America, McGill-Queen's University Press, Montreal, p. 203-215.

Washburn, A.L.
1973: Periglacial processes and environments; Edward Arnold, London, 320 p.

A CONTACT BETWEEN MASSIVE ICE AND WEDGE ICE, TUKTOYAKTUK COAST, DISTRICT OF MACKENZIE (107 C)

Project 680047

A. Gell*
Terrain Sciences Division

Introduction

Ground ice along the Beaufort Sea coast near Tuktoyaktuk has been studied in cliff exposures and core samples. Standard petrologic techniques have been employed.

Massive-ice bodies underlie topographic highs. Superimposed on these highs are ice-wedge polygons; however, ice wedges may occur without such surface expression. Ice wedges may penetrate the massive ice at depth. The characteristics of each ice type examined are discussed to aid in field or laboratory distinction of the ice types from small samples.

Site Description

A massive-ice body greater than 20 m thick contains bands of clear ice, bubbly ice, and discontinuous sediment-rich layers (Rampton and Mackay, 1971, Fig. 11). The layers are generally subhorizontal, but at the sides of the mass open folds have formed during long-term creep. Overlying the massive ice is 5 m of stony clay, which thins to 1.5 m over anticlines. Here, ice wedges have penetrated the ice and further deformed the banding.

Differences between Massive Ice and Wedge Ice

The two ice types are discussed in terms of sediment content, foliation, bubble type, and crystal size, shape, preferred dimensional and lattice orientations (cf. Black, 1951; Shumskii, 1964).

Bubble Bands

In wedge ice, bubble foliations are approximately vertical, parallel to the axial plane of the wedge and 5 m thick. No clear ice bands occur. Organic and inorganic material may be incorporated in some foliations. Bubble bands in massive ice vary from 5 cm to 1 m in thickness, alternating with clear ice and thinner, less-continuous, sand-rich ice bands. Foliation orientation is usually subhorizontal but may be locally deformed.

Bubble Type

Bubble type varies with ice type. In wedge ice, high concentrations of spherical bubbles less than 0.3 mm in diameter give the ice a milky appearance. Additionally, bubbles elongated up to 1 cm vertically may be present. Bubbles occur within crystals, on grain boundaries, and across such boundaries. Massive ice contains elongate, ellipsoidal, and spherical bubbles. Major axes of elongate bubbles trend normal to the local foliation and reach 1.2 cm in length. Both spherical bubbles, which range in diameter up to 5 mm, and ellipsoidal bubbles occur in a given band, in concentrations as high as 100 per cm^3. On surfaces exposed to solar radiation, Tyndall figures are found - flat, hexagonal figures parallel to the basal plane of the containing crystal.

Crystal Size

Crystal size varies with position in each ice type. In wedge ice, crystals range from 1 mm^2 in area near the central crack to 1 cm^2 at wedge edges. In massive ice, crystals reach over 4 cm^2 in both clear and bubbly layers, but interstitial ice crystals in sediment-rich bands are less than 1 mm^2.

Crystal Shape

In wedges, crystals are usually anhedral or subhedral, some euhedral crystals growing in the contraction crack. Massive-ice grains are generally anhedral with some subhedral. Most grain boundaries show single curvature; where strong curvatures occur they are associated with bubbles that have retarded migration of the grain boundary.

Dimensional Orientation

Long axes of crystals vary widely in orientation in both ice types. In wedges, crystals are commonly elongated vertically, parallel to the bubble foliation; preferred orientations normal to the foliation also occur. In massive ice, crystals are elongated normal to foliation where the foliation is undisturbed. No strong orientation pattern occurs in the sediment bands. Adjacent to the wedge, massive ice is subject to the lateral stress associated with the wedge and some flattening of crystals occurs. This is partly masked by micro-faulting, parallel to the wedge, that offsets some crystals.

Lattice Preferred Orientations

Orientations of optic axes vary with grain size and position in wedges. Small crystals at wedge centres have horizontal c-axes; this pattern is rotated with distance from the centre of the wedge and as crystals become larger. In massive ice away from wedges, optic axes are approximately normal to folia-

*Department of Geography, University of British Columbia, Vancouver, B.C. V6T 1W5.

tion. Adjacent to wedges, lattice orientations trend toward those of outer wedge crystals.

Summary

Petrologic characteristics of massive ice and wedge ice have been enumerated to aid in recognition of ice type from limited core samples or from poor exposure.

References

Black, R. F.
1951: Structures in ice wedges of Northern Alaska; Geol. Soc. Am. Bull., v. 62, p. 1423-1424 (Abstract).

Rampton, V. N., and Mackay, J. R.
1971: Massive ice and icy sediments throughout the Tuktoyaktuk Peninsula, Richards Island, and nearby areas, District of Mackenzie; Geol. Surv. Can., Paper 71-72, 16 p.

Shumskii, P. A.
1964: Principles of structural glaciology; Dover Publications, New York, 497 p.

95. FLUME STUDIES OF ISOLATE GRAVEL FABRIC ON A SAND BED

Project 710070

E. H. Koster*
Terrain Sciences Division

Introduction

As a complementary study to fieldwork concerning modern coarse-grained fluvioglacial outwash in southwest Yukon, the Geological Survey of Canada sedimentation flume (McDonald, 1972) has been used to examine selected sedimentary phenomena observed in the field. This report describes the findings of the first suite of experiments that involved isolate gravel fabric on a sand bed. Laming (1966) distinguished between 'isolate' and 'contact' imbrication on morphogenetic grounds; the latter type will be the subject of further flume studies.

The purpose of these experimental studies is twofold:

1) to gain a better understanding of the hydrodynamic and sediment parameters influencing development of 'anisotropic apposition fabrics' (Pettijohn, 1957) in coarse modern alluvium; and
2) to extend these findings to reconstruction of ancient paleoflow regimes in similar deposits.

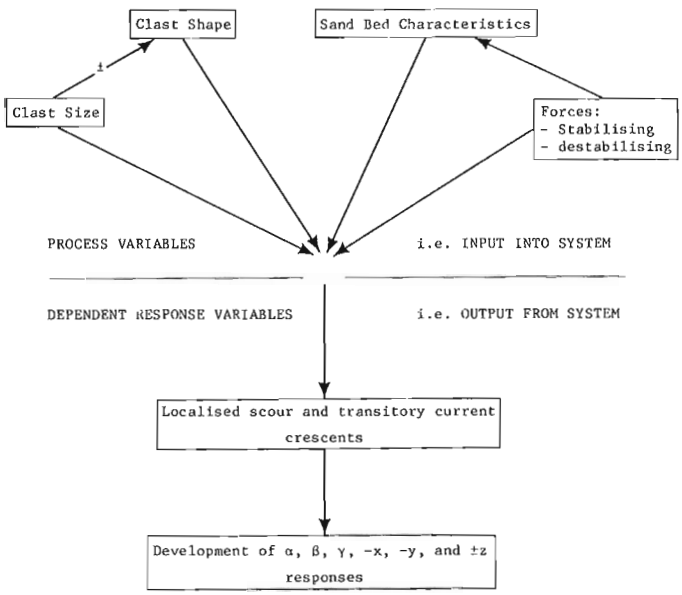

Figure 1. The dynamic system of isolate gravel fabric on a sand bed.

*Geology Department,
University of Ottawa,
Ottawa. K1N 6N5.

Material and Experimental Methods

A large heterogeneous gravel population was collected from local Pleistocene deposits. Each clast was numbered, and numerous measures of size and 'form' (Whalley, 1972) were obtained for each. The clasts varied in weight from 50 to 2,500 grams. Morphological parameters used include those listed by Johansson (1963).

Selected compact, blade, and rod-shaped clasts were spaced uniformly with a-axes transverse to flow and a-b planes parallel to bed slope in each run.

The flume was flooded before each experiment in order to avoid surge effects. Runs were continued until all the clasts had attained a stable configuration through the action of local scour and transitory current crescents. Routine measurements were made during each run to enable calculation of the various flow parameters; Froude number was utilized as the main index of run differentiation.

The lower and upper flow regimes were spanned at intervals of approximately 0.05 Froude number by adjusting slope, discharge, and tailgate height for each run. A 'depth-velocity diagram' (Southard, 1971) had already been established for the sand in use.

The analysis has employed a 'process-response' model (Fig. 1; Krumbein, 1964). The method involves the inference of 'process', on statistical grounds, from the observed 'response'. The response variables measured for each clast (following run shut-down, drying of the sand bed, and exposure by spatula) are listed in Table 1.

Preliminary Analysis of Response

α Response

While there exists significant correlation of a-b dip with clast flatness ($r = -0.692$) and with clast size, expressed as the intermediate b-axis ($r = -0.437$), a complete explanation of the α response lies in a consideration of the clast mass and the cross-sectional area facing the +x flow direction. Each run yields a distinct relationship of the form $m = a\,(A_{\alpha\ \text{stable}})^b$ where m denotes mass (grams) and $A_{\alpha\ \text{stable}}$ denotes the aforementioned area when hydrodynamic stability has been attained by the imbricated clast with respect to the flow. Correlation coefficients of these double logarithmic plots are consistently above 0.95. The coefficient a and the exponent b display systematic variation through the lower and upper flow regimes in response to the changing balance of stabilizing and destabilizing forces (Allen, 1970, p. 61). Paired values of a and b have the relationship $a = 5.2b^{-4.7}$ ($r = -0.989$). Individually, a and b when plotted

Table 1

Types of response

Variable Notation	Description of Variable
α^{o}	dip of the a-b plane
β^{o}	azimuth of the a-axis
γ^{o}	inclination of the a-axis
-x cm	negative movement parallel to the x flow axis (i.e. upstream)
-y cm	negative movement parallel to the y flow axis (i.e. downward, into the bed)
±z cm	movement parallel to the z flow axis (i.e. across the flow)

against their corresponding Froude number display parabolic relationships. In the dune regime, the exponent and coefficient attain maximum and minimum values respectively.

Field measurements from single sedimentation units in gravel, that enable a determination of a and b, might therefore allow deduction of paleoflow strength by substitution in the empirical quadratic relations.

β Response

Directional data have been treated according to the 'angular deviation' method of the Sedimentary Petrology Seminar (1965) and the 'unit vector' method of Curray (1956); each permits a slightly different approach to process determination.

The stable clast configuration was found to be a current-normal orientation of the a-b plane and the a-axis. Increasing clast size expressed as the a-axis and increasing elongation, however, yield higher vector magnitudes. The variability attributable to size alone was detected by Rust (1972). Also, pronounced clast asymmetry is effective in causing high deviation despite an otherwise favourable clast morphology. The β response with varying Froude number is variable according to the equilibrium bedform. As the bedform irregularity increases from ripples to dunes, the vector magnitude decreases, but a maximum is attained at the transitional planebed situation. Then, as antidune activity becomes increasingly vigorous, the magnitude again decreases.

γ Response

The theoretical consequence of clast asymmetry is for the a-axis to be inclined in the direction of greater mass concentration. This relationship does prevail. The portion of the gravel population that lies within ±1 standard deviation of the mean density value (gm/cm^3) correlates highly with a-axis inclination ($r = 0.942$). The least-squares regression line correctly predicts a γ response of zero when the clast is perfectly symmetrical. Anomalous values of γ are obtained when, despite low clast asymmetry, the downstream migration of sinuous-crested bedforms in the lower regime and the high turbulence beneath breaking antidunes in the upper regime effects a randomness in the response.

-x Response

In conjunction with the scour processes, which eventually produce a stable α response, clasts undergo varying distances of upstream movement. Fahnestock and Haushild (1962) described upstream movement by rolling of high-sphericity clasts at flows below their transport threshold. For the gravel population used in the present experiments, the movement is by sliding, except for compact clasts with high circularity in the b-c plane. The important process variables which explain the -x response are log (mass) and the 'angle of sliding friction' (Van Burkalow, 1945) of each clast; correlation coefficients are -0.505 and 0.579, respectively. However, for compact clasts alone the coefficients are -0.963 and 0.919. The angle of sliding friction was determined experimentally according to the method used by Van Burkalow using a tiltable surface of medium sand paper (to simulate sliding on the sand bed in the scour hollow). On account of the inequidimensional nature of the clasts employed in the present study, the main control on the angle of sliding friction is not log (mass) for which $r = 0.043$ but the maximum projection sphericity (Sneed and Folk, 1958) which yields a coefficient of -0.638.

The lower-regime bedforms involving a relatively high fluctuation of local bed elevation are conducive to maximum values of -x response; a secondary maxima is developed at high Froude number where the bed is characterized by antidunes.

-y Response

On a priori grounds it was considered more instructive to combine the -x and -y response of each clast into the angle q, calculated as tan (x/y), which represents the angle at which the clast moved simultaneously upstream and down into the sand bed during the imbrication process. The precise path of the downward movement is probably concave-up and not straight as calculated, since the Reynolds number of the imbricating clast (Karcz, 1968) decreases as a full logarithmic function of the relative roughness (i.e. a concave-upward curve on cartesian co-ordinates). Furthermore, monitoring of the imbrication process for the same blade-shaped clast in each run indicates that it is also exponential with respect to time, and the exponent displays systematic variation with flow regime.

The process variables which influence a relatively large q response each attain their maximum effect at differing flow conditions, indicating a delicate interplay of the factors responsible for scour and -x response.

±z Response

This response, as perhaps anticipated, is somewhat related to clast asymmetry although the correlation coefficient is just below the 95% significance level. As already noted, the clast asymmetry partially is responsible for a-axis inclination. This in turn causes a lateral component, transverse to flow, to be developed in conjunction with upstream motion. The most pronounced relationship realized for the ±z response is its perfect in-phase relation with the -x response (i. e. mean values obtained for these two responses in each run are linearly related with near perfect correlation). The absence of lag between this pair of responses is interesting in view of the generally diverse nature of important process variables which control each of the six responses.

Conclusions

1) Movement and reorientation of isolate pebbles and cobbles on a sand bed is an extremely complex sedimentological phenomenon. In general, the present work concurs with the earlier findings of Kelling and Williams (1967), Fahnestock and Haushild (1962), and Johansson (1963). The statement of Briggs and Middleton (1965, p. 11) that "no single shape factor is sufficient to express the hydraulic behaviour" of sedimentary particles is firmly endorsed.

2) The α response would appear to be the most fundamental in that it exerts a strong control on the hydrodynamics of scour. It is considered therefore that the other five types of response develop in accordance with the requirements that satisfy the relationship between clast mass and A_α stable.

3) The study attempts an explanation of a hitherto poorly understood phenomenon, and tentatively offers certain relationships between clast orientation and flow that may be of use in reconstructing paleoflow conditions of modern and ancient coarse-grained fluvial sediments.

References

Allen, J.R.L.
1970: Physical processes of sedimentation; Unwin University Books.

Briggs, L.I., and Middleton, G.V.
1965: Hydromechanical principles of sediment structure formation; p. 5-16 in Primary Sedimentary Structures and their Hydrodynamic Interpretation (ed. G.V. Middleton), Soc. Econ. Paleontol. Mineral., Spec. Pub. No. 12, 265 p.

Curray, J.R.
1956: The analysis of two-dimensional orientation data; J. Geol., v. 64, p. 117-131.

Fahnestock, R.K., and Haushild, W.L.
1962: Flume studies of the transport of pebbles and cobbles on a sand bed; Geol. Soc. Am. Bull., v. 73, p. 1431-1436.

Johansson, C.E.
1963: Orientation of pebbles in running water. A laboratory study; Geog. Annal., v. 45, p. 85-112.

Karcz, I.
1968: Fluviatile obstacle marks from the wadis of the Negev (southern Israel); J. Sediment. Petrol., v. 38, p. 1000-1012.

Kelling, G., and Williams, P.F.
1967: Flume studies of the reorientation of pebbles and shells; J. Geol., v. 75, p. 243-267.

Krumbein, W.C.
1964: The cyclothem as a response to sedimentary environment and tectonism; Kansas State Geol. Surv., v. 169, p. 239-247.

Laming, D.J.C.
1966: Imbrication, paleocurrents and other sedimentary features in the Lower New Red Sandstone, Devonshire, England; J. Sediment. Petrol., v. 36, p. 940-957.

McDonald, B.C.
1972: The Geological Survey of Canada sedimentation flume; Geol. Surv. Can., Paper 71-46.

Pettijohn, F.J.
1957: Sedimentary rocks; New York, 2nd ed., 718 p.

Rust, B.R.
1972: Pebble orientation in fluvial sediments; J. Sediment. Petrol., v. 42, p. 384-388.

Sedimentary Petrology Seminar
1965: Gravel fabric in Wolf Run; Sedimentology, v. 4, p. 273-283.

Sneed, E.D., and Folk, R.L.
1958: Pebbles in the lower Colorado River, Texas - a study in particle morphogenesis; J. Geol., v. 66, p. 114-150.

Southard, J.B.
1971: Representation of bed configurations in depth-velocity-size diagrams; J. Sediment. Petrol., v. 41, p. 903-915.

Van Burkalow, A.
1945: Angle of repose and angle of sliding friction: an experimental study; Bull. Geol. Soc. Am., v. 56, part I, p. 669-708.

Whalley, W.B.
1972: The description and measurement of sedimentary particles and the concept of form; J. Sediment. Petrol., v. 42, p. 961-965.

MEASUREMENT OF UPWARD FREEZING ABOVE PERMAFROST WITH A SELF-POSITIONING THERMISTOR PROBE

Project 680047

J. Ross Mackay*
Terrain Sciences Division

Introduction

The active layer above permafrost undergoes an annual freeze-thaw cycle. During the autumn months two freezing fronts are in motion, one moving downward from the ground surface and the other moving upward from the summer depth of maximum thaw. The downward-advancing front usually moves faster, because it is driven by a steeper temperature gradient. The two fronts commonly meet in the lower third of the active layer but the depth varies yearly, depending on factors such as snow cover, air temperature, and water content of the soil. When a natural site is disturbed so as to deepen the active layer or where there is a thick artificial fill which causes an upward rise of the permafrost table, it may be advantageous to monitor the change, because such sites are conducive to ice lensing. It is the purpose of this paper to describe a selfpositioning thermistor probe which can be used to measure the rate of upward freezing. Field tests have been carried out for three years at Garry Island, N.W.T., 160 km northwest of Inuvik, N.W.T.

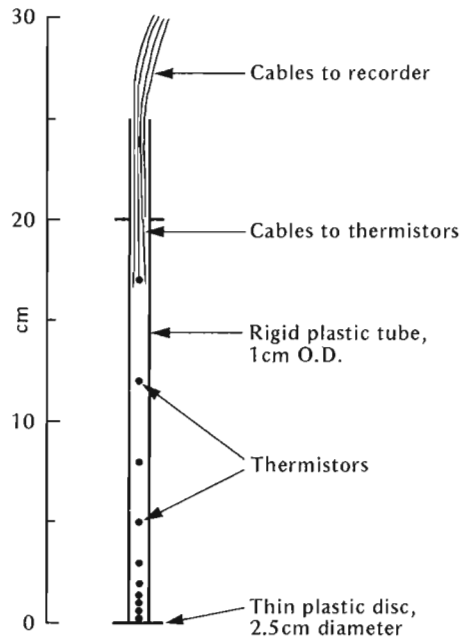

Figure 1.

Sketch of a self-positioning thermistor probe designed to fit inside a frost tube. Where the active layer is thick or there is a deep artificial fill, the probe should be made much longer.

Measurement

The downward and upward freezing of the active layer customarily is measured with temperature sensors spaced appropriate to the active layer thickness and recording equipment available. The measurement of downward freezing is straightforward, because freezing starts at a known position - - the ground surface. But measurement of the upward freezing is much more difficult, because the position of the frost table rarely will be known in advance, especially at an artificially disturbed site.

Self-Positioning Thermistor Probe

A self-positioning thermistor probe (Fig. 1) may be used in conjunction with a conventional frost tube to measure upward freezing from the frost table of late summer. A frost tube consists of an outer rigid casing, installed vertically into the ground, and a removable water- (ice-) filled inner frost tube (Mackay, 1973). In winter, water in the inner frost tube

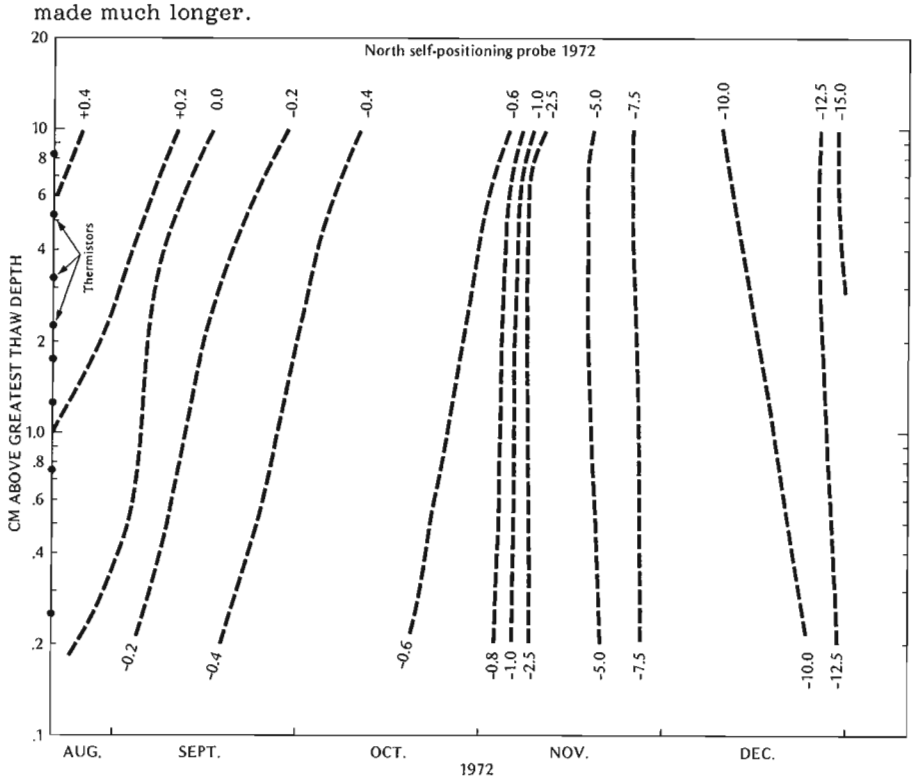

Figure 2. Temperature data (°C) for August to December 1972 for a self-positioning probe. A logarithmic depth scale has been used because of the closely spaced thermistors.

*Department of Geography, Univer- University of British Columbia, Vancouver, B.C. V6T 1W5.

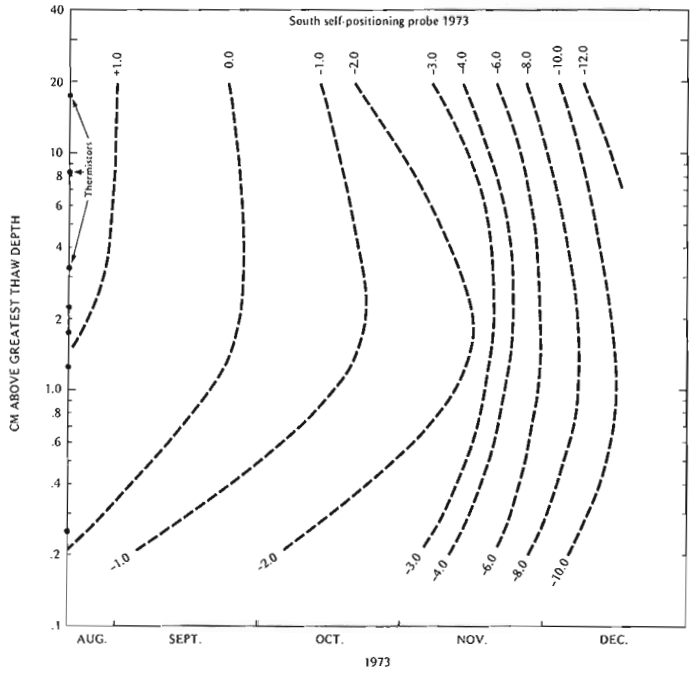

Figure 3. Temperature data (°C) for August to December 1973 for a self-positioning probe, located 21 m from the one in Figure 2. A logarithmic depth scale has been used.

freezes; in the following summer, thaw in the frost tube coincides reasonably well with that in the active layer; in the autumn freeze-back, water in the frost tube freezes downward from the ground surface and upward from the frost table until the two freezing fronts meet. The self-positioning thermistor probe is inserted into a frost tube in summer. The probe, which rests on the ice in the frost tube, descends as the ice melts in response to active layer thaw. Therefore, the probe is self positioned at the frost table when upward freezing starts, and closely spaced temperature measurements can be recorded.

The self-positioning probes, which have been used to measure upward freezing, have 10 thermistors inside a 25-cm long plastic tube (Fig. 1) which fits into an inner frost tube. The thermistors are spaced more closely together at the bottom, where upward freezing commences, in order to provide better resolution of data. Teflon insulated cables, which remain flexible at low temperatures, are used for the thermistor leads. The teflon cables are coiled loosely above the probe to permit unimpeded descent of the probe. The cables are connected outside the top of the frost tube to a multiconductor cable leading to a recorder in a nearby field cabin.

Discussion

Figures 2 and 3 show freeze-back temperature records for two self-positioning probes for 1972 and 1973 at two similar sites about 21 m apart on a wind-blown hummocky ridge. The active layer depth ranges from 25 cm to 80 cm, and is deepest beneath earth hummocks. The snowdepth rarely exceeds 5 to 10 cm and the mean annual ground temperature is about $-8^{\circ}C$. Figures 2 and 3 show that upward freezing commenced in late August and it was not until mid-December that cooling from downward freezing was more effective than cooling from upward freezing at the bottom of the active layer. Upward freezing resulted in considerable ice lensing.

Comparison with temperature measurements at nearby sites, supplemented with probing, show that the principal source of error lies in heat conduction along the frost tube in summer. Heat conduction can be minimized by keeping the top of the outer frost tube flush with the ground surface, but care must be taken to ensure that any winter frost heave of the active layer does not detach the cap.

Conclusion

The self-positioning thermistor probe can give good results in the measurement of upward freezing. The results obtained show a considerable year to year and site to site variation in the amount of upward freezing. Self-positioning probes, with lengths appropriate to side conditions, should be suitable for measuring the rise of the upper permafrost surface under areas of deep fill or to monitor degradation at disturbance sites.

Reference

Mackay, J.R.
1973: A frost tube for the determination of freezing in the active layer above permafrost; Can. Geotech. J., v. 10, p. 392-396.

PERFORMANCE OF A HEAT TRANSFER DEVICE, GARRY ISLAND, N.W.T.

Project 680047

J. Ross Mackay*
Terrain Sciences Division, Vancouver

Introduction

Heat transfer devices have been used to cool the ground by means of natural convection, utilizing summer-winter temperature contrasts (Babb et al., 1971; Jahns et al., 1973; Johnson, 1971; Long, 1966). In permafrost areas, the heat transfer devices may be designed to prevent thawing of soils, stabilize the ground, minimize heat conduction along piles, and so forth. In the summer of 1971, six heat transfer devices (Thermo Tubes[1]) were installed at Garry Island, N.W.T., 160 km northwest of Inuvik, N.W.T. The objective was to induce cooling at the top of permafrost and thus to simulate a climatic change, by means of which the active layer would be thinned and resulting permafrost effects could be studied. Because heat transfer devices are of applied interest and field data from arctic areas are few, the purpose of this paper is to report on the cooling effect of the Thermo Tubes for one calendar year, August 1971 to August 1972.

Thermo Tube

A Thermo Tube comprises, basically, steel pipe, filled with an appropriate heat transfer liquid, inserted vertically into the ground with an internal flow dividing system near ground level (Fig. 1). In winter, the above-ground portion is subjected to much colder temperatures than the lower portion in the ground. Natural convection occurs in the liquid-filled pipe, with flow channeled by a system of internal flow dividers. The liquid then circulates as long as the top part above ground is colder than the lower part in the ground. In summer, with a temperature inversion, circulation ceases. In theory, the Thermo Tube acts as an irreversible one-way heat transfer device (a thermal diode) which requires no power and minimal maintenance.

The Thermo Tubes in use at Garry Island are relatively small (Type 211 HC) measuring 2.4 m in length,

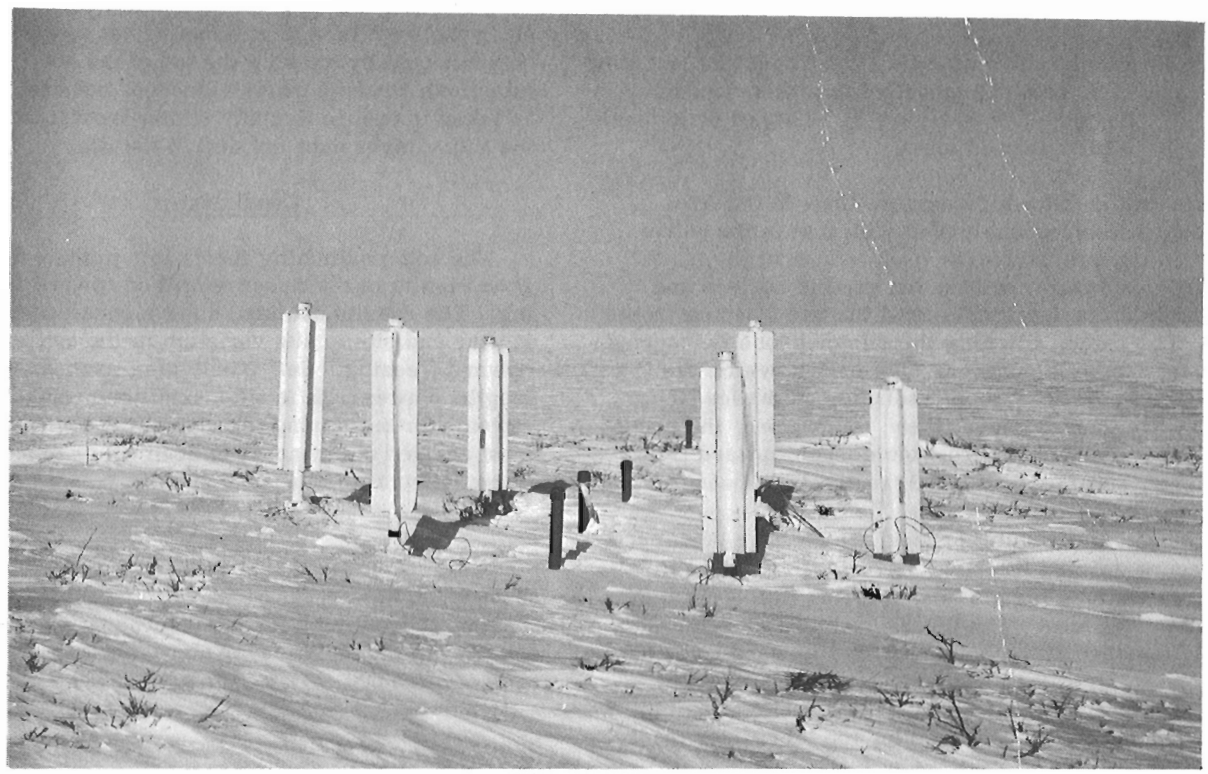

Figure 1. Six Thermo Tubes arranged in a hexagon. The four small dark pipes are frost tubes to follow freezing in the active layer. Garry Island, Northwest Territories, March, 1972.

*Department of Geography, University of British Columbia, Vancouver, B.C. V6T 1W5.

[1]Thermo-Dynamics Inc., Seattle, Washington.

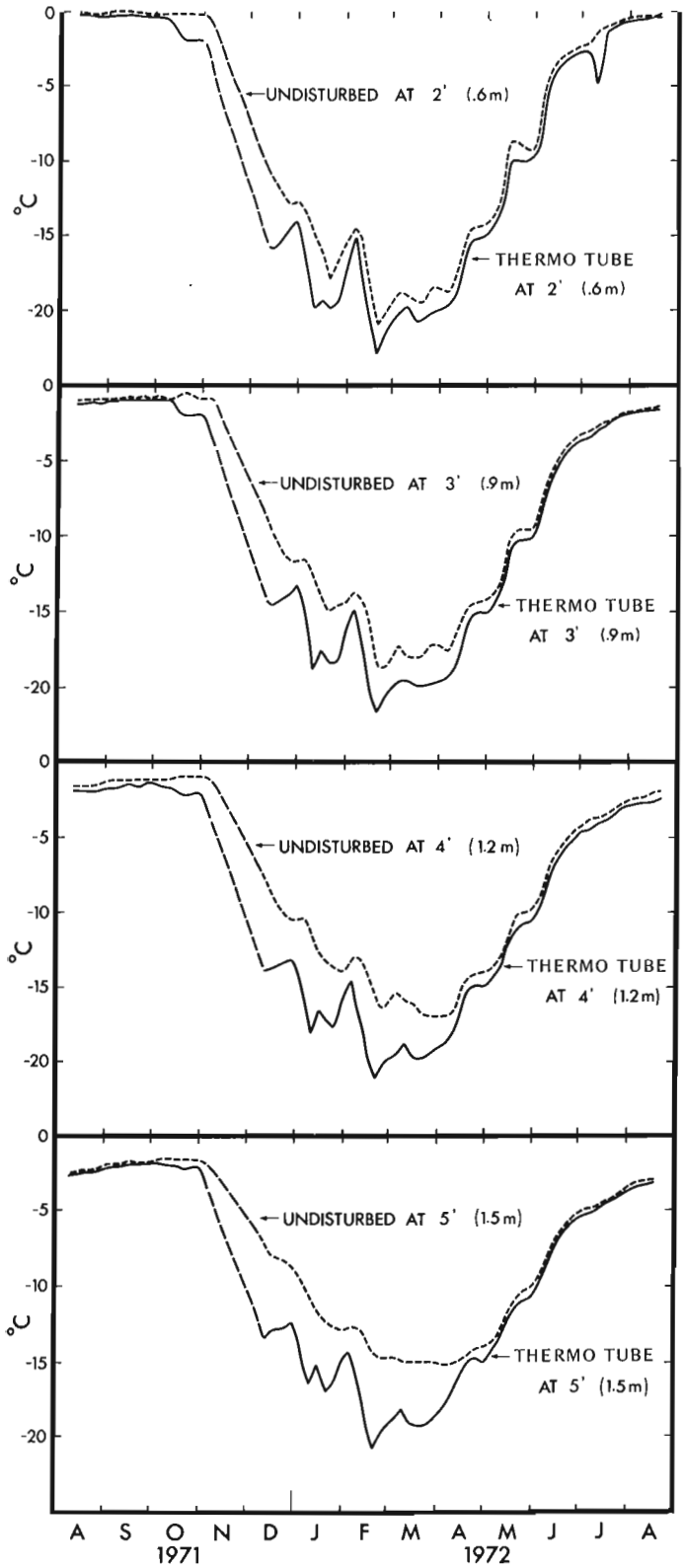

Figure 2. Temperature measurements (1971-72) for one Thermo Tube and an undisturbed site nearby. Garry Island, Northwest Territories.

90 cm of which is above ground and 1.5 m below ground. The liquid-filled steel pipe, 4.8 cm in outer diameter, is plugged at both ends. The above-ground portion has six radial fins, each 75 cm long and 10 cm wide. The fins accelerate winter cooling of the pipe. The flow dividers are close to ground level. In order to reduce heat conduction down the pipe in summer, a slight modification was made in the model by inserting a flange break in the pipe, separated by a 1.5 cm PVC coupling just above ground level.

Six Thermo Tubes were installed at the vertexes of a hexagon with 1.25-m sides (Fig. 1). Thermistors were attached at a 0.3-m depth to four Thermo Tubes; for the other two Thermo Tubes, thermistors were placed at depths of 0.3 m, 0.6 m, 0.9 m, 1.2 m, and 1.5 m. The thermistors at depths of 0.6 m, 0.9 m, 1.2 m, and 1.5 m for one of the Thermo Tubes were connected to a recorder in a nearby field cabin. For control purposes, ground temperatures at the same thermistor depths as for the Thermo Tubes at an undisturbed site located 13.5 m from the centre of the Thermo Tube array also were recorded. In addition, four frost tubes, to measure upward and downward freezing (Mackay, 1973), also were installed in the hexagon array (Fig. 1).

Field checks have been made of the Thermo Tube installation at least twice in the winter and twice in the summer from August 1971 to December 1973. During the field checks, temperatures were read manually, the snow depth was noted in winter, and thaw depths were probed in summer. The Thermo Tube site is on the crest of a wind-blown ridge where just enough snow accumulates to smooth the hummocky surface. The tops of the hummocks rarely have more than 5 cm of snow. The soil is a stony silty clay (reworked till).

Discussion

The temperature data for one Thermo Tube and an adjoining undisturbed site for 1971-72 are plotted in Figure 2. Field checks for 1972-73 have shown a similar temperature pattern. Figure 2 shows that in winter the Thermo Tube was very effective in cooling the ground from November to April. The amount of cooling increased with depth, and as expected, the greatest cooling was at 1.5 m. The short period fluctuations at the Thermo Tube site also exceeded those at the undisturbed site.

In summer, the temperature differences between the Thermo Tubes and undisturbed sites, depth for depth, have been negligible for the 1971-73 period, amounting to only about 0.5°C. With little doubt, the Thermo Tube site is warmed by heat conduction along the steel pipes. The PVC separator reduces, but by no means eliminates, undesirable heat conduction. Probing showed a slight depression of the frost table around the Thermo Tubes and also around the PVC frost tubes shown in Figure 1; when the tops of the frost tubes subsequently were cut off at ground level in summer, the frost table surrounding the tubes rose many centimetres within a few days.

Conclusion

The Thermo Tubes were quite effective in lowering the ground temperature in winter by as much as 5°C at a 1.5 m depth. Heat conduction along the pipes in spring and summer, however, largely negated the winter cooling. Consequently, the mean annual ground temperature at the top of permafrost was lowered only about 1°C by the Thermo Tubes as compared to a nearby undisturbed site. As the thaw stability of the ground is related to temperatures close to 0°C and not to temperatures well below freezing, the Thermo Tubes were not effective in keeping summer temperatures colder than in adjacent areas. However, if an artificial support structure (e.g. small pile) of equivalent conductivity to the Thermo Tube were used, but without its heat transfer properties, then thaw likely would occur under similar summer conditions. If heat conduction along the pipes could be reduced, such as by using a thicker insulating flange, and a longer model were used, the cooling results doubtless would be greatly increased.

During the installation of the six Thermo Tubes and the three frost tubes, the ground surface unavoidably was disturbed and the vegetation cover trampled. These disturbances would tend to accentuate summer thaw in 1971-73. It is still too early to determine what effects may take place in the active layer as a result of cooling by the Thermo Tubes, but a slight thinning seems likely.

References

Babb, A.L., Chow, D.M., Garlid, K.L., Popovich, R.P., and Woodruff, E.M.
1971: The Thermo Tube, a natural convection heat transfer device for stabilization of arctic soils in oil producing regions; Paper presented at 46th Annual Fall Meeting, Society of Petroleum Engineers of AIME, New Orleans, La., Oct. 3-6, 1971, 12 p.

Jahns, H.O., Miller, T.W., Power, L.D., Rickey, W. P., Taylor, T.P., and Wheeler, J.A.
1973: Permafrost protection for pipelines; Permafrost: North Amer. Contribution Sec. Intern. Conf., Washington, National Academy of Sciences, p. 673-684.

Johnson, P.R.
1971: The IAEE heat sink refrigeration system; Proc. Symp. on Cold Regions Engineering, J.L. Burdick (ed.), Univ. Alaska, p. 621-632.

Long, E.L.
1966: The Long thermopile; Proc. Permafrost Intern. Conf., Lafayette, Indiana, November 1963, Washington, National Academy of Sciences, N.R.C. Publ. No. 1287, p. 487-491.

Mackay, J.R.
1973: A frost tube for the determination of freezing in the active layer above permafrost; Can. Geotech. J., v. 10, p. 392-396.

IONIC AND OXYGEN ISOTOPIC FRACTIONATION IN PERMAFROST GROWTH

Project 680047

J. Ross Mackay* and L.M. Lavkulich**
Terrain Sciences Division

Introduction

The growth of permafrost at any given site is accompanied by the freezing of pore water in situ or its migration to form ice lenses -- in some soils there is also movement by water expulsion. As ionic and oxygen isotope fractionation are known to be affected by freezing and diffusion rates, vertical gradients would be expected to result from permafrost growth even in homogeneous material with an initial uniform groundwater quality. The purposes of this report are: 1) to show that ionic and oxygen isotope fractionation are occurring at two sites where permafrost is now growing; and 2) to suggest that such fractionation profiles may be helpful in interpreting the history of permafrost sites.

Methods

During the past several years, some hundreds of soil and ice (water) samples have been obtained from drillholes in permafrost from the Lower Mackenzie Valley and along the Western Arctic Coast by the Geological Survey and several oil and gas companies. Two drained lake bottom sites near Tuktoyaktuk, N.W.T. where permafrost is growing are discussed in this report. The drilling program was carried out by the Geological Survey. Samples obtained have been analyzed for ionic composition and oxygen isotope ratios.

Site 1

Site 1 is on the bottom of a large lake, 15 km east of Tuktoyaktuk, N.W.T. The lake drained about 150 years ago. Permafrost, which started to grow after drainage, is still growing. Permafrost ranges from about 20 to 35 m in thickness. The subpermafrost water is under artesian pressure, as a result of water expulsion from the downward advancing freezing front. The compositional differences between the surface water of a residual lake, the bottom of permafrost, and the subpermafrost water are shown in Table 1.

Table 1

Composition of water (ice) in mg/l

	Site 1			Site 2	
	Surface Water	Permafrost (at 20.5 m)	Subpermafrost Water (at 21.5)	Surface Water	Subpermafrost Water (at 17 m)
$\delta H_2{}^{18}O$ (in o/oo)	-21.6	-16.2 (at 14.5 m)	28.8	19.7	-27.7
Specific Conductance (μ mho/cm)	188	190	1224	134	1714
Chloride	16	-	106	18	141
Magnesium	7	2.3	49	4	148
Potassium	2.4	2	5.6	1.5	7.3
Calcium	14	17	93	10	54
Sodium	12	4	83	9	92

Site 2

Between 1935 and 1950, a lake some 25 km southwest of Tuktoyaktuk, N.W.T. drained. Permafrost is now 15 to 20 m thick; it is still aggrading; and the subpermafrost groundwater is under artesian pressure. Table 1 gives a comparison of water quality for the residual lake and subpermafrost groundwater.

*Department of Geography, University of British Columbia.

**Department of Soil Science, University of British Columbia.

Discussion

Although the compositions of the lake bottom groundwaters, prior to drainage, are unknown for Sites 1 and 2, it seems reasonable to assume that the waters were similar in composition to the lake waters of today. If this assumption is valid, then the compositional differences between the surface water, ice (water) in permafrost, and subpermafrost waters would result primarily from fractionation during permafrost growth.

Table 1 shows that the ionic concentrations of the subpermafrost waters are much higher than those for the surface waters. For Site 1, a sample from the subpermafrost water at 21.5 m is far more concentrated than that of ice (water) in permafrost at 20.5 m, a difference in height of only one metre.

The oxygen isotope ($H_2{}^{18}O/H_2{}^{16}O$) ratios for surface waters, compared to Standard Mean Ocean Water, have $\delta H_2{}^{18}O$ values of about $-10^{o}/oo$ to $-20^{o}/oo$, depending upon the time of year. The surface water (Table 1) for Site 1 was collected on June 28, 1973, and for Site 2 on July 16, 1973. The ice (water) samples from permafrost for both sites have values ranging from about $-18^{o}/oo$ to about $-23^{o}/oo$, but the subpermafrost water for four samples ranges from $-27.7^{o}/oo$ to $-29.8^{o}/oo$, an appreciable difference and considerably lower. Thus, fractionation seems apparent.

Although slow diffusion in frozen soils eventually might alter the profiles, fractionation is clearly recognizable in permafrost that is now growing at Sites 1 and 2. Similar appearing profiles in "old" permafrost suggest that any diffusion must necessarily be extremely slow. Consequently, compositional differences should be of assistance in the interpretation of permafrost histories, such as whether permafrost grew in open or closed groundwater systems, or in the recognition of thaw unconformities, where the upper part of thick permafrost has thawed during a warm period and has then refrozen.

Acknowledgments

The writers would like to express their thanks to several oil and gas companies for providing samples and to the National Research Council and the Department of Indian and Northern Affairs for research support.

99. ARCTIC DIVING OBSERVATIONS AT RESOLUTE BAY, N.W.T. AND THE NORTH POLE

Project 730020

Patrick McLaren
Terrain Sciences Division

While conducting coastal studies on Melville Island, N.W.T. (McLaren, 1974), the author concluded that direct sea bottom observation using SCUBA would enhance conventional marine sampling and sensing techniques. Diving would permit the geologist to exploit his training in observing and interpreting small-scale diagnostic sea bed features that would result in an enormously greater understanding of coastal environments, particularly the Arctic ice environment.

From April 19 to May 3, 1974, the author, with David Frobel, enjoyed an opportunity to dive with Dr. J.B. MacInnes', Arctic IV diving expedition at Resolute Bay, N.W.T. and the North Pole. The purposes were as follows: -

(1) To obtain diving experience in Arctic water with a professional diving team.

(2) To assess the feasibility of performing simple measurement and sampling techniques underwater.

(3) To make observations on sea ice and sediment pertinent to drift-ice geological processes.

A total of 10 dives comprising 9 underwater hours were made by Geological Survey personnel in support of these objectives.

At Resolute, access to the water was made by chipping a hole through 1.60 m of ice. In each dive a geological technique including underwater photography with a Nikonos camera system, sampling, hand augering, and the installation of permanent stakes with a hand-driven portable pile driver was practised. Each technique had been planned previously and will be utilized in future coastal studies on Melville Island.

The bottom of Resolute Bay is an organic-rich ooze containing small pebbles of ice-rafted sandstone. Contrary to Smith's speculation (Smith, 1974) that thin sediment (8 cm) overlies bedrock, the augering proved that the sediments are at least 1.50 m thick. Sedimentation is extremely slow as evidenced by the lack of particulate deposition on the pig-iron ballast of Dr. MacInnis' underwater habitat, sub-igloo (MacInnis, 1973, 1974). The pig-iron, which had been emplaced in steel trays on the sea floor, had been seen last in December, 1972. In over two years there was essentially no deposition on it.

From April 26 to 30, the author participated in a dive at the North Pole. Logistic support for this expedition was provided by the Canadian Armed Forces. During the flight from Alert to the Pole, the following observations were made on pressure ridge occurrence:

(1) A strongly oriented or preferred pressure ridge pattern did not appear to exist.

(2) Although the enormous variability of the ridges precluded development of an inclusive classification system, the following scheme accounts for many observed ridge types:

(i) Very straight linear ridges extending many miles

(ii) "Zipper" type ridges where ice relief takes the form of tightly meshed zig-zag masses making angles of approximately 60 degrees with each other

(iii) Large plates of ice bordered on all sides by ridges

(iv) Random piles

(3) Many ridges occur as branching sinuous embankments similar to eskers in topographic morphology.

(4) Old ridges are distinguished by subdued relief, and can be truncated by newer ridge systems.

(5) At 86.5°N, the size and concentration of pressure ridges seemed to decline.

(6) Leads commonly split a ridge longitudinally.

At the Pole, a camp was set up near the intersection of a small pressure ridge and a newly frozen lead. The ridge trended perpendicular to the lead and was truncated abruptly by it, thereby presenting an underwater cross-section of a pressure ridge for study. The thin lead ice (30-40 cm) offered easy access into the water (Fig. 1) as well as making a solid dive platform. Underwater visibility was excellent at 100 m or more.

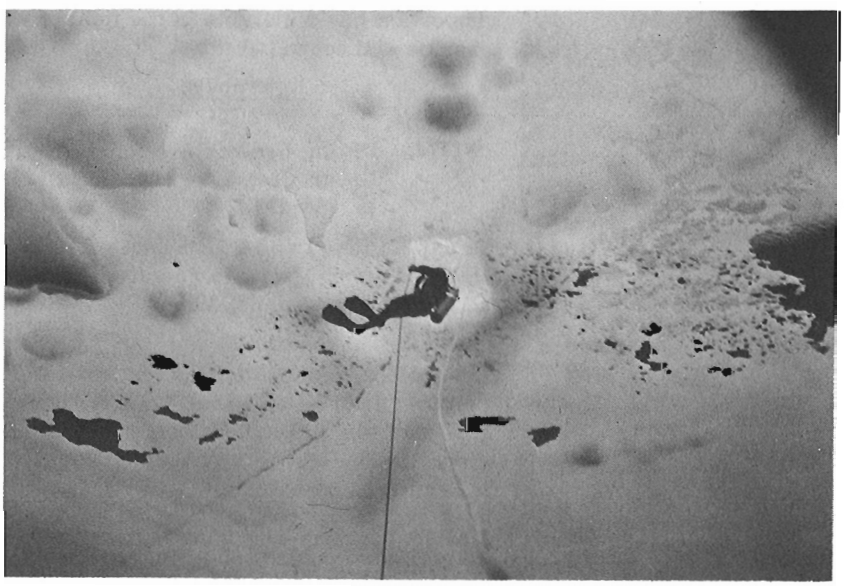

Figure 1. Diver descending through hole in new lead ice at the North Pole. Pieces of older and thicker ice can be seen frozen into the younger ice. The patches of black are air expelled by the divers and trapped beneath the ice.

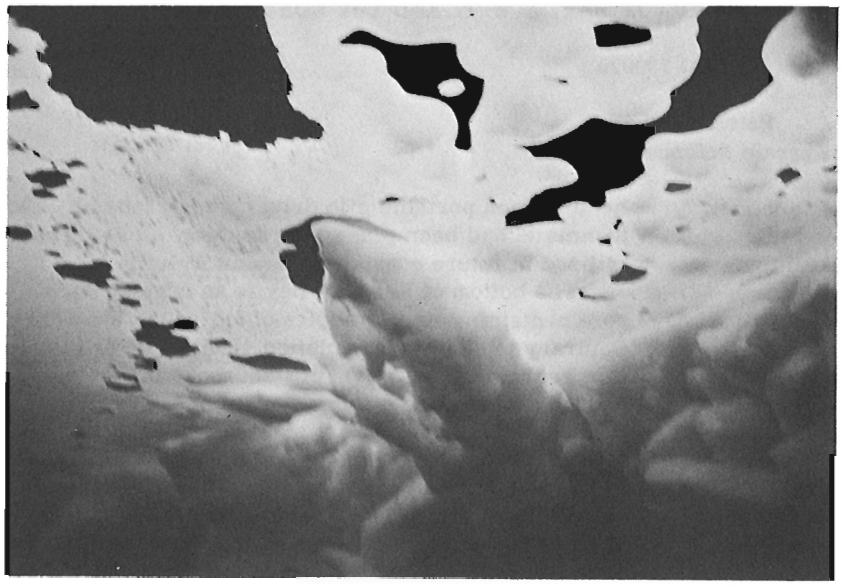

Figure 2. Upper part of keel showing plates of thin ice.

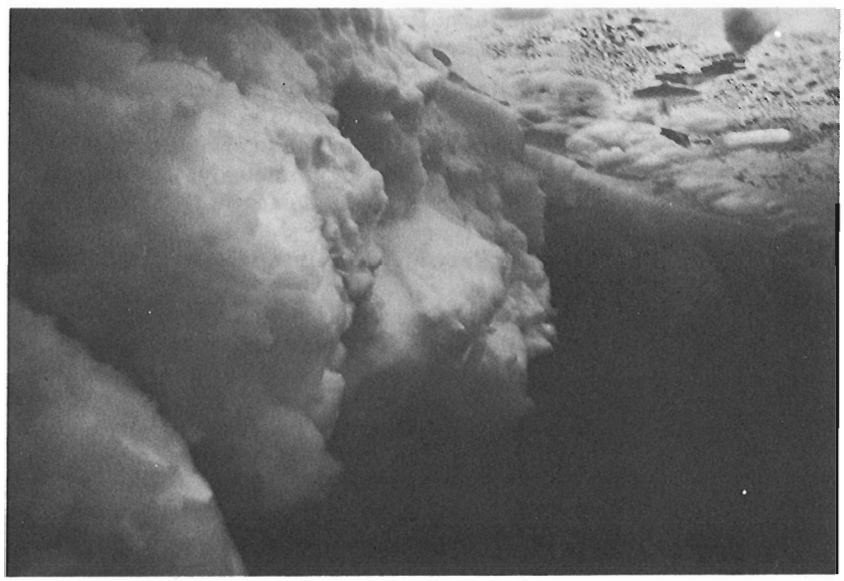

Figure 3. Massive ice in keel of pressure ridge. Note dive hole in the new lead ice in upper right-hand corner.

The ridge was measured to be approximately 4 m high by 30 m wide on the surface. The author dove to the ridge bottom at 19 m, however individual "fingers" of ice extended deeper. The keel appeared to be composed of large platelets of ice (20-30 m square) similar in thickness to the new ice in the lead (Fig. 2), as well as more massive blocks (Fig. 3). The brine-ice interface was characterized by a crystalline mush. Samples of the different ice types were extracted to compare salinities (analyses by Guildline Instruments Ltd.). They are as follows:

(1) New lead ice - 9.95 ppt
(2) Massive ice within keel - 4.80 ppt
(3) Thin ice within keel - 0.40 ppt.

The first two salinities are typical of newly frozen ice and first-year ice respectively; however, the low salinity of the thin ice is not readily explainable. It is suggested that the thin ice may be derived from refrozen, melt-water ponds that were present prior to ridge formation. In refreezing, the ponds would lose much of their salinity. This would account for the presence of two different ice types which might behave independently during ridge formation (A.R. Milne, I.M. Dunbar, pers. comm.).

Structurally, the components of both keel and sail appeared to be entirely random. The fact that adjacent ice blocks maintained distinct individuality and commonly formed substantial caves between them suggests a relatively young ridge. The interstices were not filled yet with new ice nor were the jagged blocks rounded by currents (No currents were felt by the divers, however, the pack had moved the camp two miles in the three days it was occupied).

It is concluded that the technology of SCUBA opens exciting new opportunities and viewpoints to the research geologist. Furthermore, SCUBA is easily learnt, and in comparison to cost of field operations, is extremely cheap. Zenkovich (1967), a prominent Soviet researcher of coastal geology, wondered why Americans seemed to be so reticent about using this technology for geology. With some exceptions, Canadians too, are equally reserved about using a technique that undoubtedly will provide important basic insights in the field of marine and coastal studies.

References

McInnis, J.B.
1973: Diving beneath Arctic ice; Nat. Geogr. Mag., v. 144, no. 2, p. 248-267.

1974: Arctic Expeditions I and II, Summary Report; The James Allister MacInnis Foundation, Arctic Diving Expeditions, Vol. 1.

McLaren, P.
1974: Coastal erosion-sedimentation, southeast Melville and western Byam Martin Islands, District of Franklin; in Rept. of Activities, April to October 1973, Geol. Surv. Can., Paper 74-1, Part A, p. 267.

Smith, R.W.
1974: Sedimentological-micropaleontological analysis of bottom sediments from Resolute Bay; The James Allister MacInnis Foundation, Arctic Diving Expeditions, Vol. III.

Zenkovich, V.P.
1967: Processes of coastal development; London, Oliver and Boyd, 738 p.

100. EFFECT OF ANTECEDENT FAULTS ON "LARAMIDE" STRUCTURE, MACKENZIE ARC

Project 670068

J.D. Aitken and D.G. Cook
Institute of Sedimentary and Petroleum Geology, Calgary

Introduction

In Canyon and Backbone Ranges of Mackenzie Mountains, a well-developed set of steeply dipping, presumably normal faults with predominant north 5°-20° west strikes, can be demonstrated at many localities to predate Upper Cambrian strata and, because it does not appear to involve Hadrynian strata, is assumed to be of pre-Hadrynian (pre-Rapitan Group) age (Aitken et al., 1973). If the Racklan (sub-Hadrynian)orogeny has any expression in the part of Mackenzie Mountains considered, then it is logical to view the subject fault set as Racklan. In any event it is appropriate to view these old faults as *antecedent* to Laramide (*sensu lato*) structures.

Because the trend of Laramide structures swings from about north 20° west at Keele River to north 70°-80° west at Arctic Red River, the apparent axis of greatest Laramide principal stress lay at different angles to the old (antecedent) faults at different places. Some of the antecedent faults have not suffered any demonstrable renewed movement during the Laramide, but others have had profound effects on the development of Laramide structures, among which are the following:

1) Rejuvenation of antecedent normal faults as strike-slip faults.
2) Propagation of antecedent faults into younger cover at the time of rejuvenation.
3) Independent development of folds and contractional faults on opposite sides of antecedent faults.
4) Localization of plunge-terminations of individual folds and of fold sets by antecedent faults and fault-zones.

It is hoped that illustration of these clear-cut relationships in the Mackenzie Mountains may help other geologists in the interpretation of structures elsewhere that may have similar origins.

The phenomena listed above are illustrated by maps of parts of Mount Eduni map-area (106A) (Figs. 3, 4, and 5). Accuracy of the maps is limited by the reconnaissance nature of the field work and the quality and completeness of the airphoto coverage, which was used extensively to interpolate geology between field observations. Nevertheless, the maps are considered to be essentially correct at the scale of presentation. The maps are generalized from the writers' completed manuscript of Mount Eduni map-area, at 1:125,000 scale. Future field work is planned to verify critical relationships in detail.

Summaries of the stratigraphy and stratigraphic nomenclature are given in the following sources:

1) Proterozoic to Upper Cambrian - Aitken, Macqueen and Usher (1973).
2) Upper Cambrian to Silurian - Macqueen (1970); Aitken and Cook (in press); Norford and Macqueen (in prep.).
3) Silurian and Devonian - Gabrielse, Blusson and Roddick (1973); Aitken and Cook (in press).

Topographic names in quotation marks are subject to approval by the Canadian Permanent Committee on Geographic Names. The names of individual structures are informal at this time.

Several faults, e.g., faults 1 and 2, are clearly bevelled by the sub-Upper Cambrian unconformity. Fault 3 is occupied by a gabbro dyke. This relationship supports a pre-Hadrynian age for the antecedent faults, because the gabbro intrusions of the region clearly are associated with Helikian strata (Aitken, Macqueen and Usher, 1974).

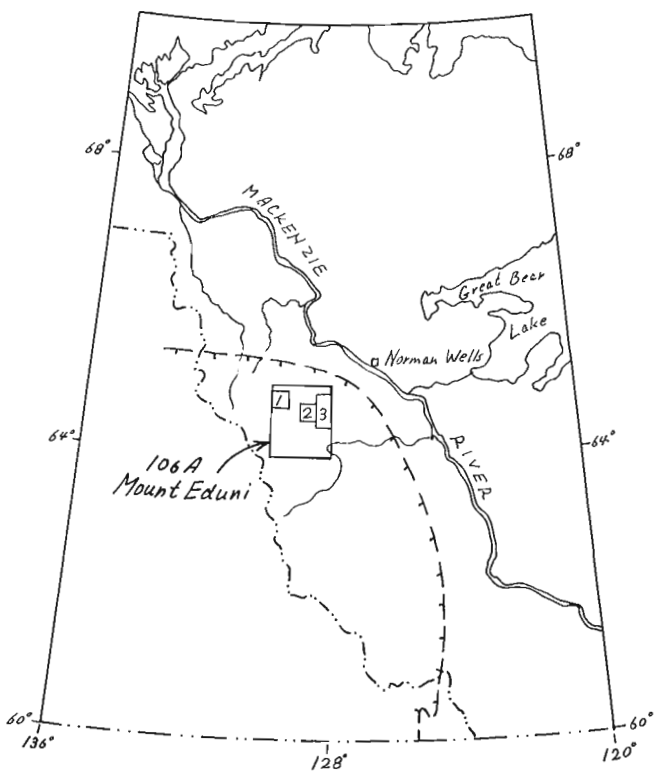

Figure 1. Index map. Mackenzie Mountains front shown thus: ⊤ ⊤⊤

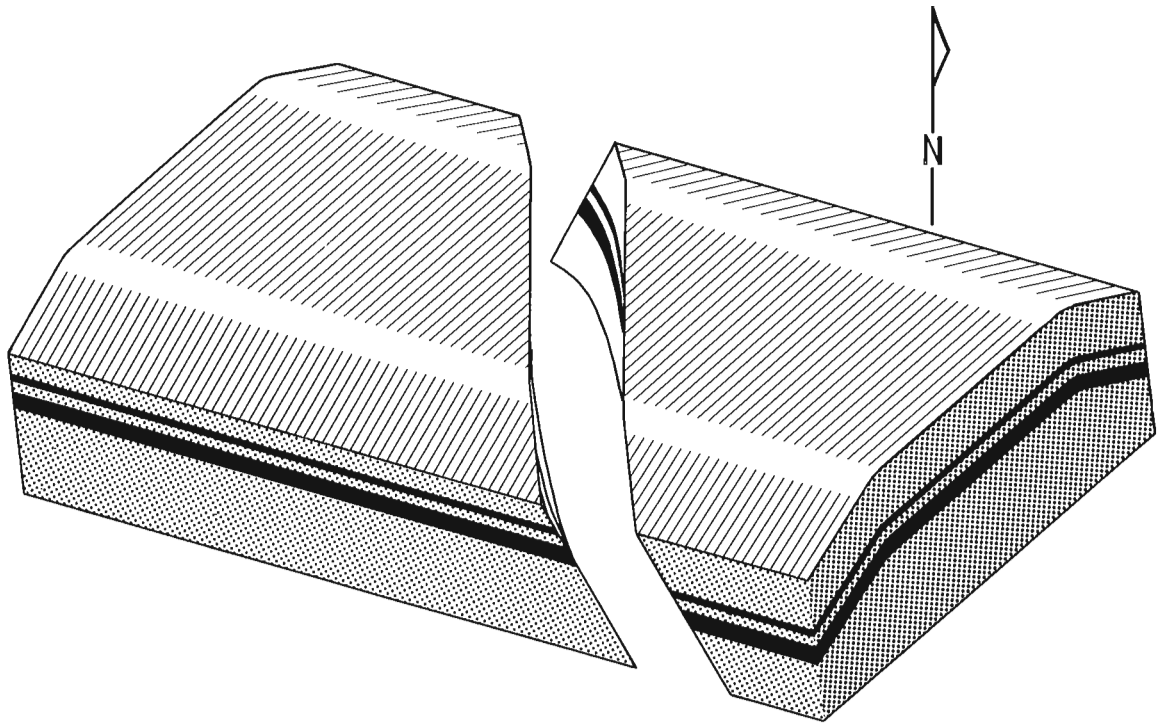

Figure 2. Deformation of a north-striking normal fault within a box-anticline trending west-northwest. If the fault undergoes rejuvenated movement during folding, the displacement will be dextral strike-slip.

LEGEND

(Figures 3, 4 and 5)

P3 Devonian clastic rocks, mainly shales (Hare Indian, Canol, Imperial Formations)

P2 Devonian carbonate rocks (Delorme, Arnica, Landry, Hume Formations)

P1 Upper Cambrian to Silurian carbonate rocks (Franklin Mountain and Mount Kindle Formations)

Hd Helikian (?) gabbro

Hc Helikian (?) carbonates, shales, local gypsum (Unit H_5 and Little Dal Formation)

Hb Helikian (?) Katherine Group, upper division: quartzite, dolomite, shale

Ha Helikian (?) Katherine Group, lower division: quartzite, minor shale, dolomite

Geological contact (observed, approximate, assumed)

Fault, steeply dipping, with normal, strike-slip, or polyphase displacement

Fault, with thrust or reverse displacement

Anticline

Syncline

Monoclinal bend, anticlinal arrow on steeper limb)

Fault 4, although it cuts post-Helikian strata, is an antecedent fault. In the first place, it shares the north-northwest trend of the old faults. Secondly, and conclusively, its sigmoid trace is precisely what would be predicted as a consequence of the folding, along an axis trending 110 degrees, of a package of strata containing a near-vertical, northerly trending fault; the fault retains its original strike through the flat crestal area of the anticline, but is deflected ("shortened") to a more northwesterly strike on the steep limbs (Fig. 2). At the same time, the fault acquires a southwesterly dip on the northeast limb of the anticline, and a northeasterly dip on the southwest limb. These rotated dips will affect only the older fault surface in Helikian rocks. The propagated portion in Paleozoic rocks, resulting from strike-slip rejuvenation, would be expected to be near vertical. Fault 4 displays such propagation upward into Paleozoic rocks.

Careful examination of the map will reveal that many of the north-northwest trending faults have contradictory senses of apparent relative vertical displacement along their traces. This is strongly suggestive of strike-slip displacement, interpreted by the writers as strike-slip displacement along faults that had originally developed as normal faults.

Flat-topped anticlinal folds in the region are defined by back-to-back pairs of monoclinal hinges (Aitken and Cook, in press). The offsets in the traces of the hinge-planes across antecedent faults are not to be interpreted literally as fault displacements, but rather as illustrations of the independent development of folding on opposite sides of these faults.

The most striking feature of the map is the abrupt northwestward expansion of the Shattered Range Anticline as it passes from the relatively narrow "Biscuitboard Range" to the broader "Shattered Range". The expansion takes place at a cluster of north-northwest to northwest-trending faults, interpreted as antecedent faults. One of these, fault A, has been rejuvenated during the Laramide as a dextral tear-fault that terminates the thrust to the northwest that locally defines the northeast limit of "Shattered Range". The thrust,

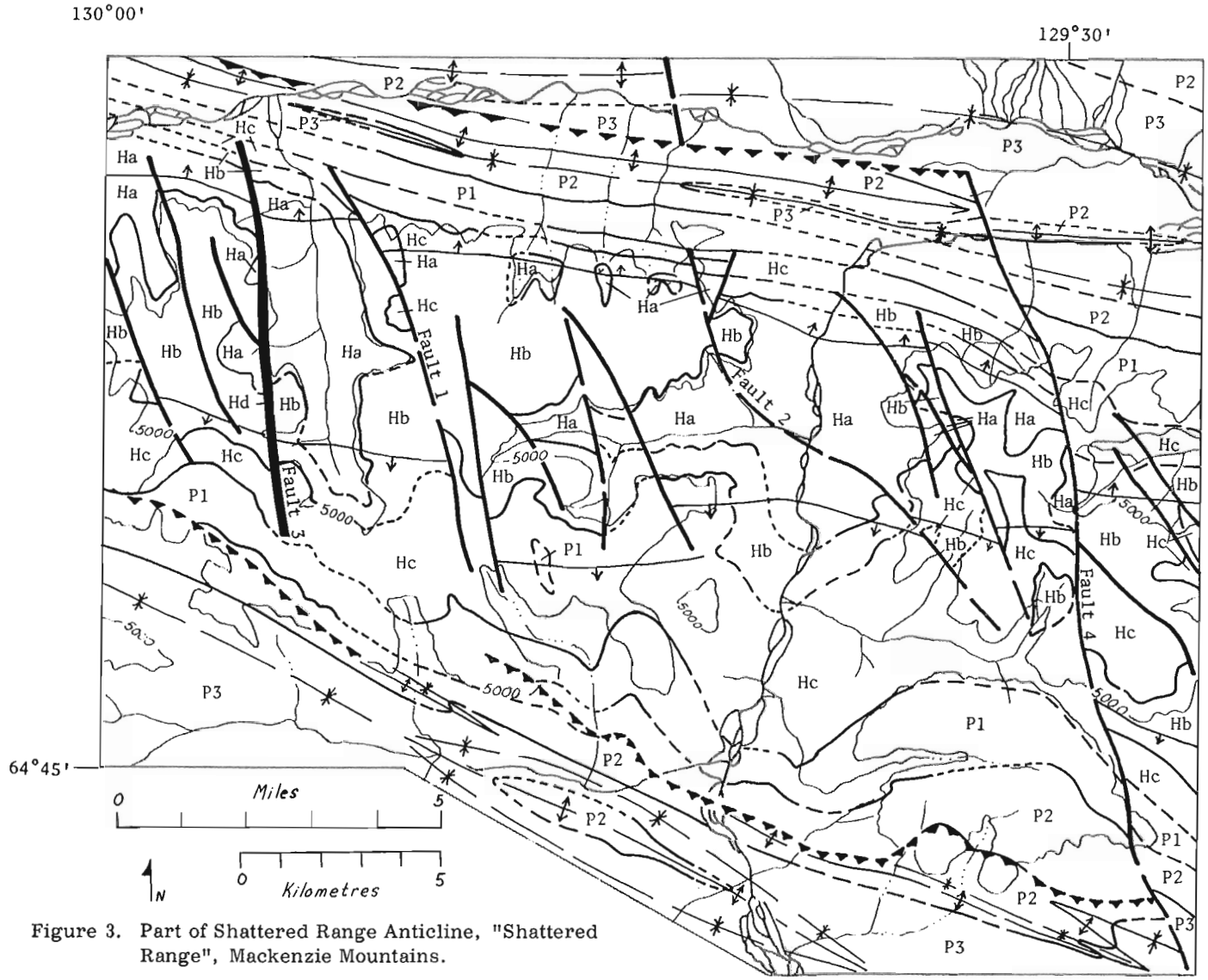

Figure 3. Part of Shattered Range Anticline, "Shattered Range", Mackenzie Mountains.

having no offset counterpart southwest of the rejuvenated fault, is a clear example of independent development of structures on opposite sides of an antecedent fault. The dextral displacement that is characteristic of such faults in the region (*see* also, faults B, C, D and Figs. 3 and 5) is predicted by compression of an existing north-northwest-trending fracture along a compression axis oriented northeast-southwest (Fig. 2).

Also obvious from the map is the abrupt thickening of map-unit Hc across the zone of antecedent faults. This may record deeper erosion of the uplifted (east) side of the faults prior to Upper Cambrian deposition; other evidence suggests however that depositional thickening also occurred, and the thickening may record synsedimentary movement on the zone of old faults.

The most striking feature of this map is the independent development of structures in adjacent blocks marked by the alignment of fold terminations, by plunge northwest or southeast, along a line marking the eastern boundary of a zone of north-northwest-trending, antecedent faults. The one through-going anticline, Tawu Anticline, also shows independent development across

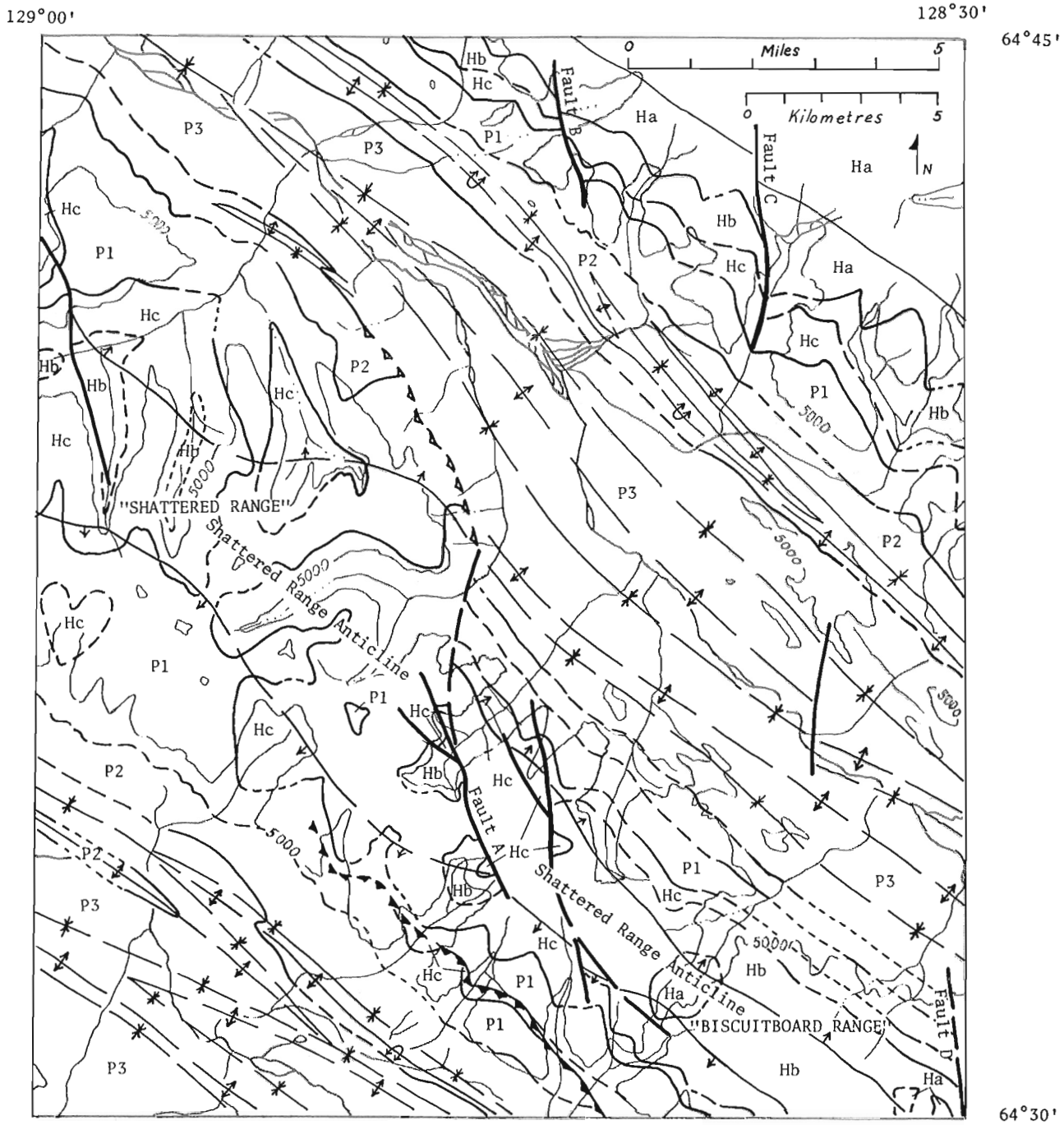

Figure 4. Shattered Range Anticline Southeast and Tawu Anticline, "Shattered" and "Biscuitboard" Ranges, Mackenzie Mountains.

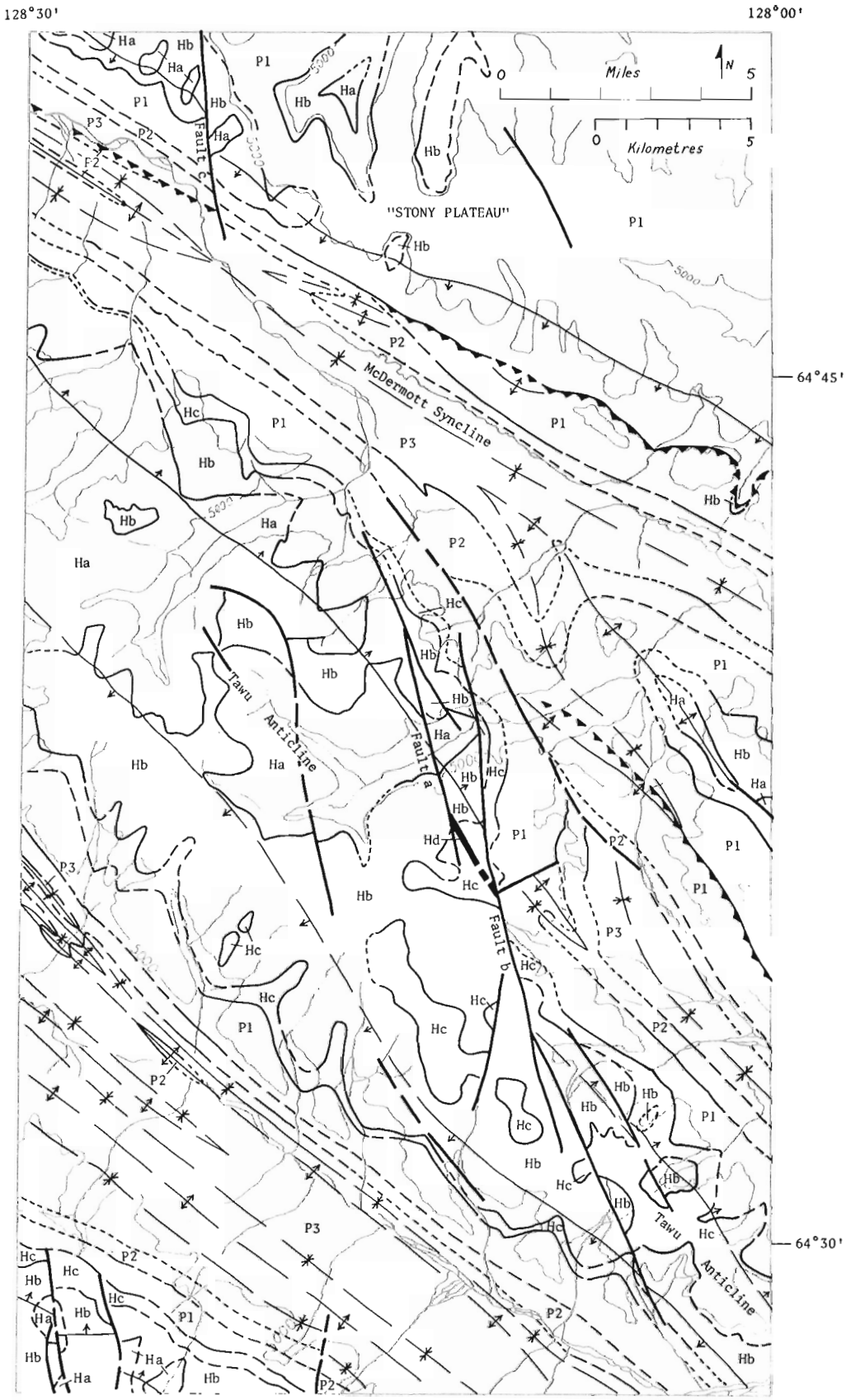

Figure 5. Tawu Anticline and "Stony Plateau", Canyon Ranges, Mackenzie Mountains.

the antecedent faults as it undergoes a marked expansion *without* notable change in the stratigraphic package involved.

Of further interest is the position of Stony Plateau Fault (c) almost on trend with the fault zone, north of McDermott Syncline. Although there is no through-going break in Paleozoic rocks, it appears to be a continuation of either fault a or fault b and, if so, its misalignment provides a means of estimating the tectonic shortening across McDermott Syncline. Again, its inferred sigmoid trace is that which would be expected (*see* fault 4, Fig. 3), in a synclinally folded antecedent fault.

References

Aitken, J.D., Macqueen, R.W., and Usher, J.L.
1973: Reconnaissance studies of Proterozoic and Cambrian stratigraphy, lower Mackenzie River area (Operation Norman), District of Mackenzie; Geol. Surv. Can., Paper 73-9.

Aitken, J.D. and Cook, D.G.
Carcajou Canyon map-area (96D), District of Mackenzie, Northwest Territories; Geol. Surv. Can., Paper 74-13 (with Map 1390A). (in press)

Gabrielse, H., Blusson, S.L., and Roddick, J.A.
1973: Geology of Flat River, Glacier Lake, and Wrigley Lake map-areas, District of Mackenzie and Yukon Territories; Geol. Surv. Can., Mem. 366.

Macqueen, R.W.
1970: Lower Paleozoic stratigraphy and sedimentology; eastern Mackenzie Mountains, northern Franklin Mountains (96 C,D,E,F; 106 G,H); in Report of Activities, April to October 1969, Geol. Surv. Can., Paper 70-1, pt. A, p. 225-230.

Norford, B.S. and Macqueen, R.W.
Mount Kindle, Franklin Mountain Formations, District of Mackenzie: type sections, regional relationships; Geol. Surv. Can. (in preparation).

101. LOWER PALEOZOIC CARBONATES C.D.R. TENLEN LAKE A-73 WELL, NORTHWEST TERRITORIES

Projects 710010 and 710013

W.S. MacKenzie
Institute of Sedimentary and Petroleum Geology, Calgary, Alberta

Introduction

Lower Paleozoic carbonate rocks, described in this report, range in age from Late Cambrian (Macqueen and MacKenzie, 1973, p. 185) to Early Devonian (Thorsteinsson, pers. comm.). At the C.D.R. Tenlen Lake A-73 well they have been divided (from oldest to youngest) into the Franklin Mountain and Mount Kindle Formations, and an overlying sequence of Lower Devonian and Upper Silurian carbonate rocks, probably lateral equivalents of the Delorme Formation.

Fossils collected by the writer from the Mount Kindle Formation and from the Lower Devonian-Upper Silurian carbonate sequence were identified by B.S. Norford and R. Thorsteinsson of the Geological Survey. With the exception of a few scattered ghosts of presumed skeletal remains, zones of soft sediment burrowing by organisms, and thin intervals with algal-laminated fenestral textures, no fossils were observed in the Franklin Mountain Formation.

There are no outcrops of lower Paleozoic strata closer than about 150 miles (240 km) to the Tenlen Lake A-73 well. The continuous sequence of cores recovered from between 200 feet (61 m) and the final total depth of 8,510 feet (259 m) at the Tenlen Lake A-73 well thus provides important data with which to further elucidate Paleozoic geology in the area, and at the same time serves to illustrate the useful complementary nature of surface and subsurface studies. For example, characteristic attributes that in outcrop serve to identify some lithologic units are either absent or not easily seen in rocks recovered from the subsurface; lithologic units that have not heretofore been observed in outcrop are present in subsurface at the Tenlen Lake well.

Description of Rock Units

Franklin Mountain Formation

The name Franklin Mountain Formation was given by Williams (1922, p. 60B; 1923, p. 78B) to about 500 feet (152 m) of partly talus-covered "pea green shales and sandy shales" and "buff-weathering calcareous shales with red interbeds, grading upward into buff limestones", on the eastern slope of Mount Kindle.

At the Tenlen Lake A-73 well, strata assigned to this formation are 2,727 feet (832 m) thick and consist mainly of dolomite. Five lithologic units have been recognized within the dolomite sequence; lower cyclic, rhythmic, and cherty units (Macqueen, 1970), a zone with floating sand grains (occurs here within the cherty unit), and an upper porous dolomite unit.

The lowermost cyclic unit, given a thickness of 226 feet (69 m) in the Tenlen Lake well, lacks the pale yellowish orange weathering colours and individual lithic cycles noted as identifying characteristics in surface exposures along the Franklin and Mackenzie Mountains. Thin shale interbeds and thin beds of flat-pebble conglomerate occur intermittently throughout the unit as in the mountains and in the subsurface near Colville Lake. Quartz silt and sand occur throughout the lowermost 32 feet of the unit. A probable source area for the sand is near Arctic Red River where, according to Aitken et al. (1973), Cambrian carbonate rocks unconformably overlie Proterozoic quartzites.

The presence of an overlying rhythmic unit (Macqueen, 1970, p. 227), 1,000 feet (305 m) thick at the Tenlen Lake A-73 well, is indicated on the accompanying columnar section (Fig. 2), even though the distinctive sedimentary rhythms characteristic of surface exposures in the northern Franklin Mountains and eastern Mackenzie Mountains were not observed in cores. The most striking rhythms occur in outcrop far to the south along the lower part of Keele River (Macqueen, 1970, Fig. 2). The rhythms are conspicuous also in the lower Mackenzie River region, but occur only in the lower 100 to 200 feet (30 to 61 m) of the sequence farther north near Arctic Red River (Macqueen, 1970). Perhaps weathering is required to accentuate the rhythms in order for them to be recognized. In any case, rhythms diagnostic of the unit in surface outcrops are tentatively presumed to be absent in the subsurface near Tenlen Lake.

The overlying cherty unit (Fig. 2) is appreciably thinner than in the Colville Lake region to the east where it reaches 2,040 feet (612 m), almost twice its thickness of 1,120 feet (341 m) at Tenlen Lake. Thin beds and lenses of white chert, abundant clear silica as vug lining, euhedral quartz crystals and silicified oolites are common in both areas. The thin oolite beds do not seem to persist far laterally. Their stratigraphic position is different in the Colville and Tenlen Lake wells.

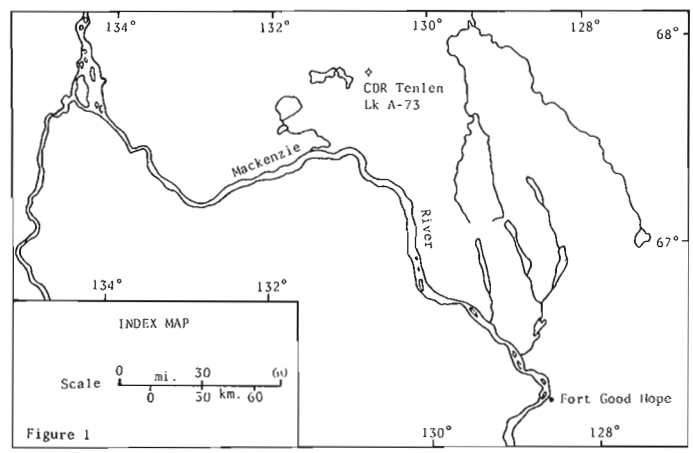

Figure 1

Rounded grains of randomly distributed quartz sand are characteristic of an informal unit called here a zone of floating sand grains. The quartz sand grains commonly occur in finely and medium crystalline, in part slightly silty, carbonate rock. At Tenlen Lake the sandy zone is 302 feet (92 m) thick and lies within the upper part of the cherty unit (Fig. 2). The same zone of floating sand grains is present in surrounding wells but its stratigraphic position relative to the cherty unit varies from partly within and partly above to entirely above the chert. The value as a correlation tool of either the cherty unit or the zone of floating sand grains has not yet been satisfactorily assessed. The sand grain unit appears to have no predictable stratigraphic relationship to the cherty unit or to the upper boundary of the Franklin Mountain Formation, except that it occurs within, partly within, or above the chert. The cherty unit, in turn, varies in thickness and in stratigraphic position within the upper part of the Franklin Mountain Formation. Chert, being diagenetic, is perhaps less reliable as a time stratigraphic marker than the quartz sand grains which presumably might all have been disturbed over a wide area at about the same time.

The stratigraphically highest unit is an informal porous dolomite unit, 381 feet (116 m) thick (Fig. 2). It is conspicuous because it lacks chert and consists mainly of light brown and almost white porous dolomite. These strata have a comparable thickness in nearby wells but are absent in the Mackenzie Mountains (Macqueen, 1970, p. 229) and in the subsurface near Colville Lake in the east (Macqueen and MacKenzie, 1973, p. 183).

Mount Kindle Formation

The overlying Mount Kindle Formation was named by Williams (1922, p. 60B) for a sequence of "grey argillaceous limestone" about 500 feet (152 m) thick forming part of the crest and western slopes of Mount Kindle. At the Tenlen Lake well the strata are 787 feet (240 m) thick. They consist mainly of dark brown argillaceous and siliceous dolomite, commonly with silicified solitary and colonial corals, crinoids, gastropods, and bryozoans and by the presence of nodules and thin beds of brown and white chert. The formation is conspicuously siliceous and fossiliferous throughout.

Lower Devonian and Upper Silurian Carbonates

Seven hundred and fifty-eight feet (231 m) of carbonate strata, referred to in this report as "Lower Devonian and Upper Silurian carbonates", overlie the Mount Kindle Formation at the Tenlen Lake A-73 well (Fig. 2). They may be wholly or in part lateral equivalents of the Delorme Formation of Douglas and Norris (1971, p. 10). The name Delorme Formation is used frequently by industry for this part of the stratigraphic sequence. The probable age of these beds, based on a fauna of pteraspidid and cyathaspidid fish remains collected from cores in the upper part of the sequence, ranges from Late Silurian to Early Devonian (Thorsteinsson, pers. comm.). Tassonyi's (1969) Lower Limestone Member of the Gossage Formation (Fig. 2) probably should be included in this sequence of carbonate rocks. The change upward from these light coloured, presumably shallow water limestones with interbedded silty and sandy green waxy shale, to overlying dark brown argillaceous dolomites of the Gossage Formation marks a conspicuous change in sedimentary regime from a relatively shallow to an appreciably deeper water environment. Despite the fact that a disconformity is present below the Gossage Formation elsewhere, along the Horton River for example (Yorath et al., 1969, p. 11), evidence for such a period of erosion prior to deposition of the deeper water Gossage Formation dolomites appears to be absent in the Tenlen Lake area. A cursory look at data from other wells permits an interpretation of

Figure 2

CDR TENLEN LAKE A-73
(67°52'07"N; 130°43'21"W)

COLUMNAR SECTION

LEGEND

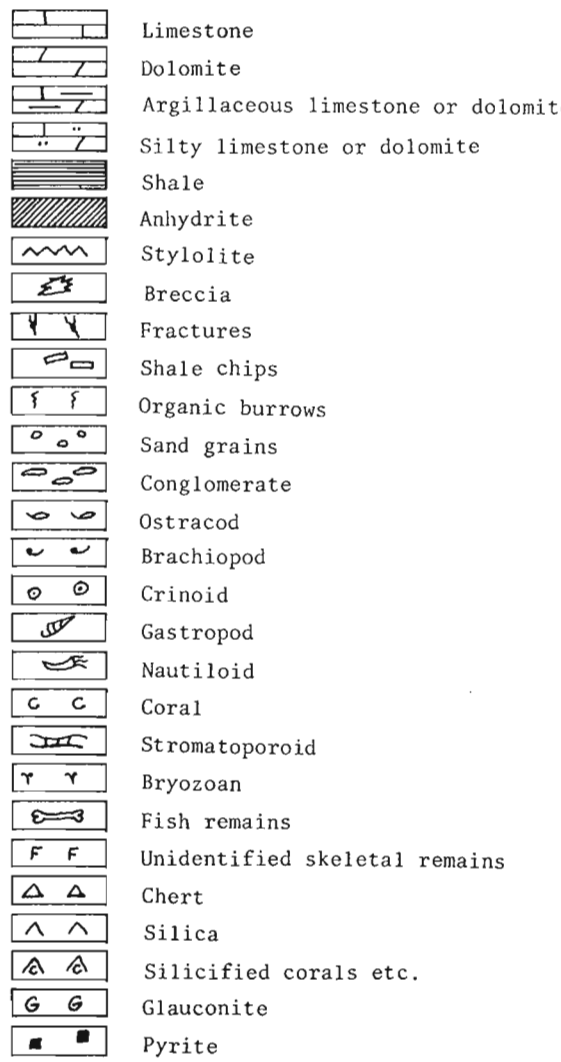

Figure 2(cont'd)

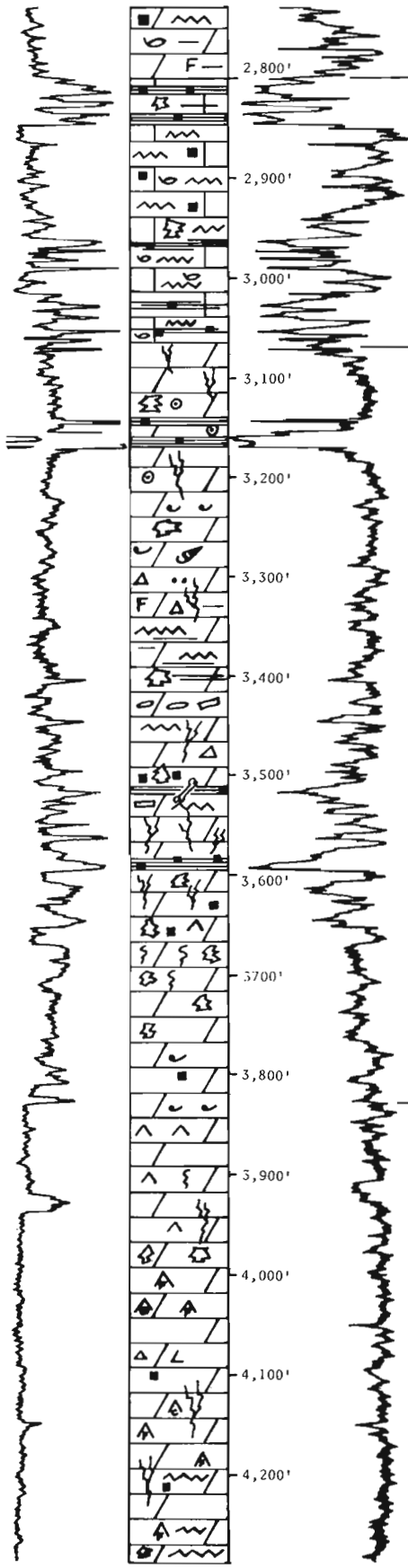

GOSSAGE FORMATION

Dolomite member (2,800')

Lower limestone member

Limestone, light brown, mainly lime mudstone, intermittently burrowed, intervals of algal-laminated fenestral texture, grainstone, rudite and limestone conglomerate, stylolites particularly abundant throughout, thin interbeds green waxy shale, dolomite interbeds, breccia and pyrite abundant in upper fifty feet.

(3,072')

LOWER DEVONIAN AND UPPER SILURIAN CARBONATES (758')
(Delorme Formation equivalent?)

Dolomite, mainly grey and brown, varyingly argillaceous; intermittent light and dark brown conspicuously bedded and banded intervals, frequently with micro erosional surfaces, occur where textures have not been obliterated by extensive burrowing and reworking of the sediment; burrowed algal-laminated fenestral textures are also common in the lighter coloured carbonates. A few beds of dark brown dolomitic shale occur as well as scattered thin partings, floating chips, and rounded fragments of green waxy pyritic shale. A little silica associated with leached skeletal fragments and open vugs, and white chert nodules with preserved primary grainstone textures is present mainly in the upper part of the formation. Organic remains consist of coral, brachiopod, crinoid, and gastropod remains and scattered unidentifiable skeletal fragments. Sub-vertical calcite-cemented fractures, commonly with associated local brecciation and pyrite mineralization and minor breccias occur throughout the formation.

Fish fragments (GSC loc. C-28116) were collected from a thin shale bed at 3517 feet. The family represented ranges in age from Late Silurian (Wenlockian) to Early Devonian (Gedinnian) but is most likely Late Silurian.

(3,830')

MOUNT KINDLE FORMATION (787')

Dolomite, intervals of dark brown and grey finely crystalline argillaceous dolomite and medium brown, medium and coarsely crystalline dolomite with more coarsely srystalline sucrosic textures common in the lower part of the formation. Burrow mottling, soft sediment deformation, local brecciation and sub-vertical fracturing with associated calcite cementation, pyrite mineralization, and geopetal fabrics are common throughout; bedded intervals occur where the sediments have been undisturbed. Silicified fossil remains (GSC loc. C-28261, C-28262, C-28264) consist mainly of solitary and colonial corals; small crinoids, gastropods, bryozoans, and nautiloids, also silicified, occur sporadically in the more argillaceous parts of the sequence. Nodules and thin beds of white chert occur occasionally; euhedral quartz crystals are present in the lower about 300 feet lining the interior of small open vugs.

Figure 2(cont'd)

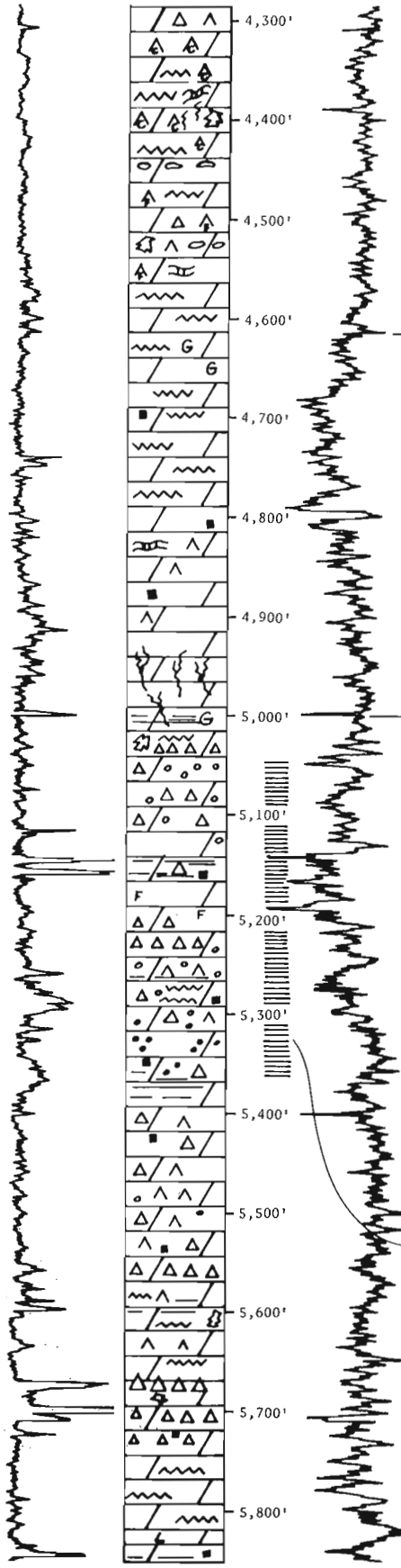

(4617')

FRANKLIN MOUNTAIN FM (2727')

Porous dolomite unit (381')

Dolomite, mainly light brown, coarsely crystalline and sucrosic; consists of randomly distributed broken tabular plates and irregularly shaped angular fragments of light brown and white dolomite in a matrix of dark brown, finely crystalline argillaceous dolomite. Graded textures are common in the dark brown presumably cavity-filling dolomite matrix; patches of algal laminated sediment with fenestral textures occur sporadically. Secondary glauconite occurs in the upper few feet of the unit; lower 153 feet, brown finely crystalline dolomite, argillaceous and partly siliceous with intermittent bedded and burrow-mottled areas.

(4998')

Cherty unit (1120')

Dolomite, light, medium, and dark brown, with fine, coarse crystalline and sucrosic textures, varyingly argillaceous, silty, and sandy, with intermittent bedded, banded, and burrow-mottled areas more common in the lower part of the unit. Chert in the form of thin, mainly white but also grey, brown and black beds and nodules is characteristic of the unit; primary sedimentary features such as algal laminated bedding, and grainstone and oolite textures have been preserved in some of the chert beds and nodules. Intervals of appreciable thickness have been strongly silicified, many vugs are lined with silica in the form of euhedral quartz crystals; strongly silicified areas frequently consist of coarsely crystalline sucrosic dolomite in a silica cement. Floating rounded quartz sand and silt grains and floating chips of chert are common in the upper part of the unit. A few stylolites, scattered pyrite crystals and occasional indeterminate fossil ghosts occur throughout the unit.

Zone of floating sand grains (302')
Round grains of quartz sand randomly distributed in the carbonate rock.

Figure 2 (cont'd)

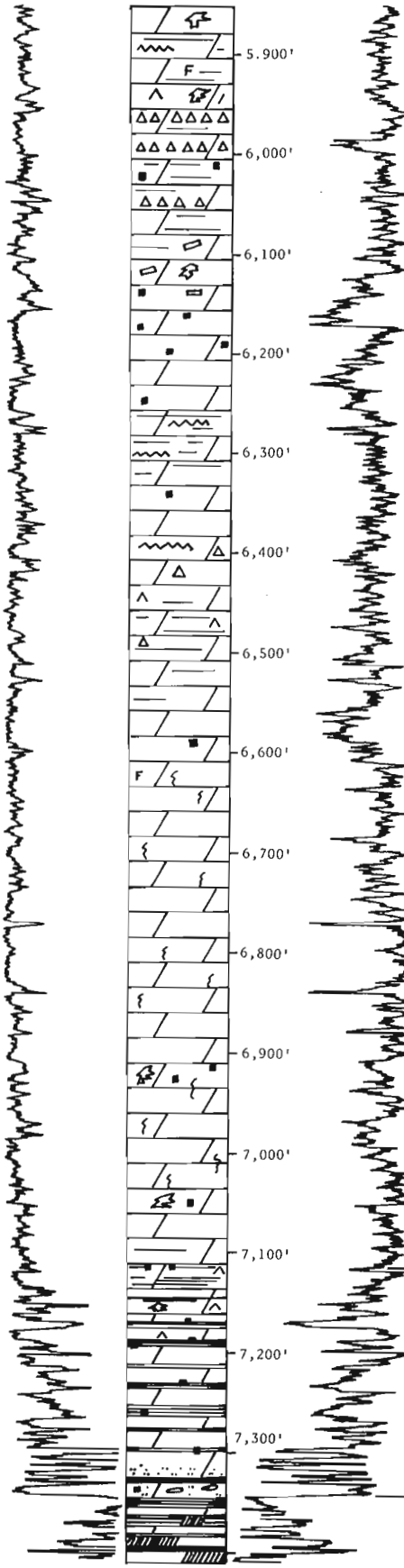

(6118')

Rhythmic Unit (1000')

Dolomite, light and dark brown and dark grey, with fine, medium, coarse crystalline and sucrosic textures, varyingly argillaceous; finely crystalline intervals intermittently bedded, banded, and burrow mottled; bedding made manifest by concentrations of dark argillaceous material and frequently by thin partings of waxy green pyritic shale; soft sediment slump structures, crenulated bedding and occasional fine scale crossbedding also present. Green waxy shale frequently occurs as matrix material in dolomites with coarse sucrosic texture and also partially infilling open vugs; some vugs lined with euhedral quartz crystals, traces of chert in small nodules. Scattered fossil ghosts, low amplitude stylolites and finely disseminated pyrite crystals occur sporadically throughout the unit.

(7118')

Cyclic Unit (226')

Dolomite, mainly grey and brown, finely crystalline, argillaceous, commonly with soft sediment structures, occasional flat pebble conglomerates, a few thin beds of light brown, algal-laminated dolomite, local minor fracturing and brecciation, partly siliceous; lower 32 feet with quartz silt, sand, and fine conglomerate in thin beds of green shale and brown dolomite.

(7344')

SALINE RIVER FM

Maroon and green shale, dolomite and anhydrite.

lateral truncation of beds, suggesting that there may have been a hiatus in deposition prior to accumulation of the Lower Devonian-Upper Silurian carbonate sequence and, moreover, that this hiatus is the sub-Gossage or sub-Bear Rock Formation unconformity that has been documented in other areas. Proposed further study of available data may resolve the problem.

Mean and standard deviation calculations, based on per cent organic carbon determinations by A. Foscolos of the Geological Survey, showed significant differences in the percentage of organic carbon present in each of the formations described above. The Lower Devonian-Upper Silurian sequence of carbonate rocks contained the least amount of organic carbon. The greatest amount was present in the Mount Kindle Formation. All of the formations contained organic carbon in amounts significantly greater than the mean organic carbon content of limestone reported by Gehman (1962, p. 885) for collections from many parts of the world.

References

Aitken, J.D., Macqueen, R.W., and Usher, J.L.
1973: Reconnaissance studies of Proterozoic and Cambrian stratigraphy, lower Mackenzie River area (Operation Norman), District of Mackenzie; Geol. Surv. Can., Paper 73-9.

Douglas, R.J.W., and Norris, A.W.
1961: Camsell Bend and Root River map-areas, District of Mackenzie, Northwest Territories; Geol. Surv. Can., Paper 61-13.

Gehman, H.M.
1962: Organic matter in limestones; Geochim. Cosmochim. Acta, v. 26, p. 885-897.

Macqueen, R.W.
1970: Lower Paleozoic stratigraphy and sedimentology, eastern Mackenzie Mountains, northern Franklin Mountains (96C, D, E, F; 106G, H); in Report of Activities, Part A, April to October, 1969, Geol. Surv. Can., Paper 70-1, pt. A, p. 225-230.

Macqueen, R.W. and MacKenzie, W.S.
1973: Lower Paleozoic and Proterozoic stratigraphy, Mobil Colville Hills E-15 well and environs, Interior Platform, District of Mackenzie; in Report of Activities, Part B, November 1972 to March 1973, Geol. Surv. Can., Paper 73-1, pt. B, p. 183-187.

Tassonyi, E.J.
1969: Subsurface geology, lower Mackenzie River and Anderson River area, District of Mackenzie; Geol. Surv. Can., Paper 68-25.

Williams, M.Y.
1922: Exploration east of Mackenzie River between Simpson and Wrigley; Geol. Surv. Can., Summ. Rept. 1921, pt. B, p. 55-66.

1923: Reconnaissance across northeastern British Columbia and the geology of the northern extension of Franklin Mountains, Northwest Territories; Geol. Surv. Can., Summ. Rept. 1922, pt. B, p. 65-87.

Yorath, C.J., Balkwill, H.R., and Klassen, R.W.
1969: Geology of the eastern part of the Northern Interior and Arctic Coastal Plains, Northwest Territories; Geol. Surv. Can., Paper 68-27.

102. STRATIGRAPHIC RELATIONSHIPS AT THE WESTERN EDGE OF THE MIDDLE CAMBRIAN CARBONATE FACIES BELT, FIELD, BRITISH COLUMBIA

Project 720050

I. A. McIlreath
Institute of Sedimentary and Petroleum Geology, Calgary

Prior to the field study by Cook (1970), theories on the relationship of the Chancellor Formation to Cambrian units farther east were variously interpreted as juxtaposition of facies by a normal fault, a normal fault with subsequent thrust motion and a thrust fault. Cook (1967, 1970), however, found no substantial fault but an intertonguing facies transition between a predominantly carbonate eastern facies and a predominantly argillaceous, western facies.

On the basis of lithology, Cook (1967, 1970) correlated the lower Chancellor with the Middle Cambrian Mount Whyte, Cathedral, Stephen, Eldon and Pika formations. The upper Chancellor was correlated with the Sullivan Formation on the basis of lithology substantiated by *Cedaria* Zone fossils from both formations. The middle Chancellor, on the basis of relative position in the sequence and lithologic similarity, was correlated with the Arctomys and Waterfowl formations. A single fossil collection from near the top of the middle Chancellor contained the genus *Lejopyge* which indicates proximity to the Middle-Upper Cambrian boundary. This implies that the uppermost middle Chancellor and the upper portion of the Waterfowl Formation are of similar age.

Cook (1967, 1970) cited four areas where the transition from lower Chancellor to rocks of the Cathedral, Stephen, Eldon and Pika formations can be observed. These four localities (see Fig. 1) include the best exposure in the west wall of Prospector's Valley, Dennis Pass, Park Mountain and head of Duchesnay Creek. The first two localities were studied by the writer in the summer of 1973 in a much more detailed manner than was possible for Cook in his extended study, and new observations further modify the understanding of this facies change.

Cook (1970) stated that, in the west wall of Prospector's Valley (see Fig. 2a), the Cathedral, Stephen, Eldon and Pika formations become increasingly shaly from north to south until they become indistinguishable across a narrow zone, shown by the dashed line (FT). However, the writer traced the Cathedral, Stephen and basal portion of the Eldon formations, completely unchanged, southward across the area of supposed facies changes (see Fig. 2a) to where each unit, because of a southerly plunge, disappears into the talus. The first manifestation of the facies transition occurs with the introduction of minor shale tongues in the upper Eldon limestone (see Fig. 2a). These shale tongues can be traced southward, subparallel to the ridge line across the full extent of the valley wall and, therefore, there is no narrow lateral transitional zone. The facies change in the Eldon Formation at Prospector's Valley occurs east of the escarpment in the upper Cathedral Formation as it does on Park Mountain (see Fig. 1). This escarpment recently has been described by McIlreath (1974).

In tracing the Cathedral and Stephen formations southward across the originally supposed area of facies change, a localized collapse-breccia zone was found in the uppermost Cathedral (see Fig. 2a). In this breccia zone, Stephen and basal Eldon beds have collapsed into the uppermost Cathedral and are preserved as breccia in a coarse, white dolomite. Away from the breccia zone, the uppermost Cathedral consists of laminated, buff-coloured dolomite with some interbedded gypsum. This local collapse may have been due to localized solution of the gypsum in very early Eldon time.

A second locality studied by the writer was Dennis Pass between Mount Stephen and Mount Dennis (see Fig. 2b), where the essential continuity of strata from eastern to western facies was described by Cook (1970). The dashed line marked FT (see Fig. 2b) indicates the most recently postulated position of the facies change

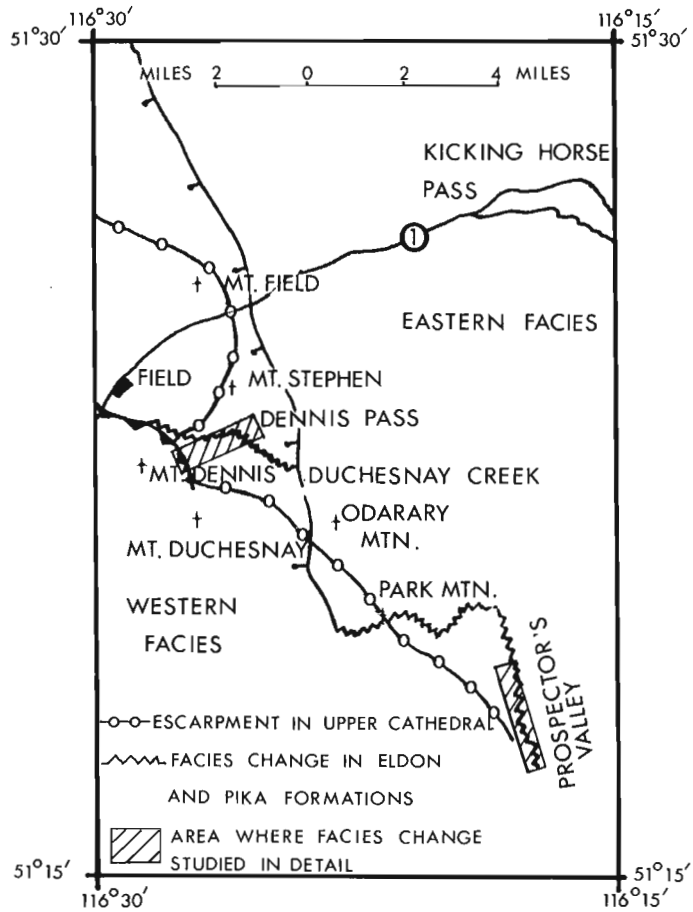

Figure 1. Location map showing trend of facies change in Eldon and Pika formations.

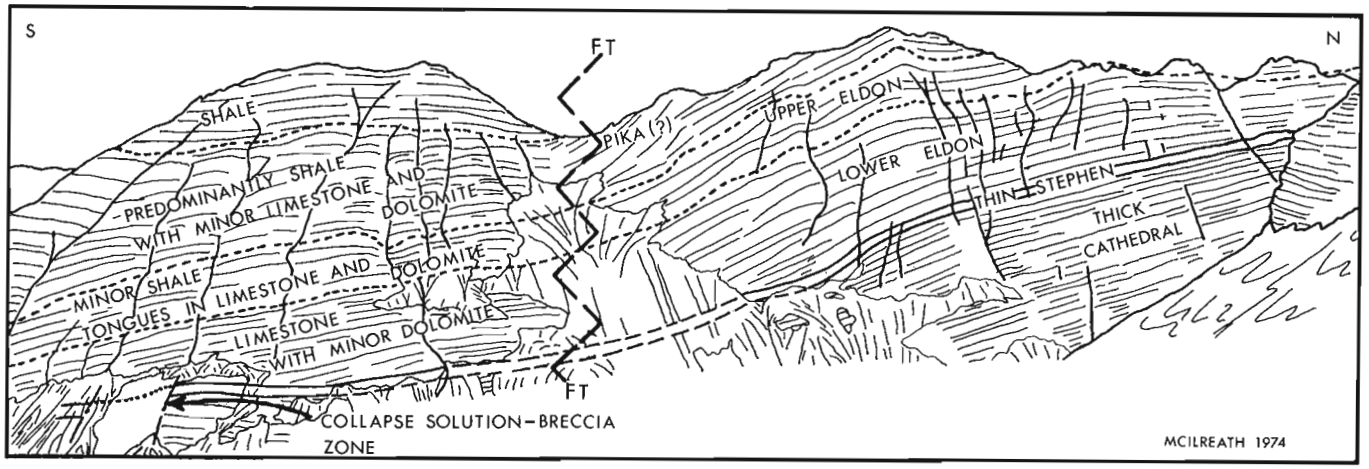

Figure 2a. Facies change in west wall of Prospector's Valley. Cathedral, Stephen and lower portion of the Eldon formations can be traced across area of originally supposed position of facies change near vertical dashed line (FT). First manifestation of facies change is the introduction of shale tongues into limestones of the upper Eldon Formation. View is looking west from Neptuak Mountain.

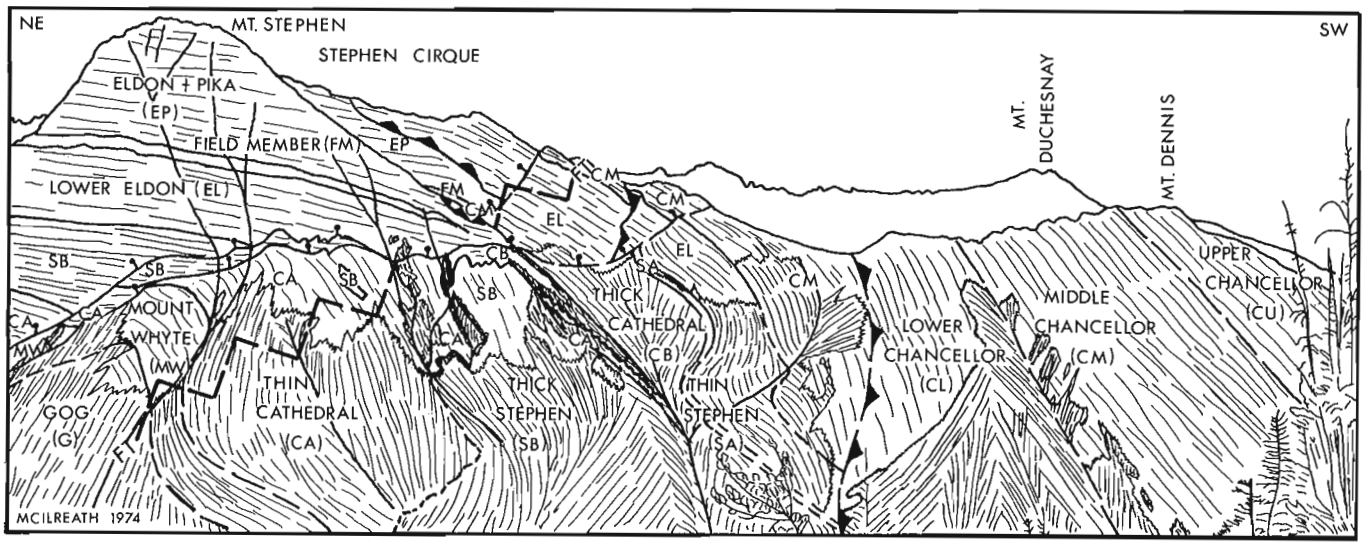

Figure 2b. Facies change in Dennis Pass between Mount Stephen and Mount Dennis. First manifestation of the facies change occurs in the ridge line where well-defined shale tongues can be observed in the lower Eldon limestones. There is no transition to western facies on the west flank of Mount Stephen in the area indicated by the dashed line (FT), as previously believed. View is looking southwards from Mount Burgess.

shown by Cook (Fig. 38 in Balkwill et al., 1972). By detailed walking-out of the Mount Whyte, Cathedral and Stephen formations, the writer established that the west flank of Mount Stephen consists entirely of eastern facies (see Fig. 2b) as was suggested by Cook in an earlier interpretation (1970). As previously described by McIlreath (1974), eastern facies, Cathedral and Stephen outcrop at the entrance to Stephen cirque and in the adjacent ridge line between Mount Stephen and Mount Dennis. In the ridge, the facies change begins with well-defined shale tongues in lower Eldon limestone. Compared to the occurrence at Prospector's Valley the facies change can be observed at a lower level in the Eldon Formation. Like Prospector's Valley and Park Mountain, the facies transition in the Eldon occurs east of the escarpment in the upper Cathedral (see Fig. 1). To the northwest of Dennis Pass, the facies change in the Eldon occurs progressively west of the upper Cathedral escarpment. Therefore, the writer believes that the escarpment in the upper Cathedral did not exert any control on the development of the western bank-edge in the overlying Eldon carbonates.

In the ridge between Mount Stephen and Mount Dennis (see Fig. 2b), middle Chancellor strata directly overlie lower Eldon in depositional contact at approximately the same stratigraphic position as the Field member which overlies lower Eldon on Mount Stephen. Therefore, the Field member (an outer detrital tongue in the Eldon Formation; Aitken, 1971) may be associated with the lower part of the middle Chancellor. If this

correlation is correct, the lower part of the middle Chancellor, instead of being equivalent to Arctomys Formation (Cook, 1967, 1970), would be, at least, equivalent to Arctomys, Picka and uppermost Eldon formations. Also, if the Field member is a tongue from the middle Chancellor, there is a progressive change in the lithology of this unit eastward from a slate (Dennis Pass) to an argillaceous, platy limestone capped by a thin argillite bed (west side, Mount Stephen) to limestone which is dolomitized and becomes indistinguishable from eastern facies carbonates (east side, Mount Stephen).

References

Aitken, J.D.
1971: Control of lower Paleozoic sedimentary facies by the Kicking Horse Rim, southern Rocky Mountains, Canada; Bull. Can. Pet. Geol., v. 19, no. 3, p. 557-569.

Balkwill, H.R., Cook, D.G., and Price, R.A.
1972: Main Ranges and Western Ranges - Kicking Horse Pass - Rogers Pass section in The Canadian Rockies and tectonic evolution of the southeastern Canadian Cordillera; XXIV Int. Geol. Congr., Field Excursion Guidebook A15-C15, p. 58-68.

Cook, D.G.
1967: Structural style influenced by a Cambrian regional facies change in the Mount Stephen-Mount Dennis area, Alberta-British Columbia; unpubl. Ph.D. thesis, Queen's University.

1970: A Cambrian facies change and its effects on structure, Mount Stephen-Mount Dennis area, Alberta-British Columbia in Structure of the southern Canadian Cordillera, J.O. Wheeler, ed.; Geol. Assoc. Can., Spec. Paper No. 6, p. 27-40.

McIlreath, I.A.
1974: Stratigraphic relationships at the western edge of the Middle Cambrian carbonate facies belt, Field, British Columbia; in Report of Activities, Part A, Geol. Surv. Can., Paper 74-1, pt. A, p. 333, 334.

103.

GEOLOGY OF THE "BULMER LAKE HIGH", A GRAVITY FEATURE IN THE SOUTHERN GREAT BEAR PLAIN, DISTRICT OF MACKENZIE

Project 710011

N. C. Meijer-Drees
Institute of Sedimentary and Petroleum Geology, Calgary

Hornal et al. (1970), in their discussion of the Wrigley-Providence Bouguer anomaly map (Gravity Map Series 117) described a relatively positive anomaly of over 50 mgal, extending from the Trout River northward through Bulmer Lake and Keller Lake to McVicar Arm on Great Bear Lake. They named this feature the "Bulmer Lake High" and suggested that the origin of the high is in the Precambrian basement. Models which would fit the observed field data require a near-surface trough or ridge of high density granulites or basic igneous rocks, which is fault-bounded on the east, has a maximum thickness of 27,000 feet east of Bulmer Lake and then thins rapidly to the west.

On the Bouguer anomaly map the "Bulmer Lake High" extends northeast and merges on Leith Peninsula, with a relatively positive gravity anomaly, which coincides with a ridge of Precambrian granite mapped by Balkwill (1971). This ridge is 1,100 feet above the base of nearby Cambrian sandstone. The Precambrian salient is flanked on its southeastern side near Hottah Lake by approximately 325 feet of Cambrian rocks. On the northwestern flank it is capped by Proterozoic rocks of the Hornby Bay Group (Balkwill, 1971), which dip gently to the northwest and are estimated to be about 1,000 feet thick. The Hornby Bay Group is, in turn, flanked on the northwest side by Cambrian rocks of the combined Mount Cap and Saline River formations, by the cyclic unit of the Franklin Mountain Formation and by the Mount Kindle Formation (see Fig. 2).

Studies of the lower Paleozoic formations in the subsurface of the Fort Simpson area (see Fig. 1) suggest the existence of a similar Precambrian basement high, which was a positive element during Cambrian sedimentation (Meijer Drees, ms in prep.). In the subsurface north of Fort Simpson, rocks of the lower Paleozoic Mount Clark, Mount Cap, Saline River and Franklin Mountain formations thin and disappear eastward from the McConnell Range toward Bulmer Lake and reappear again in the Lac la Martre area (see Fig. 3). West of the basement high these formations overlie a thick succession of Proterozoic rocks similar to the ?Helikian succession described by Aitken et al. (1973) from Cap Mountain, McConnell Range. East of the high, in the Imperial Windflower Lake G-77 (62° 56'26"N, 118° 29'02"W), the Horn River Shell Levis D-76 (62° 25'06"N, 118° 29'34"W) and the Imperial Davidson Creek P-2 (62° 11'45"N, 118° 15'00"W) wells a succession consisting of the Mount Cap, Saline River and Franklin Mountain formations directly overlies a pink granite resembling the Hudsonian granite found in the Wopmay Belt of the Bear Province.

Two wells have been drilled on the Bulmer Lake gravity anomaly: Imperial Cartridge B-72 (63° 11'19"N, 129° 29'04"W) and Chevron Harris River A-31 (62° 30' 02"N, 120° 06'00"W). In the Cartridge well pink granite is overlain by 157 feet of Proterozoic sandstone which is, in turn, overlain by 37 feet of sandstone and sandy dolomite of the Franklin Mountain Formation. In the Harris River well Proterozoic sandstone is directly overlain by dolomite of the Mount Kindle Formation. In both wells Lower and Middle Cambrian strata are missing and a positive Cambrian area is postulated in the area between Bulmer Lake and Keller Lake.

The subsurface geology of the southern Great Bear Plain, therefore, appears to be strikingly analogous to the geology of Leith Peninsula as described by Balkwill, although the Precambrian high cannot be defined precisely at present because of scattered well control. The similarity of geology in the two areas permits the suggestion that the eastern boundary of the "Bulmer Lake High" (see Fig. 1) may be the subsurface extension of the boundary between the Wopmay Belt and the Coppermine Homocline of the Bear Province (Stockwell, 1970, Fig. IV-1, p. 46). It must be pointed out, however, that this suggestion does not completely explain the gravity anomaly in the Bulmer Lake area, since the difference in elevation from the top to the base of the Precambrian high probably does not exceed 300 feet (the combined thickness of the Cambrian sediments that onlap the high in the east). The steep gravity gradient east of Bulmer Lake must have its origin in the granitic basement, either in the form of a change in lithology or as a significant fault.

The writer proposes to apply the name "Bulmer Lake Arch" for the paleotopographic and tectonic Precambrian feature in the Bulmer Lake area. It is concluded that the Bulmer Lake Arch consists of a Precambrian granitic high, flanked on the west by a thick succession of Proterozoic quartzites and argillites. This arch was a positive element during Cambrian sedimentation and its internal structure is the cause of Bulmer Lake gravity anomaly, which can be traced to the Precambrian salient present on Leith Peninsula.

References

Aitken, J. D., Macqueen, R. W., and Usher, J. L.
1973: Reconnaissance studies of Proterozoic and Cambrian stratigraphy, lower Mackenzie River area (Operation Norman), District of Mackenzie; Geol. Surv. Can., Paper 73-9.

Balkwill, H. R.
1971: Reconnaissance geology, southern Great Bear Plains, District of Mackenzie; Geol. Surv. Can., Paper 71-11.

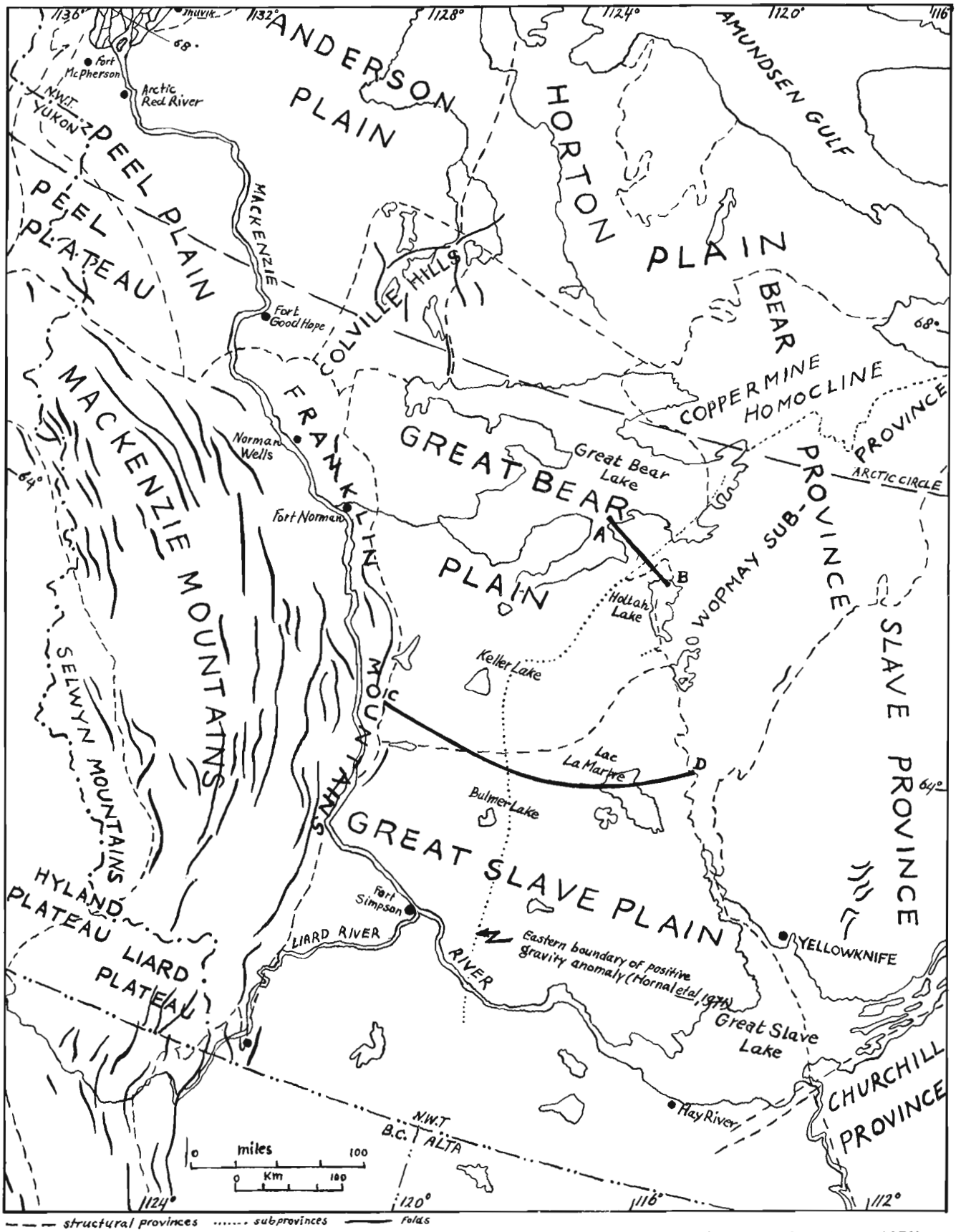

Figure 1. Structural Provinces, northern Interior Plains and environs. (Modified from Douglas et al., 1970).

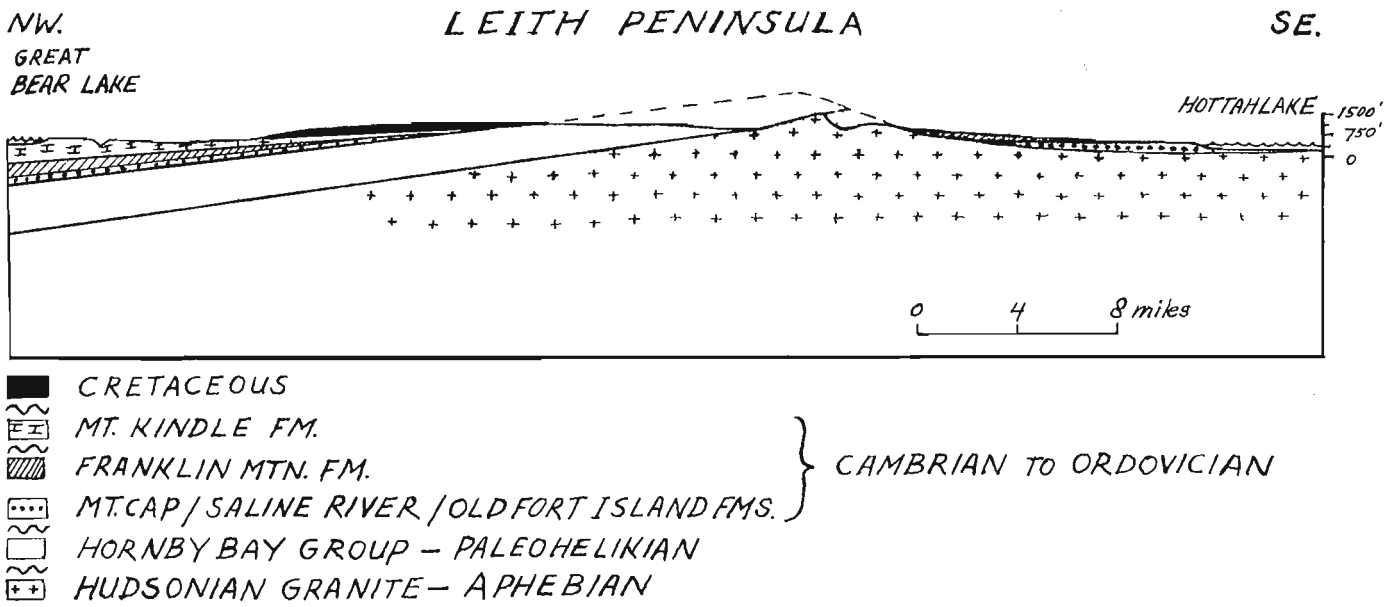

Figure 2. Schematic structural cross-section A-B across Leith Peninsula.

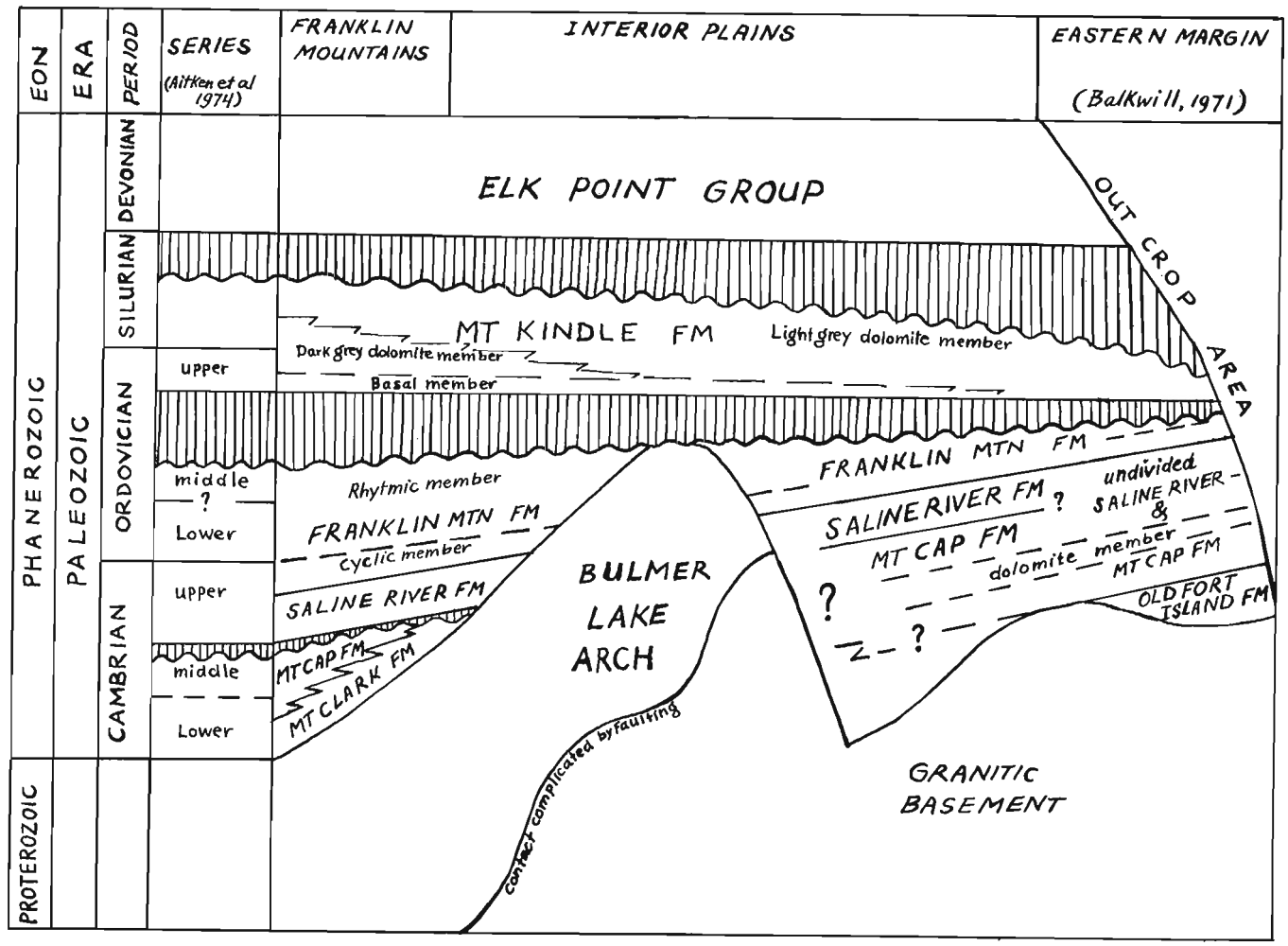

Figure 3. Schematic east-west structural and stratigraphical cross-section (C-D on Figure 1). (Note: Some of the time lines in this section are not horizontal).

Fraser, J.A.
1960: North-central District of Mackenzie, Northwest Territories; Geol. Surv. Can., Map 18-1960.

Hornal, R.W., Sobczak, L.W., Burke, W.E.F., and Stephens, L.E.
1970: Preliminary results of gravity surveys over the Mackenzie Basin and Beaufort Sea; Dept. of Energy, Mines and Resources, Gravity Map Series of the Earth Physics Branch.

Meijer Drees, N.C.
Geology of the lower Paleozoic succession in the subsurface of the Fort Simpson area, District of Mackenzie, N.W.T. (in preparation)

Stockwell, C.H. et al.
1970: Geology of the Canadian Shield, chapter IV, in Douglas, R.J.W., ed.; Geol. Surv. Can., Econ. Geol. Ser., no. 1, p. 44-45 and 77-84.

Project 720061

A. D. Miall
Institute of Sedimentary and Petroleum Geology

Introduction

The first of a series of short reports on the subsurface geology of the Banks Island area has appeared elsewhere (Miall, 1974a). In that paper, the stratigraphy of the Elf et al. Storkerson Bay A-15 well was described briefly. The present report discussed the stratigraphy of two more wells which recently have been released from confidential status. These are the Elf Nanuk D-76 well and the Elf Uminmak H-07 well. The stratigraphy of these boreholes is summarized in Tables 1 and 2. Figure 1 is a diagrammatic stratigraphic cross-section through all three wells.

Paleozoic Stratigraphy

The oldest unit penetrated in the three wells is composed of limestone of Late Emsian or Early Eifelian age in the Storkerson Bay well (Miall, 1974a). This is succeeded by a shale formation dated tentatively as Eifelian. The same unit is present in the Nanuk well where it is 823 feet thick. The top of the shale at the Nanuk well corresponds to the eroded top of the Paleozoic strata. The base of the shale was not penetrated by the well, and thus the recorded thickness is a minimum for the complete formation.

In the Nanuk well, the shale may be subdivided into two members: a siliceous shale unit occurring in the interval between 3,695 and 4,140 feet, and a calcareous shale unit occurring between 4,140 and 4,518 feet (T.D.). The lower member contains scattered pyrite and, near the base, stringers of dark grey, argillaceous, microcrystalline dolomite. The upper member contains interbeds of medium grey, micaceous siltstone and a unit of light grey or black, massive chert in the interval between 3,990 and 4,075 feet. Scattered pyrite is present in the upper part of the calcareous shale member. X-ray diffraction analyses of the siliceous shale reveal a silica content of up to 91 per cent. Thus, although the lithology may be classified as a shale on the basis of hand-specimen examination, much of it should be termed more accurately as argillaceous chert.

Several samples from the calcareous and siliceous shale units were analyzed for spores by A.R. Sweet and for conodonts by T.T. Uyeno, all without success. *Tentaculites* and *Styliolina* are present in the 4,160- to 4,260-foot interval. The *Tentaculites* specimens were examined by A.W. Norris, who dated them as late Early Devonian (Late Emsian) in age. This is the same age as indicated for the limestone in the Storkerson Bay well. A lateral facies change between the two wells is, therefore, presumed to exist, unless one or both of the dates are proved to be imprecise.

No exact analogues of this limestone-shale sequence are present on the mainland or elsewhere in the Arctic Islands. The units thus have not been formally named at the present time. However, the siliceous shale is similar to the Ibbett Bay Formation of Melville Island, and the calcareous shale is similar to the Eids.

The only other Paleozoic unit present in these three wells is an incomplete section through the Melville Island Group in the Uminmak well. The succession is 2,715 feet thick and consists of interbedded sandstone, siltstone, shale and coal. The sandstone is pale grey, very fine grained, slightly calcareous, quartzose, well cemented, of low porosity and contains disseminated grains of carbonaceous material. The siltstone is similar in texture. The shale is medium grey, silty and micaceous or dark grey and carbonaceous. Two dolomite stringers are present at 4,220 and 4,410 feet. Plant fragments are scattered throughout.

These beds have yielded a megaspore assemblage indicating that the succession ranges in age from early Frasnian at the base to middle Famennian at the top (palynology by A.R. Sweet). Age, lithology and thickness correlations with the Upper Devonian sediments exposed on northeastern Banks Island (Klovan and Embry, 1971) are very close, with the exception that the Mercy Bay member is not represented in the Uminmak well.

The subdivision of the Melville Island Group given in Table 2 corresponds to that used by Klovan and Embry (1971) in their study of the surface exposures. However, in the type area of the Melville Island Group (Melville Island) and on Bathurst Island, virtually all beds of early Frasnian to middle Famennian age are placed within the Griper Bay Formation (McGregor and Uyeno, 1972). A considerable thickness of Givetian strata (Hecla Bay and Weatherall formations of the original definition) may be present below the oldest beds penetrated in the Uminmak well. According to A.F. Embry (pers. comm., 1974) recent work in other parts of the Arctic Islands has shown that major revisions in the 1971 terminology are required but, until these are published, the earlier version must be used for comparative purposes within the Banks Island area.

Mesozoic and Tertiary Stratigraphy

The Christopher, Kanguk and Eureka Sound formations are similar in lithology in all three wells. Descriptions of these formations as they occur in the Storkerson Bay well have been provided by Miall (1974a). Differences in the other two wells are discussed briefly below.

The Christopher Formation consists predominantly of silty shale. Minor sand and silt interbeds are present in both wells but are more common in the

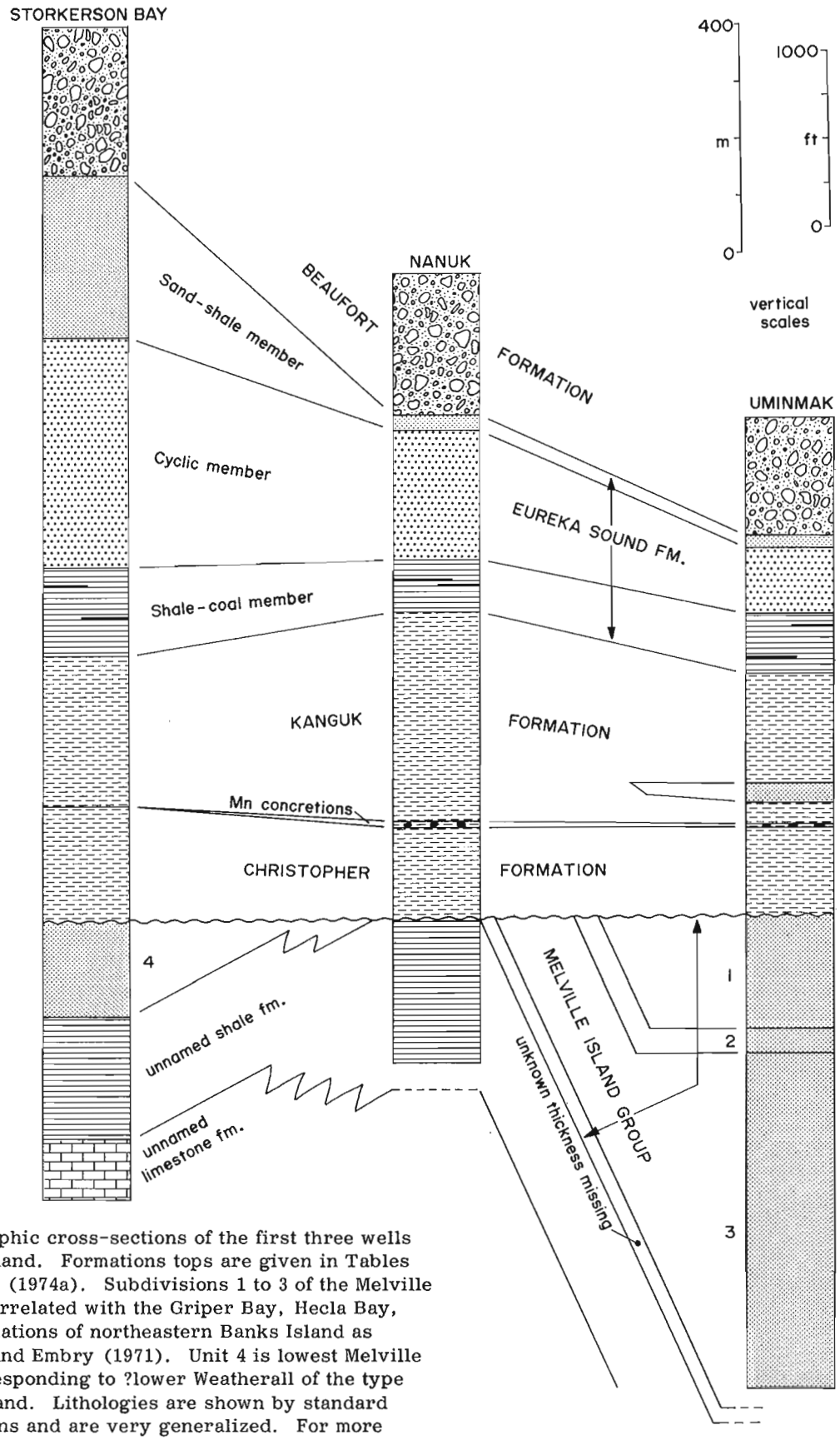

Figure 1.

Simplified stratigraphic cross-sections of the first three wells drilled on Banks Island. Formations tops are given in Tables 1 and 2 and in Miall (1974a). Subdivisions 1 to 3 of the Melville Island Group are correlated with the Griper Bay, Hecla Bay, and Weatherall formations of northeastern Banks Island as defined by Klovan and Embry (1971). Unit 4 is lowest Melville Island Group, corresponding to ?lower Weatherall of the type area on Melville Island. Lithologies are shown by standard lithologic conventions and are very generalized. For more detailed lithologic information see the text.

TABLE 1

Table of formations in the Elk Nanuk D-76 well

Age	Formation	Log depth	Subsea elevation	Thickness
Quaternary	Beaufort Formation	0	327	813
Maastrichtian-Eocene	Eureka Sound Formation	813	-486	1,127
	Sand-shale member	813	-486	89
	Cyclic member	902	-575	741
	Shale-coal member	1,643	-1,316	297
Santonian-Maastrichtian	Kanguk Formation	1,940	-1,613	1,198
	Upper Kanguk	1,940	-1,613	963
	Lower Kanguk	2,903	-2,576	235
Cenomanian?	Spherulitic concretion bed	3,138	-2,811	37
Albian	Christopher Formation	3,175	-2,848	520
Emsian-Eifelian	Unnamed shale formation	3,695	-3,368	823
	Siliceous shale member	3,695	-3,368	445
	Calcareous shale member	4,140	-3,813	378
	Total depth	4,518	-4,191	

TABLE 2

Table of formations in the Elk Uminmak H-07 well

Age	Formation	Log depth	Subsea Elevation	Thickness
Quaternary	Beaufort Formation	0	368	680
Maastrichtian-Eocene	Eureka Sound Formation	680	-312	796
	Sand-shale member	680	-312	75
	Cyclic member	755	-387	380
	Shale-coal member	1,135	-767	341
Santonian-Maastrichtian	Kanguk Formation	1,476	-1,108	861
	Upper Kanguk	1,476	-1,108	624
	Sandstone Member	2,100	-1,732	117
	Lower Kanguk	2,217	-1,849	120
Cenomanian?	Spherulitic concretion bed	2,337	-1,969	19
Albian	Christopher Formation	2,356	-1,988	502
Early to Middle Famennian	Griper Bay Formation*	2,858	-2,490	744
Late Frasnian	Hecla Bay Formation*	3,500	-3,132	140
Early to Late Frasnian	Weatherall Formation*	3,640	-3,272	1,933
	Total depth	5,573	-5,205	

* terminology of Klovan and Embry (1971)

Uminmak well. Early to Late Albian foraminifera (identifications by W. V. Sliter and T. P. Chamney) and Albian palynomorphs (identifications by W. S. Hopkins, Jr.) are present in this formation. The Christopher is thinner in the Uminmak and Nanuk wells than at Storkerson Bay. This is probably a reflection of the tectonic position of the two wells on the flanks of Storkerson Uplift (Miall, 1974b).

The contact between the Lower and Upper Cretaceous strata is marked by a distinctive unit of calcareous and dolomitic shale containing sand-size spherulitic concretions of rhodochrosite ($MnCO_3$). Traces of this bed are present in the Storkerson Bay well, but the unit is much thicker in the Nanuk and Uminmak wells. The manganese may have been derived from continental erosion of mafic igneous or metamorphic rocks, or from the decomposition of contemporaneous submarine volcanic material. A separate report discussing the implications of this unusual lithology is in preparation.

The Kanguk Formation consists predominantly of silty shale and argillaceous, calcareous siltstone. At both localities, pyrite and bentonite are minor accessories, and plant debris is scattered throughout. Differences between the two sections are that, at the Nanuk location, the Kanguk contains several beds of cone-in-cone limestone (as at Storkerson Bay), whereas this lithology is absent in the Uminmak well. Conversely, a prominent sandstone member is present in the 2,100- to 2,217-foot interval in the Uminmak section, and this unit is absent in the Nanuk well. The sandstone is quartzose and contains minor detrital chert and feldspar grains. A marine origin for the unit is suggested by the presence of glauconite. There is a patchy dolomite cement and a porosity, where cemented, of approximately 7 per cent (measured in thin section). Mechanical log interpretation suggests that shale interbeds are present in the lower part of the section and that these diminish in importance upwards and the sand becomes coarser in grain size. The unit is interpreted as a beach shoreface or barrier island sand, the origin of which is related to shoaling over Storkerson Uplift.

The Kanguk is dated as Santonian to Maastrichtian in age at the Uminmak and Nanuk locations. This compares with a Turonian to Maastrichtian age for the formation in the Storkerson Bay well (revised slightly from the age given by Miall, 1974a). The base of the Kanguk therefore appears to represent a marine transgression out of Big River Basin, covering the flanks of Storkerson Uplift only in Santonian times. Between the end of the Albian and the early part of the Santonian stage the uplift was emergent.

The Eureka Sound Formation shows a marked thinning between the Storkerson Bay location and the Uminmak and Nanuk wells. The latter are located on the flank of Storkerson Uplift, which presumably underwent less subsidence at this time. The same three members may be recognized in the Nanuk and Uminmak sections as were recognized at Storkerson Bay, although each member is thinner than at the latter locality. Lithologies are very similar; the middle member shows the same prograding clastic cycles and the sandstones are abundantly pebbly. They contain abundant fragments of siliceous shale and argillaceous chert, which probably were derived from exposures of the Middle Devonian rocks on Storkerson Uplift.

References

Klovan, J. E., and Embry, A. F., III
1971: Upper Devonian stratigraphy, northeastern Banks Island, N. W. T.; Bull. Can. Soc. Pet. Geol., v. 19, p. 705-729.

McGregor, D. C., and Uyeno, T. T.
1972: Devonian spores and conodonts of Melville and Bathurst Islands, District of Franklin; Geol. Surv. Can., Paper 71-13.

Miall, A. D.
1974a: Stratigraphy of the Elf et al. Storkerson Bay A-15 well; Geol. Surv. Can., Paper 74-1, pt. A, p. 335, 336.

1974b: Bedrock geology of Banks Island, District of Franklin; in Report of Activities, Part A, April to October 1973, Geol. Surv. Can., Paper 74-1, pt. A, p. 336-342.

105. A SHALLOW SHELF COASTAL ENVIRONMENT INTERPRETED FROM LITHOSTRATIGRAPHY OF LOWER CRETACEOUS CORES IN THE GULF-MOBIL EAST REINDEER G-04 BOREHOLE, N.W.T.

Project 710036

D.W. Myhr
Institute of Sedimentary and Petroleum Geology, Calgary

Introduction

Core No. 4 (9,580'-9,611') and core No. 5 (9,615'-9,647') of Early Cretaceous age were examined from the well, Gulf-Mobil East Reindeer G-04, located 16 miles northeast of the East Channel, modern Mackenzie Delta (Fig. 1) in the Northwest Territories (Lat. 68°53'15.9"N, Long. 133°46'03.3"W). The cored interval has an age ranging from Hauterivian to Aptian (Brideaux, 1973 and pers. comm.) and, therefore, is equivalent to the Coal-bearing division and Upper shale-siltstone division of northern Richardson Mountains (Jeletzky, 1958; 1960). Based on lithology, the interval from 9,210'-9,825' (including the cored interval) is correlative with the Upper shale-siltstone division; a succession of interstratified shale, siltstone and sandstone with abundant clay-ironstone concretions of (?)Upper Hauterivian-Barremian age (Jeletzky, 1958). From evidence based on lithology, sedimentary structures, micropaleontology, and inferred depositional processes, the depositional environment appears to have been somewhat brackish to marine, shallow and influenced by tractive currents and burrowing organisms. The depositional processes are in part cyclic as evidenced from sedimentary microcycles which may have been generated by periodic storms on a shallow shelf platform. The sublittoral sheet deposits onlap older deltaic deposits and represent the initial phase of late Neocomian transgression.

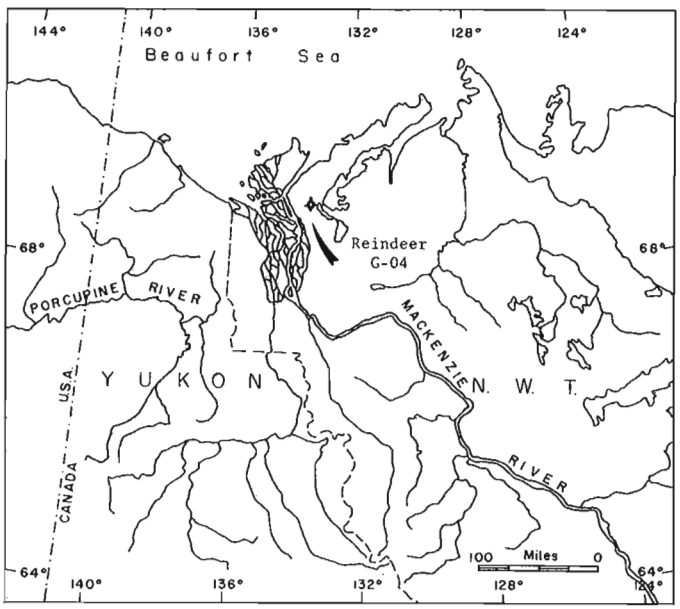

Figure 1. Location map of Gulf-Mobil East Reindeer G-04 borehole.

Description and Environmental Implications

The cored interval (9,580'-9,647') consists of an interstratified succession of siltstone and silty shale with a very fine sandstone unit near the base of the interval (9,632'-9,640'). The siltstone beds and silty shale interbeds are light brown to grey-brown (argillaceous units) in colour. The arenites are cemented with silica. Visible coal clasts are absent but organic detritus is common in samples processed for palynological identification. Bed thicknesses vary from 0.5-inch to 1.0-foot-thick and evenly bedded, microlaminated, plane bedded and wavy to horizontal and subhorizontal (up to 10° dip from vertical edge of core). Laminae consist of clay partings (stylolitic in the sandstone unit) and on one bedding (9,615') surface the partings consist of bimodal (very fine and coarse) shale clasts that are pelletoidal in shape. Their origin may be organic (faecal pellets; Reineck, 1961) or inorganic (clay floccules; Oomkens, 1970).

Sedimentary structures influenced by tractive currents include small-scale asymmetrical ripples (Fig. 2, photo 1), small-scale cross-laminations (tangential and wedge sets, photographs 1 and 2), climbing ripples up to 2 inches high, climbing ripple-drift laminations (indicative of rapid supply of sediment from suspension) and plane-bed, horizontal to subhorizontal laminations (lower phase of upper flow regime). Bioturbation structures are common in the silty shales. Individual ichnocoenose include simple burrow shafts, a smooth tubed U-shaped burrow, chevron-like grazing burrows (top of sandstone unit and not unlike those described by Howard, 1966 and Howard et al., 1972) and a few sinuous traces on bedding planes. Most common are disruptive structures (Frey, 1973b) which impart a mottled and mixed texture to the destratified shaly interbeds. The extensively bioturbated zones reflect a change in energy conditions allowing detritus feeders to recolonize the substrate (Howard, 1966) during periods of quiescence and deposition of suspended fine particles enriched in organic matter. Clay-ironstone concretions randomly occur in the siltstone and shaly interbeds and mineralogical analysis of one nodule yielded a composition of 63 per cent quartz, 37 per cent siderite and a significant amount of amorphous iron (Heinrich, 1974). The concretions are brown to pale yellowish brown and 10 mm to 50 mm in size. They are commonly ovoid and occasionally irregular to discoid in shape. In some cases the nodules reflect the original shape of the carbonized plant fragment nuclei. Two nodules contain carbonaceous microlaminae which pass into the adjoining siltstone beds and are unequivocal evidence for an autochthon-

Core Photographs Gulf-Mobil East Reindeer G-04

Photograph #1

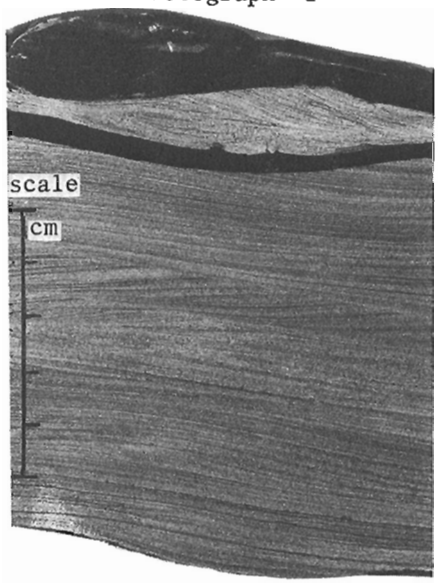

shale

asymmetrical ripple

plane bed wavy

microlaminated siltstone

"truncated" tangential crosslaminae

small-scale climbing-ripple drift laminations

9,593

Photograph #2

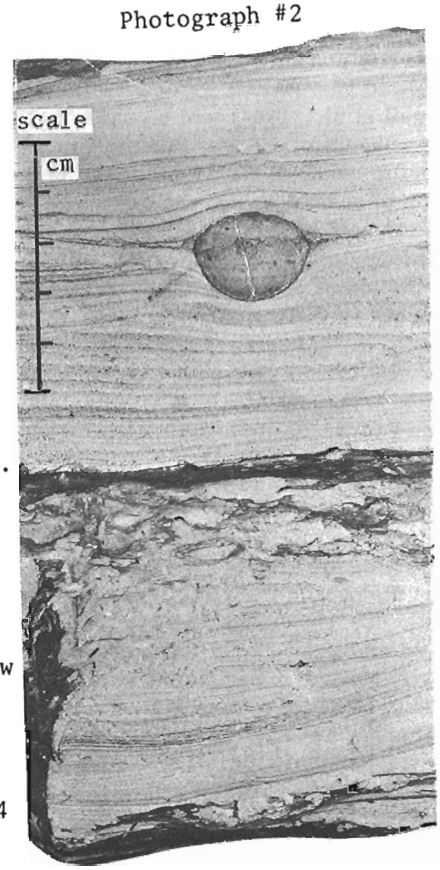

siltstone

autochthonous concretion

trunc. bioturb. text. slst.

vertical burrow infilled with shale

9,584

Mechanical Logs

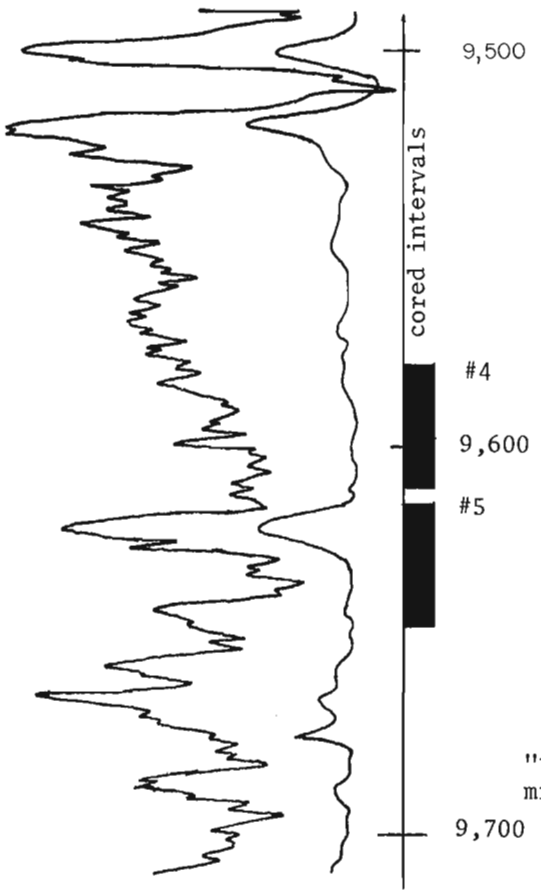

9,500

9,600

9,700

Photograph #3

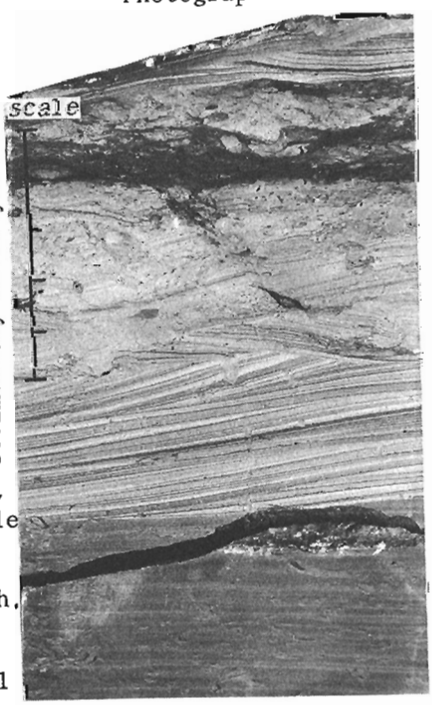

bed sole

destratified silty shale & siltstone with bioturb. texture.

burrowed crosslaminations

microlaminated siltstone

bed sole

"truncated" plane bed microlaminated slty. sh.

9,601

ous origin (Fig. 2, photo 2 illustrates one such nodule). Sideritic nodules are believed to form in the early stages of diagenesis (Müller, 1967; Gagliano, 1972; Coleman et al., 1972) and most commonly occur in brackish water environments such as swamps, lakes and marshes (Gagliano, 1972). They have been recorded also from a shallow nearshore deposit (Macdougall et al., 1964) and an outer delta-platform setting (Mazzullo, 1973). Shelton (1973) employs clayey sideritic concretions as one set of criteria for recognition of coastal sediments deposited in a brackish environment (e.g. delta-front or margin and distributary-influenced deposits). Clearly, concretions may be found in a host of environments but tend to be found in the transitional (=coastal-paralic) setting. Repetitive sedimentary microcycles are common and most obvious in core No. 4 (9,599'-9,603'=4'). Individual cycles consist of microlaminated siltstone which grades upwards into bioturbate-textured siltstone and shale (Fig. 2, photo 3), varying in thickness from a few inches to one foot thick. Bed soles are flat to undulose, truncating the older sedimentary sequence with up to 1 inch of relief. Depositional cycles begin with plane-bedded horizontal to subhorizontal laminations that grade up into micro-cross laminations of small, current- to wave-formed ripples, slightly burrowed and gradational with the extensively bioturbated silty shale unit. Sedimentary microcycles in core No. 5 are graded, of a finer texture and horizontally microlaminated, but have either noticeably thinner or no cross-laminated tops. The close association of current (?tractive) depositional processes with suspension sedimentation is recorded in the individual graded sedimentary microcycles. Various authors (Swift, 1970; Howard, 1972; Howard et al., 1972; Reineck et al., 1971) have attributed the repetitive character of depositional and biogenic structures to storm activity, thereby explaining the abrupt, erosive base and vertical variations in lithology and sedimentary structures depicting a gradual change in "flow regime" of a waning current. Swift (1970) has suggested that "storm-generated wave drift currents may be the dominant agent of sediment dispersal" on a shallow shelf platform. Other processes invoked by various authors include tidal currents, density currents (river influenced), turbidity currents (caused by floods basinward from land masses or tsunami) and less likely oceanic and rip currents.

In the ancient rocks Howard (1972) has described repetitive depositional cycles from a lower shoreface lithofacies; a regressive sedimentary sequence of Late Cretaceous age (Blackhawk Formation of Utah). He states that in the sandstone "bedding thickness at a particular outcrop is remarkably constant, and the laminations within the beds are mostly parallel and subhorizontal. The 'parallel to burrowed' vertical sequence of each bed shows progressive increase in the density of burrows upward, and the top of nearly every bed has been eroded (Fig. 5)". He attributes "the preserved record of sedimentation" to "periodic storms or strong tidal action" followed by recolonization of the substrate during periods of quiescence. In contrast with the cored interval the lower shoreface lithofacies is coarser grained and lacks the cross-laminated wave-rippled tops and bioturbated shaly-silty interbeds, but there are similarities as the sedimentary microcycles in the cored interval contain a vertical zonation of trace fossils (vertical and inclined shafts to disruptive structures), distinct bedding units of a near constant thickness and sharp bedding plane boundaries which may reflect a somewhat similar depositional process of a cyclic nature. Lithologies and sedimentary structures of the cored succession are similar to McCave's (1973) shallow marine, silty subfacies, a transgressive phase (Chemung facies) which onlaps the Catskill deltaic facies. McCave compares the silty subfacies to the German Bight transition facies of 10-15 metre water depth (Reineck et al., 1968).

In conclusion, the sedimentary structures, textural variations and repetitive depositional microcycles suggest that tractive currents and suspension-settling are the dominant sedimentary processes that are intimately associated and, in part, are cyclical in nature. The depositional site appears to have been a nearshore area on a shallow shelf platform. Brackish conditions may have prevailed as evidenced by the clay-ironstone concretions, organic constituents (megaspores, palynomorphs, rare dinoflagellates, and abundant carbonized plant detritus); indirect evidence includes the lack of glauconite and whole, marine fossils. Conversely, abundant foraminifera and rare ostracodes suggest a marine environment (Chamney, 1974). Modern environments of deposition, where comparable sedimentary deposits have formed, include the Neogene sediments of the Georgia Coast upper offshore (2-5 m water depth) lithofacies (Howard et al., 1972); the transition facies (10-15 m water depth) of a German Bight (Reineck et al., 1968) and, to a lesser degree, the delta-front deposits of the Mississippi Delta (Scruton, 1955), the Colorado River delta (Kanes, 1970), and the Niger Delta (Allen, 1964; 1970).

Stratigraphy

Palynological samples examined by Brideaux (1974) from between 9,580 and 9,605 feet range in age from latest Jurassic to Early Cretaceous. Samples collected from the interval between 9,615 and 9,647 feet yielded abundant plant debris, derived Devono-Carboniferous spores, bisaccate grains, palynomorphs and two dinoflagellate species with more restricted age ranges; *Oligosphaeridium asterigium* (Gocht) Davy and Williams has an age-range of Valanginian to Middle Albian, and *Hystrichosphaeridium*? sp. G (MS) ranges from Hauterivian to Aptian; therefore, the age of the interval is Hauterivian to Aptian (Brideaux, 1973 and pers. comm.). Megaspore analysis yielded a Lower Cretaceous assemblage with abundant algal cysts (*Leiosphaeridia* sp.), and reworked Upper Devonian and rare Carboniferous megaspores (Sweet, 1974).

The sublittoral sheet deposits described from cores No. 4 and No. 5 of the Gulf-Mobil East Reindeer G-04 well represent 63 feet of a much thicker sequence (635') of interbedded siltstone, shale, and minor

sandstone. The uppermost contact (9,210') is gradational with a thick shale and mudstone succession (=deep marine). The basal contact (9,825') is chosen at the top of the first clean, porous sandstone (75 feet thick) which is interpreted as a shoreline deposit (beach-barrier-bar). The sandstone unit is in abrupt contact with argillaceous sandstone and mudstone that are interbedded with coal and clean, porous sandstone to a depth of 10,635 feet. This lithofacies may represent a fluvial-deltaic environment. The vertical succession from 10,635 to 9,210 feet typifies a regressive-transgressive phase of sedimentation marked by prograding continental deposits that were onlapped eventually by a late Neocomian sea; the cored interval is within the marine transgression. Based on lithology (samples, core, and mechanical log response) and the vertical succession of rock units, the cored interval and genetically related lithofacies (9,210'-9,825') appears to be correlative with the Upper shale-siltstone division described by Jeletzky (1958; 1960) from surface sections in the Richardson Mountains and dated as (?)late Hauterivian to Barremian. Palynological evidence indicates that the cored interval is Hauterivian to Aptian in age and, therefore, is in part synchronous with the Upper shale-siltstone division. Jeletzky (1960) also recognized the transgressive, marine nature of the Upper shale-siltstone division which onlaps the underlying Coal-bearing division.

References

Allen, J.R.
1964: Sedimentation in the modern Niger Delta *in* Deltaic and shallow marine deposits, L.M.J.U. Van Straaten, ed.; Dev. Sedimen., v. 1, p. 29-32, Amsterdam (Elsevier).

1970: Sediments of the modern Niger Delta; a summary and review *in* Deltaic sedimentation modern and ancient, J.P. Morgan, ed.; Soc. Econ. Paleontol. Mineral., Spec. Publ. No. 15, p. 138-151.

Barnes, C.R., Brideaux, W.W., Chamney, T.P., Clowser, D.R., Dunay, R.E., Fisher, M.J., Fritz, W.H., Hopkins, W.S., Jr., Jeletzky, J.A., McGregor, D.C., Norford, B.C., Norris, A.W., Pedder, A.E.H., Rauwerda, P.J., Sherrington, P.F., Sliter, W.V., Tozer, E.T., Uyeno, T.T., and Waterhouse, J.B.
1974: Biostratigraphic determinations of fossils from the subsurface of the northwest and Yukon Territories; Geol. Surv. Can., Paper 74-11.

Brideaux, W.W.
1973: Geol. Surv. Can., Internal Paleont. Report K-2-WWB.

Chamney, T.P.
1974: Geol. Surv. Can., Internal Paleont. Report Mcs-2-TPC.

Coleman, J.M., and Gagliano, S.M.
1972: Sedimentation in a Malaysian high tide tropical delta *in* Arenaceous deposits, F.D. Crawford, ed.; Sedimentation and Diagenesis, p. 61-89.

Frey, R.W.
1973a: The Neogene of the Georgia Coast *in* 8th Annual Field Trip of the Georgia Geological Society, R.W. Frey, ed.; Dept. Geol., Univ. Georgia, p. 1-34.

1973b: Concepts in the study of biogenic sedimentary structures; J. Sediment. Petrol., v. 43, no. 1, p. 6-19.

Gagliano, S.M.
1973: The Mississippi Delta system; Part A in Arenaceous deposits, F.D. Crawford, ed.; Sedimentation and Diagenesis, p. 89-113.

Goldring, R., and Bridges, P.
1973: Sublittoral sheet sandstones; J. Sediment. Petrol., v. 43, p. 736-747.

Heinrich, A.G.
1974: Geol. Surv. Can. Internal Mineralogical Analysis, no. 74-XR-11.

Howard, J.D.
1966: Characteristic trace fossils in Upper Cretaceous sandstones of the Book Cliffs and Wasatch Plateau in Central Utah Coals - a guidebook prepared for the G.S.A. and associated societies, Bull. 80.

1972: Trace fossils as criteria for recognizing shorelines in stratigraphic record *in* recognition of ancient sedimentary environments, J.K. Rigby and W.K. Hamblin, eds.; Soc. Econ. Paleontol. Mineral., Spec. Publ. No. 16, p. 215-225.

Howard, J.D., and Reineck, H.E.
1972: Georgia coastal region, Sapelo Island, U.S.A. Sedimentology and Biology IV, physical and biogenic sedimentary structures of the nearshore shelf; Senckenbergiana maritima, no. 4, p. 81-125.

Jeletzky, J.A.
1958: Uppermost Jurassic and Cretaceous rocks of Aklavik Range, northeastern Richardson Mountains, Northwest Territories; Geol. Surv. Can., Paper 58-2.

1960: Uppermost Jurassic and Cretaceous rocks, east flank of Richardson Mountains between Stony Creek and lower Donna River, Northwest Territories; Geol. Surv. Can., Paper 59-14.

Jeletzky, J.A. (cont'd.)
1972: Stratigraphy, facies and paleogeography of Mesozoic and Tertiary rocks of northern Yukon and northwest Mackenzie District, N.W.T. (NTS 107B, 106M, 117A, 116-O (N½), 116I, 116H, 116J, 116K (E½)); Geol. Surv. Can., Open File Report 82.

Mazzullo, J.S.
1973: Deltaic depositional environments in the Hamilton Group (Middle Devonian), southeastern New York State; J. Sediment. Petrol., v. 43, no. 4, p. 1061-1071.

McCave, N.I.
1973: The sedimentology of a transgression: Portland Point and Cooksburg Members (Middle Devonian), New York State; J. Sediment. Petrol., v. 43, p. 490-495.

McDougall, J.D.S., and Prentice, J.E.
1964: Sedimentary environments of the Weald Clay of southeastern England *in* deltaic and shallow marine deposits, L.M.J.U. Van Straatan, ed.; Dev. Sedimentol., v. 1, p. 257-263, Amsterdam (Elsevier).

Müller, G.
1967: Diagenesis in argillaceous sediments *in* Diagenesis in sediments, L.M.J.U. Van Straatan, ed.; Dev. Sedimentol., v. 8, p. 154, 155, Amsterdam (Elsevier).

Oomkens, E.
1970: Postglacial Rhône delta complex *in* Deltaic sedimentation modern and ancient, J.P. Morgan, ed.; Soc. Econ. Paleontol. Mineral., Spec. Publ. No. 15, p. 204-207.

Reineck, H.-E.
1961: Versteinerte Nordsee; Natur und Volk, v. 91, p. 151-162.

Reineck, H.-E., Dorjes, J., Gadow, S., and Hertweck, G.
1968: Sedimentologie, Faunenzonierung und Faziesabfolge van der Ostkuste der inneren Deutschen Bucht; Senckenbergiana Lethaea, v. 49, p. 261-309.

Reineck, H.-E., and Singh, I.B.
1971: Der Golf von Gaeta (Tyrrhenisches Meir). III Die Gefüge von Vorstrand und Schelfsedimenten; Senckenbergiana marit., v. 3, p. 185-201.

Scruton, R.C.
1955: Sediments of the eastern Mississippi Delta *in* Finding ancient shorelines, J.L. Hough and H.W. Menard, eds.; Soc. Econ. Paleontol. Mineral., Spec. Publ. No. 3, p. 21-50.

Shelton, J.W.
1973: Models of sand and sandstone deposits: A methodology for determining sand geneses and trend; Oklahoma Geol. Surv., Bull. 118.

Sweet, A.R.
1974: Geol. Surv. Can., Paleont. Internal Report No. As-1-1974.

Swift, D.J.P.
1969: The Carolina Cretaceous: Petrographic reconnaissance of a graded shelf; J. Sediment. Petrol., v. 39, p. 18-33.

1970: Quaternary shelves and return to grade; Mar. Geol., v. 8, p. 5-30.

106. LOWER PALEOZOIC, SLAVE RIVER MAP-AREA, DISTRICT OF MACKENZIE (NTS 85)

Project 710033

G. K. Williams
Institute of Sedimentary and Petroleum Geology, Calgary

Pre-Devonian sediments outcrop sporadically west of the North Arm of Great Slave Lake. Norris (1965) introduced the terms "Chedabucto Lake Formation", "La Martre Falls Formation" (with the Mazenod member) and "Old Fort Island Formation" for an Upper Ordovician dolomite; and underlying shale, siltstone, sandstone, and dolomite unit; and the basal Paleozoic sandstone respectively. Subsequent field mapping by personnel of the Geological Survey of Canada (Operation Norman) has established the continuity of several map units from the Franklin Mountains eastward to the Shield. In the area immediately north of the Slave River map-area Balkwill (1971) used the older lower Paleozoic nomenclature of Williams (1922, 1923) in part redefined by Macqueen (1970) with the addition of Norris' term "Old Fort Island Formation".

The relationship of the two systems of nomenclature must be approximately as shown on Figure 2. The Mount Kindle and Chedabucto Lake formations outcrop belts are continuous. The precise relationship of the pre-Mount Kindle sediments is less certain. A regional unconformity at the base of the Mount Kindle Formation is known from surface and subsurface information in the Franklin Mountains, Mackenzie Mountains and adjacent plains. The unconformity cuts deeper down section to the east. In the west the Mount Kindle Formation lies on a thick dolomite succession, the Franklin Mountain Formation, which has three mappable units, from the top down: the "cherty", "rhythmic" and "cyclic" units. In the southern Great Bear Plain, mapped by Balkwill (1971), the Mount Kindle Formation lies directly on the "cyclic" unit; the higher two units of the Franklin Mountain Formation are missing through pre-Mount Kindle erosion.

The sub-Mount Kindle unconformity apparently cuts even lower in the section from north to south, as illustrated in Figure 2. This can be inferred from the sections described by Norris (1965). Norris' northernmost sections 10 and 11 (Norris, 1965, p. 104 and 105) contain, at the top of the La Martre Falls Formation, a few feet of dolomite which, from the descriptions, belong in the "cyclic unit". South of about latitude 63°40' Norris' sections 1, 12, 14 and 15 (Norris, 1965, p. 100, 110 and 112), the "cyclic unit" type of dolomite is not present.

The upper 40 feet of the La Martre Falls Formation at the type section (Norris, 1965, Sec. 13, p. 108) consists of interbedded dolomite and shale with fossils.

> "This assemblage, according to G. W. Sinclair, indicates an Ordovician age, younger than Chazyan.... On the above evidence all of the La Martre Falls Formation is provisionally dated as Middle Ordovician" (Norris, 1965, p. 20)."

The above fossil evidence is in apparent conflict with more recent field evidence. North of the map-area, in beds which are lithologically and stratigraphically equivalent to part of the La Martre Falls Formation, Cominco Ltd. have discovered fossils which indicate a Middle Cambrian age. These are discussed in Balkwill (1971, p. 14), and it is partly on this evidence that the beds can be correlated with the Saline River and Mount Cap Formations. The overlying "cyclic" unit also is considered to be Cambrian (Balkwill, 1971, p. 18).

The solution to this apparent inconsistency may be that the upper 40 feet or so of the La Martre Falls type section actually belong with the Mount Kindle Formation (younger than Chazyan). The pre-Mount Kindle unconformity may be near the dolomite/sandstone contact (footage 79.3 of Norris' type section) or perhaps a few feet higher, and marked by the chert pebbles just below the fossils in unit 16 of the type section (Norris, pers. comm.).

The older system of nomenclature is applicable over a vast area of the Northwest Territories from the northern boundary of the Slave River map-area to the Arctic coast (see Macqueen and MacKenzie, 1973). The same nomenclature is applicable also to the subsurface (see Gilbert, 1973; Kunst, 1973). As the outcrops in the Slave River map-area can be described adequately by the northern nomenclature, it seems inevitable that the terms "Chedabucto Lake" and "La Martre Falls" will be abandoned. The term "Old Fort Island" should be retained for the basal sandstone in areas where recognizable Cambrian strata are preserved. To the south where the oldest known rocks are Devonian, for example over the Tathlina high, the term "Old Fort Island" is not appropriate for the basal sandstone. The term "Mazenod Member" also is useful locally and should be retained. Unfortunately it is uncertain whether this dolomite is a member of the Saline River or of the Mount Cap Formation; probably it lies within the lower part of the section equivalent to the Mount Cap Formation.

In the subsurface, two wells, Imperial Windflower G-77 and Horn River Shell Levis D-76, penetrated an early Paleozoic section comparable with that at the surface; these are illustrated on Figure 3. In three other wells, which lie closer to the southern limit of the early Paleozoic, the correlation is less obvious. In Imperial Triad Davidson Creek P-2, the basal few feet of sediments are green shale, unlike anything to be expected in the early Devonian deposits; this shale may be a remnant of the Mount Cap Formation. Farther west in Imperial Willowlake B-20 and Chevron Hornell Lake G-24 wells, there is a basal reddish or pink dolomite; in the former well this dolomite lies on crystalline basement. This dolomite is interpreted as the Mount Kindle Formation. Red and pink coloration in the Mount Kindle dolomite is described by Norris in the southernmost exposures.

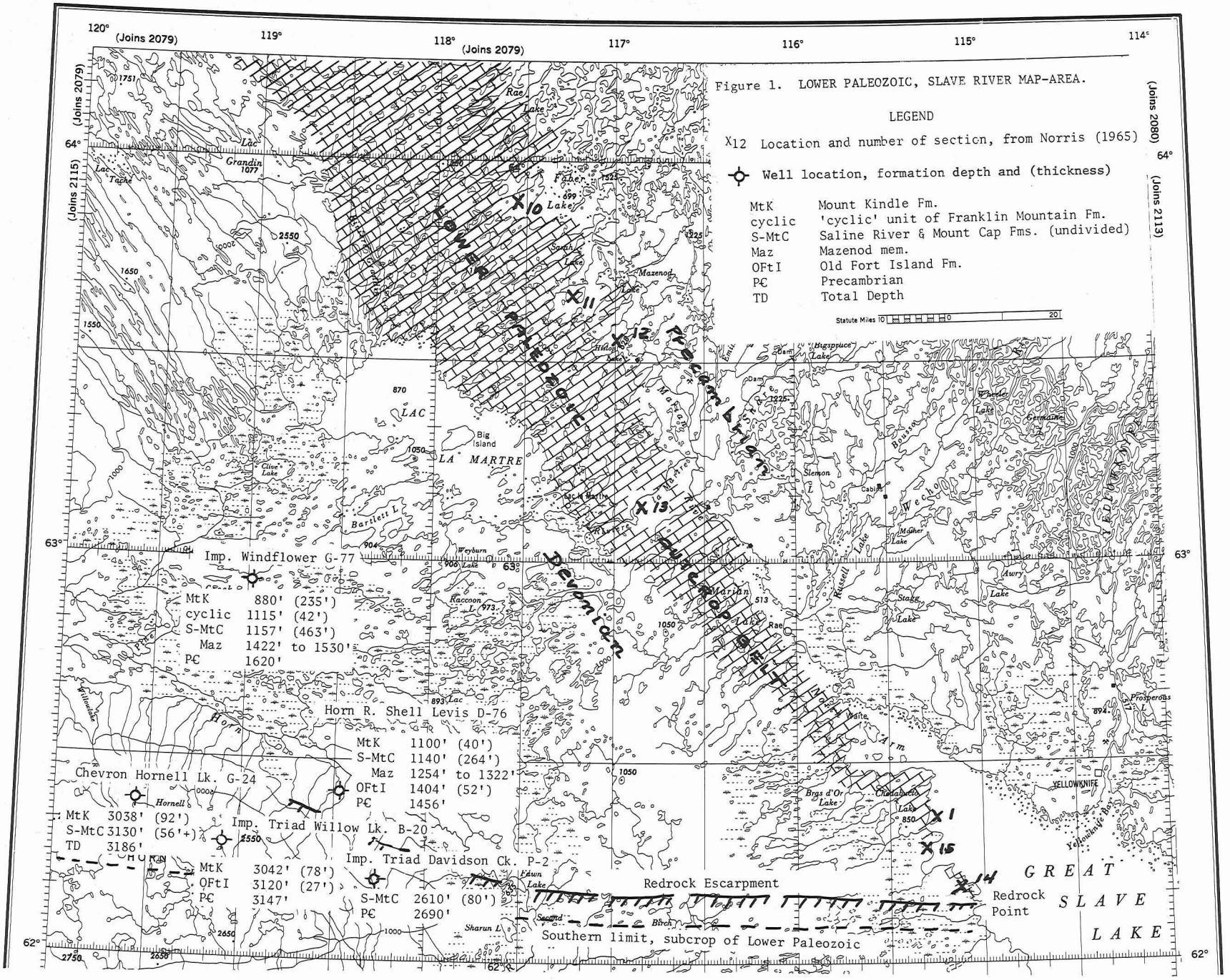

Figure 1. LOWER PALEOZOIC, SLAVE RIVER MAP-AREA.

LEGEND

X12 Location and number of section, from Norris (1965)

Well location, formation depth and (thickness)

MtK	Mount Kindle Fm.
cyclic	'cyclic' unit of Franklin Mountain Fm.
S-MtC	Saline River & Mount Cap Fms. (undivided)
Maz	Mazenod mem.
OFtI	Old Fort Island Fm.
PC	Precambrian
TD	Total Depth

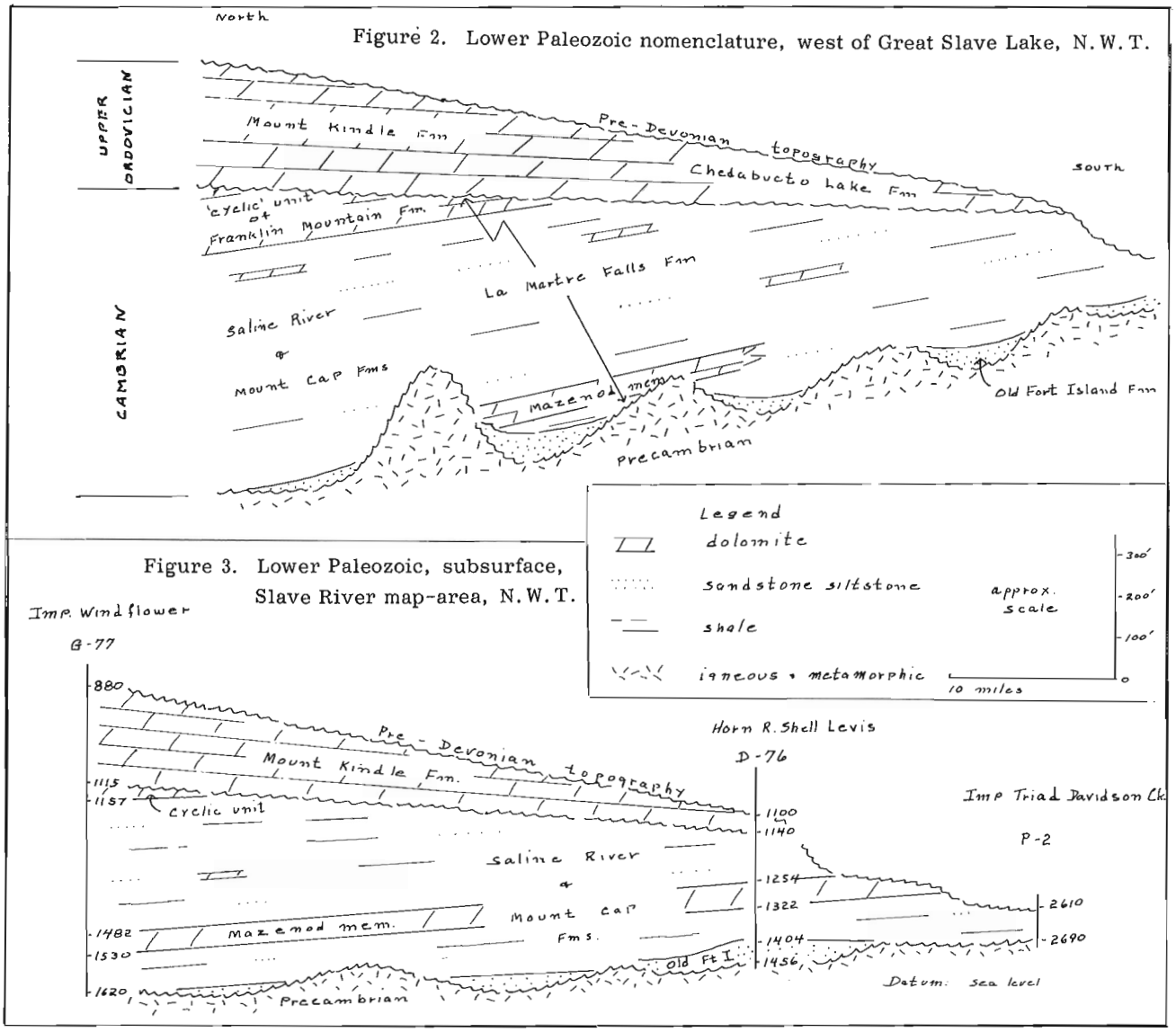

Figure 2. Lower Paleozoic nomenclature, west of Great Slave Lake, N.W.T.

Figure 3. Lower Paleozoic, subsurface, Slave River map-area, N.W.T.

Figure 4 illustrates a diagrammatic interpretation of the pre-Devonian relief of a part of the Slave River Sheet. In the east is a low escarpment capped by a thin remnant of the resistant Mount Kindle dolomite which overlies the recessive Cambrian clastic rocks. The evidence for such an escarpment comes largely from subsurface data, illustrated on Figure 3. If the outcrop belt is interpreted in similar fashion, the Mirage Point Formation is a sequence of early Devonian evaporites and red beds which filled the depression south of the escarpment. Toward the west the escarpment disappears. In this area, which is part of the northern flank of the Tathlina high, Mount Kindle rocks apparently lie directly on the basement. Where no recessive sediments lie below the Mount Kindle dolomite, an escarpment did not form.

This south-facing escarpment is a mirror image of the north-facing Meadow Lake escarpment, described by van Hees (1958). Both escarpments are formed by rocks of roughly equivalent age and lithology. The northern escarpment has only about half of the vertical relief of that to the south. The maps of van Hees, and Porter and Fuller (in McCrossan, 1964) illustrate that there is no known occurrence of Cambrian or Ordovician rocks in the area between these two escarpments. The term "Redrock escarpment" is proposed for the northern feature, from Redrock Point on Great Slave Lake on which occurs the southernmost outcrop of the Mount Kindle Formation.

References

Balkwill, H.R.
1971: Reconnaissance geology, southern Great Bear Plain, District of Mackenzie; Geol. Surv. Can., Paper 71-11.

Gilbert, D.L.F.
1973: Anderson Plain, northern District of Mackenzie; in Future Petroleum Provinces of Canada, R.G. McCrossan, ed., Can. Soc. Pet. Geol., Mem. 1.

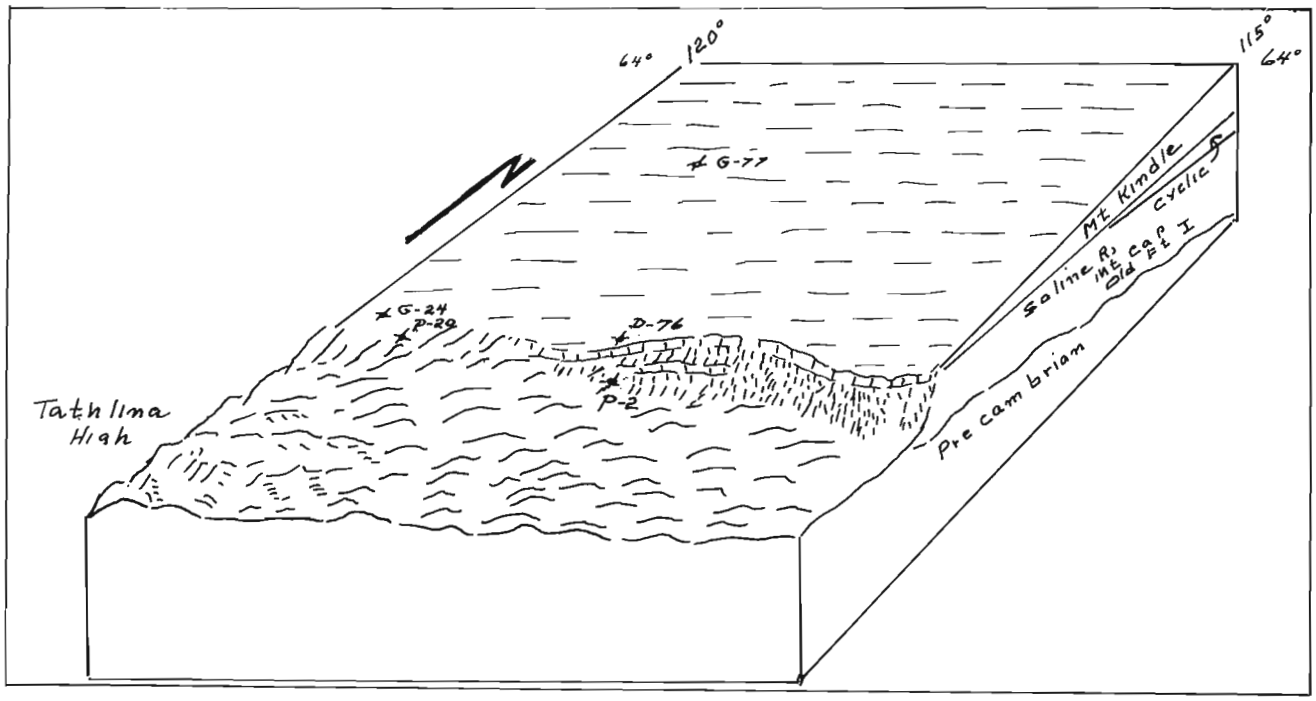

Figure 4. Pre-Devonian topography, west of Great Slave Lake, N.W.T.

Kunst, H.
1973: Peel Plateau; in Future Petroleum Provinces of Canada, R.G. McCrossan, ed., Can. Soc. Pet. Geol., Mem. 1.

Macqueen, R.W.
1970: Lower Paleozoic stratigraphy and sedimentology, eastern Mackenzie Mountains, northern Franklin Mountains; in Report of Activities, April to October 1969, Geol. Surv. Can., Paper 70-1A, p. 225-230.

Macqueen, R.W. and MacKenzie, W.S.
1973: Lower Paleozoic and Proterozoic stratigraphy, Mobil Colville Hills E-15 well and environs, Interior Platform, District of Mackenzie; in Report of Activities, November 1972 to March 1973, Geol. Surv. Can., Paper 73-1B, p. 183.

McCrossan, R.G. and Glaister, R.P. (eds.)
1964: Geological History of Western Canada; Alberta Soc. Pet. Geol.

Norris, A.W.
1965: Stratigraphy of Middle Devonian and older Paleozoic rocks of the Great Slave Lake region, Northwest Territories; Geol. Surv. Can., Mem. 322.

van Hees, H.
1958: The Meadow Lake escarpment - its regional significance to Lower Paleozoic stratigraphy; Ind. Intern. Symp. on the Williston Basin, Sask. Geol. Soc. and North Dakota Geol. Soc., p. 70-78.

Williams, M.Y.
1922: Exploration east of Mackenzie between Simpson and Wrigley; Geol. Surv. Can., Sum. Rept. 1921, Part B.

1923: Reconnaissance across northeastern British Columbia and the geology of the northern extension of the Franklin Mountains, N.W.T.; Geol. Surv. Can., Sum. Rept. 1922, Part B.

107. CRETACEOUS STRATIGRAPHIC DISPLACEMENTS ACROSS BLOW FAULT ZONE, NORTHERN YUKON TERRITORY

Projects 700068, 710036

F.G. Young
Institute of Sedimentary and Petroleum Geology, Calgary

Introduction

Norris (in press) recently has called attention to the possible tectonic significance of the Kaltag Fault of central Alaska with regard to offset crustal plates in northern Canada. The extension of the Kaltag Fault can be shown to be the Porcupine Fault (ibid.) of east-central Alaska and northern Yukon. This fault swings to an almost north-south orientation where it meets the Yukon Fault in northwestern Richardson Mountains (Fig. 1). From there, northward toward the offshore area, the faults diverge into the Rapid Fault Array (Norris, 1971). This paper attempts to show that (i) right lateral offsets within or near the fault array are unlikely to have occurred after Aptian time, but may have occurred before then; (ii) vertical displacements in which the western block was uplifted took place in Early Cretaceous tectonic episodes; and (iii) displacements in the first two episodes (?Hauterivian and Aptian) and possibly the third (Albian) were concentrated in a five-mile-wide zone trending north-south, located eight miles east of Bonnet Lake. Because of its importance to the tectonics and stratigraphy of the area this zone is here termed the Blow Fault Zone (Fig. 1).

Early Lower Cretaceous (Neocomian) Rocks

Numerous stratigraphic sections of Neocomian rocks have been measured by the writer and J.A. Jeletzky within and surrounding the critical area. Summary versions of these were plotted on a map (not shown) and compared over the north slope region. Internal Neocomian stratigraphy and its relationship to the Aptian unconformity undergo profound changes across the western edge of Rapid Fault Array in the Blow Fault Zone.

In northwest Richardson Mountains virtually every Lower Cretaceous stratigraphic unit thickens from east to west (Fig. 3); especially marked thickenings occur within the Valanginian-Hauterivian interval which includes the Blue-grey shale to Coaly quartzite divisions. In crossing Blow Fault Zone, however, these great thicknesses of quartzitic sandstone and shale disappear, to be replaced in the periphery of Barn Uplift by very much thinner rock-units. The Upper sandstone division, which is in the order of 1,000 feet thick east of the fault zone, is absent to the west of it. It reappears in a thinner form southwest of Barn Mountains, twenty miles or more west of the fault zone.

The abrupt disappearance of Lower Cretaceous units is expressed by the markedly different stratigraphic levels upon which the Aptian-Albian flysch deposits lie on either side of Blow Fault Zone (Fig. 3). East of it, within Rapid Fault Array, the flyschoid depositional phase appears to begin within the Aptian Upper sandstone division, above a disconformity representing an insignificant stratigraphic omission. West of Blow Fault Zone, however, the flysch commences with the Aptian Lower shale-siltstone unit, which lies above an unconformity truncating increasingly older Mesozoic sediments from west to east (Fig. 3). Immediately west of the fault zone, approximately 6,000 feet of Lower Cretaceous and Uppper Jurassic sediments are apparently differentially truncated relative to the east side.

The Aptian Unconformity

Evidence to support the stratigraphic levels below the Aptian unconformity (B, Fig. 3) is derived from the writer's measured sections and auxiliary field observations, interpretations of Jeletzky's published data, and geological mapping. Within Blow River valley, including Bonnet Lake area, no stratigraphic units younger than Blue-grey shale division (Valanginian) are encountered except the Aptian-Albian flysch. The absence of much of the intervening Neocomian section, which is so prominently exposed only a few miles to the east, is anomalous if indeed it does exist in this area.

The stratigraphic succession at the headwaters of Fitton Creek along the east flank of Barn Uplift clearly indicates a large stratigraphic hiatus (Young, 1973). There, chert-pebble conglomerates, assumed to represent the base of the Aptian-Albian flysch division, form buttes and low mesas and lie only 300 to 400 feet above shaly sandstone containing the Berriasian *B. okensis* faunal zone. To the southeast in Blow Valley, Jurassic and Aptian rocks commonly alterate perpendicular to strike. Jeletzky (1971, p. 205) has interpreted this as entirely due to faulting, but the writer believes the Aptian rocks lie unconformably on the Jurassic shale and this set is repeated by faults. In one continuous exposure, pebbly Aptian shale overlies Jurassic bioturbated silty shale without any evidence of a fault between them. Higher in the outcrop Jurassic shale overlies, in turn, the Lower Cretaceous shale, hence a fault must separate them at this level.

From Jeletzky's published data, it can be noted that no rocks of an age between early Valanginian and latest Aptian are recorded in the Bonnet Lake area west of the "Bonnet Alps" (Sects. 6, 7, 8 in Jeletzky, 1961; Area 2 in Jeletzky, 1971; Area 9 in Jeletzky, 1973). The absence of strata of these ages supports the contention that a hiatus representing this interval exists in a belt about 18 miles wide immediately west of, and parallel to, the Blow Fault Zone.

East of Blow Fault Zone, the Aptian unconformity appears to represent little stratigraphic omission, but

Figure 1. Location map with tectonic elements (after D. K. Norris, 1973; in press).

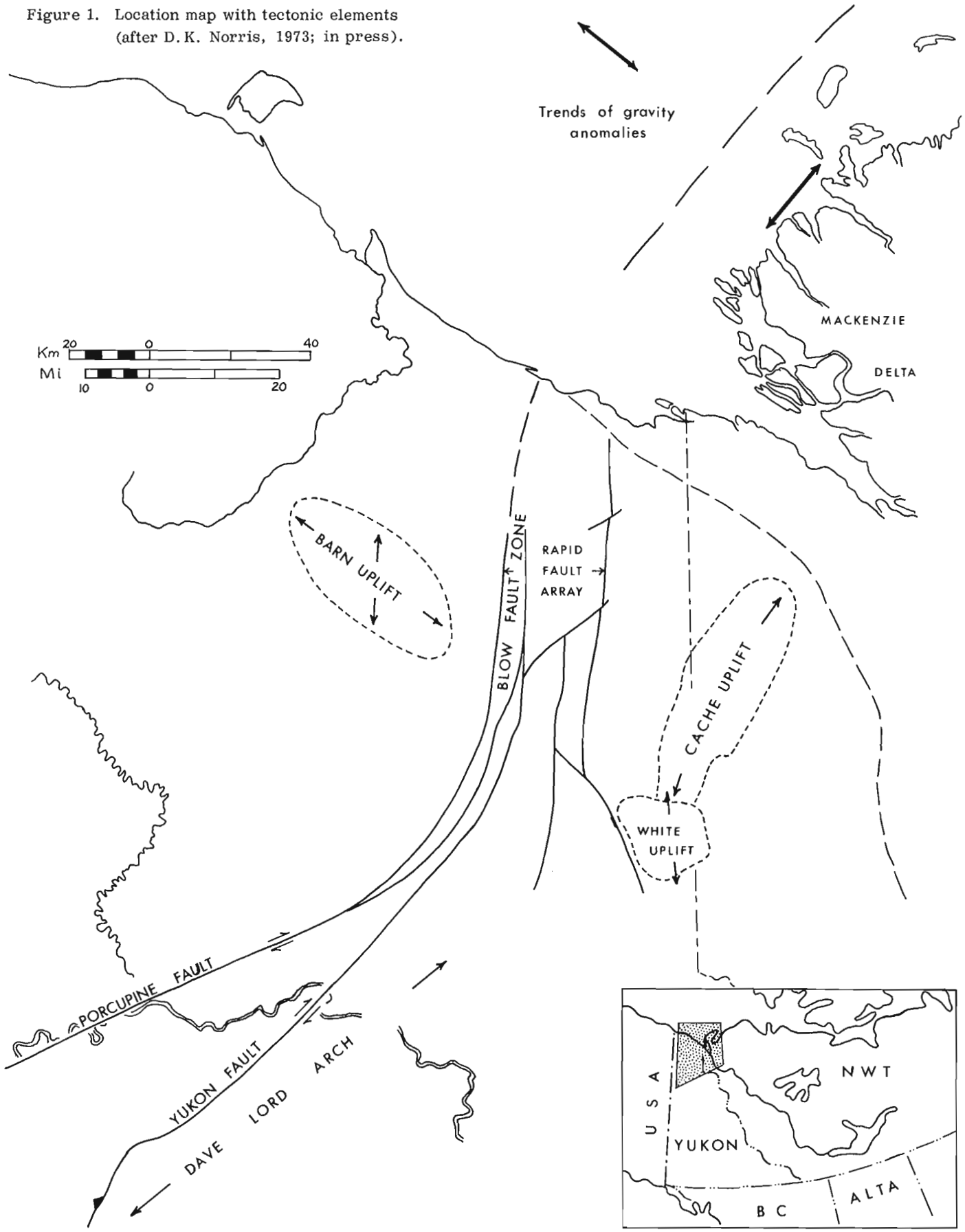

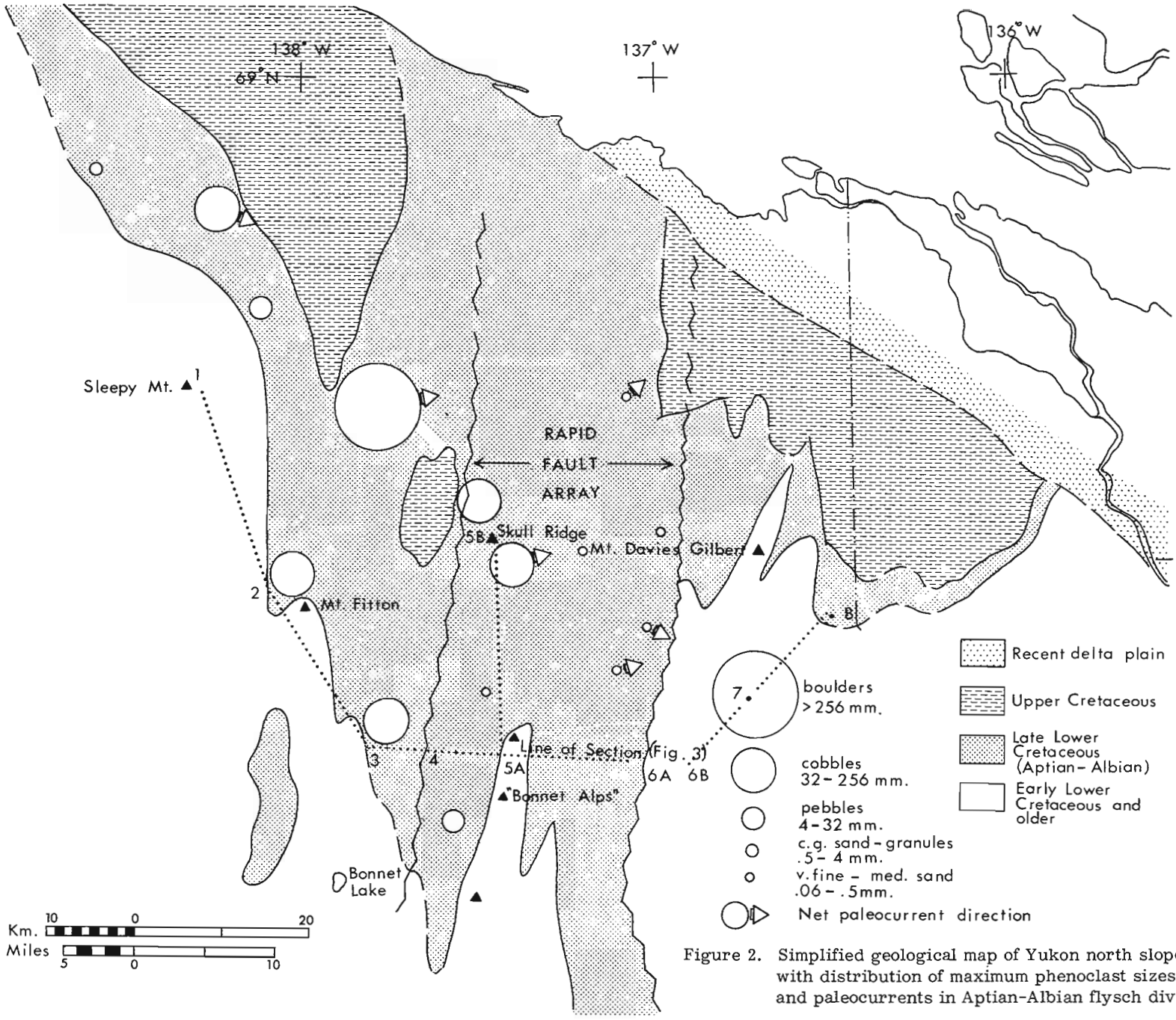

Figure 2. Simplified geological map of Yukon north slope, with distribution of maximum phenoclast sizes and paleocurrents in Aptian-Albian flysch division.

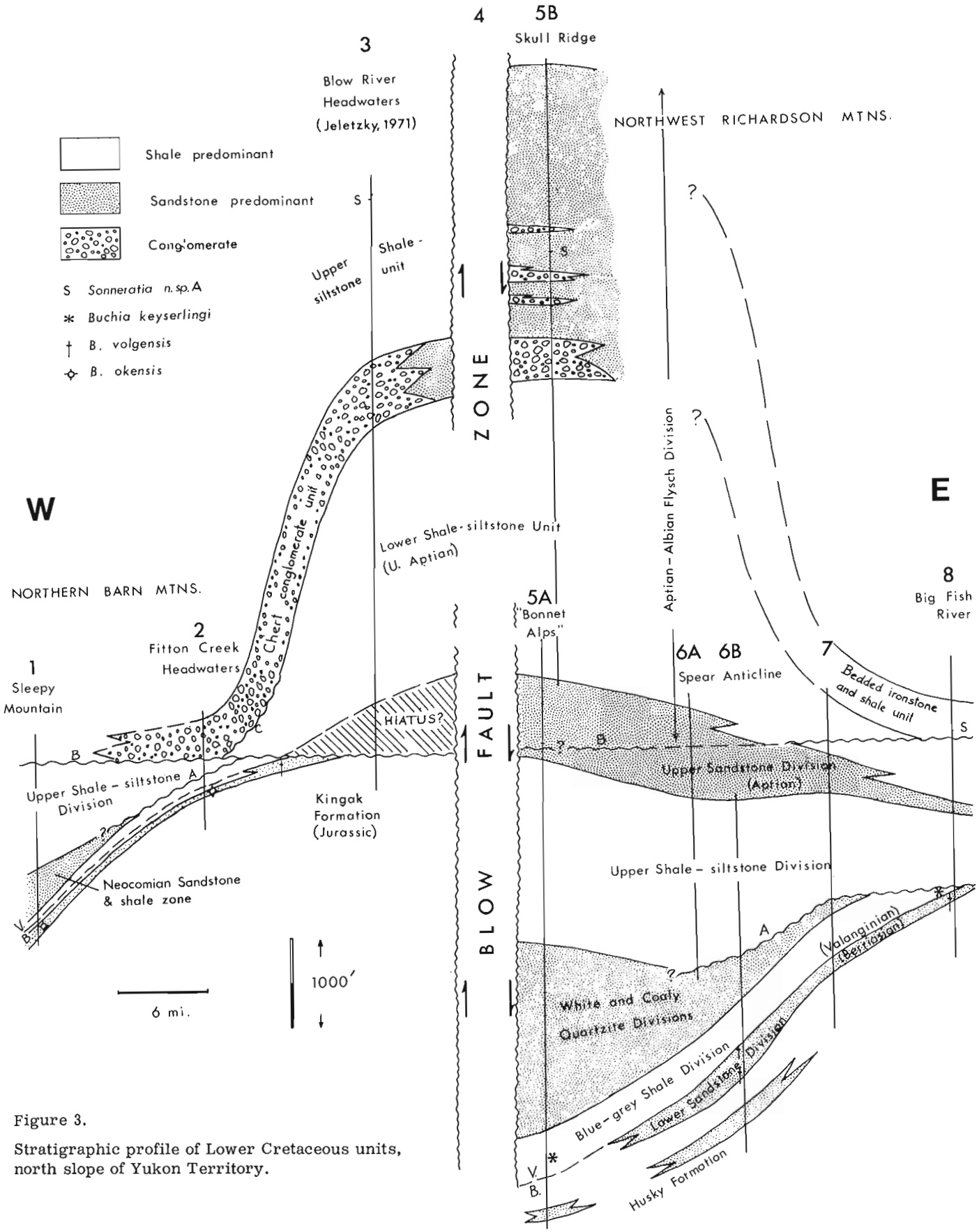

Figure 3.

Stratigraphic profile of Lower Cretaceous units, north slope of Yukon Territory.

marks a change in source-area and dispersal directions. The unconformity is identified in a section 3 miles northeast of the "Bonnet Alps" by a hematitic granular conglomerate containing mostly quartz-arenite sandstone clasts (?Neocomian sandstone) about 100 feet above the base of the Upper sandstone division. Sandstones below this level are very quartzose; however, above the unconformity they are rich in limestone, sandstone and chert fragments. This change, as well as paleocurrent data, suggest a western derivation of clastics above the unconformity, but a southeastern source is indicated for those below. Farther eastward the unconformity cannot be recognized until one reaches the area of Mount Davies Gilbert.

Upper Lower Cretaceous (Late Aptian and Albian) Rocks

The youngest sedimentary rocks of the area (Fig. 2), including those from the Upper Cretaceous and upper Lower Cretaceous (Aptian and Albian stages), have not undergone major lateral displacements according to present knowledge of local stratigraphy and sedimentology.

The Aptian-Albian flysch division is thickest within Rapid Fault Array, and is evenly distributed on each side of it. From the east near Mackenzie Delta, this sequence thickens westerly by a factor of ten (Young, 1972), and essentially maintains its thick trough-fill character well to the west of Blow River. Hence, its general thickness trend is undisturbed by the presence of Rapid Fault Array.

The lowest stratigraphic unit within the flysch division seems unaffected by Rapid Fault Array. This unit, a thick marine shale of probable latest Aptian age, referred to as the "lower shale-siltstone unit" in Blow River-Bonnet Lake area by Jeletzky (1971, p. 210) can be traced eastward across the fault array and is more or less identical with the "lower mudstone member" of Young (1972, p. 231) on the eastern side of the array.

Sedimentary features in the Albian part of the flysch do not suggest the presence of lateral displacements within the array. Maximum phenoclast sizes, within Albian conglomerates and sandstones, were plotted (Fig. 2) on a map together with dominant paleocurrent trends in order to show possible discontinuities in trends. A general easterly fining trend with local aberrations is indicated, paralleling downcurrent paleodispersal directions. Axial flow in a north-south sense occurred on the trough floor located in the middle of Rapid Fault Array but, farther to the east, even finer sands continued to be dispersed towards the east.

A 3,500-foot accumulation of conglomerate and sandstone at Skull Ridge (Fig. 3), located along the western margin of Rapid Fault Array, attests to a considerable downwarp of the basin relative to the area immediately to the west. Equivalent rocks in the chert conglomerate unit (Jeletzky, 1971) west of Skull Ridge are relatively thin and are separated from the Skull Ridge sandstones by a narrow fault zone, assumed to be a northerly extension of the Blow Fault Zone. This fault zone may represent the locus of downward displacements of the eastern part of the flysch trough during the time of Albian sedimentation, with the result that sands largely bypassed the western side and accumulated in the eastern downwarp.

The foregoing interpretation requires that the Upper shale-siltstone unit which overlies the chert conglomerate unit west of Blow Fault Zone be younger than most of Skull Ridge sandstones. The fact that both contain the early Albian ammonite *Sonneratia* n. sp. A may be accounted for by the rapid rates of sedimentation which occurred in the flysch trough, such that a single fossil zone is represented by a great thickness of rocks.

Significance of Stratigraphic Contrasts

The stratigraphic contrasts in Lower Cretaceous rocks outlined above indicate that large displacements occurred along the Blow Fault Zone in Early Cretaceous time. The stratigraphic successions preserved on either side indicate that the west side was displaced upward relative to the east side, during three main episodes in Early Cretaceous time.

The timing of the first episode is poorly defined due to lack of paleontological control. This uplift caused marked thinning of the Neocomian sandstone and shale zone northeastward from Barn Mountains (Unconformity A). Truncation of sandstone units of near-equivalent age below the Upper shale-siltstone division has been recorded elsewhere in the region to the east (Jeletzky, 1961, p. 537-539; Young, 1972, p. 230) and to the south (Jeletzky, 1973, p. 25-27), and probably is related to regional mid-Valanginian to early Hauterivian tectonic movements. Some or all of the detritus in the very thick Coaly quartzite division in the "Bonnet Alps" may have been derived from an uplifted block adjacent to the west.

The second episode of fault displacements is recorded by the Aptian unconformity and associated marked stratigraphic differences in rocks below the unconformity from one side of the fault zone to the other, as discussed above. This episode occurred during the regional Aptian orogeny (Jeletzky, 1961b) which resulted in a pronounced restructuring of the depositional framework in northern Yukon (Young, 1974).

An early Albian uplift of a western block is indicated by the presence of the Chert conglomerate unit within the Aptian-Albian flysch division. This uplift was not localized along the Blow Fault Zone, however, but occurred primarily in Barn Uplift (Dyke, 1974) some ten miles to the west, where the Chert conglomerate unit lies unconformably (Unconformity C) on older Cretaceous shales (Fig. 3) (Young, 1973). Practically coeval with this uplift were downward displacements of the eastern part of the flysch basin along the Blow Fault Zone.

The uplift of the western block is indicated by the Bouguer gravity anomaly map in the Beaufort Sea (Sobczak et al., 1973). The gravity field indicates generally higher anomalies west of a line extending offshore from the Blow Fault Zone, indicating relatively denser rocks (basement?) in that area. This map also shows a marked discontinuity in the trends of gravity

fields from one side of the line to the other (Fig. 1). These differences are due probably to contrasting structural grains in underlying rock sequences.

Good stratigraphic evidence for lateral displacements along Blow Fault Zone generally is lacking, although in rocks older than Albian, differences in facies and thicknesses could be explained in part as due to lateral off-sets.

Significant lateral displacements need not be expected along Blow Fault Zone, however, because the latter merges with the Porcupine and Yukon faults at a 45° angle (Fig. 1). Hence, purely transcurrent movements on the Porcupine Fault must have been partly transformed into compressive translational components in the Blow Fault Zone. This type of transition is illustrated and discussed by Wilcox, Harding and Seely (Fig. 14, 1973), whereby right lateral wrenching can result in a series of uplifted blocks within a zone of low-angle convergent wrench-faulting. As shown above, a western uplifted block is indeed the observed feature associated with Blow Fault Zone.

Acknowledgments

The writer benefitted greatly from discussions with, and critical comments by, D.K. Norris and C.J. Yorath in preparing this paper.

References

Dyke, L.D.
1974: Structural investigations in Barn Mountains, northern Yukon Territory; in Report of Activities, April to October, 1973, Geol. Surv. Can., Paper 74-1, Part A, p. 303-308.

Jeletzky, J.A.
1961a: Upper Jurassic and Lower Cretaceous rocks, west flank of Richardson Mountains between the headwaters of Blow River and Bell River, Yukon Territory; Geol. Surv. Can., Paper 61-9.

1961b: Eastern slope, Richardson Mountains: Cretaceous and Tertiary structural history and regional significance; in Geology of the Arctic, Proc. First Intern. Symp. on Arctic Geology, v. 1, Univ. of Toronto Press, p. 532-583.

1971: Stratigraphy, facies and paleogeography of Mesozoic rocks of northern and west-central Yukon; in Report of Activities, April to October 1970, Geol. Surv. Can., Paper 71-1, Part A, p. 203-221.

Jeletzky, J.A. (cont'd)
1973: Stratigraphy, facies and paleogeography of Jurassic and Cretaceous rocks of north Yukon and Mackenzie District, N.W.T.; Open File report 177, Geol. Surv. Can., 53 p.

Norris, D.K.
1971: Tectonic complex, northern Yukon Territory and western District of Mackenzie, Canada (abstr.); Geol. Soc. Am., Rocky Mtn. Sect., 24th Ann. Mtg., Calgary, Alta., May 10-15, 1971, oral presentation and abstract, in Geol. Soc. Am. Bull., v. 3, p. 398-399.

1973: Tectonic styles of northern Yukon Territory and northwestern District of Mackenzie, Canada; in Arctic Geology, Am. Assoc. Pet. Geol., Mem. 19, p. 23-40.

Structural geometry and geological history of the northern Canadian Cordillera; in Proc. 1973 Can. Soc. Exploration Geophysicists Nat. Convention, Calgary, Alta., R.B. Cruz, ed. (in press)

Sobczak, L.W., Stephens, L.E., Winter, P.J., and Hearty, D.B.
1973: Gravity measurements over the Beaufort Sea, Banks Island and Mackenzie Delta; Gravity Map Series of the Earth Physics Branch, Dept. of Energy, Mines and Resources, Canada, 16 p.

Wilcox, R.E., Harding, T.P., and Seely, D.R.
1973: Basic wrench tectonics; Am. Assoc. Pet. Geol. Bull., v. 57, p. 74-96.

Young, F.G.
1972: Cretaceous stratigraphy between Blow and Fish Rivers, Yukon Territory; in Report of Activities, April to October, 1971, Geol. Surv. Can., Paper 72-1, Part A, p. 229-235.

1973: Jurassic and Cretaceous stratigraphy between Babbage and Blow Rivers, Yukon Territory; in Report of Activities, April to October, 1972, Geol. Surv. Can., Paper 73-1, Part A, p. 277-281.

1974: Mesozoic epicontinental, flyschoid and molassoid depositional phases of Yukon's north slope; in Proc. of the Symp. on the Geology of the Canadian Arctic, May, 1973, Saskatoon, J.D. Aitken and D.J. Glass eds., Can. Soc. Pet. Geol. and Geol. Assoc. Can., p. 181-202.

AUTHOR INDEX